ADVANCES IN THE RESEARCH OF DIABETIC RETINOPATHY

EDITED BY: Michele Lanza, Khalid Siddiqui and Subrata Chakrabarti
PUBLISHED IN: Frontiers in Endocrinology and Frontiers in Public Health

frontiers Research Topics

ISSN 1664-8714
ISBN 978-2-83250-736-0
DOI 10.3389/978-2-83250-736-0

About Frontiers

Frontiers is more than just an open-access publisher of scholarly articles: it is a pioneering approach to the world of academia, radically improving the way scholarly research is managed. The grand vision of Frontiers is a world where all people have an equal opportunity to seek, share and generate knowledge. Frontiers provides immediate and permanent online open access to all its publications, but this alone is not enough to realize our grand goals.

Frontiers Journal Series

The Frontiers Journal Series is a multi-tier and interdisciplinary set of open-access, online journals, promising a paradigm shift from the current review, selection and dissemination processes in academic publishing. All Frontiers journals are driven by researchers for researchers; therefore, they constitute a service to the scholarly community. At the same time, the Frontiers Journal Series operates on a revolutionary invention, the tiered publishing system, initially addressing specific communities of scholars, and gradually climbing up to broader public understanding, thus serving the interests of the lay society, too.

Dedication to Quality

Each Frontiers article is a landmark of the highest quality, thanks to genuinely collaborative interactions between authors and review editors, who include some of the world's best academicians. Research must be certified by peers before entering a stream of knowledge that may eventually reach the public - and shape society; therefore, Frontiers only applies the most rigorous and unbiased reviews.
Frontiers revolutionizes research publishing by freely delivering the most outstanding research, evaluated with no bias from both the academic and social point of view. By applying the most advanced information technologies, Frontiers is catapulting scholarly publishing into a new generation.

What are Frontiers Research Topics?

Frontiers Research Topics are very popular trademarks of the Frontiers Journals Series: they are collections of at least ten articles, all centered on a particular subject. With their unique mix of varied contributions from Original Research to Review Articles, Frontiers Research Topics unify the most influential researchers, the latest key findings and historical advances in a hot research area! Find out more on how to host your own Frontiers Research Topic or contribute to one as an author by contacting the Frontiers Editorial Office: frontiersin.org/about/contact

ADVANCES IN THE RESEARCH OF DIABETIC RETINOPATHY

Topic Editors:
Michele Lanza, University of Campania Luigi Vanvitelli, Italy
Khalid Siddiqui, King Saud University, Saudi Arabia
Subrata Chakrabarti, Western University, Canada

The authors declare that the research was conducted in the absence of any commercial or financial relationships that could be construed as a potential conflict of interest.

Citation: Lanza, M., Siddiqui, K., Chakrabarti, S., eds. (2022). Advances in the Research of Diabetic Retinopathy. Lausanne: Frontiers Media SA.
doi: 10.3389/978-2-83250-736-0

Table of Contents

frontiers | Frontiers in Endocrinology

TYPE Editorial
PUBLISHED 25 October 2022
DOI 10.3389/fendo.2022.1038056

OPEN ACCESS

EDITED BY
Åke Sjöholm,
Gävle Hospital, Sweden

REVIEWED BY
Renu Kowluru,
Wayne State University, United States

*CORRESPONDENCE
Subrata Chakrabarti
subrata.chakrabarti@lhsc.on.ca

SPECIALTY SECTION
This article was submitted to Clinical Diabetes, a section of the journal Frontiers in Endocrinology

RECEIVED 06 September 2022
ACCEPTED 12 October 2022
PUBLISHED 25 October 2022

CITATION
Chakrabarti S, Lanza M and Siddiqui K (2022) Editorial: Advances in the research of diabetic retinopathy. *Front. Endocrinol.* 13:1038056. doi: 10.3389/fendo.2022.1038056

Editorial: Advances in the research of diabetic retinopathy

Subrata Chakrabarti[1]*, Michele Lanza[2] and Khalid Siddiqui[3]

[1]Western University, London, ON, Canada, [2]University of Campania Luigi Vanvitelli, Caserta, Italy, [3]Strategic Center for Diabetes Research, College of Medicine, King Saud University, Riyadh, Saudi Arabia

KEYWORDS

diabetic retinopathy, pathogenesis, mechanisms, diagnosis, treatment

Editorial on the Research Topic
Advances in the research of diabetic retinopathy

Diabetes remains a planetary crisis with its prevalence estimated to increase by nearly 50% in the next 25 years (1, 2) One of the main challenges for the diabetic patients is the development of chronic complications, leading to end organ damage. Chronic diabetic complications are a major cause of mortality and morbidity for the people living with diabetes. Retinal damage in diabetics, also known as diabetic retinopathy (DR) is a leading cause of blindness in working-aged adults (3, 4). Although DR begins with asymptomatic hyperglycemic damage to the retinal microvasculature, in particularly endothelial cells, it eventually causes a symphony of abnormalities at various levels, creating cellular dysfunction and damage, ultimately leading to functional and structural changes in the retina that result in vision impairment and blindness (5–7). Current treatment approaches serve as band-aid solutions that address the root of the problem in a very limited perspective (8, 9). To develop a solid preventive and therapeutic approach for DR, a better understanding of this disease is essential.

This Research Topic presents a large number of articles including original research as well as review to improve our understanding of DR. The specific topics represent various levels of complexities. The publications address issues ranging from the molecular level to cellular level to animal levels and finally to DR patients. The articles investigate and discuss specific pathogenetic mechanisms, effects of current treatment modalities and treatment outcomes.

It was also to be noted that this collection also identifies potential upcoming treatment modalities and diagnostic approach using various RNA molecules as well as application of artificial intelligence and machine learning for DR diagnosis and assessment of prognosis.

Among the review topics Zhang et al. compared effectiveness of panretinal photocoagulation alone along with in combination of anti VEGF treatment. Guo et al. discussed uric acid abnormalities, an understudied area in DR. Similarly, Zheng et al. reviewed another relatively unappreciated topic, i.e, relationship of sleep quality with risk

of developing DR. Furthermore, Zhang et al. reviewed the effects of calcium dobesylate treatments in patients with non-proliferative DR.

As we are entering in an area of RNA based therapy and diagnosis, two of the presented articles provided valuable insight in this area. Niu et al. reviewed exosomes/microRNAs in the treatment of DR and Kowluru discussed Long Noncoding RNAs and Mitochondrial Homeostasis in the Development of DR. Practical applications of these reviews these reviews were also supported by original research articles. In one such article Biswas et al. described the use of a serum lncRNAs panel to diagnose DR. In the other article Yang et al. characterised small RNAs and microRNAs in the vitreous Humor of proliferative DR. It was also revealed that plasma metabolomic profiling (Sun et al.) growth differentiation factor 15 levels (Niu et al.) may also be effective in the assessment of DR.

Several researchers presented original research describing roles of various additional molecules in DR, including secreted cystine rich acidic protein (Luo et al.), homocysteine (Luo et al.) and retinal inflammation and macrophage infiltration (Meng et al.).

The articles presented in this Research Topic further showed the impact of glycemic control on photoreceptor Layers and RPE in type 2 Diabetes (Ishibashi et al.). Furthermore, Xie et al. showed assessment of fundus structure using OCT may act as a predictive model for treatment effect for diabetic macular edema. Best corrected visual acuity in macular edema may also be predicted by OCT (Li et al.). Deng et al. proposed the use of hand-held ERG device for DR Screening. In addition, it was shown that artificial intelligence and machine learning may also predict DR in type 2 diabetic patients (Zhao et al.). It was also important to note the data of Kailuan eye study (Yongpeng et al), showing that DR is an independent risk factor for dry AMD.

In conclusion, this Research Topic brings insights and a wealth of knowledge regarding DR, involving its pathogenesis, diagnostic modalities, clinical presentation and treatment. We sincerely feel that these set of articles have set the stage for new knowledge creation and their clinical application in this area in future.

Author contributions

SC drafted the manuscript. ML and KS reviewed, provided input and approved the content.

Conflict of interest

The authors declare that the research was conducted in the absence of any commercial or financial relationships that could be construed as a potential conflict of interest.

Publisher's note

References

1. Saeedi P, Petersohn I, Salpea P, Malanda B, Karuranga S, Unwin N, et al. Global and regional diabetes prevalence estimates for 2019 and projections for 2030 and 2045: Results from the international diabetes federation diabetes atlas, 9th edition. *Diabetes Res Clin Pract* (2019) 157:107843. doi: 10.1016/j.diabres.2019.107843

2. Cheung N, Mitchell P, Wong TY. Diabetic retinopathy. *Lancet (Lond Engl)* (2010) 376(9735):124–36. doi: 10.1016/S0140-6736(09)62124-3

3. Leasher JL, Bourne RRA, Flaxman SR. Global estimates on the number of people blind or visually impaired by diabetic retinopathy: A meta-analysis from 1990 to 2010. *Dia Care* (2016) 39:1643–9. doi: 10.2337/dc15-2171

4. Teo ZL, Tham YC, Yu M, Chee ML, Rim TH, Cheung N, et al. Global prevalence of diabetic retinopathy and projection of burden through 2045. *Ophthalmology* (2021) 128(11):1580–91. doi: 10.1016/j.ophtha.2021.04.027

5. Khan ZA, Chakrabarti S. Chronic diabetic complications: Endothelial cells at the frontline. chapter 9. In: Rahman AU, Choudhary I, editors. *Front Cardiovasc Drug Discov*. Sharjah, U.A.E: Bentham Science publishers (2010). p. pp121–137.

6. Gui F, You Z, Fu S, Wu H, Zhang Y. Endothelial dysfunction in diabetic retinopathy. *Front Endocrinol (Lausanne)* (2020) 11:591. doi: 10.3389/fendo.2020.00591

7. Brownlee M. The pathobiology of diabetic complications: A unifying mechanism. *Diabetes* (2005) 54:1615–25. doi: 10.2337/diabetes.54.6.1615

8. Duh EJ, Sun JK, Stitt AW. Diabetic retinopathy: current understanding, mechanisms, and treatment strategies. *JCI Insight* (2017) 2(14):e93751. doi: 10.1172/jci.insight.93751

9. Tomita Y, Lee D, Tsubota K, Negishi K, Kurihara T. Updates on the current treatments for diabetic retinopathy and possibility of future oral therapy. *J Clin Med* (2021) 10:4666. doi: 10.3390/jcm10204666

frontiers in Endocrinology

ORIGINAL RESEARCH
published: 15 March 2021
doi: 10.3389/fendo.2021.627395

The Relationship Between Circulating Growth Differentiation Factor 15 Levels and Diabetic Retinopathy in Patients With Type 2 Diabetes

Yixin Niu†, Weiwei Zhang†, Jie Shi†, Yueming Liu, Hongmei Zhang, Ning Lin, Xiaoyong Li, Li Qin, Zhen Yang and Qing Su**

Department of Endocrinology, Xinhua Hospital, Shanghai Jiaotong University School of Medicine, Shanghai, China

OPEN ACCESS

Edited by:
Khalid Siddiqui, King Saud University, Saudi Arabia

Reviewed by:
Claudio Bucolo, University of Catania, Italy
Reema Bansal, Post Graduate Institute of Medical Education and Research (PGIMER), India

***Correspondence:**
Zhen Yang
yangzhen@xinhuamed.com.cn
Qing Su
suqing@xinhuamed.com.cn

†These authors have contributed equally to this work

Specialty section:
This article was submitted to Clinical Diabetes, a section of the journal Frontiers in Endocrinology

Received: *09 November 2020*
Accepted: *25 February 2021*
Published: *15 March 2021*

Citation:
Niu Y, Zhang W, Shi J, Liu Y, Zhang H, Lin N, Li X, Qin L, Yang Z and Su Q (2021) The Relationship Between Circulating Growth Differentiation Factor 15 Levels and Diabetic Retinopathy in Patients With Type 2 Diabetes. Front. Endocrinol. 12:627395. doi: 10.3389/fendo.2021.627395

Objective: Growth differentiation factor 15 (GDF-15) is a member of the TGF-β superfamily that has anti-inflammatory properties. The objective of this study was to evaluate the relationship between circulating GDF-15 levels and diabetic retinopathy (DR) in patients with type 2 diabetes.

Materials/Methods: A case–control study was performed in which 402 patients with type 2 diabetes were enrolled. Of these, 171 patients had DR and the remaining 231 patients without DR acted as controls. The plasma GDF-15 levels were measured using ELISA, while DR was diagnosed using the canon ophthalmic digital imaging system and the Canon EOS 10D digital camera (Canon, Tokyo, Japan) through a non-pharmacologically dilated pupil.

Results: The levels of GDF-15 were significantly higher in patients with DR [168.9 (112.9–228.3) pg/ml *vs*. 127.8 (96.1–202.8) pg/ml, $P < 0.001$] compared to controls. Results of the Spearman correlation analysis showed that the GDF-15 levels were positively associated with the duration of diabetes morbidity, fasting plasma glucose, systolic blood pressure, albumin/creatinine ratio, creatinine, and liver enzymes, but negatively associated with eGFR (both $P < 0.001$). The participants in the highest GDF-15 quartile had a significantly increased risk for DR (OR = 2.15, 95% CI 1.53–3.02) after adjusting for potential cofounders.

Conclusions: The circulating GDF-15 levels are positively associated with DR independent of potential cofounders.

Keywords: GDF-15, type 2 diabetes, mild non-proliferative DR, moderate NPDR, vision-threatening DR

INTRODUCTION

The prevalence of diabetes in China has become a major public health concern with ~9.7% of all adults affected (1). Diabetic retinopathy (DR) is a microvascular complication of diabetes and is the leading cause of blindness among adults of working-age around the world (2). Although DR is initially asymptomatic, its progression is characterized by damage to the retinal microvasculature due to inflammation and oxidative stress caused by chronic hyperglycemia. Recently, studies have

focused on inflammatory biomarkers and risk factors for endothelial dysfunction, such as C-reactive protein (CRP), and tumor necrosis factor-α (TNF-α) that are considered to be prognostic factors for the development of DR. These studies have also shown that some cytokines may be associated with the development of DR (3–5).

Growth differentiation factor 15 (GDF-15), also known as macrophage inhibitory cytokine-1(MIC-1) (6), placental transformation growth factor-b (PTGF-b) (7–9), prostate derived factor (PDF) (10), placental bone morphogenetic protein (PLAB) (11, 12), NSAID activated gene-1 (NAG-1) (13, 14), and PL74 (15), are divergent members of the transforming growth factor-β (TGF-β) superfamily with anti-inflammatory properties. GDF-15 is highly expressed in cardiomyocytes, adipocytes, macrophages, endothelial cells, and vascular smooth muscle cells during tissue injury and inflammatory states. It plays a crucial role in the development and progression of cardiovascular diseases such as heart failure, coronary artery diseases, atrial fibrillation, diabetes, cancer, and cognitive impairment (16, 17). In type 2 diabetes, GDF-15 predicts the development of proteinuria in patients with diabetic nephropathy, suggesting that GDF-15 may be a part of an anti-inflammatory response to microvascular damages (18). Moreover, GDF-15 is associated with a number of circulating proangiogenic endothelial progenitor cells in patients with type 2 diabetes (19). Furthermore, GDF-15 expression is markedly increased before the onset of type 2 diabetes (20), which suggests that GDF-15 is a potential biomarker of DR (21).

Therefore, the current study aimed to investigate the relationship between plasma GDF-15 levels and the risk of DR in a large cohort of type 2 diabetic patients.

METHODS

Study Population

This was a cohort study aimed at assessing the risk factors associated with the development of diabetic complications. Study participants were type 2 diabetes patients recruited from the Department of Endocrinology at Xinhua Hospital Affiliated to Shanghai Jiaotong University School of Medicine between 2013 and 2014. Diabetes was defined according to the 2008 American Diabetes Association diagnostic criteria (22).

Individuals with the following conditions were excluded from the study: cancer, acquired immune deficiency syndrome, severe psychological disorders, clinical signs or symptoms of inborn errors of metabolism, a history of vitreal surgery, senile dementia, tuberculosis, a cataract on examination, or any other communicable disease. A total of 402 participants with type 2 diabetes were included in this study. Written informed consent was obtained from all participants. The Ethics Committee of Xinhua Hospital Affiliated to Shanghai Jiaotong University School of Medicine approved this study.

Clinical Data Collection and Biochemical Measurements

Anthropometric measurements, questionnaire, physical examination, and laboratory measurements were performed. The waist circumference was defined as the midway level between the costal margins and the iliac crests. Blood pressure was assessed twice on the right arm after a 15-min rest in a sitting position using a standard mercury sphygmomanometer. BMI was calculated as the weight in kilograms divided by the square height in meters (kg/m^2). Age, alcohol consumption (yes/no, history of alcohol consumption was defined as "yes", lack of history was defined as "no"), smoking (yes/no, history of smoking was defined as "yes"; lack of history was defined as "no"), education status, and duration of diabetes morbidity were assessed using interviews. Based on the International Physical Activity Questionnaire scoring protocol, the physical activity level was classified as low, moderate, or high level.

The A1c was measured using high-performance liquid chromatography (BIO-RAD, D10, CA), while fasting plasma glucose levels were tested using the glucose oxidase method (ADVIA-1650 Chemistry System, Bayer, Leverkusen, Germany). Lipid profiles, liver enzyme profiles, and creatinine (Cr) were determined using a Hitachi 7080 analyzer (Hitachi 7080; Tokyo, Japan), while fasting insulin was determined using the radioimmunoassay method (Linco Research, St. Charles, MO). The albumin/creatinine ratio (ACR) was calculated as milligrams of urinary albumin excretion per gram of urinary creatinine. Glomerular filtration rate (eGFR) was estimated using a simplified Modification of Diet in Renal Disease formula recalibrated for the Chinese: $186 \times (\text{serum creatinine} \times 0.011)^{-1.154} \times (\text{age})^{-0.203} \times (0.742 \text{ if female}) \times 1.233$ (23). The homoeostasis model assessment (HOMA) value for insulin resistance (HOMA-IR) was evaluated with the following formula: fasting insulin × fasting glucose/22.5. The HOMA-β was calculated using the formula described by Matthews et al. (24).

Circulating GDF-15 Levels, Adiponectin and CRP

The circulating levels of GDF-15 were determined in duplicate using the Duoset kit for ELISA (DY805; R&D Systems, Minneapolis, MN) according to the instructions of the manufacturer. The ELISA system had an intra-assay coefficient of variation of 3 to 9% and an inter-assay coefficient of variation of 4 to 10.2%.

The circulating adiponectin and C-reactive protein (CRP) were measured using ELISA kits (DY1065 and DY1707, respectively; R&D Systems, Minneapolis, MN) according to the instructions of the manufacturer.

Diagnosis of Diabetic Retinopathy

Dilated ophthalmic eye examinations including fundus photography were performed by an experienced ophthalmologist. DR was classified as cases without diabetic retinopathy (non-DR), mild non-proliferative DR (NPDR), moderate NPDR and vision-threatening DR (VTDR).

Assessment of Diabetic Retinopathy

Fundus photography was performed using digital non-mydriatic camera (CR6-45NM; Canon, Lake Success, NY) according to the International Classification of Diabetic Retinopathy (25).

The severity of DR was classified as 1) non-DR; 2) mild non-proliferative DR (NPDR); 3) moderate NPDR; 4) severe NPDR; and 5) proliferative DR (PDR). Due to the limited number of study participants with PDR (n = 2), PDR cases were combined with severe NPDR cases to give the vision-threatening DR (VTDR) group. When binocular DR was present and unequal, we used the more advanced DR measurement for analyses. Patients with ungradable retinal fundus photographs of both eyes were excluded from the study.

Statistical Analysis

Continuous variables with normal distribution were shown as means with SDs, whereas variables with skewed distribution were presented as median with interquartile range. For comparisons between groups, continuous variables were compared using Student *t* tests or Mann–Whitney U tests. Categorical variables were expressed as proportions and compared across groups using X^2 tests. Spearman correlation analysis was used to calculate the correlation coefficients between GDF-15 and metabolic parameters. Multivariate logistic regression models were performed to determine the potential relationship between GDF-15 levels and the risk of DR. To minimize the potential confounding factors, covariates were selected based on biologic interest, well established risk factors for DR, or associated exposures and outcomes. Variables showing P < 0.05 in the univariable regression were entered into the multivariable model. All statistical analyses were performed with the SPSS software (version 25.0). A two-sided P < 0.05 was considered to be statistically significant.

RESULTS

Baseline Characteristics

Out of a study population of 402 participants, 171 individuals (42.5%) had DR. The plasma GDF-15 levels were significantly higher in patients with DR (168.9 [112.9–228.3] pg/ml *vs.* 127.8 [96.1–202.8] pg/ml, P < 0.001) compared to controls. Moreover, there was an increasing trend in the median (inter-quartile range) of GDF-15 concentrations from the patients with no DR, mild NPDR, moderate NPDR, to VTDR (P < 0.001 for trend) (**Figure 1**). The clinical characteristics of the study participants are shown in **Table 1**.

Results of the Spearman correlation analysis showed that GDF-15 was positively correlated with age (r = 0.14, P < 0.0001), duration of morbidity (r = 0.40, P < 0.0001), fasting plasma glucose (r = 0.13, P < 0.0001), systolic blood pressure (r = 0.15, P < 0.0001), Cr (r = 0.21, P < 0.0001), and ACR (r = 0.13, P < 0.0001), but was negatively correlated with eGFR (r = −0.21, P < 0.0001) (**Figure 2**). Multiple regression analysis with a stepwise model was used to assess the independent variables that affect the GDF-15 plasma levels. The variables entered in the model were as follows: age, gender, CRP, BMI, WC, SBP, DBP, ALT, AST, GGT, HbA1c, fasting plasma glucose, fasting plasma insulin, triglycerides, total cholesterol, LDL-c and HDL-c. The main determinants of GDF-15 were age (β = 0.304, P < 0.001), ALT (β = 0.153, P < 0.001) and Cr (β = 0.152, P < 0.001).

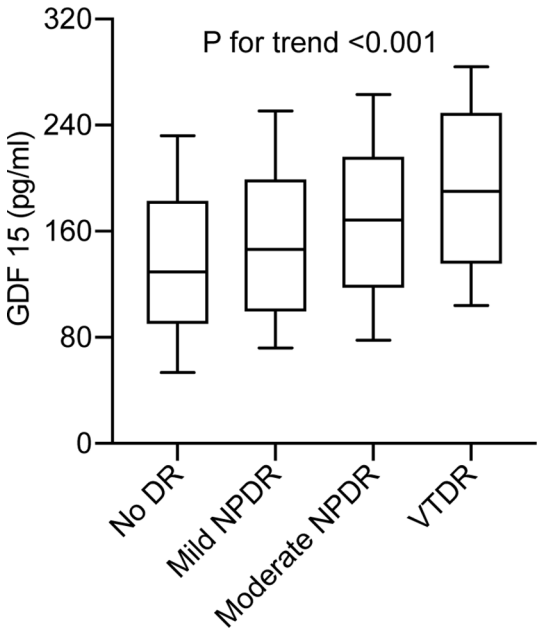

FIGURE 1 | Plasma GDF-15 levels in type 2 diabetes without DR compared with patients with mild non-proliferative DR (NPDR), moderate NPDR, or vision-threatening DR (VTDR). Boxes represent the inter-quartile range, with the median superimposed as a horizontal line. Error bars indicate ranges of plasma GDF-15 levels. *P* < 0.001 for trend.

Association Between GDF-15 and DR

Table 2 displays the odds ratios (ORs) for DR based on the GDF-15 quartiles. As expected, there was an increase in the ORs for DR from the 1st to the 4th GDF-15 quartiles in the study cohort (P < 0.001 for trend). In the highest GDF-15 quartile, the adjusted OR of DR was 2.15 [95% confidence interval (CI) 1.53–3.02] after adjusting for age, gender, smoking, alcohol consumption, education status, physical activity, BMI, waist circumference, CRP, adiponectin, HOMA-IR, liver enzymes, diabetes duration, FPG, eGFR, Cr, and ACR. A positive linear dose–response relationship was evident in the cubic spline regression model (**Figure 3**, P for non-linearity > 0.1).

Subgroup Analyses

Subgroup analyses were performed to examine potential effect modifiers, stratified by age (<65 *versus* ≥65 years), sex (male *versus* female), SBP (<140 *versus* ≥140 mmHg), waist circumference (<90 *versus* ≥90 cm for men and <85 *versus* ≥85 cm for women and), CRP (<3.0 *versus* ≥3.0 mg/L), and ACR (<30 *versus* ≥30 mg/g). Results of stratified analyses showed that the positive associations between GDF-15 levels and the presence of DR remained consistent across all subgroups (**Figure 4**). No interaction was observed with any of the variables (all P for interaction > 0.1).

DISCUSSION

In this cohort study, we found a significantly positive association between circulating GDF-15 levels and the risk of DR in

TABLE 1 | Characteristics of subjects according to the presence or absence of diabetic retinopathy (DR) (n = 402).

Characteristics	NDR (n = 231)	DR (n = 171)	P value
Case (male/female)	119/112	91/80	0.736
Age (year)	57.8 ± 8.3	57.3 ± 9.2	0.569
Duration (year)	5 (1–10)	10 (7–14)	<0.001
BMI (kg/m^2)	25.6 ± 3.8	25.3 ± 3.6	0.424
WC (cm)	86.5 ± 8.6	86.9 ± 8.7	0.647
SBP (mmHg)	127.1 ± 11.9	134.5 ± 12.5	<0.001
DBP (mmHg)	75.6 ± 9.2	78.7 ± 10.1	0.002
FPG (mmol/L)	7.6 (5.8–9.7)	9.4 (7.0–11.9)	<0.001
HbA1c (%)	9.1 ± 1.3	9.6 ± 1.5	<0.001
HOMA-IR	2.69 (1.79–3.89)	2.87 (1.85–3.99)	<0.001
TC (mmol/L)	4.83 ± 1.25	4.92 ± 1.31	0.485
TG (mmol/L)	1.68 (1.19–2.53)	1.77 (1.28–2.87)	<0.001
HDL (mmol/L)	1.39 (1.21–1.59)	1.32 (1.16–1.49)	0.009
LDL (mmol/L)	2.91 ± 0.94	2.98 ± 0.95	0.463
CRP (mg/L)	1.92 (1.26–2.70)	2.46 (1.38–3.61)	<0.001
Adiponectin (mg/L)	3.13 (2.39–3.95)	2.87 (2.06–3.73)	0.008
ALT (U/L)	16 (12–25)	22 (14–31)	<0.001
AST (U/L)	20 (16–25)	24 (19–31)	<0.001
GGT (U/L)	22 (16–28)	28 (19–39)	<0.001
Cr (μmol/L)	68.7 ± 18.6	77.9 ± 19.3	<0.001
ACR	10.1 ± 3.6	17.3 ± 3.9	<0.001
eGFR (mL/min/1.73 m^2)	104.3 (99.9-110.1)	93.6 (88.9–100.3)	<0.001
Hypoglycemic treatments			0.006
Insulin (%)	87 (37.7)	64 (37.4)	
OHA (%)	112 (48.5)	63 (36.8)	
Insulin + OHA (%)	32 (13.9)	44 (25.7)	
GDF-15 (pg/ml)	127.8 (96.1–202.8)	168.9 (112.9–228.3)	<0.001

ACR, albumin/creatinine ratio; ALT, alanine aminotransferase; AST, aspartate transaminase; BMI, body mass index; CRP, C-reactive protein; Cr, creatinine; DBP, diastolic blood pressure; eGFR, estimated glomerular filtration rate; FPG, fasting plasma glucose; GDF15, growth differentiation factor 15; GGT, γ-glutamyltransferase; HbA1c, glycated hemoglobin; HDL-C, high-density lipoprotein cholesterol; HOMA-IR, homeostasis model assessment-insulin resistance; LDL-C, low-density lipoprotein cholesterol; OHA, oral hypoglycemic agent; SBP, systolic blood pressure; TC, total cholesterol; TG, triglycerides; WC, waist circumference.

individuals with type 2 diabetes. This association remained even after extensively adjusting for potential confounders through the stratification of several potential risk factors that may have an effect on the GDF-15–DR relationship.

In our study, plasma levels of GDF-15 were significantly higher in patients with DR compared to patients without DR. Moreover, results of our study showed that plasma GDF-15 concentrations were associated with progression of DR in individuals with type 2 diabetes, after controlling for confounding risk factors. Glycemia, blood pressure, and duration of diabetes morbidity have been identified as risk factors for DR although there are still some controversies (26, 27). This is consistent with the findings from our study that showed that the duration of diabetes morbidity, HbA1c, CRP, and systolic blood pressure was a risk factor for DR in patients with type 2 diabetes. In line with a previous study (28), we also found that the plasma levels of GDF-15 were significantly associated with renal damage and could predict the development of diabetic retinopathy in patients with type 2 diabetes. Importantly, the association between circulating plasma GDF-15 concentrations and the progression of DR in type 2 diabetic patients in our study was independent of the traditional DR risk factors mentioned above.

GDF-15 was discovered and cloned as a divergent member of the TGF-β superfamily in the late 1990s (6). The GDF-15 gene is composed of two exons and contains one single intron that interrupts the coding sequences at identical positions within the pre-pro-domain of the corresponding proteins (7, 29). It is widely expressed in almost all tissues indicating that it has numerous vital cellular functions such as proliferation, migration, maintenance, and homeostasis (10). This suggests that alterations of serum GDF-15 levels may be associated with various diseases including heart failure, coronary artery diseases, cancer, diabetes, and diabetic renal damage (16–18). Circulating GDF-15 is likely to be secreted by endothelial cells such that the serum levels of GDF-15 are a general indication of endothelial and microvascular damage. This may explain the association between GDF-15 and DR since DR is primarily caused by microvascular injury during diabetes (30).

The mechanism of the microvascular effects of GDF-15 on DR in patients with type 2 diabetes has not been elucidated yet. Previous studies have shown that DR is characterized by a decrease in retinal perfusion caused by the constriction of arterioles, endothelial cell degeneration, microvascular destabilization caused by the retinal pericyte loss, and a release of proangiogenic factors that promote the development of many abnormal new vessels (26, 30). In addition, GDF-15 plays a major role in regulating the recruitment of inflammatory cells by directly interfering with leukocyte integrin activation and inhibiting leukocyte arrest and extravasation on the endothelium (30). Due to the anti-inflammatory role of GDF-15 in the vascular endothelial cell, the plasma levels of GDF-15 tend to rise with the progress of microvascular injury (31).

Alternatively, as a member of the TGF-β family, GDF-15 may signal through an alternate, non-TGF-β receptor mediated mechanism instead of the classical TGF-β signaling pathway through Smad phosphorylation (32–34). It may also play an important role in angiogenesis (34). GDF-15 impairs *in vitro* angiogenesis by blocking connective tissue growth factor 2 (CCN-2)-mediated tube formation in human umbilical vein endothelial (HUVEC) cells as well as inhibiting the CCN-2-dependent activation of focal adhesion kinase and subsequent decrease in $\alpha_V\beta_3$ integrin clustering. In the same vein, GDF-15, in combination with BMP-2, has been shown to mediate the inhibition of fenretidine-dependent tumor vessel growth by interfering with endothelial cell growth, migration, and invasion (35). There have been reports that angiogenesis in hypoxic HUVEC cells is promoted by a signaling pathway, which includes hypoxia-inducible factor 1-alpha (HIF-1alpha), VEGF, and p53 (36). Moreover, GDF-15 regulates endothelial cells through altered endothelial caveolar signaling (37). Increased circulating levels of GDF-15 have been attributed, inter alia, to endothelial dysfunction (38). It is possible that the increase in the plasma levels of GDF-15 in the patients with diabetes may cause a counter-regulatory and compensatory mechanism which protects against angiogenesis, but not sufficient to protect against DR. Interestingly, consistent with our hypothesis, we observed that the incidence of DR increased with the plasma GDF-15 quartiles in this study.

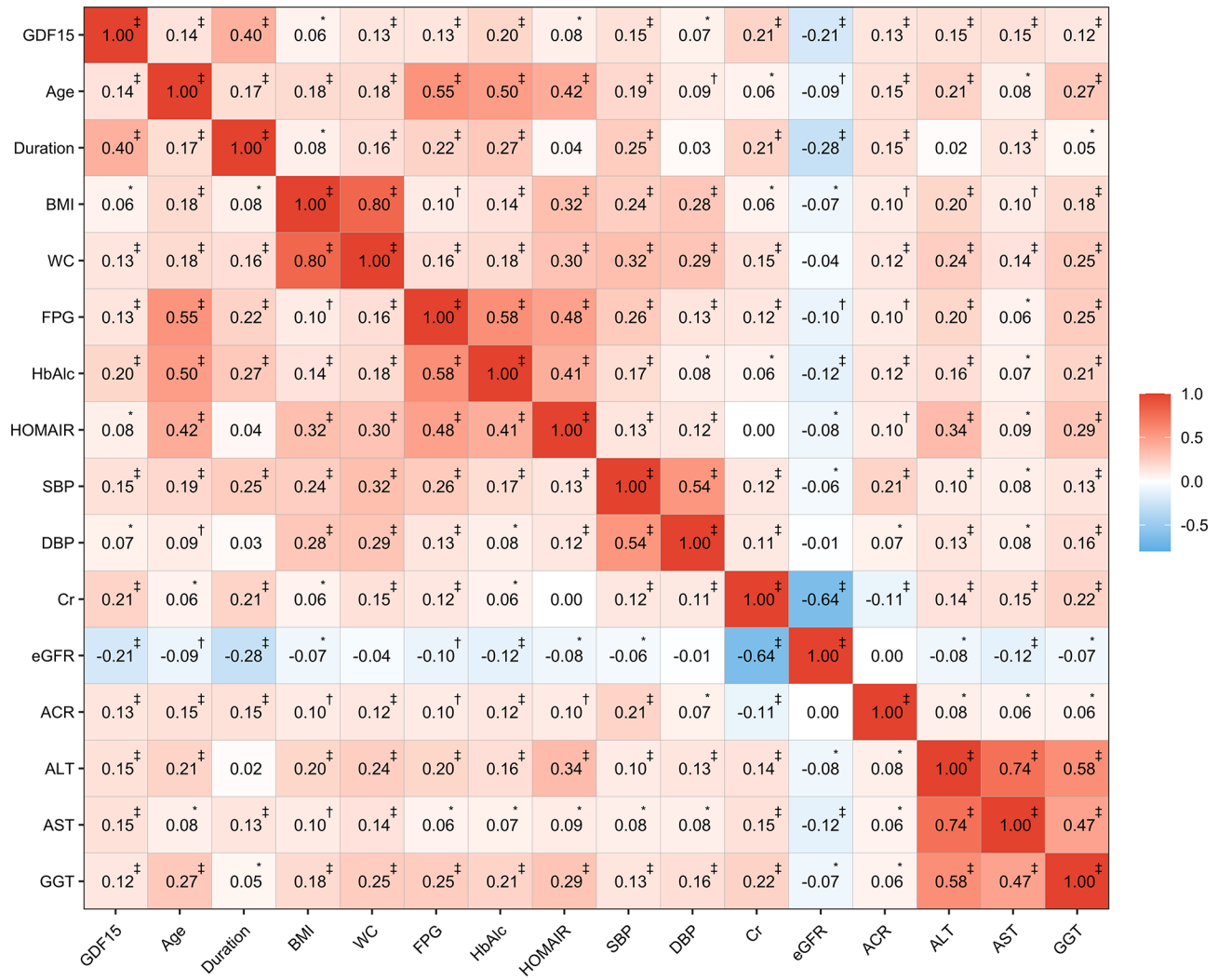

FIGURE 2 | Correlations between GDF-15 and clinical characteristics. The values in the cell represent the correlation coefficients based on spearman correlation. *P < 0.05; †P < 0.001; ‡P < 0.0001.

TABLE 2 | Adjusted odds ratios (ORs) of diabetic retinopathy according to quartiles of plasma growth differentiation factor 15 (GDF-15) levels.

	GDF15				P for trend
	Q1 n = 100	Q2 n = 101	Q3 n = 101	Q4 n = 100	
Model 1 OR (95% CI)	1.00	1.54 (1.16–2.03)	1.72 (1.31–2.26)	2.61 (1.99–3.40)	<0.001
Model 2 OR (95% CI)	1.00	1.50 (1.13–1.98)	1.64 (1.25–2.17)	2.30 (1.75–3.01)	<0.001
Model 3 OR (95% CI)	1.00	1.47 (1.11–1.95)	1.59 (1.21–2.10)	2.20 (1.67–2.89)	<0.001
Model 4 OR (95% CI)	1.00	1.46 (1.08–1.98)	1.58 (1.15–2.16)	2.15 (1.53–3.02)	<0.001

Model 1 was adjusted for age, gender, smoking, alcohol drinking, educational attainment, and physical activity. Model 2 was further adjusted for BMI and waist circumference. Model 3 was further adjusted for CRP, adiponectin, HOMA-IR, and liver enzymes. Model 4 was further adjusted for duration, FPG, eGFR, Cr, and ACR. Q, quartile. The quartile ranges of Q1, Q2, Q3, and Q4 of plasma GDF-15 level were <96.5, 96.5–141.7, 141.8–210.3, and >210.3 pg/ml, respectively. Q1 is the reference group. Multivariate logistic regression models were used to estimate the odds ratios (ORs) with corresponding 95% confidence intervals (CIs) for diabetic retinopathy.

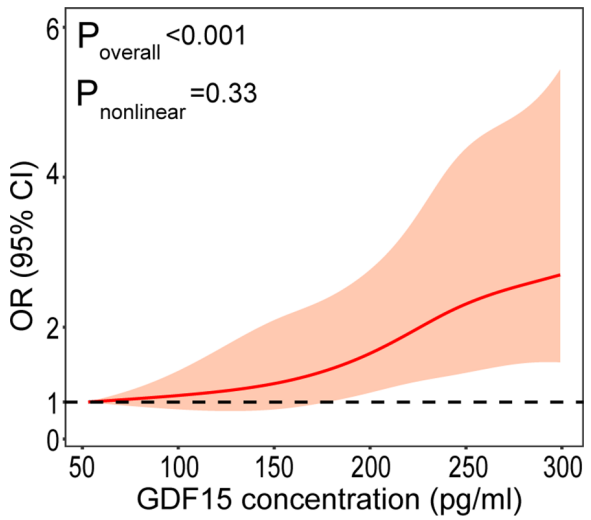

FIGURE 3 | Plasma GDF-15 levels on a continuous scale and the presence of DR. The solid line represents the odds ratio (OR) and the gray area represents the 95% confidence interval (CI). Model was adjusted for age, gender, smoking, drinking, physical activity, educational attainment, BMI, waist circumference, CRP, adiponectin, HOMA-IR, liver enzymes, duration, FPG, eGFR, Cr, and ACR.

This study establishes the association between DR and GDF-15 in type 2 diabetes. There are several limitations to this study. First, due to the cross-sectional nature of the present study, we could not determine whether GDF-15 plays a causal role in the pathogenesis of DR. Accordingly, prospective studies in the future are of vital importance. Second, plasma GDF-15 levels may vary among different populations, and it is unclear how local and ocular factors can influence DR. Third, the sample size was relatively small. Further studies are also required to determine the GDF-15 levels in a larger population. Moreover, VEGF levels in patients with type 2 diabetes may be associated with the development of DR. However, due to the limitations in the study design, we did not measure VEGF levels in the patients. Lastly, given the limited number of study participants with PDR (n = 2), we did not analyze the differences in GDF-15 levels between PDR and NPDR. Based on a previous study (39), PDR was combined with severe NPDR in our study to give the vision-threatening DR (VTDR) group. There is therefore need to investigate the differences between PDR and NPDR.

In conclusion, the results from our study suggest that there is a significant and independent association between the increased plasma levels of GDF-15 and DR. Future prospective studies with greater numbers of patients should be done to provide a link between increased circulating plasma GDF-15 concentration and the severity of DR.

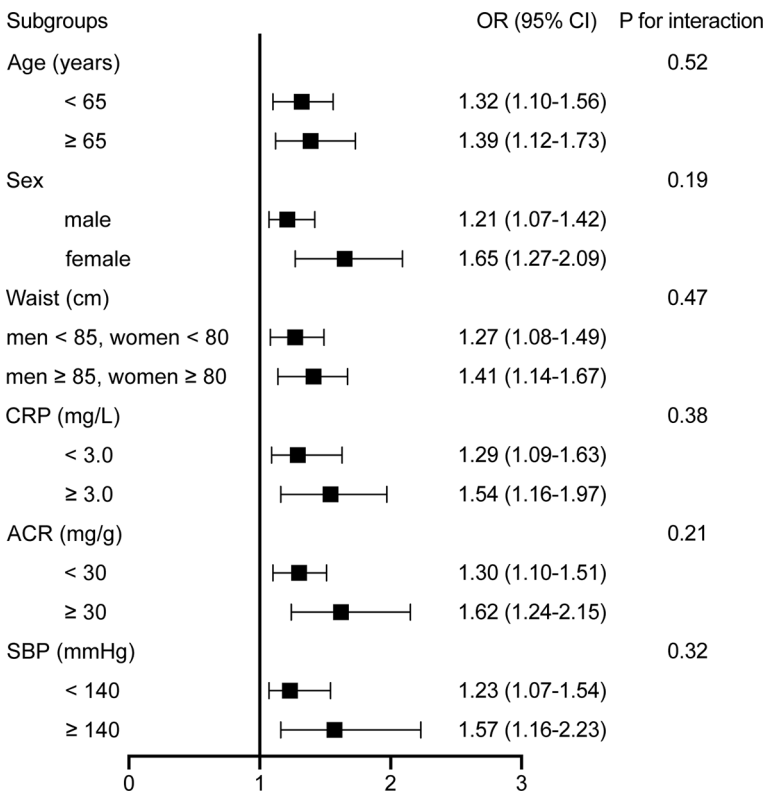

FIGURE 4 | Stratified analyses of the associations [odds ratio (95% confidence interval)] between plasma GDF-15 levels (per 50 pg/ml increment) and DR. Model was adjusted for age, gender, smoking, drinking, physical activity, education status, BMI, waist circumference, CRP, adiponectin, HOMA-IR, liver enzymes, duration, FPG, eGFR, Cr, and ACR. Subgroup variable was excluded from the model.

DATA AVAILABILITY STATEMENT

The raw data supporting the conclusions of this article will be made available by the authors, without undue reservation.

ETHICS STATEMENT

The studies involving human participants were reviewed and approved by the Xinhua Hospital Ethics Committee Affiliated to Shanghai Jiaotong University School of Medicine. The patients/participants provided their written informed consent to participate in this study.

AUTHOR CONTRIBUTIONS

Conceived and designed the experiments: ZY and QS. Analyzed the data: YN, WZ, and JS. Contributed reagents/materials/analysis tools: YN, ZY, JS, YL, XL, NL, HZ, and LQ. Wrote the paper: YN, WZ, and JS. All authors contributed to the article and approved the submitted version.

FUNDING

This work was supported by grants from National Key R&D Program of China(2016YFC0901200, 2016YFC0901203), the Shanghai Sailing Program (18YF1415800), the Shanghai Science and Technology Commission (15411953200, 10411956600, 14ZR1427400), National Natural Science Foundation of China (81300667, 81370953, 81370935, 81670743), Shanghai Health System Outstanding Young Talents Training Program (XYQ2013098), Shanghai Education Committee Key Program (14zz110), and State Key Development Program for Basic Research of China (2012CB517501).

REFERENCES

1. Yang SH, Dou KF, Song WJ. Prevalence of diabetes among men and women in China. *N Engl J Med* (2010) 362(25):2425–6. doi: 10.1056/NEJMc1004671
2. Abougalambou SSI, Abougalambou AS. Risk factors associated with diabetic retinopathy among type 2 diabetes patients at teaching hospital in Malaysia. *Diabetes Metab Syndr* (2015) 9(2):98–103. doi: 10.1016/j.dsx.2014.04.019
3. Cekić S, Cvetković T, Jovanović I, Jovanović P, Pesić M, Stanković Babić G, et al. C-reactive protein and chitinase 3-like protein 1 as biomarkers of spatial redistribution of retinal blood vessels on digital retinal photography in patients with diabetic retinopathy. *Bosn J Basic Med Sci* (2014) 14(3):177–84. doi: 10.17305/bjbms.2014.3.21
4. Kuo JZ, Guo X, Klein R, Klein BE, Cui J, Rotter JI, et al. Systemic soluble tumor necrosis factor receptors 1 and 2 are associated with severity of diabetic retinopathy in Hispanics. *Ophthalmology* (2012) 119(5):1041–6. doi: 10.1016/j.ophtha.2011.10.040
5. Roy MS, Janal MN, Crosby J, Donnelly R. Inflammatory biomarkers and progression of diabetic retinopathy in African Americans with type 1 diabetes. *Invest Ophthalmol Vis Sci* (2013) 54(8):5471–80. doi: 10.1167/iovs.13-12212
6. Bootcov MR, Bauskin AR, Valenzuela SM, Moore AG, Bansal M, He XY, et al. MIC-1, a novel macrophage inhibitory cytokine, is a divergent member of the TGF-beta superfamily. *Proc Natl Acad Sci USA* (1997) 94(21):11514–9. doi: 10.1073/pnas.94.21.11514
7. Lawton LN, Bonaldo MF, Jelenc PC, Qiu L, Baumes SA, Marcelino RA, et al. Identification of a novel member of the TGF-beta superfamily highly expressed in human placenta. *Gene* (1997) 203(1):17–26. doi: 10.1016/S0378-1119(97)00485-X
8. Yokoyama-Kobayashi M, Saeki M, Sekine S, Kato S. Human cDNA encoding a novel TGF-beta superfamily protein highly expressed in placenta. *J Biochem* (1997) 122(3):622–6. doi: 10.1093/oxfordjournals.jbchem.a021798
9. Tan M, Wang Y, Guan K, Sun Y. PTGF-beta, a type beta transforming growth factor (TGF-beta) superfamily member, is a p53 target gene that inhibits tumor cell growth via TGF-beta signaling pathway. *Proc Natl Acad Sci USA* (2000) 97(1):109–14. doi: 10.1073/pnas.97.1.109
10. Paralkar VM, Vail AL, Grasser WA, Brown TA, Xu H, Vukicevic S, et al. Cloning and characterization of a novel member of the transforming growth factor-beta/bone morphogenetic protein family. *J Biol Chem* (1998) 273 (22):13760–7. doi: 10.1074/jbc.273.22.13760
11. Hromas R, Hufford M, Sutton J, Xu D, Li Y, Lu L. PLAB, a novel placental bone morphogenetic protein. *Biochim Biophys Acta* (1997) 1354(1):40–4. doi: 10.1016/S0167-4781(97)00122-X
12. Appierto V, Tiberio P, Villani MG, Cavadini E, Formelli F. PLAB induction in fenretinide-induced apoptosis of ovarian cancer cells occurs via a ROS-dependent mechanism involving ER stress and JNK activation. *Carcinogenesis* (2009) 30(5):824–31. doi: 10.1093/carcin/bgp067
13. Yan M, Rerko RM, Platzer P, Dawson D, Willis J, Tong M, et al. 15-Hydroxyprostaglandin dehydrogenase, a COX-2 oncogene antagonist, is a TGF-beta-induced suppressor of human gastrointestinal cancers. *Proc Natl Acad Sci USA* (2004) 101(50):17468–73. doi: 10.1073/pnas.0406142101
14. Baek SJ, Eling TE. Changes in gene expression contribute to cancer prevention by COX inhibitors. *Prog Lipid Res* (2006) 45(1):1–16. doi: 10.1016/j.plipres.2005.10.001
15. Li H, Dakour J, Guilbert LJ, Winkler-Lowen B, Lyall F, Morrish DW. PL74, a novel member of the transforming growth factor-beta superfamily, is overexpressed in preeclampsia and causes apoptosis in trophoblast cells. *J Clin Endocrinol Metab* (2005) 90(5):3045–53. doi: 10.1210/jc.2004-0808
16. Lindahl B. The story of growth differentiation factor 15: another piece of the puzzle. *Clin Chem* (2013) 59(11):1550–2. doi: 10.1373/clinchem.2013.212811
17. Wallentin L, Hijazi Z, Andersson U, Alexander JH, De Caterina R, Hanna M, et al. Growth differentiation factor 15, a marker of oxidative stress and inflammation, for risk assessment in patients with atrial fibrillation: insights from the Apixaban for Reduction in Stroke and Other Thromboembolic Events in Atrial Fibrillation (ARISTOTLE) trial. *Circulation* (2014) 130 (21):1847–58. doi: 10.1161/CIRCULATIONAHA.114.011204
18. Hellemons ME, Mazagova M, Gansevoort RT, Henning RH, de Zeeuw D, Bakker SJL, et al. Growth-differentiation factor 15 predicts worsening of albuminuria in patients with type 2 diabetes. *Diabetes Care* (2012) 35 (11):2340–6. doi: 10.2337/dc12-0180
19. Berezin AE. Circulating Biomarkers in Heart Failure. *Adv Exp Med Biol* (2018) 1067:89–108. doi: 10.1007/5584_2017_140
20. Carstensen M, Herder C, Brunner EJ, Strassburger K, Tabak AG, Roden M, et al. Macrophage inhibitory cytokine-1 is increased in individuals before type 2 diabetes diagnosis but is not an independent predictor of type 2 diabetes: the Whitehall II study. *Eur J Endocrinol* (2010) 162(5):913–7. doi: 10.1530/EJE-09-1066
21. Chung JO, Park S-Y, Cho DH, Chung DJ, Chung MY. Relationship between plasma growth differentiation factor-15 levels and diabetic retinopathy in individuals with type 2 diabetes. *Sci Rep* (2020) 10(1):20568. doi: 10.1038/s41598-020-77584-z
22. Diagnosis and classification of diabetes mellitus. *Diabetes Care* (2013) 36 Suppl 1:S67–74. doi: 10.2337/dc13-S067
23. Ma Y-C, Zuo L, Chen J-H, Luo Q, Yu X-Q, Li Y, et al. Modified glomerular filtration rate estimating equation for Chinese patients with chronic kidney disease. *J Am Soc Nephrol* (2006) 17(10):2937–44. doi: 10.1681/ASN.2006040368
24. Matthews DR, Hosker JP, Rudenski AS, Naylor BA, Treacher DF, Turner RC. Homeostasis model assessment: insulin resistance and beta-cell function from

fasting plasma glucose and insulin concentrations in man. *Diabetologia* (1985) 28(7):412–9. doi: 10.1007/BF00280883
25. Wilkinson CP, Ferris FL, Klein RE, Lee PP, Agardh CD, Davis M, et al. Proposed international clinical diabetic retinopathy and diabetic macular edema disease severity scales. *Ophthalmology* (2003) 110(9):1677–82. doi: 10.1016/S0161-6420(03)00475-5
26. Lajer M, Jorsal A, Tarnow L, Parving H-H, Rossing P. Plasma growth differentiation factor-15 independently predicts all-cause and cardiovascular mortality as well as deterioration of kidney function in type 1 diabetic patients with nephropathy. *Diabetes Care* (2010) 33(7):1567–72. doi: 10.2337/dc09-2174
27. Dirani M, Xie J, Fenwick E, Benarous R, Rees G, Wong TY, et al. Are obesity and anthropometry risk factors for diabetic retinopathy? The diabetes management project. *Invest Ophthalmol Vis Sci* (2011) 52(7):4416–21. doi: 10.1167/iovs.11-7208
28. Frimodt-Møller M, von Scholten BJ, Reinhard H, Jacobsen PK, Hansen TW, Persson FI, et al. Growth differentiation factor-15 and fibroblast growth factor-23 are associated with mortality in type 2 diabetes - An observational follow-up study. *PloS One* (2018) 13(4):e0196634. doi: 10.1371/journal.pone.0196634
29. Böttner M, Suter-Crazzolara C, Schober A, Unsicker K. Expression of a novel member of the TGF-beta superfamily, growth/differentiation factor-15/macrophage-inhibiting cytokine-1 (GDF-15/MIC-1) in adult rat tissues. *Cell Tissue Res* (1999) 297(1):103–10. doi: 10.1007/s004410051337
30. Kempf T, Zarbock A, Widera C, Butz S, Stadtmann A, Rossaint J, et al. GDF-15 is an inhibitor of leukocyte integrin activation required for survival after myocardial infarction in mice. *Nat Med* (2011) 17(5):581–8. doi: 10.1038/nm.2354
31. Bonfiglio V, Platania CBM, Lazzara F, Conti F, Pizzo C, Reibaldi M, et al. TGF-β Serum Levels in Diabetic Retinopathy Patients and the Role of Anti-VEGF Therapy. *Int J Mol Sci* (2020) 21(24):9558. doi: 10.3390/ijms21249558
32. Heger J, Schiegnitz E, von Waldthausen D, Anwar MM, Piper HM, Euler G. Growth differentiation factor 15 acts anti-apoptotic and pro-hypertrophic in adult cardiomyocytes. *J Cell Physiol* (2010) 224(1):120–6. doi: 10.1002/jcp.22102
33. Johnen H, Lin S, Kuffner T, Brown DA, Tsai VW-W, Bauskin AR, et al. Tumor-induced anorexia and weight loss are mediated by the TGF-beta superfamily cytokine MIC-1. *Nat Med* (2007) 13(11):1333–40. doi: 10.1038/nm1677
34. Whitson RJ, Lucia MS, Lambert JR. Growth differentiation factor-15 (GDF-15) suppresses in vitro angiogenesis through a novel interaction with connective tissue growth factor (CCN2). *J Cell Biochem* (2013) 114(6):1424–33. doi: 10.1002/jcb.24484
35. Ferrari N, Pfeffer U, Dell'Eva R, Ambrosini C, Noonan DM, Albini A. The transforming growth factor-beta family members bone morphogenetic protein-2 and macrophage inhibitory cytokine-1 as mediators of the antiangiogenic activity of N-(4-hydroxyphenyl)retinamide. *Clin Cancer Res* (2005) 11(12):4610–9. doi: 10.1158/1078-0432.CCR-04-2210
36. Song H, Yin D, Liu Z. GDF-15 promotes angiogenesis through modulating p53/HIF-1α signaling pathway in hypoxic human umbilical vein endothelial cells. *Mol Biol Rep* (2012) 39(4):4017–22. doi: 10.1007/s11033-011-1182-7
37. Mazagova M, Buikema H, Landheer SW, Vavrinec P, Av B, Henning RH, et al. Growth differentiation factor 15 impairs aortic contractile and relaxing function through altered caveolar signaling of the endothelium. *Am J Physiol Heart Circ Physiol* (2013) 304(5):H709–18. doi: 10.1152/ajpheart.00543.2012
38. Tchou I, Margeli A, Tsironi M, Skenderi K, Barnet M, Kanaka-Gantenbein C, et al. Growth-differentiation factor-15, endoglin and N-terminal pro-brain natriuretic peptide induction in athletes participating in an ultramarathon foot race. *Biomarkers* (2009) 14(6):418–22. doi: 10.1080/13547500903062976
39. Lu J, Ma X, Zhou J, Zhang L, Mo Y, Ying L, et al. Association of Time in Range, as Assessed by Continuous Glucose Monitoring, With Diabetic Retinopathy in Type 2 Diabetes. *Diabetes Care* (2018) 41(11):2370–6. doi: 10.2337/dc18-1131

Conflict of Interest: The authors declare that the research was conducted in the absence of any commercial or financial relationships that could be construed as a potential conflict of interest.

frontiers in Endocrinology

ORIGINAL RESEARCH
published: 12 April 2021
doi: 10.3389/fendo.2021.632457

A Diagnostic Model for Screening Diabetic Retinopathy Using the Hand-Held Electroretinogram Device RETeval

Xiaowen Deng[1,2†], *Zijing Li*[1,2†], *Peng Zeng*[1,2†], *Jing Wang*[1,2], *Jiaqi Liang*[1,2] *and Yuqing Lan*[1,2*]

[1] Department of Ophthalmology, Sun Yat-sen Memorial Hospital, Sun Yat-sen University, Guangzhou, China, [2] Guangdong Provincial Key Laboratory of Malignant Tumor Epigenetics and Gene Regulation, Sun Yat-sen Memorial Hospital, Sun Yat-sen University, Guangzhou, China

Purpose: To construct a proper model to screen for diabetic retinopathy (DR) with the RETeval.

Method: This was a cross-sectional study. Two hundred thirty-two diabetic patients and seventy controls were recruited. The DR risk assessment protocol was performed to obtain subjects' DR risk score using the RETeval. Afterwards, the receiver operating characteristic (ROC) curve was used to determine the best cutoff for diagnosing DR. Random forest and decision tree models were constructed.

Results: With increasing DR severity, the DR score gradually increased. When the DR score was used to diagnose DR, the ROC curve had an area under the curve of 0.881 (95% confidence interval: 0.836-0.927, $P < 0.001$), with a best cutoff value of 22.95, a sensitivity of 74.3% (95 CI: 66.0%~82.6%), and a specificity of 90.6% (95 CI: 83.7% ~94.8%). The top four risk factors selected by the random forest were used to construct the decision tree for diagnosing DR, which had a sensitivity of 93.3% (95% CI: 86.3%~97.0%) and a specificity of 80.3% (95% CI: 72.1% ~86.6%).

Conclusions: The DR risk assessment protocol combined with the decision tree model was innovatively used to evaluate the risk of DR, improving the sensitivity of diagnosis, which makes this method more suitable than the current protocol for DR screening.

Keywords: diabetic retinopathy, electroretinogram, diagnostic model, risk factor, decision tree

OPEN ACCESS

Edited by:
Michele Lanza, University of Campania Luigi Vanvitelli, Italy

Reviewed by:
Tony Fitzgerald, University College Cork, Ireland
Francesco Maria D'Alterio, Imperial College Healthcare NHS Trust, United Kingdom

***Correspondence:**
Yuqing Lan
lanyq@mail.sysu.edu.cn

†These authors have contributed equally to the work

Specialty section:
This article was submitted to Clinical Diabetes, a section of the journal Frontiers in Endocrinology

Received: *24 November 2020*
Accepted: *11 March 2021*
Published: *12 April 2021*

Citation:
Deng X, Li Z, Zeng P, Wang J, Liang J and Lan Y (2021) A Diagnostic Model for Screening Diabetic Retinopathy Using the Hand-Held Electroretinogram Device RETeval. Front. Endocrinol. 12:632457. doi: 10.3389/fendo.2021.632457

INTRODUCTION

Diabetic retinopathy (DR) is a serious chronic complications of diabetes mellitus (DM), and it is the main cause of sight loss among the working population worldwide (1). With the continuously increasing prevalence of diabetes in recent years (2), early diagnosis and treatment of DR has become increasingly important. China has the largest population of diabetes patients in the world (3), and the prevalence of DR in rural areas with insufficient medical resources is higher than that in urban areas (4). At present, the diagnostic methods of DR mainly rely on professional

ophthalmologists. In primary medical institutions, such as community hospitals, where there is a lack of professional ophthalmologists and examination equipment, it is difficult to conduct professional eye examinations, which also makes clinical follow-up more difficult.

In the past few years, there has been increasing evidence that neurodegenerative changes in diabetic patients occur during preclinical DR (before microvascular changes occur) (5, 6). However, traditional flash electroretinogram (FERG) devices and multifocal electroretinogram (mfERG) devices are time consuming to use. In addition, traditional electroretinogram devices require pupil dilation, the use of invasive corneal electrodes, and professional analyses (7, 8), which greatly reduce the efficiency of the device. The advent of the RETeval, a hand-held ERG device, has made it much easier to make general judgments about retinal function in the community and to perform initial DR screening. The RETeval (LKC Tech. Inc., Gaithersburg, MD, USA) is a small, handheld FERG-recording device that uses special skin electrodes to capture ERGs. The device can perform a FERG test without pupil dilation noninvasively and quickly. Traditional FERG and mfERG reports have no intuitive judgment criteria and need professional interpretation. The DR risk assessment protocol of the device calculates the implicit time, amplitude, and pupillary response of flicker ERGs at 30 Hz to obtain a DR risk score. Compared to traditional ERG examinations, DR screening, even by nonprofessionals in primary care settings, can reduce subjective errors and make it more feasible. This device has been effective in studies of ERG in diabetic retinopathy (9–11) and has good reproducibility (12), but it has a high misdiagnosis rate in early DR screening when using the device directly. In addition, there may be differences among different races. The purposes of this study were to find the appropriate diagnostic threshold in South Chinese diabetic patients and to establish a simple and effective screening model, so as to popularize the screening for DRin the community. The risk factors from its use were also assessed.

METHODS

Subjects

This was a cross-sectional observational study. The study adhered to the tenets of the Declaration of Helsinki and was approved by the research ethics committee of Sun Yat-sen Memorial Hospital, Sun Yat-sen University. Two hundred thirty-two patients with type 2 diabetes mellitus (T2DM) recruited from the DM center between March 2019 and January 2020 and seventy healthy controls were included in the study. All were ethnically Chinese, mostly from southern China. DR stages were determined according to the criteria published by the ADA in 2017 (13). A randomly selected eye was included from each healthy, no-DR (NDR) control patient and each DR patient with the same DR stage in both eyes, while the worst eye was selected if the patient had uneven DR severity in the two eyes. Vision-threatening diabetic retinopathy (VTDR) was defined as severe nonproliferative diabetic retinopathy (NPDR), proliferative diabetic retinopathy (PDR), or clinically significant macular edema (CSME) with any stage of DR. The diagnosis of CSME was based on slit lamp fundus examination, fundus photography, and optical coherence tomography (OCT) examination and was defined as: (1) retinal thickening within 500 μm of the macular fovea, (2) macular fovea showing hard exudation within 500 μm and related to the thickening of the adjacent retina, or (3) retinal thickening in one or more places ≥1 papilla diameter and distance from macular fovea <1 papilla diameter. The exclusion criteria were as follows: (1) eye diseases such as glaucoma, uveitis, spherical equivalent >6 diopters, etc.; (2) ocular trauma or ocular surgical history (including retinal photocoagulation and intravitreal injection); (3) craniocerebral trauma or surgeries and ischemic diseases; (4) acute kidney disease or malignant hypertension; (5) photosensitive epilepsy; and (6) opaque refractive media or an ungradable fundus.

All subjects underwent a detailed ocular examination, including LogMAR best-corrected visual acuity (BCVA), noncontact tonometer intraocular pressure (IOP) (NIDEK, Inc., Aichi, Japan), axial lengths (by the IOLmaster, Zeiss, Inc., Jena, Germany), fundus photography (Canon, Inc., Tokyo, Japan), optical coherence tomography (OCT), and mydriatic slit-lamp fundus examination. The OCT examination was performed with the RTVue XR Avanti device (Optovue, Inc., Fremont, CA, USA) in 6.0×6.0 mm B-Scan mode after mydriasis. The stage of DR was confirmed by two experienced ophthalmologists according to the results of slit-lamp fundus examination, color fundus photographs, OCT, and fundus fluorescein angiography (FFA, Microclear, Inc., Suzhou, China) in suspected PDR patients. FFA images were collected as 9-field 60° fundus photographs after mydriasis. Age, sex, DM duration, glycosylated hemoglobin (HbA1c) levels, and body mass index (BMI) were collected. Moreover, the presence of systemic diseases, including high blood pressure(HBP), impaired renal function (IRF), dyslipidemia, and diabetic complications, including diabetic peripheral neuropathy (DPN), diabetic peripheral vasculopathy (DPV), and diabetic foot, was also recorded. IRF was defined as: (1) a history of chronic kidney diseases or diabetic nephropathy, (2) estimated glomerular filtration rate (eGFR) <60 ml/min/1.73 m2, (3) urinary albumin:creatinine ratio >30 mg/g for more than 3 months, and (4) need for a renal biopsy in suspected patients. eGFR was calculated from serum creatinine according to the Xiangya equation (14). All the above indexes were classified as dichotomous variables (Yes/No) based on the presence or absence of diseases or dysfunctions. A diagnosis of hypertension (>130/80 mmHg) was made according to associated guidelines updated in 2017 by the American College of Cardiology/American Heart Association (ACC/AHA) (15).

FERG Examination

The FERG examination was performed by the RETeval. Special skin electrodes of the RETeval device and the nondilated pupil mode of the DR risk assessment protocol were used for examination. The DR risk assessment protocol of the device was provided by the manufacturer. The original calculation method was established based on multiperson research by Maa et al. to screen VTDR (9). A 30-Hz flicker ERG, as set in the

electrophysiological standard by the International Society for Clinical Electrophysiology of Vision (ISCEV) (8), was used to observe the cone cell response. The time delay (implicit time) between the stimulus and the peak electrical response, as well as the peak-to-peak amplitude of the electrical response, was recorded after the scintillation photostimulus was administered. The device provides fixed retinal illuminating (Td-s) stimulation by adjusting brightness (cd-s/m2); therefore, FERG can be recorded without dilated pupils to compensate for changes in pupil area (mm^2) (16). A flashing white-light stimulus is made up of brief (< 5 ms) flashes from red, green, and blue LEDs at a frequency of 28.3 Hz with a background light of 0 Td-s. After it recorded the implicit time and amplitude of 16 Td-s and 32 Td-s flashes, as well as the pupil area ratio between 4 Td-s and 32 Td-s flashes, it generated a report including the parameters above and a DR risk assessment score (called DR score) calculated from them for each eye. The default normal value range is 7-19.9, and a DR score greater than or equal to 20 suggests a high risk of VTDR.

Statistical Analysis

The comparative analysis of data was done with SPSS 25.0 (SPSS Inc. Chicago, IL, USA), a commercial statistical program. One-way ANOVA was used to analyze the numerical variables among the groups, and Bonferroni's *post hoc* analysis was applied to evaluate statistical significance. Categorical variables were analyzed by the chi-square test. In all diabetic patients (DM with no DR, NPDR, or PDR), the receiver operating characteristic (ROC) curve to screen DR or VTDR was constructed by using the DR score and the stages of DR, and the area under the curve (AUC) was determined. The sensitivity and specificity were obtained according to the ROC curve, and the optimal diagnostic cutoff point was obtained by using the maximum value of the Youden index (YI= sensitivity + specificity -1). The significance levels of all the above statistical tests were set at 0.05.

R software (http://www.r-project.org) was used to analyze the risk factors and construct the DR screening model. The randomforest package was applied to analyze the risk factors and build the random forest. The mean decrease Gini (MDG) obtained by randomforest indicated the correlation between various factors and DR, in which a larger MDG of the factor meant a greater influence on DR. The out-of-bag (OOB) error estimate, which was computed by the OBB classifier on the training set, was as accurate as the error rate obtained by using the test set with the same size as the training set and let us avoid creating a separate set of tests. The Rpart package of R software was applied to obtain a decision tree. A decision tree is a nonlinear discriminant method that can divide the sample into subgroups. In the current model, the target variable was whether DR or VTDR was present. Starting at the root, the data were divided into two groups at each node according to whether the most correlated factors met the criteria. The process was then repeated for each node until all subjects were assigned to either a high-risk or a low-risk group. The confidence intervals of the ROC curves and decision trees were calculated by the efficient-score method (17).

RESULT

Subject Characteristics

Two hundred thirty-two eyes of 232 T2DM subjects (127 NDR and 105 DR) and seventy eyes of 70 matched healthy controls were included in this study. There were no significant differences in age or sex among the three groups. Compared with the NDR group, the patients in the DR group had a longer course of diabetes, a higher level of glycosylated hemoglobin, and a higher prevalence of HBP, IRF, diabetic foot, and DPN ($P < 0.05$), while there was no significant difference between the two groups in terms of dyslipidemia and DPV. BCVA showed no significant difference between the healthy control group and the NDR group, while visual acuity decreased significantly in the DR group compared with the controls and the NDR group ($P < 0.001$). There was no significant difference in the ocular axis or IOP among the three groups. Details are given in **Table 1**.

FERG Findings

The features of FERG at each stage of DR are shown in **Figure 1**. In this study, as DR severity increased, the amplitude of ERG gradually decreased, the implicit time gradually extended, and the pupillary response gradually deteriorated. The details and comparison of the parameters in the DR assessment protocol are shown in **Table 2**. The DR score increased successively from the healthy control group to the NDR group to the DR group (18.35 ± 2.56 in the healthy control group, 19.74 ± 2.69 in the NDR group and 28.37 ± 6.43 in the DR group). The implicit time of 16Td-s and 32Td-s grew successively longer from the healthy control group to the NDR group to the DR group. The amplitudes of 16Td-s and 32Td-s and the pupillary area were decreased from the healthy control group to the NDR group to the DR group. Between the healthy control group and NDR group, only the amplitudes of 16Td-s and 32Td-s flashes were significantly different (P=0.001), while there was no significant difference in DR score, latency, or pupil response between the two groups ($P > 0.05$). All values showed statistically significant differences between the healthy control group and DR group and between the NDR and DR groups ($P < 0.05$). As shown in **Figure 2**, when all DM patients were divided into no-DR, mild NPDR, moderate NPDR, mild/moderate NPDR with CSME, severe NPDR, and PDR groups, the DR score tended to increase with the progression of DR.

ROC Curves

In all diabetic patients (NDR and DR), the ROC curves for detecting DR and VTDR using the DR score are shown in **Figure 3**. To screen for DR, the area under the ROC curve (AUC) was 0.881 (95% confidence interval (CI) 0.836-0.927, $P < 0.001$), and the optimal cutoff value was 22.95, with a sensitivity of 74.3% (95 CI: 66.0%~82.6%), a specificity of 90.6% (95 CI: 83.7% ~94.8%), and a YI of 0.648. If the default threshold of 20.0 of the DR risk assessment protocol were used to diagnose DR, the sensitivity would be 87.6% (95 CI: 79.4% ~93.0%), with a specificity of 48.8% (95 CI: 39.9% ~57.8%), and a YI of 0.364. When detecting VTDR using the

TABLE 1 | Subject characteristics.

Group	Controls	NDR	DR	P VALUE		
	(n=70)	(n=127)	(n=105)	Controls vs NDR	Controls vs DR	NDR vs DR
Genger (M/F)	36/34	77/50	67/38		χ^2 = 2.770,*P* =0.250	
Age (Year)	54.24 ± 9.55	55.73 ± 12.97	57.37 ± 8.39	1.0	0.186	0.739
BMI (kg/m^2)	NA	24.79 ± 3.49	23.96 ± 3.17	NA	NA	0.06
HbAlc%	NA	8.40 ± 2.06	9.69 ± 2.44	NA	NA	<0.001*
Duration of DM (Year)	NA	7.36 ± 6.78	11.32 ± 5.84	NA	NA	<0.001*
HBP (YES/NO)	NA	64/63	68/37	NA	χ^2 = 4.839,*P*=0.028*	
IRF (YES/NO)	NA	25/102	51/54	NA	χ^2 = 21.774,*P*<0.001*	
Diabetic Foot (YES/NO)	NA	2/125	12/93	NA	χ^2 = 9.842,*P*=0.002*	
DPV (YES/NO)	NA	55/72	49/56	NA	χ^2 = 0.262,*P*=0.609	
DPN (YES/NO)	NA	58/69	74/31	NA	χ^2 = 14.423,*P*<0.001*	
Dyslipidemia (YES/NO)	NA	62/65	54/51	NA	χ^2 = 0.157,*P*=0.692	
Axial length (mm)	23.28 ± 1.00	23.70 ± 1.23	23.31 ± 0.76	0.231	1.0	0.101
IOP (mmHg)	14.97 ± 2.36	15.01 ± 2.58	16.00 ± 3.81	1.0	0.315	0.193
BCVA (Logmar)	-0.03 ± 0.11	-0.03 ± 0.06	0.31 ± 0.39	1.0	<0.001*	<0.001*

NDR, no diabetic retinopathy; DR, diabetic retinopathy; M, male; F, female; BMI, body mass index; HBP, high blood pressure; IRF, impaired renal function; DPV, diabetic peripheral vasculopathy; DPN, diabetic peripheral neuropathy; IOP, intraocular pressure; BCVA, best-corrected visual acuity.
**Statistically significant.*

DR score, the AUC was 0.972 (95% CI: 0.954-0.991, P < 0.001) with the best threshold of 26.45, a sensitivity of 95.7% (95% CI: 84.3% ~99.3%), a specificity of 93.5% (95% CI: 88.7% ~96.5%), and a YI of 0.894.

Random Forest

Figure 4 demonstrates the random forest map based on the presence of DR and the DR score, as well as the related risk factors mentioned above. Red dots represent DR subjects, blue dots represent NDR subjects, and the OOB estimate of the error rate is 4.74%. **Figure 5** shows the MDG values of the factors. The top several were DR score (36.05), BCVA (23.21), duration of DM (15.14), HbA1c (14.58), BMI (9.13), and IRF (3.06), while the MDG values of the other indexes (gender, HBP, dyslipidemia, diabetic foot, DPV, and DPN) were less than 3.

Decision Trees

When the decision trees were constructed, the 232 eyes of the DM patients were divided into 160 eyes for the training set (approximately 7/10) and 72 eyes for the test set (approximately 3/10). **Figures 6** and **7** show the decision trees of DR and VTDR, respectively, decided by only the DR score using the training set. In the simple model for DR, it had a sensitivity of 70.6% (95% CI:52.3%~84.2%) in the training set and 72.4% (95% CI:62.6%~80.4%) in the test set, and a specificity of 92.1% (95% CI:77.5%~97.9%) in the training set and 91.3% (95% CI:84.6%~95.4%) in the test set. For VTDR, the simple decision tree had a sensitivity of 100.0% (95% CI:85.0% ~100.0%) in the training set and 100.0% (95% CI:79.1%~100.0%) in the test set, and a specificity of 94.6%(95% CI:89.0%~97.7%) in the training set and 92.5%(95% CI:80.9%~97.6%) in the test set.

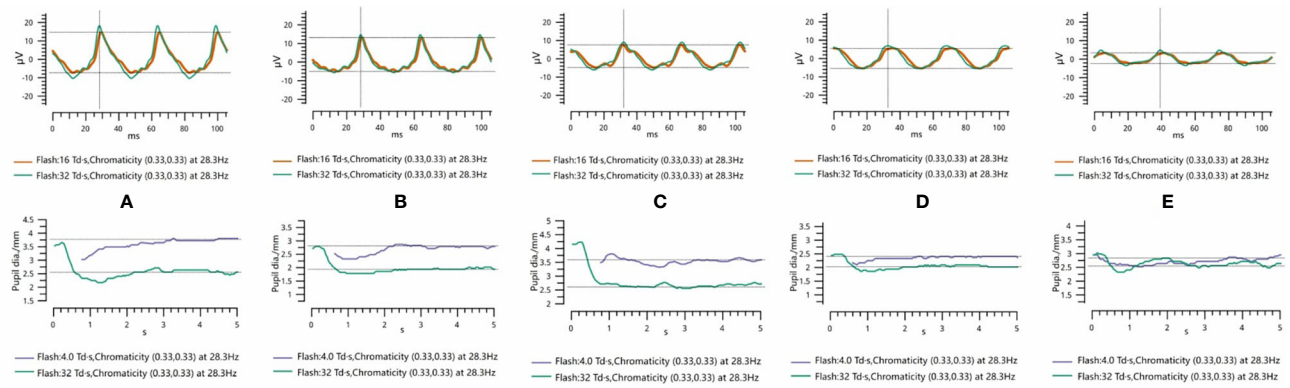

FIGURE 1 | The representative 30Hz flicker ERG performances and pupil diameter ratios of control **(A)**, no DR **(B)**, mild NPDR **(C)**, moderate-severe NPDR **(D)**, and PDR **(E)**.

TABLE 2 | Parameters of the DR risk assessment protocol.

Group	Controls	NDR	DR	P VALUE		
	(n=70)	(n=127)	(n=105)	Controls vs NDR	Controls vs DR	NDR vs DR
DR score	18.35 ± 2.56	19.74 ± 2.69	28.37 ± 6.43	0.099	<0.001*	<0.001*
16 Td-s implicit time(ms)	28.71 ± 1.46	29.66 ± 2.19	35.28 ± 4.73	0.305	<0.001*	<0.001*
16 Td-s amplitude(μV)	19.81 ± 4.96	16.04 ± 6.61	10.39 ± 5.44	0.001*	<0.001*	<0.001*
32 Td-s implicit time(ms)	27.64 ± 1.22	28.53 ± 1.83	34.37 ± 4.90	0.359	<0.001*	<0.001*
32 Td-s amplitude(μV)	23.56 ± 5.46	19.08 ± 7.57	12.55 ± 6.10	0.001*	<0.001*	0.001*
Pupil area ratio	2.01 ± 0.39	1.91 ± 0.48	1.53 ± 0.29	0.440	<0.001*	<0.001*

NDR, no diabetic retinopathy; DR, diabetic retinopathy.
**Statistically significant.*

Figure 8 displays the decision rules of the factor-combined decision tree for detecting DR using the training set. The top several factors (DR score, BCVA, duration of DM, HbA1c%, BMI, and IRF) obtained from the random forest were included in the Rpart package, and DR score, BCVA, duration of DM, and HbA1c% were selected by the program to build the decision tree. **Tables 3–5** show the results of DR screening in the training set, the test set, and the summation, respectively, of which display the comparison of the factors-combined model and the DR score-only model. Adding up the results, the decision tree with risk factors to detect DR had a sensitivity of 93.3% (95% CI: 86.3%~97.0%) and a specificity of 80.3% (95% CI: 72.1% ~86.6%), while the DR-score-only model had a sensitivity of 72.4% (95% CI: 62.6%~80.4%) and a specificity of 91.3% (95% CI: 84.6%~95.4%).

DISCUSSION

In this study, with the progression of DR, DR scores gradually increased, with longer implicit times and decreased amplitudes of 30-Hz flicker ERG, as well as worse pupil responses. Previous studies on DR assessment protocols have shown the same trend

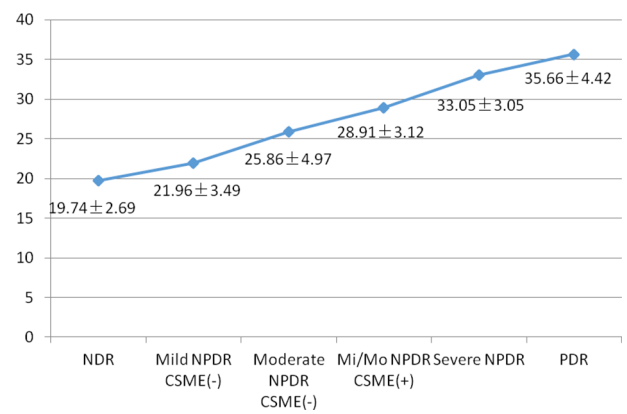

FIGURE 2 | Mean DR score in various stages of DR. NDR, no diabetic retinopathy; NPDR, non-proliferative diabetic retinopthy; Mi/Mo NPDR, mild or moderate non-proliferative diabetic retinopthy; PDR, proliferative diabetic retinopthy.

(9, 11, 18). Changes in flicker ERG at 30 Hz were associated with the severity of DR. When DR progresses with increased retinal ischemia, apoptosis of retinal cells, especially ganglion cells (19), leads to impaired retinal function, which induces a prolonged implicit time and a decreased amplitude (20). The speed and amplitude of pupillary contraction after light stimulation decreases with increasing DR severity, and an impaired pupillary dilatation and light reflex response in diabetes, may be due to sympathetic neuropathy or parasympathetic dysfunction (21). When the pupil is not artificially dilated, it can act as an independent indicator of the severity of DR (9).

Although the DR score showed no significant difference between the healthy control and NDR groups, we believe that the decreased amplitudes of 16Td-s and 32Td-s flicker stimuli suggested that functional impairment may have occurred before identifiable retinopathy appeared in the diabetes patients. Zeng's research showed that NDR patients had a lower amplitude and longer implicit time than healthy people by 30-Hz flicker ERG (22), while Tyrberg's study showed only a longer implicit time (23). In Fukuo's studies, both the amplitude and implicit time of 8Td-s flash were not significantly different between the healthy control group and the NDR group (10), which we suspect may be related to the weaker intensity of light stimulation (24). The results of animal experiments have also varied (25, 26). The 30-Hz flicker ERG is the response of the cones (8), where the density of cone cells in the macular fovea is higher (27); therefore, only if the entire retina or the macula is involved, there is a significant change. In other words, if the macula is involved, the test becomes more sensitive and helpful to evaluate the effectiveness of treatment (28). In addition, traditional ERG examinations required dark adaptation (8) and were time consuming, while a 30-Hz flicker ERG check can be done in a few minutes.

In this study, compared with the use of the RETeval to diagnose any DR, the sensitivity and specificity for detecting VTDR were increased, which suggested that its diagnostic value in early DR is not as good as that in a more serious stage of DR. Previous studies have shown the same trend. In Fukuo's studies, the sensitivity and specificity of the optimal cutoff point for any DR diagnosis were 0.70 and 0.81, while the sensitivity and specificity for the diagnosis of severe NPDR were 0.85 and 0.85, respectively (10). In Zeng's research, the sensitivity and specificity for any DR were 80.2% and 81.7%, respectively,

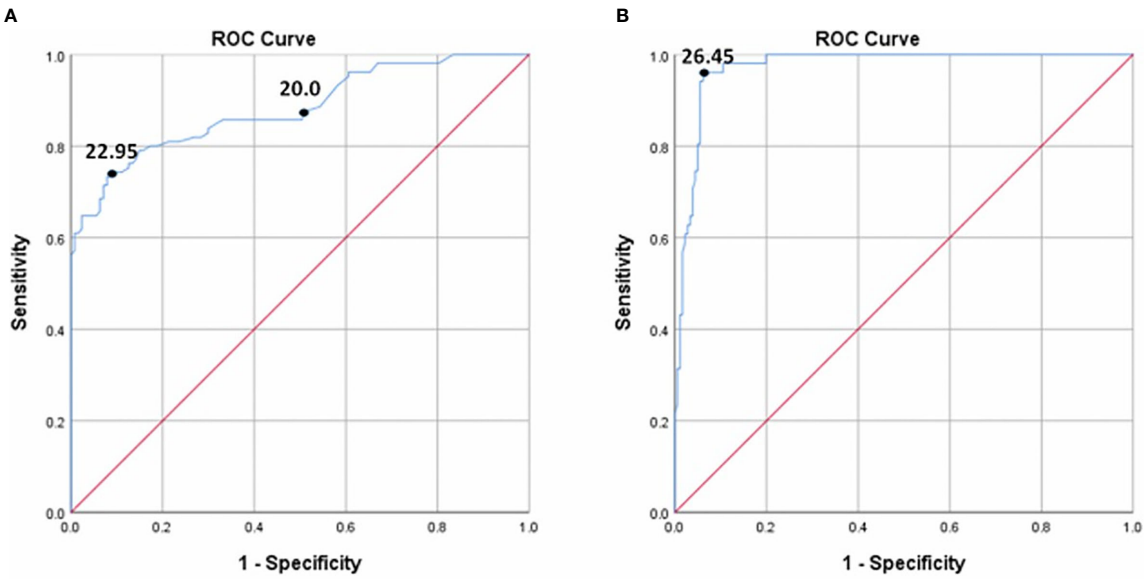

FIGURE 3 | The ROC curve for DR score to detect DR **(A)** and VTDR **(B)**.

while the sensitivity and specificity for VTDR were 94.6% and 88.8%, respectively (18). Therefore, more information should be used to assess a patient's fundus. A random forest model was introduced for the first time to analyze the DM and DR-related risk factors of patients. A random forest with a low classification error rate (OBB error estimate=4.74%) was established. The sensitivity of the decision tree model combined with the top several risk factors (DR SCORE, BCVA, duration of DM, and HbA1c%) calculated by the random forest model can also offer an improvement. In this way, we can get an overall impression of DM patients by performing RETeval and obtain some simple indexes, such as best corrected visual acuity, diabetes course, and the level of blood glucose, which are effective and useful, especially in community and clinical follow-ups. Given the 18.45%–23% prevalence of DR in Chinese diabetes patients (29, 30), we assumed there are 200 DR patients out of 1000 diabetes subjects. If we used the best cutoff of 22.95 obtained from the ROC curve of this study to screen for DR, 149 patients

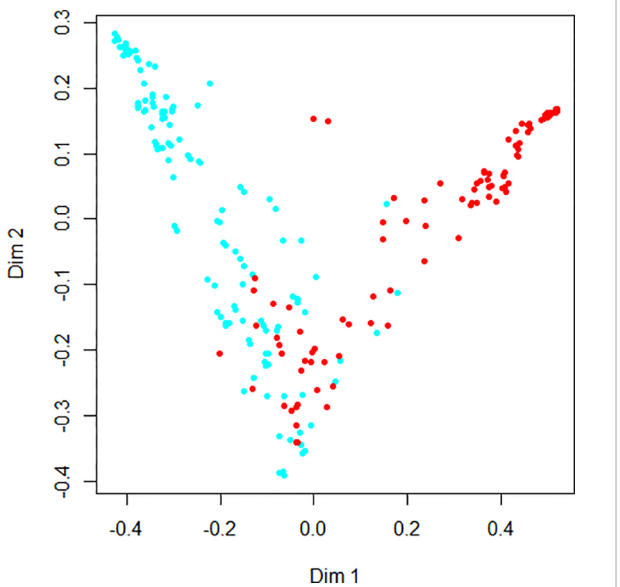

FIGURE 4 | The random forest map for diabetic retinopathy detection.

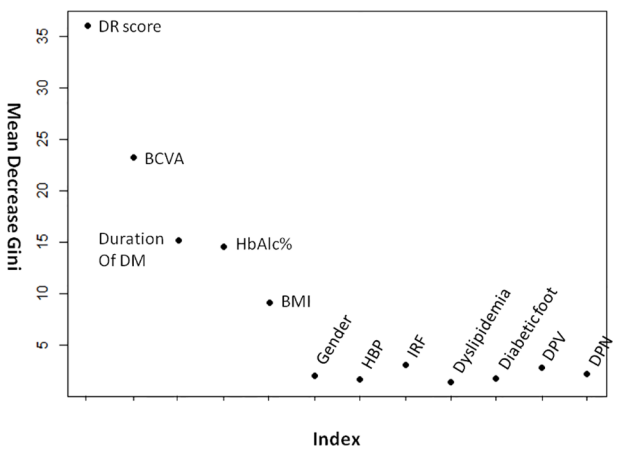

FIGURE 5 | The mean decrease gini values of DR- related factors. BCVA, best-corrected visual acuity; BMI, body mass index; HBP, high blood pressure; IRF, impaired renal function; DPV, diabetic peripheral vasculopathy; DPN, diabetic peripheral neuropathy.

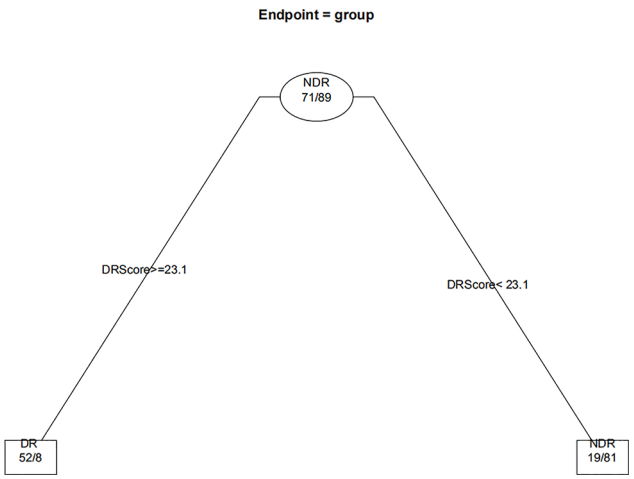

FIGURE 6 | Decision tree for detecting DR using only DR score.

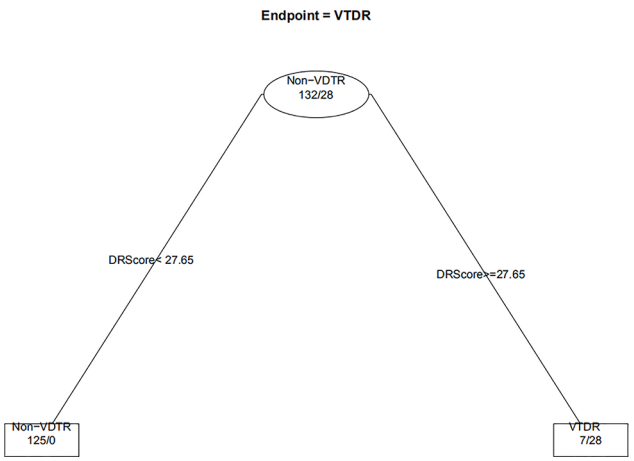

FIGURE 7 | Decision tree for detecting VTDR using only DR score.

would be screened out, and 51 patients would be missed. At the same time, 725 of the 800 patients with no DR were considered low risk for DR, and 75 were considered high risk for DR. In conclusion, the positive predictive value and negative predictive value of DR screening using the DR score alone were 66.5% and 93.4%, respectively. Similarly, the positive predictive value and negative predictive value of VTDR screened by DR score were 78.6% and 98.8%, respectively, and the positive predictive value and negative predictive value of the decision tree model combining several risk factors were 54.2% and 98.0%, respectively. The model combining risk factors increased the number of patients who were misidentified as high risk by 83, but it also reduced the number of missed diagnoses by 38.

In the current study, the top several factors related to DR arranged according to the MDG value were, respectively, DR score (36.05), BCVA (23.21), duration of DM (15.14), HbA1c (14.58), and BMI (9.13). The MDG values of other indexes (IRF, sex, HBP, dyslipidemia, diabetic foot, DPV, and DPN) were around or less than 3. Previous studies have found that poorer blood glucose control and longer diabetes duration are strongly associated with DR (1, 31), and high blood glucose levels can lead to pericyte loss, capillary occlusion, microangioma formation, and other problems (32). With the increase in the duration of diabetes, the deterioration of retinal function might be correlated with the increase in vascular endothelial growth factor level (33). Van's study showed that obesity was associated with retinopathy, while others found no association (34). Another study found that hypertension, dyslipidemia, vascular risk factors, diabetic peripheral neuropathy, and renal function were correlated with retinopathy (34–37), while this study found no such associations. We suspect this discrepancy was related to the selection of subjects and the sample size. In addition to the DR score, these indicators (BCVA, duration of DM, and HbA1c) were also selected to build a decision tree, suggesting that their correlation with DR may be stronger. Therefore, diabetic patients should pay close attention to the control of blood glucose and check whether there is any change in BCVA, and patients with long diabetes durations should be especially vigilant.

In China, no national DR screening system has been established, and DR screening has not been carried out in most parts of China (38). If not treated in time, DR will seriously impair vision, which often creates great familial and socioeconomic burdens (39) and eventually leads to blindness (1). The DR assessment protocol of the RETeval detects abnormalities in retinal function that come from diabetes and produces an objective DR risk score. The RETeval can be operated and read through simple training without specialized ophthalmologists. Moreover, ERG data can be documented for pretreatment and posttreatment follow-ups (40). At present, it is generally believed that, compared with fundus photography and optical coherence tomography, electrophysiological examinations in cases of affected intraocular refractive media, such as cataracts and vitreous hemorrhage, are more effective and can be used as prognostic assessments of postoperative visual acuity (41, 42). Although Miura's study claimed that the device was affected by cataracts (43, 44), Ratanapakorn's study showed that the differences were not statistically significant (45). In the current study, subjects with other ocular diseases that may affect ERG results were also excluded. However, these patients could also benefit from the device if they could be directed to ophthalmic specialists after examination by the device.

The current study and Mehmet's study examined each eye to generate a separate DR risk assessment report (11). Maa and Zeng combined two-eye tests to produce a DR score (9, 15). We wanted to detect DR monocularly to set the scope, rather than to assess the overall risk of DR. Although most DR patients follow the principle of binocular congruence, and using both eyes can assess the risk of DR as a whole, we still found many DR patients; 18.1% (19/105) of DR subjects in this study had unequal severities of DR in two eyes, and seven patients had only the worst eye reach the level of VTDR, which needed further treatment soon. The use of binocular grading does not reflect each eye alone, and for patients with only one eye, it is necessary to evaluate one eye separately. The purposes of the two examination modes are different. Therefore, compared with Maa's

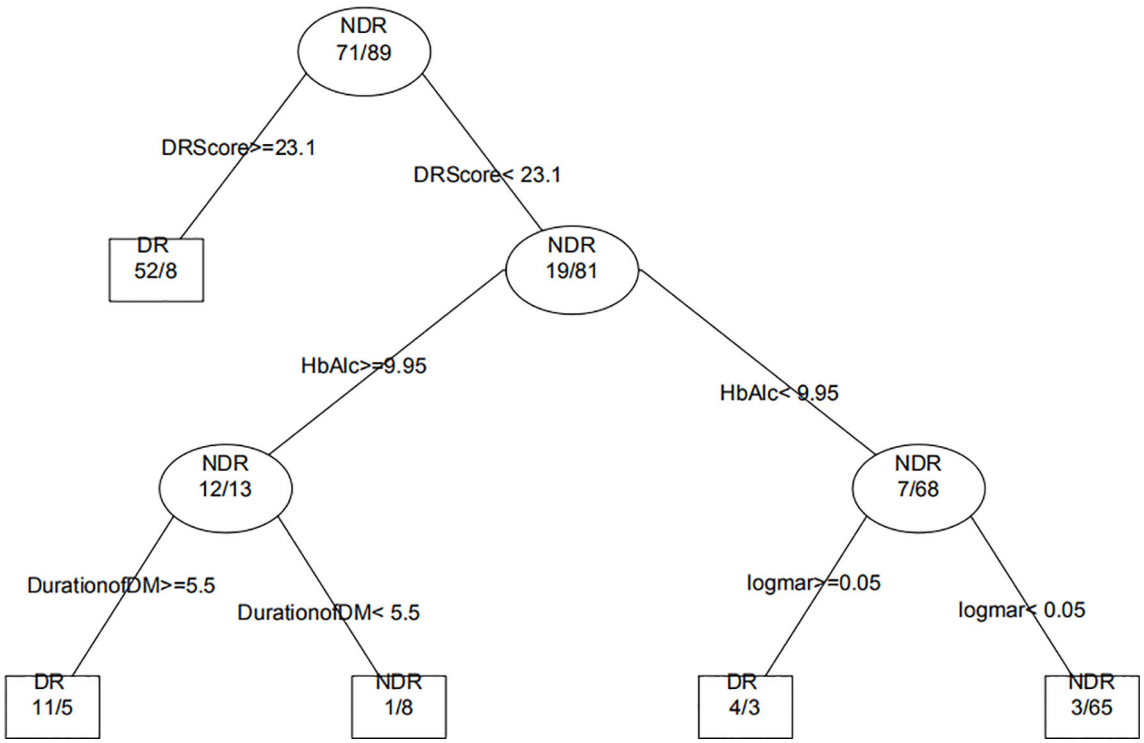

FIGURE 8 | Decision tree for detecting diabetic retinopathy using DR score combined with several factors. The subsets in ellipses means the classification had not been completed, while the subsets in the boxes mean completed. Subsets in "DR" boxes mean " high risk of DR", while "NDR" subsets mean "low risk of DR". The numbers in every subset mean "true DR subjects/true NDR subjects". For example, the first box in the upper left corner means 60 subjects were considered to be at high risk for DR, of which 52 were true cases of DR and eight were actually NDR subjects. For the last box, it means 68 subjects were considered to be at low risk for DR, of which three were actually cases of DR and 65 were true NDR subjects.

TABLE 3 | The classification results of the train sets for screening DR.

	True value	Predicted value		sensitivity	specificity
		case	control		
Factor-combined model	case	67	4	94.4% (95% CI:85.5%~98.2%)	82.0% (95% CI:72.1%~89.1%)
	control	16	73		
DR score only model	case	52	19	73.2% (95% CI:61.2%~82.7%)	91.0% (95% CI:82.6%~95.8%)
	control	8	81		

TABLE 4 | The classification results of the test sets for screening DR.

	True value	Predicted value		sensitivity	specificity
		case	control		
Factor-combined model	case	31	3	91.2% (95% CI:75.2%~97.7%)	76.3% (95% CI:59.34%~88.0%)
	control	9	29		
DR score only model	case	24	10	70.6% (95% CI:52.3%~84.2%)	92.1% (95% CI:77.5%~97.9%)
	control	3	35		

TABLE 5 | The classification results of all diabetes subjects for screening DR.

	True value	Predicted value		sensitivity	specificity
		case	control		
Factor-combined model	case	98	7	93.3% (95% CI:86.3%~97.0%)	80.3% (95% CI:72. 1%~86.6%)
	control	25	102		
DR score only model	case	76	29	72.4% (95% CI:62.6%~80.4%)	91.3%(95% CI:84.6%~95.4%)
	control	11	116		

study (sensitivity of 83% and specificity of 78%) (9) and Zeng's study (sensitivity of 94.6% and specificity of 88.8%) (15), ours may be more sensitive (96.1%) in detecting VTDR. Therefore, it is necessary to further optimize techniques, correct algorithms, or combine this method with other factors or devices to reduce classification mistakes.

We found that the mean DR scores in this study were higher than those of previous studies. Maa's study was primarily in Caucasian and African subjects, with a best cutoff of 20.0 for screening VTDR (9). In Mehmet's study, Turkish subjects were selected, and the best cutoff for screening moderate NPDR or more severe DR was 22 (11). Previous studies showed that the amplitudes of people with light-colored choroids were higher than those with dark pigmentation (46). All of our subjects were Chinese, and had dark-colored choroids, which might lead to a decrease in amplitude (47). This would be related to increased resistance associated with melanin or reduced effective illumination of the retina, thus reducing ERG amplitude (47, 48). Moreover, the worst eyes were selected, which meant lower amplitudes, prolonged implicit times, and poorer pupil responses. In addition, the higher DR scores in our study may be related to the poor blood glucose control of the subjects (mean HbA1c% of 8.40 in NDR subjects, mean HbA1c% of 9.69 in DR subjects) (31, 32), who were recruited from a DM center. Therefore, it is recommended that each examination room establish its own normal range and reference boundaries due to the differences between races, regions, and instruments (8).

Limitations

Due to the small sample size and uneven group distribution, the ROC curve, random forest, and decision tree for DR detection may have been deficient. In addition, there was no detailed classification of systemic diseases or risk factors, and some indexes, such as diabetic foot, may have been undervalued due to the small number of subjects. In the future, more factors and more detailed classifications, such as IRF and HBP classifications, may be included to make the model more complete and thereby lower the misdiagnosis rate.

Conclusion

The DR risk assessment protocol using the RETeval can be used for DR screening, but there is a relatively high missed diagnosis rate in the early stages of DR. In this study, FERG combined with the decision tree model was innovatively used to evaluate the risk of DR and improve the sensitivity of the protocol, which would be more suitable for DR screening.

DATA AVAILABILITY STATEMENT

The raw data supporting the conclusions of this article will be made available by the authors, without undue reservation.

ETHICS STATEMENT

The studies involving human participants were reviewed and approved by the research ethics committee of Sun Yat-sen Memorial Hospital, Sun Yat-sen University. The patients/participants provided their written informed consent to participate in this study.

AUTHOR CONTRIBUTIONS

XD, ZL, and PZ have contributed equally to the work. All authors contributed to the article and approved the submitted version.

FUNDING

Supported by the Natural Science Foundation of Guangdong Province (No.2015A030313019) and the Sun Yat-sen Clinical Research Cultivation Project (No.SYS-C-201705).

REFERENCES

1. Wong TY, Cheung CM, Larsen M, Sharma S, Simó R. Diabetic retinopathy. *Nat Rev* (2016) 2:16012. doi: 10.1038/nrdp.2016.12
2. Shaw JE, Sicree RA, Zimmet PZ. Global estimates of the prevalence of diabetes for 2010 and 2030. *J Diabetes Res* (2010) 87(1):4–14. doi: 10.1016/j.diabres.2009.10.007
3. Yang W, Lu J, Weng J, Jia W, Ji L, Xiao J, et al. Prevalence of diabetes among men and women in China. *J New Engl J Med* (2010) 362(12):1090–101. doi: 10.1056/NEJMoa0908292
4. Liu L, Wu X, Liu L, Geng J, Yuan Z, Shan Z, et al. Prevalence of diabetic retinopathy in mainland China: a meta-analysis. *PloS One* (2012) 7(9):e45264. doi: 10.1371/journal.pone.0045264
5. Moran EP, Wang Z, Chen J, Sapieha P, Smith LE, Ma JX, et al. Neurovascular cross talk in diabetic retinopathy: Pathophysiological roles and therapeutic implications. *Am J Physiol* (2016) 311(3):H738–49. doi: 10.1152/ajpheart.00005.2016
6. Carpineto P, Toto L, Aloia R, Ciciarelli V, Borrelli E, Vitacolonna E, et al. Neuroretinal alterations in the early stages of diabetic retinopathy in patients

with type 2 diabetes mellitus. *Eye* (2016) 30(5):673–9. doi: 10.1038/eye.2016.13
7. Hood DC, Bach M, Brigell M, Keating D, Kondo M, Lyons JS, et al. ISCEV standard for clinical multifocal electroretinography (mfERG) (2011 edition). *Doc Ophthalmol* (2012) 124(1):1–13. doi: 10.1007/s10633-011-9296-8
8. McCulloch DL, Marmor MF, Brigell MG, Hamilton R, Holder GE, Tzekov R, et al. ISCEV Standard for full-field clinical electroretinography (2015 update). *Doc Ophthalmol* (2015) 130(1):1–12. doi: 10.1007/s10633-014-9473-7
9. Maa AY, Feuer WJ, Davis CQ, Pillow EK, Brown TD, Caywood RM, et al. A novel device for accurate and efficient testing for vision-threatening diabetic retinopathy. *J Diabetes* (2016) 30(3):524–32. doi: 10.1016/j.jdiacomp.2015.12.005
10. Fukuo M, Kondo M, Hirose A, Fukushima H, Ikesugi K, Sugimoto M, et al. Screening for diabetic retinopathy using new mydriasis-free, full-field flicker ERG recording device. *Sci Rep* (2016) 6:36591. doi: 10.1038/srep36591
11. Değirmenci MFK, Demirel S, Batıoğlu F, Özmert E. Role of a mydriasis-free, full-field flicker ERG device in the detection of diabetic retinopathy. *Doc Ophthalmol* (2018) 137(3):131–41. doi: 10.1007/s10633-018-9656-8
12. Asakawa K, Amino K, Iwase M, Kusayanagi Y, Nakamura A, Suzuki R, et al. New Mydriasis-Free Electroretinogram Recorded with Skin Electrodes in Healthy Subjects. *BioMed Res Int* (2017) 2017:8539747. doi: 10.1155/2017/8539747
13. Solomon SD, Chew E, Duh EJ, Sobrin L, Sun JK, VanderBeek BL, et al. Erratum. Diabetic Retinopathy: A Position Statement by the American Diabetes Association. *Diabetes Care* (2017) 40(9):1285. doi: 10.2337/dc17-er09
14. Li DY, Yin WJ, Yi YH, Zhang BK, Zhao J, Zhu CN, et al. Development and validation of a more accurate estimating equation for glomerular filtration rate in a Chinese population. *J Kidney Int* (2019) 95(3):636–46. doi: 10.1016/j.kint.2018.10.019
15. Whelton PK, Carey RM, Aronow WS, Casey DE Jr, Collins KJ, Dennison Himmelfarb C, et al. 2017 ACC/AHA/AAPA/ABC/ACPM/AGS/APhA/ASH/ASPC/NMA/PCNA Guideline for the Prevention, Detection, Evaluation, and Management of High Blood Pressure in Adults: Executive Summary: A Report of the American College of Cardiology/American Heart Association Task Force on Clinical Practice Guidelines. *J Am Soc Hypertens* (2018) 12(8):579. doi: 10.1016/j.jash.2018.06.010
16. Kato K, Kondo M, Sugimoto M, Ikesugi K, Matsubara H. Effect of Pupil Size on Flicker ERGs Recorded With RETeval System: New Mydriasis-Free Full-Field ERG System. *J Invest Ophthalmol* (2015) 56(6):3684–90. doi: 10.1167/iovs.14-16349
17. Newcombe RG. Two-sided confidence intervals for the single proportion: comparison of seven methods. *J Stat Med* (1998) 17(8):857–72. doi: 10.1002/(sici)1097-0258(19980430)17:8<857::aid-sim777>3.0.co;2-e
18. Zeng Y, Cao D, Yang D, Zhuang X, Yu H, Hu Y, et al. Screening for diabetic retinopathy in diabetic patients with a mydriasis-free, full-field flicker electroretinogram recording device. *Doc Ophthalmol* (2020) 140(3):211–20. doi: 10.1007/s10633-019-09734-2
19. Barber AJ, Lieth E, Khin SA, Antonetti DA, Buchanan AG, Gardner TW, et al. Neural apoptosis in the retina during experimental and human diabetes. Early onset and effect of insulin. *J Clin Invest* (1998) 102(4):783–91. doi: 10.1172/jci2425
20. Tahara K, Matsuura T, Otori T. Diagnostic evaluation of diabetic retinopathy by 30-Hz flicker electroretinography. *Japanese J Ophthalmol* (1993) 37(2):204–10.
21. Smith SA, Smith SE. Reduced pupillary light reflexes in diabetic autonomic neuropathy. *J Diabetol* (1983) 24(5):330–2. doi: 10.1007/bf00251818
22. Zeng Y, Cao D, Yu H, Yang D, Zhuang X, Hu Y, et al. Early retinal neurovascular impairment in patients with diabetes without clinically detectable retinopathy. *Br J Ophthalmol* (2019) 103(12):1747–52. doi: 10.1136/bjophthalmol-2018-313582
23. Tyrberg M, Lindblad U, Melander A, Lövestam-Adrian M, Ponjavic V, Andréasson S. Electrophysiological studies in newly onset type 2 diabetes without visible vascular retinopathy. *Doc Ophthalmol* (2011) 123(3):193–8. doi: 10.1007/s10633-011-9298-6
24. Pardue MT, Barnes CS, Kim MK, Aung MH, Amarnath R, Olson DE, et al . Rodent Hyperglycemia-Induced Inner Retinal Deficits are Mirrored in Human Diabetes. *Transl Vision Sci* (2014) 3(3):6. doi: 10.1167/tvst.3.3.6
25. Li Q, Zemel E, Miller B. Early retinal damage in experimental diabetes: electroretinographical and morphological observations. *Exp Eye Res* (2002) 74(5):615–625. doi: 10.1006/exer.2002.1170
26. Ramsey DJ, Ripps H, Qian H, et al. An electrophysiological study of retinal function in the diabetic female rat. *J Invest Ophthalmol* (2006) 47(11):5116–24. doi: 10.1167/iovs.06-0364
27. Curcio CA, Sloan KR, Kalina RE, Hendrickson AE. Human photoreceptor topography. *J Comp Neurol* (1990) 292(4):497–523. doi: 10.1002/cne.902920402
28. Ichio A, Sugimoto M, Matsubara H, Mochida D, Kato K, Kondo M. Effects of Intravitreal Aflibercept on Retinal Function and Improvement of Macular Edema Associated With Diabetic Retinopathy. *Transl Vision Sci* (2020) 9(11):2. doi: 10.1167/tvst.9.11.2
29. Zhong Y, Wu J, Yue S, Zhang G, Liu L, Chen L. Burden of diabetic retinopathy in mainland China: Protocol for an updated systematic review and meta-analysis of prevalence and risk factors to identify prevention policies. *Medicine* (2018) 97(50):e13678. doi: 10.1097/md.0000000000013678
30. Song P, Yu J, Chan KY, Theodoratou E. Prevalence, risk factors and burden of diabetic retinopathy in China: a systematic review and meta-analysis. *J Global Health* (2018) 8(1):010803. doi: 10.7189/jogh.08.010803
31. Yau JW, Rogers SL, Kawasaki R, Lamoureux EL, Kowalski JW, Bek T, et al. Global prevalence and major risk factors of diabetic retinopathy. *J Diabetes Care* (2012) 35(3):556–64. doi: 10.2337/dc11-1909
32. Chiu CJ, Taylor A. Dietary hyperglycemia, glycemic index and metabolic retinal diseases. *J Prog Retinal Eye Res* (2011) 30(1):18–53. doi: 10.1016/j.preteyeres.2010.09.001
33. Semeran K, Pawłowski P, Lisowski Ł, Szczepaniak I, Wójtowicz J, Lawicki S, et al. Plasma levels of IL-17, VEGF, and adrenomedullin and S-cone dysfunction of the retina in children and adolescents without signs of retinopathy and with varied duration of diabetes. *Mediators Inflamm* (2013) 2013:274726. doi: 10.1155/2013/274726
34. van Leiden HA, Dekker JM, Moll AC, Nijpels G, Heine RJ, Bouter LM, et al. Blood pressure, lipids, and obesity are associated with retinopathy: the hoorn study. *J Diabetes Care* (2002) 25(8):1320–25. doi: 10.2337/diacare.25.8.1320
35. Chen YH, Chen HS, Tarng DC. More impact of microalbuminuria on retinopathy than moderately reduced GFR among type 2 diabetic patients. *J Diabetes Care* (2012) 35(4):803–8. doi: 10.2337/dc11-1955
36. Klein R, Sharrett AR, Klein BE, Moss SE, Folsom AR, Wong TY, et al. The association of atherosclerosis, vascular risk factors, and retinopathy in adults with diabetes: the atherosclerosis risk in communities study. *J Ophthalmol* (2002) 109(7):1225–34. doi: 10.1016/s0161-6420(02)01074-6
37. Liu X, Xu Y, An M, Zeng Q. The risk factors for diabetic peripheral neuropathy: A meta-analysis. *PloS One* (2019) 14(2):e0212574. doi: 10.1371/journal.pone.0212574
38. Zhang G, Chen H, Chen W, Zhang M. Prevalence and risk factors for diabetic retinopathy in China: a multi-hospital-based cross-sectional study. *British J Ophthalmol* (2017) 101(12):1591–5. doi: 10.1136/bjophthalmol-2017-310316
39. Mazhar K, Varma R, Choudhury F, McKean-Cowdin R, Shtir CJ, Azen SP, et al. Severity of diabetic retinopathy and health-related quality of life: the Los Angeles Latino Eye Study. *J Ophthalmol* (2011) 118(4):649–55. doi: 10.1016/j.ophtha.2010.08.003
40. Yasuda S, Kachi S, Ueno S, Piao CH. Flicker electroretinograms before and after intravitreal ranibizumab injection in eyes with central retinal vein occlusion. *Acta Ophthalmol* (2015) 93(6):e465–8. doi: 10.1111/aos.12674
41. An J, Zhang L, Wang Y, Zhang Z. The Success of Cataract Surgery and the Preoperative Measurement of Retinal Function by Electrophysiological Techniques. *J Ophthalmol* (2015) 2015:401281. doi: 10.1155/2015/401281
42. Yamauchi Y, Mochizuki JI, Hirakata A, Uda S. Single flash electroretinograms of mature cataractous and fellow eyes. *J Clin Ophthalmol* (2016) 10:2031–34. doi: 10.2147/opth.S118677
43. Miura G, Baba T, Oshitari T, Yamamoto S. Flicker electroretinograms of eyes with cataract recorded with RETeval system before and after mydriasis. *J Clin Ophthalmol* (2018) 12:427–32. doi: 10.2147/opth.S157505

44. Miura G, Nakamura Y, Sato E, Yamamoto S. Effects of cataracts on flicker electroretinograms recorded with RETeval™ system: new mydriasis-free ERG device. *BMC Ophthalmol* (2016) 16:22. doi: 10.1186/s12886-016-0200-x
45. Ratanapakorn T, Patarakittam T, Sinawat S, Sanguansak T, Bhoomibunchoo C, Kaewpanna S, et al. Effect of cataract on electroretinographic response. *J Med Assoc Thailand* (2010) 93(10):1196–9.
46. Wali N, Leguire LE. Fundus pigmentation and the dark-adapted electroretinogram. *J Documenta Ophthalmol Adv Ophthalmol* (1992) 80 (1):1–11. doi: 10.1007/bf00161226
47. Al Abdlseaed A, McTaggart Y, Ramage T, Hamilton R, McCulloch DL. Light- and dark-adapted electroretinograms (ERGs) and ocular pigmentation: comparison of brown- and blue-eyed cohorts. *Doc Ophthalmol* (2010) 121 (2):135–146. doi: 10.1007/s10633-010-9240-3
48. Wali N, Leguire LE. Fundus pigmentation and the electroretinographic luminance-response function. *J Documenta Ophthalmol Adv Ophthalmol* (1993) 84(1):61–69. doi: 10.1007/bf01203283

Conflict of Interest: The authors declare that the research was conducted in the absence of any commercial or financial relationships that could be construed as a potential conflict of interest.

frontiers in Endocrinology

ORIGINAL RESEARCH
published: 23 April 2021
doi: 10.3389/fendo.2021.614161

The Impact of Glycemic Control on Retinal Photoreceptor Layers and Retinal Pigment Epithelium in Patients With Type 2 Diabetes Without Diabetic Retinopathy: A Follow-Up Study

Fukashi Ishibashi[1], *Aiko Kosaka*[1] *and Mitra Tavakoli*[2*]

[1] Internal Medicine, Ishibashi Clinic, Hiroshima, Japan, [2] Diabetes and Vascular Research Centre (DVRC), NIHR Exeter Clinical Research Facility, University of Exeter Medical School, Exeter, United Kingdom

Aims: To establish the sequential changes by glycemic control in the mean thickness, volume and reflectance of the macular photoreceptor layers (MPRLs) and retinal pigment epithelium in patients with type 2 diabetes without diabetic retinopathy.

Methods: Thirty-one poorly controlled (HbA1c > 8.0%) patients with type 2 diabetes without diabetic retinopathy undergoing glycemic control and 39 control subjects with normal HbA1c levels (< 5.9%) underwent periodical full medical, neurological and ophthalmological examinations over 2 years. Glycemic variability was evaluated by standard deviation and coefficient of variation of monthly measured HbA1c levels and casual plasma glucose. 3D swept source-optical coherence tomography (OCT) and OCT-Explorer-generated enface thickness, volume and reflectance images for 9 subfields defined by Early Treatment Diabetic Retinopathy Study of 4 MPRLs {outer nuclear layer, ellipsoid zone, photoreceptor outer segment (PROS) and interdigitation zone} and retinal pigment epithelium were acquired every 3 months.

Results: Glycemic control sequentially restored the thickness and volume at 6, 4 and 5 subfields of outer nuclear layer, ellipsoid zone and PROS, respectively. The thickness and volume of outer nuclear layer were restored related to the decrease in HbA1c and casual plasma glucose levels, but not related to glycemic variability and neurological tests. The reflectance of MPRLs and retinal pigment epithelium in patients was marginally weaker than controls, and further decreased at 6 or 15 months during glycemic control. The reduction at 6 months coincided with high HbA1c levels.

Conclusion: Glycemic control sequentially restored the some MPRL thickness, especially of outer nuclear layer. In contrast, high glucose during glycemic control decreased reflectance and may lead to the development of diabetic retinopathy induced by glycemic control. The repeated OCT examinations can clarify the benefit and hazard of glycemic control to the diabetic retinopathy.

Keywords: macular photoreceptor layers, retinal pigment epithelium, enface optical coherence tomography, glycemic control, type 2 diabetes, microvascular complications, diabetic neuropathy, diabetic retinopatathy

OPEN ACCESS

Edited by:
Hans Ulrich Häring, Tübingen University Hospital, Germany

Reviewed by:
Koichi Kato, Aichi Gakuin University, Japan
Yukihiro Fujita, Shiga University of Medical Science, Japan

***Correspondence:**
Mitra Tavakoli
m.tavakoli@exeter.ac.uk

Specialty section:
This article was submitted to Clinical Diabetes, a section of the journal Frontiers in Endocrinology

Received: *05 October 2020*
Accepted: *19 March 2021*
Published: *23 April 2021*

Citation:
Ishibashi F, Kosaka A and Tavakoli M (2021) The Impact of Glycemic Control on Retinal Photoreceptor Layers and Retinal Pigment Epithelium in Patients With Type 2 Diabetes Without Diabetic Retinopathy: A Follow-Up Study. Front. Endocrinol. 12:614161. doi: 10.3389/fendo.2021.614161

INTRODUCTION

Diabetic retinopathy, the leading cause of blindness in working-age individuals has been viewed traditionally as a microvascular complication in diabetes. Indeed, the clinical classification system for diabetic retinopathy is based solely on the changes in the retinal microvasculature, because the microvasculature is visible using the routine fundus imaging. The advent of the high-resolution spectral-domain and swept-source-optical coherence tomography (OCT) and image segmentation algorithms permit depth-resolved enface OCT imaging for viewing the retinal layers in the coronal plane, enabling to measure the metrics (spatial thickness, volume and reflectance) of individual macular photoreceptor layers (MPRLs) and retinal pigment epithelium (RPE) (1).

It has been shown that glycemic variability induces retinal neurodegeneration in type 1 diabetes (2), but this has not been studied in type 2 diabetes.

However, studies on the impact of diabetes on the metrics of MPRLs and RPE using enface OCT had been cross-sectional (3) and inconsistent (4, 5). Because the thickness of individual MPRLs, except for outer nuclear layer (ONL), and RPE is < 20 μm, and because OCT image quality depends on the instrument reliability and measurement variability (6), the excellent OCT repeatability is essential to measure the metrics of the individual layers of MPRLs and RPE. We measured the metrics of RPE, because RPE has the close functional and morphological relationship with MPRLs.

For evaluating the impact of glycemic control on the structures of individual layers of MPRLs and RPE, the sequential measurements during follow-up are necessary. The sequential changes by glycemic control in the metrics of individual MPRLs and RPE using enface OCT in diabetes had never been studied.

The current study aimed to investigate the impact of glycemic control and glycemic variability on the sequential changes in the metrics of individual MPRLs and RPE in type 2 diabetic patients without diabetic retinopathy using enface OCT.

SUBJECTS AND METHODS

Subjects

Thirty-one patients with type 2 diabetes under poor glycemic control (HbA1c > 8.0%) at the baseline undergoing a subsequent glycemic control, and 39 healthy gender- and age-matched control subjects with normal HbA1c levels (HbA1c < 5.9%) were studied. All subjects were enrolled at the period from January 2016 to December 2017 at the Ishibashi Clinic, Hiroshima Japan, and were followed up for 24 months. The exclusion criteria of all subjects were as follows; best-corrected visual acuity < 1.0, color blindness, diabetic retinopathy of any grade, macular edema, glaucoma, history of intraocular disease, refractive surgery, using hard contact lenses, neurodegenerative diseases, and significant media opacities. Written informed consent was obtained from all subjects based on the Declaration of Helsinki. The ethics committee of the Ishibashi Clinic approved the protocol of the present research.

Abbreviations: ANOVA, analysis of variance; CNF, corneal nerve fiber; CPPG, casual postprandial plasma glucose; DPP4-I, dipeptidyl peptidase4-inhibitor; ETDRS, Early Treatment Diabetic Retinopathy Study; MPRL, macular photoreceptor layer; OCT, optical coherence tomography; ONL, outer nuclear layer; PROS, photoreceptor outer segment; RPE, retinal pigment epithelium.

Clinical and Laboratory Data

The BMI, blood pressure, casual postprandial plasma glucose (CPPG), and HbA1c levels were measured monthly during the terms of study in patients with type 2 diabetes, and at the baseline and endpoint in control subjects. In patients, the standard deviation and coefficient of variation of CPPG and HbA1c levels over the whole follow-up period were calculated for estimating glycemic variability. The serum lipid levels (LDL-cholesterol, HDL-cholesterol and triglycerides), and urinary creatinine and albumin levels were assessed every 3 months in patients. An albumin-to-creatinine ratio > 30mg/g creatinine twice a year was labeled as nephropathy (7).

Ophthalmic Examinations

The visual acuity was measured using the international type visual acuity chart (Tsutsumi, Tokyo, Japan). The color vision was assessed by the Ishihara color test. The bilateral fundus images were captured (the field of assessment: 45°) without pupil dilatation every 6 months for patients with type 2 diabetes, and at the baseline and endpoint for control subjects.

Corneal Confocal Microscopy

All subjects were examined at the baseline and endpoint using a Heidelberg Retina Tomograph III *in vivo* corneal confocal microscope with Rostock Corneal Module (Heidelberg Engineering, Heidelberg, Germany) (8). Six high-quality images per subject from Bowman's layer were captured for quantifying the following corneal nerve fiber (CNF) morphological parameters: 1) CNF density: total number of major nerve fibers/mm^2 of corneal tissue; 2) CNF length: total length of all nerve fibers (mm/mm^2); 3) corneal nerve branch density: number of branches emanating from all major nerve trunks/mm^2; 4) beading frequency/0.1mm; and 5) bead size (μm^2) (9). Except for bead size, all measurements were performed using ImageJ (Texelcraft, Tokyo, Japan). The examiners and team members analyzing the images were all blinded and masked to the study groups.

3D Swept-Source-OCT, Automated Segmentation, Mean Thickness, Volume, and Reflectance of MPRLs and RPE

The OCT images of the right eye were obtained every 3 months for 24 months using 3D swept-source-OCT (DRI OCT Triton, Topcon Corp., Tokyo, Japan) for all subjects. Macula was scanned using standard 6x6 mm protocol, in which 3D acquisition consisted of 256 B-scan slices. Only the high-quality images without artifact were included. The raw 256 jpg images were exported to OCT-Explorer (image size; 512 x 992 x 256 voxels) (10) which automatically assess the segmentation, enface thickness (**Figure 1A**), volume and reflectance images of the following MPRLs {1) ONL, 2) ellipsoid zone, 3) photoreceptor

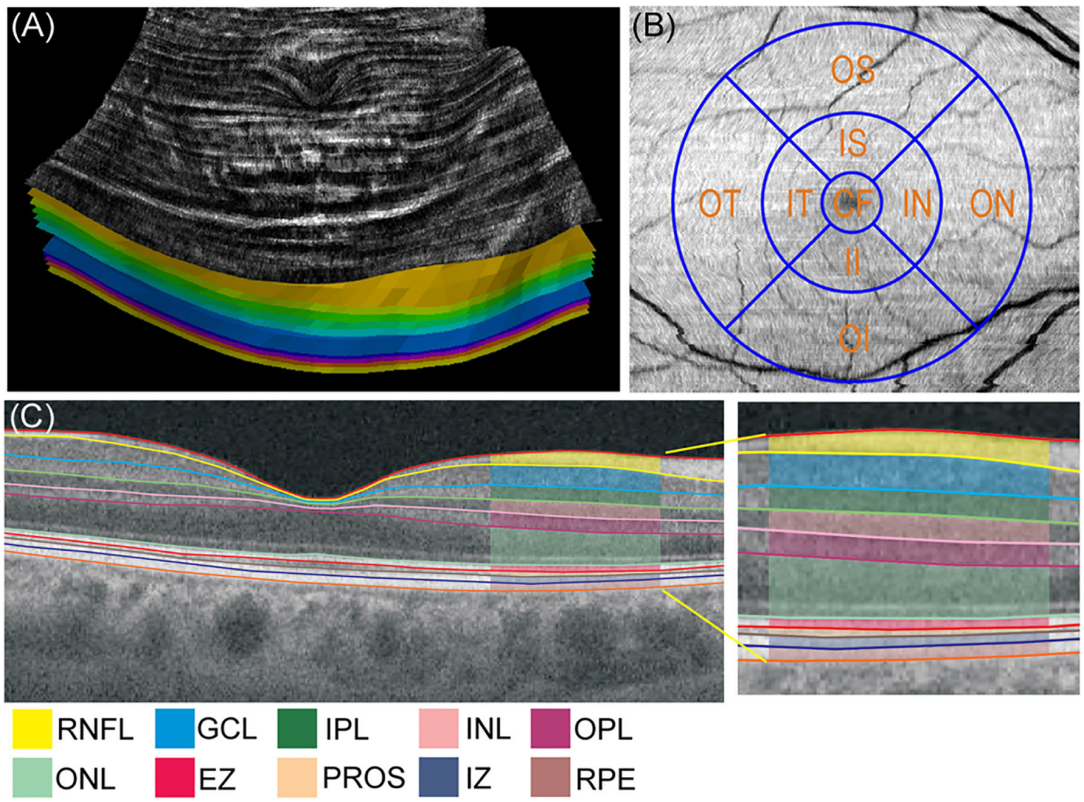

FIGURE 1 | **(A)** Enface thickness image generated by OCT-Explorer of control subject. The innermost layer was inner limiting membrane, and the outermost layer was retinal pigment epithelium. **(B)** Three concentric circles of 1, 3, and 6 mm diameter and 9 Early Treatment Diabetic Retinopathy Study grids. **(C)** Representative optical coherence tomography (OCT) image presenting the mean thickness of macular neuroretinal layers and retinal pigment epithelium in control subject visualized by swept-source OCT and OCT-Explorer. CF, central fovea; EZ, ellipsoid zone; GCL, ganglion cell layer; II, inner inferior; IN, inner nasal; INL, inner nuclear layer; IPL, inner plexiform layer; IS, inner superior; IT, inner temporal; IZ, interdigitation zone; OI, outer inferior; ON, outer nasal; ONL, outer nuclear layer; OPL, outer plexiform layer; OS, outer superior; OT, outer temporal; PROS, photoreceptor outer segment; RNFL, retinal nerve fiber layer; RPE, retinal pigment epithelium.

outer segment (PROS), 4) interdigitation zone} and RPE. The layer-specific mean reflectance was evaluated for each layer and each grid defined by the Early Treatment Diabetic Retinopathy Study (ETDRS). The raw scanned data were interpreted as 16-bit grayscale image, and reflectance was expressed in arbitrary unit (0～256). These metrics were assessed at the central, pericentral, and peripheral rings with diameters of 1, 3, and 6 mm defined by the ETDRS at the following 9 grids: central fovea, inner and outer nasal, superior, temporal, and inferior grids (**Figure 1B**).

Assessment of Neuropathy and Neurophysiological Examinations

The severity of the neuropathy and neurological deficits were assessed using the modified neuropathy disability score (11) which includes the evaluation of vibration, pin prick, temperature perception and ankle reflexes to establish the severity of neuropathy.

All subjects underwent neurophysiological examinations at the baseline and endpoint. Electrophysiology and nerve conduction velocity studies were performed using an electromyography instrument (Neuropak S1, NIHON KOHDEN, Tokyo, Japan). The motor (median nerve) and sensory (sural nerve) nerve conduction velocity, and their action potential amplitudes were determined. The patients with neuropathy disability score > 2 and sensory nerve conduction velocity of the sural nerve < 42 m/s were labeled with neuropathy based on the Toronto consensus (12) as previously reported (13).

The vibration perception threshold was measured at the left medial malleolus using a biothesiometer (Biomedical Instruments, Newbury, OH, USA). The warm and cold perception thresholds at the dorsum of the foot were determined using a thermal stimulator (Intercross-200, Intercross Co., Tokyo, Japan). The autonomic neuropathy and the cardiovagal function were assessed with the coefficient of variation of R-R intervals which was calculated from the R-R intervals of 200 samples on an electrocardiogram.

Statistical Analysis

The *post hoc* analysis of sample power using G power 3.1 (http://gpower.software.informer.com/3.1/) revealed that the statistical power provided by the present study population was 0.96～1.00 for the interaction of the metrics of MPRLs and RPE using the

mixed analysis of variance (ANOVA) (significance of 0.05) and 0.83～0.95 for the multiple regression analysis of the OCT metrics. All statistical analyses were performed using the SPSS (verion19, Chicago, IL, USA). All values are presented as the mean ± standard error of the mean (SEM). All data sets were tested for the normality using the Shapiro-Wilk test. For normally distributed variables, the comparisons between controls and patients with type 2 diabetes at the baseline or endpoint were made by Student t-test for continuous variables and the χ^2-test for categorical variables. For non-normally-distributed continuous variables, Mann-Whitney's U-test was applied and χ^2-test for categorical variables. The differences between baseline and endpoint in each cohort were assessed using the paired t-test, and Wilcoxon signed-rank test for normally and non-normally distributed continuous variables, respectively, and χ^2-test and McNemar test for normally and non-normally distributed categorical variables, respectively. The longitudinal changes in the metrics of MPRLs and RPE were estimated using a mixed ANOVA, which included 2 participant groups as a between-subjects factor, 9-time points as a within-subject factor and the OCT metrics as dependent variables. The sphericity of the within-subjects factors for 2 cohorts was estimated by Mauchly's test. The degree of freedom was adjusted by Greenhouse-Geisser correction for violations of the sphericity assumption. The *post hoc* analyses were performed by Bonferroni's multiple comparison test. The correlations between the changes in the OCT metrics at 9 ETDRS grids and parameters of clinical factors, HbA1c, CPPG, or neurological measures were assessed by the multiple regression analysis.

RESULTS

Demographic Data

Table 1 presents the summary of the demographic and clinical results. Patients with type 2 diabetes and control subjects were age- and gender-matched. At the baseline and endpoint the BMI, systolic blood pressure, CPPG, and HbA1c levels in patients were higher, and HDL-cholesterol was lower than controls. At the baseline LDL-cholesterol, triglycerides and urinary albumin-to-creatinine ratio in patients were higher than controls. During the follow-up period, systolic and diastolic blood pressure, CPPG, HbA1c levels, LDL-cholesterol, and estimated glomerular filtration rate in patients were significantly decreased. The insulin-sensitizing agent (6.5→58.1%) and dipeptidyl peptidase-4 inhibitor (DPP4-I, 9.7→80.6%) were more prescribed at the endpoint than baseline (**Table 1**).

HbA1c levels at baseline (10.3 ± 0.34%) was intensively decreased to 7.0 ± 0.10% at 3 months with adequate speed (1.1%/month). Thereafter, HbA1c levels were kept between 6.5%～6.7%.

Neurophysiological and CNF Measures, and Microvascular Complications

Neuropathy disability score, neurophysiological and CNF measures at the baseline and endpoint in patients were altered compared with controls. Glycemic control did not alleviate neurophysiological measures, while improving some CNF measures. There was no diabetic retinopathy at the baseline and no new incidences of retinopathy in patients with type 2 diabetes. Glycemic control in patients with type 2 diabetes reduced the prevalence of neuropathy, but this did not reach the statistical significance ($p = 0.453$) (**Table 2**).

The Mean Thickness at ETDRS Grids of MPRLs and RPE

Figure 1C shows the representative image of the mean thickness of neuroretinal layers and RPE in a control subject. **Figure 2** compared the sequential changes in the mean thickness at 9 ETDRS grids of MPRLs and RPE between control subjects and patients with type 2 diabetes undergoing glycemic control for 24 months. The thickness at 7 grids of ONL and at inner tempoal grid at the baseline and 3 months in patients was thinner than control. The thickness at 5 ONL grids in patients was significantly increased from the baseline. The baseline thickness at 4 grids of ellipsoid zone in patients was thinner than controls, and glycemic control restored them to the control levels at endpoint. Glycemic control increased the thickness at 5 PROS grids from the baseline. The thickness at 7 grids of interdigitation zone and one RPE grid in patients was thinner than controls. The glycemic control did not restore them (**Figure 2**).

As the volumes at grids of MPRLs and RPE were automatically determined by OCT-Explorer by multiplying the mean thickness by the area of each ETDRS grids, changes in the volume by glycemic control in patients were quite similar to those in the mean thickness.

The Reflectance at ETDRS Grids of MPRLs and RPE

In patients with type 2 diabetes, the reflectance at ONL grids at 6 or 15 months during glycemic control seems to decrease. The reflectances at 6 ONL grids in patients were weaker than controls. There was scarcely any group difference in the reflectances of ellipsoid zone. In ellipsoid zone of patients the reflectances at 3 grids were temporally decreased. In PROS of patients the reflectances at 2 grids were weaker than controls, and reflectances at 2 grids were temporally decreased. In patients, the reflectances at 2 grids of interdigitation zone were weaker than controls, and temporal decrease was found at one grid. At RPE of patients the reflectances at 3 grids were weaker than controls. The temporal decreases were seen at 2 grids. At inner nasal grid of parients the reflectances at 6 and 15 months were weaker than those of controls (**Figure 3**). At 6 months the refrectance at the inner nasal grid was clearly weaker than at 3 and 9 months in patients and at 6 months in controls (**Figure 4**).

Multiple Regression Analysis between Metrics of MPRLs or RPE and Clinical Factors

By multiple regression analysis, the thickness at some ONL grids in patients increased negatively related with the decrease and mean of HbA1c levels over the whole follow-up period and those

TABLE 1 | Demographic data and clinical characteristics at baseline and endpoint in patients with type 2 diabetes and control subjects.

	Patients with type 2 diabetes		Control subjects	
	Baseline	**Endpoint**	**Baseline**	**Endpoint**
Number (Male/Female, %)	31 (64.5/35.5)	31 (64.5/35.5)	39 (64.1 /35.9)	39 (64.1/35.9)
Age (year)	49.8±1.8	51.8±1.8	49.2±1.2	51.2±1.2
Body mass index (kg/m^2)	25.6±0.88*	25.9±1.02†	22.5±0.41	22.6±0.43
Follow up period (year)	-	2.07±0.02	-	2.04±0.01
Duration of diabetes (year)	5.5±1.4	7.5±1.4	-	-
Systolic blood pressure (mmHg)	141±3.6‡	131±2.3§,†	120±1.7	122±1.5
Diastolic blood pressure (mmHg)	85.3±2.2$^{\prime\prime}$	76.4±1.5§	78.5±1.0	79.5±0.9
No. treated with ARB (%)	5 (16.1)$^{\prime\prime}$	7 (22.6)¶	0 (0)	1 (2.6)
Casual postprandial plasma glucose (mg/dL)	272±19.4‡	162±10.3$^{\#,**}$	97.5±2.3	104±2.5
Mean (mg/dL)		156±6.7		
Standard deviation (mg/dL)		43.8±3.2		
Coefficient of variation (%)		29.0±2.3		
HbA1c (%)	10.3±0.34‡	6.7±0.07$^{\#,**}$	5.4±0.05	5.5±0.03
Mean (%)	-	7.05±0.08	-	-
Standard deviation (%)	-	0.94±0.09	-	-
Coefficient of variation (%)	-	13.4±1.3	-	-
LDL-cholesterol (mmol/L)	3.46±0.16 $^{\prime\prime}$	3.08±0.16††	3.02±0.12	2.90±0.09
No. treated with statins (%)	2 (6.5)	1 (3.2)	3 (7.7)	3 (7.7)
HDL-cholesterol (mmol/L)	1.45±0.07 $^{\prime\prime}$	1.48±0.07†	1.71±0.07	1.74±0.06
Triglycerides (mmol/L)	2.25±0.34*	1.68±0.16	1.53±0.25	1.40±0.18
No. treated with fibrates (%)	0 (0)	0 (0)	0 (0)	0 (0)
Estimated glomerular filtration rate (mL/min)	91.5±4.17	85.1±3.16††	86.4±2.46	83.5±2.54
Urinary albumin to creatinine ratio (mg/gCr)	20.1±4.52‡	18.8±4.93¶	8.49±1.22	8.61±0.95
Hypoglycemic treatment				
None/SU/ISA/DPP4-I/diet alone (no.)	26/3/2/3/0	0** /6/18** /25** /1		

Data are the mean ± standard error of the mean in patients with type 2 diabetes and control subjects at baseline and endpoint.
**p < 0.01 compared with control subjects at baseline, †p < 0.01 compared with control subjects at endpoint, ‡p <0.001 compared with control subjects at baseline, §p < 0.01 compared with baseline, $^{\prime\prime}$p < 0.05 compared with control subjects at baseline, ¶p < 0.05 compared with control subjects at endpoint, $^{\#}$p < 0.001 compared with control subjects at endpoint, **p < 0.001 compared with baseline, ††p < 0.05 compared with baseline.*
ARB, angiotensin receptor blocker; DPP4-I, dipeptidyl peptidase-4 inhibitor; HDL, high-density lipoprotein; ISA, insulin-sensitizing agent; LDL, low-density lipoprotein; SU, sulfonylurea.

TABLE 2 | Neurophysiological measures, corneal nerve fiber measures and microvascular complications at baseline and endpoint in patients with type 2 diabetes and control subjects.

	Patients with type 2 diabetes		Control subjects	
	Baseline	**Endpoint**	**Baseline**	**Endpoint**
Neurophysiological measures				
Neuropathy disability score	4.39±0.50*	3.84±0.42†	0.44±0.08	0.49±0.08
MCV of median nerve (m/s)	52.5±0.60*	53.7±0.54†	59.0±0.70	58.3±0.57
Amplitude of median nerve (mV)	8.03±0.57‡	7.12±0.60†	9.18±0.44	9.53±0.39
SCV of sural nerve (m/s)	45.1±1.00§	46.3±0.86†	49.4±0.72	50.0±0.63
Amplitude of sural nerve (μV)	11.5±0.93§	13.0±1.00	15.9±1.15	15.7±1.02
Vibration perception threshold (μ/120c/s)	3.30±0.37*	2.75±0.36	1.67±0.16	1.78±0.12
Coefficient of variation of R-R interval (%)	3.15±0.24§	3.06±0.25†	4.13±0.24	4.25±0.18
Warm perception threshold (W/m^2)	-635±45.4‡	-616±42.3$^{\prime\prime}$	-497±20.5	-489±16.0
Cold perception threshold (W/m^2)	544±25.1	509±20.7	490±19.3	496±11.8
Corneal nerve fiber measures				
Corneal nerve fiber density (no/mm^2)	19.9±0.53*	20.2±0.50†	30.8±0.83	30.3±0.57
Corneal nerve fiber length (mm/mm^2)	10.7±0.26*	11.4±0.27¶,†	15.1±0.30	15.4±0.34
Corneal nerve branch density (no/mm^2)	9.84±0.50*	11.3±0.42¶,†	14.2±0.77	14.5±0.56
Beading frequency (no/0.1mm)	19.4±0.25*	19.6±0.28†	23.6±0.33	24.0±0.27
Bead size (μm^2)	11.7±0.10*	10.3±0.12$^{\#,\dagger}$	8.09±0.074	8.11±0.051
Microvascular complications				
Prevalence of retinopathy (%)	0	0	0	0
Prevalence of neuropathy (%)	25.8	16.1	0	0
Prevalence of nephropathy (%)	16.1	19.4	0	0

Data are the mean ± standard error of the mean in patients with type 2 diabetes and control subjects at baseline and endpoint.
**p < 0.001 compared with control subjects at baseline, †p < 0.001 compared with control subjects at endpoint, ‡p < 0.05 compared with control subjects at baseline, §p < 0.01 compared with control subjects at baseline, $^{\prime\prime}$p < 0.05 compared with control subjects at endpoint, ¶p < 0.05 compared with baseline, $^{\#}$p < 0.001 compared with baseline.*
MCV, motor nerve conduction velocity; SCV, sensory nerve conduction velocity.

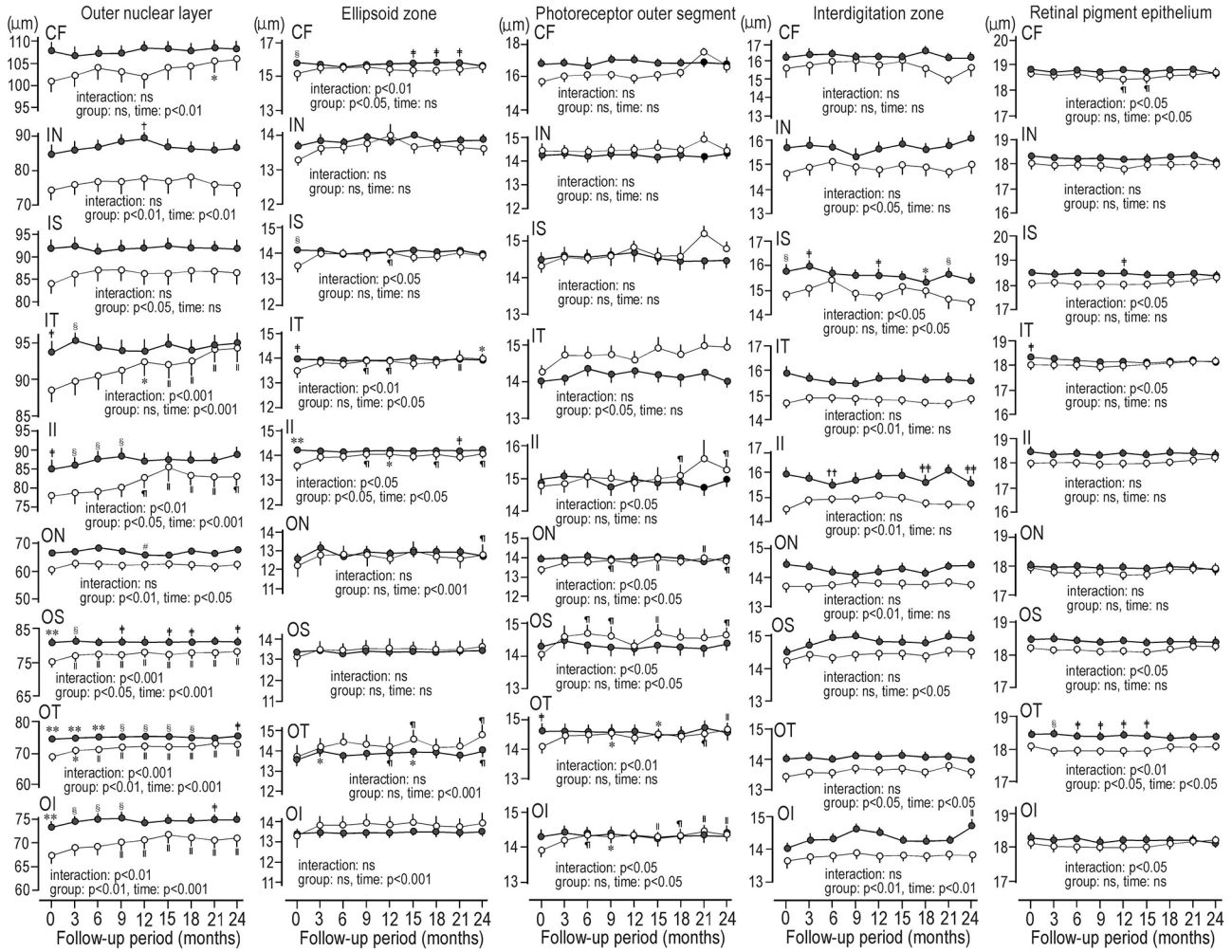

FIGURE 2 | Sequential changes for 2 years in the mean thickness at grids defined by Early Treatment Diabetic Retinopathy Study of individual macular photoreceptor layers and retinal pigment epithelium in patients with type 2 diabetes undergoing glycemic control (open circle) and control subjects (solid circle). Values were mean ± SEM. *p < 0.01 compared with baseline, †p < 0.05 compared with 3 months, ‡p < 0.05 compared with patients with type 2 diabetes, §p < 0.01 compared with patients with type 2 diabetes, ‟p < 0.001 compared with baseline, ¶p < 0.05 compared with baseline, #p < 0.05 compared with 6 months, **p < 0.001 compared with patients with type 2 diabetes, ††p < 0.01 compared with 21 months, ‡‡p < 0.05 compared with 21 months. CF, central fovea; II, inner inferior; IN, inner nasal; IS, inner superior; IT, inner temporal; OI, outer inferior; ON, outer nasal, OS; outer superior; OT, outer temporal.

at 6-24 months, and positively related with baseline HbA1c levels. The mean CPPG and those at 12,18 and 21 months were negatively related with the increase in the thickness at the outer temporal ONL grid. The decrease in the reflectance at 6 months during glycemic control at outer inferior grid of ellipsoid zone or PROS was inversely associated with the HbA1c levels at that time (**Table 3**).

The mean levels (β:-0.220～0.060, p:0.268～0.782) or improvements (β:-0.257～0.092, p:0.232～0.784) of the metabolic syndrome components during glycemic control did not influence the ONL thickness and the reflectances of ellipsoid zone or PROS. The interval changes in neurophysiological tests (β:-0.227～0.348, p:0.133～0.942) and CNF measures (β:-0.349～0.275, p:0.090～0.992) were not associated with the increase in thickness at inner temporal and outer temporal grids of ONL nor weaker reflectance at outer inferior grid of ellipsoid zone or PROS. The increased prescription of DPP4-I and insulin sensitizing agent at the endpoint did not influence the ONL thickness (β:-0.353～0.339, p:0.067～0.603) nor the reflectance of ellipsoid zone or PROS (β:-0.249～0.197, p:0.400～0.930).

DISCUSSION

The present study investigated the sequential changes during glycemic control in the mean thickness, volume and reflectance

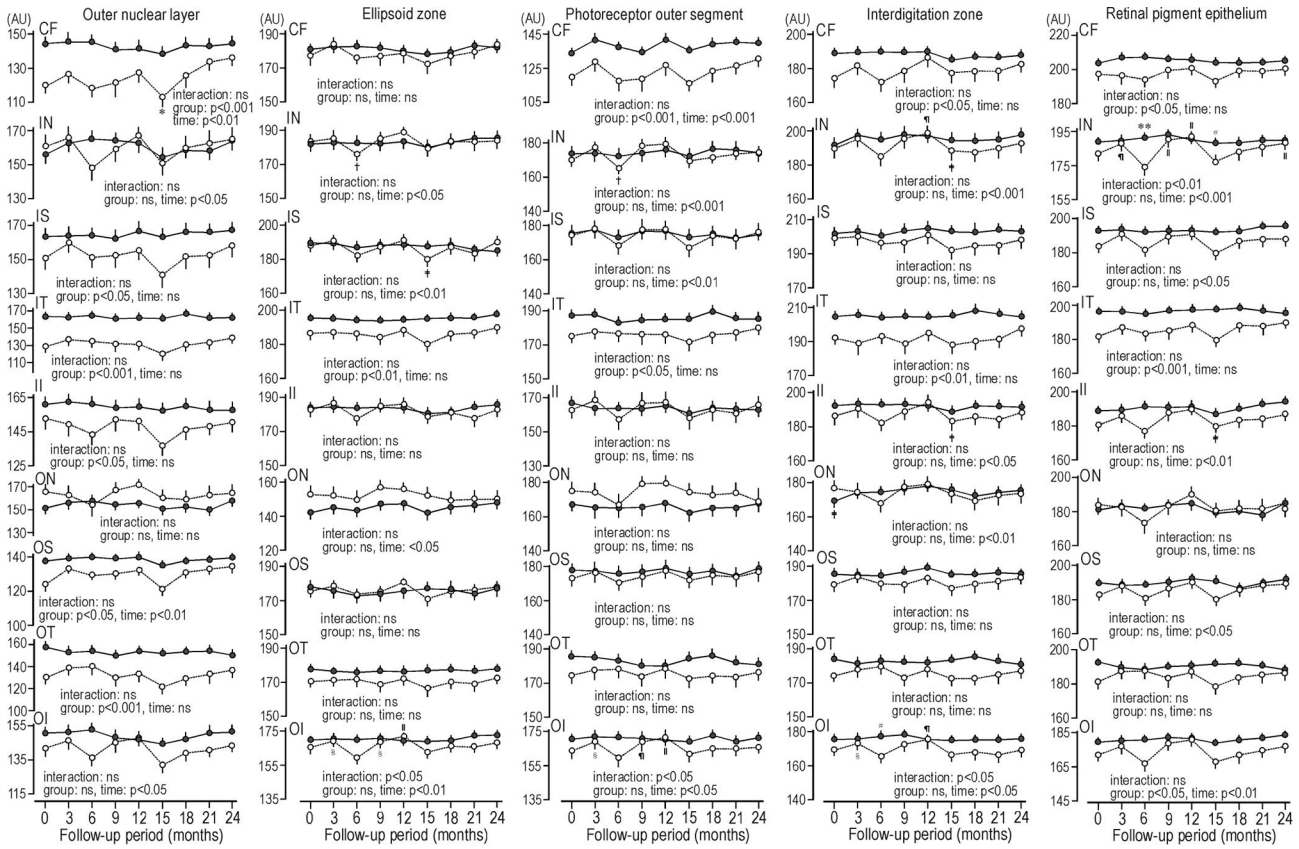

FIGURE 3 | Sequential changes for 2 years in the reflectance at grids defined by Early Treatment Diabetic Retinopathy Study of individual macular photoreceptor layers and retinal pigment epithelium in patients with type 2 diabetes undergoing glycemic control (open circle) and control subjects (solid circle). Values were mean ± SEM. *$p < 0.05$ compared with endpoint, †$p < 0.01$ compared with 12 months, ‡$p < 0.05$ compared with 12 months, §$p < 0.05$ compared with 6 months, ‖$p < 0.001$ compared with 6 months, ¶$p < 0.01$ compared with 6 months, #$p < 0.05$ compared with patients with type 2 diabetes, **$p < 0.001$ compared with patients with type 2 diabetes. AU, arbitrary unit; CF, central fovea; II, inner inferior; IN, inner nasal; IS, inner superior; IT, inner temporal; OI, outer inferior; ON, outer nasal, OS; outer superior; OT, outer temporal.

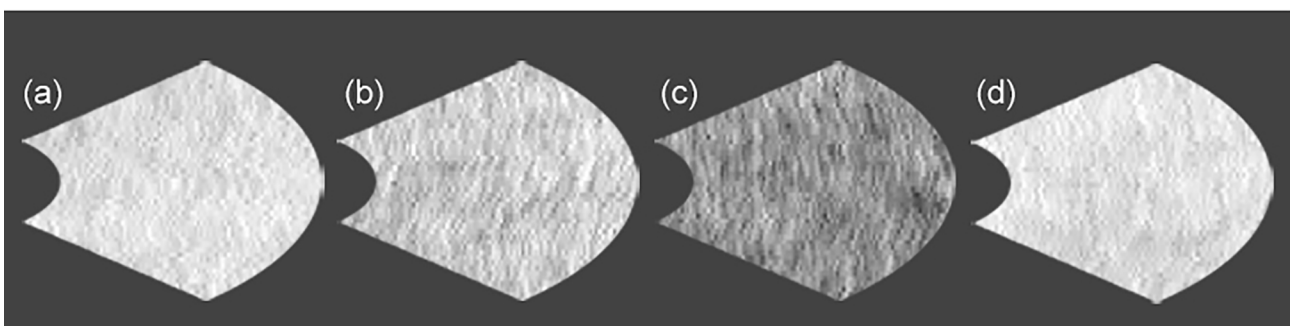

FIGURE 4 | The comparison of the reflectances at inner nasal grid of retinal pigment epithelium between control subject and patient with type 2 diabetes under glycemic control. (a) control subject at 6 months (223), (b) patient with type 2 diabetes at 3 months (204), (c) patient with type 2 diabetes at 6 months (147), and (d) patient with type 2 diabetes at 9 months (224). No. in the parenthesis reveals reflectance in arbitrary unit.

TABLE 3 | Correlations between the increase in the thickness at grids of the outer nuclear layer or the decrease in reflectance at EZ and PROS grids and parameters of HbA1c, CPPG, and their variability during the follow-up period in patients with type 2 diabetes undergoing glycemic control for 24 months.

		Increase in the thickness at grids of outer nuclear layer by glycemic control				Decrease in reflectance at the outer inferior grid of EZ and PROS at 6 months during glycemic control			
		Inner temporal grid		Outer temporal grid		Outer inferior grid of EZ		Outer inferior grid of PROS	
		Standard β	p	Standard β	p	Standard β	p	Standard β	p
HbA1c levels	decrease	-0.545	**0.004**	-0.588	**0.004**	-0.041	0.854	-0.160	0.463
	mean	-0.473	**0.026**	-0.570	**0.008**	-0.021	0.929	0.101	0.667
	standard deviation	0.321	0.273	0.227	0.485	-0.478	0.126	-0.534	0.084
	coefficient of variation	0.486	0.077	0.447	0.138	-0.411	0.166	-0.501	0.087
	baseline	0.450	**0.020**	0.547	**0.008**	0.095	0.664	0.227	0.292
	3 months	-0.102	0.648	-0.153	0.526	-0.226	0.338	0.011	0.964
	6 months	-0.388	0.082	-0.631	**0.006**	-0.803	**<0.001**	-0.665	**0.001**
	9 months	-0.581	**0.033**	-0.634	**0.003**	-0.044	0.847	0.099	0.661
	12 months	-0.534	**0.007**	-0.639	**0.003**	0.072	0.754	0.163	0.472
	15 months	-0.572	**0.004**	0.816	**<0.001**	-0.021	0.929	0.214	0.346
	18 months	-0.578	**0.002**	-0.686	**0.001**	-0.013	0.952	0.101	0.647
	21 months	-0.561	**0.003**	-0.656	**0.001**	-0.024	0.913	0.226	0.303
	endpoint	-0.705	**<0.001**	-0.783	**<0.001**	0.264	0.267	0.279	0.237
CPPG	decrease	-0.171	0.394	-0.328	0.124	-0.257	0.225	-0.331	0.111
	mean	-0.070	0.736	-0.498	**0.019**	-0.145	0.509	-0.138	0.526
	standard deviation	0.138	0.512	0.076	0.740	-0.295	0.180	-0.117	0.599
	coefficient of variation	0.223	0.276	0.255	0.250	-0.279	0.198	-0.105	0.631
	baseline	0.109	0.573	0.170	0.416	0.182	0.376	0.234	0.249
	3 months	0.080	0.688	-0.227	0.289	-0.195	0.354	-0.312	0.131
	6 months	-0.033	0.874	-0.398	0.070	0.255	0.221	0.231	0.191
	9 months	0.003	0.987	-0.321	0.125	-0.132	0.531	-0.196	0.347
	12 months	-0.251	0.263	-0.464	**0.049**	-0.220	0.358	-0.364	0.120
	15 months	0.030	0.887	-0.215	0.343	-0.323	0.142	-0.257	0.243
	18 months	-0.202	0.335	-0.548	**0.010**	-0.132	0.555	0.164	0.460
	21 months	-0.153	0.463	-0.494	**0.021**	-0.067	0.763	-0.071	0.748
	endpoint	-0.174	0.443	-0.420	0.078	-0.222	0.354	-0.288	0.225

Decrease in HbA1c = value at endpoint – value at baseline. Increase in thickness = value at endpoint – value at baseline. Decrease in reflectance = reflectance at 6 months – reflectance at 3 months after the start of glycemic control. CPPG, casual postprandial plasma glucose; EZ, ellipsoid zone; PROS; photoreceptor outer segment.
Statistically significant correlations appear in boldface type.

of individual MPRLs and RPE using enface OCT in type 2 diabetic patients without diabetic retinopathy. In patients with diabetes, evidences showing photoreceptor death is equivocal (4, 14). Therefore, not much has been clarified what occurs in the metrics of individual MPRLs and RPE during glycemic control in type 2 diabetes. Indeed the glycemic control has the potential transient negative influence on diabetic retinopathy (15). In patients with type 2 diabetes 4 months after starting glycemic control, retinal nerve fiber layer got thinner related with the decrease in HbA1c levels (16). Therefore, the sequential OCT examinations during glycemic control is crucial to clarify the dynamic influence of glycemic control on the metrics and neuroretinal structures. This may enable to predict the future incidences of diabetic retinopathy. Because the thickness of most MPRLs and RPE is < 20 μm, the precise measurement and good repeatability are necessary to elucidate the impact of glycemic control on the small but significant changes in the OCT metrics in diabetic patients. In control subjects, the coefficients of variation in 9 measurements of the mean thickness and volume over 2 years at 9 ETDRS grids of ONL, ellipsoid zone, PROS, interdigitation zone and RPE were 1.6-5.3%, 1.6-3.7%, 1.9-3.8%, 1.7-5.5%, and 1.2-1.8%, respectively, indicating good repeatablility, although some significant fluctuations even in control subjects were seen. In contrast, the coefficients of variation in 9 reflectance measurements at these layers in controls were 8.8-11.0%, 4.5-6.5%, 4.8-7.3%, 4.4-5.8% and 4.6-6.0%, respectively, indicating poorer repeatablility than the mean thickness and volume. The sequential changes in the reflectance by the intervention such as glycemic control should be cautiously interpreted.

In the present study, the thickness of 7 grids of ONL over whole follow-up period, and partially at inner temporal grid in patients was thinner than controls. Glycemic control significantly increased the thickness at 6 grids of ONL from the baseline. In patients the mean thickness at the inner temporal grid was restored to the control level after 24 months follow-up. Because glycemic variability plays a causative role in diabetic complications independent of HbA1c levels (17), we associated the recovery of some ONL thickness with parameters of glycemic control and glycemic variability. The recovery of some ONL grid thickness was robustly associated with overall HbA1c decrease from the baseline and monthly low HbA1c levels during the second year of follow-up period. The mean HbA1c and CPPG levels also contributed to ONL recovery. The baseline HbA1c levels did not influence any baseline ONL thickness (P = 0.205～0.966), but positively related with the recovery of some ONL

thickness. Because the HbA1c levels at the endpoint in patients were similar (6.5～6.7%), the decrease in HbA1c levels was highly correlated with the baseline HbA1c levels ($p < 0.001$). Then, the high baseline HbA1c levels positively correlated with the increase in ONL thickness. In contract, glycemic variability was not significantly related with the recovery of ONL thickness. However, glycated albumin has been reported to be better marker of glycemic variability than HbA1c levels, especially for short term (18). Because the present study did not measure glycated albumin, we could not clarify the relationship between the variability of glycated albumin and the metrics of MPRLs and RPE.

A reduced ONL thickness may represent photoreceptor cell death (19). Therefore, the ONL thickness, especially at inner temporal grid, can provide a measure for the photoreceptor recovery by glycemic control. The cone density near central fovea is highest and abruptly decreases toward the periphery, and the rod occupies 90% of photoreceptors (20). Because glycemic control increased the thickness at central fovea, pericentral and peripheral grids, glycemic control might restore ONL of the cones and rods.

The thickness at 4 grids of ellipsoid zone at the baseline in patients with type 2 diabetes was thinner than control subjects. Glycemic control significantly increased the thickness at 3 inner and 2 outer grids of ellipsoid zone from the baseline. The ellipsoid zone contains mitochondria which are the main focus of hyperglycemia-induced retinal oxidative stress (21). The recovery of ellipsoid zone by glycemic control may represent the amelioration in photoreceptor oxidative stress and mitochondrial degeneration.

As previously reported (3, 4), the most baseline PROS thickness in patients with type 2 diabetes was similar to that of control subjects, and glycemic control increased the thickness from the baseline at all peripheral and one pericentral grids, suggesting the PROS of the rod in patients might be more amenable to glycemic control than cone which located near the central fovea. This was compatible with less severe demand in blood supply and metabolism in the peripheral retina than central fovea (4).

The mean thickness of 6 grids of interdigitation zone and one grid of RPE in patients was thinner than controls (22). Glycemic control did not restore the thickness of interdigitation zone and RPE. The influence of glycemic control on these layers had never been investigated and the current study is the first to our knowledge that reports these findings.

The influence of glycemic control on the volume of MPRLs and RPE was quite similar to that on the mean thickness, because OCT-Explorer automatically calculated the volume by multiplying the mean thickness by the each grid area defined by the ETDRS.

The second aspect of these novel findings is the sequential assessment of reflectance in MPRLs and RPE during glycemic control in diabetic patients without diabetic retinopathy. This may disclose the alterations occurring before the development of new diabetic retinopathy, as reported in cross-sectional study of type 1 diabetes (23). The reflectance at baseline and during follow-up in patients was similar or less than controls. The transient weaker reflectance occurred at 6 and 15 months during glycemic control. To rule out the shadowing effect by high reflectance at inner retinal layers to outer retinal layers (24), we measured reflectances at all inner retinal layers. There were no high reflectances, and weaker reflectances were found at all inner retinal layers at the same time points as MPRLs and RPE. The weaker reflectance at outer inner grid of ellipsoid zone and PROS at 6 months during glycemic control was robustly related with high HbA1c levels at that time point. This means that the temporal glycemic deterioration during glycemic control may cause weaker reflectance of MPRLs, suggesting the possible derangement of MPRLs. The erratically high blood glucose rather than constant high glucose exposure was shown to have more harmful consequences associated with oxidative stress and endothelial dysfunction (25). Because the ellipsoid zone contains mitochondria which are the main focus of hyperglycemia-induced retinal oxidative stress (21), the temporal glycemic deterioration during glycemic control may result in the derangement of MPRLs. In the perifoveal region, the reflectances in ellipsoid zone and interdigitation zone are closely related to the cone density (26). The weaker reflectance may result from the disarray of the mosaic cone and rod distribution, as found in various retinal diseases (27). If the hyperglycemia-induced hyperosmolarity may enhance dehydration in situ, the baseline thickness was reduced, and reflectance was increased. The subsequent glycemic control may restore normal osmolarity and improve the thickness and reflectance toward the endpoint. We think this was unlikely, because the thickness in some grids at baseline was sequentially and significantly increased toward the endpoint, while the reflectance at endpoint did not significantly changed from baseline at all grids of MPRLs and RPE, and the weaker reflectances were transient at specific time points and reversible, and because chronic hyperglycemia could increase the permeability of retinal vasculature (28), which may have led to the thickening of the retinal layers due to edema (3) at baseline.

The thickness and reflectance in patients with diabetes seem to be variable compared with those in control subjects. The metrics of MPRLs and RPE are influenced by not only glycemic levels (28), but also many clinical factors including anthropometric values, blood pressure and serum lipid levels (22). In control subjects, these clinical factors were stable and existed in a narrow range during the follow-up period, while in the present study all values in patients except for BMI were significantly different between baseline and endpoint. Furthermore, clinical background of diabetes such as disease duration and severity of hyperglycemia was different among patients with diabetes. These diverse clinical factors in patients may induce variability in the metrics of MPRLs and RPE. The fovea has the highest density of cones, and therefore has an increased metabolic demand, and the temporal regions have the thinnest retina. The foveal and temporal regions of retina may be susceptible to diabetic harm (28). Therefore, the influence of diabetes on neuroretina may be variable among

ETDRS grids, and cause regional variability in the metrics of MPRLs and RPE.

The causative mechanisms of the transient weaker reflectances of MPRLs and RPE are unknown. According to the neurodegenerative theory of diabetic retinopathy, the apoptosis of neuronal cells, including photoreceptor cells, observed at an early stage of diabetes, might lead to microvascular changes (29). In type 1 diabetes without diabetic retinopathy, the weaker reflectance in some retinal layers is supposed to predict the new development of diabetic retinopathy (23). Therefore, transient weaker reflectances in the present study may be relevant to the development of diabetic retinopathy induced by glycemic control.

Because the increase in ONL thickness during glycemic control was not associated with the improvement in CNF and neurophysiological measures, and because glycemic control did not ameliorate the neurophysiological measures, the recovery of ONL thickness by glycemic control might be a novel morphological marker for investigating the benefit of glycemic control on the diabetic neuropathy. Although glycemic control improved some CNF measures, all measures at endpoint were still inferior to those in control subjects. In contrast, glycemic control increased the mean thickness and volume at some grids of ONL, ellipsoid zone and PROS to the levels of control subjects, indicating that glycemic control had potential to normalize the thickness and volume of some MPRLs.

Because the normal HbA1c levels (< 5.9%) (13) or HbA1c levels < 6.5% (30) are mandatory for improving neuro physiological and CNF measures by glycemic control, the average HbA1c levels in the current study beyond these levels could not improve the neuropathy measures.

Although chronic hyperglycemia clearly plays a causative role in the retinal neurodegeneration in type 2 diabetes, metabolic syndrome components are likely to cause it (31). In our study, the mean levels or changes in metabolic syndrome components during follow-up period were not associated with the increase in ONL thickness.

Strengths and Limitations

The longitudinal impact of glycemic control on the OCT metrics in type 2 diabetes had never been investigated. For excluding time-dependent variability in OCT metrics, this study repeated OCT examinations every 3 months for 2 years. The current study measured the main factors influencing the metrics of MPRLs and RPE monthly or every 3 months during the follow-up period. Therefore, the mean clinical factors influencing the OCT metrics are representative; the contribution of controlling hyperglycemia and other risk factors to the restoration of altered MPRLs and RPE was reliably evaluated by multiple regression analysis.

Our study has some limitations. First, the follow-up period of 2 years may need to be extended. Ideally, the glycemic control needs to be maintained for over 3-5 years to yield definite benefit (32). Two years might be too short to restore the morphology of all MPRLs and RPE, and neurological deficits. Second, we did not examine the retinal function such as electroretinography. The simultaneous examinations using electroretinography and OCT strengthen the role of glycemic control on the restoration of MPRLs and RPE. Third, because we aimed to unveil changes in MPRL metrics before the development of diabetic retinopathy, patients with diabetic retinopathy were excluded. Therefore, we could not assess the influence of diabetic retinopathy on the metrics of MPRLs. Fourth, the weaker reflectances at the specific time points occurred in relation to coincident HbA1c increase during glycemic control. The future research, including many diabetic patients developing new diabetic retinopathy during glycemic control is indicated to clarify the role of transient weaker reflectance for the development of diabetic retinopathy induced by glycemic control.

In conclusion, the longitudinal impact of glycemic control on the OCT metrics in type 2 diabetes had never been investigated. In this paper for the first time, we conducted such a follow-up study. The glycemic control in type 2 diabetes sequentially restored the mean thickness and volume at some MPRL gids over 24 months follow-up period. Some reflectances of MPRLs and RPE at specific time points during glycemic control were weaker than those at adjacent time points coincident with high HbA1c levels. The causative mechanisms of transient weaker reflectance during glycemic control should be investigated for predicting the development of diabetic retinopathy.

DATA AVAILABILITY STATEMENT

The raw data supporting the conclusions of this article will be made available by the authors, without undue reservation.

ETHICS STATEMENT

Written informed consent was obtained from all subjects based on the Declaration of Helsinki. The ethics committee of Ishibashi Clinic approved the protocol of this study.

AUTHOR CONTRIBUTIONS

FI designed the study, researched data, and wrote the entire manuscript. AK gathered clinical and laboratory data and statistically analyzed all data. MT advised on the statistical analysis, interpreted the results, and reviewed and revised the whole manuscript. FI and MT are the guarantors of this work, and, as such, had full access to all data in the study and take responsibility for the integrity of the data and the accuracy of the data analysis and interpretation. All authors contributed to the article and approved the submitted version.

ACKNOWLEDGMENTS

The authors wish to acknowledge the contribution by Ms. Harumi Uetake for secretarial work.

REFERENCES

1. Francis AW, Wanek J, Lim JI, Shahidi M. Enface thickness mapping and reflectance imaging of retinal layers in diabetic retinopathy. *PloS One* (2015) 10(12):e0145628. doi: 10.1371/journal.pone.0145628
2. Picconi F, Parravano M, Ylli D, Pasqualetti P, Coluzzi S, Giordani I, et al. Retinal neurodegeneration in patients with type 1 diabetes mellitus: the role of glycemic variability. *Acta Diabetol* (2017) 54(5):489–97. doi: 10.1007/s00592-017-0971-4
3. Wanek J, Blair NP, Chau FY, Lim JI, Leiderman YI, Shahidi M. Alterations in retinal layer thickness and reflectance at different stages of diabetic retinopathy by en face optical coherence tomography. *Invest Ophthalmol Vis Sci* (2016) 57:341–7. doi: 10.1167/iovs.15-18715
4. Ozkaya A, Alkin Z, Karakucuk Y, Karatas G, Fazil K, Gurkan Erdogan M, et al. Thickness of the retinal photoreceptor outer segment layer in healthy volunteers and in patients with diabetes mellitus without retinopathy, diabetic retinopathy, or diabetic macular edema. *Saudi J Ophthalmol* (2017) 31(2):69–75. doi: 10.1016/j.sjopt.2016.12.006
5. Gella L, Raman R, Sharma T. Quantitative spectral-domain optical coherence tomography thickness parameters in type II diabetes. *Oman J Ophthalmol* (2016) 9(1):32–6. doi: 10.4103/0974-620X.176098
6. Hong EH, Ryu SJ, Kang MH, Seong M, Cho H, Yeom JH, et al. Comparison of repeatability of swept-source and spectral-domain optical coherence tomography for measuring inner retinal thickness in retinal disease. *PloS One* (2019) 14(1):e0210729. doi: 10.1371/journal.pone.0210729
7. Molitch ME, DeFronzo RA, Franz MJ, Keane WF, Mogensen CE, Parving HH. Nephropathy in diabetes. *Diabetes Care* (2003) 26(Suppl. 1):S94–8. doi: 10.2337/diacare.26.2007.s94
8. Ishibashi F, Okino M, Ishibashi M, Kawasaki A, Endo N, Kosaka A, et al. Corneal nerve fiber pathology in Japanese type 1 diabetic patients and its correlation with antecedent glycemic control and blood pressure. *J Diabetes Invest* (2012) 3(2):191–8. doi: 10.1111/j.2040-1124.2011.00157.x.2012
9. Ishibashi F, Kojima R, Taniguchi M, Kosaka A, Uetake H, Tavakoli M. The expanded bead size of corneal C-nerve fibers visualized by corneal confocal microscopy is associated with slow conduction velocity of the peripheral nerves in patients with type 2 diabetes mellitus. *J Diabetes Res* (2016) 2016:9. doi: 10.1155/2016/3653459
10. Garvin MK, Abramoff MD, Kardon R, Russell SR, Wu X, Sonka M. Intraretinal layer segmentation of macular optical coherence tomography images using optimal 3-D graph search. *IEEE Trans Med Imaging* (2008) 27 (10):1495–505. doi: 10.1109/TMI.2008.923966
11. Young MJ, Boulton AJ, MacLeod AF, Williams DR, Sonksen PH. A multicentre study of the prevalence of diabetic peripheral neuropathy in the United Kingdom hospital clinic population. *Diabetologia* (1993) 36(2):150–4. doi: 10.1007/BF00400697
12. Tesfaye S, Boulton AJM, Dyck PJ, Freeman R, Horowitz M, Kempler P, et al. Toronto Diabetic Neuropathy Expert Group. Diabetic neuropathies: update on definitions, diagnostic criteria, estimation of severity, and treatments. *Diabetes Care* (2010) 33(10):2285–93. doi: 10.2337/dc10-1303
13. Ishibashi F, Taniguchi M, Kosaka A, Uetake H, Tavakoli M. Improvement in neuropathy outcomes with normalizing HbA1c in patients with type 2 diabetes. *Diabetes Care* (2019) 42(1):110–8. doi: 10.2337/dc.18-1560
14. Verma A, Rani PK, Raman R, Pal SS, Laxmi G, Gupta M, et al. Is neuronal dysfunction an early sign of diabetic retinopathy? Microperimetry and spectral domain optical coherence tomography (SD-OCT) study in individuals with diabetes, but no diabetic retinopathy. *Eye (Lond)* (2009) 23 (9):1824–30. doi: 10.1038/eye.2009.184
15. Bain SC, Klufas MA, Ho A, Matthews DR. Worsening of diabetic retinopathy with rapid improvement in systemic glucose control: a review. *Diabetes Obes Metab* (2019) 21(9):454–66. doi: 10.1111/dom.13538
16. Sugimoto M, Sasoh M, Ido M, Narushima C, Uji Y. Retinal nerve fiber layer decrease during glycemic control in type 2 diabetes. *J Ophthalmol* (2010) 2010:6. doi: 10.1155/2010/569215
17. Gorst C, Kwok CS, Aslam S, Buchan I, Kontopantelis E, Myint PK, et al. Long-term glycemic variability and risk of adverse outcomes: a systematic review and meta-analysis. *Diabetes Care* (2015) 38(12):2354–69. doi: 10.2337/dc15-1188
18. Takahashi S, Uchino H, Shimizu T, Kanazawa A, Tamura Y, Sakai K, et al. Comparison of glycated albumin (GA) and glycated hemoglobin (HbA1c) in type 2 diabetic patients: usefullness of GA for evaluation of short-term changes in glycemic control. *Endocr J* (2007) 54(1):139–44. doi: 10.1507/endocrj.k06-103
19. Arroyo JG, Yang L, Bula D, Chen DF. Photoreceptor apoptosis in human retinal detachment. *Am J Ophthalmol* (2005) 139(4):605–10. doi: 10.1016/j.ajo.2004.11.046
20. Wells-Gray EM, Choi SS, Bries A, Doble N. Variation in rod and cone density from the fovea to the mid-periphery in healthy human retinas using adaptive optics scanning laser ophthalmoscopy. *Eye (Lond)* (2016) 30(5):1135–43. doi: 10.1038/eye.2016.107
21. Du Y, Veenstra A, Palczewski K, Kern TS. Photoreceptor cells are major contributors to diabetes-induced oxidative stress and local inflammation in the retina. *Proc Natl Acad Sci USA* (2013) 110(41):16586–91. doi: 10.1073/pnas.1314575110
22. Ishibashi F, Tavakoli M. Thinning of macular neuroretinal layers contributes to sleep disorder in patients with type 2 diabetes without clinical evidences of neuropathy and retinopathy. *Front Endocrinol (Lausanne)* (2020) 11:69. doi: 10.3389/fedo.2020.00069
23. DeBuc D, Tatrai E, Laurik L, Varga BE, Olvedy V, Somogyi A, et al. Identifying local structural and optical derangement in the neural retina of individuals with type 1 diabetes. *J Clin Exp Ophthalmol* (2013) 4(4):1000289. doi: 10.4172/2155-9570.1000289
24. Chen H, Chen X, Qiu Z, Xiang D, Chen W, Shi F, et al. Quantitative analysis of retinal layers' optical intensities on 3D optical coherence tomography for central retinal artery occlusion. *Sci Rep* (2015) 5:9269. doi: 10.1038/srep09269
25. Papachristoforou E, Lambadiari V, Maratou E, Makrilakis K. Association of glycemic indices (hyperglycemia, glucose variability, and hypoglycemia) with oxidative stress and diabetic complications. *J Diabetes Res* (2020) 2020:17. doi: 10.1155/2020/7489795
26. Saleh M, Flores M, Gauthier AS, Elphege E, Delbosc B. Quantitative analysis of photoreceptor layer reflectivity on en-face optical coherence tomography as an estimator of cone density. *Graefes Arch Clin Exp Ophthalmol* (2017) 255 (11):2119–26. doi: 10.1007/s00417-017-3761-3
27. Wartak A, Augustin M, Haindl R, Beer F, Salas M, Laslandes M, et al. Multi-directional optical coherence tomography for retinal imaging. *BioMed Optics Express* (2017) 8(12):5560–78. doi: 10.1364/BOE.8.005560
28. Jiang J, Liu Y, Chen Y, Ma B, Qian Y, Zhang Z, et al. Analysis of changes in retinal thickness in type 2 diabetes without diabetic retinopathy. *J Diabetes Res* (2018) 2018:7. doi: 10.1155/2018/3082893
29. Barber AJ. A new view of diabetic retinopathy: a neurodegenerative disease of the eye. *Prog Neuropsychopharmacol Biol Psychiatry* (2003) 27(2):283–90. doi: 10.1016/S0278-5846(03)00023-X
30. Ishibashi F, Tavakoli M. Impact of normoglycemia in reducing microvascular complications in patients with type 2 diabetes: a follow-up study. *Front Endocrinol (Lausanne)* (2018) 9:52. doi: 10.3389/fendo.2018.00052
31. Grisold A, Callaghan BC, Feldman EL. Mediators of diabetic neuropathy: is hyperglycemia the only culprit? *Curr Opin Endocrinol Diabetes Obes* (2017) 24 (2):103–11. doi: 10.1097/MED.0000000000000320
32. Giorgino F, Home PD, Tuomilehto J. Glucose control and vascular outcomes in type 2 diabetes: is the picture clear? *Diabetes Care* (2016) 39(suppl. 2):S187–95. doi: 10.2337/dcS15-3023

Conflict of Interest: The authors declare that the research was conducted in the absence of any commercial or financial relationships that could be construed as a potential conflict of interest.

frontiers in Endocrinology

ORIGINAL RESEARCH
published: 29 October 2021
doi: 10.3389/fendo.2021.757088

Plasma Metabolomics Reveals Metabolic Profiling For Diabetic Retinopathy and Disease Progression

Yu Sun[1,2], *Huiling Zou*[2], *Xingjia Li*[1,3], *Shuhang Xu*[1,3]* and *Chao Liu*[1,3]*

[1] Department of Endocrinology, Affiliated Hospital of Integrated Traditional Chinese and Western Medicine, Nanjing University of Traditional Chinese Medicine, Nanjing, China, [2] Department of Endocrinology and Metabolism, The Affiliated Suqian Hospital of Xuzhou Medical University, Suqian, China, [3] Treatment of Yingbing of State Administration of Traditional Chinese Medicine, Jiangsu Provincial Academy of Traditional Chinese Medicine, Nanjing, China

OPEN ACCESS

Edited by:
Lei Ye,
National Heart Centre Singapore, Singapore

Reviewed by:
Xiaocen Kong,
Nanjing Medical University, China
Wuquan Deng,
First Affiliated Hospital of Chongqing Medical University, China

***Correspondence:**
Chao Liu
profliuchao@163.com
Shuhang Xu
shuhangxu@163.com

Specialty section:
This article was submitted to Clinical Diabetes, a section of the journal Frontiers in Endocrinology

Received: *11 August 2021*
Accepted: *29 September 2021*
Published: *29 October 2021*

Citation:
Sun Y, Zou H, Li X, Xu S and Liu C (2021) Plasma Metabolomics Reveals Metabolic Profiling For Diabetic Retinopathy and Disease Progression. Front. Endocrinol. 12:757088. doi: 10.3389/fendo.2021.757088

Backgrounds: Diabetic retinopathy (DR), the main retinal vascular complication of DM, is the leading cause of visual impairment and blindness among working-age people worldwide. The aim of this study was to investigate the difference of plasma metabolic profiles in patients with DR to better understand the mechanism of this disease and disease progression.

Methods: We used ultrahigh-performance liquid Q-Exactive mass spectrometry and multivariate statistical analyses to conduct a comprehensive analysis of plasma metabolites in a population with DR and proliferative DR (PDR). A risk score based on the level of the selected metabolite was established and evaluated using the least absolute shrinkage and selection operator regularization logistic regression (LASSO-LR) based machine learning model.

Results: 22 differentially expressed metabolites which belonged to different metabolic pathway were identified and confirmed to be associated with the occurrence of DR. A risk score based on the level of the selected metabolite pseudouridine was established and evaluated to strongly associated with the occurrence of DR. Four circulating plasma metabolites (pseudouridine, glutamate, leucylleucine and N-acetyltryptophan) were identified to be differentially expressed between patients with PDR and other patients, and a risk score formula based on these plasma metabolites was developed and assessed to be significantly related to PDR.

Conclusions: Our work highlights the possible use of the risk score assessment based on the plasma metabolites not only reveal in the early diagnosis of DR and PDR but also assist in enhancing current therapeutic strategies in the clinic.

Keywords: diabetic retinopathy, plasma metabolomics, biomarkers, diabetes mellitus, machine learning

INTRODUCTION

In both developing and developed countries, the prevalence of diabetes mellitus (DM) is rising. By 2045, it is estimated that 629 million people worldwide will have DM (1). The proportion was reported to be less than 1% in the 1980s in China, while a series of large-scale and well-conducted population surveys have shown that the prevalence has risen sharply to 9-12% in the past few years, with more than one million persons affected (2, 3). Diabetic retinopathy (DR), the main retinal vascular complication of DM, is the leading cause of visual impairment and blindness among working-age people worldwide (4). In addition, the existence of DR also suggests an increased risk of life-threatening systemic vascular complications (5, 6). By 2010, worldwide, DM-related eye disease contributed to the fifth most common cause of moderate-to-severe vision loss and blindness, accounting for nearly four million cases of visual impairment and more than eight hundred thousand cases of blindness (7).

DR is a progressive and devastating disease, and much of the blindness associated with DR can be prevented with early diagnosis and therapy. DR is classified according to its severity as nonproliferative DR (NPDR) in the early stages and proliferative DR (PDR) in the later stages; while PDR is often associated with visual impairment, NPDR is often asymptomatic (8). Therefore, profiling and early detection of DR are specifically vital in preventing NPDR from progressing to PDR. One challenge associated with the use of common retinal imaging methods widely utilized to screen and diagnose DR is training primary healthcare workers to assess these retinal images (9). However, an exciting area of research is the diagnosis and assessment of the occurrence, development and prognosis of disease based on liquid biopsy and the identification of easily accessible biomarkers; notably, plasma/serum multiomics can disclose systemic changes associated with biological dysfunction (10, 11). Thus, the development of DR diagnosis and PDR monitoring biomarkers must be advanced from a modern perspective so that treatment efforts for DR can be enhanced in the clinic.

Metabolomics research has been applied to qualitatively and quantitatively analyze all low-molecular-weight metabolites in a sample, identify metabolites with significant differences and important biological significance between different groups, and further clarify the metabolic processes and pathophysiological changes in an organism during the disease process (12, 13). This type of research moves from the genome to providing a complete illustration of the phenotype (14). Metabolomics is a powerful technology that can be leveraged to study biomarkers of various diseases, including DM. Several recent studies have revealed that the development of DM is closely related to amino acid metabolism, including that of branched chain amino acids, aromatic amino acids, tyrosine and other aromatic amino-containing acids, glycine, glutamine and glutamic acid (15). Despite the biological function of DM becoming increasingly apparent, the role of metabolites in regulating microvascular complications of DM such as DR remains under investigation.

In our work, we investigated plasma metabolomic biomarker profiling of DR patients and disease progression. We used ultrahigh-performance liquid Q-Exactive mass spectrometry (UPLC-QE-MS) and multivariate statistical analyses to conduct a comprehensive analysis of plasma metabolites in a population with DR and PDR. A risk score based on the level of the selected metabolite pseudouridine was established and evaluated using the least absolute shrinkage and selection operator regularization logistic regression (LASSO-LR) based machine learning method, and this score was strongly associated with the occurrence of DR. Subsequently, four circulating plasma metabolites (pseudouridine, glutamate, leucylleucine and N-acetyltryptophan) were identified to be differentially expressed between patients with PDR and other patients, and a risk score formula based on these plasma metabolites was developed and assessed to be significantly related to the severity of DR.

METHODS

Chemicals and Reagents

HPLC-grade methanol was supplied by Tedia Company, Inc. (Fairfield, OH, USA). Formic acid (FA) was provided by Sigma-Aldrich Co., Ltd (St. Louis, MO, USA).

Plasma Sample Collection

This study was managed at the The Affiliated Suqian Hospital of Xuzhou Medical University between August 2019 and January 2021, and the ethics committee of The Affiliated Suqian Hospital of Xuzhou Medical University (2019–102–07) approved the study, which was conducted according to the ethical standards for human experimentation and the World Medical Association (WMA) Declaration of Helsinki. The cases were T2DM patients with DR, and the controls were T2DM patients without DR. T2DM was diagnosed according to standard criteria recommended by WHO since 1999. All participants received detailed ophthalmic examinations and were separately assessed based on digital retinal photographs, while different stages of DR was diagnosed with fundus fluorescence angiography method (16). The inclusion criteria were as follows (1): T2DM (2); ≥18 years old (3); following the same therapy programs consists of basal insulin (Insulin Degludec) and metformin. Participants with following situation would be excluded (1): any other eye diseases or history of eye surgery (2); acute or chronic inflammatory disease, cardiovascular diseases, malignancy, liver or renal dysfunction and any other severe chronic systemic disease (3); poor quality of fundus photographs, which were not clear for DR diagnosis. According to inclusion criteria and exclusion criteria, 42 patients with clinical and histopathology-confirmed DR, including 21 PDR and 21 NPDR patients, and 32 age- and sex-matched T2DM patients without DR, were recruited between August 2019 and January 2021 at the Hospital of The Affiliated Suqian Hospital of Xuzhou Medical University. According to diabetic nephropathy diagnostic criteria (17), 6.25% (2/32) in T2DM group, 19.0 (4/21) in DR group and 61.9% (13/21) in PDR group were assessed to diabetic nephropathy.

Sample Preparations for Metabolomics

Peripheral venous blood samples including 42 DR patients and 32 T2DM patients without DR, were drawn from the elbow vein in the fasting state in the morning and stored in ethylenediaminetetraacetic

acid vacuum tubes (BD Vacutainer, Franklin Lakes, NJ, USA) and then centrifuged at 1300 g for 10 min at 4°C. Plasma was immediately separated and stored at -80°C. Sample preparation for nontargeted metabolomics was performed according to the manufacturer's instructions. One hundred microliters of each sample were slowly lysed at 4°C, 400 μL of precooled methanol was added, vortexed for 60 s, and incubated at -80°C for 8 hours, and the protein was precipitated by centrifugation at 16,000 g for 10 min at 4°C. The supernatant was used for UHPLC analysis.

Metabolite Profile Analysis and Metabolite Identification

The samples were separated by UHPLC and then analyzed by a Thermo QE HF-X mass spectrometer carried out by Clinical Mass Company (Nanjing, China). Electrospray ionization (ESI) positive and negative ion modes were applied. The ESI source conditions after C18 chromatographic separation were as follows: sheath gas flow rate: 50; Aux gas flow rate: 13; sweep gas flow rate: 0; capillary temperature: 300°C; spray voltage: ± 3.5 kV; scan m/z range: 67-1000 Da; and product ion scan m/z range: 67-1000 Da. Secondary mass spectra were obtained using information-dependent acquisition (IDA) and high sensitivity mode, with an N collision energy of 15, 30, 45 eV. Aliquots of samples were mixed for the preparation of QC samples. QC samples were inserted in the sample cohort throughout the analysis to monitor and evaluate system stability. The MSdial program was used for peak extraction of the data, and the SIMCA program was used for principal component analysis (PCA) and orthogonal partial least-squares discriminant analysis (OPLS-DA). Then, metabolite structure identification was performed by exact mass number matching and secondary spectrum matching by searching public databases.

Correlation-Based Metabolic Network Analysis and Metabolic Pathway Analysis

The MS signal intensities confirmed that significantly changed metabolites were converted by log transformation and autoscaling and applied to calculate Pearson's correlation coefficient, followed by correlation-based metabolic networking analysis using Cytoscape 3.7. Variable metabolites were imported and analyzed using MetaboAnalyst software (http://www.metaboanalyst.ca) to perform pathway analysis to display the role of disturbed metabolic pathways.

Biochemical Measurements

All patients' medical histories were acquired, and age, sex, body mass index (BMI), and duration were obtained after a physical examination. Patients underwent blood and urine laboratory tests that included fasting plasma glucose (FPG), glycated hemoglobin | glycosylated hemoglobin (HbA1c), urine Albumin to creatinine (UACR), triglycerides, high-density lipoprotein cholesterol (HDL-c), low-density lipoprotein cholesterol (LDL-c) and total cholesterol (TC).

Statistical Analysis

Data are presented as the mean ± SD. Continuous data were analyzed with Student's t-test or the Mann-Whitney U test using SPSS 22.0 software (SPSS, Chicago, IL, USA). As the association of HbA1c level with severity of retinopathy has been investigated and assessed, Pearson correlation and partial correlation were used to analyze the relationships between plasma HbA1c level and risk score (GraphPad Prism). LASSO-LR based machine learning model was then performed to derive an DR or PDR diagnosis risk score. Receiver operating characteristic (ROC) analysis was utilized to estimate the sensitivity and specificity by the standard method. The general acceptance level of significance was $P < 0.05$.

RESULTS

Clinical Features of Subjects

In the present work, we explored the association between the plasma metabolite fingerprint and proliferative retinopathy in DM patients. Detailed demographic characteristics of the enrolled participants are shown in **Table 1**, FPG, HbA1c and UACR levels were markedly higher in DR patients ($P < 0.001$). In addition, no significant differences were found for BMI, or levels of triglycerides, HDL-c, LDL-c and TC between the DR and control groups ($P > 0.05$).

Metabolomics Workflow

The study workflow is shown in **Figure 1**. Plasma samples were collected from subjects and analyzed with the UHPLC-QE MS platform with both the electrospray ionization positive (ESI+) and negative (ESI-) modes. Raw data were normalized using Pareto scaling for subsequent data analysis after extraction of the background and alignment of the metabolic peaks. Different metabolic features and metabolites were extracted by combining the criteria of fold change (FC) >1.2 and $P<0.05$ and visualized with volcano plots and heat maps. Thirty significantly different metabolites were screened by the threshold of variable important in projection (VIP) value >1 and P value <0.05, of which correlation analysis and pathway analysis were performed.

TABLE 1 | Detailed demographics of the enrolled patient.

Detailed demographics of the enrolled patients		
	DR	**NDR**
n	42	32
Gender (male/female)	18/24	15/17
Age (years)	52 (45–62)	50 (45–61)
Dibabets duration (years)	13 (11.4-19)	12.5 (10.5-18.5)
BMI (kg/m2)	26.8 (23.8-29.4)	25.4 (22.3-28.9)
triglycerides (mmol/L)	1.3 (0.78-1.9)	1.7 (0.86-2.3)
HDL-c (mmol/L)	0.89 (0.59-1.23)	0.92 (0.63-1.29)
LDL-c (mmol/L)	2.96 (2.03-3.61)	2.78 (2.13-3.53)
TC (mmol/L)	4.86 (3.62-5.52)	4.72 (3.30-5.38)
FPG (mmol/L)	10.05 (8.97-11.31)	8.11 (6.71-8.93)
UACR (mg/g)	37.4 (6–213)	17.3 (4.1-45.2)
HbA1c (1%)	9.47 (8.78-10.69)	8.03 (7.58-8.63)

DR, Diabetic retinopathy; BMI, body mass index; FPG, fasting plasma glucose; HbA1c, glycated hemoglobin glycosylated hemoglobin; HDL-c, high-density lipoprotein cholesterol; LDL-c, low-density lipoprotein cholesterol; TC, total cholesterol; UACR, urine albumin to creatinine.

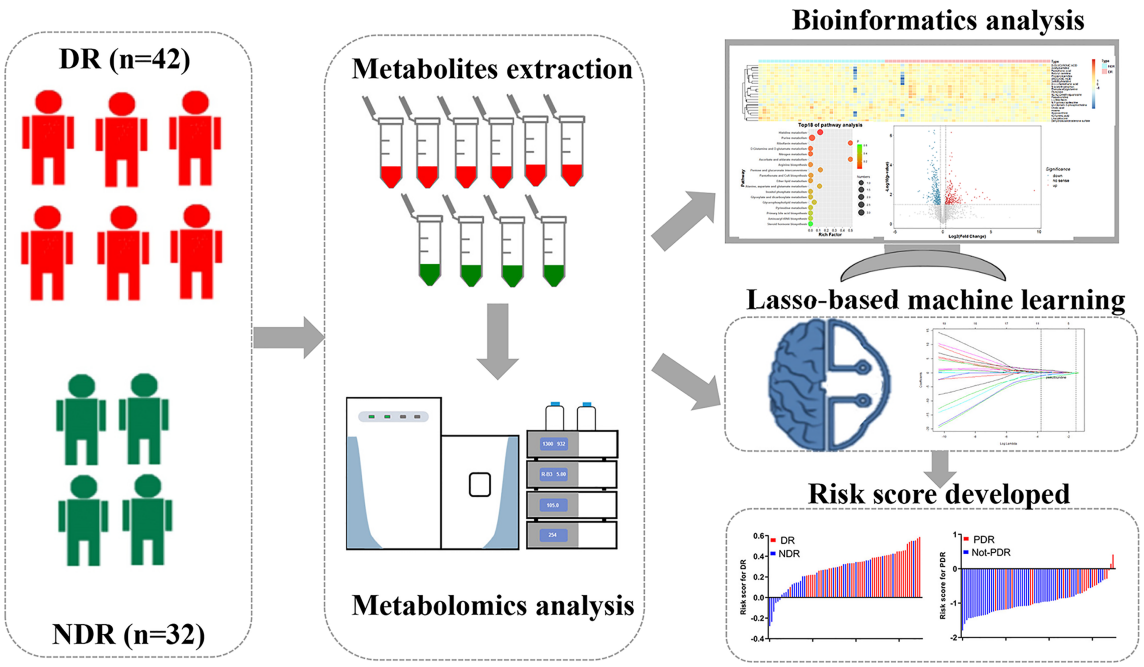

FIGURE 1 | Workflow of metabolomics for metabolomic profiling and data interpretation of plasma samples from DR and NDR.

The LASSO-LR was utilized to select diagnostic markers to predict DR and PDR among the subjects *via* penalized maximum likelihood. Evaluation of the risk score formula was performed using ROC analysis, and the relationship between the risk score and HbA1c level was investigated.

Metabolic Profiling of DR

We first compared the metabolic signatures between DR and control T2DM patients in both ESI+ and ESI− modes of untargeted metabolomics. In total, more than 50,000 metabolic features were consistently found in all plasma samples from the discovery cohort, including 25742 features in ESI+ mode and 31374 features in ESI- mode. QC samples were tightly clustered in principal component analysis (PCA), validating the stability and reproducibility of the instrumental analysis (**Figures 2A, B**). The OPLS-DA score plot displays a clear demarcation between the DR group and the control group in ESI+ mode with R^2Y = 0.939 and in ESI- mode with R^2Y = 0.991, suggesting significant changes in plasma metabolites in the DR group (**Figures 2C, D**).

Identification of Differential Metabolites

To reveal the plasma metabolic characteristics in DR patients and identify and confirm high-confidence metabolites that contribute to DR, we distinguished the differences by ESI+ and ESI- based on the criteria of FC>1.2 and P<0.05, respectively. In addition, a VIP value greater than 1.0, which was calculated by OPLS-DA scoring, was selected as a significantly different metabolic feature for analysis. Thus, metabolic characteristics with significant differences were extracted and visualized by volcano plots (**Figures 3A, B**). According to a public metabolite library, 22 metabolites were identified and confirmed after inputting the refined significant metabolic features, containing 13 and 5 metabolites from the ESI+ and ESI- models, respectively, and 4 metabolites with dual mode. They were classified into 13 subcategories according to the chemical taxonomy in the Human Metabolome Database (HMDB) with the largest proportion of the significantly different metabolites which was classified as amino acid (7/22) (**Table 2**). Hierarchical clustering analysis also revealed differentially expressed metabolites between DR and NDR (**Figure 3C**).

Metabolite Correlation Analysis and Pathway Enrichment Analysis

To further investigate the interrelationships between the significantly different metabolites, we utilized the Metscape plugin (http://metscape.ncibi.org/) in Cytoscape (https://cytoscape.org/), a tool available for interactive exploration and visualization of metabolic networks in metabolite changes, and constructed the metabolic network (**Figure 3D**). We identified 45 pairs of correlations with correlation coefficients ≥0.4 or ≤-0.4 among the 22 significantly different metabolites. KEGG pathway enrichment analysis was performed for 22 dysregulated metabolites involving 18 metabolic pathways. Based on the enrichment factor and P-value, histidine metabolism, purine metabolism, riboflavin metabolism, d-glutamine metabolism and nitrogen metabolism were the five most significantly enriched metabolic pathways (**Figure 3E**).

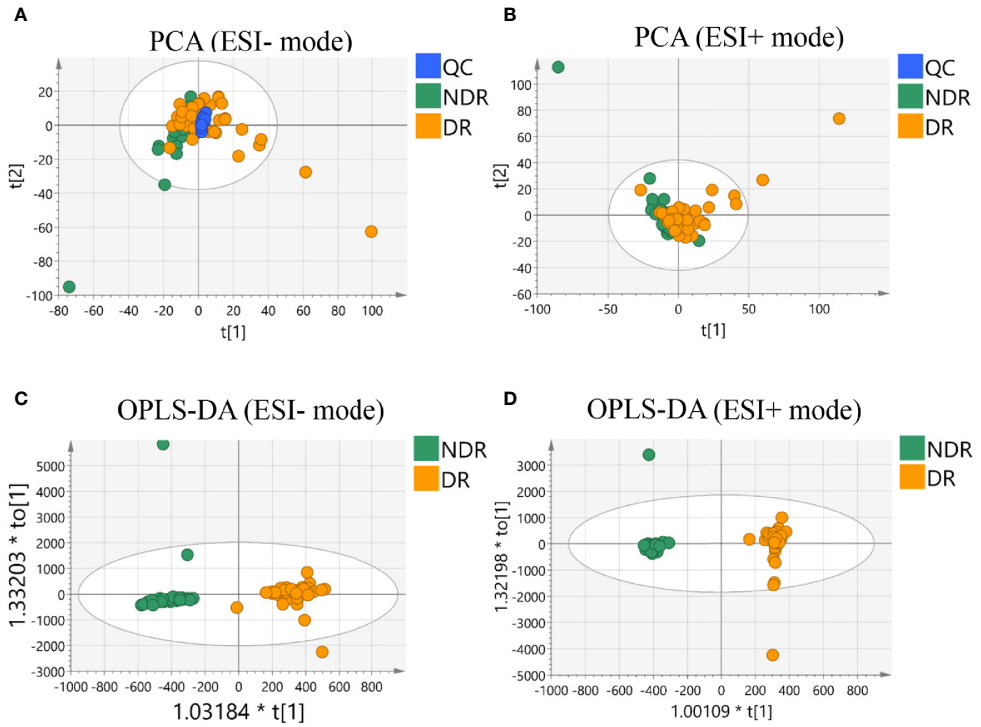

FIGURE 2 | Multivariate statistical analysis results. PCA score plot of the analysis in ESI (–) mode **(A)** and ESI (+) mode **(B)**. OPLS-DA score plot of the analysis in ESI (–) mode **(C)** and ESI (+) mode **(D)**.

Development and Evaluation of a Diagnostic Panel for DR

To further elucidate the metabolite signature for DR, a LASSO-LR model was utilized to select diagnostic metabolites to predict DR among the subjects *via* penalized maximum likelihood, which gives the most normalized model for the application of one or ten markers (**Figure 3A**). The normalization path was calculated for the LASSO-LR model at a grid of values for the normalization parameter lambda, which identified one (pseudouridine) or ten differentially expressed metabolites (**Figure 4A**). The OPLS-DA score plot displays a clear demarcation between the DR group and the control group at the level of pseudouridine with R2Y = 0.867 (**Figure 4B**). According to the levels of the selected metabolites, the following formula was derived to calculate the DR risk score for each patient: risk score (DR) = -0.23× Ln (pseudouridine) + 1.88. Based on the study of the relationship between the risk score distribution and DR status, the results showed that the rate of DR in the low-risk score party was primarily lower than that in the high-risk score party (**Figure 4C**). In addition, the risk scores for the DR group were predominantly higher than those for the NDR group (**Figure 4D**). The sensitivity and specificity of the risk score for DR were 97.6% and 53.1%, respectively, with an AUC of 0.80 (95% CI = 0.70 to 0.90) (**Figure 4E**). Then, it was also shown that the risk score was positively correlated with the level of HbA1c according to a linear correlation analysis (R = 0.603, P < 0.001) (**Figure 4F**).

Plasma Metabolomics Approach to Monitor the Progression of DR

According to the International Clinical DR and Diabetic Macular Edema Disease Severity Scale, 21 PDR patients and 53 non-PDR patients, including 32 control cases and 21 NPDR patients, were distinguished. Then, the same procedure of LASSO-LR analysis was performed to select metabolites to monitor PDR. The normalization path was calculated for the LASSO-LR model at a grid of values for the normalization parameter lambda, which identified four (pseudouridine, glutamate, leucylleucine and N-acetyltryptophan) differentially expressed metabolites (**Figure 5A**). As shown in **Figure 5B**, the plasma concentrations of pseudouridine, N-acetyltryptophan and glutamate were predominantly upregulated, whereas that of leucylleucine was found to be downregulated in PDR patients. According to the levels of the four selected metabolites, the following formula was derived to calculate the PDR risk score for each patient: risk score = 0.23 × Ln(pseudouridine) + 0.16 × Ln(N-acetyltryptophan) - 0.065 × Ln(leucylleucine) + 0.11 × Ln(glutamate) -3.63. Based on the relationship between the risk score distribution and DR status, the results showed that the rate of PDR cases in the low-risk score party was primarily lower than that in the high-risk score party (**Figure 5C**). Statistical analysis showed that the risk scores of the PDR group were significantly higher than those of the non-PDR group (**Figure 5D**). The sensitivity and specificity of the risk score for DR were 76.2% and 77.4%, respectively, with an AUC of 0.82 (95% CI = 0.71 to 0.90) (**Figure 5E**). Ultimately, it was also shown

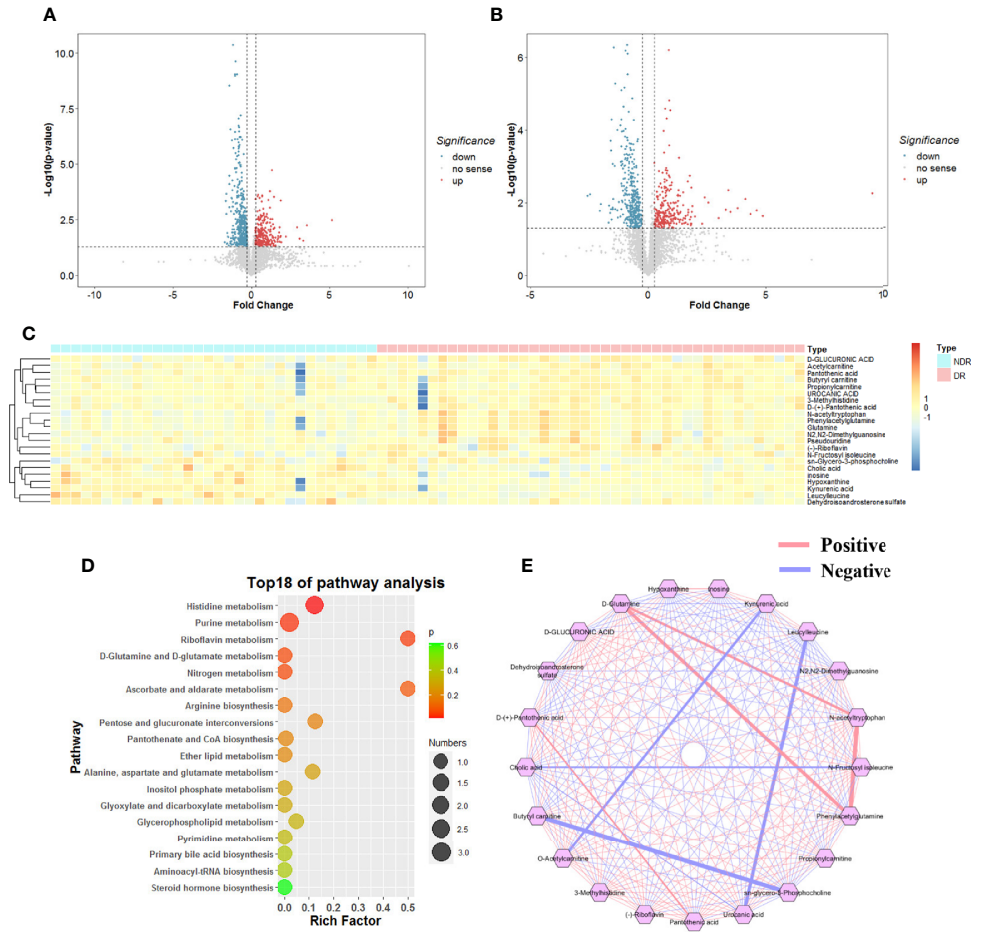

FIGURE 3 | Representative Volcano plot (fold change >1.2 and p-value < 0.05) in ESI (+) mode **(A)** and ESI (+) mode **(B)** metabolomics data. **(C)** Representative heatmap of significant different metabolites (fold change >1.2, VIP>1 and p-value < 0.05). **(D)** Correlation-based metabolic network analysis. **(E)** Metabolic pathway analysis.

that the risk score was positively correlated with the level of HbA1c according to a linear correlation analysis (R = 0.36, P < 0.01) (**Figure 5F**).

DISCUSSION

DR, the main retinal vascular complication of DM, is the leading cause of visual impairment and blindness among working-age people worldwide. Therefore, early and accurate identification of DR and disease progression among T2DM patients is essential for clinicians when evaluating the disease status of patients and formulating suitable therapy efforts such as anti-vascular endothelial growth-factor agents, intraocular injection of steroids or timely laser therapy for preservation of sight in DR patients. In our work, we demonstrated that the levels of circulating plasma metabolites were significantly differentially expressed between the DR and NDR groups. A risk score based on the level of pseudouridine was established and evaluated using the LASSO-LR model, which was strongly associated with the occurrence of DR. Subsequently, four circulating plasma metabolites, including pseudouridine, glutamate, leucylleucine and N-acetyltryptophan, were identified to be differentially expressed between PDR and not-PDR, and a risk score formula based on these four plasma metabolites was developed in the same way and assessed to be significantly related to the severity of DR. Our work highlights the possible use of plasma metabolites in the early diagnosis of DR and PDR in the clinic.

A panel of differentially expressed plasma metabolites was first identified after comparing DR and NDR subjects and was found to be significantly enriched in histidine metabolism, purine metabolism, riboflavin metabolism, d-glutamine/d-glutamate metabolism and others. Histidine, an essential amino acid (EAA) in mammals, is derived from growth and amino acid composition in tissues. An increasing number of studies have revealed the effect of histidine catabolism on carnosine synthesis, which contributes to strong antioxidant effects (18) and the efficiency of chemotherapy agents (19), preventing cataracts

TABLE 2 | Differential metabolites identified from metabolomics profiling.

Metabolite name	Mode	VIP	FC	P Value	Subclass
Pantothenic acid	POS	1.53	1.553	0.0057	vitamin
(–)-Riboflavin	POS	2.05	2.819	0.0076	vitamin
D-(+)-Pantothenic acid	NEG	1.16	1.357	0.0310	vitamin
Pseudouridine	NEG	1.63	1.720	0.0047	uridine
D-GLUCURONIC ACID	NEG	1.30	1.316	0.0455	sugars
Dehydroisoandrosterone sulfate	NEG	1.19	0.598	0.0456	steroids
Hypoxanthine	NEG/POS	2.60	0.360	0.0079	purine derivatives
N2,N2-Dimethylguanosine	POS	1.11	1.439	0.0331	nucleoside
sn-Glycero-3-phosphocholine	POS	1.01	0.705	0.0301	lipid
Propionylcarnitine	POS	1.05	1.276	0.0267	lipid
Acetylcarnitine	POS	1.38	1.584	0.0088	enzyme
Inosine	NEG/POS	2.18	0.315	0.0363	creatinine
Cholic acid	NEG/POS	2.53	0.244	0.0172	cholic acid
Butyryl carnitine	POS	1.48	1.561	0.0024	carnitine
UROCANIC ACID	POS	1.33	1.373	0.0002	azole
N-Fructosyl isoleucine	POS	1.09	1.496	0.0474	amino acid
N-acetyltryptophan	POS	1.95	3.762	0.0341	amino acid
Leucylleucine	POS	3.24	0.329	0.0002	amino acid
Kynurenic acid	POS	1.90	0.541	0.0000	amino acid
3-Methylhistidine	POS	1.86	2.264	0.0010	amino acid
Phenylacetylglutamine	NEG/POS	2.10	3.262	0.0188	amino acid
Glutamine	NEG	1.98	2.560	0.0196	amino acid

POS, Positive; NEG, Negative; FC, Fold change; VIP, Variable important in projection.

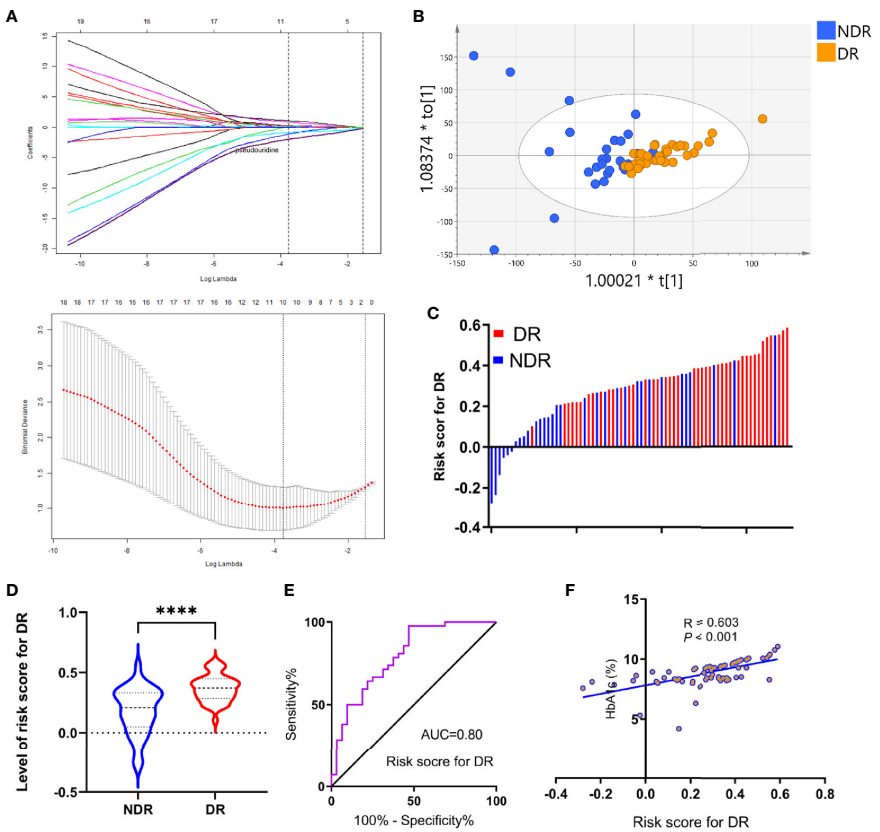

FIGURE 4 | Development of risk score for DR using the least absolute shrinkage and selection operator regularization (LASSO-LR) model. **(A)** Dotted vertical lines were drawn at the optimal values with Lambda (log), by using the minimum criteria and the 1 standard error of the minimum criteria (the 1-SE criteria). **(B)** OPLS-DA score plot of the analysis using selected metabolite. **(C)** Distribution of the risk score in the group. **(D)** Statistical analysis for distribution of risk score between DR and NDR (****p<0.0001). **(E)** ROC curves were created to evaluate the power of risk score. **(F)** A linear correlation analysis between risk score and HbA1c levels.

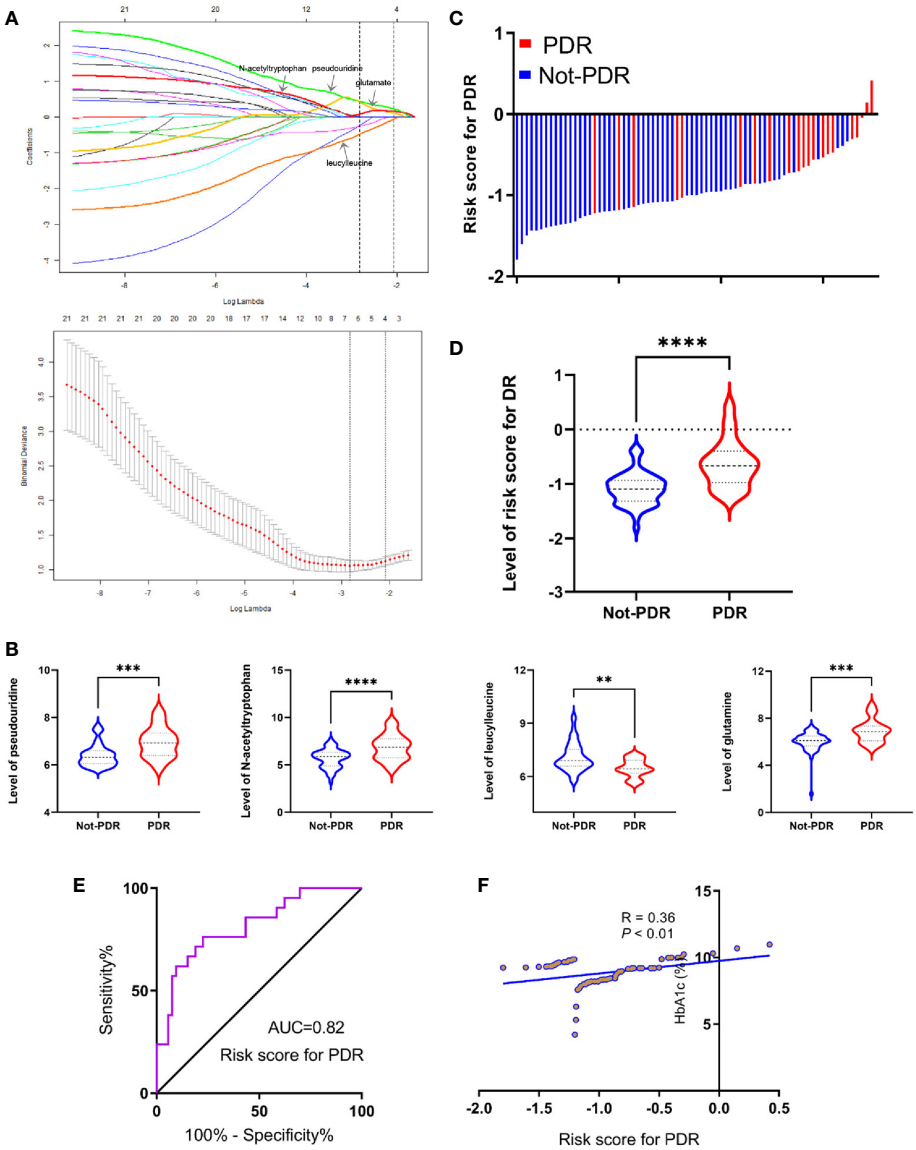

FIGURE 5 | Development of risk score for PDR using the least absolute shrinkage and selection operator regularization (LASSO-LR) model. **(A)** Dotted vertical lines were drawn at the optimal values with Lambda (log), by using the minimum criteria and the 1 standard error of the minimum criteria (the 1-SE criteria). **(B)** Statistical analysis of pseudouridine, glutamate, leucylleucine and N-acetyltryptophan between PDR and not-PDR group (**p < 0.01; ***p < 0.001; ****p < 0.0001). **(C)** Distribution of the risk score in the group. **(D)** Statistical analysis for distribution of risk score between PDR and not-PDR group (****p < 0.0001). **(E)** ROC curves were created to evaluate the power of risk score. **(F)** A linear correlation analysis between risk score and HbA1c levels.

(20). The major pathway of histidine catabolism could proceed in four steps to yield glutamate, with many functions, including the development of DM (21). Our data are in accordance with previous studies showing that purine metabolism plays a role in the development of DR (22). Purines, the basic composition of nucleotides in the process of cell proliferation, are associated with various molecular functions, such as cell cycle regulation, signal transduction and immune function. Uric acid, the final product of purine metabolism, is an independent predictor of cardiac allograft vasculopathy after heart transplantation (23). Additionally, uric acid has been reported to be a risk factor related to extremity vasculopathy in T2DM (24). Riboflavin, a water-soluble vitamin, is an essential nutrient in higher organisms and is involved in oxidation-reduction reactions in many metabolic pathways and in energy production in the respiratory chain that occurs in the mitochondria. Impairment of flavin homeostasis may lead to multisystem dysfunction, including neuromuscular disorders and cardiovascular disease (25). Moreover, diabetic patients have been reported to suffer from riboflavin deficiency, and flavin imbalance plays a vital role in the

appearance of DR (26). The above evidence indicates that metabolic pathways may contribute to the process of DR.

Our results also showed that the pseudouridine gradient increased in DR and PDR subjects. From screening and fitting results based on LASSO-LR analysis, variable selection and regularization were performed when fitting a generalized linear curve. The variable profiling here mentions not setting all the variables into the model for fitting but to selectively set the variables into the model to obtain better performance parameters to avoid overfitting (27). Through LASSO-LR based machine learning methods, the optimal number of metabolites can be screened from a large number of variables, and equations based on these metabolites can be established. To our knowledge, there has been no metabolomics research on the impact of pseudouridine in patients who have undergone DR and disease progression. It has generally been acknowledged that pseudouridine, a fundamental metabolite, is a c-glycosyl pyrimidine that consists of uracil having a beta-D-ribofuranosyl residue attached at position 5. Pseudouridine is also associated with RNA modification (28), owing to the relative abundance and inertness of the isomer compared with other mNS in cells, and comprises approximately 5% of all cellular RNA nucleotides (29). The unique structural properties of pseudouridine contribute to the folding of tRNAs and rRNA, and recent research suggests that pseudouridylation influences the coding potential of mRNA. Recently, pseudouridine has been identified and observed in the plasma, urine or tissue of cancer patients with multiple malignancies, including prostate cancer (30), hepatocellular carcinoma lymphoma (31), colorectal cancer (32) and chronic kidney disease (33). Pseudouridine has also been shown to be a novel diagnostic metabolic marker of heart failure, which is similar to the observation of the Alexander D team, who found that pseudouridine was elevated in dilated cardiomyopathy patients (34). Besides, the relationship of pseudouridine and the risk of diabetes had been disclosed. Pseudouridine inhibits glucose utilization at the postreceptor level through lowering the intracellular Ca concentration to affect the progression of T2DM (35), and plasma pseudouridine predict both the risk and prevalence (36) and insulin resistance of T2DM (37). Moreover, plasma pseudouridine has been shown to be correlated with declining renal function and albuminuria in diabetic kidney disease (38, 39), suggesting a close relationship between the level of plasma pseudouridine and diabetic microangiopathy.

Glutamate, another metabolite that was shown to be associated with DR and PDR in our work, is the most abundant and versatile amino acid in the body. Under normal conditions, glutamate is the principal excitatory neurotransmitter in the brain and is involved in learning and memory (40). In addition, glutamate may play a role in acute brain damage after traumatic brain injury, cerebral ischemia and status epilepticus (41, 42), immune system (43), the endocrine system (44), kidney and coronary artery disease (45) and others. The roles of plasma glutamine acid in DR and disease progression have not yet been illustrated. However, some evidence has revealed their effect on the development of DM and DM-related complications. Glutamate is significantly associated with the risk of developing T2DM (45, 46). In addition, other studies have suggested that DM is accompanied by an accumulation of glutamate in the retina, which causes neurotoxicity and the development of DR (47, 48), while glutamine is regarded as the most individual metabolite for the presence of DR (49).

There were a few limitations in our study, one of which is its small sample size with only 78 plasma samples applicable for metabolomic analysis, which is unfavorable for investigating the robustness of the model. Therefore, the sensitivity and specificity of the diagnostic model should be assessed with an expanded number of patients as well as in a prospective cohort. In addition, the absolute concentration of candidate metabolites was not quantified and validated in our study, making them difficult to apply in the clinic.

In brief, liquid biopsy metabolomics could be applied to discriminate metabolic subphenotypes of DR and disease progression, with the identification and validation of specific circulating discriminant metabolites. Based on the aforementioned results, we were able to develop a risk score according to the level of metabolites for DR and PDR. Further investigations are required to quantitatively detect candidate metabolites in an expanded cohort. Nevertheless, our work demonstrated that this risk score based on molecular signatures should enable the monitoring of the appearance of disease and disease progression at an early stage.

DATA AVAILABILITY STATEMENT

The original contributions presented in the study are included in the article/supplementary material. Further inquiries can be directed to the corresponding authors.

ETHICS STATEMENT

Written informed consent was obtained from the individual(s) for the publication of any potentially identifiable images or data included in this article.

AUTHOR CONTRIBUTIONS

CL and SX conceived of and designed the experiments. YS, HZ, and XL performed the experiments. YS and HZ analyzed the data and YS wrote the manuscript. All authors contributed to the article and approved the submitted version.

ACKNOWLEDGMENTS

Suqian Key Research and Development Program (No. S201807) is gratefully acknowledged. The authors would also like to thank American Journal Experts for proofreading the article.

REFERENCES

1. Ogurtsova K, da Rocha Fernandes JD, Huang Y, Linnenkamp U, Guariguata L, Cho NH, et al. IDF Diabetes Atlas: Global Estimates for the Prevalence of Diabetes for 2015 and 2040. *Diabetes Res Clin Pract* (2017) 128:40–50. doi: 10.1016/j.diabres.2017.03.024
2. Wang L, Gao P, Zhang M, Huang Z, Zhang D, Deng Q, et al. Prevalence and Ethnic Pattern of Diabetes and Prediabetes in China in 2013. *JAMA* (2017) 317:2515–23. doi: 10.1001/jama.2017.7596
3. Xu Y, Wang L, He J, Bi Y, Li M, Wang T, et al. Prevalence and Control of Diabetes in Chinese Adults. *JAMA* (2013) 310:948–59. doi: 10.1001/jama.2013.168118
4. Song P, Yu J, Chan KY, Theodoratou E, Rudan I. Prevalence, Risk Factors and Burden of Diabetic Retinopathy in China: A Systematic Review and Meta-Analysis. *J Glob Health* (2018) 8:010803. doi: 10.7189/jogh.08.010803
5. Sabanayagam C, Banu R, Chee ML, Lee R, Wang YX, Tan G, et al. Incidence and Progression of Diabetic Retinopathy: A Systematic Review. *Lancet Diabetes Endocrinol* (2019) 7:140–9. doi: 10.1016/S2213-8587(18)30128-1
6. Xu XH, Sun B, Zhong S, Wei DD, Hong Z, Dong AQ. Diabetic Retinopathy Predicts Cardiovascular Mortality in Diabetes: A Meta-Analysis. *BMC Cardiovasc Disord* (2020) 20:478. doi: 10.1186/s12872-020-01763-z
7. Leasher JL, Bourne RR, Flaxman SR, Jonas JB, Keeffe J, Naidoo K, et al. Global Estimates on the Number of People Blind or Visually Impaired by Diabetic Retinopathy: A Meta-Analysis From 1990 to 2010. *Diabetes Care* (2016) 39:1643–9. doi: 10.2337/dc15-2171
8. Wong TY, Cheung CM, Larsen M, Sharma S, Simo R. Diabetic Retinopathy. *Nat Rev Dis Primers* (2016) 2:16012. doi: 10.1038/nrdp.2016.12
9. Wang LZ, Cheung CY, Tapp RJ, Hamzah H, Tan G, Ting D, et al. Availability and Variability in Guidelines on Diabetic Retinopathy Screening in Asian Countries. *Br J Ophthalmol* (2017) 101:1352–60. doi: 10.1136/bjophthalmol-2016-310002
10. Mader S, Pantel K. Liquid Biopsy: Current Status and Future Perspectives. *Oncol Res Treat* (2017) 40:404–8. doi: 10.1159/000478018
11. Drabovich AP, Saraon P, Drabovich M, Karakosta TD, Dimitromanolakis A, Hyndman ME, et al. Multi-Omics Biomarker Pipeline Reveals Elevated Levels of Protein-Glutamine Gamma-Glutamyltransferase 4 in Seminal Plasma of Prostate Cancer Patients. *Mol Cell Proteomics* (2019) 18:1807–23. doi: 10.1074/mcp.RA119.001612
12. Bujak R, Struck-Lewicka W, Markuszewski MJ, Kaliszan R. Metabolomics for Laboratory Diagnostics. *J Pharm BioMed Anal* (2015) 113:108–20. doi: 10.1016/j.jpba.2014.12.017
13. Wishart DS. Metabolomics for Investigating Physiological and Pathophysiological Processes. *Physiol Rev* (2019) 99:1819–75. doi: 10.1152/physrev.00035.2018
14. Evangelatos N, Bauer P, Reumann M, Satyamoorthy K, Lehrach H, Brand A. Metabolomics in Sepsis and Its Impact on Public Health. *Public Health Genomics* (2017) 20:274–85. doi: 10.1159/000486362
15. Chen T, Ni Y, Ma X, Bao Y, Liu J, Huang F, et al. Branched-Chain and Aromatic Amino Acid Profiles and Diabetes Risk in Chinese Populations. *Sci Rep* (2016) 6:20594. doi: 10.1038/srep20594
16. American Diabetes A. 2. Classification and Diagnosis of Diabetes: Standards of Medical Care in Diabetes-2021. *Diabetes Care* (2021) 44:S15–33. doi: 10.2337/dc21-S002
17. American Diabetes A. 11. Microvascular Complications and Foot Care: Standards of Medical Care in Diabetes-2021. *Diabetes Care* (2021) 44:S151–67. doi: 10.2337/dc21-S011
18. Taylor RG, Levy HL, McInnes RR. Histidase and Histidinemia. Clinical and Molecular Considerations. *Mol Biol Med* (1991) 8:101–16.
19. Kanarek N, Keys HR, Cantor JR, Lewis CA, Chan SH, Kunchok T, et al. Histidine Catabolism is a Major Determinant of Methotrexate Sensitivity. *Nature* (2018) 559:632–6. doi: 10.1038/s41586-018-0316-7
20. Remo SC, Hevroy EM, Olsvik PA, Fontanillas R, Breck O, Waagbo R. Dietary Histidine Requirement to Reduce the Risk and Severity of Cataracts is Higher Than the Requirement for Growth in Atlantic Salmon Smolts, Independently of the Dietary Lipid Source. *Br J Nutr* (2014) 111:1759–72. doi: 10.1017/S0007114513004418
21. Brosnan ME, Brosnan JT. Histidine Metabolism and Function. *J Nutr* (2020) 150:2570S–5S. doi: 10.1093/jn/nxaa079
22. Zhu XR, Yang FY, Lu J, Zhang HR, Sun R, Zhou JB, et al. Plasma Metabolomic Profiling of Proliferative Diabetic Retinopathy. *Nutr Metab (Lond)* (2019) 16:37. doi: 10.1186/s12986-019-0358-3
23. Asleh R, Prasad M, Briasoulis A, Nardi V, Adigun R, Edwards BS, et al. Uric Acid is an Independent Predictor of Cardiac Allograft Vasculopathy After Heart Transplantation. *J Heart Lung Transplant* (2018) 37:1083–92. doi: 10.1016/j.healun.2018.04.017
24. Xu J, Wang G, Fu D, Su N, Wang L, Gao F, et al. High-Resolution Color Doppler Ultrasound Examination and Related Risk Factor Analysis of Lower Extremity Vasculopathy in Type 2 Diabetes Patients. *Genet Mol Res* (2015) 14:3939–47. doi: 10.4238/2015.April.27.8
25. Balasubramaniam S, Christodoulou J, Rahman S. Disorders of Riboflavin Metabolism. *J Inherit Metab Dis* (2019) 42:608–19. doi: 10.1002/jimd.12058
26. Sinha T, Al-Ubaidi MR, Naash MI. Flavin Imbalance as an Important Player in Diabetic Retinopathy. *Adv Exp Med Biol* (2019) 1185:575–9. doi: 10.1007/978-3-030-27378-1_94
27. Merdan S, Subramanian K, Ayer T, Van Weyenbergh J, Chang A, Koff JL, et al. Gene Expression Profiling-Based Risk Prediction and Profiles of Immune Infiltration in Diffuse Large B-Cell Lymphoma. *Blood Cancer J* (2021) 11:2. doi: 10.1038/s41408-020-00404-0
28. Helm M. Post-Transcriptional Nucleotide Modification and Alternative Folding of RNA. *Nucleic Acids Res* (2006) 34:721–33. doi: 10.1093/nar/gkj471
29. Kihara H. Pseudouridinuria in Mentally Defective Siblings. *Am J Ment Defic* (1967) 71:593–6.
30. Stockert JA, Weil R, Yadav KK, Kyprianou N, Tewari AK. Pseudouridine as a Novel Biomarker in Prostate Cancer. *Urol Oncol* (2021) 39:63–71. doi: 10.1016/j.urolonc.2020.06.026
31. Amuro Y, Nakaoka H, Shimomura S, Fujikura M, Yamamoto T, Tamura S, et al. Serum Pseudouridine as a Biochemical Marker in Patients With Hepatocellular Carcinoma. *Clin Chim Acta* (1988) 178:151–8. doi: 10.1016/0009-8981(88)90221-5
32. Feng B, Zheng MH, Zheng YF, Lu AG, Li JW, Wang ML, et al. Normal and Modified Urinary Nucleosides Represent Novel Biomarkers for Colorectal Cancer Diagnosis and Surgery Monitoring. *J Gastroenterol Hepatol* (2005) 20:1913–9. doi: 10.1111/j.1440-1746.2005.03888.x
33. Sekula P, Dettmer K, Vogl FC, Gronwald W, Ellmann L, Mohney RP, et al. From Discovery to Translation: Characterization of C-Mannosyltryptophan and Pseudouridine as Markers of Kidney Function. *Sci Rep* (2017) 7:17400. doi: 10.1038/s41598-017-17107-5
34. Alexander D, Lombardi R, Rodriguez G, Mitchell MM, Marian AJ. Metabolomic Distinction and Insights Into the Pathogenesis of Human Primary Dilated Cardiomyopathy. *Eur J Clin Invest* (2011) 41:527–38. doi: 10.1111/j.1365-2362.2010.02441.x
35. Eldin WS, Ragheb A, Klassen J, Shoker A. Evidence for Increased Risk of Prediabetes in the Uremic Patient. *Nephron Clin Pract* (2008) 108:c47–55. doi: 10.1159/000112529
36. Yu D, Moore SC, Matthews CE, Xiang YB, Zhang X, Gao YT, et al. Plasma Metabolomic Profiles in Association With Type 2 Diabetes Risk and Prevalence in Chinese Adults. *Metabolomics* (2016) 12:3. doi: 10.1007/s11306-015-0890-8
37. Papandreou C, Bullo M, Ruiz-Canela M, Dennis C, Deik A, Wang D, et al. Plasma Metabolites Predict Both Insulin Resistance and Incident Type 2 Diabetes: A Metabolomics Approach Within the Prevencion Con Dieta Mediterranea (PREDIMED) Study. *Am J Clin Nutr* (2019) 109:626–34. doi: 10.1093/ajcn/nqy262
38. Niewczas MA, Sirich TL, Mathew AV, Skupien J, Mohney RP, Warram JH, et al. Uremic Solutes and Risk of End-Stage Renal Disease in Type 2 Diabetes: Metabolomic Study. *Kidney Int* (2014) 85:1214–24. doi: 10.1038/ki.2013.497
39. Solini A, Manca ML, Penno G, Pugliese G, Cobb JE, Ferrannini E. Prediction of Declining Renal Function and Albuminuria in Patients With Type 2 Diabetes by Metabolomics. *J Clin Endocrinol Metab* (2016) 101:696–704. doi: 10.1210/jc.2015-3345
40. Zhou Y, Danbolt NC. Glutamate as a Neurotransmitter in the Healthy Brain. *J Neural Transm (Vienna)* (2014) 121:799–817. doi: 10.1007/s00702-014-1180-8
41. Meldrum BS. Glutamate as a Neurotransmitter in the Brain: Review of Physiology and Pathology. *J Nutr* (2000) 130:1007S–15S. doi: 10.1093/jn/130.4.1007S
42. Iovino L, Tremblay ME, Civiero L. Glutamate-Induced Excitotoxicity in Parkinson's Disease: The Role of Glial Cells. *J Pharmacol Sci* (2020) 144:151–64. doi: 10.1016/j.jphs.2020.07.011

43. Marazziti D, Albert U, Mucci F, Piccinni A. The Glutamate and the Immune Systems: New Targets for the Pharmacological Treatment of OCD. *Curr Med Chem* (2018) 25:5731–8. doi: 10.2174/0929867324666171108152035
44. Maechler P. Glutamate Pathways of the Beta-Cell and the Control of Insulin Secretion. *Diabetes Res Clin Pract* (2017) 131:149–53. doi: 10.1016/j.diabres.2017.07.009
45. Ottosson F, Smith E, Melander O, Fernandez C. Altered Asparagine and Glutamate Homeostasis Precede Coronary Artery Disease and Type 2 Diabetes. *J Clin Endocrinol Metab* (2018) 103:3060–9. doi: 10.1210/jc.2018-00546
46. Sriboonvorakul N, Pan-Ngum W, Poovorawan K, Winterberg M, Tarning J, Muangnoicharoen S. Assessment of the Amino Acid Profile in Thai Patients With Type 2 Diabetes Mellitus Using Liquid Chromatography-Mass Spectrometry. *Int Health* (2020) 13:367–73. doi: 10.1093/inthealth/ihaa083
47. Kowluru RA, Engerman RL, Case GL, Kern TS. Retinal Glutamate in Diabetes and Effect of Antioxidants. *Neurochem Int* (2001) 38:385–90. doi: 10.1016/S0197-0186(00)00112-1
48. Li Q, Puro DG. Diabetes-Induced Dysfunction of the Glutamate Transporter in Retinal Muller Cells. *Invest Ophthalmol Vis Sci* (2002) 43:3109–16.
49. Rhee SY, Jung ES, Park HM, Jeong SJ, Kim K, Chon S, et al. Plasma Glutamine and Glutamic Acid are Potential Biomarkers for Predicting Diabetic Retinopathy. *Metabolomics* (2018) 14:89. doi: 10.1007/s11306-018-1383-3

Conflict of Interest: The authors declare that the research was conducted in the absence of any commercial or financial relationships that could be construed as a potential conflict of interest.

Publisher's Note: All claims expressed in this article are solely those of the authors and do not necessarily represent those of their affiliated organizations, or those of the publisher, the editors and the reviewers. Any product that may be evaluated in this article, or claim that may be made by its manufacturer, is not guaranteed or endorsed by the publisher.

frontiers in Endocrinology

SYSTEMATIC REVIEW
published: 14 March 2022
doi: 10.3389/fendo.2022.799337

Effect of Chinese Patent Medicines on Ocular Fundus Signs and Vision in Calcium Dobesilate-Treated Persons With Non-Proliferative Diabetic Retinopathy: A Systematic Review and Meta-Analysis

Yuehong Zhang[1†], Xuedong An[1†], Liyun Duan[1†], De Jin[1], Yingying Duan[2], Rongrong Zhou[1], Yuqing Zhang[1], Xiaomin Kang[2] and Fengmei Lian[1]*

[1] Department of Endocrinology, Guang'anmen Hospital, China Academy of Chinese Medical Sciences, Beijing, China, [2] Clinical Department of Traditional Chinese Medicine, Beijing University of Chinese Medicine, Beijing, China

Background: Diabetic retinopathy (DR), one of the commonest microvascular complications in diabetic patients, is featured by a series of fundus lesions. Conventional Western medicine therapies for DR are always with modest treatment outcome. This paper is to assess the ocular fundus signs, vision and safety of Chinese patent medicines (CPMs) as an add-on treatment for DR.

Method: 7 electronic databases were searched to determine eligible trials. Randomized controlled trials (RCTs) of non-proliferative diabetic retinopathy (NPDR) in which the intervention group received CPMs combined with calcium dobesilate (CD), and the control group received only CD were included for analysis. Two reviewers extracted the data independently. Results expressing as mean differences (MD) and relative risks (RR) were analyzed with a fixed-effects or random-effects models.

Results: 19 RCTs involved 1568 participants with 1622 eyes met our inclusion criteria. The results suggested that compared with CD alone, CPMs plus CD for NPDR was superior at reducing the microaneurysm volume (MD -3.37; 95% confidence interval [CI], -3.59 to -3.14), microaneurysm counts (MD -2.29; 95%CI -2.97 to -1.61), hemorrhage area (MD -0.79; 95%CI -0.83 to -0.75), and macular thickness (MD -59.72; 95%CI -63.24 to -56.20). Participants in CPMs plus CD group also achieved a better vision. No obvious adverse events occurred.

OPEN ACCESS

Edited by:
Khalid Siddiqui,
King Saud University, Saudi Arabia

Reviewed by:
Satyanarayana Alleboina,
University of Tennessee Health Science Center (UTHSC), United States
Ferdinando Carlo Sasso,
Università della Campania Luigi Vanvitelli, Italy

****Correspondence:***
Fengmei Lian
lfm565@sohu.com

†These authors have contributed equally to this work and share first authorship

Specialty section:
This article was submitted to Clinical Diabetes, a section of the journal Frontiers in Endocrinology

Received: *21 October 2021*
Accepted: *14 February 2022*
Published: *14 March 2022*

Citation:
Zhang Y, An X, Duan L, Jin D, Duan Y, Zhou R, Zhang Y, Kang X and Lian F (2022) Effect of Chinese Patent Medicines on Ocular Fundus Signs and Vision in Calcium Dobesilate-Treated Persons With Non-Proliferative Diabetic Retinopathy: A Systematic Review and Meta-Analysis. Front. Endocrinol. 13:799337. doi: 10.3389/fendo.2022.799337

Conclusion: CPMs as an add-on therapy for NPDR have additional benefits and be generally safe. This meta-analysis demonstrated that CPMs combined with CD could improve retinal microaneurysm, hemorrhage, macular thickness, visual acuity, fasting blood glucose (FBG), and glycosylated hemoglobin (HbAlc) compared with CD alone. Further studies are needed to provide more conclusive evidence.

Systematic Review Registration: PROSPERO https://www.crd.york.ac.uk/prospero/, identifier CRD42021257999.

Keywords: chinese patent medicines, efficacy, non-proliferative diabetic retinopathy, randomized controlled trials (RCT), calcium dobesilate

HIGHLIGHTS

1. CPMs as an add-on therapy showed clinically and statistically significant reductions in microaneurysm, hemorrhage, macular thickness, visual acuity, FBG, and HbAlc for NPDR.
2. The outcomes can evaluate the therapeutic effects of CPMs in the treatment of NPDR objectively, indicating that CPMs might be used as a complementary and alternative approach to prevent, delay and reverse DR progression.

INTRODUCTION

In parallel with the soaring prevalence of diabetes mellitus (DM) to an epidemic proportion (1), the incidence of diabetic retinopathy (DR) is inevitably increasing. A meta-analysis that included 35 epidemiological studies around the world showed that the prevalence of DR was as high as 34.6% among diabetic patients, respectively (2). In China which is home to the largest number of people with DM in the world, DR incidence fluctuated dramatically by region between 7.4% and 43.1%, and after 10 to 20 years, the incidence will increase to 54% (3–6). DR, a common retinal microvascular complication of DM, is responsible for progressive vision impairment and ultimately blindness (7). The quality of life, psychological aspects, as well as social behavior are irreversibly and seriously affected in patients with sight-threatening retinopathy. Moreover, apart from diabetic medication, patients with DR also need fundus examination and treatment resulting in substantial social and economic burden, which increases with retinopathy severity and visual impairment (8, 9).

According to the international staging system, DR is mainly divided into non-proliferative diabetic retinopathy (NPDR) characterized by microaneurysms, retinal dot and blot hemorrhages, hard exudates or cotton wool spots and proliferative diabetic retinopathy (PDR) characterized by neovascularization, vitreous or preretinal hemorrhages identified in fundoscopic examination (10, 11). The main therapeutic strategies for NPDR involve control of risk factors and microcirculation improvement. In this stage, screening and early effective intervention can prevent or delay the occurrence of the disease and avoid severe loss of vision. While PDR is usually treated with anti-vascular endothelial growth factor (VEGF) agents, laser and surgery (10, 12). Calcium dobesilate (CD), registered in more than 20 countries, is an established vasoactive and angioprotective drug that has been prescribed as the routine medication for decades to patients with NPDR to ameliorate microcirculatory disturbance (12, 13). As detailed in the meta-analysis study published in 2015, CD can reduce the hyperviscosity of blood, inhibit the synthesis and release of platelet aggregator, and improve retinal microangioma and hemorrhage (14). However, some patients did not benefit from CD treatment alone (15).

From another perspective, as the most important part of traditional Chinese medicine (TCM), Chinese patent medicines (CPMs), widely and conveniently used in clinical practice by TCM or non-TCM persons, are always based on well-established and long-standing prescriptions to meet the demands of TCM for syndrome differentiation. Remarkable progress has been made toward the treatment of DM and its complications with CPMs (16–18). In recent years, several RCTs indicated that CPMs as an adjunct therapy can enhance the therapeutic efficacy (e.g. improving ocular fundus signs including microaneurysm, hemorrhage and macular thickness, and vision) of CD (19, 20). Nevertheless, for now, there has been no systematic review data available concerning the ocular fundus signs, vision and safety of CPMs in combination with CD in treating NPDR. Therefore, we conducted a meta-analysis to evaluate the ocular fundus signs, vision and safety of CPMs as an adjunct therapy for the treatment of NPDR to provide high-quality evidence to help clinicians select better treatment strategy.

METHODS

This study complied with the Preferred Reporting Project (PRISMA) (21) statement for systematic reviews and meta-analysis and was registered through PROSPERO (PROSPERO Registration number: CRD42021257999).

Search Strategy

We comprehensively searched the following databases from their start date to the present (up to 30 May 2021) and updated the search on 29 January 2022 to obtain more up-to-date and comprehensive evidence: PubMed, Embase, Cochrane Library,

Wanfang database, Weipu database, China National Knowledge Infrastructure, Chinese biomedical literature database and clinical trial registration centers, such as ChiCTR and clinical Trials.gov.

To fully retrieve eligible studies, a combination of Medical subject headings (MeSH) and free text words were used. English search terms include: (Diabetic Retinopathy OR Diabetic Retinopathies OR Retinopathies, Diabetic OR Retinopathy, Diabetic) AND [Calcium Dobesilate OR Dobesilate, Calcium OR Dobesilate Calcium OR Calcium, Dobesilate OR 2,5-Dihydroxybenzenesulfonate OR 2,5 Dihydroxybenzenesulfonate OR 2,5-Dihydroxybenzenesulfonic Acid OR 2,5 Dihydroxybenzenesulfonic Acid OR Doxium OR Calcium Dobesilate Monoammonium Salt OR Calcium Dobesilate Monopotassium Salt OR Dexium OR Dobica OR Calcium Dobesilate (1:1)] AND (danshen OR dan shen OR xueshuantong OR xue shuan tong OR qiming OR qi ming OR qijudihuang OR qi ju di huang OR shuangdanmingmu OR shuang dan ming mu). All titles and abstracts of articles were then separately screened by two authors (Yuehong Zhang, Xuedong An). Any discrepancies in extraction were resolved through discussion.

Study Selection

The Inclusion Criteria Were as Follows

1. The study included the patients who suffered from NPDR in accordance with international or domestic diagnostic criteria.
2. CD in combination with CPMs was used as an intervention, and CD alone was used as a control. Both groups received basic treatment (eg, glycemic control, blood pressure control and lipid modulation).
3. The outcomes included microaneurysm, hemorrhage, macular thickness, visual acuity, FBG, HbAlc, as well as adverse events (AEs).
4. We merely included trials whose treatment duration continued for 12 weeks or more.
5. The study design was a two-arm, randomized controlled trial.

The Exclusion Criteria Were as Follows

1. Non-randomized controlled clinical trials.
2. Studies with a treatment duration of less than 12 weeks.
3. Duplicate publication, only abstract or lack of outcome data and no access to obtain the full text.

Data Extraction

The relevant information was extracted independently by 2 authors (Yuehong Zhang, Xuedong An). The details included title, authors, year published, duration of disease, sample size, age, gender, outcome indicators, intervention and control, intervention time, and AEs. Discrepancies were settled by consensus or third-party adjudication (Fengmei Lian).

Quality Assessment

Two authors (Yuehong Zhang, Xuedong An) independently evaluated risk of bias of each of all included RCTs using the Cochrane Bias Risk Tool (CRBT) (22). This tool includes random sequence generation, allocation concealment, blinding, incomplete outcome data, selective reporting, and other biases. The results of the assessment were expressed as low bias risk, high bias risk and unclear bias risk.

Statistical Analysis

RevMan5.4 software provided by the Cochrane collaboration network was used for system evaluation and meta-analysis. The heterogeneity of the included studies was assessed using the I^2 statistics. $I^2 < 50\%$ indicates that heterogeneity is reasonable among the groups, thus the fixed-effect model is adopted for analysis; otherwise, a random-effects model will be applied. Mean differences (MDs) were employed in continuous variables. All effect quantities were reported with 95% CI, and $P \leq 0.05$ was considered a significant statistical difference. We also examined potential publication bias by constructing a funnel plot according to the Cochrane Handbook.

RESULTS

A total of 592 articles was retrieved by searching the literature databases, and *via* a search of clinical trial registries, we retrieved 5 records. After 351 duplicated studies were excluded, 241 studies remained. According to the understanding of the titles, abstracts, or summaries, we eliminated 138 articles that were not randomized, controlled trials, or the trial participants and the interventions did not meet our inclusion criteria. Then, after reading the full-text reading, 84 articles that full texts could not be retrieved, outcome data were missing, or the intervention did not match the criteria for integration strategies were deemed unsuitable and were therefore excluded. Finally, 19 trials were included in the present study (23–41). The specific literature screening and selection is shown in **Figure 1**.

A total of 1568 patients with 1622 eyes in the 19 RCTs met the inclusion criteria (23–41) (**Table 1**). The application of the treatment was assigned to two groups, control group (n=782, 809 eyes) that was treated with CD and intervention group (n=786, 813 eyes) that was treated with CPMs including Compound Xueshuantong (CX), Compound Danshen Dripping Pill (CDDP) and Shuangdan Mingmu Capsule (SMC) in combination with CD.

Hypoglycemic therapy was concomitantly administered to both groups to control glycemia. All 1568 patients were treated for at least 3 months. 8 studies (24, 29, 30, 33, 35, 36, 40, 41) mentioned the generation of random sequences (used random number tables), 2 RCTs (32, 34) used a semi-randomization method, and participants were assigned according to the visiting sequence, the remaining 9 RCTs (23, 25–28, 31, 37–39) referred to "random" but no method in detail. No study clearly mentioned the allocation concealment or the use of blind method, thus, all of them were judged to be at high or unclear risk of bias concerning the 2 items. None of the studies described the number of dropouts or lost to follow-up cases. We considered most studies to be at of low risk of reporting bias (**Figure 2**).

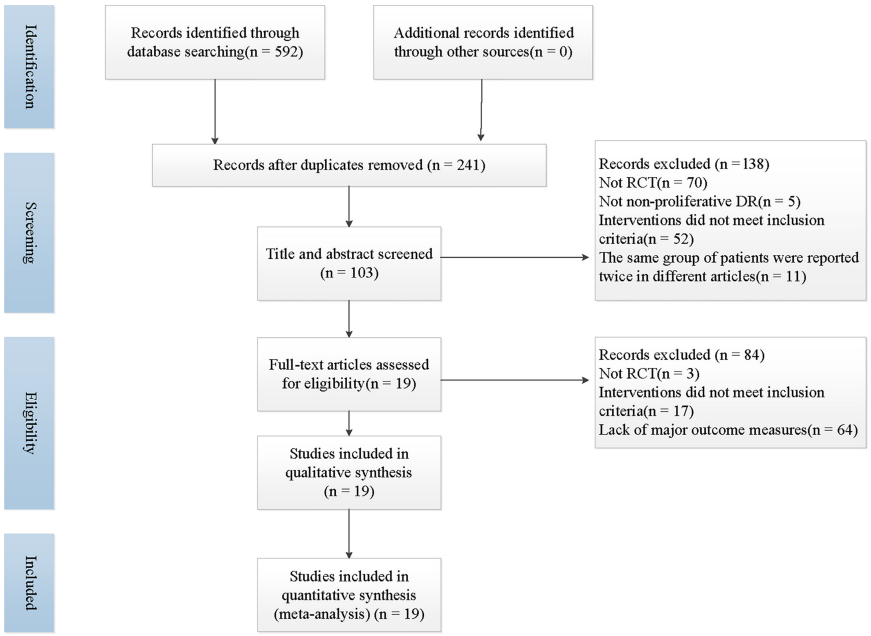

FIGURE 1 | The screening process summarized in a flow diagram.

Microaneurysm Volume

A total of 15 RCTs (23, 24, 26–28, 30–34, 37–41) with 1241 eyes provided data for microaneurysm volume. There was no significant heterogeneity reported, and a fixed-effects model was used. Meta-analysis result showed that CPMs combined with CD was significantly superior to control group in reducing microaneurysm volume (n=1241, MD -3.37, 95% CI -3.59 to -3.14), and the difference had statistical significance (P < 0.00001). According to the different CPMs, subgroup analysis was performed. 11 studies (23, 26, 28, 30, 31, 33, 34, 37–39, 41) reported the information of CX concerning the reduction of microaneurysm volume. The results revealed that a statistically significant decrease in microaneurysm volume with CX plus CD, compared to the CD group (n=965, MD -3.62, 95% CI -3.95 to -3.30). There was also a significant difference between the subgroups of the CDDP plus CD and CD groups (24, 27, 32, 40) (n=276, MD -3.14, 95% CI -3.45 to -2.83) (**Figure 3A**).

Microaneurysm Counts

2 RCTs (25, 36)reported the number of microaneurysm to be the outcome. A fixed-effects model was used to analyze the dependent variables according to the heterogeneity without significant difference. Pooled analysis showed a statistically significant decrease in microaneurysm counts with CMPs plus CD group, compared to the CD group (n=175, MD -2.29, 95% CI -2.97 to -1.61) (**Figure 3B**).

Hemorrhage Area

No significant heterogeneity was exhibited within 17 RCTs (24–39, 41) with available hemorrhage area data. Hence, we applied the fixed effect model. The results showed that hemorrhage area of CMPs in combination with CD in the treatment of NPDR was significantly smaller than that of CD alone (n=1462, MD -0.79, 95% CI -0.83 to -0.75). Subgroup analyses revealed that the pooled mean difference of hemorrhage area reduction was -0.77 mm^2 (n=1070, 95%CI -0.82 to -0.72, P<0.00001) between CX plus CD and CD alone groups (25, 26, 28, 30, 31, 33, 34, 36–39, 41). In the CDDP combined with CD group versus the CD alone subgroup, 4 trials (24, 27, 32, 35) reported the hemorrhage area data. There was also a significant difference between the 2 groups (n=272, MD -0.80, 95% CI -0.88 to -0.72, P<0.00001). In 1 RCT (29) of SMC, results indicated that there was statistical difference (n=120, MD -0.92, 95% CI -1.05 to -0.79, P<0.00001) (**Figure 4**).

Macular Thickness

17 included studies (23–33, 35–39, 41)compared the effect of CPMs and CD on macular thickness. Significant heterogeneity was found (P < 0.00001, I^2 = 90%), so a random effect model was used. The pooled mean differences of macular thickness reduction were -59.72μm (n=1440, 95% CI -63.24 to -56.20, P < 0.00001), and -61.15μm (n=1048, 95% CI -64.16 to -58.14, P < 0.00001), -60.37μm (n=272, 95% CI -69.66 to -51.07, P < 0.00001) and -48.94μm (n=120, 95% CI -53.32 to -44.56, P < 0.00001) for the CX plus CD and CD alone groups (23, 25, 26, 28, 30, 31, 33, 36–39, 41), the CDDP plus CD and CD alone groups (24, 27, 32, 35) and the SMC plus CD and CD alone groups (29), respectively (**Figure 5**).

Visual Acuity

2 RCTs (24, 27) provided specific information concerning the improvement of visual acuity. Significant heterogeneity was not

TABLE 1 | Basic characteristics of included studies.

Study ID	Sample size (eyes)	Gender M/F; Age, yr		Disease course		Intervention time(month)	Main indicators	Method of random allocation
		Intervention group	Control group	Intervention group	Control group			
An 2020 (23)	70 (70)	19/16;51.17 ± 17.83	20/15;52.12 ± 15.76	3.71 ± 1.31, yr	3.51 ± 1.44, yr	3	A,D	Random grouping
Bai 2017 (24)	76(76)	20/18;62	21/17;51	N	N	4	A,C,D,E	Random number table method
Chai 2018 (25)	107(107)	32/22;61.11 ± 6.01	30/23;61.19 ± 6.03	2.77 ± 0.32, yr	2.79 ± 0.30, yr	3	B,C,D	Random grouping
Chen 2019 (26)	78(78)	21/18;59.34 ± 3.27	20/19;58.17 ± 3.82	2.24 ± 1.08, yr	2.38 ± 1.14, yr	3	A,C,D,E	Random grouping
Huang 2020 (27)	40(40)	9/11;53.16 ± 2.26	10/10;52.16 ± 2.45	N	N	4	A,C,D,E,F, G	Random grouping
Li 2018 (28)	60(60)	18/12;56.68 ± 2.52	17/13;55.72 ± 2.31	35.49 ± 1.04, mo	35.91 ± 1.23, mo	5	A,D	Random grouping
Liu 2019 (29)	120(120)	33/27;57.54 ± 8.11	32/28;57.10 ± 9.26	10.46 ± 8.16, yr	10.46 ± 8.16, yr	4	C,D	Random number table method
Ma 2018 (30)	54(68)	16(19)/11(15); 53.02 ± 4.13	15(20)/12(14);53.08 ± 4.25	3.51 ± 0.30, yr	3.67 ± 0.75, yr	5	A,C,D,E,F, G	Random number table method
Pei 2015 (31)	64(64)	17/15;56.4 ± 2.1	16/16;55.3 ± 1.2	35.8 ± 1.3, mo	40.2 ± 1.4, mo	5	A,C,D	Random grouping
Ruan 2017 (32)	70(70)	18/17;52.5 ± 1.1	20/15;52.8 ± 1.7	N	N	4	A,C,D,E,F, G	According to the order of visit
Wang 2020 (33)	86(86)	25/19;69.52 ± 7.11	23/19;68.35 ± 6.82	3.14 ± 1.45, yr	3.05 ± 1.32, yr	5	A,C,D	Random number table method
Wu 2018 (34)	72(92)	20(26)/16(20); 52.97 ± 4.17	20(26)/16(20); 52.97 ± 4.17	3.47 ± 0.81, yr	3.47 ± 0.81, yr	3	A,C,D,F,G	According to the order of visit
Xu 2019 (35)	86(86)	24/19;53.11 ± 4.41	25/18;53.06 ± 4.39	N	N	4	A,C,D	Random number table method
Yu 2017 (36)	68(68)	19/15;57.4 ± 8.3	17/17;58.1 ± 7.9	33.6 ± 2.7, mo	33.8 ± 2.6, mo	3	B,C,D	Random number table method
Zhang 2020a (37)	200(220)	60(68)/40(42); 53.86 ± 4.27	60(68)/40(42); 53.86 ± 4.27	3.48 ± 0.90, yr	3.48 ± 0.90, yr	12	A,C,D	Random grouping
Zhang 2020b (38)	80(80)	23/17;53.60 ± 5.20	24/16;53.30 ± 5.60	3.20 ± 1.60, yr	3.10 ± 1.50, yr	3	A,C,D	Random grouping
Zhao 2019 (39)	87(87)	22/22;53.66 ± 5.49	22/21;53.71 ± 5.52	N	N	6	A,C,D	Random grouping
Huang 2021a (40)	90(90)	28/17;67.5 ± 5.30	29/16;67.30 ± 5.10	2.60 ± 1.20	2.40 ± 1.10	6	A,G	Random number table method
Huang 2021b (41)	60(60)	17/13; 52.85 ± 6.38	18/12; 51.86 ± 6.16	3.21 ± 0.66	3.18 ± 0.72	5	A,C,D	Random number table method

A, Microaneurysm Volume; B, Microaneurysm counts; C, Hemorrhage area; D, Macular thickness; E, Visual acuity; F, FBG; G, HbAlc.

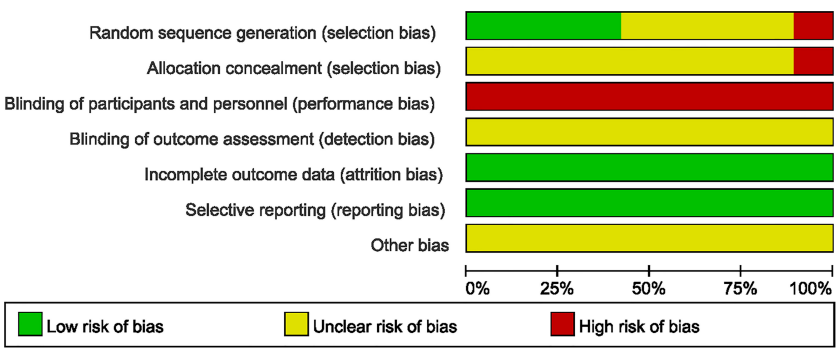

FIGURE 2 | Quality assessment of the included trials-Risk of bias graph.

observed between these RCTs. A fixed-effect model revealed that the CPMs group was statistically different than the CD group in decreasing the visual acuity (n=116, MD 0.15, 95% CI 0.10 to 0.20, P < 0.00001) (**Figure 6**).

FBG

4 trials (27, 30, 32, 34) provided the data concerning the FBG. The pooled effect was generated using a random-effects model because of the significant heterogeneity. The results showed

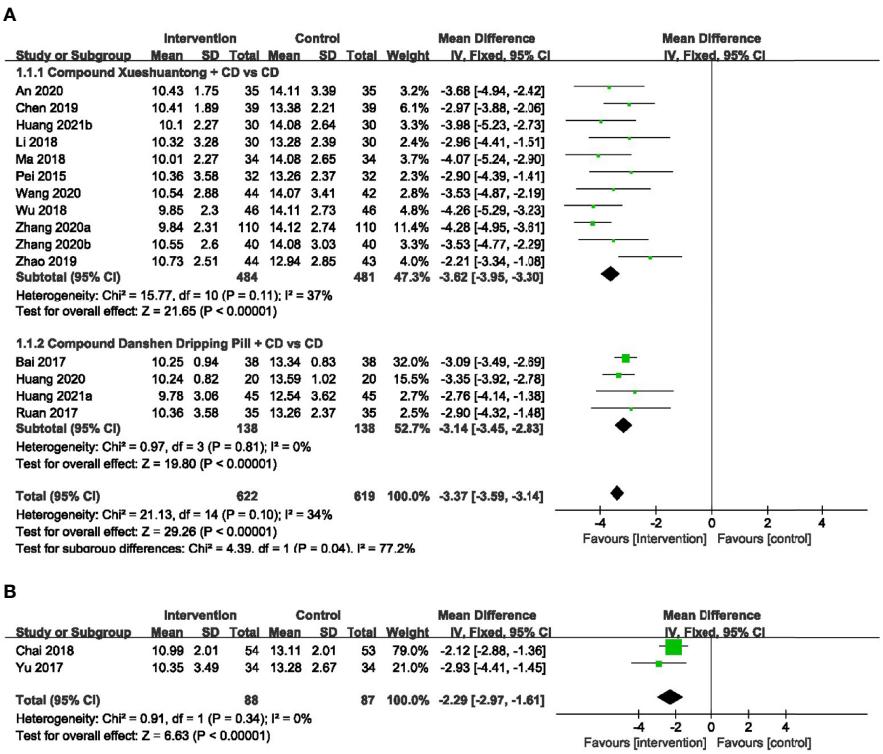

FIGURE 3 | Forest plots of comparison of ocular fundus signs for CPMs plus CD versus CD alone. **(A)** Microaneurysm volume, **(B)** Microaneurysm counts.

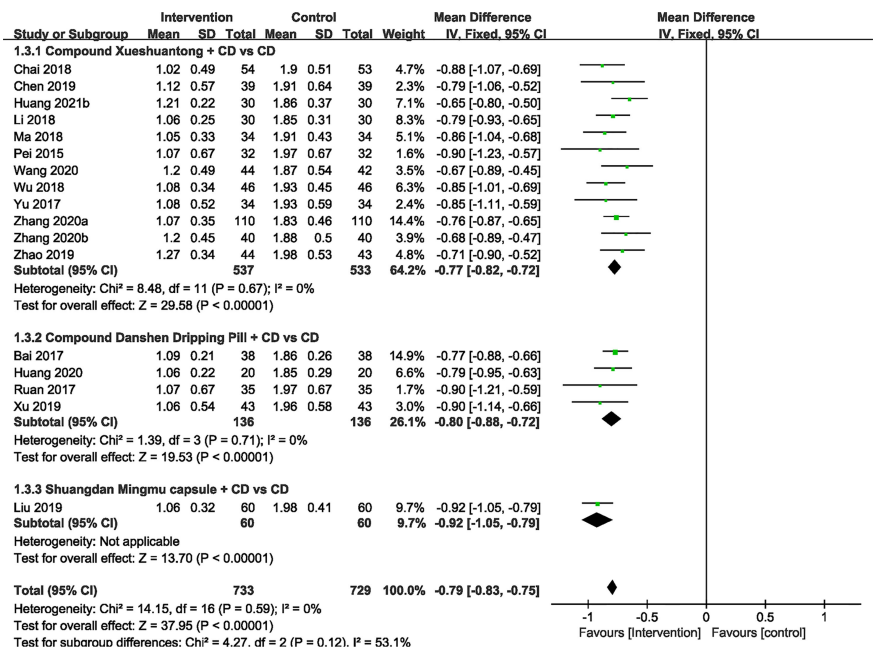

FIGURE 4 | Forest plots of comparison of ocular fundus signs for CPMs plus CD versus CD alone. Hemorrhage area.

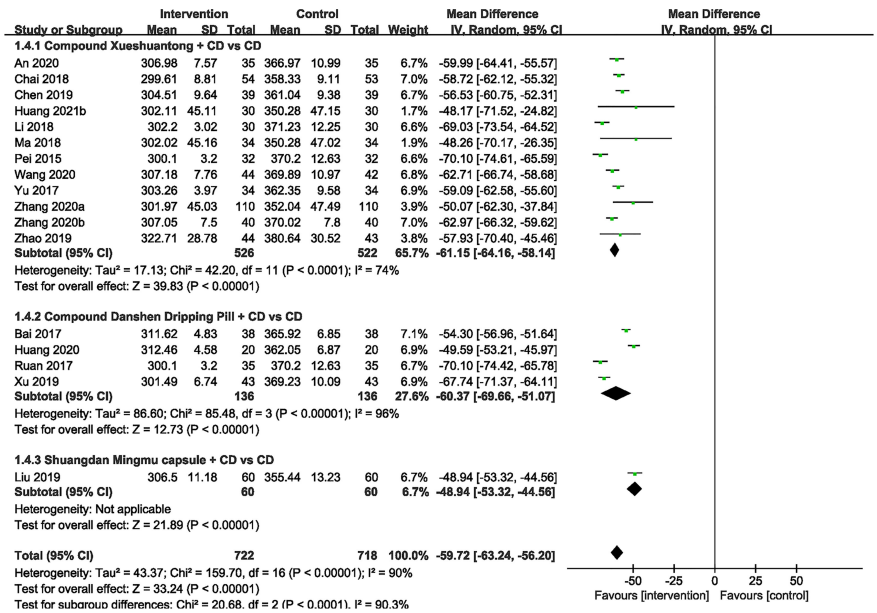

FIGURE 5 | Forest plots of comparison of ocular fundus signs for CPMs plus CD versus CD alone. Macular thickness.

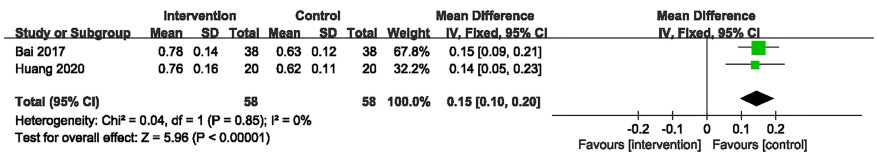

FIGURE 6 | Forest plots of comparison of visual acuity for CPMs plus CD versus CD alone.

that FBG in CX combined group presented significantly lower than the CD group (30, 34) (n=140, MD -1.39, 95% CI -1.78 to -1.00, P<0.00001). Significant reduction was also found between the subgroups of the CDDP Combined group and CD group (27, 32) (n=110, MD -0.80, 95% CI -1.59 to -0.00, P<0.00001) (**Figure 7A**).

HbAlc

5 trials (27, 30, 32, 34, 40) reported HbAlc data. As we found no heterogeneity among them, the fixed-effects model was selected. A pooled analysis of 2 trials (30, 34) showed a statistically significant decrease in HbAlc with CX combined group, compared to the CD group (n=140, MD -1.24, 95% CI -1.89 to -0.60, P=0.0002). HbAlc was also significantly lower in CDDP combined group versus CD group (27, 32, 40) (n=200, MD -0.99, 95% CI -1.09 to -0.89, P<0.00001) (**Figure 7B**).

Adverse Events

Of the 19 studies (23–41), 6 reported no evident adverse reaction (24, 29–32, 35). 5 trials (23, 33, 38, 40, 41) showed that there was no significant difference in AEs between the CPMs plus CD and CD groups (n=370, RR 0.99, 95% CI 0.54 to 1.82) **Figure 8**. Adverse reactions in both groups were mainly concerned with stomach discomfort, nausea and decreased appetite.

Publication Bias

Funnel plots of microaneurysm volume was shown in **Figure 9**. Shape of the funnel plots was not completely symmetrical, suggesting probable publication bias. The following factors were linked with publication bias: positive results are easier to publish than negative results; the small sample size of the included studies brings a small sample effect.

DISCUSSION

Once patients have entered the stage of advanced DR, they are more susceptible to developing more severe forms of the disease such as macular edema, vitreous hemorrhage and retinal detachment. Even with surgical intervention, visual function suffers serious damage. Therefore, the early diagnosis of DR and adequate initiating therapy are essential, which remain a

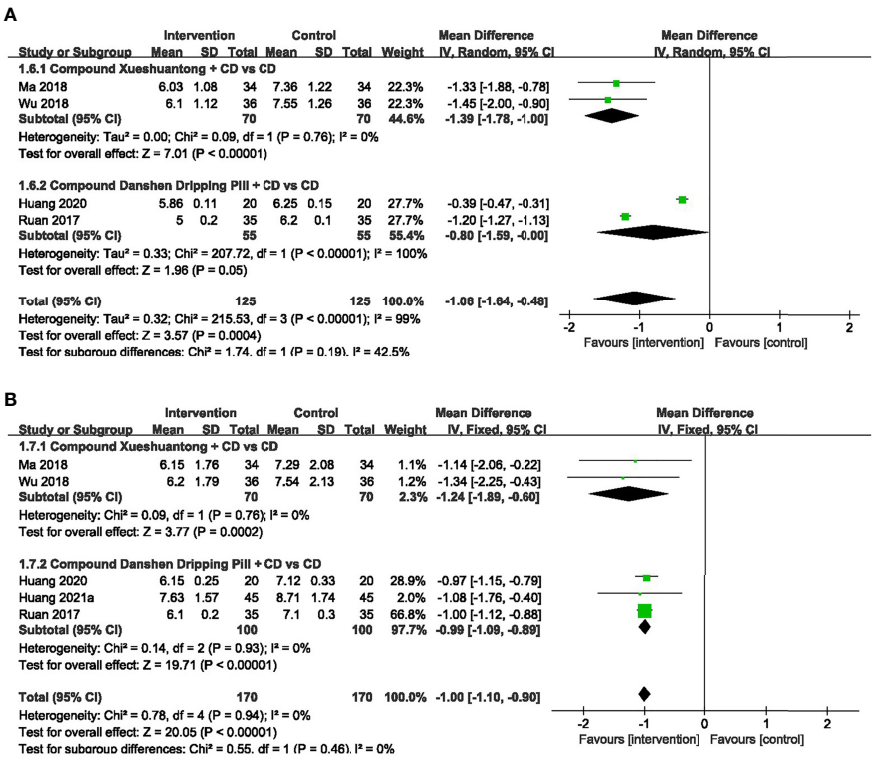

FIGURE 7 | Forest plots of comparison of blood sugar for CPMs plus CD versus CD alone. **(A)** FBG, **(B)** HbAlc.

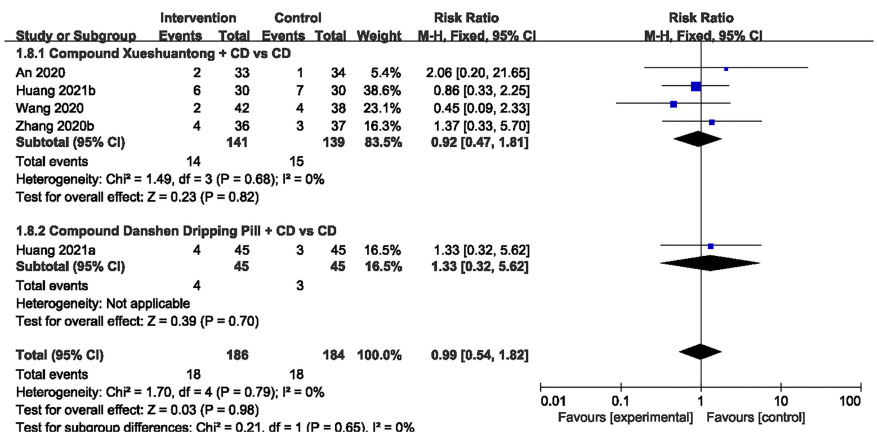

FIGURE 8 | Forest plots of comparison of adverse events for CPMs plus CD versus CD alone.

challenge (42). Telemedicine seems to be a worthy alternative, which can provide an easy, smart specialist fundus oculi examination, especially in times of pandemic, to bring the specialist closer to clinical centers allowing screening and follow-up of DR (43, 44). The other way round, screening for an early-stage diagnosis of DR allows not only to avoid the risk of severe vision loss but also to estimate high cardiovascular disease risk in diabetic patients (45), particularly if associated with additional important forms of diabetic microangiopathies, such as albuminuria (46).

As for therapy, the past decades have witnessed significant advances in the treatment options for DR. CD, as the most widely accepted oral vascular protective agent for NPDR, contributes a lot to the successful management in arresting or

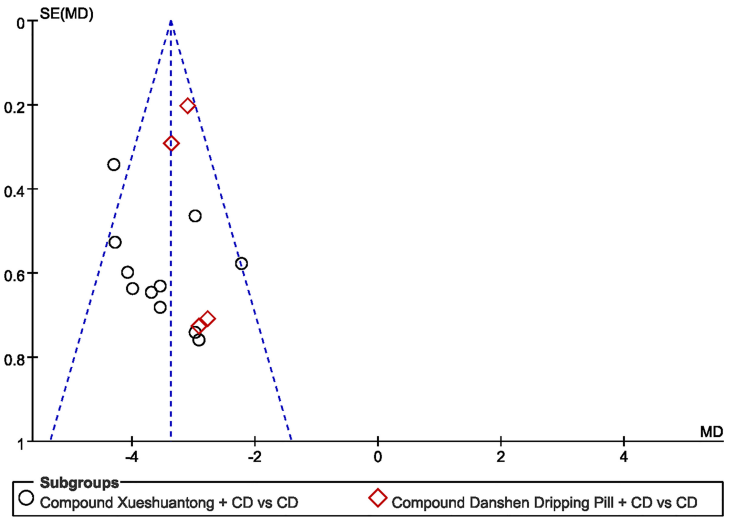

FIGURE 9 | Funnel plot of the trials that compared CPMs plus CD group with CD group; Microaneurysm volume.

reversing the progression of the disease. The possible protective mechanisms of CD responsible for DR are mainly achieved by decreasing retinal albumin leakage and capillary permeability, suppressing oxidative stress, inhibiting aldose reductase (47–49). However, in parallel, TCM, as an adjuvant therapy option has gotten more and more attention among the public for its remarkable effects in clinical practice. It states that the occurrence of diseases is due to the imbalance of Yin, Yang, Qi and Blood, and CPMs are prescribed accordingly to rebuild that balance.

Previous studies have proven that CPMs are a safe and effective therapeutic option in NPDR treatment (18, 50, 51). Our research team has completed a controlled trial enrolled with 223 NPDR patients indicating that significant effect was observed in CDDP (composed of three herbs: *Salvia miltiorrhiza, Panax notoginseng* and *Borneol*) treated group (18). We find that at 24 weeks, for the fluorescein fundus angiography, the percent of "Excellent" and "Effective" in the high-dose and mid-dose CDDP groups (540mg, 3 times/day) was 74% and 77%, respectively, that is significantly higher than 28% in the placebo group (P<0.001) (18). CDDP may exert its action mainly by improving retinal microcirculation and alleviating retinal tissue ischemia observed in an animal study (52). In the meantime, the research has also revealed that CDDP improved retinal damage in diabetic rats through attenuating oxidative injury (52). CX with daily doses used in therapy range from 1.5g up to 4.5g per day consists of four herbs including *Panax notoginseng, Salvia miltiorrhiza, Astragalus membranaceus* and *Scrophulariae Radix*. It counteracts DR may be related to the HIF-1 pathway, TNF pathway, VEGF pathway and Hippo pathway (53–55), thereby improving retinal hypoxic microenvironment, retinal inflammation and vascular proliferation. On the other hand, CX causes the hemodynamics and morphological alterations in diabetic rat retinas, which may *via* regulating the PPAR pathway and complement and coagulation cascades (56). SMC based on Chinese ancient prescriptions named Liuwei Dihuang Pill and Erzhi Pill is composed of *Ligustrum lucidum Ait., Eclipta prostrata, Cornus officinalis Sieb, Dioscorea polystachya Turczaninow, Salvia miltiorrhiza Bunge, Panax notoginseng, Paeonia suffruticosa Andr., Alismatis Rhizoma, Poria cocos (Schw.), Smilax glabra Roxb.* and *Achyranthes bidentata Blume*. The usual dose of SMC is a 2 g single dose three times daily for 4 months. As to the underlying mechanisms of SMC in the treatment of DR may be bound up with the down-regulation of the expressions of hypoxia-inducible factor 1α (HIF-1α) and nuclear factor-βK (NF-κB), as well as an attenuation of oxidative stress-induced apoptosis of pericytes through PARP/GAPDH pathway and inhibition of retinal angiogenesis *via* Ras pathway consequently exerting retinal tissue-protective effects (57–59). The major mechanisms involved in the treatment of DR with CPMs mentioned above are shown in **Figure 10**. Additionally, it was shown that all these CPMs contained *Salvia miltiorrhiza* and *Panax notoginseng*, so the information can be used to support further single herb studies.

Effectiveness and Safety of CPMs Combined With CD for NPDR

The aim of this meta-analysis was to assess the ocular fundus signs, vision and safety of CPMs as an adjuvant therapy for DR. 19 studies (23–41)with 1622 eyes meet the criterion. The results demonstrated that CPMs provided additional benefits for the NPDR population, which displayed a significant improvement in ocular fundus signs including microaneurysm volume/counts, hemorrhage area and macular thickness as well as visual acuity, FBG and HbAlc compared to CD alone. The effects of the combination of CPMs and CD may be related to their mechanisms of the synergistic effect between the two drugs, which remain to be further studied.

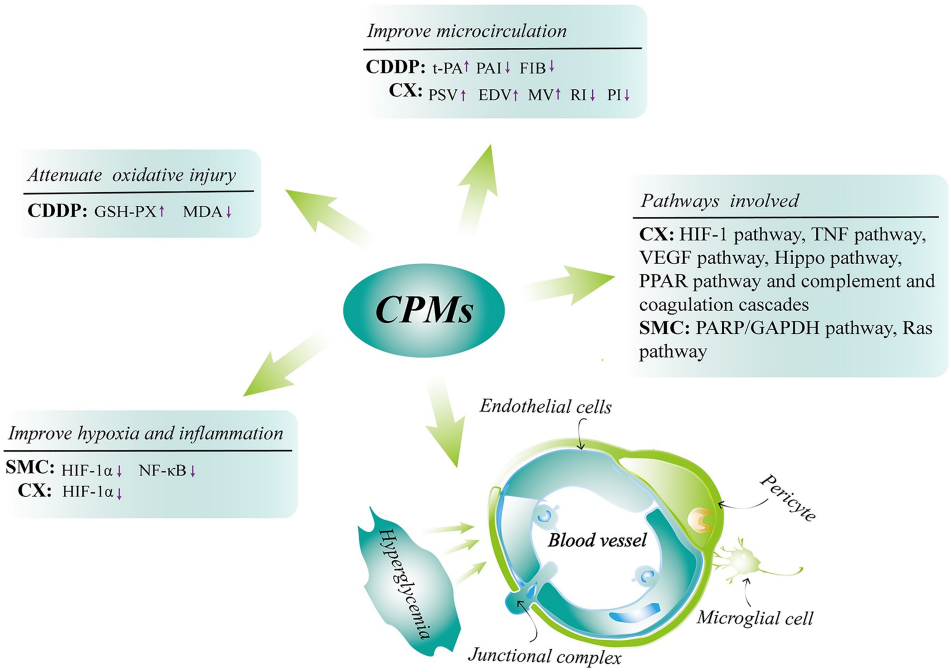

FIGURE 10 | The major underlying mechanisms involved in the treatment of DR with CPMs (CX, CDDP and SMC). Chinese patent medicines (CPMs); Compound Xueshuantong (CX); Compound Danshen Dripping Pill (CDDP); Shuangdan Mingmu Capsule (SMC); tissue plasminogen activator (t-PA); plasminogen activator inhibitor (PAI); fibrinogen (FIB); peak systolic velocity (PSV); end diastolic velocity (EDV); mean velocity (MV); resistance index (RI); pulsatility index (PI); glutathione peroxidase (GSH-PX); malondialdehyde (MDA); hypoxia-inducible factor 1α (HIF-1α); nuclear factor-κB (NF-κB).

The data to the analyses on treatment-associated AEs was provided in 5 (23, 33, 38, 40, 41) out of 19 studies (23–41). Stomach discomfort, nausea and appetite loss were the manly common AEs. Meta-analysis results were basically consistent with relevant study results with no significant differences between the two groups, demonstrating that a combination of CPMs and CD is safe for the treatment of DR. However, due to lack of long-term follow-up data, long-term efficacy and safety could not be determined. Thus, the safety of the combination with CPMs and CD still needs to be observed.

Description of the Outcomes

NPDR, the early stage of DR, is often asymptomatic and mostly accompanied by microaneurysms and hemorrhages as the ocular fundus signs (60). Microaneurysms, the signature lesion of NPDR, appear as dilations of capillaries on the fundus that is widely performed to measure the severity of DR and assess the risk of future DR progression (61). Hemorrhage resulting from the rupture of microaneurysms is another essential diagnostic criterion to assess the severity level of DR (11). Therefore, microaneurysms and hemorrhage can be used as suitable indicators to evaluate drug effects. The macula is particularly prone to fluid accumulation leading to macular edema which is the abnormal thickening of the macula (62). This thickening always threatens or actually causes vision loss. Thus, it is particularly important to evaluate macular thickness. The main causative pathogenic factor in the progression of DR is hyperglycemia, and better glycemic control may be beneficial in reducing the incidence of DR and increasing the odds of improvement of DR (14). In our study, CMPs as an add-on therapy for NPDR could better control the FBG and HbAlc of the subjects. However, significant heterogeneity remained in the CDDP subgroups under the heading of FPG, several potential causes could be associated with the severity of disease and different hypoglycemic agents with different pharmacokinetic parameters.

Potential Limitations of the Study

Several limitations of our study have to be acknowledged. First, none of the 19 articles (23–41) provided a complete trial protocol, making the data questionable in terms of standardization and transparency. Second, only 8 literature (24, 29, 30, 33, 35, 36, 40, 41) reported that participants were randomized using table of random numbers, more than half of the studies did not state the randomization process, which exposed the results to selection bias. Third, none of the 19 studies (23–41) mentioned how allocation concealment or blinding was performed, and participants withdraw and drop out, which may result in selection bias, information bias and publication bias. Fourth, the included populations were all Asian populations, and no studies of CPMs on other races were retrieved, thus the efficacy of CPMs combined with CD on NPDR in other races is unknown. Since the concern in methodological quality, multicenter, large-sample, well-designed RCTs following

the Consolidated Standards of Reporting Trials (CONSORT) guidelines (63) are needed.

CONCLUSION

In summary, combination therapies hold great potential for NPDR. Compared with the use of CD alone, CPMs (CX, CDDP OR SMC) plus CD has additional benefits in the treatment of NPDR, especially in ocular fundus signs involving microaneurysm, hemorrhage and macular thickness, and visual acuity. It also had advantages in the reduction of FBG and HbAlc without serious adverse reactions. These effects largely arrest progression of DR and save vision efficaciously. However, due to the moderate study quality and possible publication bias, the results should be treated with caution. In the future, large-scale RCTs with powerful study design are desired to provide a higher grade of evidence.

DATA AVAILABILITY STATEMENT

The original contributions presented in the study are included in the article/supplementary material. Further inquiries can be directed to the corresponding author.

AUTHOR CONTRIBUTIONS

FL designed the study and as the corresponding author. DJ, YD, and RZ carried out the literature search. YueZ and XA contributed to data extraction and quality assessment and drafted the manuscript with LD. YuqZ and XK provided statistical supports for meta-analysis. All authors contributed to the article and approved the submitted version.

FUNDING

This work was supported by 2015 Traditional Chinese Medicine Scientific Research (201507001-11) and Innovation Team and Talents Cultivation Program of National Administration of Traditional Chinese Medicine (No: ZYYCXTD-D-202001). The funders had no role in the study design, data collection, data analysis, interpretation, or writing of the report.

ACKNOWLEDGMENTS

We would like to acknowledge all the authors of the research articles used for the analysis.

REFERENCES

1. Sun H, Saeedi P, Karuranga S, Pinkepank M, Ogurtsova K, Duncan BB, et al. IDF Diabetes Atlas: Global, Regional and Country-Level Diabetes Prevalence Estimates for 2021 and Projections for 2045. *Diabetes Res Clin Pract* (2021) 109119. doi: 10.1016/j.diabres.2021.109119
2. Yau JW, Rogers SL, Kawasaki R, Lamoureux EL, Kowalski JW, Bek T, et al. Global Prevalence and Major Risk Factors of Diabetic Retinopathy. *Diabetes Care* (2012) 35(3):556–64. doi: 10.2337/dc11-1909
3. Zhang GS, Morigejilit, Ren FM, Hui YN. Epidemiological Investigation of Diabetic Retinopathy in Hohhot. *Chin J Pract Ophthalmol* (2017) 04):428–33. doi: 10.3760/cma.j.issn.1006-4443.2017.04.020
4. Wang WJ, Liu YN, Yan YJ, Yao BD, Zhou F, Li LQ. The Investigation of Risk Factors of Diabetic Retinopathy in Type 2 Diabetes Mellitus in Minhang, Shanghai. *Chin Primary Health Care* (2015) 29(08):66–8. doi: 10.3969/j.issn.1001-568X.2015.08.0029
5. Xie XW, Xu L, Jonas JB, Wang YX. Prevalence of Diabetic Retinopathy Among Subjects With Known Diabetes in China: The Beijing Eye Study. *Eur J Ophthalmol* (2009) 19(1):91–9. doi: 10.1177/112067210901900114
6. Wang FH, Liang YB, Peng XY, Wang JJ, Zhang F, Wei WB, et al. Risk Factors for Diabetic Retinopathy in a Rural Chinese Population With Type 2 Diabetes: The Handan Eye Study. *Acta Ophthalmol* (2011) 89(4):e336–43. doi: 10.1111/j.1755-3768.2010.02062.x
7. Willis JR, Doan QV, Gleeson M, Haskova Z, Ramulu P, Morse L, et al. Vision-Related Functional Burden of Diabetic Retinopathy Across Severity Levels in the United States. *JAMA Ophthalmol* (2017) 135(9):926–32. doi: 10.1001/jamaophthalmol.2017.2553
8. Tóth G, Nagy ZZ, Németh J. Model-Based Economic Burden of Diabetic Retinopathy in Hungary. *Orv Hetil* (2021) 162(8):298–305. doi: 10.1556/650.2021.32031
9. Orji A, Rani PK, Narayanan R, Sahoo NK, Das T. The Economic Burden of Diabetic Retinopathy Care at a Tertiary Eye Care Center in South India. *Indian J Ophthalmol* (2021) 69(3):666–70. doi: 10.4103/ijo.IJO_1538_20
10. Flaxel CJ, Adelman RA, Bailey ST, Fawzi A, Lim JI, Vemulakonda GA, et al. Diabetic Retinopathy Preferred Practice Pattern®. *Ophthalmology* (2020) 127 (1):66–145. doi: 10.1016/j.ophtha.2019.09.025
11. Wong TY, Cheung CM, Larsen M, Sharma S, Simó R. Diabetic Retinopathy. *Nat Rev Dis Primers* (2016) 2:16012. doi: 10.1038/nrdp.2016.12
12. Retinopathy Group CDS. Expert Consensus on Prevention and Treatment of Diabetic Retinopathy. *Chin J Diabetes Mellitus* (2018) 10(4):241–7. doi: 10.3760/cma.j.issn.1674-5809.2018.04.001
13. Ribeiro ML, Seres AI, Carneiro AM, Stur M, Zourdani A, Caillon P, et al. Effect of Calcium Dobesilate on Progression of Early Diabetic Retinopathy: A Randomised Double-Blind Study. *Graefes Arch Clin Exp Ophthalmol* (2006) 244(12):1591–600. doi: 10.1007/s00417-006-0318-2
14. Zhang X, Liu W, Wu S, Jin J, Li W, Wang N. Calcium Dobesilate for Diabetic Retinopathy: A Systematic Review and Meta-Analysis. *Sci China Life Sci* (2015) 58(1):101–7. doi: 10.1007/s11427-014-4792-1
15. Stamper RL, Smith ME, Aronson SB, Cavender JC, Cleasby GW, Fung WE, et al. The Effect of Calcium Dobesilate on Nonproliferative Diabetic Retinopathy: A Controlled Study. *Ophthalmology* (1978) 85(6):594–606. doi: 10.1016/s0161-6420(78)35643-8
16. Lian F, Jin D, Bao Q, Zhao Y, Tong X. Effectiveness of Traditional Chinese Medicine Jinlida Granules as an Add-on Therapy for Type 2 Diabetes: A System Review and Meta-Analysis of Randomized Controlled Trials. *J Diabetes* (2019) 11(7):540–51. doi: 10.1111/1753-0407.12877
17. Piao C, Zhang Q, Jin D, Shao M, Bi C, Wang L, et al. Treatment of Type 2 Diabetes With Tianqi Jiangtang Capsule: A Systematic Review and Meta-Analysis of Randomized Controlled Trials. *Med (Baltimore)* (2020) 99(21): e19702. doi: 10.1097/md.0000000000019702
18. Lian F, Wu L, Tian J, Jin M, Zhou S, Zhao M, et al. The Effectiveness and Safety of a Danshen-Containing Chinese Herbal Medicine for Diabetic Retinopathy: A Randomized, Double-Blind, Placebo-Controlled Multicenter Clinical Trial. *J Ethnopharmacol* (2015) 164:71–7. doi: 10.1016/j.jep.2015.01.048
19. Sui HL, Yu CY, Xue HM, Wang RN. The Clinical Curative Observation on Qiming Granule Combined With Calcium Dobesilate Capsules in Treatment of Patients With Nonproliferative Diabetic Retinopathy. *Chin Med Innovations* (2014) 20):99–102. doi: 10.3969/j.issn.1674-4985.2014.20.036
20. Rao XJ, Wu YM, Wei LJ, Ma Y. Comparison of Efficacy Between Traditional Chinese Medicine Combined With Western Medicine and Simple Western Medicine for Patients With NPDR. *Int Eye Sci* (2017) 17(01):148–50. doi: 10.3980/j.issn.1672-5123.2017.1.41

21. Moher D, Liberati A, Tetzlaff J, Altman DG. Preferred Reporting Items for Systematic Reviews and Meta-Analyses: The PRISMA Statement. *PloS Med* (2009) 6(7):e1000097. doi: 10.1371/journal.pmed.1000097
22. Higgins JP, Altman DG, Gøtzsche PC, Jüni P, Moher D, Oxman AD, et al. The Cochrane Collaboration's Tool for Assessing Risk of Bias in Randomised Trials. *Bmj* (2011) 343:d5928. doi: 10.1136/bmj.d5928
23. An LN. Clinical Study of Compound Xueshuantong Combined With Calcium Dobesilate in the Treatment of Diabetic Retinopathy. *Pract Clin J Integrated Traditional Chin Western Med* (2020) 20:69–71. doi: 10.13638/j.issn.1671-4040.2020.14.034
24. Bai YX. Therapeutic Effect of Calcium Dobesilate Combined With Compound Danshen Dripping Pills on Diabetic Retinopathy and Its Influence on Serum Inflammatory Factors. *J Qiqihar Med Coll* (2017) 38(22):2641–3. doi: 10.3969/j.issn.1002-1256.2017.22.014
25. Chai F, Wang Y, Huang Q. Effect of Compound Xueshuantong Capsule Combined With Calcium Dobesilate on IGF-1, VEGF and Hemodynamic Parameters in Patients With Early Diabetic Retinopathy. *J Pract Traditional Chin Med* (2018) 34(11):1360–2. doi: 10.3969/j.issn.1004-2814.2018.11.068
26. Chen KF. Clinical Observation of Compound Xueshuantong Combined With Calcium Dobesilate in the Treatment of Early Diabetic Retinopathy. *J Huaihai Med* (2019) 37(01):72–4. doi: 10.14126/j.cnki.1008-7044.2019.01.026
27. Huang H. Effect of Danshen Dripping Pills on Diabetic Retinopathy. *J North Pharm* (2020) 17(04):100–1. doi: 10.3969/j.issn.1672-8351.2020.04.072
28. Li Q. Effect of Calcium Dobesilate Combined With Compound Xueshuantong Capsule on Clinical Efficacy and VEGF and IGF-1 Levels in Patients With Early Diabetic Retinopathy. *World Latest Med Inf* (2018) 18(37):99+101. doi: 10.19613/j.cnki.1671-3141.2018.37.068
29. Liu JP, Kong HY, Wang L. Clinical Efficacy of Shuangdan Mingmu Capsules Combined With Calcium Dobesilate in the Treatment of Diabetic Retinopathy and Its Effects on Serum Levels of Vascular Endothelial Growth Factor, Platelet-Derived Growth Factor and Interleukin-1. *Eval Anal Drug-Use Hospitals China* (2019) 19(11):1332–4+8. doi: 10.14009/j.issn.1672-2124.2019.11.015
30. Ma JP. Compound Xueshuantong Capsules Combined With Calcium Dobesilate in the Treatment of Early Diabetic Retinopathy. *Int Eye Sci* (2018) 18(02):305–8. doi: 10.3980/j.issn.1672-5123.2018.2.25
31. Pei R, Gao H. Clinical Effects and Hs-CRP, VEGF and IGF-1 Levels of Xueshuantong Capsule Combined With Calcium Dobesilate in Treatment of Early Diabetic Retinopathy. *Modern J Integrated Traditional Chin Western Med* (2015) 24(35):3896–8+907. doi: 10.3969/j.issn.1008-8849.2015.35.007
32. Ruan YX, Chen M, Liu ZQ, Wang YL, Sun N, Huang X, et al. Clinical Study on the Treatment of Diabetic Retinopathy by Oral Compound Danshen Dripping Pill Combined With Calcium Dobesilate. *Med Sci J Cent South China* (2017) 45(01):18–20+3. doi: 10.15972/j.cnki.43-1509/r.2017.01.004
33. Wang J, Du W, Li Y. Therapeutic Effect of Calcium Dobesilate Combined With Compound Xueshuantong Capsule on Diabetic Retinopathy Among Older Adults and Its Influence on Hemorheology. *Chin J Gerontology* (2020) 40(08):1603–6. doi: 10.3969/j.issn.1005-9202.2020.08.010
34. Wu XS. Clinical Analysis of Compound Xueshuantong Capsule Combined With Calcium Hydroxybenzenesul Fonate in Treating Early Diabetic Retinopathy. *Capital Med* (2018) 25(22):34–6. doi: 10.3969/j.issn.1005-8257.2018.22.028
35. Xu HT. Effect of Compound Danshen Dripping Pills Combined With Calcium Dobesilate on Diabetic Retinopathy. *Chin J Convalescent Med* (2019) 28(08):884–6. doi: 10.13517/j.cnki.ccm.2019.08.041
36. Yu W, Lin BS, Ma SF, Zhang WW, Wu QL. Effect of Calcium Dobesilate Combined With Compound Xueshuantong Capsule on Early Diabetic Retinopathy and Its Influence on Serum IGF-1 and VEGF Levels. *Chin J Gerontology* (2017) 37(21):5311–3. doi: 10.3969/j.issn.1005-9202.2017.21.041
37. Zhang W. Compound Xueshuantong Capsules Combined With Calcium Dobesilate in the Treatment of Early Diabetic Retinopathy. *Health Horizon* (2020) 20:75.
38. Zhang WW. Analysis of Therapeutic Effect of Calcium Dobesilate Combined With Compound Xueshuantong Capsule on Early Diabetic Retinopathy. *J Clin Med literature* (2020) 7(79):155,7.
39. Zhao YL. Clinical Observation of Compound Xueshuantong Combined With Calcium Dobesilate in the Treatment of Early Diabetic Retinopathy. *Capital Med* (2020) 27(09):95. doi: 10.3969/j.issn.1005-8257.2020.09.077
40. Huang YX, Sun HP, Tang YQ, Chen X. Effect of Compound Danshen Dripping Pills on Inflammatory Mediators, Cytokines and Visual Function in Patients With Diabetic Retinopathy. *Chin J Integr Med Cardio-/Cerebrovascuiar Dis* (2021) 19 (08):1364–6+408. doi: 10.12102/j.issn.1672-1349.2021.08.030
41. Huang W, Tang AD, Liu J. Therapeutic Effect of Calcium Dobesilate Combined With Compound Xueshuantong Capsule on Diabetic Retinopathy. *Contemp Med* (2021) 27(31):162–4. doi: 10.3969/j.issn.1009-4393.2021.31.066
42. Vujosevic S, Aldington SJ, Silva P, Hernández C, Scanlon P, Peto T, et al. Screening for Diabetic Retinopathy: New Perspectives and Challenges. *Lancet Diabetes Endocrinol* (2020) 8(4):337–47. doi: 10.1016/s2213-8587(19)30411-5
43. Galiero R, Pafundi PC, Nevola R, Rinaldi L, Acierno C, Caturano A, et al. The Importance of Telemedicine During COVID-19 Pandemic: A Focus on Diabetic Retinopathy. *J Diabetes Res* (2020) 2020:9036847. doi: 10.1155/2020/9036847
44. Sasso FC, Pafundi PC, Gelso A, Bono V, Costagliola C, Marfella R, et al. Telemedicine for Screening Diabetic Retinopathy: The NO BLIND Italian Multicenter Study. *Diabetes Metab Res Rev* (2019) 35(3):e3113. doi: 10.1002/dmrr.3113
45. Shoeibi N, Bonakdaran S. Is There Any Correlation Between Diabetic Retinopathy and Risk of Cardiovascular Disease? *Curr Diabetes Rev* (2017) 13(1):81–6. doi: 10.2174/1573399812666151012115355
46. Sasso FC, Pafundi PC, Simeon V, De Nicola L, Chiodini P, Galiero R, et al. Efficacy and Durability of Multifactorial Intervention on Mortality and MACEs: A Randomized Clinical Trial in Type-2 Diabetic Kidney Disease. *Cardiovasc Diabetol* (2021) 20(1):145. doi: 10.1186/s12933-021-01343-1
47. Ribeiro ML, Caillon P, Gamba G, Cunha–Vaz JGroup DS. Efficacy of Calcium Dobesilate (Doxium(R)) on the Blood-Retinal Barrier Permeability in Early Diabetic Retinopathy: A Double-Blind Study. *Invest Ophthalmol Vis* (2004) 45:4153.
48. Leal EC, Martins J, Voabil P, Liberal J, Chiavaroli C, Bauer J, et al. Calcium Dobesilate Inhibits the Alterations in Tight Junction Proteins and Leukocyte Adhesion to Retinal Endothelial Cells Induced by Diabetes. *Diabetes* (2010) 59 (10):2637–45. doi: 10.2337/db09-1421
49. Velpandian T, Nirmal J, Gupta P, Vijayakumar AR, Ghose S. Evaluation of Calcium Dobesilate for Its Anti-Cataract Potential in Experimental Animal Models. *Methods Find Exp Clin Pharmacol* (2010) 32(3):171–9. doi: 10.1358/mf.2010.32.3.1423888
50. Zhu YX, Li J, Ying J. Efficacy of Compound Xueshuantong Capsules in the Treatment of Nonproliferative Diabetic Retinopathy. *China Modern Doctor* (2016) 54(24):60–2,6.
51. Qin YH, Li F, Tu LY, Qiu B, Zhang ML, Cao JH, et al. Multicentric Clinical Study of Shuangdan Mingmu Capsule on Diabetic Retinopathy. *J Hunan Univ Chin Med* (2010) 30(1):46–51. doi: 10.3969/j.issn.1674-070X.2010.01.015
52. Zhou SP, Guo ZX, Tong XL, Pan L, Zhao JB. Effect of Composite Salvia Pellet on Diabetic Retinopathy in Streptozotocin Induced Diabetic Rats. *Chin J Integrated Traditional Western Med* (2002) S1):174–8.
53. Yang Y, Zhang WF, Li YT, Zhao X, Zhang JH, Zhang DM, et al. Protective Effect of Complex Thrombolysis Capsule on High Altitude Retinopathy in Rat Models. *Int Eye Sci* (2021) 21(2):211–6. doi: 10.3980/j.issn.1672-5123.2021.2.04
54. Li H, Li B, Zheng Y. Exploring the Mechanism of Action Compound-Xueshuantong Capsule in Diabetic Retinopathy Treatment Based on Network Pharmacology. *Evid Based Complement Alternat Med* (2020) 2020:8467046. doi: 10.1155/2020/8467046
55. Hao GM, Lv TT, Wu Y, Wang HL, Xing W, Wang Y, et al. The Hippo Signaling Pathway: A Potential Therapeutic Target Is Reversed by a Chinese Patent Drug in Rats With Diabetic Retinopathy. *BMC Complement Altern Med* (2017) 17(1):187. doi: 10.1186/s12906-017-1678-3
56. Sun HH, Chai XL, Li HL, Tian JY, Jiang KX, Song XZ, et al. Fufang Xueshuantong Alleviates Diabetic Retinopathy by Activating the PPAR Signalling Pathway and Complement and Coagulation Cascades. *J Ethnopharmacol* (2021) 265:113324. doi: 10.1016/j.jep.2020.113324
57. Fu CJ, Ling YJ, Yan JZ, Zhao HQ, Lv Y, He WL, et al. Effects of Shuangdan Mingmu Capsules on Expressions of HIF-1α and NF-κb in Retina of Diabetic Retinopathy Rats. *Chin J Inf Traditional Chin Med* (2018) 25(6):44–7. doi: 10.3969/j.issn.1005-5304.2018.06.011
58. Nie F, Yan J, Ling Y, Liu Z, Fu C, Li X, et al. Effect of Shuangdan Mingmu Capsule, a Chinese Herbal Formula, on Oxidative Stress-Induced Apoptosis of

Pericytes Through PARP/GAPDH Pathway. *BMC Complement Med Ther* (2021) 21(1):118. doi: 10.1186/s12906-021-03238-w
59. Fu CJ, Ling YJ, Yan JC, Zhao HQ, Qin YH. Effect of Shuangdan Mingmu Capsule on the Ras-Raf-1-MEK-ERK Pathway in Retinal Tissue in Rats With Diabetic Retinopath. *J Hunan Univ Chin Med* (2018) 38(7):728–31. doi: 10.3969/j.issn.1674-070X.2018.07.003
60. Cheung N, Mitchell P, Wong TY. Diabetic Retinopathy. *Lancet* (2010) 376 (9735):124–36. doi: 10.1016/s0140-6736(09)62124-3
61. Durzhinskaya MK. [Microaneurysms as a Biomarker of Diabetic Retinopathy]. *Vestn Oftalmol* (2021) 137(5. Vyp. 2):300–5. doi: 10.17116/oftalma2021137052300
62. Johnson MW. Etiology and Treatment of Macular Edema. *Am J Ophthalmol* (2009) 147(1):11–21.e1. doi: 10.1016/j.ajo.2008.07.024
63. Boutron I, Altman DG, Moher D, Schulz KF, Ravaud P. CONSORT Statement for Randomized Trials of Nonpharmacologic Treatments: A 2017 Update and a CONSORT Extension for Nonpharmacologic Trial Abstracts. *Ann Intern Med* (2017) 167(1):40–7. doi: 10.7326/m17-0046

Conflict of Interest: The authors declare that the research was conducted in the absence of any commercial or financial relationships that could be construed as a potential conflict of interest.

frontiers in Endocrinology

ORIGINAL RESEARCH
published: 29 March 2022
doi: 10.3389/fendo.2022.865211

The Fundus Structural and Functional Predictions of DME Patients After Anti-VEGF Treatments

Hang Xie[1†], Shihao Huang[1†], Qingliang Liu[2†], Yifan Xiang[3], Fabao Xu[4], Xiaoyan Li[4] and Chun-Hung Chiu[1]*

[1] Business School, Sun Yat-Sen University, Guangzhou, China, [2] School of Computer Science and Engineering, Sun Yat-Sen University, Guangzhou, China, [3] State Key Laboratory of Ophthalmology, Zhongshan Ophthalmic Center, Sun Yat-Sen University, Guangzhou, China, [4] Department of Ophthalmology, Qilu Hospital, Cheeloo College of Medicine, Shandong University, Jinan, China

OPEN ACCESS

Edited by:
Khalid Siddiqui, King Saud University, Saudi Arabia

Reviewed by:
Mohamed El-Sherbiny, Almaarefa University, Saudi Arabia
Subrata Chakrabarti, Western University, Canada

***Correspondence:**
Chun-Hung Chiu
zhaojx5@mail.sysu.edu.cn

[†]*These authors have contributed equally to this work*

Specialty section:
This article was submitted to Clinical Diabetes, a section of the journal Frontiers in Endocrinology

Received: *29 January 2022*
Accepted: *01 March 2022*
Published: *29 March 2022*

Citation:
Xie H, Huang S, Liu Q, Xiang Y, Xu F, Li X and Chiu C-H (2022) The Fundus Structural and Functional Predictions of DME Patients After Anti-VEGF Treatments. Front. Endocrinol. 13:865211. doi: 10.3389/fendo.2022.865211

Diabetic retinopathy (DR) is an important complication with a high incidence of 34.6% in the diabetic populations. DR could finally lead to vision impairment without effective interventions, during which, diabetic macular edema (DME) is a key phase causing visual loss. Up to date, antivascular endothelial growth factor (anti-VEGF) therapy is the first-line treatment for DME which has achieved relatively better clinical outcomes than traditional treatments. However, there are several kinds of anti-VEGF medicines, and patients are sensitive to different anti-VEGF treatments. In addition, its effectiveness is unstable. Considering the patients' need to accept continual anti-VEGF treatments and its price is comparatively high, it is clinically important to predict the prognosis after different anti-VEGF treatments. In our research, we used the demographic and clinical data of 254 DME patients and 2,763 optical coherence tomography (OCT) images from three countries to predict the fundus structural and functional parameters and treatment plan in 6 months after different anti-VEGF treatments. Eight baseline features combined with 11 models were applied to conduct seven prediction tasks. Accuracy (ACC), the area under curve (AUC), mean absolute error (MAE), and mean square error (MSE) were respectively used to evaluate the classification and regression tasks. The ACC and AUC of structural predictions of retinal pigment epithelial detachment were close to 1.000. The MAE and MSE of visual acuity predictions were nearly 0.3 to 0.4 logMAR. The ACC of treatment plan regarding continuous injection was approaching 70%. Our research has achieved great performance in the predictions of fundus structural and functional parameters as well as treatment plan, which can help ophthalmologists improve the treatment compliance of DME patients.

Keywords: diabetic macular edema, optical coherence tomography, visual acuity, clinical effectiveness, prognosis prediction

INTRODUCTION

Diabetes is a global public health issue (1). According to published results, 1 in 11 adults had diabetes worldwide in 2015, and the diabetic population will increase to 642 million by 2040 (2–4). Diabetic retinopathy (DR) is an important complication with a high incidence of 24.7% to 37.5% in the diabetic populations (5). DR could gradually progress and finally lead to vision impairment without effective intervention, during which diabetic macular edema (DME) is a key phase causing visual loss. The morbidity of DME is 3.1% to 7.9% in the diabetic populations, and most of them need prompt and effective treatment to avoid severe visual impairment (6).

Up to date, antivascular endothelial growth factor (anti-VEGF) therapy is the first-line treatment for DME and has achieved relatively better clinical outcomes than traditional treatments of retinal photocoagulation and surgery (7–9). There are several kinds of anti-VEGF medicines, involving bevacizumab, ranibizumab, aflibercept, and so on. However, patients are sensitive to different anti-VEGF treatments and its effectiveness is unstable (10–12). Considering that patients need to accept repetitive anti-VEGF treatments and its price is comparatively high, it is clinically important to predict the prognosis after different anti-VEGF treatments (13, 14).

In our study, we established intelligent models for fundus structural and functional predictions of DME patients after different anti-VEGF treatments. Based on the multinational data, we applied several algorithms to predict the functional parameter of visual acuity (VA), structural parameters of central retinal thickness (CRT) and other four parameters, and clinical advice of continuing injection (CI) 6 months in advance. Our models have achieved great performance in different prediction tasks, which can help ophthalmologists make treatment plans for DME patients and provide research basis for other retinopathies.

MATERIALS AND METHODS

The data were downloaded from the open dataset provided by the Asia Pacific Tele-Ophthalmology Society (APTOS) and the Department of Ophthalmology, Qilu Hospital, Shandong University, from October 2018 to May 2021. The APTOS data were applied to train and test the models. The Qilu data were applied for external validation. Our ethics committee ruled that written informed consent was not required because our study was retrospective in nature and all the images were fully anonymized. Moreover, this study adhered to the tenets of the Declaration of Helsinki (2020KYPJ024).

DATA COLLECTION

The APTOS data were obtained from the Rajavithi Hospital of Thailand and the Aravind Eye Hospital of India, then labeled by the Zhongshan Ophthalmic Center of China. The Qilu data were extracted from the clinical records. Only patients diagnosed with DME and accepting anti-VEGF treatments are enrolled. The inclusion criteria were as follows (1): aged greater or equal to 18 years; (2) diagnosed with DME; and (3) accepting consecutive monthly anti-VEGF therapy of bevacizumab, aflibercept, conbercept, ranibizumab, or combination for 6 months. The exclusion criteria were as follows: (1) presence of any other retinal diseases including age-related macular degeneration (AMD), retinal vein occlusion (RVO), polypoidal choroidal vasculopathy (PCV), and so on; (2) low image quality caused by media opacities; or (3) an abnormal signal strength index of images. The follow-up points were at 6 months after anti-VEGF therapy.

The demographic information of age and gender were recorded. Pretherapeutic visual acuity (pre-VA) and visual acuity (VA) after anti-VEGF therapy for 6 months were tested. Based on the optical coherence tomography (OCT) of patients before and after anti-VEGF therapy, five imaging characteristics of central retinal thickness (CRT), and presence of retinal interlayer fluid (RIF), subretinal pigment epithelium fluid (SRF), retinal pigment epithelial detachment (PED), and retinal hyperreflexia (RHF) were measured and recorded by ophthalmologists with clinical work experience of more than 5 years. The clinical decision label of suggesting continuous injection (CI) of anti-VEGF medicine was made based on its therapeutic effect after 6 months according to changes of VA and imaging characteristics, which was labeled by professors with clinical work experience of more than 10 years. As the appearance and treatment of binocular DME are usually asynchronous, we treated each eye as a separate case in data collection.

MODEL TRAINING AND EVALUATION

The research procedure is shown in **Figure 1**. Eight parameters were applied to train the prediction models, including age, gender, pre-VA, pre-CRT, pre-RIF, pre-SRF, pre-PED, and pre-RHF at baseline. Five classification prediction models were constructed to predict the CI and the presence of RIF, SRF, PED, and RHF. Six regression prediction models were established to predict VA and CRT 6 months in advance.

The classification prediction models included classical random forest (RF), generalized regression neural network (GRNN), probabilistic neural network (PNN), extreme learning machine (ELM), and support vector machine (SVM) modeling. Also, their classification performances were evaluated by classification accuracy (ACC) and area under the curve (AUC). ACC is defined as the proportion of the sum of true-positive samples (TP) and the true-negative samples (TN) to the total number of samples (N) to be predicted, as follows,

$$\mathrm{ACC} = \frac{TP + TN}{N}.$$

AUC represents the area under the ROC curve, and AUC takes values between 0 and 1, where a larger AUC indicates a better model performance.

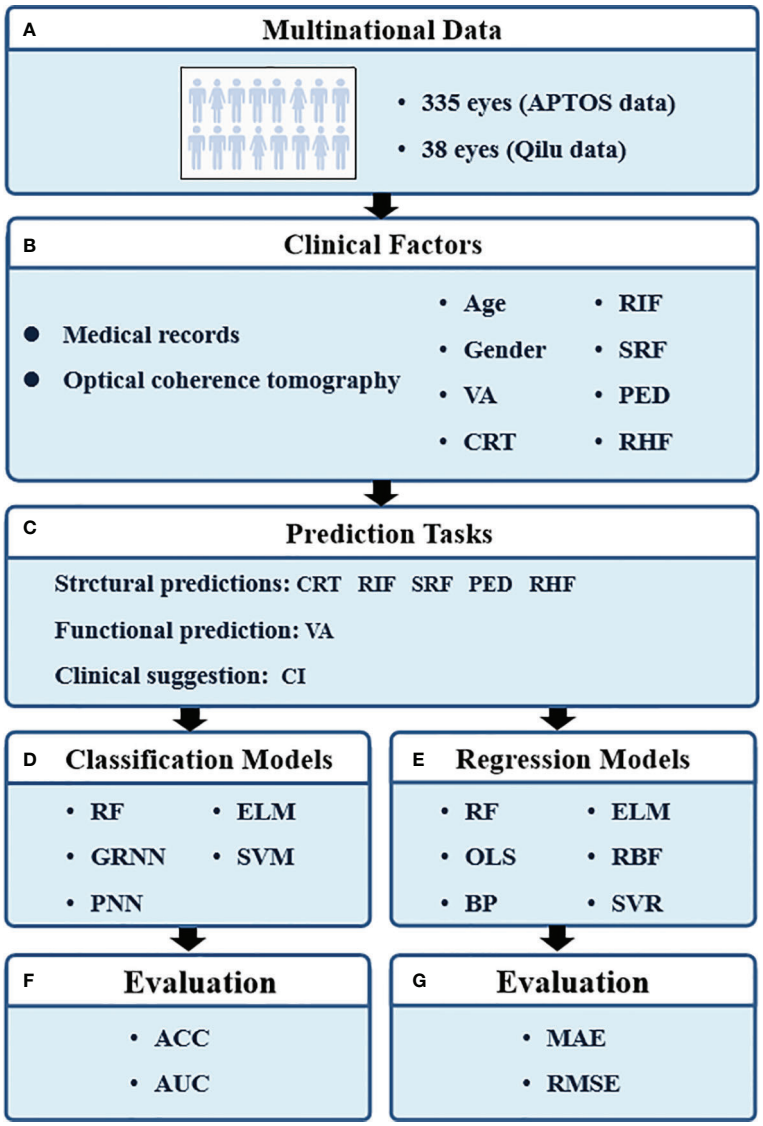

FIGURE 1 | The pipeline of our study. VA, visual acuity; CRT, central retinal thickness; RIF, retinal interlayer fluid; SRF, subretinal pigment epithelium fluid; PED, retinal pigment epithelial detachment; RHF, retinal hyperreflexia; CI, continuous injection; RF, random forest; GRNN, generalized regression neural network; PNN, probabilistic neural network; ELM, extreme learning machine; SVM, support vector machines; OLS, ordinary least squares; BP, back propagation network; RBF, radial basis function network; SVR, support vector regression; ACC, classification accuracy; AUC, area under curve; MAE, mean absolute error; RMSE, root mean square error.

The regression prediction models contained RF, ordinary least squares (OLS), back propagation (BP) network, ELM, radial basis function (RBF) network, and support vector regression (SVR) modeling. The prediction performances of regression models were quantified with the mean absolute error (MAE) and root mean square error (RMSE). The MAE is defined as the average value of the absolute error of the prediction results, which directly reflects the deviation of the predicted values from the actual values, as follows,

$$\mathrm{MAE} = \frac{1}{N}\sum_{i=1}^{N}|\widetilde{y}_i - y_i|,$$

where $\widetilde{y}_i$ and y_i represent the model prediction value and the real value for the ith sample, respectively. The RMSE is the square root of mean square error (MSE), which is calculated as the average value of the square of the error of the prediction results, as follows,

$$\mathrm{RMSE} = \sqrt{\frac{1}{N}\sum_{i=1}^{N}(\widetilde{y}_i - y_i)^2}.$$

RESULTS

Of 216 patients, 335 eyes were included from APTOS data and 38 eyes of 38 patients were enrolled form Qilu data (**Table 1**).

The DME patients were aged 26 to 84 years old with a mean age of nearly 56 years old. One hundred fourteen (34.0%) patients and 22 (57.9%) patients were men in the APTOS and Qilu data, respectively. The pre-VAs were 0.74 ± 0.60 (0–3) logMAR and 1.20 ± 0.63 (0–3) logMAR in two datasets ($p < 0.001$). The pre-CRTs ranged from 151 to 1,345 μm with mean values of 426.71 ± 177.88, 415.21 ± 131.98, and 699.87 ± 921.63 μm in the training, test, and external validation groups, respectively. The statistical differences of all characteristics before and after treatments between the APTOS and Qilu data are shown in **Table 1**. Except for the baseline age, pre-VA and pre-RHF, there was no statistical difference between two datasets. DME patients of three groups showed VA improvement, CRT decrease, and percentage changes of RIF, SRF, PED, and RHF, which are described in detail in **Table 1**.

Five structural prediction models obtained ACCs and AUCs at different levels, of which the RF and SVM models achieved best performances (**Table 2**). In the internal test, ACCs of presence predictions regarding RIF, SRF, PED, and RHF were 0.902, 0.825, 0.937, and 0.939 with the RF model and 0.912, 0.787, 0.965, and 0.948 with the SVM model. AUCs of presence predictions regarding RIF, SRF, PED, and RHF were 0.844, 0.645, 0.772, and 0.891 with the RF model and 0.865, 0.525, 0.906, and 0.890 with the SVM model. In the external validation, these two models also obtained high-level accuracies that ACCs of presence predictions regarding RIF, SRF, PED, and RHF were 0.858, 0.783, 1.000, and 0.917 with the RF model and 0.868, 0.777, 1.000, and 0.895 with the SVM model. AUCs of presence predictions regarding RIF, SRF, PED, and RHF were 0.782, 0.654, 1.000, and 0.944 with the RF model and 0.812, 0.622, 1.000, and 0.911 with the SVM model, which have achieved excellent performance in the PED predictions with an AUC of 1.000 in external validation. The predictions of RIF and RHF obtained high accuracies of more than 0.900 as well. In the clinical suggestions of CI predictions, the accuracy is close to 0.700. In the internal test, the ACCs of CI predictions were 0.671 with the RF model and 0.697 with the SVM model. The AUCs were 0.607 with the RF model and 0.634 with the SVM model. In the external validation, ACCs were 0.674 and 0.656 and AUCs were 0.649 and 0.671 respectively in the RF and SVM models.

The SVR and RF models obtained the best performances in VA and CRT predictions (**Table 2**). MAEs of VA predictions were 0.262 and 0.302 logMAR in internal tests and 0.387 and 0.485 logMAR in external validations. Prediction errors were equivalent to nearly three lines of visual chart. Predictions errors of CRT were exhibited in **Table 2**. Prediction errors of MAE and RMSE were close to 100 to 150 μm.

Feature weights of CI and VA predictions of the best two models are indicated in **Figure 2**. Two models showed different weight patterns in the same tasks. In the CI predictions, the most important features were pre-RIF (0.345), pre-PED (0.236), and pre-RHF (0.419) according to the SVM model. However, in the RF model, the most important features were pre-VA (0.257), pre-CRT (0.366), and pre-RHF (0.175). In the VA predictions, the pre-VA had the highest weights of 0.826 and 0.319 in the SVR and RF models, respectively. The pre-CRT (0.321) also played an important role in VA predictions based on the RF model.

DISCUSSION

Our study established classification and prediction models with multinational data to predict the treatment effects of anti-VEGF therapy for DME patients. The models have achieved excellent performance in prediction tasks of structural and functional parameters as well as clinical suggestions 6 months in advance, which can help ophthalmologists with DME patients.

TABLE 1 | The characteristics of patients according to groups.

Characteristics	Training group	Test group	External validation	*p*-values
Patients	182	34	38	
Gender (men)	98 (53.85%)	16 (47.06%)	22 (57.89%)	0.726
Age (year)	56.55 ± 9.98	57.59 ± 10.27	61.84 ± 11.19	0.005
Eyes	301	34	38	
Baseline				
Pre-VA (logMAR)	0.74 ± 0.60	0.60 ± 0.42	1.20 ± 0.63	<0.001
Pre-CRT (μm)	426.71 ± 177.88	415.21 ± 131.98	699.87 ± 921.63	0.08
Pre-RIF	243 (80.73%)	27 (79.41%)	34 (89.47%)	0.355
Pre-SRF	98 (32.56%)	10 (29.41%)	18 (47.37%)	0.260
Pre-PED	26 (8.64%)	1 (2.94%)	2 (5.26%)	0.609
Pre-RHF	205 (68.11%)	20 (58.82%)	20 (52.63%)	0.039
Posttreatment				
VA (logMAR)	0.69 ± 0.59	0.52 ± 0.31	0.87 ± 0.64	0.184
CRT (μm)	391.08 ± 157.26	392.56 ± 140.09	355.55 ± 132.69	0.243
RIF	242 (80.40%)	25 (73.53%)	29 (76.32%)	0.359
SRF	66 (21.93%)	4 (11.76%)	8 (21.05%)	0.676
PED	26 (8.64%)	1 (2.94%)	2 (5.26%)	0.638
RHF	202 (67.11%)	19 (55.88%)	20 (52.63%)	0.056
CI	203 (67.44%)	25 (73.53%)	21 (55.26%)	0.052

p-values showed the statistical differences of characteristics between the APTOS and Qilu data.
VA, visual acuity; CRT, central retinal thickness; RIF, retinal interlayer fluid; SRF, subretinal pigment epithelium fluid; PED, retinal pigment epithelial detachment; RHF, retinal hyperreflexia; CI, continuous injection.

TABLE 2 | The prediction performances of the best two models in classification and regression tasks.

Classification models	RF				SVM			
	ACC		AUC		ACC		AUC	
Factors	Test	Validation	Test	Validation	Test	Validation	Test	Validation
RIF	0.901	0.857	0.843	0.781	0.911	0.868	0.864	0.812
SRF	0.824	0.782	0.645	0.654	0.787	0.776	0.525	0.622
PED	0.936	1.000	0.772	1.000	0.964	1.000	0.905	1.000
RHF	0.938	0.916	0.890	0.943	0.947	0.894	0.887	0.911
CI	0.671	0.607	0.674	0.656	0.697	0.634	0.649	0.671
Regression models	**SVR**				**RF**			
	MAE		RMSE		MAE		RMSE	
Factors	Test	Validation	Test	Validation	Test	Validation	Test	Validation
VA (logMAR)	0.262	0.387	0.414	0.511	0.302	0.485	0.446	0.585
CRT (μm)	99.91	162.34	140.36	330.86	94.86	131.26	128.94	159.24

RF, random forest; SVM, support vector machines; SVR, support vector regression; ACC, classification accuracy; AUC, area under curve; MAE, mean absolute error; RMSE, root mean square error; RIF, retinal interlayer fluid; SRF, subretinal pigment epithelium fluid; PED, retinal pigment epithelial detachment; RHF, retinal hyperreflexia; CI, continuous injection; VA, visual acuity; CRT, central retinal thickness.

DME is an important stage of RD, which needs timely treatment, otherwise may cause severe visual impairment (15). Anti-VEGF treatment is the first-line treatment of DME (16, 17). Increasing researches were conducted to explore the clinical effect and limitation of anti-VEGF treatment (11, 18–21). Although anti-VEGF treatment was proved to function better than previous therapies of laser therapy and steroid therapy, it had some limitations as well (22–24). Patients need long-term and consecutive anti-VEGF injections, and the complication morbidity will increase with the treatment progress (7, 25, 26). The potential ocular complications include entophthalmia, glaucoma, and retinal detachment, which can lead to a more severe visual loss (27, 28). Consequently, to predict the therapeutic effect of anti-VEGF treatment can provide basis to make intervention plan for both ophthalmologists and patients. The functional prediction of VA and treatment plan prediction of CI both serve as key roles in treatment guidance. The prediction of CI is an impossible task for human ophthalmologists, even for experienced fundus professors. Our models achieved nearly 70% accuracy in the CI predictions, which provided a new sight in the understanding treatment effectiveness.

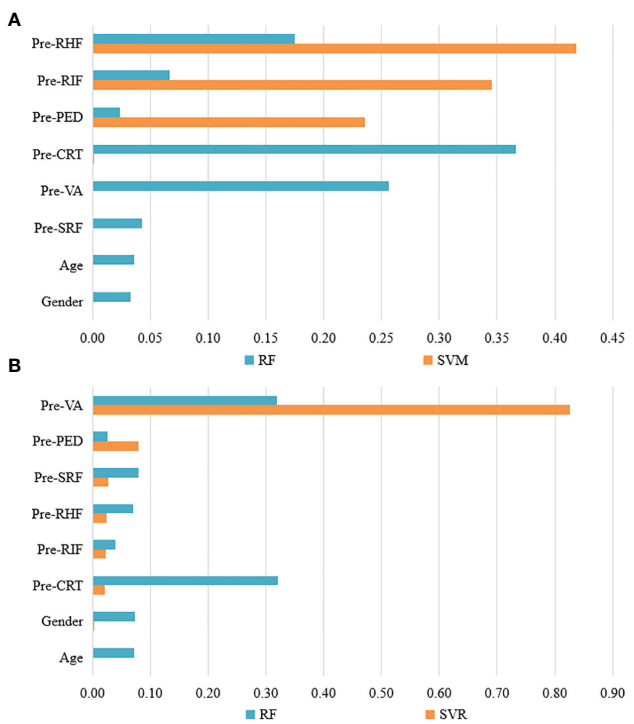

FIGURE 2 | The feature weights of CI and VA predictions of the best two models. **(A)** The feature weights of CI predictions with RF and SVW models. **(B)** The feature weights of VA predictions with RF and SVR models. VA, visual acuity; CI, continuous injection; CRT, central retinal thickness; RIF, retinal interlayer fluid; SRF, sub retinal pigment epithelium fluid; PED, retinal pigment epithelial detachment; RHF, retinal hyperreflexia; RF, random forest; SVM, support vector machines; SVR, support vector regression.

In our research, we finished the structural prediction tasks of five parameters, including CRT, RIF, SRF, PED, and RHF, which are all relatively important in the DME process and prognosis (29). Thick CRT and the presence of RIF, SRF, PED, and RHF all indicate there are still effusion and exudation in the lesion areas and that the prognosis is unsatisfactory (12, 30, 31). Previous studies have published relative prediction results, and some studies accurately predicted the VA and CRT of DME patients after anti-VEGF treatment by clinical information and OCT data (32–35). Honghua Yu and his team have published results predicting the VA and CRT of DME patients 1 month after anti-VEGF treatments (36). Our research has achieved earlier predictions of 6 months with more parameters. Our models obtained high accuracies in the presence predictions of more structural parameters, including RIF, SRF, PED, and RHF, especially the presence of PED, which provided more information about the treatment effects. Moreover, some other retinopathies, such as central serous chorioretinopathy and age-related macular degeneration, have similar pathological changes

(37–39). Our results may offer a research basis for the intelligent structural predictions of other retinopathies.

The two best models in VA and CI predictions exhibited different weight patterns according to the analysis. Based on the SVM models, the patients showing the presence of pre-RIF, pre-PED, and pre-RHF may need anti-VEGF treatment more and may obtain higher clinical effectiveness with CI. The presence of these structural lesions indicates there are chronic vascular leakage and fluid accumulation, which may cause angiogenesis (40, 41). As a result, anti-VEGF treatment is beneficial to patients with these structural lesions. Our study found the clinical basis to support the continuous injection of anti-VEGF medicine, which may provide a new idea for studied on the effectiveness of anti-VEGF treatment.

LIMITATION

Some limitations of our research should be considered. Larger samples of DME patients are needed to enrich the data and to improve the prediction accuracy. Moreover, data form more external validations are necessary to test the stability of prediction models. Additionally, the intelligent models for predicting the effect of different anti-VEGF treatments are essential to assist doctors in making a clinical plan.

DATA AVAILABILITY STATEMENT

The raw data supporting the conclusions of this article will be made available by the authors, without undue reservation.

ETHICS STATEMENT

Our ethics committee ruled that written informed consent was not required because our study was retrospective in nature and all the images were fully anonymized. Moreover, this study adhered to the tenets of the Declaration of Helsinki (2020KYPJ024). The patients/participants provided their written informed consent to participate in this study.

AUTHOR CONTRIBUTIONS

HX, SH, and C-HC conceived and designed the experiments. FX and XL collected the data. YX, FX, and XL labeled the data. SH and QL performed the experiments and analyzed the data. HX wrote the paper, and SH and CHC revised it. All authors read and approved the final manuscript.

FUNDING

This study was funded by the National Natural Science Foundation of China (Grant No. 71971224 and 71721001) and Guangdong Basic and Applied Basic Research Foundation (Grant No. 2020A1515011081). The sponsors of the study played no role in the study protocol design; data collection, analysis, or interpretation; manuscript preparation; or the decision to submit the manuscript for publication.

ACKNOWLEDGMENTS

The authors are grateful to the open APTOS data and all DME patients for supporting our study.

REFERENCES

1. Zimmet PZ. Diabetes and Its Drivers: The Largest Epidemic in Human History. *Clin Diabetes Endocrinol* (2017) 3:1. doi: 10.1186/s40842-016-0039-3
2. Bellary S, Kyrou I, Brown JE, Bailey CJ. Type 2 Diabetes Mellitus in Older Adults: Clinical Considerations and Management. *Nat Rev Endocrinol* (2021) 17:534–48. doi: 10.1038/s41574-021-00512-2
3. Zheng Y, Ley SH, Hu FB. Global Aetiology and Epidemiology of Type 2 Diabetes Mellitus and Its Complications. *Nat Rev Endocrinol* (2018) 14:88–98. doi: 10.1038/nrendo.2017.151
4. Holman N, Young B, Gadsby R. Current Prevalence of Type 1 and Type 2 Diabetes in Adults and Children in the UK. *Diabetes Med* (2015) 32:1119–20. doi: 10.1111/dme.12791
5. Flaxel CJ, Adelman RA, Bailey ST, Fawzi A, Lim JI, Vemulakonda GA, et al. Diabetic Retinopathy Preferred Practice Pattern®. *Ophthalmology* (2020) 127: P66–66P145. doi: 10.1016/j.ophtha.2019.09.025
6. Wang FH, Liang YB, Zhang F, Wang JJ, Wei WB, Tao QS, et al. Prevalence of Diabetic Retinopathy in Rural China: The Handan Eye Study. *Ophthalmology* (2009) 116:461–7. doi: 10.1016/j.ophtha.2008.10.003
7. Malhotra NA, Greenlee TE, Iyer AI, Conti TF, Chen AX, Singh RP. Racial, Ethnic, and Insurance-Based Disparities Upon Initiation of Anti-Vascular Endothelial Growth Factor Therapy for Diabetic Macular Edema in the US. *Ophthalmology* (2021) 128:1438–47. doi: 10.1016/j.ophtha.2021.03.010
8. Bressler SB, Odia I, Maguire MG, Dhoot DS, Glassman AR, Jampol LM, et al. Factors Associated With Visual Acuity and Central Subfield Thickness Changes When Treating Diabetic Macular Edema With Anti-Vascular Endothelial Growth Factor Therapy: An Exploratory Analysis of the Protocol T Randomized Clinical Trial. *JAMA Ophthalmol* (2019) 137:382–9. doi: 10.1001/jamaophthalmol.2018.6786
9. Brown DM, Ou WC, Wong TP, Kim RY, Croft DE, Wykoff CC. Targeted Retinal Photocoagulation for Diabetic Macular Edema With Peripheral Retinal Nonperfusion: Three-Year Randomized DAVE Trial. *Ophthalmology* (2018) 125:683–90. doi: 10.1016/j.ophtha.2017.11.026
10. Bhandari S, Nguyen V, Fraser-Bell S, Mehta H, Viola F, Baudin F, et al. Ranibizumab or Aflibercept for Diabetic Macular Edema: Comparison of 1-Year Outcomes From the Fight Retinal Blindness! Registry. *Ophthalmology* (2020) 127:608–15. doi: 10.1016/j.ophtha.2019.11.018
11. Glassman AR, Wells JA3rd, Josic K, Maguire MG, Antoszyk AN, Baker C, et al. Five-Year Outcomes After Initial Aflibercept, Bevacizumab, or Ranibizumab Treatment for Diabetic Macular Edema (Protocol T Extension Study). *Ophthalmology* (2020) 127:1201–10. doi: 10.1016/j.ophtha.2020.03.021
12. Bressler NM, Beaulieu WT, Glassman AR, Blinder KJ, Bressler SB, Jampol LM, et al. Persistent Macular Thickening Following Intravitreous Aflibercept, Bevacizumab, or Ranibizumab for Central-Involved Diabetic Macular Edema With Vision Impairment: A Secondary Analysis of a Randomized Clinical Trial. *JAMA Ophthalmol* (2018) 136:257–69. doi: 10.1001/jamaophthalmol.2017.6565
13. Wells JA, Glassman AR, Jampol LM, Aiello LP, Antoszyk AN, Baker CW, et al. Association of Baseline Visual Acuity and Retinal Thickness With 1-Year Efficacy of Aflibercept, Bevacizumab, and Ranibizumab for Diabetic Macular Edema. *JAMA Ophthalmol* (2016) 134:127–34. doi: 10.1001/jamaophthalmol.2015.4599
14. Reddy RK, Pieramici DJ, Gune S, Ghanekar A, Lu N, Quezada-Ruiz C, et al. Efficacy of Ranibizumab in Eyes With Diabetic Macular Edema and Macular

Nonperfusion in RIDE and RISE. *Ophthalmology* (2018) 125:1568–74. doi: 10.1016/j.ophtha.2018.04.002
15. Bandello F, Battaglia Parodi M, Lanzetta P, Loewenstein A, Massin P, Menchini F, et al. Diabetic Macular Edema. *Dev Ophthalmol* (2017) 58:102–38. doi: 10.1159/000455277
16. Kim EJ, Lin WV, Rodriguez SM, Chen A, Loya A, Weng CY. Treatment of Diabetic Macular Edema. *Curr Diabetes Rep* (2019) 19:68. doi: 10.1007/s11892-019-1188-4
17. Schmidt-Erfurth U, Garcia-Arumi J, Bandello F, Berg K, Chakravarthy U, Gerendas BS, et al. Guidelines for the Management of Diabetic Macular Edema by the European Society of Retina Specialists (EURETINA). *Ophthalmologica* (2017) 237:185–222. doi: 10.1159/000458539
18. Arima M, Nakao S, Yamaguchi M, Feng H, Fujii Y, Shibata K, et al. Claudin-5 Redistribution Induced by Inflammation Leads to Anti-VEGF-Resistant Diabetic Macular Edema. *Diabetes* (2020) 69:981–99. doi: 10.2337/db19-1121
19. Wells JA, Glassman AR, Ayala AR, Jampol LM, Bressler NM, Bressler SB, et al. Aflibercept, Bevacizumab, or Ranibizumab for Diabetic Macular Edema: Two-Year Results From a Comparative Effectiveness Randomized Clinical Trial. *Ophthalmology* (2016) 123:1351–9. doi: 10.1016/j.ophtha.2016.02.022
20. Banaee T, Ashraf M, Conti FF, Singh RP. Switching Anti-VEGF Drugs in the Treatment of Diabetic Macular Edema. *Ophthalmic Surg Lasers Imaging Retina* (2017) 48:748–54. doi: 10.3928/23258160-20170829-10
21. Virgili G, Parravano M, Evans JR, Gordon I, Lucenteforte E. Anti-Vascular Endothelial Growth Factor for Diabetic Macular Oedema: A Network Meta-Analysis. *Cochrane Database Syst Rev* (2017) 6:CD007419. doi: 10.1002/14651858.CD007419.pub5
22. Sun JK. Intravitreal Anti-VEGF Therapy With Prompt or Deferred Laser Compared With Steroid With Prompt Laser and Prompt Laser Alone for Treatment of Diabetic Macular Edema. *Curr Diabetes Rep* (2011) 11:227–9. doi: 10.1007/s11892-011-0201-3
23. Hussain RM, Ciulla TA. Treatment Strategies for Refractory Diabetic Macular Edema: Switching Anti-VEGF Treatments, Adopting Corticosteroid-Based Treatments, and Combination Therapy. *Expert Opin Biol Ther* (2016) 16:365–74. doi: 10.1517/14712598.2016.1131265
24. Mansour SE, Browning DJ, Wong K, Flynn HW Jr, Bhavsar AR. The Evolving Treatment of Diabetic Retinopathy. *Clin Ophthalmol* (2020) 14:653–78. doi: 10.2147/OPTH.S236637
25. Chang CK, Cheng CK, Peng CH. The Incidence and Risk Factors for the Development of Vitreomacular Interface Abnormality in Diabetic Macular Edema Treated With Intravitreal Injection of Anti-VEGF. *Eye (Lond)* (2017) 31:762–70. doi: 10.1038/eye.2016.317
26. Gabrielle PH, Massin P, Arnould L, Couturier A, Bouché-Pillon J, Maupin E, et al. Development of a 1-Year Risk-Prediction Nomogram for Good Functional Response With Anti-VEGF Agents in Naive Diabetic Macular Oedema. *Acta Ophthalmol* (2020) 98:e975–82. doi: 10.1111/aos.14428
27. Durand ML. Endophthalmitis. *Clin Microbiol Infect* (2013) 19:227–34. doi: 10.1111/1469-0691.12118
28. Cox JT, Eliott D, Sobrin L. Inflammatory Complications of Intravitreal Anti-VEGF Injections. *J Clin Med* (2021) 10:981–96. doi: 10.3390/jcm10050981
29. Lally DR, Shah CP, Heier JS. Vascular Endothelial Growth Factor and Diabetic Macular Edema. *Surv Ophthalmol* (2016) 61:759–68. doi: 10.1016/j.survophthal.2016.03.010
30. Wong TY, Cheung CM, Larsen M, Sharma S, Simó R. Diabetic Retinopathy. *Nat Rev Dis Primers* (2016) 2:16012. doi: 10.1038/nrdp.2016.12
31. Sun JK, Lin MM, Lammer J, Prager S, Sarangi R, Silva PS, et al. Disorganization of the Retinal Inner Layers as a Predictor of Visual Acuity in Eyes With Center-Involved Diabetic Macular Edema. *JAMA Ophthalmol* (2014) 132:1309–16. doi: 10.1001/jamaophthalmol.2014.2350
32. Chakroborty S, Gupta M, Devishamani CS, Patel K, Ankit C, Ganesh Babu TC, et al. Narrative Review of Artificial Intelligence in Diabetic Macular Edema: Diagnosis and Predicting Treatment Response Using Optical Coherence Tomography. *Indian J Ophthalmol* (2021) 69:2999–3008. doi: 10.4103/ijo.IJO_1482_21
33. Gunasekeran DV, Ting D, Tan G, Wong TY. Artificial Intelligence for Diabetic Retinopathy Screening, Prediction and Management. *Curr Opin Ophthalmol* (2020) 31:357–65. doi: 10.1097/ICU.0000000000000693
34. Gallardo M, Munk MR, Kurmann T, De Zanet S, Mosinska A, Karagoz IK, et al. Machine Learning Can Predict Anti-VEGF Treatment Demand in a Treat-And-Extend Regimen for Patients With Neovascular AMD, DME, and RVO Associated Macular Edema. *Ophthalmol Retina* (2021) 5:604–24. doi: 10.1016/j.oret.2021.05.002
35. Cao J, You K, Jin K, Lou L, Wang Y, Chen M, et al. Prediction of Response to Anti-Vascular Endothelial Growth Factor Treatment in Diabetic Macular Oedema Using an Optical Coherence Tomography-Based Machine Learning Method. *Acta Ophthalmol* (2021) 99:e19–19e27. doi: 10.1111/aos.14514
36. Liu B, Zhang B, Hu Y, Cao D, Yang D, Wu Q, et al. Automatic Prediction of Treatment Outcomes in Patients With Diabetic Macular Edema Using Ensemble Machine Learning. *Ann Transl Med* (2021) 9:43. doi: 10.21037/atm-20-1431
37. Kaye R, Chandra S, Sheth J, Boon C, Sivaprasad S, Lotery A. Central Serous Chorioretinopathy: An Update on Risk Factors, Pathophysiology and Imaging Modalities. *Prog Retin Eye Res* (2020) 79:100865. doi: 10.1016/j.preteyeres.2020.100865
38. van Lookeren Campagne M, LeCouter J, Yaspan BL, Ye W. Mechanisms of Age-Related Macular Degeneration and Therapeutic Opportunities. *J Pathol* (2014) 232:151–64. doi: 10.1002/path.4266
39. Ding X, Patel M, Chan CC. Molecular Pathology of Age-Related Macular Degeneration. *Prog Retin Eye Res* (2009) 28:1–18. doi: 10.1016/j.preteyeres.2008.10.001
40. Romero-Aroca P, Baget-Bernaldiz M, Pareja-Rios A, Lopez-Galvez M, Navarro-Gil R, Verges R. Diabetic Macular Edema Pathophysiology: Vasogenic Versus Inflammatory. *J Diabetes Res* (2016) 2016:2156273. doi: 10.1155/2016/2156273
41. Gandorfer A. Diffuse Diabetic Macular Edema: Pathology and Implications for Surgery. *Dev Ophthalmol* (2007) 39:88–95. doi: 10.1159/000098501

Conflict of Interest: The authors declare that the research was conducted in the absence of any commercial or financial relationships that could be construed as a potential conflict of interest.

frontiers in Endocrinology

SYSTEMATIC REVIEW
published: 29 March 2022
doi: 10.3389/fendo.2022.807687

Effectiveness of Panretinal Photocoagulation Plus Intravitreal Anti-VEGF Treatment Against PRP Alone for Diabetic Retinopathy: A Systematic Review With Meta-Analysis

Wuyue Zhang[1], *Jinsong Geng*[2] *and Aimin Sang*[3]*

[1] School of Medicine, Nantong University, Nantong, China, [2] Department of Medical Informatics, School of Medicine, Nantong University, Nantong, China, [3] Affiliated Hospital of Nantong University, Nantong, China

OPEN ACCESS

Edited by:
Subrata Chakrabarti,
Western University, Canada

Reviewed by:
Arup Das,
University of New Mexico,
United States
Biao Feng,
Western University, Canada

***Correspondence:**
Aimin Sang
sangam@ntu.edu.cn

Specialty section:
This article was submitted to Clinical Diabetes, a section of the journal Frontiers in Endocrinology

Received: 02 November 2021
Accepted: 31 January 2022
Published: 29 March 2022

Citation:
Zhang W, Geng J and Sang A (2022) Effectiveness of Panretinal Photocoagulation Plus Intravitreal Anti-VEGF Treatment Against PRP Alone for Diabetic Retinopathy: A Systematic Review With Meta-Analysis. Front. Endocrinol. 13:807687. doi: 10.3389/fendo.2022.807687

Objective: To compare the efficacy and safety of panretinal photocoagulation (PRP) combined with intravitreal anti-vascular endothelial growth factor (anti-VEGF) against PRP monotherapy for diabetic retinopathy (DR).

Methods: We searched Pubmed, Cochrane Library, Web of Science, Embase, and Science Direct Register of Controlled Trials from April 2011 to January 2021 to identify the randomized trials that compared the efficacy and safety between PRP combined with intravitreal anti-VEGF and PRP monotherapy for DR. We searched in the following databases between April 2011 and January 2021: Pubmed, Cochrane Library, Web of Science, Embase, and Science Direct without any restriction of countries or article type. The outcome measures were the best-corrected visual acuity (BCVA), neovascularization on the disc (NVD), neovascularization elsewhere (NVE), central macula thickness (CMT), and total retinal volume over time (FAS), and we also observed the adverse events (AEs) between the two groups.

Results: A total of 351 studies were identified, of which 11 studies were included in this meta-analysis (N = 1,182 eyes). Compared with PRP monotherapy, PRP plus anti-VEGF combination treatment produced a mean reduction in BCVA in units of logMAR of -0.23 [95% CI -0.32, -0.15] or a mean improvement in BCVA in units of letters of 4.99 [95% CI 3.79, 6.19], and also yielded a mean reduction in NVD of -28.41 [95% CI -30.30, -26.52], in NVE of -1.33 [95% CI -1.52, -1.14], in CMT of -1.33 [95% CI -1.52, -1.14], or in total FAS. No significant difference was observed on the risk of AEs as vitreous hemorrhage, elevation in intraocular pressure, and cataract between the two different treatments.

Conclusion: PRP with anti-VEGF combination treatment can achieve the ideal efficacy on DR by improving BCVA and NV regression, with no potential increased incidence of AEs, which proves that the combination therapy is an efficient therapeutic strategy that could improve the management of patients with DR.

Keywords: panretinal photocoagulation, anti-vascular endothelial growth factor, diabetic retinopathy, meta-analysis, combination therapy

INTRODUCTION

Diabetic retinopathy (DR) has become a leading cause of visual impairment in working age in industrialized countries. DR can be divided into two classifications including non-proliferative diabetic retinopathy (NPDR) and proliferative diabetic retinopathy (PDR), of which PDR is the more advanced stage leading to visual impairment and loss in the nearly total absence of symptoms (1). In recent decades, there have been a variety of treatments for DR, among which panretinal photocoagulation (PRP) and anti-vascular endothelial growth factor (anti-VEGF) therapy are commonly used. VEGF is a kind of homodimeric glycoprotein, including PLGF, VEGF-A, VEGF-B, VEGF-C, and VEGF-D. VEGF can promote endothelial cell-specific mitogen, increase vascular permeability, and promote inflammation (2). Under the condition of high glucose, oxidative stress, hemodynamic changes, and inflammatory reactions are involved in the regulation of VEGF expression and increase the concentration of VEGF. VEGF increases capillary permeability by the phosphorylation of tight-junction protein, leading to macular edema and angiogenesis (3). Therefore, inhibition of VEGF has become an important part of anti-neovascularization therapy. Anti-VEGF agents available include bevacizumab, ranibizumab, and aflibercept and are gaining popularity by intravitreal injection while the mainstay of surgical treatment for PDR is Scatter, or panretinal, photocoagulation (4).

Both treatments have a positive effect on delaying the progression of DR, and they also have been combined many times in clinical practice. However, the efficacy of monotherapy and combined treatment may be different. Some adverse events can be found in the follow-up of both therapies. Administration or surgery methods may cause some ocular disorders such as vitreous hemorrhage, elevation in intraocular pressure, and cataract, and pesticide effects may result in some non-ocular disorders such as hypertension.

In order to inform in clinical decision-making which treatment can be preferred to use clinically, this meta-analysis examined 11 randomized controlled trials (RCTs), with patients from Canada, the United States, Pakistan, Brazil, and other countries, trying to compare the efficacy and safety of PRP with intravitreal anti-VEGF-combined treatment against PRP monotherapy.

METHODS

Search Strategy and Selection Criteria

This meta-analysis is reported in accordance with the Systematic Reviews and Meta-Analyses (PRISMA) Statement. The registration number in PROSPERO is CRD42021254750.

We searched Pubmed, Cochrane Library, Web of Science, Embase, and Science Direct Register of Controlled Trials between April 2011 and January 2021 to identify the randomized trials that compared the efficacy and safety between PRP combined with intravitreal anti-VEGF and PRP monotherapy for DR. We selected several studies published between April 2011 and January 2021. We searched the following databases: Pubmed, Cochrane Library, Web of Science, Embase, and Science Direct without any restriction of countries or article type. The reference list of all selected articles is independently screened to identify additional studies left out in the initial search. We used the combined search strategy with text and MESH terms as follows: ((“Diabetic Retinopathy”[Mesh]) OR ((proliferative diabetic retinopathy[Title/Abstract]) OR PDR[Title/Abstract])) AND (((“retinal laser photocoagulation”[Mesh]) OR retinal laser photocoagulation [Title/Abstract])) AND (((((((VEGF[Title/Abstract]) OR anti VEGF [Title/Abstract]) OR anti-VEGF [Title/Abstract]) OR lucentis[Title/Abstract]) OR bevacizumab[Title/Abstract]) OR ranibizumab [Title/Abstract]) OR aflibercept[Title/Abstract])) AND (“Randomized Controlled Trial” [Publication Type]).

Eligibility Criteria

Eligible studies are regarded as RCTs, comparing PRP plus anti-VEGF with PRP alone, reporting changes in best-corrected visual acuity (BCVA), neovascularization on the disc (NVD), neovascularization elsewhere (NVE), central macula thickness (CMT), or total retinal volume over time (FAS). We exclude studies in adherence to the following criteria: non-RCT studies, studies done in patients treated with drug monotherapy, and combination therapy on DR. We did not impose restriction on history of systemic treatment.

The primary outcomes were assessed as follows: the changes of BCVA (logMAR, letters), the regression of neovascularization defined as NVD (percentage of disc surface, DD%), NVE (disc diameter, DD), CMT (μm), and total retinal volume. The incidences of adverse events (AEs) were estimated as secondary outcomes, including vitreous hemorrhage, elevation in intraocular pressure, and cataract.

Data Extraction

Two investigators collaborated on assessing these studies together, reviewing the titles and abstracts and retrieving studies satisfied for full-text assessment. Studies qualified were selected by two investigators with an agreement value of 99.4%. Disagreements were settled by a third investigator.

We extracted data in a standardized form from each selected study. The data included the first author and year of each study,

total number of patients participated, age, follow-up period, details of therapeutic method, change in BCVA (mean [SD]), change in CMT (mean [SD]), change in BCVA (mean [SD]), change in NVD (mean [SD]), change in NVE (mean [SD]), change in total retinal volume (mean [SD]), and incidence of AEs.

In some cases where the data were ambiguous, we emailed some of the relevant corresponding authors to refine the data obtained.

Statistical Analysis

We assessed the efficacy of PRP plus anti-VEGF agents versus PRP monotherapy on four outcomes: BCVA, regression of neovascularization (NVD, NVE, CMT), total retinal volume, and incidence of any AEs.

We analyzed BCVA, NVD, NVE, CMT, and total retinal volume as continuous variables and calculated pooled estimates of the mean differences (MD) in changes of BCVA, NVD, NVE, CMT, and total retinal volume of study groups and control groups by using a random-effect (RE) model to depict the characteristics of each group.

The incidence of AEs common in eligible studies was analyzed, from which an overall relative risk (ORR) was calculated. The pooled estimates of the relative risk with an RE model were also calculated.

As we divided studies into groups with data in common and the data set that counted changes in CMT contained a relatively large number of studies, which was seven, we assessed publication bias of the CMT group using Egger test and defined significant publication bias as a p value <0.05 (5).

Risk-of-Bias Assessment

Cochran Q test and the I^2 statistics were employed to assess heterogeneity between studies. I^2 values greater than 50% represent moderate to high heterogeneity, while I^2 values lower than 50% represent low heterogeneity (6). We investigated sources of heterogeneity through subgroup analyses. Review Manager (version 5.4, Cochrane Collaboration) and STATA (version 15.1, STATA Corp) were used for all statistical analyses. Further sensitivity analysis was also performed to confirm whether the heterogeneity had an impact on the conclusions.

RESULTS

We identified 351 studies initially, of which 11 studies were included in this meta-analysis (**Figure 1**). The 11 studies were published from April 2011 to January 2021 (**Table 1**) (7–17). Follow-up duration ranges from 1 to 12 months. 9 studies (7, 8, 11–17) reported changes of BCVA, among which 4 studies (7, 12, 16, 17) specified the changes of BCVA in logMAR and 5 studies (8, 11, 13–15) in letters. 7 studies (9–11, 13, 15–17) measured the changes of CMT. 2 studies (7, 16) reported changes of NVD and NVE, which were specified in DD% and DD. One study (10) measured the change of mean total retinal volume over time in units of mm^3 while the other study measured the changes of neovascularization total (NVT) in units of disc area (DA) (8). Adverse events were assessed by 6 studies (8, 10, 11, 13–15), of which 3 reported vitreous hemorrhage (8, 11, 15), 3 reported elevation in intraocular pressure (8, 10, 11), and 4 reported cataract (8, 11, 13, 14). One study (9) observed no adverse effects. We also assessed the risk of bias of all the 11 RCTs (**Figure 2**).

In the pooled analysis of 9 trials, the results showed that combination therapy had a better impact on improving or

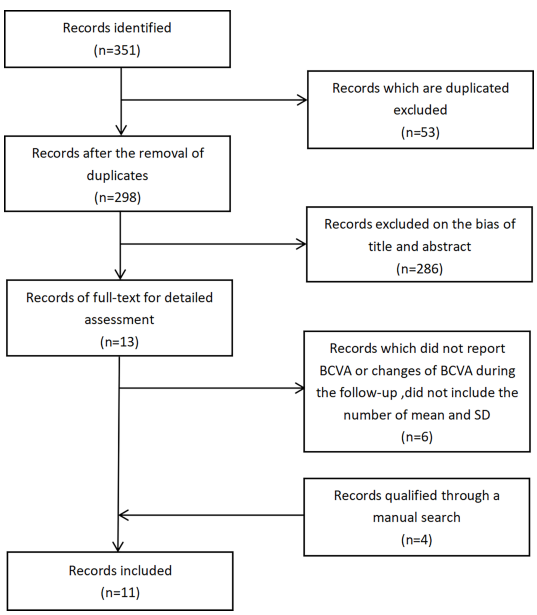

FIGURE 1 | Process of study selection.

TABLE 1 | Characteristics of included studies.

Study ID (first author)	Year	Design	Sample size (eyes)	Case/control (PRP plus IVB/PRP)	Average age/age range (case/control)	Details of anti-VEGF agent injection	Details of laser photocoagulation	Intraoperative and postoperative evaluating parameters	Follow-up periods (months)
Ali et al. (7)	2018	RCT	60	30/30	(40–52)/(53–65); (52.27 ± 6.8)	IVB (1.25 mg 0.05 ml) 15 days prior to PRP session	1,500–2,000 shots (200–500 μm spots), 0.05–0.1-s duration, 0.1 interval, 300–500-W power per episode, under topical anesthesia	BCVA, NVE, NVD	3
Figueira et al. (8)	2018	RCT	87	41/46	(58.8 ± 13.3)/(52.0 ± 11.9)	IVR, in month 0, month 1, and month 2 combined with the standard PRP treatment, that is, with 1, 2, or 3 laser sessions	1,200–1,600 scatter laser burns (500 μm spots)	BCVA, NVE, NVD, NVT, CMT, AEs	12
Preti et al. (9)	2017	RCT	38	19/19	(53.4 ± 9.3)/(53.4 ± 9.3)	IVB (1.25 mg/0.05 ml) 7 days prior to PRP session and at the end of the third PRP episode.	A spot size of 250 μm, an exposure time between 0.1 and 0.2-m, and a moderate intensity (200 to 500 mW)	CMT, choroidal thickness, AEs	1
Lang et al. (10)	2018	RCT	128	85/43	(63.5 ± 9.3)/(63.5 ± 10.5)	IVR (0.5 mg), 4 monthly	Focal laser and ranibizumab injections were administered on the same day with a minimum interval of 30 min between the two treatments	BCVA, FCS, and FCP thickness, CMT, AEs	6.2 ± 2.7
Berger et al. (11)	2015	RCT	145	73/72	(60.8 ± 10.2)/(62.8 ± 9.4)	IVR (0.5 mg ranibizumab intravitreal injections), 3 monthly injections followed by as-needed therapy	On day one. If required, the initial photocoagulation could be split into 2 sessions, 4 weeks apart	BCVA, CMT, VFQ-25 (Visual Function Questionnaire-25), AEs	12
Messias et al. (12)	2012	RCT	20	11/9	(59 ± 12)/(64 ± 8)	IVR ((0.5 mg/0.05 ml), at weeks 16 and 32	Six to eight hundred 500 lm spots were applied per session	BCVA, duration of diabetes, FLA	6
Mitchell et al. (13)	2011	RCT	229	118/111	(64.0 ± 8.15)/(63.5 ± 8.81)	IVR (0.5 mg), at months 0–2; treatment initiation phase	2 sessions, 4 weeks apart	BCVA, CMT, AEs	12
Ishibashi et al. (14)	2015	RCT	263	132/131	(61.2 ± 10.52)/(61.5 ± 9.68)	IVR (0.5 mg), on day 1 and continued monthly until stable vision was achieved	On day 1 (if needed, the first laser treatment session could be split into 2 sessions 4 weeks apart)	BCVA, AEs	12
Ferraz et al. (15)	2015	RCT	60	30/30	52.3 ± 7.8	IVR (0.5 mg) and were given again at Month 1	Full-scatter PRP treatment, performed in three sessions according to the ETDRS guidelines	BCVA, CMT, AEs	6
Rebecca et al. (16)	2021	RCT	76	38/38	(51.1 ± 5.9)/(50.7 ± 6.9)	IVB (1.25 mg/0.05 ml). In Group B subjects, first intravitreal bevacizumab injection (1.25 mg/0.05 ml) was given followed by PRP after the 1st week, likewise 2 more PRP episodes were done, and a second IVB injection was given at the end of the 3rd PRP session.	Three sessions of PRP were done with a 1-week interval; two thousand burns were applied at the 1st session with a 200-μm spot size, duration of 20-ms pulse, and from 400 to 500 mW power to achieve grayish burns; and further PRP was done at 1 and 2 months with supplementary 800–1,000 burns	BCVA, NVE, NVD, CMT	6
Sameen et al. (17)	2017	RCT	76	38/38	(57.47 ± 6.08)/(55.69 ± 6.58)	IVB (2.5 mg/0.1 ml) 1 day after PRP session and repeated monthly for 3 months.	Two thousand burns were applied at the 1st session with a 20-ms pulse duration, 200-μm spot size, and power ranging from 350 to 600 mW, titrating the burn intensity until a mild gray reaction was achieved, repeating at 4 weeks and 8 weeks with an additional 800–1,000 burns	BCVA, CMT	3

delaying vision deterioration in BCVA, compared to monotherapy, with a statistically significant between-study heterogeneity (**Figure 3**). Sensitivity analysis was performed in the BCVA group with LogMAR as the unit. Since one of the studies (17) enrolled patients with PDR and DME, while the other studies included patients with or without DME, this might be the reason for the heterogeneity. However, the removal of the study had no effect on the results, which still showed the priority of the combination therapy on improvements of BCVA after the exclusion. The other indicators (NVD, NVE, CMT) (**Figure 4**)

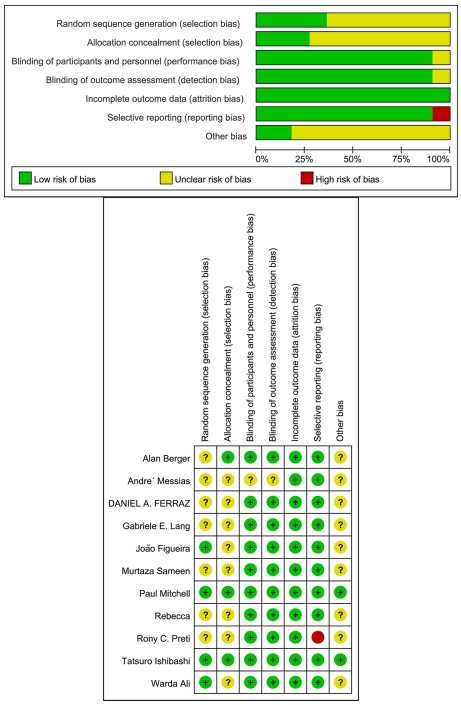

FIGURE 2 | Risk of bias.

all showed a mean overall reduction in favor of PRP plus anti-VEGF treatment, with no significant between-study heterogeneity. For the assessment of publication bias of the CMT group shown in the table (p value >0.05) (**Figure 5**), no significant publication bias was detected.

In addition, two studies separately reported changes of NVT (8) and the mean total retinal volume (10), supporting the findings above (**Figure 6**).

6 studies reported the incidence of adverse events, including intraocular or extraocular disorders if present. The pooled

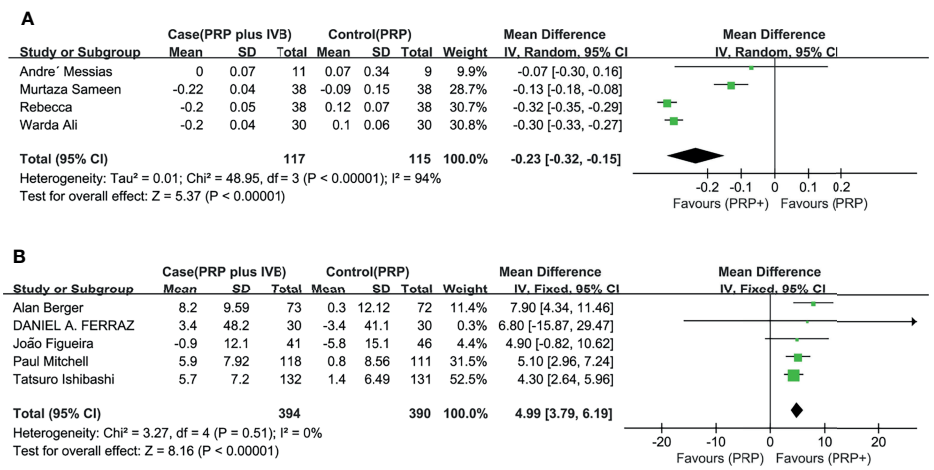

FIGURE 3 | Meta-analyses of PRP+anti-VEGF treatment and PRP monotherapy, comparing changes of BCVA (logMAR, letters). **(A)** BCVA (logMAR), **(B)** BCVA (letters). Outcomes assessed: BCVA in studies that compared combination treatment with PRP monotherapy. The shaded area is the weight of the estimate in proportion to the overall effect.

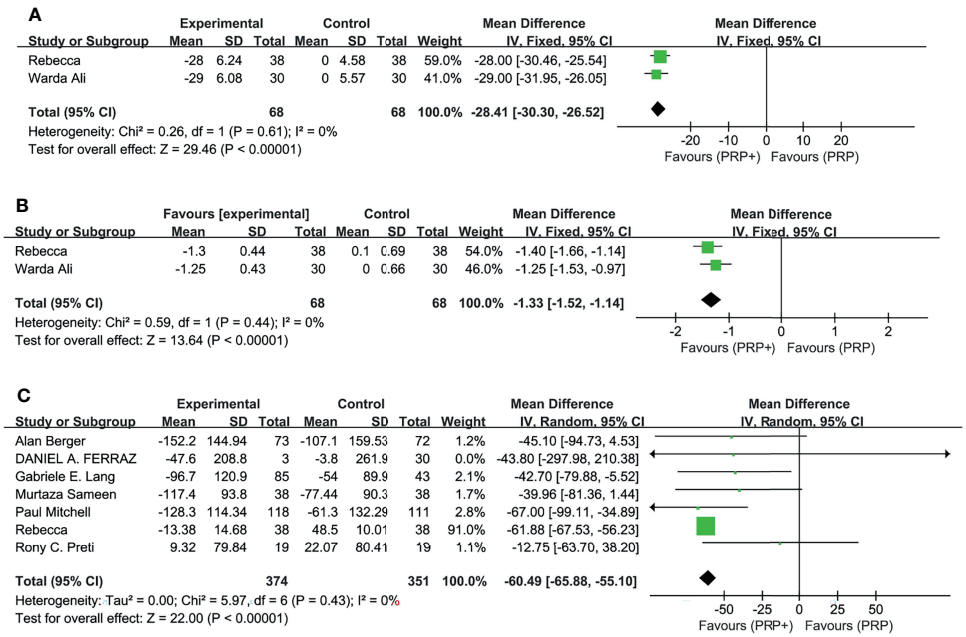

FIGURE 4 | Meta-analyses of PRP+anti-VEGF treatment and PRP monotherapy, comparing changes of NVD (DD%), NVE (DD), and CMT (μm). **(A)** NVD (DD%), **(B)** NVE (DD), and **(C)** CMT (μm). Outcomes assessed: NVD, NVE, and CMT in studies that compared combination treatment with PRP monotherapy. The shaded area is the weight of the estimate in proportion to the overall effect.

analysis (**Figure 7**) showed no significant difference in the RR of the study group compared with the control group, with no significant between-study heterogeneity. Combination therapy or monotherapy had little effect on the incidence of adverse events such as vitreous hemorrhage, elevation in intraocular pressure, and cataract.

DISCUSSION

In the previous study, anti-VEGF monotherapy has been reported to show potential benefits compared to PRP monotherapy. However, anti-VEGF monotherapy also carries a certain degree of risk for PDR. For example, anti-VEGF

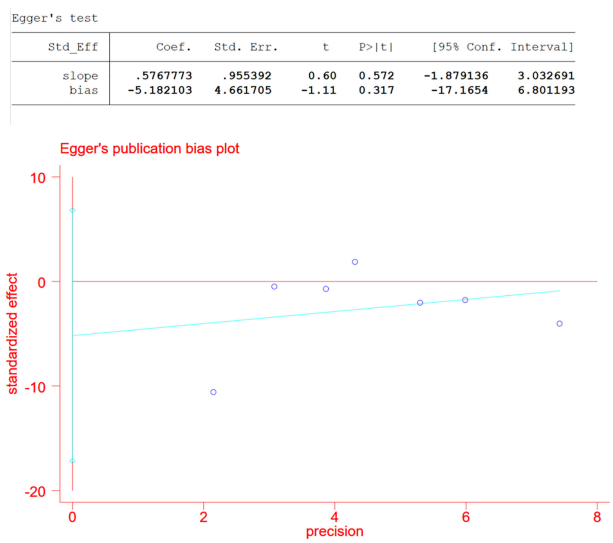

FIGURE 5 | Estimate of publication bias of CMT.

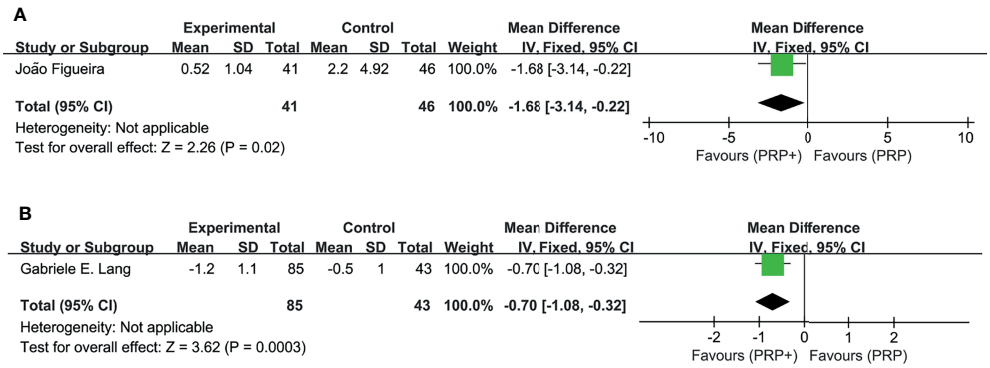

FIGURE 6 | Meta-analyses of PRP+anti-VEGF treatment and PRP monotherapy, comparing changes of NVT (DA) and total retinal volume (mm3). **(A)** NVT (DA). **(B)** Total retinal volume (mm3). Outcomes assessed: BCVA in studies that compared combination treatment with PRP monotherapy. The shaded area is the weight ofthe estimate in proportion to the overall effect.

treatment is expensive, time-consuming, and not cost-effective. In countries and regions with limited resources, this treatment is easily restricted. In addition, it is easy for patients who are treated exclusively with anti-VEGF to cause complications such as tractional retinal detachment and neovascular glaucoma, leading to blindness (18). Our study showed that the combination therapy is even more beneficial. The PRP plus anti-VEGF treatment is better at delaying vision loss associated with DR and also contributing to the reduction of NVD, NVE, and CMT, compared to PRP monotherapy. It is worth mentioning that application of a more complex therapeutic method did not cause more adverse effects than monotherapy. Previous studies have reported the role of anti-VEGF agents as adjuncts to surgical treatment, regressing neovascularization and

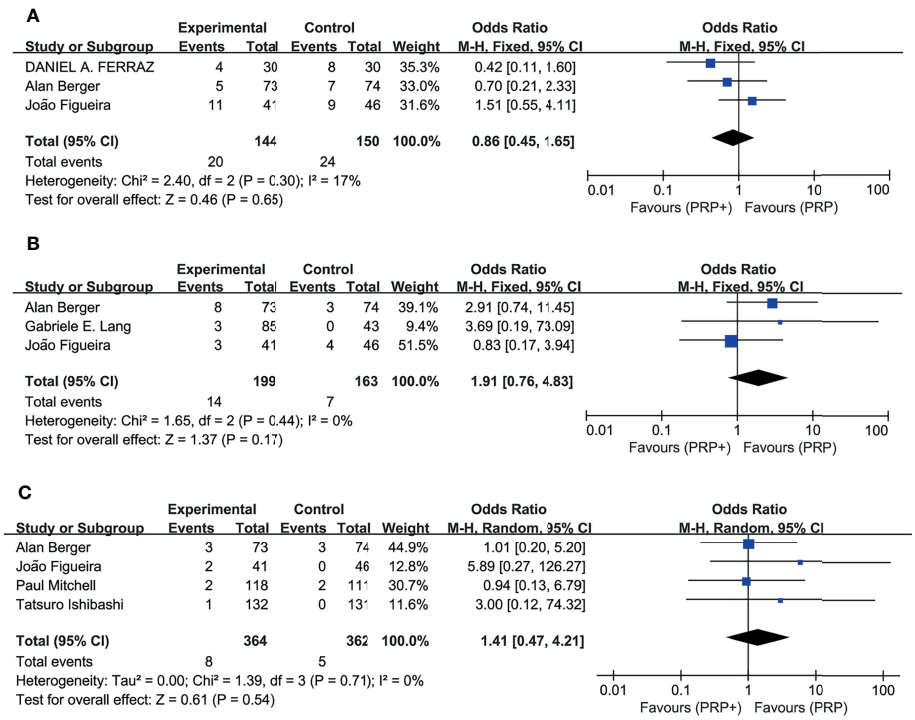

FIGURE 7 | Meta-analyses of PRP+anti-VEGF treatment and PRP monotherapy, comparing incidence of AEs. **(A)** Vitreous hemorrhage. **(B)** Elevation in intraocular pressure. **(C)** Cataract. Outcomes assessed: incidence of vitreous hemorrhage, elevation in intraocular pressure, and cataract in studies that compared combination treatment with PRP monotherapy. The shaded area is the weight of the estimate in proportion to the overall effect.

minimizing bleeding and complications followed by vitrectomy and endolaser for a vitreous hemorrhage (19). Findings in these meta-analyses proved the well-documented efficacy and safety of anti-VEGF.

Retinal detachments have been observed in some PRP groups, which is likely to be associated with anti-VEGF injections in PDR eyes (20), but studies included in this analysis did not have any cases of this probably because eyes were excluded with fibrovascular proliferation with retinal traction.

Most of the studies identified the included patients as DME, PDR, or high-risk PDR (HR-PDR) (7–14, 16, 17). Retinal ischemia has been reported to be present in high-risk PDR in the previous study (21). Preoperative anti-VEGF injections in DR may reduce the bleeding during an operation and decrease the complications (22). Our findings showed that the combination might benefit patients with DME and PDR, by reducing the incidence of complications. In addition, combination therapy consistently improved BCVA and reduced CMT across all the patients with PDR, including patients with DME. Further studies are needed to confirm the beneficial effect of additional anti-VEGF treatment in NPDR patients.

Our results compared anti-VEGF monotherapy with combination therapy in terms of effects on visual improvement, retinal angiogenesis, and the incidence of adverse events, which would give some feasible suggestions on evidence-based clinical practice. A limitation of this analysis is that all the follow-up periods are less than 1 year. Longer follow-up studies may establish the benefit or adverse effects more clearly. Another limitation is the fact that the difference between the DME and non-DME groups cannot be concluded from the data in the RCTs, due to the short follow-up duration or the small sample sizes. The long-term results from relevant studies further showed that response to anti-VEGF is sustained through the period of 2 years (23), and 3 years (24), and the longer the duration, the fewer the injections to control edema, from which we hypothesized that a longer follow-up period would help reveal the relationship between lesion severity and response to treatment.

It has been reported that the intensity of anti-VEGF treatment has a statistically significant effect on BCVA, but there is no confirmed clinical evidence (25). Compared with clinical treatment, the injection intensity in clinical trials is often very high, while in clinical practice, the treatment intensity of many treatment plans is not high in the first year resulting in poorer visual effect and more inaccurate estimation.

In conclusion, Intravitreal anti-VEGF agents for a certain duration are effective as adjunctive treatment to PRP with less foveal thickness, early and greater rate of retinal neovessel regression, and better vision improvement rates than PRP alone in patients of DR.

AUTHOR CONTRIBUTIONS

WZ was in charge of the writing of manuscript and analyzing of data while JG was in charge of collecting the data. AS was the corresponding author. All authors contributed to the article and approved the submitted version.

REFERENCES

1. Porta M, Maldari P, Mazzaglia F. New Approaches to the Treatment of Diabetic Retinopathy. *Diabetes Obes Metab* (2011) 13(9):784–90. doi: 10.1111/j.1463-1326.2011.01415.x
2. Takahashi H, Shibuya M. The Vascular Endothelial Growth Factor (VEGF)/ VEGF Receptor System and Its Role Under Physiological and Pathological Condition. *Clin Sci (Lond)* (2005) 109(3):227–41. doi: 10.1042/CS20040370
3. Zheng B, Li T, Chen H, Xu X, Zheng Z. Correlation Between Ficolin-3 and Vascular Endothelial Growth Factor-to-Pigment Epithelium-Derived Factor Ratio in the Vitreous of Eyes With Proliferative Diabetic Retinopathy. *Am J Ophthalmol* (2011) 152(6):1039–43. doi: 10.1016/j.ajo.2011.05.022
4. Bressler NM, Beck RW, Ferris FL3rd. Panretinal Photocoagulation for Proliferative Diabetic Retinopathy. *N Engl J Med* (2011) 365(16):1520–6. doi: 10.1056/NEJMct0908432
5. Higgins JP, Thompson SG, Deeks JJ, Altman DG. Measuring Inconsistency in Meta-Analyses. *BMJ* (2003) 327(7414):557–60. doi: 10.1136/bmj.327.7414.557
6. Higgins JP, Thompson SG. Quantifying Heterogeneity in a Meta-Analysis. *Stat Med* (2002) 21(11):1539–58. doi: 10.1002/sim.1186
7. Ali W, Abbasi KZ, Raza A. Panretinal Photocoagulation Plus Intravitreal Bevacizumab Versus Panretinal Photocoagulation Alone for Proliferative Diabetic Retinopathy. *J Coll Physicians Surg Pak* (2018) 28(12):923–7. doi: 10.29271/jcpsp.2018.12.923
8. Figueira J, Fletcher E, Massin P, Silva R, Bandello F, Midena E, et al. Ranibizumab Plus Panretinal Photocoagulation Versus Panretinal Photocoagulation Alone for High-Risk Proliferative Diabetic Retinopathy (PROTEUS Study). *Ophthalmology* (2018) 125(5):691–700. doi: 10.1016/j.ophtha.2017.12.008
9. Preti RC, Mutti A, Ferraz DA, Zacharias LC, Nakashima Y, Takahashi WY, et al. The Effect of Laser Pan-Retinal Photocoagulation With or Without Intravitreal Bevacizumab Injections on the OCT-Measured Macular Choroidal Thickness of Eyes With Proliferative Diabetic Retinopathy. *Clinics* (2017) 72(2):81–6. doi: 10.6061/clinics/2017(02)03
10. Lang GE, Liakopoulos S, Vogeler J, Weiss C, Spital G, Gamulescu MA, et al. The RELATION Study: Efficacy and Safety of Ranibizumab Combined With Laser Photocoagulation Treatment Versus Laser Monotherapy in NPDR and PDR Patients With Diabetic Macular Oedema. *Acta Ophthalmol* (2018) 96(3): e377–85. doi: 10.1111/aos.13574
11. Berger A, Sheidow T, Cruess AF, Arbour JD, Courseau AS, Takacsy F. Efficacy/safety of Ranibizumab Monotherapy or With Laser Versus Laser Monotherapy in DME. *Can J Ophthalmol* (2015) 50(3):209–16. doi: 10.1016/j.jcjo.2014.12.014
12. Messias A, Ramos Filho JA, Messias K, Almeida FP, Costa RA, Scott IU, et al. Electroretinographic Findings Associated With Panretinal Photocoagulation (PRP) Versus PRP Plus Intravitreal Ranibizumab Treatment for High-Risk Proliferative Diabetic Retinopathy. *Doc Ophthalmol* (2012) 124(3):225–36. doi: 10.1007/s10633-012-9322-5
13. Mitchell P, Bandello F, Schmidt-Erfurth U, Lang GE, Massin P, Schlingemann RO, et al. The RESTORE Study: Ranibizumab Monotherapy or Combined With Laser Versus Laser Monotherapy for Diabetic Macular Edema. *Ophthalmology* (2011) 118(4):615–25. doi: 10.1016/j.ophtha.2011.01.031
14. Ishibashi T, Li X, Koh A, Lai TY, Lee FL, Lee WK, et al. The REVEAL Study: Ranibizumab Monotherapy or Combined With Laser Versus Laser Monotherapy in Asian Patients With Diabetic Macular Edema. *Ophthalmology* (2015) 122(7):1402–15. doi: 10.1016/j.ophtha.2015.02.006
15. Ferraz DA, Vasquez LM, Preti RC, Motta A, Sophie R, Bittencourt MG, et al. A Randomized Controlled Trial of Panretinal Photocoagulation With and Without Intravitreal Ranibizumab in Treatment-Naive Eyes With Non-High-Risk Proliferative Diabetic Retinopathy. *Retina* (2015) 35(2):280–7. doi: 10.1097/IAE.0000000000000363

16. Rebecca, Shaikh FF, Jatoi SM. Comparison of Efficacy of Combination Therapy of an Intravitreal Injection of Bevacizumab and Photocoagulation Versus Pan Retinal Photocoagulation Alone in High Risk Proliferative Diabetic Retinopathy. *Pak J Med Sci* (2021) 37(1):157–61. doi: 10.12669/pjms.37.1.3141
17. Sameen M, Khan MS, Mukhtar A, Yaqub MA, Ishaq M. Efficacy of Intravitreal Bevacizumab Combined With Pan Retinal Photocoagulation Versus Panretinal Photocoagulation Alone in Treatment of Proliferative Diabetic Retinopathy. *Pak J Med Sci* (2017) 33(1):142–5. doi: 10.12669/pjms.331.11497
18. Yates WB, Mammo Z, Simunovic MP. Intravitreal Anti-Vascular Endothelial Growth Factor Versus Panretinal LASER Photocoagulation for Proliferative Diabetic Retinopathy: A Systematic Review and Meta-Analysis. *Can J Ophthalmol* (2021) 56(6):355–63. doi: 10.1016/j.jcjo.2021.01.017
19. Jardeleza MS, Miller JW. Review of Anti-VEGF Therapy in Proliferative Diabetic Retinopathy. *Semin Ophthalmol* (2009) 24(2):87–92. doi: 10.1080/08820530902800330
20. Arevalo JF, Maia M, Flynn HWJr., Saravia M, Avery RL, Wu L, et al. Tractional Retinal Detachment Following Intravitreal Bevacizumab (Avastin) in Patients With Severe Proliferative Diabetic Retinopathy. *Br J Ophthalmol* (2008) 92(2):213–6. doi: 10.1136/bjo.2007.127142
21. Nilsson SE. Human Retinal Vascular Obstructions. A Quantitative Correlation of Angiographic and Electroretinographic Findings. *Acta Ophthalmol (Copenh)* (1971) 49:111–33.
22. Han XX, Guo CM, Li Y, Hui YN. Effects of Bevacizumab on the Neovascular Membrane of Proliferative Diabetic Retinopathy: Reduction of Endothelial Cells and Expressions of VEGF and HIF-1α. *Mol Vision* (2012) 18:1–9.
23. Nguyen QD, Shah SM, Khwaja AA, Channa R, Hatef E, V Do D, et al. Two-Year Outcomes of the Ranibizumab for Edema of the Macula in Diabetes (READ-2) Study. *Ophthalmology* (2010) 117:2146–51. doi: 10.1016/j.ophtha.2010.08.016
24. Schmidt-Erfurth U, Lang GE, Holz FG, Schlingemann RO, Lanzetta P, Massin P, et al. Three-Year Outcomes of Individualized Ranibizumab Treatment in Patients With Diabetic Macular Edema: The RESTORE Extension Study. *Ophthalmology* (2014) 121(5):1045–53. doi: 10.1016/j.ophtha.2013.11.041
25. Li E, Donati S, Lindsley KB, Krzystolik MG, Virgili G. Treatment Regimens for Administration of Anti-Vascular Endothelial Growth Factor Agents for Neovascular Age-Related Macular Degeneration. *Cochrane Database Syst Rev* (2020) 5(5):8. doi: 10.1002/14651858.CD012208.pub2

Conflict of Interest: The authors declare that the research was conducted in the absence of any commercial or financial relationships that could be construed as a potential conflict of interest.

frontiers | Frontiers in Endocrinology

ORIGINAL RESEARCH
published: 07 April 2022
doi: 10.3389/fendo.2022.851967

Expressions of Serum lncRNAs in Diabetic Retinopathy – A Potential Diagnostic Tool

Saumik Biswas[1†], *Ali Coyle*[2†], *Shali Chen*[1], *Miso Gostimir*[3], *John Gonder*[3] *and Subrata Chakrabarti*[1*]

[1] Department of Pathology and Laboratory Medicine, Western University, London, ON, Canada, [2] School of Biomedical Engineering, Western University, London, ON, Canada, [3] Department of Ophthalmology, Western University, London, ON, Canada

OPEN ACCESS

Edited by:
Ping Wang,
Michigan State University,
United States

Reviewed by:
Xuan Shi,
Peking University People's Hospital,
China
Donato Santovito,
National Research Council (CNR), Italy
Aixia Sun,
Michigan State University,
United States

***Correspondence:**
Subrata Chakrabarti
subrata.chakrabarti@lhsc.on.ca

[†]*These authors have contributed equally to this work*

Specialty section:
This article was submitted to Clinical Diabetes, a section of the journal Frontiers in Endocrinology

Received: *11 January 2022*
Accepted: *03 March 2022*
Published: *07 April 2022*

Citation:
Biswas S, Coyle A, Chen S, Gostimir M, Gonder J and Chakrabarti S (2022) Expressions of Serum lncRNAs in Diabetic Retinopathy – A Potential Diagnostic Tool. Front. Endocrinol. 13:851967. doi: 10.3389/fendo.2022.851967

With increasing incidence of diabetes worldwide, there is an ever-expanding number of patients with chronic diabetic complications such as diabetic retinopathy (DR), one of the leading causes of blindness in the working age population. Early screening for the onset and severity of DR is essential for timely intervention. With recent advancements in genomic technologies, epigenetic alterations in DR are beginning to unravel. Long non-coding RNAs (lncRNAs), which are key epigenetic mediators, have demonstrated implications in several (DR) related processes. Based on the previous research, we have developed a serum-based, multi-panel PCR test using 9 lncRNAs (*ANRIL*, *MALAT1*, *WISPER*, *ZFAS1*, *H19*, *HOTAIR*, *HULC*, *MEG3*, and *MIAT*) to identify and validate whether this panel could be used as a diagnostic and prognostic tool for DR. We initially used a cell culture model (human retinal endothelial cells) and confirmed that 25 mM glucose induces upregulations of *ANRIL*, *HOTAIR*, *HULC*, *MALAT1*, and *ZFAS1*, and downregulation of *H19* compared to 5 mM glucose controls. Then as an initial proof-of-concept, we tested vitreous humor and serum samples from a small cohort of non-diabetic (N=10) and diabetic patients with proliferative retinopathy (PDR, N=11) and measured the levels of the 9 lncRNAs. Differential expressions of lncRNAs were found in the vitreous and serum of patients and showed significant correlations. We expanded our approach and assessed the same lncRNAs using samples from a larger cohort of diabetic (n= 59; M/F:44/15) and non-diabetic patients (n= 11; M/F:4/7). Significant increased lncRNA expressions of *ANRIL*, *H19*, *HOTAIR*, *HULC*, *MIAT*, *WISPER* and *ZFAS1* were observed in the serum of diabetic patients (with varying stages of DR) compared to non-diabetics. No significant correlations were demonstrated between lncRNA expressions and creatinine or glycated hemoglobin (HbA1C) levels. Using ROC and further analyses, we identified distinct lncRNA phenotype combinations, which may be used to identify patients with DR. Data from this study indicate that a panel of serum lncRNAs may be used for a potential screening test for DR. Further large-scale studies are needed to validate this notion.

Keywords: lncRNA, epigenetics, diabetic retinopathy, biomarker, diagnosis

INTRODUCTION

Diabetes mellitus (DM) continues to wreak havoc across the world, where 463 million of the global population are estimated to have DM, while 700 million are projected to have DM by 2045 (1). DM is characterized by chronic hyperglycemia and the sustained elevation of blood glucose levels promotes cellular and tissue damage, which consequently leads to the development of diabetic complications. Among these complications, diabetic retinopathy (DR) is a prevalent microvascular complication of DM and one of the leading causes of preventable blindness in the working age population (2). To prevent irreversible visual loss from DR, screening for the onset and severity of DR has become critical for timely and necessary ophthalmic examination and treatment (3). To bridge this gap in healthcare delivery, here we describe a novel lncRNA-based serum test which may facilitate effective screening and identification of DR.

According to the International Council of Ophthalmology classification, DR can be categorized into five progressive stages of retinopathy: no retinopathy, mild non-proliferative, moderate non-proliferative, severe non-proliferative, and proliferative retinopathy (4). Each stage of DR is categorized by distinct clinical observations, which can include retinal vascular-related abnormalities (microaneurysms, intraretinal hemorrhages, and venous beading), retinal thickening (edema), accumulation of lipid deposits, presence of neovascularization, and/or vitreous/preretinal hemorrhage (4). According to one study in the US involving 4617 patients, 6.6% of patients with non-proliferative DR (NPDR) progressed to proliferative DR (PDR). Proliferative DR is considered the more advanced stage of DR and is characterized by the onset of neovascularization at various retinal regions (including new vessels at the inner surface of the retina, on or near the optic disc and new vessels elsewhere in the retina) compared to non-proliferative stages of DR (4, 5). These vessels are prone to bleeding and may undergo fibrosis and contraction, which can ultimately lead to blindness and a profound impact on the quality of life for patients (6).

Presently, there are several relevant risk factors that are used to monitor potential development of DR, including the duration of diabetes, poor glycemic control (high glycated hemoglobin [HbA1c levels]), presence of hypertension, dyslipidemia, and a higher body mass index (7). However, based on several large population-based clinical studies, substantial variation in the onset and severity of DR have been documented in patients living with DM that is not completely explained by the known risk factors. For example, total glycemic exposure (duration of diabetes and HbA1c values) explained only ~11% of the variation in DR risk for the entire study population in the Diabetes Control and Complications Trial, which suggests that the remaining 89% of the variation risk is due to other factors (i.e., genetic determinants and/or epigenetic factors) in the diabetic milieu that are independent of HbA1c (8). As a result, to effectively monitor glycemic control and implement timely treatment protocols, it becomes imperative that research efforts are invested towards identifying these unexplained factors and novel molecular players that continue to contribute to the development and progression of microvascular complications such as DR. Furthermore, implementation of a test to effectively identify and treat patients early in the disease process will result in considerable cost savings, since the cost of caring for patients with PDR is much greater than the costs of managing patients with NPDR (9, 10).

Given the advent of novel genomic technologies within the last decade, recent studies examining the epigenetic landscape in DR have shed light on the 'dark matter' of the epi/genome and have opened the door for the selective targeting of promising molecular candidates in the diagnosis and/or therapy of DR. Among these molecules, long non-coding RNAs (lncRNAs), which do not have protein-coding potential and are greater than 200 nucleotides in length, have demonstrated critical implications in a number of DR-related processes including angiogenesis (11–13), inflammation (14), and even fibrosis-related mechanisms (i.e., endothelial-to-mesenchymal transition) (15).

In this study, based on the collective findings from our previous lncRNA microarray involving human retinal endothelial cells (HRECs) subjected to basal and high glucose conditions (GEO ID: 122189) and existing mechanistic-based research performed by us and others (11–19), we selected 9 prominent lncRNAs (*ANRIL*, *MALAT1*, *WISPER*, *ZFAS1*, *H19*, *HOTAIR*, *HULC*, *MEG3*, and *MIAT*) and developed a multi-lncRNA PCR panel in order to investigate and validate whether a diagnostic biomarker panel could be used to distinguish between patients with non-DR and DR. We then carried out additional statistical analyses to determine the potential discriminative ability of this lncRNA-panel to diagnose and identify the various sub-stages of DR.

MATERIALS AND METHODS

Development of the Multi-lncRNA PCR Panel

Customized human lncRNA primers were developed (**Table 1**) and subsequently aliquoted and air dried into a 96-well plastic qPCR plate. Custom qPCR plates were stored in -20°C prior to use. A single panel (consisting of 10 wells) in the lncRNA PCR plate examined 9 distinct lncRNAs (*MALAT1, HOTAIR, H19, MEG3, ANRIL, MIAT, WISPER, ZFAS1*, and *HULC*) and one house-keeping gene (β-actin). Synthesized cDNA (following the protocol below) was diluted and combined with SYBR-green master mix (Takara Bio, Mountain View, CA, USA), and then

Abbreviations: DR, diabetic retinopathy; lncRNA, long non-coding RNA; DM, diabetes mellitus; ECs, endothelial cells; NPDR, non-proliferative DR; PDR, proliferative DR; VEGF, vascular endothelial growth factor; MALAT1, metastasis associated lung adenocarcinoma transcript 1; HOTAIR, HOX transcript anti-sense RNA; H19, H19 imprinted maternally expressed transcript; WISPER, Wisp2 super-enhancer-associated RNA; ZFAS1, ZNFX1 antisense RNA 1; MIAT, myocardial infarction-associated transcript; HULC, highly up-regulated in liver cancer; ANRIL, antisense non-coding RNA in the INK4 locus; MEG3, maternally expressed gene 3; NG, normoglycemia; HG, hyperglycemia or high glucose; HRECs, human retinal microvascular endothelial cells.

TABLE 1 | Human lncRNA qPCR primers used for the PCR panel.

Target Gene (Human):	Oligonucleotide Sequence (5'→3'):
ACTB (B-actin)	F: CCTCTATGCCAACACAGTGC
	R: CATCGTACTCCTGCTTGCTG
HOTAIR	F: GGGGCTTCCTTGCTCTTCTTATC
	R: CTGACACTGAACGGACTCTGTTTG
H19	F: AAAGACACCATCGGAACAGC
	R: AGAGTCGTCGAGGCTTTGAA
WISPER	F: CCATCTGTGGGACATCTGTG
	R: TGGGGGCTGTGGAGATAGTA
ZNFX1-AS1 (ZFAS1)	F: CAGCGGGTACAGAATGGA
	R: TCAGGAGATCGAAGGTTGTAGA
HULC	F: ATCTGCAAGCCAGGAAGAGTC
	R: CTTGCTTGATGCTTTGGTCTGT
ANRIL	F: CCCTTATTTATTCCTGGCTCC
	R: GACCTCGCTTTCCTTTCTTCC
MALAT1	F: TCTTAGAGGGTGGGCTTTTGTT
	R: CTGCATCTAGGCCATCATACTG
MIAT	F: GGGAGGGGAAATGGGTGATGTA
	R: TAACGCCAAATGTGAAGTGTGA
MEG3	F: CGGCTGGGTCGGCTGAAGAACT
	R: CCGCCCAAACCAGGAAGGAGAC

aliquoted into the 96-well PCR plate containing the pre-aliquoted PCR panel. The panel was then inserted into the LightCycler 96 System (Roche Diagnostics, Laval, QC, CAN) for amplification.

RNA Isolation and Quantitative Real-Time Polymerase Chain Reaction (RT-qPCR)

As described by us previously (12–15), total RNA was extracted using the TRIzol reagent (Invitrogen). RNA concentrations were quantified using a spectrophotometer (260 nm; Gene Quant, Pharmacia Biotech, USA) and 1-2 μg of total RNA was reverse transcribed to complementary DNA (cDNA) using a high-capacity cDNA reverse-transcription kit (Applied Biosystems/Thermo Fisher Scientific). cDNA was then amplified in the LightCycler 96 System (Roche Diagnostics, Laval, QC, CAN) using the multi-lncRNA PCR panel. RT-qPCR results were analyzed using the LightCycler 96 SW 1.1 software (Roche) and expression levels were calculated by the relative standard curve method using β-actin as an internal control for sample normalization.

Cell Culture

Prior to the clinical validation of our panel, we first validated our assay *in vitro*. Human retinal microvascular endothelial cells (HRECs; Cell Systems, Kirkland, WA, USA; catalog number ACBRI 181) were cultured in endothelial basal media-2 (EBM-2, Lonza, Walkersville, MD, USA) containing endothelial growth media-2 (EGM-2) SingleQuots (Lonza). All cells were grown in 75 cm^2 culture flasks and maintained in a humidified incubator containing 5% CO_2 at 37°C. As described previously (12, 14), to reduce variability for experimentation, cells were used between passages three and six and the cellular densities were determined accordingly based on the type of culture plates used for each experiment. Generally, once 80% confluence was obtained post-seeding, ECs were cultured in serum and growth factor-free medium overnight before exposure to different D-glucose levels (final glucose concentrations of 5 mmol/L, mimicking normoglycemia [NG], and 25 mmol/L, mimicking hyperglycemia [HG]) for 48 hours; the selected glucose level is based on a large volume of previous experiments (12–15). Twenty-five mmol/L L-glucose was used as osmotic control. All *in vitro* experiments were independently repeated at least three times and performed with six replicates, unless specified.

Collection and Analyses of Vitreous and Serum Samples

The study was approved by the Western Research Ethics Board and Lawson Health Research Institute at the University of Western Ontario (London, ON, CAN). Informed consent was received from patients prior to obtaining specimens and the research was conducted following the *Declaration of Helsinki*. As an initial test to identify whether serum lncRNAs appropriately reflect the vitreous lncRNAs, we collected both serum and undiluted vitreous humor (VH) samples from patients, undergoing a pars plana vitrectomy by an experienced vitreoretinal surgeon (12). These samples were categorized into two groups: control and DR.

In the initial cohort, the DR group comprised of patients diagnosed with advanced stages of DR, including proliferative DR (PDR; n= 11; mean age ± SD= 60.9 ± 10.4 years; 10 males and 1 female, 1 type I diabetic and 10 type 2 diabetics), while the control group consisted of patients that had no previous history of DR and were diagnosed with idiopathic macular hole or a separate non-diabetic ocular condition (n= 10; mean age ± SD= 69.2 ± 8.9 years; 2 males and 8 females). PDR was defined as the presence of neovascularization or fibrous proliferation of the disc or elsewhere on the retina. Total RNA was extracted from 500 μL of VH and 200 μL of serum samples using a serum RNA extraction kit (Bio Basic Inc., Markham, ON, CAN) and was subsequently examined by RT-qPCR.

Following the results of our initial experiment, we expanded our test using only serum samples from a larger new cohort of patients. Briefly, undiluted serum samples were collected in BD gold-top serum separator tubes. Serum specimens were submitted to the research laboratory, where total RNA was extracted from 200 μL of serum samples using TRIzol and the serum RNA extraction kit mentioned above. The expression levels of the 9-specific lncRNAs (*ANRIL*, *H19*, *HOTAIR*, *HULC*, *MALAT1*, *MEG3*, *MIAT*, *WISPER* and *ZFAS1*) were assessed using RT-qPCR, where a research technician was masked to the sample type. The subjects include 7 type I diabetic and 52 type 2 diabetics. Specimens were categorized into two groups: control ('C') and diabetic retinopathy ('P'; DR). The 'P' group comprised of diabetic patients diagnosed with varying stages of DR (indicated as '0'= diabetic patients with no retinopathy, '1' = diabetic patients with non-proliferative DR [NPDR], and '2'= diabetic patients with proliferative DR [PDR]) (n= 59; mean age ± SD= 64.2 ± 11.5 years; 44 males and 15 females), while the control group consisted of non-diabetic patients who were seen at the eye clinic for conditions unrelated to diabetes (n= 11; mean age ± SD= 62.9 ± 17.3 years; 4 males and 7 females).

Statistical Analyses

Statistical differences were evaluated between groups using GraphPad Prism 7 (La Jolla, CA, USA) and Microsoft Excel (Washington, USA). Data were considered statistically significant if the p value was less than 0.05. Statistical significance for the clinical samples (with non-normal distribution) were identified using the Mann-Whitney U test (when comparing two conditions) or Kruskal-Wallis one-way ANOVA (for multiple group comparisons) and linear regression analyses wherever appropriate. ROC curves were used to elucidate clinical significance of lncRNA molecules in control versus diabetic patients with no retinopathy, NPDR and PDR by comparing sensitivities and false positive rates. AUC numbers were approximated simply by sum of the areas of rectangles in the ROC curves. Creatinine and HbA1c levels were compared between control and patient groups using Spearman's rank correlation coefficient. Two outliers from control samples I6 and A1 for *MEG3* (86096.52 and 2022.94, respectively) were removed for better graphical representation of the results.

Data Availability

All data generated or analyzed during this study are included in this published article.

RESULTS

Glucose Causes Differential Expressions of lncRNAs in Retinal Endothelial Cells

Using our established cell culture model and RT-qPCR (12–15, 17), we confirmed the lncRNA expressions of *ANRIL*, *H19*, *HOTAIR*, *HULC*, *MALAT1*, *MEG3*, *MIAT*, *WISPER*, and *ZFAS1* in HRECs exposed to 25 mM (HG) or 5 mM (NG) glucose over 48 hours from our array (**Figure 1**). As depicted in **Figure 1**, HG induced significant upregulations of *ANRIL*, *HOTAIR*, *HULC*, *MALAT1*, and *ZFAS1*, and a significant downregulation of *H19* in HRECs compared to NG controls. Although not statistically significant, in comparison to NG controls, general trends of upregulation were observed for *MIAT* and *WISPER*, while *MEG3* appeared to demonstrate decreased expressions following HG stimulation. No alterations of such lncRNA expressions were seen when the cells were exposed to 25mM L-glucose (not shown).

Expressions of lncRNAs in the Serum Correlates With Vitreous Levels in Diabetic Retinopathy

As an initial proof-of-concept experiment, we wanted to determine whether the selected lncRNAs could be detected in human DR. So, we analyzed both vitreous humor and serum samples from an initial small cohort of patients as outlined above using the customized qPCR-based panel. Similar to the trends observed *in vitro*, differential expressions of lncRNAs were found in the vitreous and serum of patients with PDR compared to non-PDR patients—further suggesting the biological significance of lncRNAs in human DR (**Figure 2**). Specifically, alterations were significantly pronounced in the serum expression levels of *ANRIL* (**Figure 2A**), *H19* (**Figure 2B**), *HOTAIR* (**Figure 2C**), *MALAT1* (**Figure 2E**), *WISPER* (**Figure 2H**) and *ZFAS1* (**Figure 2I**) in PDR. However, we did not find significant alterations with respect to the serum expressions of *HULC* (**Figure 2D**), *MEG3* (**Figure 2F**) and *MIAT* (**Figure 2G**) in PDR, and such findings may be related to the relatively small sample size. Moreover, as shown in **Figure 3**, significant expressions of *ANRIL* (**Figure 3A**), *HOTAIR* (**Figure 3B**), *H19* (**Figure 3C**), *MALAT1* (**Figure 3E**), *MIAT* (**Figure 3G**), *WISPER* (**Figure 3H**) and *ZFAS1* (**Figure 3I**) were observed in the vitreous of PDR patients, while statistical significances were

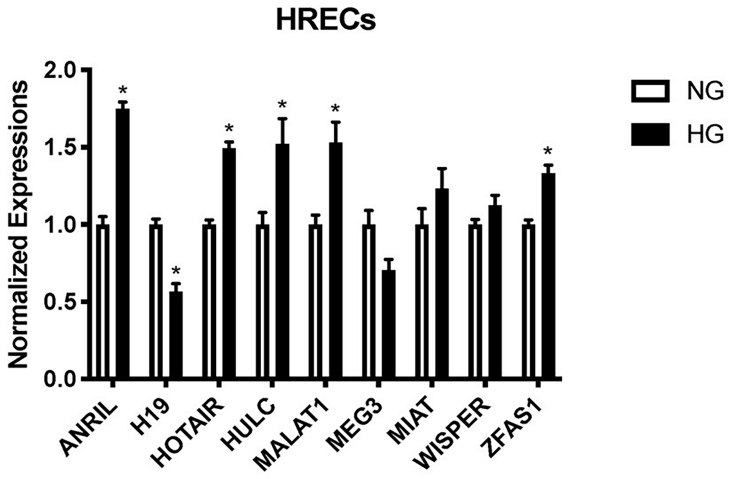

FIGURE 1 | Glucose-treated human retinal endothelial cells (HRECs) demonstrate differential expressions of lncRNAs at 48 hours. RT-qPCR analysis of *ANRIL*, *H19*, *HOTAIR*, *HULC*, *MALAT1*, *MEG3*, *MIAT*, *WISPER* and *ZFAS1* expressions in HRECs exposed to 25 mM (HG) or 5 mM (NG) glucose over 48 hours [data (mean ± SEM); N=6 per group; normalized to β-actin and expressed as a fold change of NG; *p<0.05 compared to NG].

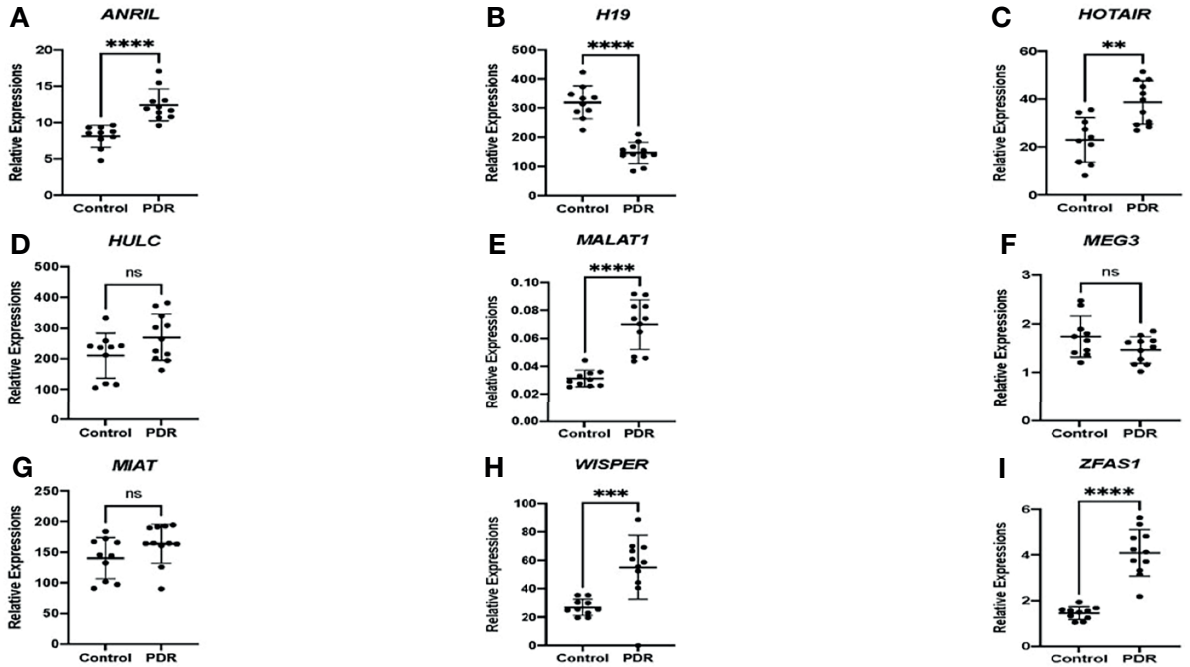

FIGURE 2 | Differential expressions of lncRNAs in the serum of patients. RT-qPCR analyses of **(A)** *ANRIL*, **(B)** *H19*, **(C)** *HOTAIR*, **(D)** *HULC*, **(E)** *MALAT1*, **(F)** *MEG3*, **(G)** *MIAT*, **(H)** *WISPER*, and **(I)** *ZFAS1* expressions in the serum of patients with proliferative diabetic retinopathy (PDR) compared to controls (non-diabetic patients). Data is expressed as a ratio to β-actin. Statistical significance was assessed using the Mann-Whitney U test. Data represents the mean ± SD (N=10 per control group or N=11 per PDR group; ns, not significant, $^{**}p<0.01$, $^{***}p<0.001$, or $^{****}p<0.0001$).

not observed for *HULC* (**Figure 3D**) and *MEG3* expressions (**Figure 3F**).

When comparing the level of lncRNA expressions between serum and vitreous samples, significant correlations were observed for *HOTAIR* (**Figure 4A**), *ANRIL* (**Figure 4B**), *H19* (**Figure 4C**), *MALAT1* (**Figure 4E**), *WISPER* (**Figure 4H**) and *ZFAS1* (**Figure 4I**), which suggests that the level of expression for these lncRNAs in the serum parallels that of the lncRNA expression levels in the vitreous. We did not find significant correlations between serum and vitreous concentrations of *HULC* (**Figure 4D**), *MEG3* (**Figure 4F**), and *MIAT* (**Figure 4G**).

Demographic Data and Disease Characteristics of the Study Population

Following the results from our proof-of-concept experiment, we expanded our study by examining the expression of the above lncRNAs in the serum of a new cohort of non-diabetic patients and diabetic patients with various stages of DR. As shown in **Table 2**, males were more predominant in the diabetic patient group, while females were more prevalent in the control group. As expected, the diabetic patient group also had a slightly higher means of BMI, hemoglobin A1c [HbA1c], and creatinine levels compared to the control group. However, when examining the diabetic patient groups according to the presence of retinopathy, no significant differences were observed for age, BMI, or creatinine levels, while significances were observed for HbA1c and gender distribution between diabetic patients with retinopathy and those without. Furthermore, when comparing between NPDR and PDR patients, no significant differences were observed across age, type of diabetes, BMI, creatinine, HbA1c, and gender distribution.

A Pattern of lncRNA Alterations Were Observed in the Serum in Diabetes

As shown in **Figure 5**, significant increased lncRNA expressions of *ANRIL*, *H19*, *HOTAIR*, *HULC*, *MIAT*, *WISPER* and *ZFAS1* were observed in the serum of diabetic patients (with varying stages of DR; group 'P') compared to non-diabetic patients (without DR; group 'C'). Interestingly, although not significant, *MEG3* lncRNA levels demonstrated decreasing trends in diabetic patients compared to control patients ($p = 0.67$), while *MALAT1* levels exhibited increasing trends in the diabetic patient group ($p = 0.09$). No significant correlations were demonstrated between the lncRNA expression profiles and the creatinine (**Table 3**) or HbA1C levels (**Table 4**) in the non-diabetic and diabetic patient groups.

Stage Dependent Alterations of lncRNAs in DR

When the data of various patient subgroups were analyzed, the average expression levels for 8 lncRNAs were generally increased across all diabetic patient sub-groups ('DM', 'NPDR', and 'PDR') when compared to controls (**Figure 6**). Such alterations were not observed with *MEG3*. Interestingly, when comparing between

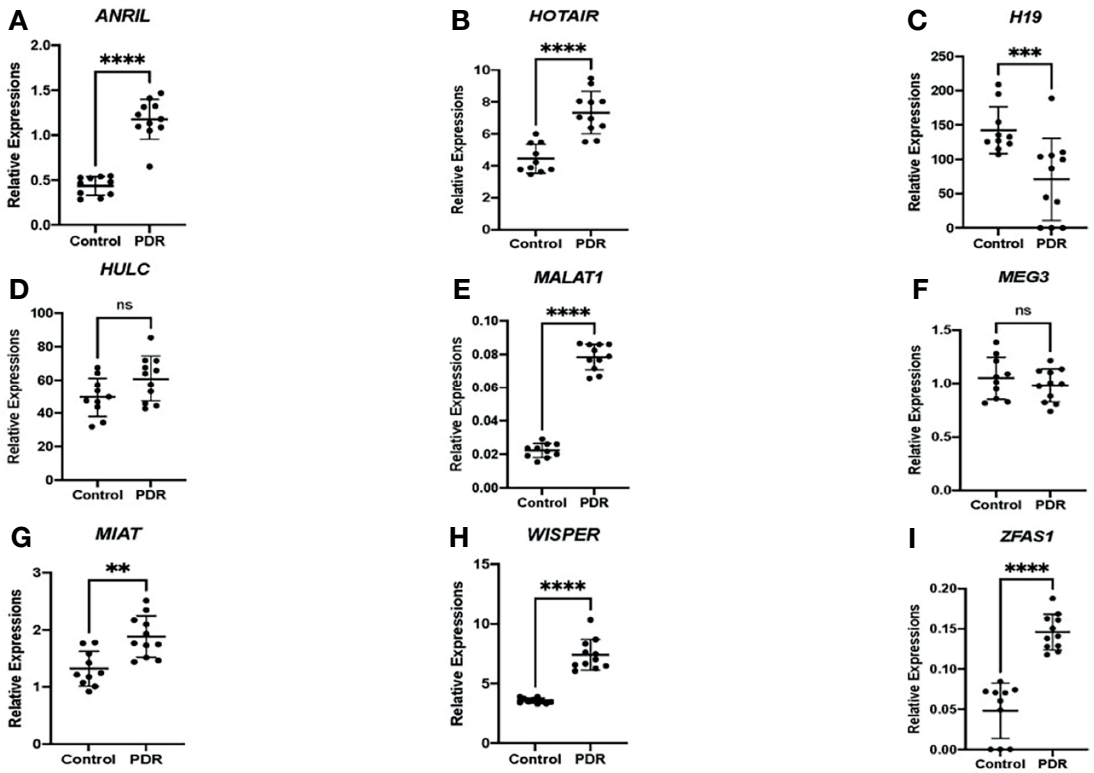

FIGURE 3 | Differential expressions of lncRNAs in the vitreous fluid of patients. RT-qPCR analyses of **(A)** *ANRIL*, **(B)** *HOTAIR*, **(C)** *H19*, **(D)** *HULC*, **(E)** *MALAT1*, **(F)** *MEG3*, **(G)** *MIAT*, **(H)** *WISPER*, and **(I)** *ZFAS1* expressions in the vitreous of patients with proliferative diabetic retinopathy (PDR) compared to controls (non-diabetic patients). Data is expressed as a ratio to β-actin. Statistical significance was assessed using the Mann-Whitney U test. Data represents the mean ± SD (N=10 per control group or N=11 per PDR group; ns, not significant, $^{**}p<0.01$, $^{***}p<0.001$, or $^{****}p<0.0001$).

control and 'DM' groups, significances were observed for the lncRNAs *ANRIL, H19, HULC, MIAT, WISPER*, and *ZFAS1*. In addition, when the control group was compared with the 'NPDR' sub-group, significances were observed for 8 out of the 9 lncRNAs, apart from *MEG3*. Additionally, comparing the lncRNA expression levels between control and PDR groups also demonstrated statistical significance for *ANRIL*, *H19*, *HOTAIR*, *HULC*, *MIAT*, *ZFAS1*, and *WISPER*, while *MEG3* and *MALAT1* did not show significance. These observations suggest a duration-dependent change in the lncRNA expression profiles in the serum, where the duration of diabetes may reflect distinct lncRNA expression patterns. Collectively, the results suggest that these 9 lncRNAs can be used as biomarkers of DR.

To further examine significance of the serum levels of the analytes, area under the curve (AUC) was calculated. AUC analyses demonstrated that the lncRNAs of interest have potential diagnostic value in discriminating diabetic patient sub-groups (diabetes, NPDR, and PDR) from control non-diabetic patients. (95% CI, two-tailed Z-critical values were used to calculate p-values) (**Table 5**). Specifically, using AUC, comparison between control patients and diabetic patients with no DR demonstrated a significant difference in 9 lncRNAs, where *HULC* had the highest AUC ($p < 0.05$) and *MEG3* had the lowest AUC ($p < 0.05$). Furthermore, when analyzing the AUC values for control and NPDR patients, all 9 lncRNAs demonstrated statistical significance and 7 out of 9 lncRNAs had AUC values greater than 0.7, except for *MEG3* and *MALAT1*. Additionally, comparison of AUC values between control patients and PDR patients demonstrated significance for all the lncRNA markers and 6 out of the 9 lncRNAs had AUC values greater than or equal to 0.7, apart from *H19*, *MEG3* and *MALAT1*. Interestingly, when comparing between diabetic patients with no retinopathy and diabetic patients with DR (NPDR or PDR), all 9 lncRNAs demonstrated AUC values ranging between 0.460 to 0.570 with significant statistical differences. Furthermore, although significant, AUC values for the 9 lncRNAs ranged between 0.290 to 0.420 when comparing between NPDR and PDR patients. Collectively, these results demonstrate that the 9 examined lncRNAs may be used as a prognostic tool to discriminate between non-diabetic and diabetic patients with DR, as well as potentially discriminate various stages of DR (mild NPDR to severe PDR) from diabetic patients without DR.

Alteration of Specific lncRNAs Phenotypes May Be Predictive of DR

Given the various lncRNA expression profiles, we wanted to further determine whether combinations of specific lncRNA phenotypes existed across control and diabetic patient sub-groups. Through Z-

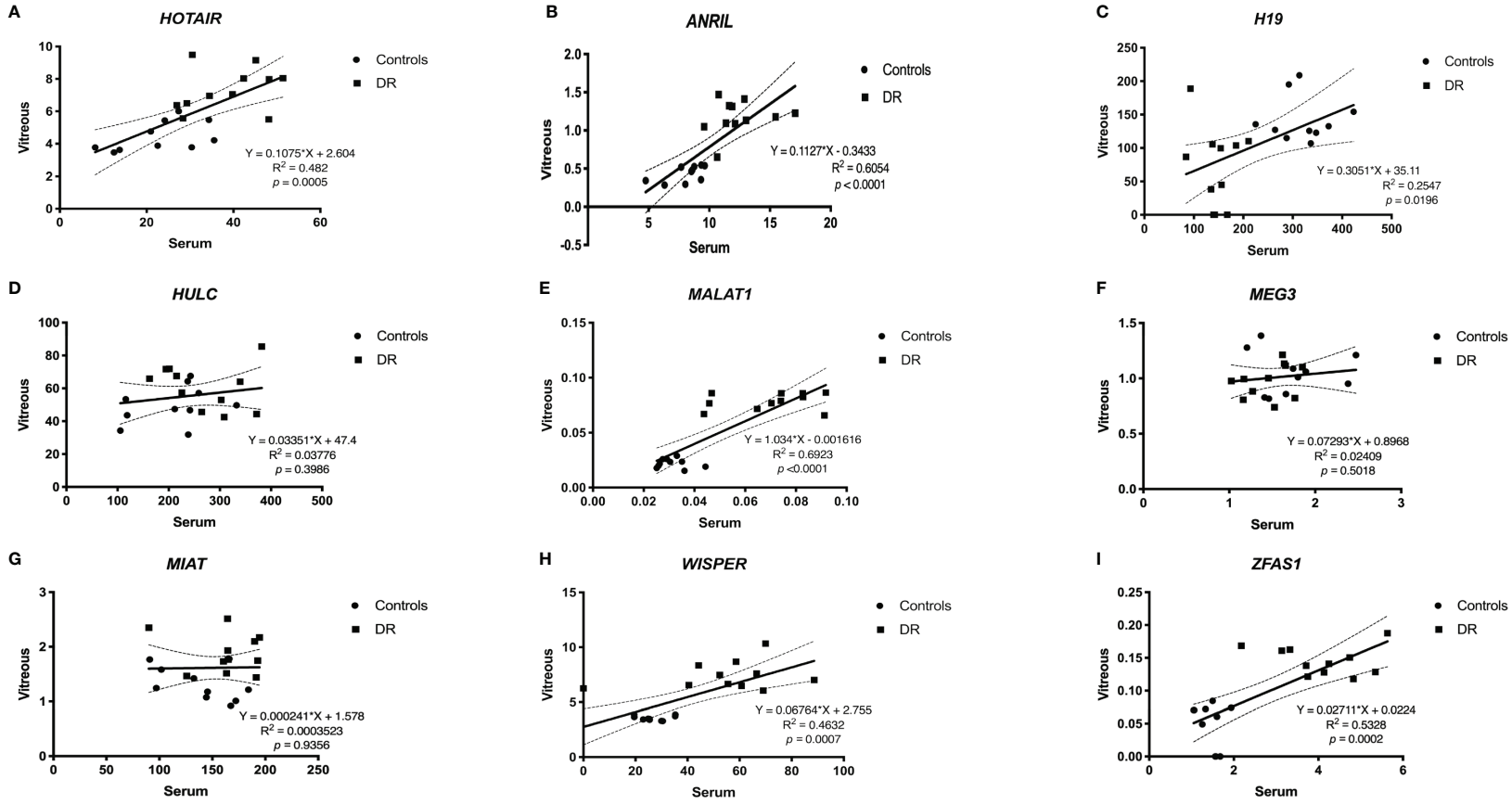

FIGURE 4 | Pearson correlation analyses between serum and vitreous samples. When comparing between serum and vitreous samples, significant correlations were observed for **(A)** *ANRIL*, **(B)** *H19*, **(C)** *HOTAIR*, **(E)** *MALAT1*, **(H)** *WISPER* and **(I)** *ZFAS1*, which suggests that the expressions of these lncRNAs can be reflected from the serum and vitreous of patients with DR. Although we did find significant correlations between serum and vitreous concentrations of **(D)** *HULC*, **(F)** *MEG3*, and **(G)** *MIAT*, including a larger sample size may further help confirm the relationships between these markers and sample types [$p<0.05$ was considered significant; dotted lines represent 95% confidence intervals. N= 10 for control group and N= 11 for diabetic group; and normalized to β-actin]. DR, diabetic retinopathy.

TABLE 2 | Demographic data and disease characteristics of the study groups.

Variables	Control	All Patients	Control vs. All Patients		DM	DR	DM vs. DR		Control vs. DR		NPDR	PDR	NPDR vs. PDR	
			p	OR (95% CI)			*p*	OR (95% CI)	*p*	OR (95% CI)			*p*	OR (95% CI)
Number	11	59			10	49					26	23		
Age														
Mean ± SD	62.9 ± 17.29	64.2 ± 11.49	0.52		70.7 ± 7.13	62.9 ± 11.75	0.9		0.62		65.6 ± 11.16	59.7 ± 11.63	0.9	
≤ 50	3 (27.3)	5 (8.5)	0.07	Reference	0 (0)	5 (10.2)	0.29	Reference	0.13	Reference	1 (3.8)	4 (17.4)	0.12	Reference
> 50	8 (72.7)	54 (91.5)		4.05 (0.81-20.31)	10 (100)	44 (89.8)		0		3.3 (0.65-16.63)	25 (96.2)	19 (82.6)		0.19 (0.02-1.84)
Sex														
Female	7 (63.6)	15 (25.4)	*0.01*	Reference	4 (40)	11 (22.4)	*0.01*	Reference	*0.007*	Reference	5 (19.2)	6 (26.1)	0.6	Reference
Male	4 (36.4)	44 (74.6)		*5.13 (1.32-20.02)*	6 (60)	38 (77.6)		*2.3 (0.55-9.64)*		*6.05 (1.49-24.51)*	21 (80.8)	17 (73.9)		*0.67 (0.18-2.6)*
Other														
BMI (kg/m^2)	29.3 ± 3.08	31.1 ± 6.29	0.24	NA	30.4 ± 4.53	31.2 ± 6.54	0.4	NA	0.25	NA	31.9 ± 5.56	30.5 ± 7.26	0.9	NA
HbA1c (µmol/L)	5.6 ± 0.74	7.5 ± 2.63	*< 0.001*	*NA*	6.6 ± 1.12	7.7 ± 2.82	*0.02*	*NA*	*< 0.001*	*NA*	6.9 ± 2.88	8.3 ± 2.6	0.06	*NA*
Creatinine	75.8 ± 21.58	95.5 ± 48.58	0.1	NA	82 ± 14.71	97.9 ± 52.07	0.25	NA	0.1	NA	101.3 ± 48.68	94.8 ± 54.79	0.8	NA

Data are represented as number (percentage) or mean ± standard deviation (SD). DM, diabetes mellitus patients without retinopathy; NPDR, non-proliferative diabetic retinopathy; PDR, proliferative diabetic retinopathy. OR (95% CI), odds ratio and 95% confidence interval. Mann Whitney u test for quantitative variables and chi-square test for qualitative data were applied. Items in italics indicate p < 0.05. NA, not applicable.

score calculations and by comparing the mean and standard deviations for each lncRNA expression levels in diabetic patients against controls, we found that the ANRIL+/HOTAIR+/HULC +/(H19), (MIAT)/WISPER+/ZFAS1+/(H19), and ANRIL +/HOTAIR+/HULC+/WISPER+/ZFAS1+/(H19) phenotypes were prevalent in 33.9%, 35.6%, and 30.5% of all diabetic patients (n = 59 patients), respectively (**Table 6**). Interestingly, when examining both diabetic patients with either NPDR or PDR against control patients (n = 49 patients), 34.7% of these patients presented with the ANRIL +/HOTAIR+/HULC+/(H19) phenotype, 38.8% exhibited the (MIAT)/WISPER+/ZFAS1+/(H19) phenotype, and 30.6% of these patients demonstrated the ANRIL+/HOTAIR+/HULC+/WISPER +/ZFAS1+/(H19) phenotype. Specifically, in just the NPDR group (n = 26 patients), the most prevalent phenotypes included ANRIL +/HOTAIR+/HULC+/(H19) (46.2%), (MIAT)/WISPER+/ZFAS1 +/(H19) (53.8%), and ANRIL+/HOTAIR+/HULC+/WISPER +/ZFAS1+/(H19) (38.5%). While the prevalent lncRNA phenotypes in the PDR group (n = 23 patients) included ANRIL +/HOTAIR+/HULC+/(H19) (21.7%), (MIAT)/WISPER+/ZFAS1 +/(H19) (21.7%) and ANRIL+/HOTAIR+/HULC+/WISPER +/ZFAS1+/(H19) (21.7%). These findings suggest that unique lncRNA phenotypes could exist for specific diabetic patients, particularly those presenting at a certain stage of DR. We further applied regression model in this analysis (**Supplementary Table 1**). However, no further improvement in the diagnostic accuracy was seen.

DISCUSSION

The emergence of diabetes as a global epidemic is a major challenge to human health in the 21st century, with a global prevalence of 8.8% of the global adult population in 2017 (20). Among the diabetic population, a recent meta-analysis in 2020 estimated that the global prevalence for DR was 22.27%, 6.17% for vision-threatening DR, and 4.07% for clinically significant macular edema (21). If the current rate of DR prevalence remains constant over the next 25 years, it is estimated that the global number of adults with DR will further increase by 25.9% (129.84 million) in 2030 and by 55.6% (160.50 million) in 2045 (21). Although the likelihood of DR-induced vision impairment can be greatly reduced if DR is diagnosed in its early stages and treated accordingly, nearly one-third of patients with diabetes fail to follow vision care guidelines in the US and non-adherence has reached more than 60% in developing countries, which is largely attributable to the limited accessibility of ophthalmic services and elevated costs (22). Furthermore, the current gold standard for DR screening is based on clinical examinations (with various diagnostic tools), and DR is clinically diagnosed with the onset of ophthalmoscopic signs. However, since biochemical and functional defects in the eye often precede the development of vascular lesions and the onset of clinical signs (23), it is critical that novel, accurate, low-cost, and predictive screening tools are developed that can identify the best therapeutic window for patients who have not yet developed clinically evident retinopathy and still have their visual function intact—since

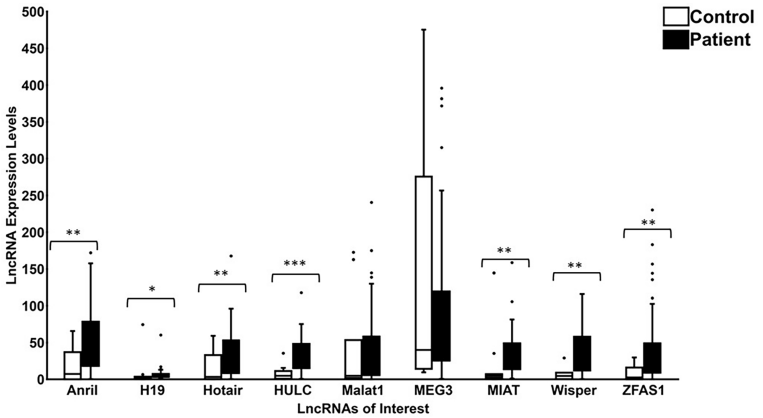

FIGURE 5 | Expression levels of lncRNAs in patients and controls. Boxplots represent comparison between expression level of 9 specific lncRNAs (*ANRIL*, *H19*, *HOTAIR*, *HULC*, *MALAT1*, *MEG3*, *MIAT*, *WISPER* and *ZFAS1*) detected by RT-qPCR in patient and control groups. The median and interquartile range (25^{th} -75^{th} percentile), are shown as solid horizontal lines. Two outliers from control samples I6 and A1 for *MEG3* (86096.52 and 2022.94, respectively) were removed for better graphical representation of the results. Statistical significance was assessed using Mann-Whitney U test (*p<0.05, **p<0.005, or ***p<0.0005; N=11 for control patients and N= 59 for diabetic patients). Statistical significance was considered at p<0.05. Legend: Control = Non-diabetic patients without any diabetic retinopathy; Patient = Diabetic patients with or without diabetic retinopathy.

TABLE 3 | Creatinine Spearman's rank correlation coefficient.

Spearman correlation coefficient ρ (Control n=6, Patient n= 55)

	ANRIL	H19	HOTAIR	HULC	MALAT1	MEG3	MIAT	WISPER	ZFAS1
Control n = 6									
ρ	-0.45	0.23	-0.42	-0.18	-0.58	0.57	-0.17	-0.40	-0.33
P-value	0.224	0.546	0.265	0.637	0.099	0.112	0.668	0.286	0.381
Patient n = 55									
ρ	0.029	-0.080	0.057	0.001	-0.070	-0.112	-0.077	0.040	-0.008
P-value	0.836	0.574	0.681	0.996	0.611	0.415	0.576	0.774	0.956
Combined P and C, n=61									
ρ	0.001	0.023	0.000	0.060	-0.135	-0.022	0.005	0.076	-0.024
P-value	0.993	0.860	0.998	0.645	0.299	0.864	0.967	0.562	0.851

Spearman's rank correlation coefficients of lncRNAs and Creatinine expression. To obtain p-values, t-statistic was used.
Method:
1. Similar to HbA1c.

TABLE 4 | HbA1c Spearman's rank correlation coefficient.

Spearman's rank correlation coefficient ρ (Control n = 7, Patient n = 51)

	ANRIL	H19	HOTAIR	HULC	MALAT1	MEG3	MIAT	WISPER	ZFAS1
Control n = 7									
ρ	0.36	-0.49	0.68	0.07	0.00	-0.74	0.14	0.34	0.52
P-value	0.427	0.268	0.090	0.878	1.000	0.058	0.758	0.452	0.229
Patient n = 51									
ρ	0.022	0.083	-0.063	-0.044	-0.143	-0.075	-0.054	-0.178	-0.106
P-value	0.879	0.564	0.662	0.760	0.318	0.602	0.705	0.211	0.459
Combined P and C, n=58									
ρ	0.237	0.103	0.164	0.167	0.034	-0.157	0.094	0.022	0.133
P-value	0.074	0.439	0.219	0.210	0.803	0.238	0.481	0.869	0.320

Spearman's rank correlation coefficients of lncRNAs and HbA1c expression. To obtain p-values, t-statistic was used.
Method:
1. lncRNA and HbA1c amounts for each sample was ranked using RANK.AVG () function.
2. Step 1 was done for control (n=7), for all patients with available HbA1c values (n=51 – some patients missing this information), and for the combination of both (n=58).
3. Correlation between the two ranks for each sample was calculated using CORREL() function.
4. T-statistic, degree of freedom was calculated for each correlation to obtain p-value using TDIST() function.

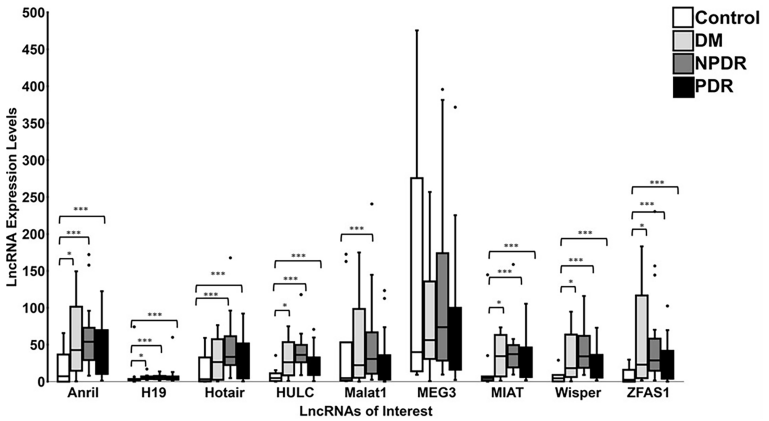

FIGURE 6 | Expression levels of lncRNAs in controls and patients diagnosed with varying stages of DR. Boxplots represent comparison between expression level of 9 specific lncRNAs (*ANRIL*, *H19*, *HOTAIR*, *HULC*, *MALAT1*, *MEG3*, *MIAT*, *WISPER* and *ZFAS1*) detected by RT-qPCR in control and patient groups (DM = diabetic patients with no retinopathy, NPDR = diabetic patients with non-proliferative DR, and PDR = diabetic patients with proliferative DR). The median and interquartile range (25^{th} -75^{th} percentile), are shown as solid horizontal lines. Two outliers from control samples I6 and A1 for *MEG3* (86096.52 and 2022.94, respectively) were removed for better graphical representation of the results. Statistical significance was assessed using Mann-Whitney U test (*p<0.05, ***p<0.0005; N=11 for control patients, N=10 for DM patients, N=26 for NPDR patients, and N=23 for PDR patients). Statistical significance was considered at p<0.05.

this sub-population of diabetic patients comprise the majority and respond better to regimented therapies early on (23). Nevertheless, the current approaches for diagnostic evaluation can be labor-intensive, time-consuming, and susceptible to diagnostic variation due to clinical subjectivity (24) and the advent of novel diagnostic technologies, which provide effective clinical utility, is greatly required, as the prevalence of DR continues to rise exponentially.

Long non-coding RNAs (lncRNAs) represent a promising class of RNA molecules that can be targeted and exploited for therapeutic and diagnostic purposes. Given their limited protein-coding capacities, research over the last decade have demonstrated the versatile and critical roles of lncRNAs in cancer progression (25), neurodegenerative diseases (26), diabetes (27), and even diabetic complications such as DR (12, 14, 15, 28). To further demonstrate the importance of lncRNAs in the context of DR screening, the present study examines the diagnostic and prognostic potential of 9 circulating lncRNAs in diabetic patients with or without DR compared to non-diabetic controls. Serum samples of diabetic patients (with varying stages of DR) exhibited significant increases in the expressions of *ANRIL*, *H19*, *HOTAIR*, *HULC*, *MIAT*, *WISPER* and *ZFAS1*, while expression levels of *MALAT1* and *MEG3* did not demonstrate statistical significance when compared to controls. However, when further stratifying the diabetic patients into distinct subsets of DR and comparing the lncRNA expression levels against controls, significant differential expressions were observed for 8 out of the 9 lncRNAs except for *MEG3*. The differential expression profiles observed for the lncRNAs in this study are consistent with previous reports that have documented the de-regulated nature of lncRNAs in DR (12, 14, 15, 29–31), which further supports the diagnostic and prognostic potential of lncRNAs for DR screening. It is to be noted that in this exploratory study, we didn't use a synthetic spike-in RNA as control. We used β-actin as internal control along with several positive controls (cell culture) and negative controls for our assays.

Although the mechanisms of action for lncRNAs continue to be elucidated, a large body of literature supports the notion that lncRNAs can govern gene expressions through various mechanisms: 1) guiding molecular complexes (e.g., chromatin-modifying enzymes) to target genomic regions (32), 2) functioning as a decoy for transcription factors (33), 3) serving as a scaffold to assist in the assembly of protein complexes (34), 4) directly enhancing the activation of neighboring genes (35), and 5) acting as a sponge that sequesters critical microRNAs (36). Although lncRNAs may exert more than one of the above mechanisms, the subcellular localization of lncRNAs can further provide insights into the structural features and distinct functionalities of lncRNAs, with nuclear-retained lncRNAs playing important roles in transcriptional regulation and cytoplasmic-retained lncRNAs being implicated in post-transcriptional regulation (37, 38). Furthermore, in the context of diabetes, chronic hyperglycemia can initiate various cellular events, such as angiogenesis, inflammation, oxidative damage, and fibrosis, which can further stimulate the transcription of various lncRNAs (28).

The lncRNAs used in the PCR panel are well-documented in literature. Specifically, *HOTAIR* is a trans-acting lncRNA that can directly interact with several epigenetic enzymes (e.g., polycomb repressive complex 2; PRC2) to regulate the expressions of multiple genes involved in various disease processes, including cancer progression, ischemic stroke, diabetes, and recently angiogenesis in DR (12, 29, 39, 40). As for the lncRNA *MALAT1* (also known as *NEAT2*), aberrant *MALAT1* expressions have been documented in the retinas of diabetic rodents and various retinal cells cultured in high glucose environments (31). Several studies have also demonstrated

TABLE 5 | Diagnostic performance of lncRNA gene expression.

lncRNA	C vs DM		C vs NPDR		C vs PDR		C vs DR		DM vs NPDR		DM vs PDR		DM vs DR		NPDR vs PDR	
	AUC ± SE	*p*	AUC ± SE	*p*	AUC ± SE	*p*	AUC ± SE	*p*	AUC ± SE	*p*	AUC ± SE	*p*	AUC ± SE	*p*	AUC ± SE	*p*
ANRIL	0.77 ± 0.1	5.2E-13	0.86 ± 0.08	2.7E-27	0.75 ± 0.1	1.6E-14	0.81 ± 0.08	4.2E-21	0.55 ± 0.11	9.5E-07	0.4 ± 0.11	1.7E-04	0.48 ± 0.1	2.4E-06	0.35 ± 0.08	1.5E-05
H19	0.78 ± 0.1	1.1E-13	0.76 ± 0.09	2.5E-15	0.69 ± 0.1	5.7E-11	0.73 ± 0.09	2.7E-14	0.56 ± 0.11	5.7E-07	0.48 ± 0.11	1.8E-05	0.52 ± 0.1	4.9E-07	0.42 ± 0.08	5.4E-07
HOTAIR	0.66 ± 0.12	5.8E-08	0.82 ± 0.08	1.3E-20	0.7 ± 0.1	1.7E-11	0.76 ± 0.09	1.4E-16	0.62 ± 0.11	1.9E-08	0.51 ± 0.11	6.3E-06	0.57 ± 0.1	5.4E-08	0.29 ± 0.07	1.3E-04
HULC	0.81 ± 0.1	4.8E-16	0.94 ± 0.05	3.6E-66	0.81 ± 0.09	9.0E-20	0.88 ± 0.07	3.8E-34	0.61 ± 0.11	3.7E-08	0.44 ± 0.11	5.8E-05	0.53 ± 0.1	3.2E-07	0.3 ± 0.08	8.4E-05
MALAT1	0.65 ± 0.12	2.0E-07	0.69 ± 0.1	2.0E-11	0.54 ± 0.11	9.3E-07	0.62 ± 0.1	7.3E-10	0.54 ± 0.11	1.3E-06	0.39 ± 0.1	2.3E-04	0.47 ± 0.1	3.4E-06	0.33 ± 0.08	3.1E-05
MEG3	0.45 ± 0.13	4.4E-04	0.51 ± 0.11	1.8E-06	0.4 ± 0.1	1.1E-04	0.46 ± 0.1	2.0E-06	0.57 ± 0.11	4.0E-07	0.44 ± 0.11	5.1E-05	0.51 ± 0.1	7.9E-07	0.36 ± 0.08	7.1E-06
MIAT	0.75 ± 0.11	7.6E-12	0.87 ± 0.07	1.7E-30	0.75 ± 0.1	2.9E-14	0.82 ± 0.08	9.1E-22	0.52 ± 0.11	3.3E-06	0.43 ± 0.11	6.6E-05	0.48 ± 0.1	2.4E-06	0.35 ± 0.08	1.3E-05
WISPER	0.75 ± 0.11	2.5E-11	0.92 ± 0.06	7.3E-51	0.76 ± 0.09	8.7E-15	0.85 ± 0.08	3.8E-26	0.62 ± 0.11	1.9E-08	0.46 ± 0.11	3.5E-05	0.54 ± 0.1	1.7E-07	0.31 ± 0.08	5.5E-05
ZFAS1	0.77 ± 0.1	5.2E-13	0.84 ± 0.08	4.5E-24	0.7 ± 0.1	1.7E-11	0.78 ± 0.09	1.3E-17	0.55 ± 0.11	6.8E-07	0.36 ± 0.1	4.2E-04	0.46 ± 0.1	3.9E-06	0.3 ± 0.08	7.4E-05

Receiver operating characteristics curve was applied to differentiate between groups. A 95% confidence interval was constructed for each AUC and two-tailed Z-critical values were used to calculate p-values, . Statistical significance was considered 0.05. DR included both NPDR and PDR. DR, diabetic retinopathy; DM, diabetes mellitus; PDR, proliferative diabetic retinopathy; NPDR, nonproliferative diabetic retinopathy.

Method:

1. Sensitivity (also called True Positive Rate - TPR) was calculated for each group [C (n=11), DM (n=10), NPDR (n=26), PDR (n=23)]. Sensitivity is the probability of testing positive given that the event (disease) is positive.

2. False Positive rate (FPR) was calculated similarly. FPR is the probability of testing positive given that the event (disease) is negative.

3. Area under the curve (AUC) was approximated by summing of all the rectangles made with two sets of consecutive TPR and FPR. Formula: middle of TPR's multiplied by change in FPR's.

4. To calculate p-values, a confidence interval was created for each AUC. First, q0, q1, and q2 were calculated using the above formula. Then the Standard Error (SE) was calculated with n being the sample size. Alpha was considered 0.05.

5. Two-tailed Z-critical value was calculated using NORM.S.INV() function. Using the z-values and SE's lower and upper bounds of the 95% confidence interval was calculated.

6. P-values were calculated using P = exp(−0.717×z − 0.416×z2). [https://www.bmj.com/content/343/bmj.d2304].

MALAT1's inflammatory functionalities in various diabetic complications (14, 41, 42). Interestingly, in alignment with our findings, Shaker et al. have demonstrated that significant increases in serum *HOTAIR* and *MALAT1* levels were evident in NPDR and PDR patients compared to healthy controls and through ROC analyses, these lncRNAs could discriminate NPDR and PDR from non-DR controls, further supporting the diagnostic and prognostic utility of lncRNAs as potential non-invasive biomarkers for DR screening and early diagnosis of PDR (29).

H19, a conserved and maternally imprinted lncRNA, is implicated in several pathophysiological processes (43). Few studies have examined *H19* in DR, however we have previously confirmed *H19*'s role in preventing the glucose-induced phenotypic switch of endothelial cells in the diabetic retina (known as endothelial-to-mesenchymal transition; EndMT) (15). Hyperglycemia was shown to promote the upregulation of mesenchymal markers and the downregulation of both *H19* and endothelial cell markers, and subsequent overexpression of *H19* in HG-treated HRECs dramatically reversed the trends evoked by hyperglycemia, suggesting a potential protective role for *H19* in preventing EndMT in DR. Interestingly, in our current findings, *H19* expression levels were relatively increased across all diabetic patient sub-groups with or without DR compared to controls, which may be attributed to patient-specific and/or biological differences (e.g., absence of EndMT). Similar to *H19*, maternally expressed gene 3 (MEG3) is a maternally imprinted gene that exerts critical developmental properties (44). Several lines of evidence also suggest that the inactivation of this gene and the subsequent loss of the *MEG3* lncRNA (along with its diseases-suppressive properties) are frequently documented in numerous cancers and diabetic environments (19, 45–47). In parallel with our findings, reduced serum levels of *MEG3* were observed in patients with DR compared to controls, which may suggest a reduction in the protective mechanisms exerted by *MEG3* (46), however additional studies are warranted to confirm this notion.

Although the lncRNAs *WISPER* (Wisp2 super-enhancer-associated RNA), *HULC* (Highly upregulated in liver cancer), and *ZFAS1* (ZNFX Antisense RNA 1) have not been extensively examined in the context of DR, these critical lncRNAs are pathologically involved in the development of cardiac fibrosis (16), metastatic progression of hepatocellular carcinoma (48), and diabetic cardiomyopathy (17), respectively. Given the increased expressions of these lncRNAs in HG-treated HRECs and the serum and vitreous specimens of DR patients observed from our study, it may be reasonable to speculate that *WISPER*, *ZFAS1* and *HULC* may have similar pathogenetic phenotypes in patients with DR, however additional mechanistic studies are warranted to further delineate their mechanisms in DR progression.

The antisense RNA to INK4 locus (*ANRIL*; also known as CDKN2B-AS1) gene gives rise to a 3.8-kb lncRNA that is prominently deregulated in many diseases, including diabetic cardiomyopathy and nephropathy (49–51). Whether *ANRIL* exerts similar functional and mechanistic capabilities in DR remains limited. However, a recent study, demonstrated for the

TABLE 6 | Diagnostic performance of lncRNA of various potential combinations of lncRNAs in the Control and Patient groups.

Phenotype	Control (n=11)	All patients (n=59)	DM (n=10)	NPDR (n=26)	PDR (n=23)	NPDR+PDR (n=49) (%total; %NPDR/%PDR)
Groups of 4						
ANRIL+/HOTAIR+/HULC+/H19+	0	0	0	0	0	0
ANRIL+/HOTAIR+/HULC+/(H19)	1 (9.1%)	20 (33.9%)	3 (30%)	12 (46.2%)	5 (21.7%)	17 (34.7%; 70.6/29.4)
(ANRIL)/(HOTAIR)/(HULC)/(H19)	8 (72.7%)	17 (28.8%)	3 (30%)	3 (11.5%)	11 (47.8%)	14 (28.6%; 21.4/78.6)
Groups of 4						
MIAT+/WISPER+/ZFAS1+/H19+	0	0	0	0	0	0
(MIAT)/WISPER+/ZFAS1+/(H19)	1 (9.1%)	21 (35.6%)	2 (20%)	14 (53.8%)	5 (21.7%)	19 (38.8%; 73.7/26.3)
(MIAT)/(WISPER)/(ZFAS1)/(H19)	8 (72.7%)	19 (32.2%)	5 (50%)	5 (19.2%)	9 (39.1%)	14 (28.6%; 35.7/64.3)
Groups of 6						
ANRIL+/HOTAIR+/HULC+/WISPER+/ZFAS1+/H19+	0	0	0	0	0	0
ANRIL+/HOTAIR+/HULC+/WISPER+/ZFAS1+/(H19)	1 (9.1%)	18 (30.5%)	3 (30%)	10 (38.5%)	5 (21.7%)	15 (30.6%; 66.7/33.3)
(ANRIL)/(HOTAIR)/(HULC)/(WISPER)/(ZFAS1)/(H19)	8 (72.7%)	14 (23.7%)	3 (30%)	2 (7.7%)	9 (39.1%)	11 (22.4%; 18.2/81.8)

+ means at least 1SD higher fold of lncRNA expression compared to control's mean. lncRNA in parenthesis indicate level of lncRNA could not fall below or rise above 1SD of control's mean. Abbreviations: DR, diabetic retinopathy; DM, diabetes mellitus; PDR, proliferative diabetic retinopathy; NPDR, nonproliferative diabetic retinopathy.

Method:

1. Mean and SD of the control (n=11) was calculated for each of the nine lncRNA.

2. A Z-score was given to each sample based on their distance from the mean and SD of the control.

3. The scores were grouped intro +1SD, +2SD +3SD or more, and -1SD.

4. Phenotypes were formed. ANRIL+ means if ANRIL is expressed at least 1SD above the control's mean calculated in step 1. (ANRIL) means the level of ANRIL could not fall or rise above 1SD of control's mean: -1SD < ANRIL < +1SD.

5. The date is shown in this format: #count (%percent) unless the value is 0.

6. Only column NPDR+PDR contains extra information for the percentage of each NPDR and PDR showing the phenotype separately. The first value shows % of NPDR (% of NPDR, % of PDR).

first time by us, alludes to the angiogenic capabilities of this lncRNA in advancing DR. As evident by the findings from both *in vitro* and *in vivo* experiments, hyperglycemia can significantly induce the upregulation of *ANRIL* in HG-treated HRECs and in the retinas of diabetic mice, and subsequent knockdown of *ANRIL* can greatly hamper glucose-induced retinal angiogenesis (13). Furthermore, in a separate study by Toraih et al., *ANRIL* and 3 additional circulating lncRNAs (*RNCR2*, *MALAT1*, and *PVT1*) did not show an association with DR progression or anti-VEGF therapy response, but the expression patterns of these lncRNAs demonstrated good diagnostic performance in differentiating DM from controls and DR (30). Another prominent lncRNA involved in the pathogenesis of DR is myocardial infarction-associated transcript (*MIAT*; also referred to as RNCR2, Gomafu, or AK028326) (11, 52). *MIAT* is significantly upregulated in the retinas of diabetic rodents, and in the fibrovascular membranes of diabetic patients compared to non-diabetic controls (11). *In vitro* experiments also indicated that expressions of *MIAT* are upregulated in several HG-treated retinal cell lines, while increased plasma levels of *MIAT* have been found to be significantly associated with the presence of DR (53). Taken together, the increased *MIAT* and *ANRIL* expressions observed in the present study confirms the pathogenetic nature of these lncRNAs documented in previous studies, and long-term clinical studies are required to further discern the diagnostic performance of these lncRNAs.

Undoubtedly, the results from the current study provide unique insights into the potential discriminative abilities of lncRNAs for identifying patients with DR from patients without DR. However, given the small sample size and cross-sectional nature of the study, additional modelling, and extrapolation of long-term outcomes between lncRNA expression levels, diabetes mellitus, and the various subsets of DR could not be determined. As well, due to the exploratory nature of this study, selection bias was inevitably introduced with respect to specimen selection. Future prospective screening studies, with larger sample sizes, should be conducted in order to increase the sensitivity of the assay and help determine whether certain sub-stages of DR can be detected, through lncRNA expression levels and/or combination of lncRNA phenotypes, before clinical diagnosis.

Nevertheless, the on-going research work on lncRNAs continues to evolve our understanding of various pathologies and their respective molecular mechanisms. Given the critical nature of lncRNAs and their involvement in disease progression, exploiting these RNA transcripts for diagnostic and/or therapeutic approaches may guide optimal treatment strategies and long-term benefits for patients. As such, the collective findings from this study highlight unique expression patterns for a subset of 9 well-studied lncRNAs (*MALAT1*, *HOTAIR*, *ANRIL*, *ZFAS1*, *HULC*, *H19*, *WISPER*, *MIAT*, and *MEG3*) for patients with and without DR, and subsequent analysis of these lncRNA signatures may provide important clinical utility for the prediction and diagnosis of DR severity. However, additional long-term and larger prospective studies are warranted in order to determine such utility of lncRNA biomarkers.

DATA AVAILABILITY STATEMENT

The original contributions presented in the study are included in the article/**Supplementary Materials**. Further inquiries can be directed to the corresponding author.

ETHICS STATEMENT

The studies involving human participants were reviewed and approved by Western Research Ethics Board and Lawson Health Research Institute at the University of Western Ontario (London, ON, CAN). The patients/participants provided their written informed consent to participate in this study.

AUTHOR CONTRIBUTIONS

SC conceived, designed, and directed the study. ShC and SB performed the *in vitro* experiments. SB, AC, MG, ShC, and SC collected clinical samples and performed data analyses. SC and JG provided reagents, materials, and analysis tools. SB, AC, and SC wrote the manuscript. All authors contributed to the article and approved the submitted version.

FUNDING

The Canadian Institutes of Health Research funded and supported this research.

SUPPLEMENTARY MATERIAL

The Supplementary Material for this article can be found online at: https://www.frontiersin.org/articles/10.3389/fendo.2022.851967/full#supplementary-material

REFERENCES

1. Saeedi P, Petersohn I, Salpea P, Malanda B, Karuranga S, Unwin N, et al. Global and Regional Diabetes Prevalence Estimates for 2019 and Projections for 2030 and 2045: Results From the International Diabetes Federation Diabetes Atlas, 9th Edition. *Diabetes Res Clin Pract* (2019) 157:107843. doi: 10.1016/j.diabres.2019.107843
2. Cheung N, Mitchell P, Wong TY. Diabetic Retinopathy. *Lancet (London England)* (2010) 376(9735):124–36. doi: 10.1016/S0140-6736(09)62124-3
3. Bascaran C, Mwangi N, D'Esposito F, Gordon I, Alberto Lopez Ulloa J, Mdala S, et al. Effectiveness of Task-Shifting for the Detection of Diabetic Retinopathy in Low- and Middle-Income Countries: A Rapid Review Protocol. *Syst Rev* (2021) 10:4. doi: 10.1186/s13643-020-01553-w
4. American Academy of Ophthalmology Retina/Vitreous Panel. Preferred Practice Pattern Guidelines. In: *Diabetic Retinopathy*. San Francisco, CA: American Academy of Ophthalmology (2016). Available at: www.aao.org/ppp.
5. Harris Nwanyanwu K, Talwar N, Gardner TW, Wrobel JS, Herman WH, Stein JD. Predicting Development of Proliferative Diabetic Retinopathy. *Diabetes Care* (2013) 36(6):1562–8. doi: 10.2337/dc12-0790
6. Gabrielian A, Hariprasad SM, Jager RD, Green JL, Mieler WF. The Utility of Visual Function Questionnaire in the Assessment of the Impact of Diabetic Retinopathy on Vision-Related Quality of Life. *Eye (London England)* (2010) 24(1):29–35. doi: 10.1038/eye.2009.56
7. Wong TY, Cheung CM, Larsen M, Sharma S, Simó R. Diabetic Retinopathy. *Nat Rev Dis Primers* (2016) 2:16012. doi: 10.1038/nrdp.2016.12
8. Lachin JM, Genuth S, Nathan DM, Zinman B, Rutledge BN. & DCCT/EDIC Research Group. Effect of Glycemic Exposure on the Risk of Microvascular Complications in the Diabetes Control and Complications Trial–Revisited. *Diabetes* (2008) 57(4):995–1001. doi: 10.2337/db07-1618
9. Woung LC, Tsai CY, Chou HK, Tsai MT, Tsai WH, Chou P, et al. Healthcare Costs Associated With Progressive Diabetic Retinopathy Among National Health Insurance Enrollees in Taiwan, 2000-2004. *BMC Health Serv Res* (2010) 10:136. doi: 10.1186/1472-6963-10-136
10. Schmier JK, Covert DW, Lau EC, Matthews GP. Medicare Expenditures Associated With Diabetes and Diabetic Retinopathy. *Retina (Philadelphia Pa.)* (2009) 29(2):199–206. doi: 10.1097/IAE.0b013e3181884f2d
11. Yan B, Yao J, Liu JY, Li XM, Wang XQ, Li YJ, et al. lncRNA-MIAT Regulates Microvascular Dysfunction by Functioning as a Competing Endogenous RNA. *Circ Res* (2015) 116(7):1143–56. doi: 10.1161/CIRCRESAHA.116.305510
12. Biswas S, Feng B, Chen S, Liu J, Aref-Eshghi E, Gonder J, et al. The Long Non-Coding RNA HOTAIR Is a Critical Epigenetic Mediator of Angiogenesis in Diabetic Retinopathy. *Invest Ophthalmol Visual Sci* (2021) 62(3):20. doi: 10.1167/iovs.62.3.20
13. Thomas AA, Feng B, Chakrabarti S. ANRIL: A Regulator of VEGF in Diabetic Retinopathy. *Invest Ophthalmol Visual Sci* (2017) 58(1):470–80. doi: 10.1167/iovs.16-20569
14. Biswas S, Thomas AA, Chen S, Aref-Eshghi E, Feng B, Gonder J, et al. MALAT1: An Epigenetic Regulator of Inflammation in Diabetic Retinopathy. *Sci Rep* (2018) 8(1):6526. doi: 10.1038/s41598-018-24907-w
15. Thomas AA, Biswas S, Feng B, Chen S, Gonder J, Chakrabarti S. lncRNA H19 Prevents Endothelial-Mesenchymal Transition in Diabetic Retinopathy. *Diabetologia* (2019) 62(3):517–30. doi: 10.1007/s00125-018-4797-6
16. Micheletti R, Plaisance I, Abraham BJ, Sarre A, Ting CC, Alexanian M, et al. The Long Noncoding RNA *Wisper* Controls Cardiac Fibrosis and Remodeling. *Sci Trans Med* (2017) 9(395):eaai9118. doi: 10.1126/scitranslmed.aai9118
17. Feng B, Chen S, Chakrabarti S. Long Noncoding RNA Zfas1 in Diabetic Cardiomyopathy. *Diabetes* (2018) 67(Supplement 1):473–P. doi: 10.2337/db18-473-P
18. Jin C, Shi W, Wang F, Shen X, Qi J, Cong H, et al. Long Non-Coding RNA HULC as a Novel Serum Biomarker for Diagnosis and Prognosis Prediction of Gastric Cancer. *Oncotarget* (2016) 7(32):51763–72. doi: 10.18632/oncotarget.10107
19. Qiu GZ, Tian W, Fu HT, Li CP, Liu B. Long Noncoding RNA-MEG3 Is Involved in Diabetes Mellitus-Related Microvascular Dysfunction. *Biochem Biophys Res Commun* (2016) 471(1):135–41. doi: 10.1016/j.bbrc.2016.01.164
20. Standl E, Khunti K, Hansen TB, Schnell O. The Global Epidemics of Diabetes in the 21st Century: Current Situation and Perspectives. *Eur J Prev Cardiol* (2019) 26(2_suppl):7–14. doi: 10.1177/2047487319881021
21. Teo ZL, Tham YC, Yu M, Chee ML, Rim TH, Cheung N, et al. Global Prevalence of Diabetic Retinopathy and Projection of Burden Through 2045: Systematic Review and Meta-Analysis. *Ophthalmology* (2021) 128(11):1580–91. doi: 10.1016/j.ophtha.2021.04.027
22. Zheng Y, He M, Congdon N. The Worldwide Epidemic of Diabetic Retinopathy. *Indian J Ophthalmol* (2012) 60(5):428–31. doi: 10.4103/0301-4738.100542
23. Antonetti DA, Barber AJ, Bronson SK, Freeman WM, Gardner TW, Jefferson LS, et al. & JDRF Diabetic Retinopathy Center Group. Diabetic Retinopathy: Seeing Beyond Glucose-Induced Microvascular Disease. *Diabetes* (2006) 55 (9):2401–11. doi: 10.2337/db05-1635
24. Heitmar R, Kalitzeos AA, Patel SR, Prabhu-Das D, Cubbidge RP. Comparison of Subjective and Objective Methods to Determine the Retinal Arterio-Venous Ratio Using Fundus Photography. *J Optomet* (2015) 8(4):252–7. doi: 10.1016/j.optom.2014.07.002
25. Jiang MC, Ni JJ, Cui WY, Wang BY, Zhuo W. Emerging Roles of lncRNA in Cancer and Therapeutic Opportunities. *Am J Cancer Res* (2019) 9(7):1354–66. doi: 10.1038/nm.3981
26. Riva P, Ratti A, Venturin M. The Long Non-Coding RNAs in Neurodegenerative Diseases: Novel Mechanisms of Pathogenesis. *Curr Alzheimer Res* (2016) 13(11):1219–31. doi: 10.2174/1567205013666160622112234

27. Leung A, Natarajan R. Long Noncoding RNAs in Diabetes and Diabetic Complications. *Antioxid Redox Signaling* (2018) 29(11):1064–73. doi: 10.1089/ars.2017.7315
28. Biswas S, Chakrabarti S. The Multifaceted Roles of lncRNAs in Diabetic Complications: A Promising, Yet Perplexing Paradigm. In: S Jurga, J Barciszewski, editors. *The Chemical Biology of Long Noncoding RNAs*. Cham: Springer Series, RNA Technologies (2020). p. 491–521. doi: 10.1007/978-3-030-44743-4_19
29. Shaker OG, Abdelaleem OO, Mahmoud RH, Abdelghaffar NK, Ahmed TI, Said OM, et al. Diagnostic and Prognostic Role of Serum miR-20b, miR-17-3p, HOTAIR, and MALAT1 in Diabetic Retinopathy. *IUBMB Life* (2019) 71 (3):310–20. doi: 10.1002/iub.1970
30. Toraih EA, Abdelghany AA, Abd El Fadeal NM, Al Ageeli E, Fawzy MS. Deciphering the Role of Circulating lncRNAs: RNCR2, NEAT2, CDKN2B-AS1, and PVT1 and the Possible Prediction of Anti-VEGF Treatment Outcomes in Diabetic Retinopathy Patients. *Graefe's Arch Clin Exp Ophthalmol = Albrecht Von Graefes Archiv Fur Klinische Und Experimentelle Ophthalmol* (2019) 257(9):1897–913. doi: 10.1007/s00417-019-04409-9
31. Yan B, Tao ZF, Li XM, Zhang H, Yao J, Jiang Q. Aberrant Expression of Long Noncoding RNAs in Early Diabetic Retinopathy. *Invest Ophthalmol Visual Sci* (2014) 55(2):941–51. doi: 10.1167/iovs.13-13221
32. Rinn JL, Kertesz M, Wang JK, Squazzo SL, Xu X, Brugmann SA, et al. Functional Demarcation of Active and Silent Chromatin Domains in Human HOX Loci by Noncoding RNAs. *Cell* (2007) 129(7):1311–23. doi: 10.1016/j.cell.2007.05.022
33. Kino T, Hurt DE, Ichijo T, Nader N, Chrousos GP. Noncoding RNA Gas5 Is a Growth Arrest- and Starvation-Associated Repressor of the Glucocorticoid Receptor. *Sci Signaling* (2010) 3(107):ra8. doi: 10.1126/scisignal.2000568
34. Zappulla DC, Cech TR. RNA as a Flexible Scaffold for Proteins: Yeast Telomerase and Beyond. *Cold Spring Harbor Symp Quant Biol* (2006) 71:217–24. doi: 10.1101/sqb.2006.71.011
35. Ørom UA, Derrien T, Beringer M, Gumireddy K, Gardini A, Bussotti G, et al. Long Noncoding RNAs With Enhancer-Like Function in Human Cells. *Cell* (2010) 143(1):46–58. doi: 10.1016/j.cell.2010.09.001
36. Wang Y, Sun L, Wang L, Liu Z, Li Q, Yao B, et al. Long Non-Coding RNA DSCR8 Acts as a Molecular Sponge for miR-485-5p to Activate Wnt/β-Catenin Signal Pathway in Hepatocellular Carcinoma. *Cell Death Dis* (2018) 9 (9):851. doi: 10.1038/s41419-018-0937-7
37. Vance KW, Ponting CP. Transcriptional Regulatory Functions of Nuclear Long Noncoding RNAs. *Trends Genet: TIG* (2014) 30(8):348–55. doi: 10.1016/j.tig.2014.06.001
38. Yoon JH, Abdelmohsen K, Gorospe M. Posttranscriptional Gene Regulation by Long Noncoding RNA. *J Mol Biol* (2013) 425(19):3723–30. doi: 10.1016/j.jmb.2012.11.024
39. Hajjari M, Salavaty A. HOTAIR: An Oncogenic Long Non-Coding RNA in Different Cancers. *Cancer Biol Med* (2015) 12(1):1–9. doi: 10.7497/j.issn.2095-3941.2015.0006
40. Wang H, Xia Y, Zhang Y. Diagnostic Significance of Serum lncRNA HOTAIR and Its Predictive Value for the Development of Chronic Complications in Patients With Type 2 Diabetes Mellitus. *Diabetol Metab Syndrome* (2021) 13 (1):97. doi: 10.1186/s13098-021-00719-3
41. Gordon AD, Biswas S, Feng B, Chakrabarti S. MALAT1: A Regulator of Inflammatory Cytokines in Diabetic Complications. *Endocrinol Diabetes Metab* (2018) 1(2):e00010. doi: 10.1002/edm2.10
42. Puthanveetil P, Chen S, Feng B, Gautam A, Chakrabarti S. Long non-Coding RNA MALAT1 Regulates Hyperglycaemia Induced Inflammatory Process in the Endothelial Cells. *J Cell Mol Med* (2015) 19(6):1418–25. doi: 10.1111/jcmm.12576
43. Wang B, Suen CW, Ma H, Wang Y, Kong L, Qin D, et al. The Roles of H19 in Regulating Inflammation and Aging. *Front Immunol* (2020) 11:579687:579687. doi: 10.3389/fimmu.2020.579687
44. da Rocha ST, Edwards CA, Ito M, Ogata T, Ferguson-Smith AC. Genomic Imprinting at the Mammalian Dlk1-Dio3 Domain. *Trends Genet: TIG* (2008) 24(6):306–16. doi: 10.1016/j.tig.2008.03.011
45. Zhou Y, Zhang X, Klibanski A. MEG3 Noncoding RNA: A Tumor Suppressor. *J Mol Endocrinol* (2012) 48(3):R45–53. doi: 10.1530/JME-12-0008
46. Zhang D, Qin H, Leng Y, Li X, Zhang L, Bai D, et al. LncRNA MEG3 Overexpression Inhibits the Development of Diabetic Retinopathy by Regulating TGF-β1 and VEGF. *Exp Ther Med* (2018) 16(3):2337–42. doi: 10.3892/etm.2018.6451
47. Tong P, Peng QH, Gu LM, Xie WW, Li WJ. LncRNA-MEG3 Alleviates High Glucose Induced Inflammation and Apoptosis of Retina Epithelial Cells *via* Regulating miR-34a/SIRT1 Axis. *Exp Mol Pathol* (2019) 107:102–9. doi: 10.1016/j.yexmp.2018.12.003
48. Li T, Xie J, Shen C, Cheng D, Shi Y, Wu Z, et al. Amplification of Long Noncoding RNA ZFAS1 Promotes Metastasis in Hepatocellular Carcinoma. *Cancer Res* (2015) 75(15):3181–91. doi: 10.1158/0008-5472.CAN-14-3721
49. Broadbent HM, Peden JF, Lorkowski S, Goel A, Ongen H, Green F, et al. & PROCARDIS Consortium. Susceptibility to Coronary Artery Disease and Diabetes Is Encoded by Distinct, Tightly Linked SNPs in the ANRIL Locus on Chromosome 9p. *Hum Mol Genet* (2008) 17(6):806–14. doi: 10.1093/hmg/ddm352
50. Li Z, Yu X, Shen J. ANRIL: A Pivotal Tumor Suppressor Long Non-Coding RNA in Human Cancers. *Tumour Biol* (2016) 37(5):5657–61. doi: 10.1007/s13277-016-4808-5
51. Thomas AA, Feng B, Chakrabarti S. ANRIL Regulates Production of Extracellular Matrix Proteins and Vasoactive Factors in Diabetic Complications. *Am J Physiol Endocrinol Metab* (2018) 314(3):E191–200. doi: 10.1152/ajpendo.00268.2017
52. Ishii N, Ozaki K, Sato H, Mizuno H, Susumu S, Takahashi A, et al. Identification of a Novel Non-Coding RNA, MIAT, That Confers Risk of Myocardial Infarction. *J Hum Genet* (2006) 51(12):1087–99. doi: 10.1007/s10038-006-0070-9
53. Li Q, Pang L, Yang W, Liu X, Su G, Dong Y. Long Non-Coding RNA of Myocardial Infarction Associated Transcript (LncRNA-MIAT) Promotes Diabetic Retinopathy by Upregulating Transforming Growth Factor-β1 (TGF-β1) Signaling. *Med Sci Monit* (2018) 24:9497–503. doi: 10.12659/MSM.911787

Conflict of Interest: The authors declare that the research was conducted in the absence of any commercial or financial relationships that could be construed as a potential conflict of interest.

Publisher's Note: All claims expressed in this article are solely those of the authors and do not necessarily represent those of their affiliated organizations, or those of the publisher, the editors and the reviewers. Any product that may be evaluated in this article, or claim that may be made by its manufacturer, is not guaranteed or endorsed by the publisher.

frontiers | Frontiers in Endocrinology

ORIGINAL RESEARCH
published: 17 May 2022
doi: 10.3389/fendo.2022.876559

Using Machine Learning Techniques to Develop Risk Prediction Models for the Risk of Incident Diabetic Retinopathy Among Patients With Type 2 Diabetes Mellitus: A Cohort Study

Yuedong Zhao[1†], Xinyu Li[1†], Shen Li[1†], Mengxing Dong[2†], Han Yu[3], Mengxian Zhang[1], Weidao Chen[2], Peihua Li[1], Qing Yu[1], Xuhan Liu[1] and Zhengnan Gao[1*]*

[1] Department of Endocrinology, Dalian Municipal Central Hospital, Dalian, China, [2] Infervision Institute of Research, Beijing, China, [3] Graduate School of Art and Science, Yale University, New Haven, CT, United States

OPEN ACCESS

Edited by:
Subrata Chakrabarti,
Western University, Canada

Reviewed by:
Matthew Cecchini,
London Health Sciences Centre, Canada
Christina A. Castellani,
Western University, Canada

***Correspondence:**
Xuhan Liu
Liuxuhan20220214@163.com
Zhengnan Gao
gao2008@163.com

†These authors have contributed equally to this work and share first authorship

Specialty section:
This article was submitted to Clinical Diabetes, a section of the journal Frontiers in Endocrinology

Received: 15 February 2022
Accepted: 12 April 2022
Published: 17 May 2022

Citation:
Zhao Y, Li X, Li S, Dong M, Yu H, Zhang M, Chen W, Li P, Yu Q, Liu X and Gao Z (2022) Using Machine Learning Techniques to Develop Risk Prediction Models for the Risk of Incident Diabetic Retinopathy Among Patients With Type 2 Diabetes Mellitus: A Cohort Study. Front. Endocrinol. 13:876559. doi: 10.3389/fendo.2022.876559

Objective: To construct and validate prediction models for the risk of diabetic retinopathy (DR) in patients with type 2 diabetes mellitus.

Methods: Patients with type 2 diabetes mellitus hospitalized over the period between January 2010 and September 2018 were retrospectively collected. Eighteen baseline demographic and clinical characteristics were used as predictors to train five machine-learning models. The model that showed favorable predictive efficacy was evaluated at annual follow-ups. Multi-point data of the patients in the test set were utilized to further evaluate the model's performance. We also assessed the relative prognostic importance of the selected risk factors for DR outcomes.

Results: Of 7943 collected patients, 1692 (21.30%) developed DR during follow-up. Among the five models, the XGBoost model achieved the highest predictive performance with an AUC, accuracy, sensitivity, and specificity of 0.803, 88.9%, 74.0%, and 81.1%, respectively. The XGBoost model's AUCs in the different follow-up periods were 0.834 to 0.966. In addition to the classical risk factors of DR, serum uric acid (SUA), low-density lipoprotein cholesterol (LDL-C), total cholesterol (TC), estimated glomerular filtration rate (eGFR), and triglyceride (TG) were also identified to be important and strong predictors for the disease. Compared with the clinical diagnosis method of DR, the XGBoost model achieved an average of 2.895 years prior to the first diagnosis.

Conclusion: The proposed model achieved high performance in predicting the risk of DR among patients with type 2 diabetes mellitus at each time point. This study established the potential of the XGBoost model to facilitate clinicians in identifying high-risk patients and making type 2 diabetes management-related decisions.

Keywords: type 2 diabetes mellitus, diabetic retinopathy, machine learning, XGBoost model, cohort study

INTRODUCTION

DR is the most common microvascular complication of diabetes mellitus. It has been demonstrated to be a leading cause of preventable blindness in the working-age population in most countries (1).

The American Academy of Ophthalmology (AAO), in 2019, stated that the prevalence of DR among diabetic patients worldwide is about 34.6%. 10.2% (28 million) diabetic patients suffer from vision-threatening DR (2). Effective management of DR requires a deep understanding of the predisposing factors, early diagnosis, and timely therapeutic intervention. Early identification of patients at risk of developing DR is the key to effective intervention, which is significant in reducing the progression of DR and thereby reducing the risk of blindness (3). Moreover, individual patients can be stratified according to different risk levels and get optimal treatment. Due to no typical symptoms in the early stage of the disease, however, most patients with DR may not seek medical evaluation until progression to the proliferative stage, resulting in irreversible visual damage (4). Therefore, methods for accurate prediction of the risk of DR are in urgent need.

At present, several DR risk prediction models based on cross-sectional studies have been developed (5–9). Deep learning algorithms were also applied (10). Although these models can predict the occurrence of DR at the index date, they cannot predict DR occurrence and development of the same patient at designated time points in the future. This will obviously restrict their clinical application. Similarly, based on the clinical characteristics related to the occurrence or development of DR, several models have been developed for optimization of the screening interval in DR screening (11, 12). However, due to the small number of cases in the studies, the proposed models have not been fully validated so far.

On the other hand, several studies investigated the pathogenesis and risk factors of DR to provide guidance for DR management. Epidemiological studies have shown that age, course of diabetes, hemoglobin A1c(HbA1c), fasting blood glucose (FBG), blood pressure, blood lipids, body mass index (BMI), smoking, proteinuria, and several others are all risk factors for DR (13, 14). Among them, duration of diabetes and hyperglycemia were demonstrated as strong risk factors for the occurrence and development of DR (15, 16). However, patients without DR were hardly unusual among those suffering from diabetes for a long time (17). The influences of other factors in DR occurrence also need to be proven. Further studies are required to elucidate the correlation and thus construct standard procedures for the management of this disease.

In this retrospective cohort study, we collected electronic health record data from hospitalized patients with type 2 diabetes and established the prediction model for future risks of DR based on a machine learning (ML) algorithm. To our knowledge, this is the first study to predict the occurrence of DR at each follow-up time point in up to 10 years. We also explore the risk factors that may affect the occurrence of DR and hope this work can provide a basis for further studies concerning the prevention and management of DR.

MATERIALS AND METHODS

Study Subjects

The study protocol was approved by the Ethics Committee of Dalian Medical University Affiliated with the Central Hospital of Dalian. The ethics committee waived the requirement of written informed consent for all patients. The data did not contain any direct patient identifiers. The study adhered to the tenets of the Declaration of Helsinki.

Datasets

In this retrospective cohort study, we recruited inpatients admitted to the Department of endocrinology of Dalian Medical University Affiliated with the Central Hospital of Dalian from January 2010 to September 2018. Patients who met the following criteria were included in the current study: 1) Age≥18 years with the diagnosis of type 2 diabetes; 2) be hospitalized at least once over the follow-up period; 3) no presence of DR at the time of the first hospitalization. Patients with other types of diabetes (type 1 diabetes, special type diabetes, or gestational diabetes) or previous eye diseases (cataract, glaucoma, or other eye diseases) were excluded. With the criteria mentioned above, 7943 patients were selected for this study, including 1692 patients diagnosed with DR in the follow-up period (DR group) and 6521 control ones without DR (non-DR group). These patients were randomly divided into a training set (n=5559) and a test set (n=2384).

Diagnostic Criteria

Diagnostic criteria of type 2 DM are according to 1999 WHO diagnostic criteria (18). DR was examined by dilated fundus examination by ophthalmologists and endocrinologists together. Diagnostic criteria of DR case meet the Diabetic Retinopathy preferred practice pattern (PPP)-2019 guideline (19). The grading of DR in this study was based on the International Clinical Diabetic Retinopathy Severity Scales (20): Grace-1 for no apparent retinopathy; Grace-2 for mild non-proliferative diabetic retinopathy (NPDR), which includes microaneurysms only; Grace-3 for moderate NPDR, which includes more than just microaneurysms but less than severe nonproliferative DR; Grace-4 for severe NPDR (any of the following can be diagnosed as Grace-4: more than 20 intraretinal hemorrhages in each of 4 quadrants, definite venous beading in 2+ quadrants, Prominent intraretinal microvascular abnormalities in 1+ quadrant); and Grace-5 for proliferative diabetic retinopathy (PDR). The individual diagnoses were described according to the diagnosis and staging of the worse one between the two eyes.

Variable Selection

Patients' information on demographics, medical history, medication, and laboratory data was extracted from the EHR at baseline and used as candidate predictor variables for developing DR (**Tables S2, S3**). These variables are commonly associated with the risk of DR, including 11 categorical variables and 20 continuous variables. The smoking status was defined as: 1) Current smokers: Patients who smoked more than 100 cigarettes and had not quit smoking at the index date; 2) Ex-smokers: Patients who smoked more than 100 cigarettes and stopped smoking 30 days before index date; 3) Never

smokers: Patients who had never smoked. The drinking status was defined as: 1) Current drinkers: Patients who have been drinking or have not abstained from alcohol for more than one year; 2) Ex-drinkers: Patients who did not drink or had abstained from drinking for more than one year; 3) Never-drinks: Patients who had never drunk. Hypertension was defined as a systolic blood pressure of ≥140 mmHg and/or a diastolic blood pressure ≥90 mmHg, measured twice or more on different days, whether antihypertensive drugs were used or not (21). Blood samples were collected the next morning after hospital admission with at least 12-h fasting. HbA1c was measured using the glycosylated hemoglobin analyzer (TOSOH company of Japan, HLC-723G8). Four items of blood lipids (high-density lipoprotein cholesterol (HDL-C), TC, LDL-C, and TG), alanine transaminase (ALT), aspartate transaminase (AST), gamma-glutamyl transpeptidase(γ-GT), serum creatinine (Scr), SUA, and FBG were detected by automatic biochemical analyzer (Siemens, Germany, ADVIA2400 biochemical system). The eGFR was calculated according to the CKD-EPI formula (22). BMI was calculated as weight (kg) divided by the square of height in meters (m^2); Blood pressure was measured on the right arm in sitting position three times consecutively at 5-min intervals, with the mean of the three measurements used for analysis.

Machine Learning Models Construction

Machine learning-based algorithms were selected according to the criteria below. First, the algorithms should show evaluation indicators based on mixed data type, including numerical variables and categorical variables. Second, the algorithms should have a wide range of applications and a history of successful usage in related fields. Based on the above criteria, we selected five machine learning algorithms, Random Forest (RF) (23), Extreme Gradient Boosting (XGBoost) (24), Logistic Regression (LR) (25), Support Vector Machine (SVM) (26), and K-Nearest Neighbor (K-NN) (27), to build the models with all the variables as predictors in this study. We used the GridSearchCV method to select the optimal key hyper-parameters of the five models as shown in **Table S3**, and other hyper-parameters were set as default. The models were then tested and internally validated by fivefold cross-validation.

Statistical Analysis

All statistical analyses were performed by using R statistical and computing software version 4.0.2 (http://www.r-project.org/). *Chi*-square test was used for categorical variables, and two-sample *t*-test for continuous variables to compare the variables between DR group and non-DR group. Two-tailed hypothesis testing was used. $P<0.05$ indicated a statistically significant result.

Performance of the proposed models was assessed mainly in terms of sensitivity, specificity, positive predictive value (PPV), negative predictive value (NPV), and accuracy. We assessed these metrics at the optimized prediction threshold identified by the Youden index. To compare performance across the models, we also calculated the area under the receiver operating characteristic curve (*AUC*). Significance testing and *LASSO* penalty were employed to identify clinical features that are associated with a high risk of DR. Nomograms were built based on the results of multivariate logistic regression analysis. The performance of the nomograms was measured using Harrell's concordance index (*C*-index).

RESULTS

Study Population

Baseline characteristics of 7943 patients with type 2 diabetes, including 1692 patients diagnosed as DR (DR group) and 6521 without DR signs (non-DR group) during the follow-up period, are presented in **Table S4**. The mean age of the patients was 63.54 years, and 45.7% were women. Mean follow-up time was 3.139 ± 2.243 years, and mean duration of diabetes mellitus was 1.449 ± 2.756 years. To further validate the performance of the model, 829 multipoint data from different follow-up time points were collected from 508 patients in the test set (supplementary test set).

Prediction Performances of the ML Models

The performances of the prediction models were assessed in terms of predefined evaluation metrics and *ROC* (**Table 1** and **Figure 1**). The XGBoost model outperformed the other models with the highest *AUC* (0.913; 95% confidence interval (*CI*), 0.901-0.925), highest accuracy (79.9%; *CI*, 76.9%-83.5%), highest sensitivity (90.2%; *CI*, 84.8%-94.9%), highest specificity (77.1&; *CI*, 72.1%- 82.7%), highest PPV (51.6%; *CI*, 47.9%-57.5%) and highest NPV (96.7%; *CI*, 95.2%-98.1%).

Prediction Performance of the XGBoost Model in Different Follow-Up Periods

The XGBoost model was further assessed as a potential tool to predict the occurrence of DR (**Table 2**). According to follow-up

TABLE 1 | The performance metrics of the cross-validated machine learning algorithms on the test data.

Model	AUC (95% CI)	Accuracy (95% CI)	Sensitivity (95% CI)	Specificity (95% CI)	PPV (95% CI)	NPV (95% CI)
RF	0.872 (0.857, 0.887)	0.764 (0.703, 0.785)	0.817 (0.793, 0.925)	0.749 (0.647, 0. 776)	0.469 (0.41, 0.498)	0.938 (0.931, 0.971)
XGBoost	0.913 (0.901, 0.925)	0.799 (0.769, 0.835)	0.902 (0.848, 0.949)	0.771 (0.721, 0. 827)	0.516 (0.479, 0.575)	0.967 (0.952, 0.981)
LR	0.808 (0.787, 0.828)	0.731 (0.659, 0.789)	0.73 (0.636, 0.852)	0.731 (0.61, 0. 828)	0.424 (0.368, 0.504)	0.909 (0.893, 0.94)
SVM	0.802 (0.781, 0.823)	0.742 (0.702, 0.776)	0.74 (0.677, 0.805)	0.742 (0.681, 0.803)	0.437 (0.398, 0.482)	0.913 (0.901, 0.93)
K-NN	0.629 (0.601, 0.656)	0.537 (0.522, 0.752)	0.689 (0.303, 0.73)	0.496 (0.478, 0.868)	0.27 (0.261, 0.399)	0.855 (0.82, 0.872)

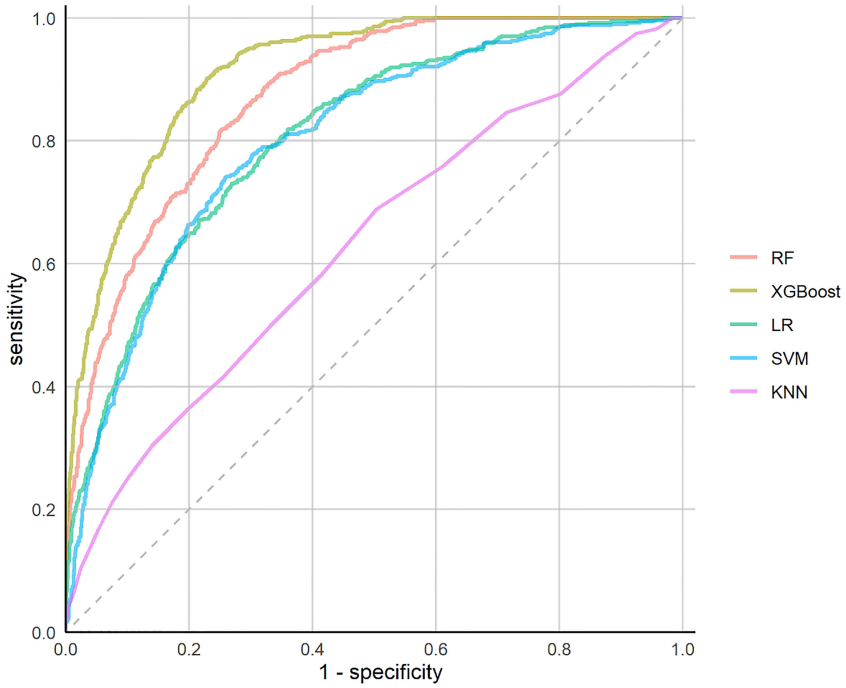

FIGURE 1 | Receiver Operating Characteristics (*ROC*) curves of the ML models.

TABLE 2 | The performance metrics of the XGBoost model for different follow-up times.

*Follow-up period	Patient number	DR patient number	AUC(95% CI)	Accuracy (95% CI)	Sensitivity (95% CI)	Specificity (95% CI)	PPV (95% CI)	NPV (95% CI)
(1, 2)	1025	93	0.966 (0.955, 0.977)	0.877 (0.855, 0.933)	0.978 (0.925, 1)	0.867 (0.841, 0.931)	0.423 (0.382, 0.578)	0.998 (0.992, 1)
(2, 3)	352	92	0.834 (0.788, 0.879)	0.733 (0.668, 0.801)	0.848 (0.739, 0.957)	0.692 (0.577, 0.812)	0.494 (0.435, 0.592)	0.928 (0.894, 0.977)
(3, 4)	283	78	0.867 (0.817, 0.918)	0.77 (0.728, 0.873)	0.859 (0.654, 0.949)	0.737 (0.659, 0.932)	0.554 (0.503, 0.797)	0.932 (0.873, 0.972)
(4, 5)	242	70	0.86 (0.809, 0.911)	0.785 (0.707, 0.851)	0.8 (0.686, 0.957)	0.779 (0.628, 0.901)	0.596 (0.496, 0.742)	0.905 (0.872, 0.977)
(5, 6)	153	49	0.835 (0.765, 0.905)	0.765 (0.719, 0.869)	0.776 (0.531, 0.898)	0.76 (0.654, 0.962)	0.603 (0.538, 0.879)	0.878 (0.809, 0.943)
(6, 7)	129	38	0.876 (0.814, 0.938)	0.837 (0.705, 0.899)	0.711 (0.605, 0.974)	0.89 (0.604, 0.967)	0.73 (0.5, 0.897)	0.88 (0.85, 0.983)
(7, 8)	116	45	0.917 (0.867, 0.966)	0.845 (0.759, 0.897)	0.822 (0.733, 0.933)	0.859 (0.732, 0.901)	0.787 (0.655, 0.841)	0.884 (0.825, 0.955)
(8, 11)	84	43	0.858 (0.779, 0.936)	0.798 (0.738, 0.881)	0.791 (0.698, 1)	0.805 (0.561, 0.927)	0.81 (0.691, 0.92)	0.786 (0.72, 1)

**Follow-up period indicated the corresponding time frame that included the former time point but not the latter one.*

intervals, the test set was divided into eight categories, respectively, each year of 1 to 8 years and more than 8 years. The highest *AUC* of 0.966 (95% *CI*, 0.955-0.977) and highest accuracy of 87.7% (95% *CI*, 85.5%-93.3%) were achieved in patients who were followed up within the timeframe of 1 to 2 years.

Information Contributions of the Features

The importance scores calculated by XGBoost are shown in **Figure 2**. Among all the features, the top five ones (HbA1c, duration, follow-up time, FBG, and age) contributed the most to identifying cases with DR risk in type 2 diabetes patients. In addition, the importance scores calculated by RF, which is the next-best performing model, are shown in **Figure S1**.

Subgroups Analysis Based on Follow-Up Period and DR Severity Level

The XGBoost model was further evaluated on the supplementary test set. Multipoint data of the same patient were used as new cases. The model showed an improved performance with an *AUC*, accuracy, sensitivity, specificity, *PPV*, and *NPV* of 0.922 (95%*CI*, 0.912-0.932), 81.5% (95% *CI*, 80.4%-84.2%), 92.6% (95% *CI*, 87.1%-94.2%), 76.6% (95% *CI*, 74.9%-82.4%), 63.6% (95% *CI*, 62.1%-68.8%), and 95.9% (95% *CI*, 93.5%-96.8%) respectively. Detailed attributes are presented in **Table S5**. Age, diuretic, fibrates, eGFR, HbA1c, duration, and follow-up time were significantly different between the cases with correct predictions and those with incorrect predictions. We then measured the time to diagnosis. The XGBoost model achieved an average of 2.895 ± 2.104 years prior to the first diagnosis by the clinical diagnosis method.

Subgroups analyses based on follow-up period and DR severity level were respectively conducted to assess the potential application of the model in clinical scenarios (**Supplementary Figure S4**). With the increase in follow-up time, the true positive prediction rate of the XGBoost model increases (**Supplementary Figure S4A**). The subgroup of patients followed up within the time frame of 7 to 8 years exhibited the highest positive prediction rate (100.0%). Data of all the others were higher than 87%. As for different DR severity subgroups, the model performed better for grade 3, reaching the highest positive prediction rate of 97.56% (**Supplementary Figure S4B**).

Nomograms for Predicting DR Risk of Patients With Type 2 Diabetes

Nomograms were developed to depict the association between the clinical variables and the occurrence of DR. After feature selection, we obtained 16 features including γGT, AST, SBP, eGFR, age, HbA1c, FBG, duration, follow-up time, insulin, diuretic, statins, fibrates, hypertension, smoking status, and drinking status. A classic LR model and an LR model integrated with the machine learning output were constructed (**Supplementary Figure S2, S3**). The C-index of the integrated LR model was 0.921, whereas that of the classic LR model was 0.836.

DISCUSSION

In this study, we constructed five ML-based models for the risk of developing DR among patients with type 2 diabetes using EHR data, the XGboost model of which demonstrated the best performance.

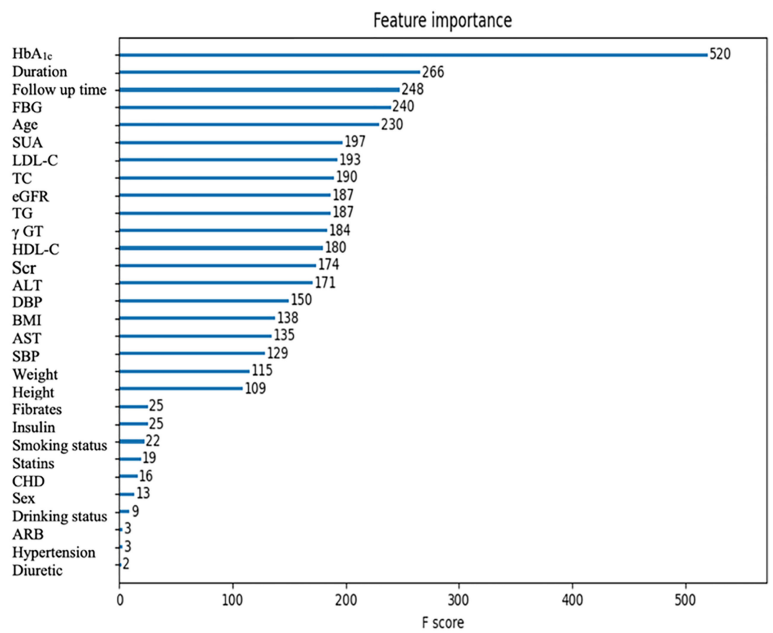

FIGURE 2 | The importance scores of the features calculated by XGBoost.

We further evaluated the predictive value of this model and found that it can accurately predict the occurrence of DR at each time point over 10 years. According to feature importance analysis, five risk factors, SUA, LDL-C, TC, eGFR, and TG, were recognized as important indicators of DR for the first time. Moreover, analysis of data from multiple time points revealed that predicting DR risk with the XGBoost model would obviously reduce the amount of time needed for the diagnosis of DR.

XGBoost algorithm is known for its good scalability and high running speed, which is thus commonly used and developed in recent years (28–30). Specifically, the XGBoost model provides the following advantages. First, the XGBoost algorithm reduces the order of magnitude of features while retaining all the features by introducing regularization terms into the objective function to avoid over-fitting. Secondly, the algorithm also used the random forest algorithm for reference, which can not only reduce the over-fitting problem but also reduce the computational complexity. We hypothesized that these reasons would be responsible for the XGBoost algorithm's outstanding prediction ability for DR risk compared with the other four methods adopted in this study.

There were several studies gaining insights into DR risk prediction, some of which developed ML-based models. However, most of them were cross-sectional studies. In a study in Iran (31), 3734 diabetic patients were included to build a logistic regression model with an *AUC* of 0.704. The input variables included sex, age, diabetes duration, BMI, blood pressure (BP), HbA1c, FPS, cholesterol, and triglycerides. In the cross-sectional study by Ein hoh et al. (7) in South Korea, a *LASSO* prediction model was constructed for predicting the risk of DR, reaching an *AUC* of 0.82 and an accuracy of 75.2%. 490 diabetic patients were selected for the study, and several variables (age, sex, smoking history, drinking history, waist circumference, BMI, physical exercise status, medication history, blood pressure, and relevant laboratory results) were used as input. In another cross-sectional study in Taiwan Province of China (6), 536 patients with type 2 diabetes were selected and 10 predictors, including systolic blood pressure, diastolic blood pressure, BMI, age, gender, duration of diabetes, family history of diabetes, whether there was a blood glucose test, whether there was exercise, and whether there was insulin treatment, were included. Then, four prediction models (SVM, DT, artificial neural network, and LR) were constructed, respectively. The model based on SVM showed the best performance with an accuracy of 79.5% and an *AUC* of 0.839. Mo et al. (5). included 4170 diabetic patients in a cross-sectional study to predict the risk of DR. Seven input variables, including age, diabetes duration, postprandial blood glucose, HbA1c, urine creatinine, urine microalbumin, and systolic blood pressure were used to construct a multivariate logistic regression model. The model showed moderate predictive ability with an *AUC* of 0.715 in the validation set. The predictive models mentioned above were developed to identify patients with DR rather than predict the occurrence of DR in the future. Therefore, they can hardly be adapted to the scenarios that require pre-diagnosis screening and prompt intervention. To our knowledge, only one follow-up study was performed for predicting the occurrence of DR (32). The study was conducted with 5034 type 2 diabetes patients not affected by retinopathy at the time of the recruitment and a median follow-up time of 1.2 years. A *Cox* risk prediction model was constructed with seven predictors including diabetes duration, HbA1c, systolic blood pressure, diastolic blood pressure, proteinuria, creatinine clearance, and diabetes drug treatment, and showed a helpful predictive ability (*C*-index=0.746). However, this model cannot meet all the clinical requirements of long-term management of type 2 diabetes and associated complications considering that it can only predict the occurrence of DR in the next 1 to 4 years.

The XGBoost model we constructed performed well in different follow-up periods (*AUC*=0.834-0.966), which indicates that it could predict whether and when a patient with type 2 diabetes will develop DR in the next 1 to 8 years or even over 8 years. Results also show the proposed model is effective to demonstrate in patients who had DR of different severity levels during follow-up. For the individuals with moderate NPDR, the model exhibited the highest performance. As a transitional stage, moderate NPDR can progress and advance to vision-threatening retinopathies. Intervention methods such as intravitreous anti-VEGF treatment can be applied to secure moderate NPDR patients. As the patient progresses to severe NPDR and PDR, it is hard to get the same treatment effect. Moreover, the method requires no extra laboratory tests since the model input was drawn from demographic and clinical characteristics and routine test results. Therefore, the model will facilitate clinicians risk-stratifying patients with type 2 diabetes. For patients at risk of DR, clinicians can provide adequate follow-up management and effective therapeutic intervention. While for the low-risk population, visit frequency will be appropriately reduced, and thus personal and societal healthcare burdens will be reduced accordingly. We further developed nomograms to depict the association between the clinical variables and the probabilities of DR. The nomogram integrating the XGBoost-based machine learning output achieved a higher predictive performance, which provides an intuitive way to interpret the model and shows its potential to be a clinical decision support tool.

To identify the key features contributing to the pre-diagnosis of DR, the importance scores of the risk factors were calculated by XGBoost. According to the feature importance analysis, HbA1c, diabetes duration, age, and FBG were highly ranked, which corresponds to the current clinical perceptions. In addition, we found that SUA, LDL-C, TC, eGFR, and TG may have the potential to be strong predictors for DR. Moreover, we further calculated the importance scores of the risk factors by RF, and found that the results were similar to and complementary to those from XGBoost. In previous studies, Krizova et al. found that an elevated level of vitreous uric acid was closely related to the development of DR, and uric acid concentration was closely related to the degree of DR progression (33). Zhu et al. found that SUA in the vitreous activates the expression of retinal inflammatory factors through the Notch signaling pathway, which will induce oxidative stress and inflammatory response and thus promote the occurrence and development of DR (34). Obesity is a metabolic disease that is

associated with insulin resistance and diabetes mellitus (35). In the Wisconsin Epidemiologic Study of Diabetic Retinopathy (WESDR), it was found that high TC levels could increase the risk of retinal hard exudation in patients with type 2 diabetes (36). High LDL-C and high TC/LDL-C levels were associated with retinal macular edema in SN-DREAMS studies (37). Besides, statin lipid-lowering drugs could significantly reduce the risk of DR (38). Since DR is a microvascular complication of diabetes, eGFR can be used as an important biochemical indicator reflecting DR. Chen et al. found that higher eGFR was positively correlated with the risk of DR (39). Therefore, the results presented in our study indicated that these risk factors could be used as early and effective predictors of DR for type 2 diabetes patients before recognizable symptoms appear.

There are still several limitations to this study. First, the prediction models were constructed with the risk factors extracted from EHR, except for those with excessive missing data including the ones that might be related to the occurrence of DR (e.g., hip circumference and neck circumference). Secondly, individualized management approaches for type 2 diabetes and associated complications were not fully described. The monitoring and tracking features were also not collected during the follow-up period. The above information will be recorded and used to optimize the XGBoost model in the future. In addition, this is a single-center retrospective study. We are planning to collect cases from several institutions and conduct a prospective study to validate the generalization ability of the proposed model.

In summary, we developed and evaluated an ML-based model for predicting the risk of DR. The results suggest that it is possible to pre-diagnose DR without fundus images. We also demonstrated the potential of applying XGBoost models to facilitate clinicians in accurately identifying the high-risk population for DR and formulating patient-specific management strategies, thereby reducing the occurrence and development of DR.

DATA AVAILABILITY STATEMENT

The original contributions presented in the study are included in the article/**Supplementary Material**. Further inquiries can be directed to the corresponding authors.

ETHICS STATEMENT

The studies involving human participants were reviewed and approved by Ethics Committee of Dalian Central Hospital. The ethics committee waived the requirement of written informed consent for participation.

AUTHOR CONTRIBUTIONS

XHL, ZG, and XYL conceived of and designed the study. YZ contributed to data collection and wrote the manuscript. MD contributed to the conceptualization of the project and edited the manuscript. SL contributed to discussion and revision of the manuscript. HY contributed to model building and wrote the corresponding manuscript. WC contributed to the modeling scheme design and technical support. MZ, PL, and QY contributed to part of manuscript proofreading. XHL, ZG, and XYL are the guarantor of this project and had full access to all of the data in the study and accuracy of the data analysis and reviewed the manuscript. All authors contributed to the article and approved the submitted version.

FUNDING

This work was funded by the National key R&D Program of China (2016YFC0901200), the Dalian Medical Science Research Project Grant Support (2011007).

ACKNOWLEDGMENTS

We would like to thank Yidu Cloud (Beijing) Technology Co, Ltd for their assistance in data searching, extraction and processing.

SUPPLEMENTARY MATERIAL

The Supplementary Material for this article can be found online at: https://www.frontiersin.org/articles/10.3389/fendo.2022.876559/full#supplementary-material

REFERENCES

1. Kempen JH, O'Colmain BJ, Leske MC, Haffner SM, Klein R, Moss SE. The Prevalence of Diabetic Retinopathy Among Adults in the United States. *Arch Ophthalmol* (2004) 122(4):552–63. doi: 10.1001/archopht.122.4.552
2. Flaxel CJ, Adelman RA, Bailey ST, Fawzi A, Lim JI, Vemulakonda GA. Diabetic Retinopathy Preferred Practice Pattern®. *Ophthalmology* (2020) 127 (1):66–145. doi: 10.1016/j.ophtha.2019.09.025
3. Liew G, Michaelides M, Bunce C. A Comparison of the Causes of Blindness Certifications in England and Wales in Working Age Adults (16-64 Years), 1999-2000 With 2009-2010. *BMJ Open* (2014) 4(2):e004015. doi: 10.1136/bmjopen-2013-004015
4. Jampol LM, Glassman AR, Sun J. Evaluation and Care of Patients With Diabetic Retinopathy. *N Engl J Med;* (2020) 382(17):1629–37. doi: 10.1056/NEJMra1909637
5. Mo R, Shi R, Hu Y, Hu F. Nomogram-Based Prediction of the Risk of Diabetic Retinopathy: A Retrospective Study. *J Diabetes Res* (2020) 2020:7261047. doi: 10.1155/2020/7261047
6. Tsao H-Y, Chan P-Y, Su EC-Y. Predicting Diabetic Retinopathy and Identifying Interpretable Biomedical Features Using Machine Learning Algorithms. *BMC Bioinf* (2018) 19(Suppl 9):283. doi: 10.1186/s12859-018-2277-0
7. Oh E, Yoo TK, Park E-C. Diabetic Retinopathy Risk Prediction for Fundus Examination Using Sparse Learning: A Cross-Sectional Study. *BMC Med Inf decision making* (2013) 13:106. doi: 10.1186/1472-6947-13-106
8. Ogunyemi O, Kermah D. Machine Learning Approaches for Detecting Diabetic Retinopathy From Clinical and Public Health Records. *AMIA Annu Symp Proc* (2015) 2015:983–90.
9. Ogunyemi OI, Gandhi M, Tayek C. Predictive Models for Diabetic Retinopathy From Non-Image Teleretinal Screening Data. *AMIA Summits Trans Sci Proc* (2019) 2019:472–7.
10. Bora A, Balasubramanian S, Babenko B, Virmani S, Venugopalan S, Mitani A. Predicting the Risk of Developing Diabetic Retinopathy Using Deep Learning. *Lancet Digit Health* (2021) 3(1):e10–9. doi: 10.1016/S2589-7500(20)30250-8
11. Mehlsen J, Erlandsen M, Poulsen PL, Bek T. Individualized Optimization of the Screening Interval for Diabetic Retinopathy: A New Model. *Acta Ophthalmol* (2012) 90(2):109–14. doi: 10.1111/j.1755-3768.2010.01882.x

12. Dagliati A, Marini S, Sacchi L, Cogni G, Teliti M, Tibollo V. Machine Learning Methods to Predict Diabetes Complications. *J Diabetes Sci Technol* (2018) 12 (2):295–302. doi: 10.1177/1932296817706375
13. Ting DSW, Cheung GCM, Wong TY. Diabetic Retinopathy: Global Prevalence, Major Risk Factors, Screening Practices and Public Health Challenges: A Review. *Clin Exp Ophthalmol* (2016) 44(4):260–77. doi: 10.1111/ceo.12696
14. Varma R, Macias GL, Torres M, Klein R, Peña FY, Azen SP. Biologic Risk Factors Associated With Diabetic Retinopathy: The Los Angeles Latino Eye Study. *Ophthalmology* (2007) 114(7):1332–40. doi: 10.1016/j.ophtha.2006.10.023
15. Nathan DM, Genuth S, Lachin J, Cleary P, Crofford O, Davis M. The Effect of Intensive Treatment of Diabetes on the Development and Progression of Long-Term Complications in Insulin-Dependent Diabetes Mellitus. *N Engl J Med* (1993) 329(14):977–86. doi: 10.1056/NEJM1993093032914
16. UK Prospective Diabetes Study (UKPDS) Group. Intensive Blood-Glucose Control With Sulphonylureas or Insulin Compared With Conventional Treatment and Risk of Complications in Patients With Type 2 Diabetes (UKPDS 33). *Lancet* (1998) 352(9131):837–53. doi: 10.1016/S0140-6736(98)07019-6
17. Keenan HA, Costacou T, Sun JK, Doria A, Cavellerano J, Coney J. Clinical Factors Associated With Resistance to Microvascular Complications in Diabetic Patients of Extreme Disease Duration: The 50-Year Medalist Study. *Diabetes Care* (2007) 30(8):1995–7. doi: 10.2337/dc06-2222
18. Alberti KG, Zimmet PZ. Definition, Diagnosis and Classification of Diabetes Mellitus and its Complications. Part 1: Diagnosis and Classification of Diabetes Mellitus Provisional Report of a WHO Consultation. *Diabetes Med* (1998) 15(7):539–53. doi: 10.1002/(SICI)1096-9136(199807)15:7<539::AID-DIA668>3.0.CO;2-S
19. Niroomand M, Afsar J, Hosseinpanah F, Afrakhteh M, Farzaneh F, Serahati S. Comparison of the International Association of Diabetes in Pregnancy Study Group Criteria With the Old American Diabetes Association Criteria for Diagnosis of Gestational Diabetes Mellitus. *Int J Endocrinol Metab* (2019) 17 (4):e88343. doi: 10.5812/ijem.88343
20. Wilkinson CP, Ferris FL3rd, Klein RE, Lee PP, Agardh CD, Davis M. Proposed International Clinical Diabetic Retinopathy and Diabetic Macular Edema Disease Severity Scales. *Ophthalmology* (2003) 110(9):1677–82. doi: 10.1016/S0161-6420(03)00475-5
21. Williams B, Mancia G, Spiering W, Agabiti Rosei E, Azizi M, Burnier M. 2018 ESC/ESH Guidelines for the Management of Arterial Hypertension'. *Eur Heart J* (2018) 39(33):3021–104. doi: 10.1093/eurheartj/ehy339
22. Levey AS, Stevens LA, Schmid CH, Zhang Y, Castro AFIII, Feldman HI. A New Equation to Estimate Glomerular Filtration Rate. *Ann Internal Med* (2009) 150(9):604–12. doi: 10.7326/0003-4819-150-9-200905050-00006
23. Breiiman L. Random Forests. *Mach Learn* (2001) 45(1):5–32. doi: 10.1023/A:1010933404324
24. Chen T, Guestrin C. XGBoost: A Scalable Tree Boosting System. KDD '16: Proceedings of the 22nd ACM SIGKDD International Conference on Knowledge Discovery and Data Mining. (2016), 785–94. doi: 10.1145/2939672.2939785
25. Sainani KL. Logistic Regression. *PMR* (2014) 6(12):1157–62 doi: 10.1016/j.pmrj.2014.10.006
26. Cortes C, Vapnik V. Support-Vector Networks. *Mach Learn* (1995) 20 (3):273–97. doi: 10.1007/BF00994018
27. Cover T, Hart P. Nearest Neighbor Pattern Classification. *IEEE Trans Inf Theory January* (1967) 13(1):21–7. doi: 10.1109/TIT.1967.1053964
28. Hou N, Li M, He L, Xie B, Wang L, Zhang R. Predicting 30-Days Mortality for MIMIC-III Patients With Sepsis-3: A Machine Learning Approach Using XGboost. *J Transl Med* (2020) 18(1):462. doi: 10.1186/s12967-020-02620-5
29. Ogunleye A, Wang QG. XGBoost Model for Chronic Kidney Disease Diagnosis. *IEEE/ACM Trans Comput Biol Bioinform*. (2020) 17(6):2131–40. doi: 10.1109/TCBB.2019.2911071
30. Zhang Y, Feng T, Wang S, Dong R, Yang J, Su J. A Novel XGBoost Method to Identify Cancer Tissue-Of-Origin Based on Copy Number Variations. *Front Genet* (2020) 11:585029. doi: 10.3389/fgene.2020.585029
31. Hosseini SM, Maracy MR, Amini M, Baradaran HR. A Risk Score Development for Diabetic Retinopathy Screening in Isfahan-Iran. *J Res Med Sci* (2009) 14(2):105–10.
32. Semeraro F, Parrinello G, Cancarini A, Pasquini L, Zarra E, Cimino A. Predicting the Risk of Diabetic Retinopathy in Type 2 Diabetic Patients. *J Diabetes its Complications* (2011) 25(5):292–7. doi: 10.1016/j.jdiacomp.2010.12.002
33. Krizova L, Kalousova M, Kubena A, Benakova H, Zima T, Kovarik Z. Increased Uric Acid and Glucose Concentrations in Vitreous and Serum of Patients With Diabetic Macular Oedema. *Ophthalmic Res* (2011) 46(2):73–9. doi: 10.1159/000322994
34. Zhu D-D, Wang Y-Z, Zou C, She X-P, Zheng Z. The Role of Uric Acid in the Pathogenesis of Diabetic Retinopathy Based on Notch Pathway'. *Biochem Biophys Res Commun* (2018) 503(2):921–9. doi: 10.1016/j.bbrc.2018.06.097
35. Li C, Qu L, Farragher C, Vella A, Zhou B. MicroRNA Regulated Macrophage Activation in Obesity. *J Trans Internal Med* (2019) 7(2):46. doi: 10.2478/jtim-2019-0011
36. LeCaire TJ, Palta M, Klein R, Klein BE, Cruickshanks KJ. Assessing Progress in Retinopathy Outcomes in Type 1 Diabetes: Comparing Findings From the Wisconsin Diabetes Registry Study and the Wisconsin Epidemiologic Study of Diabetic Retinopathy. *Diabetes Care* (2013) 36(3):631–7. doi: 10.2337/dc12-0863
37. Raman R, Ganesan S, Pal SS, Gella LL, Kulothungan V, Sharma T. Incidence and Progression of Diabetic Retinopathy in Urban India: Sankara Nethralaya-Diabetic Retinopathy Epidemiology and Molecular Genetics Study (SN-DREAMS II), Report 1. *Ophthalmic Epidemiol* (2017) 24(5):294–302. doi: 10.1080/09286586.2017.129025
38. Kang EY-C, Chen T-H, Garg SJ, Sun C-C, Kang J-H, Wu W-C. Association of Statin Therapy With Prevention of Vision-Threatening Diabetic Retinopathy. *JAMA Ophthalmol* (2019) 137(4):363–71. doi: 10.1001/jamaophthalmol.2018.6399
39. Chen Y-H, Chen H-S, Tarng D-C. More Impact of Microalbuminuria on Retinopathy Than Moderately Reduced GFR Among Type 2 Diabetic Patients. *Diabetes Care* (2012) 35(4):803–8. doi: 10.2337/dc11-1955

Conflict of Interest: MD and WC are employed by Infervision.

The remaining authors declare that the research was conducted in the absence of any commercial or financial relationships that could be construed as a potential conflict of interest.

Publisher's Note: All claims expressed in this article are solely those of the authors and do not necessarily represent those of their affiliated organizations, or those of the publisher, the editors and the reviewers. Any product that may be evaluated in this article, or claim that may be made by its manufacturer, is not guaranteed or endorsed by the publisher.

frontiers | Frontiers in Endocrinology

ORIGINAL RESEARCH
published: 27 May 2022
doi: 10.3389/fendo.2022.841813

Exploring the Immune Infiltration Landscape and M2 Macrophage-Related Biomarkers of Proliferative Diabetic Retinopathy

Zhishang Meng[1†], Yanzhu Chen[2†], Wenyi Wu[3], Bin Yan[1], Yongan Meng[1], Youling Liang[1], Xiaoxi Yao[4] and Jing Luo[1]*

[1] Department of Ophthalmology, The Second Xiangya Hospital, Central South University, Changsha, China, [2] Department of Radiation Oncology, Hunan Cancer Hospital and The Affiliated Cancer Hospital of Xiangya School of Medicine, Central South University, Changsha, China, [3] Department of Ophthalmology, Xiangya Hospital, Central South University, Changsha, China, [4] Shenzhen College of International Education, Shenzhen, China

OPEN ACCESS

Edited by:
Khalid Siddiqui,
King Saud University, Saudi Arabia

Reviewed by:
Donato Santovito,
Unit of Milan, Institute of Genetic and Biomedical Research, National Research Council (CNR), Italy
Yinan Jiang,
University of Pittsburgh, United States

****Correspondence:***
Jing Luo
luojing001@csu.edu.cn

[†]These authors have contributed equally to this work and share first authorship

Specialty section:
This article was submitted to Clinical Diabetes, a section of the journal Frontiers in Endocrinology

Received: *22 December 2021*
Accepted: *19 April 2022*
Published: *27 May 2022*

Citation:
Meng Z, Chen Y, Wu W, Yan B, Meng Y, Liang Y, Yao X and Luo J (2022) Exploring the Immune Infiltration Landscape and M2 Macrophage-Related Biomarkers of Proliferative Diabetic Retinopathy. Front. Endocrinol. 13:841813. doi: 10.3389/fendo.2022.841813

Backgrounds: Diabetic retinopathy (DR), especially proliferative diabetic retinopathy (PDR), is the major cause of irreversible blindness in the working-age population. Increasing evidence indicates that immune cells and the inflammatory microenvironment play an important role during PDR development. Herein, we aim to explore the immune landscape of PDR and then identify potential biomarkers correlated with specific infiltrating immune cells.

Methods: We mined and re-analyzed PDR-related datasets from the Gene Expression Omnibus (GEO) database. Using the cell-type identification by estimating relative subsets of RNA transcripts (CIBERSORT) algorithm, we investigated the infiltration of 22 types of immune cells in all selected samples; analyses of differences and correlations between infiltrating cells were used to reveal the immune landscape of PDR. Thereafter, weighted gene co-expression network analysis (WGCNA) and differential expression analysis were applied to identify the hub genes on M2 macrophages that may affect PDR progression.

Results: Significant differences were found between infiltration levels of immune cells in fibrovascular membranes (FVMs) from PDR and normal retinas. The percentages of follicular helper T cells, M1 macrophages, and M2 macrophages were increased significantly in FVMs. Integrative analysis combining the differential expression and co-expression revealed the M2 macrophage-related hub genes in PDR. Among these, *COL5A2, CALD1, COL6A3, CORO1C*, and *CALU* showed increased expression in FVM and may be potential biomarkers for PDR.

Conclusions: Our findings provide novel insights into the immune mechanisms involved in PDR. *COL5A2, CALD1, COL6A3, CORO1C*, and *CALU* are M2 macrophage-related biomarkers, further study of these genes could inform novel ideas and basis for the understanding of disease progression and targeted treatment of PDR.

Keywords: proliferative diabetic retinopathy, biomarkers, M2 macrophage, immune landscape, bioinformatics

INTRODUCTION

Diabetic retinopathy (DR) is a major cause of irreversible blindness in the working-age population worldwide (1, 2). Proliferative diabetic retinopathy (PDR), characterized by neovascularization (NV) and excessive proliferation, is the most advanced and refractory form of DR (3). The global incidence of PDR is 1.4% among all individuals with diabetes (4). PDR management has been one of the greatest challenges in modern ophthalmology. Recent advances in high-throughput technologies and bioinformatics analysis have improved the understanding of PDR and facilitated the development of treatment (5). Therefore, the identification of new biomarker and therapeutic strategies for retinal NV in PDR is urgent and in high demand for improved clinical outcome.

Retinal cells are privileged from systemic immune surveillance (6). Once the blood-retina barrier is breached, retinal cells gate the layer of protection by suppressing the local inflammatory response (7). Immunological activity in the central nervous system (CNS) is largely determined by an innate immune response and is heightened in PDR (8). Previous studies have shown enrichment of immune processes in DR (9, 10). In addition, therapies targeting inflammation have also been shown to be effective for patients with DR (11, 12). However, whether and how molecular pathways and immune cell populations are involved in the progress of PDR is still unknown.

Activated macrophages are generally divided into M1-like and M2-like forms (13). The activation of M2 macrophages plays a major role in cellular processes such as cell proliferation and differentiation. These processes rely on external factors including transcription factors, intrinsic-signaling pathways, cytokines, and metabolic adaptation (14). Previous studies have demonstrated the key signals involved in M2 macrophage polarization in DR (10, 15, 16). A recent study also showed that M2 Macrophages are the major immune cells that involved in the immune response of retinal neovascularization in the rat model with ischemic retinopathy (17).

In the present study, we analyzed the transcriptome data from publicly available databases using various bioinformatics algorithms to identify potential immune cell-related biomarkers in PDR and a panel of M2 macrophage-related biomarkers, and to determine the immune landscape of PDR.

MATERIALS AND METHODS

Data Collection and Preprocessing

The gene expression data and relevant clinical information were downloaded from the Gene Expression Omnibus (GEO) database (http://www.ncbi.nlm.nih.gov/geo/) with accession numbers GSE60436 (18) and GSE102485 (19). Fibrovascular membranes (FVMs) obtained from PDR patients and normal retinal tissue from donated eyes in the above two datasets were included in this study. The expression data were then normalized using the "normalizeBetweenArrays" function in the "limma" R package (20), and the "sva" R package was used to correct for batch effects between two different arrays (21).

Gene Set Enrichment Analysis

GSEA was performed between FVMs and normal retinas to explore the potential biological functions involved in the occurrence and development of PDR; the "Hallmark" gene sets (from the Molecular Signatures Database) were selected as the annotation gene sets (22). Significance was set at NOM $p<0.05$ and false discovery rate (FDR)-adjusted q-values <0.25.

Immune Cell Infiltration-Related Analysis

The CIBERSORT algorithm was applied to estimate the relative proportions of 22 types of immune cells which infiltrated into all included samples (23), those with a CIBERSORT output of $p<0.05$ were considered accurate and enrolled for further construction of the immune landscape, otherwise, samples were eliminated. Thereafter, the correlation matrix of different immune cells was constructed and visualized using the "Corrplot" R package. Principal component analysis (PCA) was then used to evaluate subsets distinguished by the extent of immune cell infiltration. The results were visualized using the R package "scatterplot3d."

Construction of Co-Expression Network Associated With PDR-Infiltrating Immune Cells

To search for genes associated with immune infiltrates, we constructed a signed hybrid co-expression network for all selected samples using weighted gene correlation network analysis (WGCNA) (Soft-power 5, mergeCutheight 0.25, minModuleSize 20) (24). After filtering out low-expression genes to remove noise, those genes with similar expression patterns were hierarchically clustered into several modules according to the topological overlap measure-based dissimilarity, and all the modules were summarized by module eigengenes (ME) which were used to measure the module membership. The hub genes in our study were defined as those with ME-based gene connectivity (kME) >0.9 within each module; those genes with higher kME tended to have higher connectivity. We then performed correlation analysis between co-expression modules and immune infiltrated cells in PDR to identify hub genes associated with the disease. Pearson's correlations were calculated between the ME and immune cells obtained from previous analysis. Associations between the module and immune cell were considered significant at $p<0.05$. Thus, we obtained the module and hub genes that likely shaped the specific immune landscape of PDR. Meanwhile, analysis of gene ontology (GO) annotation and enrichment was carried out to better understand the biological functions of these enrolled genes (R packages "clusterProfiler" and "enrichplot," $p<0.05$, $q<0.05$).

Identification Biomarkers of PDR-Infiltrating Immune Cells

In general, clues about the disease are inferred from gene expression differences between normal and pathologic tissues. Therefore, we conducted differential expression analysis of FVMs and normal retinas. The differentially expressed genes

(DEGs) were identified using the "limma" R package and filtered by |log2FoldChange| >1 and FDR<0.05. The potential biomarkers were screened by integrating the results of the differentially expressed analysis, WGCNA, and immune landscape of PDR. The expression distribution of selected genes was visualized with violin plots using R packages "ggplot2" and "reshape2." Finally, PCA was used to evaluate the discriminative capacity of these candidates to differentiate the two groups.

RESULTS

Overview of Research Design and Data Preparation

The overall design and workflow of this study are shown in **Figure 1**. An integrative analysis combining differential expression and co-expression revealed that immune cells, particularly M2 macrophages, play an essential role in the progression of DR, and further suggested that increased expression of *COL5A2, CALD1, COL6A3, CORO1C*, and *CALU* in the FVM may be potential M2 macrophage-related biomarkers for PDR.

The GSE60436 dataset used in this study is based on the platform of GPL6884 (Illumina HumanWG-6 v3.0 expression beadchip) and included 3 normal retina tissues and 6 FVM tissues. The second dataset used here, GSE102485, was analyzed on the GPL18573 Illumina NextSeq 500 platform and comprised 20 FVM samples(17 from type 2 diabetes mellitus patients and 3 from type 1 diabetes mellitus patients), 3 normal retina samples, and 7 other samples. It is clear from **Figure 2A** that the batch effects of the two different datasets were eliminated after internal correction and normalization. We finally selected 32 eligible samples (6 normal retinas and 26 FVMs) and 14,132 intersected genes from the two datasets for subsequent analysis (**Figure 2B**). Next, in the primary analysis of the biological differences between the two groups, GSEA revealed that several hallmarks of immune function were positively correlated with FVMs, including IL2-STAT5-signaling, IL6-JAK-STAT3-signaling, inflammatory response, IFN-α response, IFN-γ response, and TNF-α signaling *via* NF-κB. Other highly enriched hallmarks were angiogenesis, apoptosis, and epithelial mesenchymal transition, among others (**Figure 2C**). These results preliminarily indicate the correlation between immune activity and FVM in PDR.

Immune Landscape of FVM and Normal Retina

The CIBERSORT algorithm was used to calculate the infiltration of 22 types of immune cells in all 32 samples (26 FVMs, and 6 normal retinas). The bar plot of **Figure 3A** shows the proportions of the 22 immune cell types in 29 eligible samples. **Figure 3B** indicates the correlations between immune cell types. The strongest positive correlation was between resting mast cells and plasma cells (r=0.6), while the strongest negative correlation was between plasma cells and M1 macrophages (r=-0.55).

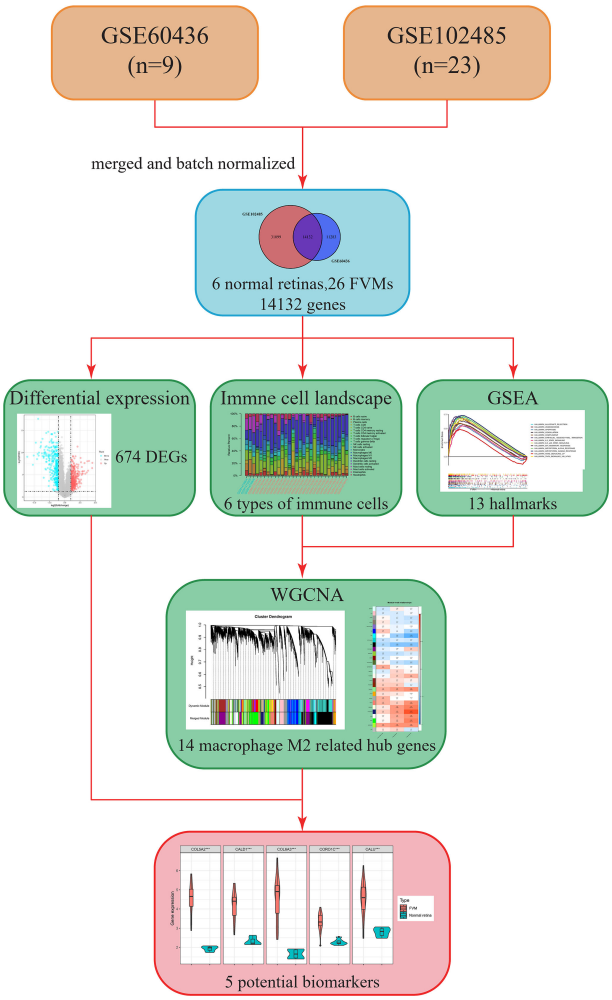

FIGURE 1 | Flow chart showing the research process in this study. FVM, fibrovascular membrane; DEG, differentially expressed gene; CIBERSORT, cell-type identification by estimating relative subsets of RNA transcripts; GSEA, gene set enrichment analysis; WGCNA, weighted gene co-expression network analysis.

The differences in proportions of immune cell infiltration between the two groups is shown in **Figure 3C**. The percentages of follicular helper T cells, M1 macrophages, and M2 macrophages were increased significantly, while those of plasma cells, active NK cells and resting mast cells were decreased significantly compared with controls. Complete separation between the FVM and normal retina groups as shown in **Figure 3D** indicates that the infiltration of immune cell types may be used as a distinguishing characteristic of FVM in PDR patients.

Identification of PDR-Infiltrating Immune Cell-Related Genes

Gene expression data and immune cell types with significantly increase were used to conduct WGCNA, a powerful scale-free network used to identify co-expressed gene clusters correlated

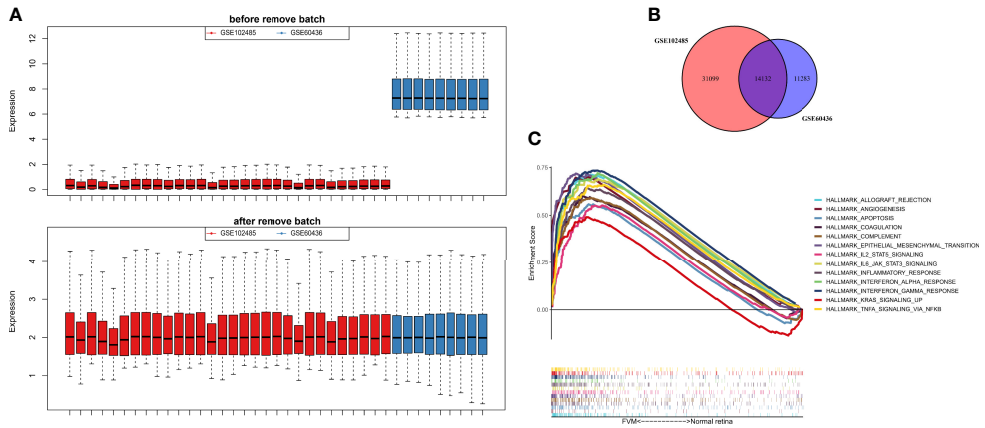

FIGURE 2 | Data preprocessing and gene set enrichment analysis (GSEA). **(A)** Box plot for the expression profiles before and after normalization. **(B)** Venn diagram showing the intersection between expressed genes from two datasets. **(C)** GSEA plot for the significant Hallmark sets for FVM group (FDR<0.25, p<0.05).

with meaningful immune cells based on the CIBERSORT algorithm, the CIBERSORT results of follicular helper T cells, M1 macrophages, and M2 macrophages in all 29 samples were selected as trait data for WGCNA. A scale-free topological network (soft-thresholding power=5, scale-free R2 = 0.9) was established (**Figure 4A**). Based on the hierarchical clustering method, genes that were highly co-expressed were clustered into different modules and color coded (**Figures 4B**). A total of 28 modules containing 14,132 genes were identified after merging modules with highly correlated eigengenes (**Figures 4B, C**). The

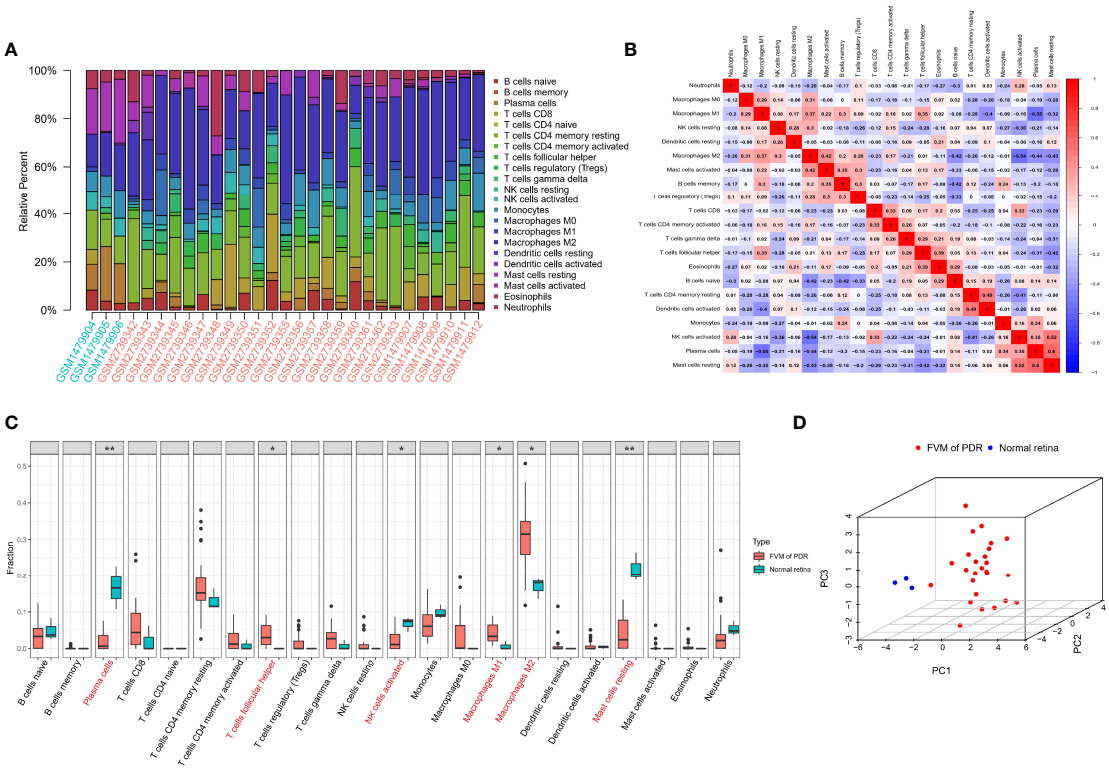

FIGURE 3 | Immune infiltration landscape in FVM and normal retinal tissue. **(A)** Bar charts of 22 immune cell types in all eligible samples. **(B)** Correlations between infiltrating immune cells. Red and blue colors indicate positive and negative correlations, color intensity represents the degree of correlation. **(C)** Box plot of the difference in immune cell content between the FVM group and control group (*p < 0.05; **p < 0.01). **(D)** 3D scatter plot of PCA results.

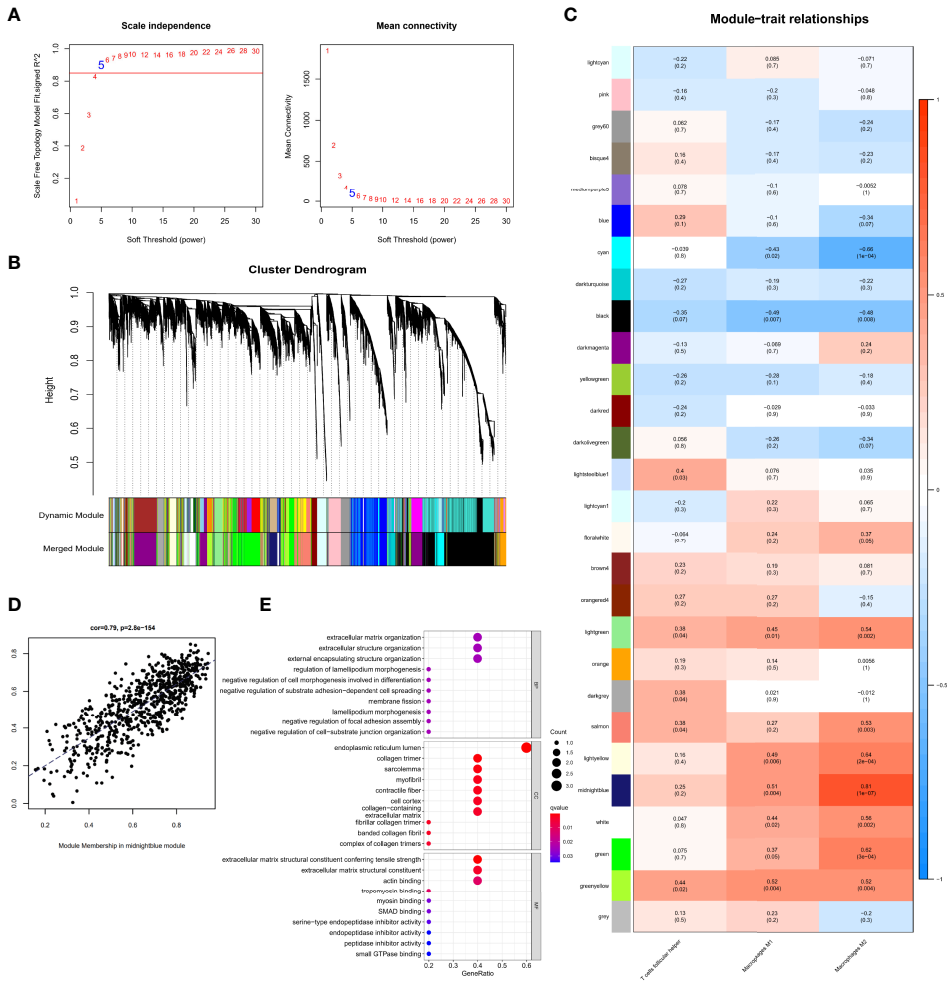

FIGURE 4 | Identification of immune cell-related genes using WGCNA. **(A)** Analysis of the scale-free fit index for soft threshold powers (β=5). **(B)** Hierarchical dendrogram of the identified co-expression modules, indicated by color coding. **(C)** Heatmap plot of correlation between the gene module and immune cell type infiltration. Strength of the correlation is depicted by its color. **(D)** Correlations between the gene module memberships and gene significance for the midnight-blue module associated with M2 macrophages. **(E)** Bubble plots of GO enrichment analysis with hub genes in the midnight-blue module.

ME, representing the expression of all the genes in this module, was associated with the characteristics of the three selected types of immune cells. Among them, we identified the midnight-blue module (r=0.81, p=1e-07) that was most closely associated with M2 macrophages (**Figures 4C, D**) as the hub module. The module contained 718 genes, of which 14 genes with kME>0.9 were considered hub genes and probably serve an essential pathobiological role (**Table S1**). GO enrichment analysis of the above 14 genes showed that several GO terms were enriched in tissue remodeling processes and fibrosis. The top 10 significant terms in the biological processes (BP), molecular functions (MF), and cellular components (CC) are shown in **Figure 4E**, including actin filament organization, extracellular matrix organization, myofibril and actin binding, among others. These provided additional evidence that these hub genes on M2 macrophages affect PDR progression.

Exploration of M2 Macrophage-Related Biomarkers

To identify possible genes that may contribute to the development of PDR, we analyzed gene expression data for all 32 samples and found 674 DEGs (**Table S2**, 328 upregulated and 346 downregulated) between FVM and normal retina (**Figure 5A**). A total of five genes (*COL5A2, CALD1, COL6A3, CORO1C*, and *CALU*) overlapped between DEGs and M2 macrophage-related genes (**Figure 5B**), and these five common genes constituted a proposed panel of possible biomarkers of PDR. GO functional enrichment analysis for these 5 genes showed that the top GO terms were also related to constructive processes like wound healing and tissue repair (**Figure 5C**), and the enrichment of these terms is consistent with the function of M2 macrophages. Furthermore, the expression of all five genes in the FVM group was significantly

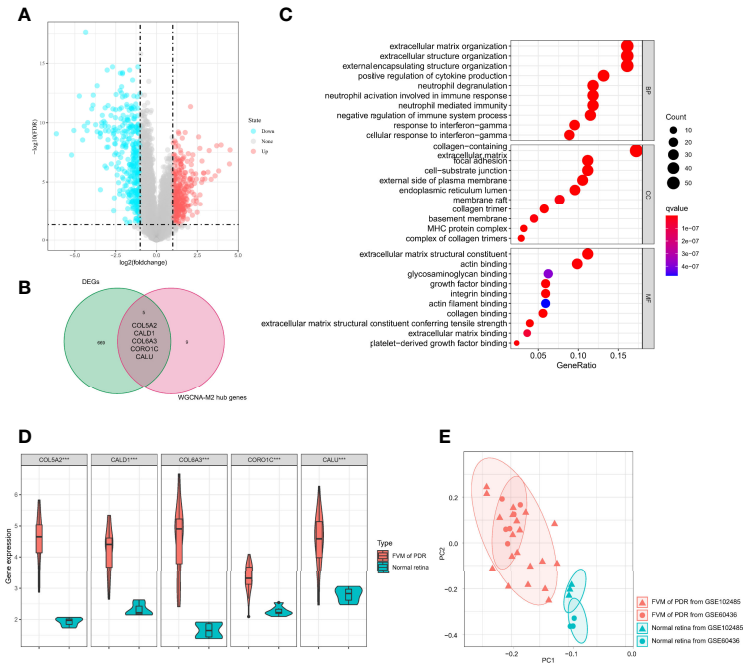

FIGURE 5 | Identification of M2 macrophage-related biomarkers. **(A)** Volcano plot of DEGs between the FVM and control group. **(B)** Venn diagram of intersection genes between DEGs and M2 macrophage-related genes. **(C)** Bubble plots of GO enrichment analysis with five possible biomarkers. **(D)** Violin plot of expression levels of selected five genes in the FVM and normal retina group (***p<0.001). **(E)** PCA plot of 32 samples from two datasets (based on selected five genes, different shapes indicate different datasets, different colors indicate different sample types).

higher than that of controls (**Figure 5D**). PCA results showed complete separation between FVM samples and normal retinal samples both in the overall datasets and even in the individual dataset (**Figure 5E**).

DISCUSSION

In this study, we sought to identify the infiltration of immune cells in PDR. The CIBERSORT algorithm was used to calculate the infiltration of 22 types of immune cells in all 32 samples, including 26 FVMs and 6 normal retinas. We then identified the difference in the proportions of infiltrating immune cell types between the two groups. Compared to normal retinas, the percentages of follicular helper T cells, M1 macrophages, and M2 macrophages were increased significantly in FVMs. Using integrative analysis combining the differential expression and co-expression, we found that *COL5A2, CALD1, COL6A3, CORO1C*, and *CALU* are M2 macrophage-related biomarkers in PDR.

The retina is highly sensitive to the fluctuation of metabolic homeostasis owing to the combination of a limited vascular supply and high metabolic demand (25). The blood-retinal barrier not only protects the retina's exposure but also regulates its supply of nutrients from the vasculature (26). Macrophages, astrocytes, and Müller cells play important cellular roles in the innate immunity of the blood-retinal barrier (27). PDR progression is closely associated with increasing abnormalities of the vasculature such as blood-retinal barrier dysfunction, neovascularization, and hemorrhage (28). However, few studies have focused on differences in composition of immune cells between PDR and normal retinal tissues. In this study, for the first time, we investigated the difference in proportions of infiltrating immune cell types between FVM and normal retina using CIBERSORT. We found that the percentages of follicular helper T cells, M1 macrophages, and M2 macrophages were increased significantly compared with controls. These findings provide new insights into the immune landscape of PDR based on bulk tissue transcriptomic profiling. However, the retina is a very complex neurosensory tissue with numerous types of cells (25), recent advances in single-cell RNA sequencing (scRNAseq) technology have provided more accurate results for characterizing different cell types in complex tissue (29). Due to the difficulty in obtaining normal retinal tissue and even complete PDR pathological samples, most of the existing single-cell based information has been established from experimental studies using diabetic animal models (30–32). In addition, currently available diabetic animal models mainly mimic non-proliferative diabetic retinopathy(NPDR) and rarely display retinal neovascularization, thereby limiting their use in PDR research (33). Accounting for the heterogeneity within normal and pathologic tissues, relevant mechanisms involved in different stages of the PDR process are worthy of further investigation according to samples with varying levels of DR severity. Future

cell or spatial resolution transcriptome analysis are warranted to investigate the infiltration status of immune cell in the PDR to determine whether the regulation of immune status could be used as a potential therapeutic approach for PDR.

Macrophages are key regulators of tissue regeneration, repair, and fibrosis (34). The dysfunctional macrophage can lead to uncontrolled generation of growth factors, impaired production of anti-inflammatory macrophages, or erroneous interactions between macrophages and endothelial cells, epithelial cells, fibroblasts, and tissue or stem progenitor cells (35). Aberrant repair contributes to sustained damage, and this could induce the progression of pathological fibrosis (36, 37). A recent study has reported that M2 macrophages participate actively in the natural process of oxygen –induced retinopathy(OIR) in mice by affecting pathological neovascularization and fibrosis (38). Another single-cell transcriptome study also showed different fibrotic, gliotic, and inflammatory profiles in microglia/macrophages subpopulations with effects on the severity of diabetic retinopathy in the Akimba mouse model (39). Which were in accordance with our results from GO enriched analysis of 14 hub genes and 5 potential biomarkers related to M2 macrophages. Meanwhile, Clinical research has also provided relevant evidence. One study used optical coherence tomography angiography (OCTA) to report that the density of macrophage-like cells was significantly increased in PDR (40). Similarly, another study suggested that the hyperreflective spots visualized by optical coherence tomography (OCT) might be related to the presence of activated microglia/macrophage in diabetic macular edema (41).

In this study, we revealed that the *COL5A2, CALD1, COL6A3, CORO1C*, and *CALU* genes associated with M2 macrophages and showed high expression in PDR by differential expression and co-expression analyses. A recent comparative analysis of the transcriptome of FVM of PDR and inner limiting membrane (ILM) of non-diabetic epiretinal membranes has shown that the signature of FVM is characterized by the expression of a variety of extracellular matrix (ECM) proteins and several collagen types, as well as the accumulation of endothelial cells, M2 macrophages and myofibroblasts (42). These results are in accordance with our findings of bioinformatics analysis. The collagen type V alpha 2 (*COL5A2*) gene offers a template for a component of type V collagen and participates in the formation of pathological scarring (43), previous studies have reported a positive association between expression of *COL5A2* and macrophages as well as proliferation, malignant transformation, and resistance to apoptosis in a variety of tumors (44). We report for the first time that *COL5A2* gene is highly expressed in PDR and associated with M2 macrophages. Further studies with a larger clinical cohort and basic research will be needed to further confirm and extend these findings. Caldesmon 1 (*CALD1*) performs as a cytoskeleton-associated protein and regulates cell morphology and motility *via* actin filament modulation. It plays roles in cytoskeletal organization, cell adhesion, and vascularization (45). Previously, it has been shown that *CALD1* may stimulate and polarize tumor-associated macrophages (46), and this is consistent with our findings but the specific mechanism remains poorly understood and further investigations are needed. Collagen Type VI Alpha 3 (*COL6A3*) is associated with insulin resistance and adipose tissue inflammation (47). Previous reports have supported a role for *COL6A3* in inflammation obesity and obesity-associated insulin resistance which may lead to a higher incidence and more rapid progression of diabetes complications (48, 49). In the current study, we report for the first time that *COL6A3* is highly expressed in FVMs and is associated with M2 macrophage cells in PDR. Further research will be necessary to gain insight into such potential mechanisms. Coronin-like actin-binding protein 1C (*CORO1C*) belongs to the coronin family of actin-binding proteins that are important for the control and remodeling of the actin filaments network (50). One report has indicated that the PI3K/AKT signaling pathway is significantly inhibited by *CORO1C* knockdown in colorectal cancer (51). The expression of *CORO1C* in PDR has not been previously reported. In this study, we found that *CORO1C* is associated with M2 macrophage cells in PDR. Further mechanistic studies are required to understand the relevant mechanism of action. Calumenin (*CALU*) is a multiple EF-hand Ca2+-binding protein (52). One report has indicated a positive correlation of *CALU* with cancer-associated fibroblasts and macrophages in bladder cancer (53). Moreover, previous analyses of *CALU* target genes were mainly focused on epithelial-mesenchymal transition-related genes (54). In this study, we found the association between CALU and M2 macrophage cells in PDR. However, the mechanisms by which CALU regulates are not clear. Combining the obtained biomarkers and the aforementioned PDR immune landscape results, immunomodulation or targeted therapy for specific therapeutic biomarkers may be potential therapeutic approaches to inhibit FVM formation and slow or even reverse the progression of PDR.

CONCLUSION

Taken together, using integrative analysis combining differential expression and co-expression, we found that the ratio of follicular helper T cells, M1 macrophages, and M2 macrophages increased significantly in PDR, while the ratio of plasma cells, activated NK cells and resting mast cells was decreased compared with controls. These findings indicate that M2 macrophages play an important role in the progression of PDR, and further study of *COL5A2, CALD1, COL6A3, CORO1C*, and *CALU* could inform novel ideas and basis for the understanding of disease progression and targeted treatment of PDR.

DATA AVAILABILITY STATEMENT

The original contributions presented in the study are included in the article/**Supplementary Material**. Further inquiries can be directed to the corresponding author.

AUTHOR CONTRIBUTIONS

Conceptualization: JL. Methodology and software: ZM, YC, and WW. Visualization: ZM and XY. Formal analysis and data

curation: BY, YM, YL, and XY. Writing: ZM and YC. Review and editing: WW and JL. Supervision and acquisition of funding: JL. All authors have read and agreed to the submitted version of the manuscript.

FUNDING

This work was supported by grants from the National Natural Science Foundation of China (81570847) and the Hunan Provincial Natural Science Foundation of China (2020JJ4800).

ACKNOWLEDGMENTS

We thank the authors of the utilized GEO dataset for providing their microarray samples to the general public, as well as the R development team and the R community for contributing packages.

SUPPLEMENTARY MATERIAL

The Supplementary Material for this article can be found online at: https://www.frontiersin.org/articles/10.3389/fendo.2022.841813/full#supplementary-material

REFERENCES

1. Sabanayagam C, Banu R, Chee ML, Lee R, Wang YX, Tan G, et al. Incidence and Progression of Diabetic Retinopathy: A Systematic Review. *Lancet Diabetes Endocrinol* (2019) 7(2):140–9. doi: 10.1016/S2213-8587(18)30128-1
2. Teo ZL, Tham YC, Yu M, Chee ML, Rim TH, Cheung N, et al. Global Prevalence of Diabetic Retinopathy and Projection of Burden Through 2045: Systematic Review and Meta-Analysis. *Ophthalmology* (2021) 128 (11):1580–91. doi: 10.1016/j.ophtha.2021.04.027
3. Antonetti DA, Klein R, Gardner TW. Diabetic Retinopathy. *N Engl J Med* (2012) 366(13):1227–39. doi: 10.1056/NEJMra1005073
4. Antoszyk AN, Glassman AR, Beaulieu WT, Jampol LM, Jhaveri CD, Punjabi OS, et al. Effect of Intravitreous Aflibercept vs Vitrectomy With Panretinal Photocoagulation on Visual Acuity in Patients With Vitreous Hemorrhage From Proliferative Diabetic Retinopathy. *JAMA* (2020) 324(23):2383. doi: 10.1001/jama.2020.23027
5. Gao X, Du Y WB, Li Y, Zhu S, Ma XL. Atg16L1 as a Novel Biomarker and Autophagy Gene for Diabetic Retinopathy. *J Diabetes Res* (2021) 2021:5398645. doi: 10.1155/2021/5398645
6. Streilein JW. Ocular Immune Privilege: Therapeutic Opportunities From an Experiment of Nature. *Nat Rev Immunol* (2003) 3(11):879–89. doi: 10.1038/nri1224
7. Chen M, Luo C, Zhao J, Devarajan G, Xu H. Immune Regulation in the Aging Retina. *Prog Retin Eye Res* (2019) 69:159–72. doi: 10.1016/j.preteyeres.2018.10.003
8. Binet F, Cagnone G, Crespo-Garcia S, Hata M, Neault M, Dejda A, et al. Neutrophil Extracellular Traps Target Senescent Vasculature for Tissue Remodeling in Retinopathy. *Science* (2020) 369(6506):eaay5356. doi: 10.1126/science.aay5356
9. Vujosevic S, Simó R. Local and Systemic Inflammatory Biomarkers of Diabetic Retinopathy: An Integrative Approach. *Invest Ophth Vis Sci* (2017) 58(6):BIO68–75. doi: 10.1167/iovs.17-21769
10. Yoshida S, Kobayashi Y, Nakama T, Zhou Y, Ishikawa K, Arita R, et al. Increased Expression of M-CSF and IL-13 in Vitreous of Patients With Proliferative Diabetic Retinopathy: Implications for M2 Macrophage-Involving Fibrovascular Membrane Formation. *Brit J Ophthalmol* (2015) 99 (5):629–34. doi: 10.1136/bjophthalmol-2014-305860
11. Rosenblatt A, Udaondo P, Cunha-Vaz J, Sivaprasad S, Bandello F, Lanzetta P, et al. A Collaborative Retrospective Study on the Efficacy and Safety of Intravitreal Dexamethasone Implant (Ozurdex) in Patients With Diabetic Macular Edema. *Ophthalmology* (2020) 127(3):377–93. doi: 10.1016/j.ophtha.2019.10.005
12. Mahaling B, Srinivasarao DA, Raghu G, Kasam RK, Bhanuprakash Reddy G, Katti DS. A non-Invasive Nanoparticle Mediated Delivery of Triamcinolone Acetonide Ameliorates Diabetic Retinopathy in Rats. *Nanoscale* (2018) 10 (35):16485–98. doi: 10.1039/C8NR00058A
13. Yunna C, Mengru H, Lei W, Weidong C. Macrophage M1/M2 Polarization. *Eur J Pharmacol* (2020) 877:173090. doi: 10.1016/j.ejphar.2020.173090
14. Nomura M, Liu J, Rovira II, Gonzalez-Hurtado E, Lee J, Wolfgang MJ, et al. Fatty Acid Oxidation in Macrophage Polarization. *Nat Immunol* (2016) 17 (3):216–7. doi: 10.1038/ni.3366
15. Wu H, Wang M, Li X, Shao Y. The Metaflammatory and Immunometabolic Role of Macrophages and Microglia in Diabetic Retinopathy. *Hum Cell* (2021) 34(6):1617–28. doi: 10.1007/s13577-021-00580-6
16. Abu El-Asrar AM, Ahmad A, Allegaert E, Siddiquei MM, Gikandi PW, De Hertogh G, et al. Interleukin-11 Overexpression and M2 Macrophage Density are Associated With Angiogenic Activity in Proliferative Diabetic Retinopathy. *Ocul Immunol Inflamm* (2020) 28(4):575–88. doi: 10.1080/09273948.2019.1616772
17. Wang JH, Kumar S, Liu GS. Bulk Gene Expression Deconvolution Reveals Infiltration of M2 Macrophages in Retinal Neovascularization. *Invest Ophthalmol Vis Sci* (2021) 62(14):22. doi: 10.1167/iovs.62.14.22
18. Ishikawa K, Yoshida S, Kobayashi Y, Zhou Y, Nakama T, Nakao S, et al. Microarray Analysis of Gene Expression in Fibrovascular Membranes Excised From Patients With Proliferative Diabetic Retinopathy. *Invest Ophthalmol Vis Sci* (2015) 56(2):932–46. doi: 10.1167/iovs.14-15589
19. Li Y, Chen D, Sun L, Wu Y, Zou Y, Liang C, et al. Induced Expression of VEGFC, ANGPT, and EFNB2 and Their Receptors Characterizes Neovascularization in Proliferative Diabetic Retinopathy. *Invest Ophthalmol Vis Sci* (2019) 60(13):4084–96. doi: 10.1167/iovs.19-26767
20. Ritchie ME, Phipson B, Wu D, Hu Y, Law CW, Shi W, et al. Limma Powers Differential Expression Analyses for RNA-sequencing and Microarray Studies. *Nucleic Acids Res* (2015) 43(7):e47. doi: 10.1093/nar/gkv007
21. Johnson WE, Li C, Rabinovic A. Adjusting Batch Effects in Microarray Expression Data Using Empirical Bayes Methods. *Biostatistics* (2007) 8 (1):118–27. doi: 10.1093/biostatistics/kxj037
22. Liberzon A, Birger C, Thorvaldsdóttir H, Ghandi M, Mesirov JP, Tamayo P. The Molecular Signatures Database Hallmark Gene Set Collection. *Cell Syst* (2015) 1(6):417–25. doi: 10.1016/j.cels.2015.12.004
23. Newman AM, Liu CL, Green MR, Gentles AJ, Feng W, Xu Y, et al. Robust Enumeration of Cell Subsets From Tissue Expression Profiles. *Nat Methods* (2015) 12(5):453–7. doi: 10.1038/nmeth.3337
24. Langfelder P, Horvath S. WGCNA: An R Package for Weighted Correlation Network Analysis. *BMC Bioinf* (2008) 9(1):559–9. doi: 10.1186/1471-2105-9-559
25. Antonetti DA, Silva PS, Stitt AW. Current Understanding of the Molecular and Cellular Pathology of Diabetic Retinopathy. *Nat Rev Endocrinol* (2021) 17 (4):195–206. doi: 10.1038/s41574-020-00451-4
26. Pan WW, Lin F, Fort PE. The Innate Immune System in Diabetic Retinopathy. *Prog Retin Eye Res* (2021) 84:100940. doi: 10.1016/j.preteyeres.2021.100940
27. Simó R, Stitt AW, Gardner TW. Neurodegeneration in Diabetic Retinopathy: Does it Really Matter? *Diabetologia* (2018) 61(9):1902–12. doi: 10.1007/s00125-018-4692-1
28. Wong TY, Cheung CMG, Larsen M, Sharma S, Simó R. Diabetic Retinopathy. *Nat Rev Dis Primers* (2016) 2(1):16012. doi: 10.1038/nrdp.2016.12
29. Hedlund E, Deng Q. Single-Cell RNA Sequencing: Technical Advancements and Biological Applications. *Mol Aspects Med* (2018) 59:36–46. doi: 10.1016/j.mam.2017.07.003
30. Lee Y, Yang J. Development of a Zebrafish Screening Model for Diabetic Retinopathy Induced by Hyperglycemia: Reproducibility Verification in Animal Model. *Biomed Pharmacother* (2021) 135:111201. doi: 10.1016/j.biopha.2020.111201

31. Niu T, Fang J, Shi X, Zhao M, Xing X, Wang Y, et al. Pathogenesis Study Based on High-Throughput Single-Cell Sequencing Analysis Reveals Novel Transcriptional Landscape and Heterogeneity of Retinal Cells in Type 2 Diabetic Mice. *Diabetes* (2021) 70(5):1185–97. doi: 10.2337/db20-0839
32. Sun L, Wang R, Hu G, Liu H, Lv K, Duan Y, et al. Single Cell RNA Sequencing (scRNA-Seq) Deciphering Pathological Alterations in Streptozotocin-Induced Diabetic Retinas. *Exp Eye Res* (2021) 210:108718. doi: 10.1016/j.exer.2021.108718
33. Pandey S, Dvorakova MC. Future Perspective of Diabetic Animal Models. *Endocr Metab Immune Disord Drug Targets* (2020) 20(1):25–38. doi: 10.2174/1871530319666190626143832
34. Wynn TA, Vannella KM. Macrophages in Tissue Repair, Regeneration, and Fibrosis. *Immun (Cambridge Mass)* (2016) 44(3):450–62. doi: 10.1016/j.immuni.2016.02.015
35. Aurora AB, Porrello ER, Tan W, Mahmoud AI, Hill JA, Bassel-Duby R, et al. Macrophages are Required for Neonatal Heart Regeneration. *J Clin Invest* (2014) 124(3):1382–92. doi: 10.1172/JCI72181
36. Alexander KA, Flynn R, Lineburg KE, Kuns RD, Teal BE, Olver SD, et al. Csf-1–dependant Donor-Derived Macrophages Mediate Chronic Graft-Versus-Host Disease. *J Clin Invest* (2014) 124(10):4266–80. doi: 10.1172/JCI75935
37. Kinuthia UM, Wolf A, Langmann T. Microglia and Inflammatory Responses in Diabetic Retinopathy. *Front Immunol* (2020) 11:564077. doi: 10.3389/fimmu.2020.564077
38. Li J, Yu S, Lu X, Cui K, Tang X, Xu Y, et al. The Phase Changes of M1/M2 Phenotype of Microglia/Macrophage Following Oxygen-Induced Retinopathy in Mice. *Inflamm Res* (2021) 70(2):183–92. doi: 10.1007/s00011-020-01427-w
39. Van Hove I, De Groef L, Boeckx B, Modave E, Hu T, Beets K, et al. Single-cell transcriptome analysis of the Akimba mouse retina reveals cell-type-specific insights into the pathobiology of diabetic retinopathy. *Diabetologia* (2020) 63(10):2235–48. doi: 10.1007/s00125-435 020-05218-0
40. Ong JX, Nesper PL, Fawzi AA, Wang JM, Lavine JA. Macrophage-Like Cell Density Is Increased in Proliferative Diabetic Retinopathy Characterized by Optical Coherence Tomography Angiography. *Invest. Ophth. Vis Sci* (2021) 62(10):2–2. doi: 10.1167/iovs.62.10.2
41. Huang H, Zhu L, Zhu W, Lin T, Los LI, Yao C, et al. Algorithm for Detection and Quantification of Hyperreflective Dots on Optical Coherence Tomography in Diabetic Macular Edema. *Front Med (Lausanne)* (2021) 8:688986. doi: 10.3389/fmed.2021.688986
42. Boneva SK, Wolf J, Hajdú RI, Prinz G, Salié H, Schlecht A, et al. In-Depth Molecular Characterization of Neovascular Membranes Suggests a Role for Hyalocyte-To-Myofibroblast Transdifferentiation in Proliferative Diabetic Retinopathy. *Front Immunol* (2021) 12:757607. doi: 10.3389/fimmu.2021.757607
43. Ilies RF, Aioanei CS, Catana A, Halmagyi SR, Lukacs I, Tokes RE, et al. Involvement of COL5A2 and TGF-Beta1 in Pathological Scarring. *Exp Ther Med* (2021) 22(4):1067. doi: 10.3892/etm.2021.10501
44. Ren X, Chen X, Fang K, Zhang X, Wei X, Zhang T, et al. COL5A2 Promotes Proliferation and Invasion in Prostate Cancer and Is One of Seven Gleason-Related Genes That Predict Recurrence-Free Survival. *Front Oncol* (2021) 11:583083. doi: 10.3389/fonc.2021.583083
45. Cheng Q, Tang A, Wang Z, Fang N, Zhang Z, Zhang L, et al. CALD1 Modulates Gliomas Progression *via* Facilitating Tumor Angiogenesis. *Cancers (Basel)* (2021) 13(11). doi: 10.3390/cancers13112705
46. Zheng H, Bai Y, Wang J, Chen S, Zhang J, Zhu J, et al. Weighted Gene Co-Expression Network Analysis Identifies CALD1 as a Biomarker Related to M2 Macrophages Infiltration in Stage III and IV Mismatch Repair-Proficient Colorectal Carcinoma. *Front Mol Biosci* (2021) 8:649363. doi: 10.3389/fmolb.2021.649363
47. Pasarica M, Gowronska-Kozak B, Burk D, Remedios I, Hymel D, Gimble J, et al. Adipose Tissue Collagen VI in Obesity. *J Clin Endocrinol Metab* (2009) 94(12):5155–62. doi: 10.1210/jc.2009-0947
48. Gesta S, Guntur K, Majumdar ID, Akella S, Vishnudas VK, Sarangarajan R, et al. Reduced Expression of Collagen VI Alpha 3 (COL6A3) Confers Resistance to Inflammation-Induced MCP1 Expression in Adipocytes. *Obes (Silver Spring)* (2016) 24(8):1695–703. doi: 10.1002/oby.21565
49. Dankel SN, Grytten E, Bjune J, Nielsen HJ, Dietrich A, Blüher M, et al. COL6A3 Expression in Adipose Tissue Cells is Associated With Levels of the Homeobox Transcription Factor PRRX1. *Sci Rep.-UK* (2020) 10(1):20164–4. doi: 10.1038/s41598-020-77406-2
50. Wang J, Tsouko E, Jonsson P, Bergh J, Hartman J, Aydogdu E, et al. miR-206 Inhibits Cell Migration Through Direct Targeting of the Actin-Binding Protein Coronin 1C in Triple-Negative Breast Cancer. *Mol Oncol* (2014) 8(8):1690–702. doi: 10.1016/j.molonc.2014.07.006
51. Wang Z, Jia L, Sun Y, Li C, Zhang L, Wang X, et al. CORO1C is Associated With Poor Prognosis and Promotes Metastasis Through PI3K/AKT Pathway in Colorectal Cancer. *Front Mol Biosci* 8:682594. doi: 10.3389/fmolb.2021.682594
52. Sahoo SK, Kim DH. Characterization of Calumenin in Mouse Heart. *BMB Rep* (2010) 43(3):158–63. doi: 10.5483/bmbrep.2010.43.3.158
53. Du Y, Miao W, Jiang X, Cao J, Wang B, Wang Y, et al. The Epithelial to Mesenchymal Transition Related Gene Calumenin Is an Adverse Prognostic Factor of Bladder Cancer Correlated With Tumor Microenvironment Remodeling, Gene Mutation, and Ferroptosis. *Front Oncol* (2021) 11:683951. doi: 10.3389/fonc.2021.683951
54. Yang Y, Wang J, Xu S, Shi F, Shan A. Calumenin Contributes to Epithelial-Mesenchymal Transition and Predicts Poor Survival in Glioma. *Transl Neurosci* (2021) 12(1):67–75. doi: 10.1515/tnsci-2021-0004

Conflict of Interest: The authors declare that the research was conducted in the absence of any commercial or financial relationships that could be construed as a potential conflict of interest.

frontiers | Frontiers in Public Health

SYSTEMATIC REVIEW
published: 31 May 2022
doi: 10.3389/fpubh.2022.906760

Uric Acid and Diabetic Retinopathy: A Systematic Review and Meta-Analysis

*Yicong Guo, Siyue Liu and Huilan Xu**

Department of Social Medicine and Health Management, Xiangya School of Public Health, Central South University, Changsha, China

Background: The relationship between uric acid (UA) and diabetic retinopathy (DR) remains ambiguous, and the results of current studies on the UA levels in patients with DR are conflicting. A meta-analysis was performed to provide a better understanding of the relationship between UA levels and DR.

Methods: PubMed, Web of Science, Embase, and the Cochrane Library databases were searched until December 11, 2021 to identify eligible studies, that compared the UA levels of the case group (patients with DR) and control group (controls with diabetes and healthy participants). The weighted mean difference (WMD) with a 95% confidence interval (CI) was used to evaluate the difference in UA levels between the case and control groups.

Results: Twenty-one studies involving 4,340 patients with DR and 8,595 controls (8,029 controls with diabetes and 566 healthy participants) were included in this meta-analysis. We found that patients with DR had significantly higher UA levels than those in the controls with diabetes (WMD = 36.28; 95% CI: 15.68, 56.89; $P < 0.001$) and healthy participants (WMD = 70.80; 95% CI: 19.85, 121.75; $P = 0.006$). There was an obvious heterogeneity among the 21 studies ($I^2 = 97\%$, $P < 0.001$). Subgroup analyses of different phases of DR showed that UA levels were significantly increased in participants with proliferative diabetic retinopathy (PDR) (WMD = 46.57; 95% CI: 28.51, 64.63; $P < 0.001$) than in controls with diabetes; however, the difference is not statistically significant when comparing UA levels in patients with non-proliferative diabetic retinopathy (NPDR) and controls with diabetes (WMD = 22.50; 95% CI: −6.07, 51.08; $P = 0.120$). In addition, UA levels were higher in participants with a body mass index (BMI) ≥25.0 kg/m^2 and over 15 years of diabetes. Univariate meta-regression analysis revealed that BMI ($P = 0.007$, Adj $R^2 = 40.12\%$) and fasting blood glucose (FBG) ($P = 0.040$, Adj $R^2 = 29.72\%$) contributed to between-study heterogeneity.

Conclusions: In conclusion, our study provides evidence that UA levels are higher in patients with DR than those in the controls, but this difference is not statistically significant in the early phases. UA might be a potential biomarker for identifying disease severity in patients with DR, rather than predicting the onset of DR among patients with diabetes.

OPEN ACCESS

Edited by:
Michele Lanza, University of Campania Luigi Vanvitelli, Italy

Reviewed by:
Taiji Nagaoka, Nihon University, Japan
Yan Zhang, Tianjin Medical University Eye Hospital, China
Qianyi Lu, The First Affiliated Hospital of Soochow University, China

****Correspondence:***
Huilan Xu
xhl_csu@163.com

Specialty section:
This article was submitted to Clinical Diabetes, a section of the journal Frontiers in Public Health

Received: *29 March 2022*
Accepted: *09 May 2022*
Published: *31 May 2022*

Citation:
Guo Y, Liu S and Xu H (2022) Uric Acid and Diabetic Retinopathy: A Systematic Review and Meta-Analysis. Front. Public Health 10:906760. doi: 10.3389/fpubh.2022.906760

However, more prospective and high-quality clinical evidence is required to confirm these present findings.

Systematic Review Registration: https://www.crd.york.ac.uk/PROSPERO/display_record.php?RecordID=297708.

Keywords: uric acid, diabetic retinopathy, systematic review, meta-analysis, non-proliferative diabetic retinopathy, proliferative diabetic retinopathy

INTRODUCTION

According to the International Diabetes Federation (IDF) estimates of the global prevalence of diabetes mellitus (DM), 700 million (10.9%) people will have diabetes by 2045, representing a 51% increase compared with that in 2019 (1). With the increasing number of people with diabetes, it is foreseeable that the prevalence of diabetic retinopathy (DR) is also expected to increase. DR is a common microvascular complication of diabetes affecting more than 30% of patients with diabetes worldwide and is one of the leading causes of acquired blindness globally in the working-age adult population (2–4). DR is divided into two progressive phases, non-proliferative (earlier) and proliferative (late), and eventually deteriorates into vision-threatening DR (VTDR) (5). The pathogenesis of DR is known as a complex interplay between neuroglial and vascular damage that results from hyperglycemia-induced metabolic oxidative stress, and improving microcirculation of the retina was proven to be effective in preventing the early development of DR (6–9). In addition, previous studies have found that DR may be associated with inflammation and dysregulation of various inflammatory mediators (10–12).

Uric acid (UA) is the final product of purine metabolism and is typically considered the predominant predictor of gout. A UA concentration of 6 mg/dL is recommended as the threshold for the definition of hyperuricemia and as the minimum uricemia target for UA-lowering therapy in patients with gout (13). In addition to being closely linked to gout, increased UA levels have been shown to be associated with the risk of diabetes and some of its complications, such as diabetic peripheral neuropathy and diabetic nephropathy (14–16). Similarly, UA is likely to contribute to DR occurrence. For example, UA has been demonstrated to promote an inflammatory response to release inflammatory factors such as tumor necrosis factor-α (TNF-α), interleukin-6 (IL-6), and C-reactive protein (CRP) (17), and a recent meta-analysis showed that IL-6 was associated with the incidence of DR (18). However, the relationship between UA levels and DR remains ambiguous, and the results of current studies on UA levels in patients with DR are conflicting. Some studies have reported increased UA levels in patients with DR compared with patients with diabetes without DR (19–21), but the results of other studies were different or even opposite (22–25).

No meta-analytical data provided the overall information on this issue. Thus, to obtain a more precise assessment of the association between DR and serum and plasma UA levels and explore the possibility of UA as a predictor for DR in patients with diabetes, we conducted a systematic review and meta-analysis to summarize the current evidence.

METHODS

This systematic review and meta-analysis followed the Preferred Reporting Items for Systematic reviews and Meta-Analyses (PRISMA) guidelines (26). The PRISMA checklist for reporting the meta-analysis results is shown in **Supplementary Table 1**. The study protocol was registered in the PROSPERO International Prospective Register of Systematic Reviews (CRD42022297708).

Literature Search

We performed a comprehensive search of PubMed, Web of Science, Embase, and the Cochrane Library databases up to December 11, 2021, to acquire original articles. A combination of keywords and mesh terms was used as a search strategy: ("uric acid" OR "urate" OR "hyperuricemia" OR "serum uric acid") AND ("diabetic retinopathy" OR "diabetic complication" OR "microvascular complication" OR "DR"). The terms were appropriately adjusted for each database. We also screened the references of relevant studies and reviewed articles to identify additional published and unpublished records.

Inclusion and Exclusion Criteria

Our meta-analysis included all studies meeting the following explicit criteria: (1) studies were designed as a comparative study, completely involving a case group (patients with diabetes with DR) and control group (patients with diabetes without DR or participants without diabetes); (2) the concentrations of UA (mean and standard deviation) and the number of individuals in each group were available; (3) studies in which UA levels were measured in blood specimens (plasma, serum, or whole blood); and (4) studies were published or written in English.

The exclusion criteria were as follows: (1) case reports, abstracts, and reviews (including systematic reviews and meta-analyses); (2) study protocols, letters, comments, and conference abstracts; (3) experimental or animal studies; and (4) duplicate studies retrieved from various databases.

Data Extraction and Quality Assessment

For each eligible study, two authors (GY-C and LS-Y) independently extracted the following data: (1) first author's last name, publication year, region of study, the grouping of each study, and sample size; (2) demographic characteristics of participants, including ages, percentage of male participants, body mass index (BMI), types of diabetes, and duration of

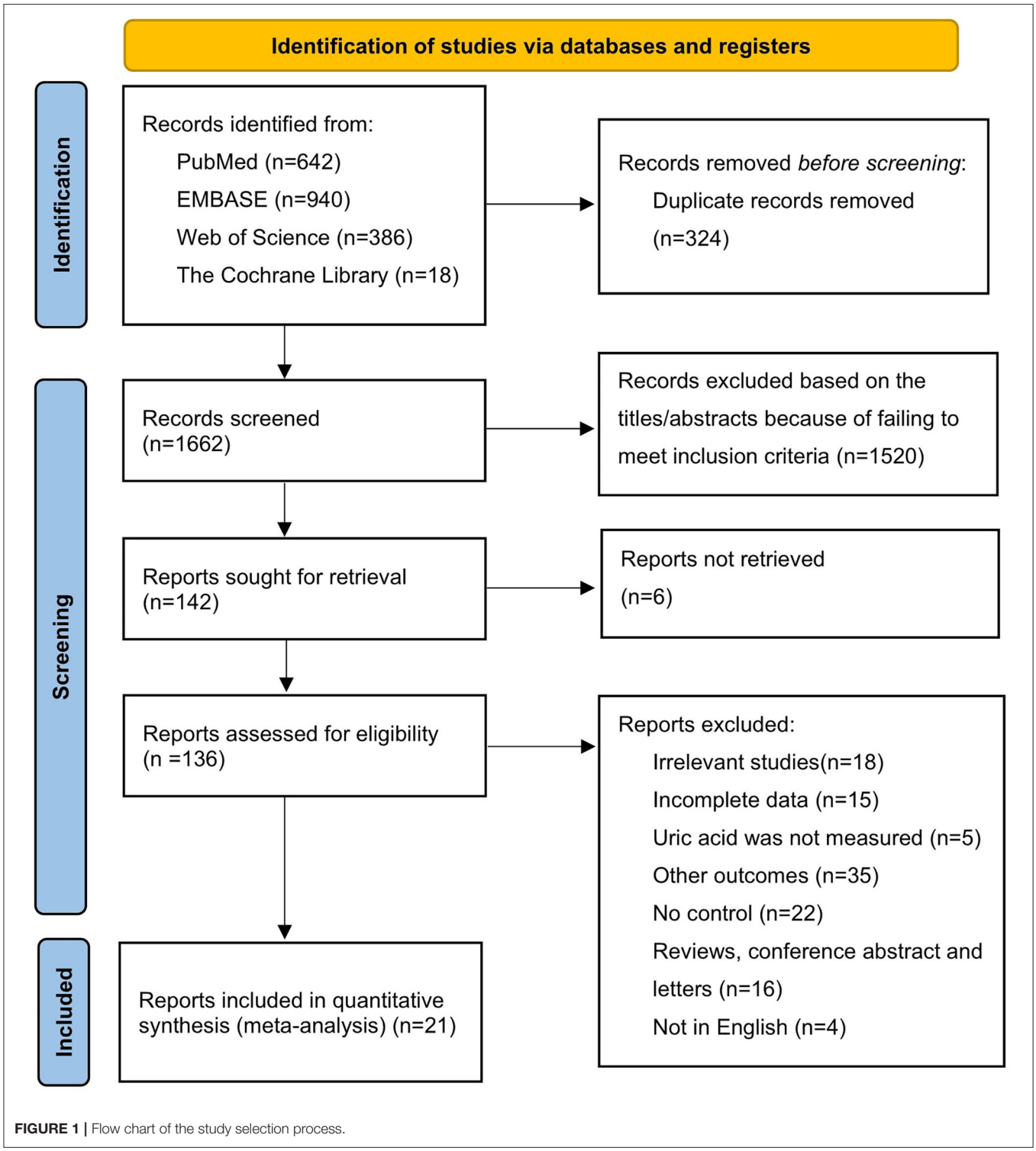

FIGURE 1 | Flow chart of the study selection process.

diabetes; (3) laboratory test results in participants with diabetes such as fasting blood glucose (FBG), glycated hemoglobin A_{1c} (HbA_{1c}), total cholesterol (TC), and low-density lipoprotein (LDL); (4) concentrations of UA (mean and standard deviation), and all of the units were converted into μmol/L (1 mg/dL = 59.48 μmol/L); and (5) detecting methods and source of specimen for UA.

The quality of the included studies was assessed using the Newcastle-Ottawa Scale (NOS) for non-randomized studies. NOS is a rating scale in which points are awarded to

studies based on selection, comparability, and exposure or outcome, where each study score ranges from 0 to 9 points (27). A study with a total quality score of more than 7 points was considered a high-quality study. Two researchers (GY-C and LS-Y) independently rated the study quality, and differences in ratings between reviewers were resolved by discussion.

Statistical Analysis

The fixed-effects (or random-effects) inverse-variance model (for continuous data) with the DerSimonian-Laird estimate of tau² was used to pool mean differences (MDs) from all included studies, and the weighted mean difference (WMD) with a 95% confidence interval (CI) was used to evaluate the difference in UA levels between the case and control groups. We generated a forest plot of the differences in UA levels between patients with DR and controls (controls with diabetes and healthy participants were separately compared). Heterogeneity was evaluated using Cochran's Q-statistic test and I-squared (I^2). A value of I^2 of 0–25% represents insignificant heterogeneity, >25% but <50% represents low heterogeneity, >50% but <75% represents moderate heterogeneity, and >75% represents high heterogeneity (46, 47). The *P*-value of the *Q*-test <0.10 was considered statistically significant. If $I^2 \geq 50\%$ and $P < 0.10$, the random-effects model was used; otherwise, the fixed-effects model was applied (48). Subgroup analysis grouped by DR phases [non-proliferative diabetic retinopathy (NPDR) vs. controls with diabetes; proliferative diabetic retinopathy (PDR) vs. controls with diabetes; and PDR vs. NPDR], region (Asia and others), diabetes type (type 1, type 2, and both), duration of diabetes (≤15 and >15 years), BMI (≤25 and >25 kg/m^2), FBG (≤150 and >150 mg/dL), HbA1c (≤8.0% and >8.0%), LDL (≤120 and >120 mg/dL), specimen types (plasma and serum), and quality score (<7 and ≥7) was performed to investigate the differences in studies or participants with different characteristics and explore the origin of heterogeneity. The UA concentrations in patients with DR were stratified (quartiles 1–4: 285.4–307.1; 307.1–333; 333–378.15; and 378.15–505.6 μmol/L) to explore a linear dose-response correlation of the pooled results in patients with DR with different ranges of UA levels. When heterogeneity was high, a univariate meta-regression analysis was performed to identify potential confounding factors and explore the sources of heterogeneity. A sensitivity analysis was performed to evaluate the effect of a particular study on the overall results by omitting one study and combining the remainders in each turn. Egger's (49) and Begg's tests (50) were used to assess potential publication bias, and a visualized funnel plot was performed as a complement.

All statistical analyses were performed using RevMan 5.4 software (The Cochrane Collaboration, Copenhagen, Denmark) and Stata v16.0 (Stata Corp LP, College Station, TX, USA). A two-sided $P < 0.05$ was considered statistically significant except for the Cochran *Q*-test. In our study, all analyses were based on previously published research; therefore, no ethical approval or patient consent was required.

RESULTS

Search Results and Study Characteristics

Our search yielded 1,986 potentially relevant articles in electronic databases: 642 from PubMed, 940 from Embase, 386 from Web of Science, and 18 from the Cochrane Library. After excluding duplicate studies, 1,662 articles were retained. Of the 1,662 studies initially identified, 1,520 were excluded because they failed to meet the inclusion criteria based on title and abstract review. The full texts of the remaining 142 articles were reviewed for eligibility, and 121 articles were excluded for various reasons, such as not being retrieved, irrelevant studies, incomplete data, other outcomes, and a review article or conference abstract. We finally selected a total of 21 qualified articles (20, 22, 23, 28–45) involving 4,340 patients with DR and 8,595 controls (containing 8,029 controls with diabetes and 566 healthy participants) in this meta-analysis. A flowchart of the literature search process is shown in **Figure 1**.

Table 1 presents the characteristics of the 21 eligible studies, including the first author's last name, publication year, region, diabetes type, specimen type, detection method for UA, grouping of each study, sample size of each group, and the NOS score. Accordingly, 16 studies were conducted in Asia (22, 23, 29–32, 34–38, 40, 42–45), and other studies were conducted in Africa (28, 33, 41), Europe (39), and South America (20). In addition, two studies were based on type 1 diabetes (20, 39) with 2,311 included participants, and the others were based on type 2 diabetes (22, 29–38, 40, 43–45) and both types of diabetes (23, 28, 32, 41, 42). The colorimetric method has been used in most studies to measure UA concentrations, and only one study applied the high-performance liquid chromatography (HPLC) method (34). Except for three studies (28, 34, 39) that measured UA concentrations using plasma, serum was utilized for the measurement of UA concentrations in other studies. Eleven studies (20, 22, 29, 34, 35, 37–40, 43, 44) that scored 7 or higher were considered high quality, and others (23, 28, 30–33, 36, 41, 42, 45) scored from 4 to 6, indicating that the overall quality of the studies was acceptable. The participants' characteristics, including age, sex, and BMI, are summarized in **Table 1**.

Comparison of UA Levels Between Patients With DR and Controls

An obvious heterogeneity was observed among the 21 included studies ($I^2 = 97\%$; $P < 0.001$); thus, the random-effects model was used. We found that patients with DR had significantly higher UA levels UA than those in the controls with diabetes (WMD = 36.28; 95% CI: 15.68, 56.89; $P < 0.001$) **(Figure 2A)**. Compared with healthy participants, the UA levels in patients with DR were higher (WMD = 70.80; 95% CI: 19.85, 121.75; $P = 0.006$; $I^2 = 98\%$; $P < 0.001$) **(Figure 2B)**.

Comparison of UA Levels Between Different Phases of DR and Controls With Diabetes

The UA levels were significantly higher in participants with PDR (WMD = 46.57; 95% CI: 28.51, 64.63; $P < 0.001$; $I^2 = 71\%$; *P*

TABLE 1 | Characteristics of included studies in the meta-analysis.

References	Region	Diabetes types	Detecting methods	Specimen types	Case group (N)/control group (N)	Male (%) (DR/DM/healthy)	Age (years) (range/mean ± SD) (DR/DM/healthy)	BMI (kg/m^2) (mean ± SD) (DR/DM/healthy)	NOS
Yanko et al. (23)	Israel	Both	NA	Serum	DR (64)/DM (104)	100/100/	>40	NA	5
Olukoga et al. (28)	Nigeria	Both	Colorimetric	Plasma	DR (30)/DM (145)+Healthy (114)	//48.2	20–70	//24.52 ± 4.82	6
Weitzman et al. (29)	Israel	2	NA	Serum	DR (124)/DM (367)	NA	65 ± 9.4/64.1 ± 0.7/	28.4 ± 3.9/28.8 ± 4.8/	7
Huang et al. (30)	Taiwan	2	Colorimetric	Serum	DR (91)/DM (166)+Healthy (204)	//43.1	//58.2 ± 12.2	NA	5
[-0.5pt] Cai et al. (31)	China	2	Colorimetric	Serum	NPDR (59)+PDR (28)/DM (103)	48.3/49.5/	61.7 ± 17.4/53.6 ± 13.6/	24.6 ± 3.7/25.1 ± 3.5/	6
Navin et al. (32)	India	Both	Colorimetric	Serum	NPDR (21)+PDR (13)/DM (30)+Healthy (30)	NA	NA	NA	4
Longo-Mbenza et al. (33)	DR Congo	2	NA	Serum	DR (66)/DM (84)+Healthy (45)	39.4/46.4/46.7	53.4 ± 13.6/56.6 ± 12.4/50.7 ± 13.0	25.2 ± 5/26.3 ± 5.0/22.4 ± 2.9	6
Xia et al. (34)	China	2	HPLC	Plasma	NPDR (39)/DM (35)+Healthy (41)	53.8/57.1/55	56.5 ± 5.4/55.87 ± 7.0/54.4 ± 5.4	25.2 ± 4.0/25.1 ± 2.6/	7
Chuengsamarn et al. (35)	Thailand	2	Colorimetric	Serum	DR (154)/DM (452)	NA	NA	NA	7
Venkatachalam et al. (36)	India	2	Colorimetric	Serum	NPDR (10)+PDR (15)/DM (25)+Healthy (50)	64/56/46	64.6 ± 8.8/57.6 ± 7.8/52.9 ± 6.9	NA	5
Cui et al. (37)	China	2	Colorimetric	Serum	DR (141)/DM (1,608)	55.5/55.6/	57.1 ± 10.3/55.9 ± 11.3/	25.9 ± 2.9/26.3 ± 3.7/	8
Zhang et al. (38)	China	2	Colorimetric	Serum	DR (533)/DM (209)	56.3/56.9/	59.7 ± 10.5/59.2 ± 10.9/	25.1 ± 2.6/24.9 ± 3.4/	7
Pilemann-Lyberg et al. (39)	Denmark	1	Colorimetric	Plasma	NPDR (277)+PDR (229)/DM (142)	NA	NA	NA	7
Melo et al. (20)	Brazil	1	Colorimetric	Serum	DR (589)/DM (1,055)	58.2/54.4/	35.8 ± 11.6/26.9 ± 11.1/	25.1 ± 4.7/23.7 ± 3.8/	8
Chen et al. (40)	China	2	Colorimetric	Serum	NPDR (184)+PDR (162)/DM (172)	52.0/51.2/	52.8 ± 11.8/49.2 ± 8.5/	23.2 ± 3.5/23.1 ± 1.6/	7

(Continued)

TABLE 1 | Continued

References	Region	Diabetes types	Detecting methods	Specimen types	Case group (N)/control group (N)	Male (%) (DR/DM/healthy)	Age (years) (range/mean ± SD) (DR/DM/healthy)	BMI (kg/m^2) (mean ± SD) (DR/DM/healthy)	NOS
Xia et al. (22)	China	2	Colorimetric	Serum	NPDR (582)+PDR (135)/DM (2,244)	46.4/52.0/	62.0 ± 10.0/60.0 ± 11.0/	NA	8
Shawki et al. (41)	Egypt	Both	Colorimetric	Serum	DR (70)/DM (40)+Healthy (40)	43/35/30	43.0 ± 10.7/45.4 ± 15.1/42.6 ± 9.4	32.4 ± 6.9/31.7 ± 6.7/30.8 ± 5.9	6
Çakir et al. (42)	Turkey	Both	Colorimetric	Serum	DR (68)/DM (54)+Healthy (42)	NA	63.4 ± 11.8/61.5 ± 11.2/59.3 ± 10.1	NA	5
Wakasugi et al. (43)	Japan	2	NA	Serum	NPDR (183)+PDR (39)/DM (777)	56.8/62/	66.0 ± 9.0/64.1 ± 9.8/	24.7 ± 3.9/24.6 ± 3.8/	7
Nakayama et al. (44)	Japan	2	Colorimetric	Serum	NPDR (72)/DM (142)	43/62/	64.0 ± 13.0/63.0 ± 10.0/	25.6 ± 4.5/25.6 ± 4.2/	7
Zhao et al. (45)	China	2	NA	Serum	NPDR (239)+PDR (104)/DM (75)	65/52/	51.7 ± 15.4/51.8 ± 14.3/	NA	6

DM, Diabetes mellitus (without diabetic retinopathy when being used as controls); DR, diabetic retinopathy; PDR, proliferative diabetic retinopathy; NPDR, non–proliferative diabetic retinopathy; NDR, non–diabetic retinopathy; HPLC, high-performance liquid chromatography; BMI, body mass index; SD, standard deviation; DR Congo, The Democratic Republic of the Congo; NA, not available; NOS, Newcastle–Ottawa scale.

= 0.001) than those in the controls with diabetes **(Figure 3A)**; however, when comparing UA levels in patients with NPDR and controls with diabetes, the difference is not statistically significant (WMD = 22.50; 95% CI:−6.07, 51.08; $P = 0.120$; $I^2 = 97\%$; $P < 0.001$) **(Figure 3B)**.

Comparison of UA Levels Between PDR and NPDR

Eight studies (22, 31, 32, 36, 39, 40, 43, 45) divided patients with DR into PDR and NPDR groups. There were significant differences in UA levels between patients with PDR and NPDR in a fixed-effects model (WMD = 28.68; 95% CI: 19.78, 37.58; $P < 0.001$; $I^2 = 44\%$; $P = 0.090$) **(Figure 3C)**.

Subgroup and Meta-Regression Analyses

Table 2 presents the results of the subgroup analyses of UA levels between patients with DR and controls with diabetes. Most of the subgroup analysis results were consistent with the overall meta-analysis results, suggesting that these results were relatively stable but with high heterogeneity. Subgroup analyses of the region and diabetes type reported that UA levels were lower in Asians (WMD = 24.67; 95% CI: 2.30, 47.03; $P = 0.031$) and participants with type 2 diabetes (WMD = 27.16; 95% CI: 2.61, 51.71; $P = 0.030$). Increased UA levels were not significant in studies including both types of diabetes (WMD = 60.51; 95% CI: −19.27, 140.29; $P = 0.137$) and studies using plasma for UA measurement (WMD = 50.15; 95% CI: −1.42, 101.72; $P = 0.057$). When stratified by quality score (NOS <7 and NOS ≥7), the results showed that the heterogeneity failed to decrease in studies where NOS <7 with an I^2 of 95.5%, and in NOS ≥7 studies, the I^2 was 97.6%. The results were statistically significant in NOS <7 (WMD = 42.26; 95% CI: 1.14, 83.38; $P = 0.044$) and NOS ≥7 (WMD = 33.15; 95% CI: 7.45, 58.84; $P = 0.011$). Further subgroup analyses demonstrated increased UA levels in participants with a longer duration of diabetes (WMD = 62.22; 95% CI: 19.16, 105.27; $P = 0.005$), higher BMI (WMD = 63.51; 95% CI: 13.11, 113.91; $P < 0.001$), FBG (WMD = 52.76; 95% CI: 10.15, 95.37; $P = 0.015$), HbA_{1c} (WMD = 55.35; 95% CI: 23.92, 86.78; $P = 0.001$), and LDL (WMD = 55.39; 95% CI: 37.11, 79.67; $P < 0.001$). In addition, we divided the UA concentrations in patients with DR [median: 333; interquartile range (IQR): 307.1–378.15, mg/dL] by quartile. The subgroup analysis of UA levels showed an insignificant difference in quartile 1 (WMD = 3.72; 95% CI: −32.87, 40.32; $P = 0.842$), while in quartiles 2–4, especially in quartile 4, there was an increase in UA levels (WMD = 128.06; 95% CI: 72.37, 183.75; $P < 0.001$) **(Figure 4)**.

According to the findings of subgroup analyses, a univariate meta-regression analysis regarding the clinical characteristics of participants, including BMI, duration of DM, FBG, HbA_{1c}, and LDL, was performed to identify possible impact factors on the

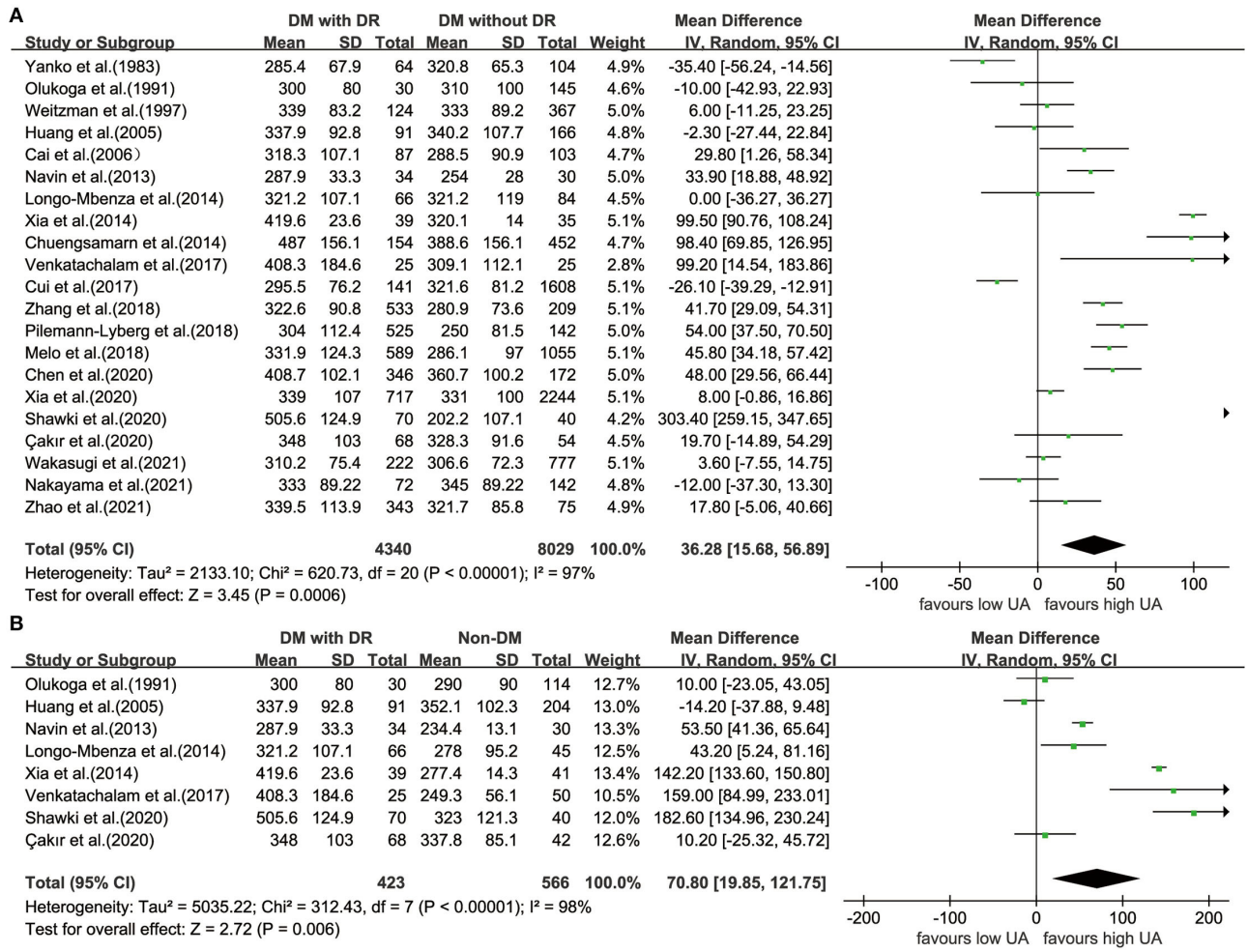

FIGURE 2 | Forest plot for WMD and the corresponding 95% confidence interval of the comparison in UA levels between case group and control group with **(A)**/without **(B)** diabetes. WMD, weighted mean difference; UA, uric acid.

relationship between UA and DR. The results showed that BMI ($P = 0.007$, Adj $R^2 = 40.12\%$) and FBG levels ($P = 0.040$, Adj $R^2 = 29.72\%$) could explain the variation in study results, whereas the duration of DM ($P = 0.099$, Adj $R^2 = 14.93\%$), LDL ($P = 0.308$, Adj $R^2 = 0.61\%$), and HbA_{1c} ($P = 0.537$, Adj $R^2 = -5.43\%$) were not significant for determining the source of heterogeneity.

Sensitivity Analysis and Publication Bias

To evaluate the stability and reliability of our results, we performed a sensitivity analysis that excluded one study from the meta-analysis. After the included studies were successively removed, the estimates were statistically significant with WMD ranging from 24.46 (95% CI: 5.85, 43.07) to 39.91 (95% CI: 19.15, 60.68), indicating that the overall results were relatively stable **(Figure 5)**. Notably, there was a marked decrease (though still obvious) in heterogeneity among studies when two sensitive studies (34, 41) were removed (WMD = 19.50; 95% CI: 5.87, 33.12; $P = 0.005$; $I^2 = 91\%$; $P < 0.001$), suggesting these two studies contributed relatively more to the heterogeneity.

The Egger funnel plot of the results of the included studies was symmetrical (**Supplementary Material**). The *P*-values of Begg's and Egger's tests of publication bias analyses were 0.291 and 0.156, respectively, suggesting that statistically significant publication bias.

DISCUSSION

To provide a better understanding of the relationship between UA and DR. We conducted a systematic review and meta-analysis to compare differences in UA levels between patients with DR and controls. We also tested whether UA levels could differ in different phases of DR, including NPDR and PDR. To the best of our knowledge, this is the first meta-analysis to show an exact association using MD with 95% CIs.

The results of our meta-analysis showed that UA levels in patients with DR were significantly higher than those in

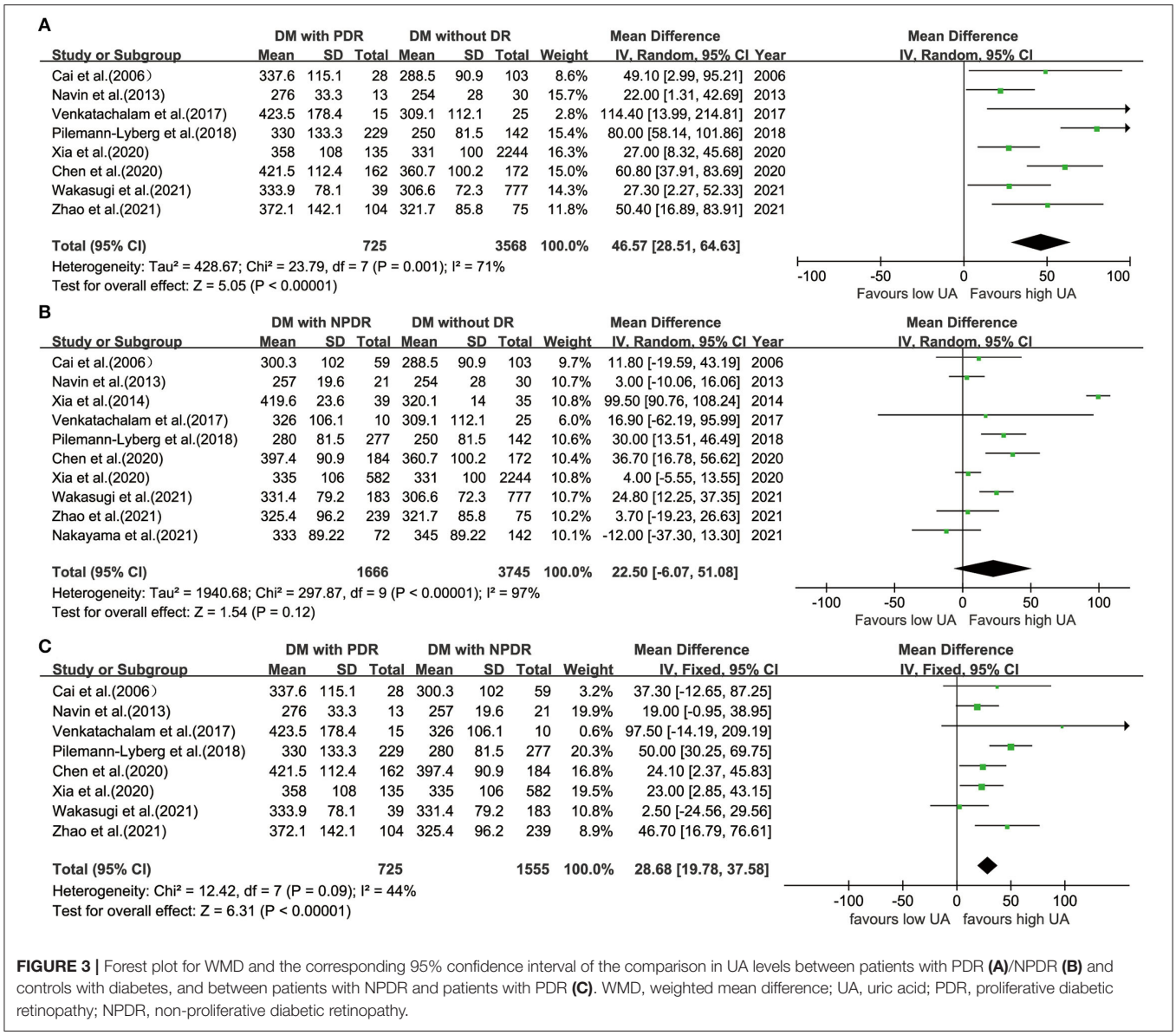

FIGURE 3 | Forest plot for WMD and the corresponding 95% confidence interval of the comparison in UA levels between patients with PDR **(A)**/NPDR **(B)** and controls with diabetes, and between patients with NPDR and patients with PDR **(C)**. WMD, weighted mean difference; UA, uric acid; PDR, proliferative diabetic retinopathy; NPDR, non-proliferative diabetic retinopathy.

the controls. For different phases of DR, UA levels increased significantly in participants with PDR than those in the controls with diabetes. No significant difference was found in patients with NPDR (WMD = 22.50; 95% CI: −6.07, 51.08; $P = 0.120$; $I^2 = 97\%$; $P < 0.001$), while the existing heterogeneity possibly influenced the robustness of this result. In the comparison between patients with NPDR and controls, we noted that the study conducted by Xia et al. (34) used different specimens and detection methods for UA measurement. When this sensitive study was removed, the heterogeneity among the studies decreased sharply, and the difference was statistically significant (WMD = 13.50; 95% CI: 3.12, 23.89; $P = 0.010$; $I^2 = 65\%$; $P = 0.003$). In addition, increased UA levels existed in patients with PDR compared with patients with NPDR in our study, with no significant heterogeneity. This finding is consistent with previous studies showing that participants with higher UA levels have an increased risk of DR severity (from NPDR to PDR) (40, 51). Furthermore, a linear dose-response correlation of the elevation in patients with DR with different UA levels revealed a gradual increase from insignificant to significant. This is in line with the epidemiological survey showing that higher UA levels (≥378.00 μmol/L) were associated with a greater risk for DR (OR: 3.42; 95% CI: 1.64, 7.14; $P = 0.001$) (52), suggesting that elevated UA may be a potential risk factor for the progression of DR.

Increased UA is likely to play a role in the pathogenesis of DR. Accumulating experimental and clinical studies have found that oxidative stress and inflammatory responses induced by UA contribute to microvascular damage in DR (53, 54). Circulating UA is regarded as a powerful antioxidant that can remove superoxide and hydroxyl radicals in plasma, which may lead to an increase in reactive oxygen species production, which has been

TABLE 2 | Subgroup analysis of the studies for the UA levels and DR.

Subgroups	Number of studies	WMD (95% CI)	*P*	Heterogeneity	
				I^2	*P*
Region					
Asia	16	24.67 (2.30; 47.03)	0.031	96.7%	<0.001
Others	5	76.30 (15.03; 137.57)	0.015	97.3%	<0.001
DR phase					
NPDR vs. DM without DR	10	22.50 (−6.07; 51.08)	0.120	97.0%	<0.001
PDR vs. DM without DR	8	46.57 (28.51; 64.63)	<0.001	70.6%	0.001
PDR vs. NPDR	8	28.68 (19.78; 37.58)	<0.001	43.6%	0.088
Diabetes types					
1	2	48.52 (39.02; 58.02)	<0.001	0.0%	0.426
2	14	27.16 (2.61; 51.71)	0.030	96.9%	<0.001
Both	5	60.51 (−19.27; 140.29)	0.137	97.9%	<0.001
Duration of diabetes, years					
≤15	10	36.52 (4.81; 68.23)	0.024	97.6%	<0.001
>15	6	62.22 (19.16; 105.27)	0.005	97.7%	<0.001
BMI, kg/m^2					
≤25	7	24.92 (8.14; 41.69)	0.004	89.5%	<0.001
>25	8	63.51 (13.11; 113.91)	0.014	98.4%	<0.001
FBG, mg/dL					
≤150	5	47.47 (−0.62; 95.56)	0.053	98.1%	<0.001
>150	7	52.76 (10.15; 95.37)	0.015	97.4%	<0.001
HbA_{1c}, %					
≤8.0	5	26.07 (2.62; 49.52)	0.029	90.4%	<0.001
>8.0	11	55.35 (23.92; 86.78)	0.001	97.4%	<0.001
LDL, mg/dL					
≤120	12	42.93 (13.78; 72.09)	0.004	97.9%	<0.001
>120	5	53.39 (37.11; 79.67)	<0.001	79.2%	0.001
Specimen types					
Plasma	3	50.15 (−1.42, 101.72)	0.057	96.4%	<0.001
Serum	18	32.77 (13.99; 51.55)	0.001	94.9%	<0.001
UA level, μmol/L					
Quartile 1 (285.4–307.1)	5	3.72 (−32.87; 40.32)	0.842	95.3%	<0.001
Quartile 2 (307.1–333)	5	25.88 (4.87; 46.90)	0.016	88.3%	<0.001
Quartile 3 (333–378.15)	6	6.83 (0.09; 13.57)	0.047	0.0%	0.531
Quartile 4 (378.15–505.6)	5	128.06 (72.37; 183.75)	0.001	96.8%	<0.001
NOS					
<7	10	42.26 (1.14; 83.38)	0.044	95.5%	<0.001
≥7	11	33.15 (7.45; 58.84)	0.011	97.6%	<0.001

DR, diabetic retinopathy; PDR, proliferative diabetic retinopathy; NPDR, non–proliferative diabetic retinopathy; NDR, non–diabetic retinopathy; BMI, body mass index; SD, standard deviation; NOS, Newcastle–Ottawa scale; HbA1c, glycated hemoglobin A1c; UA, Uric acid 1 mg/dL = 59.48 μmol/L; FBG, fasting blood glucose 1 mmol/L =18.0 mg/dL; LDL, low-density lipoprotein 1 mmol/L= 38.66 mg/dL.

proven to cause coagulation disorders in the microcirculation (55). Furthermore, previous studies have demonstrated that UA could activate the NLRP3/NALP3 inflammasome and increase the expression of inflammatory factors such as TNF-α, IL-6, and CRP (17, 56). Several meta-analyses have shown higher levels of these inflammatory factors in patients with DR than those without DR (18, 57, 58). These inflammatory mediators have been shown to induce vessel dilation, retinal edema, platelet aggregation, and other pathological changes at the onset of DR (59, 60). Moreover, UA-lowering therapy has been confirmed to significantly decrease retinal and plasma levels of inflammatory cytokines and adhesion factors in streptozotocin-induced diabetes in rats (61). The role of anti-vascular endothelial growth factor (anti-VEGF) agents in targeting inflammation treatment to slow down the progression of DR has recently been regarded as effective (62). In addition, patients with diabetes with decreased urine UA excretion have been reported to have an increased risk of DR (63).

Since obvious heterogeneity existed among the 21 studies, it was imperative to explore the sources of heterogeneity.

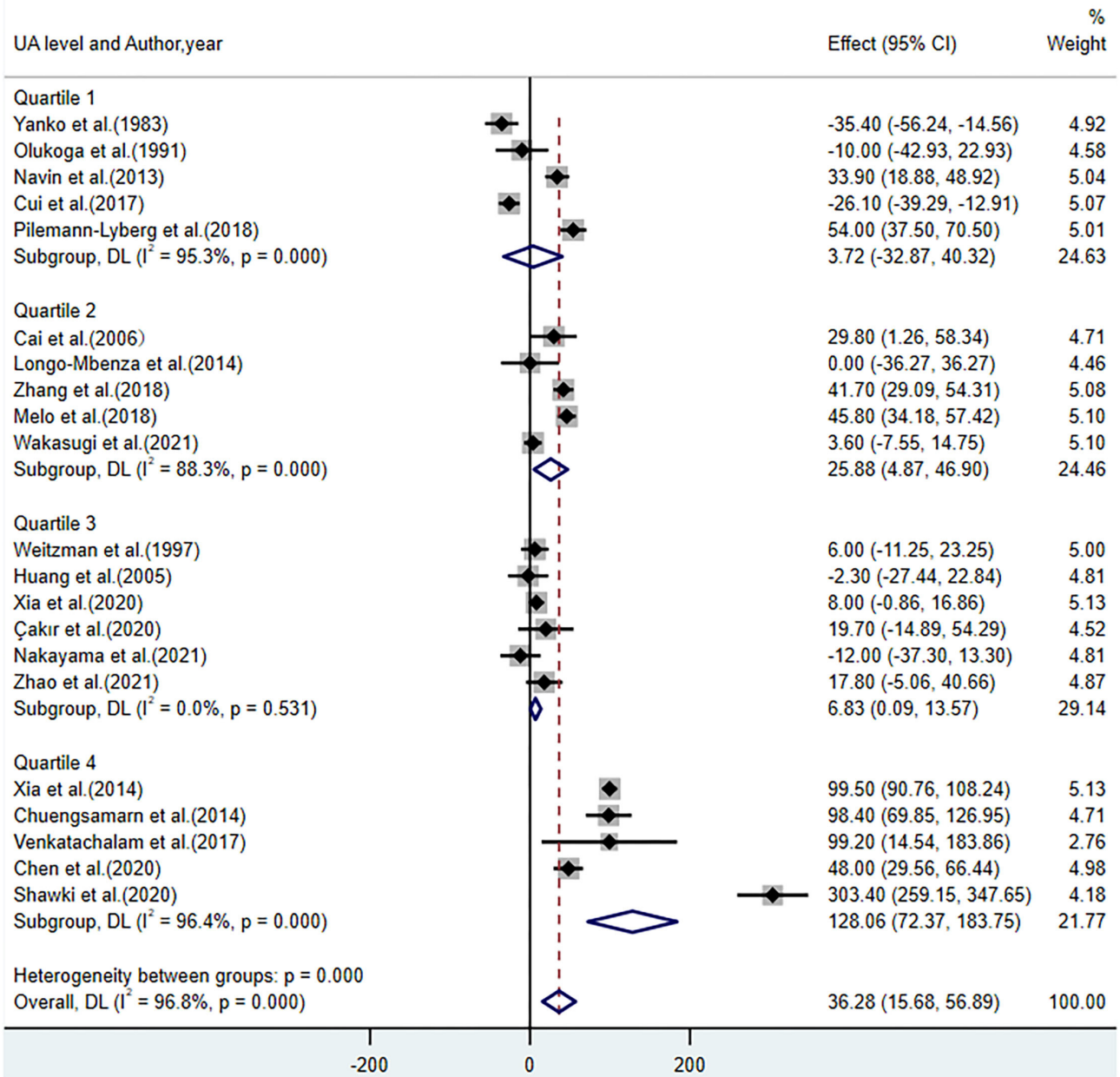

FIGURE 4 | Forest plot of the subgroup analysis on the concentrations of UA in patients with DR compared with controls with diabetes. UA, uric acid; DR, diabetic retinopathy; Quartile 1 (285.4–307.1); Quartile 2 (307.1–333); Quartile 3 (333–378.15); Quartile 4 (378.15–505.6), μmol/L.

In subgroup analyses, high heterogeneity still existed. When stratified by quality score, the results showed that the heterogeneity failed to decrease, and the pooled results for each subgroup were approached. Notably, in subgroup analyses based on participants' clinical characteristics, such as duration of diabetes, FBG, and HbA_{1c}, increased UA levels were observed in patients with DR with relatively poor health status. Further meta-regression analyses revealed that heterogeneity existed in the participants included in each study with different BMI and FBG levels. Considering the critical role of BMI and FBG levels in diabetes management (64, 65), it is rational to regard the severity of diabetes as the underlying source of heterogeneity. Possibly due to the differential therapies and health care services received by participants, diabetes severity was unevenly distributed across the included studies. For instance, unlike in developed regions, studies conducted in less-developed regions show higher UA levels (29, 41). Moreover, two sensitive studies (34, 41) were defined contributing more to the heterogeneity in sensitivity analysis.

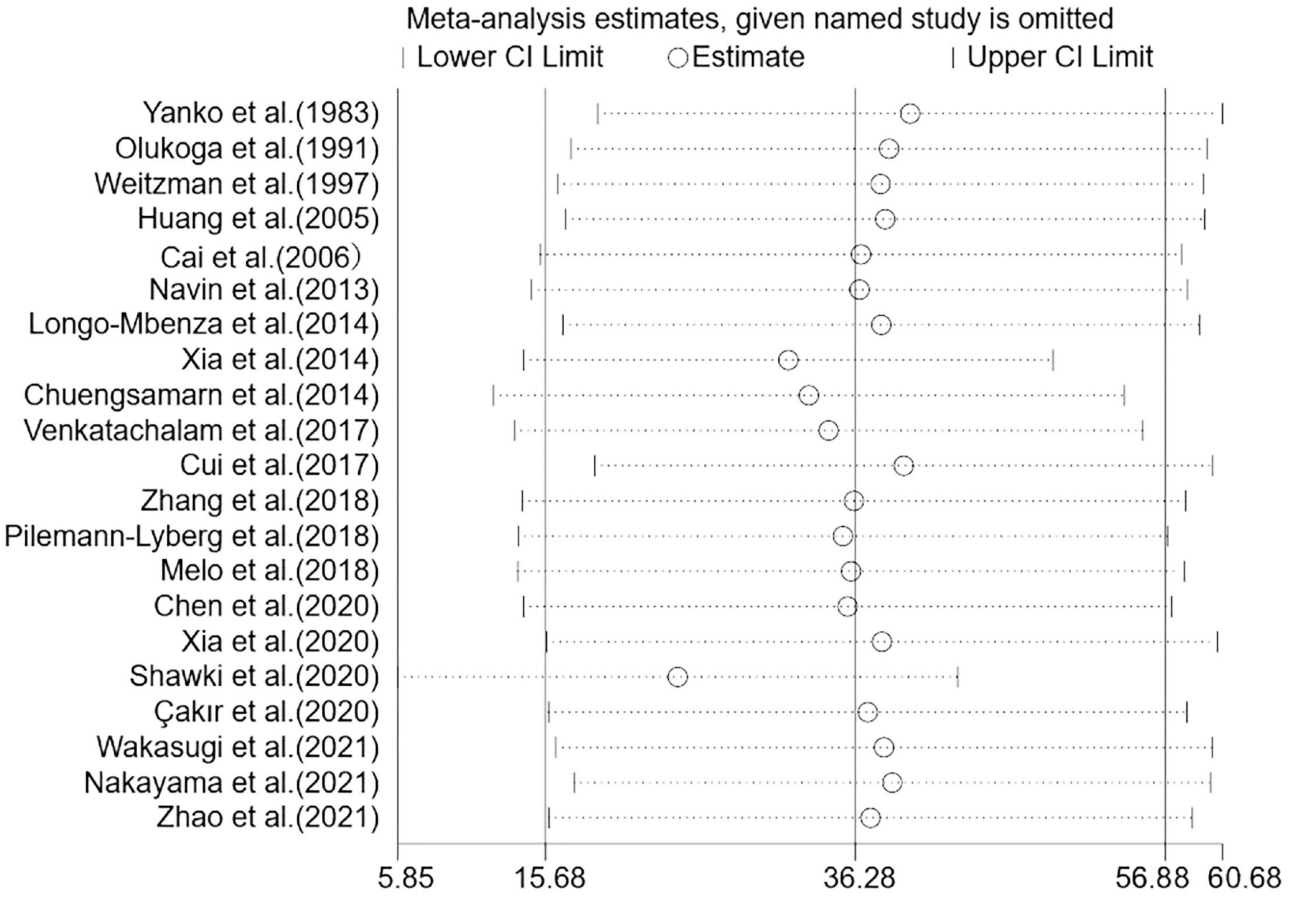

FIGURE 5 | Sensitivity analysis of the 21 studies. Sensitivity analysis was performed according to omit one study in each turn. CI, confidence interval.

Present meta-analysis had several limitations that may have affected the final conclusions. First, we failed to infer the causality of this association because of uncertainty about the temporal order. Evidence suggests that DR increases the risk of hyperuricemia in patients with diabetes (66). By summarizing the results of existing studies, we found that sex-related differences in this association remain unclear and deserve to be further elucidated. A previous cohort study reported an increased risk of newly developed DR in women [hazard ratio (HR): 2.17; 95% CI: 1.40, 3.37; $P < 0.001$] but not in men (HR: 1.08; 95% CI: 0.71, 1.66; $P = 0.998$) (19). However, Yanan Hu et al. investigated the association between UA and VTDR, showing that no sex-related difference was observed in the effect of UA on an increased risk of VTDR after adjustment (21). In addition, only a few studies have been conducted on patients with type 1 DM (20, 39, 67), which restricts the interpretation of results. Second, since the individual's continuous data, such as concentrations of UA, FBG, and BMI levels, were unavailable in each study, there were certain deviations for the subgroup analysis by transforming continuous variables into binary variables using the mean. Finally, the possibility of selection and unidentified confounding biases cannot be excluded. For example, the use of anti-hyperuricemic medications could be a potential confounder. A previous study showed that anti-hyperuricemic drugs are protective against retinal inflammation (61). However, most of the studies included in the meta-analysis did not control the use of anti-hyperuricemic medication; therefore, they possibly enrolled participants receiving UA-lowering therapy, which would limit the rigor of our results. In addition, similar to UA, homocysteine (Hcy) plays an important role in evoking oxidative stress (68), and Hcy levels are physiologically closely related to UA (69). Previous studies have also provided evidence that Hcy may also lead to endothelial injury in the retinal microvasculature at higher levels (70); this confounding factor needs to be recognized equally. Within these limitations, more prospective studies of high quality deserve launching to further confirm the association.

CONCLUSIONS

In conclusion, our study provides evidence that UA levels are higher in patients with DR than those in the controls, but this difference is not statistically significant in the early phases. UA might be a potential biomarker for identifying disease severity in patients with DR rather than predicting the onset of DR among

patients with diabetes. However, more prospective and high-quality clinical evidence is required to confirm these findings.

DATA AVAILABILITY STATEMENT

The original contributions presented in the study are included in the article/**Supplementary Material**, further inquiries can be directed to the corresponding author/s.

AUTHOR CONTRIBUTIONS

YCG and HLX contributed to the conception and design of this study. YCG and SYL performed the critical appraisal and data extraction. YCG was responsible for the subsequent analysis, interpretation of the data used in the systematic review, and meta-analysis. YCG drafted the manuscript. HLX and YCG revised it critically for important intellectual content. All authors have checked and approved this version to be submitted and finally published.

SUPPLEMENTARY MATERIAL

The Supplementary Material for this article can be found online at: https://www.frontiersin.org/articles/10.3389/fpubh.2022.906760/full#supplementary-material

REFERENCES

1. Saeedi P, Petersohn I, Salpea P, Malanda B, Karuranga S, Unwin N, et al. Global and regional diabetes prevalence estimates for 2019 and projections for 2030 and 2045: results from the international diabetes federation diabetes Atlas, 9(th) edition. *Diabetes Res Clin Pract.* (2019) 157:107843. doi: 10.1016/j.diabres.2019.107843
2. Cheung N, Mitchell P, Wong TY. Diabetic retinopathy. *Lancet.* (2010) 376:124–36. doi: 10.1016/S0140-6736(09)62124-3
3. Fong DS, Aiello L, Gardner TW, King GL, Blankenship G, Cavallerano JD, et al. Retinopathy in diabetes. *Diabetes Care.* (2004) 27(Suppl. 1):S84–7. doi: 10.2337/diacare.27.10.2540
4. Yau JW, Rogers SL, Kawasaki R, Lamoureux EL, Kowalski JW, Bek T, et al. Global prevalence and major risk factors of diabetic retinopathy. *Diabetes Care.* (2012) 35:556–64. doi: 10.2337/dc11-1909
5. Wang W, Lo ACY. Diabetic retinopathy: pathophysiology and treatments. *Int J Mol Sci.* (2018) 19:1816. doi: 10.3390/ijms19061816
6. Lechner J, O'Leary OE, Stitt AW. The pathology associated with diabetic retinopathy. *Vision Res.* (2017) 139:7–14. doi: 10.1016/j.visres.2017.04.003
7. Hernández C, Simó-Servat A, Bogdanov P, Simó R. Diabetic retinopathy: new therapeutic perspectives based on pathogenic mechanisms. *J Endocrinol Invest.* (2017) 40:925–35. doi: 10.1007/s40618-017-0648-4
8. Stitt AW. AGEs and diabetic retinopathy. *Invest Ophthalmol Visual Sci.* (2010) 51:4867–74. doi: 10.1167/iovs.10-5881
9. Kang Q, Yang C. Oxidative stress and diabetic retinopathy: molecular mechanisms, pathogenetic role and therapeutic implications. *Redox Biol.* (2020) 37:101799. doi: 10.1016/j.redox.2020.101799
10. Semeraro F, Cancarini A, dell'Omo R, Rezzola S, Romano MR, Costagliola C. Diabetic retinopathy: vascular and inflammatory disease. *J Diabetes Res.* (2015) 2015:582060. doi: 10.1155/2015/582060
11. Sheemar A, Soni D, Takkar B, Basu S, Venkatesh P. Inflammatory mediators in diabetic retinopathy: deriving clinicopathological correlations for potential targeted therapy. *Indian J Ophthalmol.* (2021) 69:3035–49. doi: 10.4103/ijo.IJO_1326_21
12. Forrester JV, Kuffova L, Delibegovic M. The role of inflammation in diabetic retinopathy. *Front Immunol.* (2020) 11:583687. doi: 10.3389/fimmu.2020.583687
13. Bardin T, Richette P. Definition of hyperuricemia and gouty conditions. *Curr Opin Rheumatol.* (2014) 26:186–91. doi: 10.1097/BOR.0000000000000028
14. Lv Q, Meng XF, He FF, Chen S, Su H, Xiong J, et al. High serum uric acid and increased risk of type 2 diabetes: a systemic review and meta-analysis of prospective cohort studies. *PLoS ONE.* (2013) 8:e56864. doi: 10.1371/journal.pone.0056864
15. Wang J, Yu Y, Li X, Li D, Xu C, Yuan J, et al. Serum uric acid levels and decreased estimated glomerular filtration rate in patients with type 2 diabetes: a cohort study and meta-analysis. *Diabetes Metabol Res Rev.* (2018) 34:e3046. doi: 10.1002/dmrr.3046
16. Yu S, Chen Y, Hou X, Xu D, Che K, Li C, et al. Serum uric acid levels and diabetic peripheral neuropathy in type 2 diabetes: a systematic review and meta-analysis. *Mol Neurobiol.* (2016) 53:1045–51. doi: 10.1007/s12035-014-9075-0
17. Lyngdoh T, Marques-Vidal P, Paccaud F, Preisig M, Waeber G, Bochud M, et al. Elevated serum uric acid is associated with high circulating inflammatory cytokines in the population-based Colaus study. *PLoS ONE.* (2011) 6:e19901. doi: 10.1371/journal.pone.0019901
18. Yao Y, Li R, Du J, Long L, Li X, Luo N. Interleukin-6 and diabetic retinopathy: a systematic review and meta-analysis. *Current Eye Res.* (2019) 44:564–74. doi: 10.1080/02713683.2019.1570274
19. Kuwata H, Okamura S, Hayashino Y, Tsujii S, Ishii H. Serum uric acid levels are associated with increased risk of newly developed diabetic retinopathy among Japanese male patients with type 2 diabetes: A prospective cohort study (diabetes distress and care registry at Tenri [DDCRT 13]). *Diabetes Metab Res Rev.* (2017) 33:e2905. doi: 10.1002/dmrr.2905
20. Melo LGN, Morales PH, Drummond KRG, Santos DC, Pizarro MH, Barros BSV, et al. Current epidemiology of diabetic retinopathy in patients with type 1 diabetes: a national multicenter study in Brazil. *BMC Public Health.* (2018) 18:989. doi: 10.1186/s12889-018-5859-x
21. Hu Y, Chan Z, Li C, Shi Y, She X, Gu C, et al. Higher serum uric acid levels are associated with an increased risk of vision-threatening diabetic retinopathy in type 2 diabetes patients. *Invest Ophthalmol Visual Sci.* (2021) 62:23. doi: 10.1167/iovs.62.4.23
22. Xia Q, Zhang SH, Yang SM, Zhu XL, Su S, Hu AP, et al. Serum uric acid is independently associated with diabetic nephropathy but not diabetic retinopathy in patients with type 2 diabetes mellitus. *JCMA.* (2020) 83:350–6. doi: 10.1097/JCMA.0000000000000285
23. Yanko L, Goldbourt U, Michaelson IC, Shapiro A, Yaari S. Prevalence and 15-year incidence of retinopathy and associated characteristics in middle-aged and elderly diabetic men. *Bri J Ophthalmol.* (1983) 67:759–65. doi: 10.1136/bjo.67.11.759
24. Segato T, Midena E, Grigoletto F, Zucchetto M, Fedele D, Piermarocchi S, et al. The epidemiology and prevalence of diabetic retinopathy in the Veneto region of north east Italy. Veneto Group for Diabetic Retinopathy. *Diabetic Med.* (1991) 8:S11–6. doi: 10.1111/j.1464-5491.1991.tb02149.x
25. Hu Y, Li Q, Min R, Deng Y, Xu Y, Gao L. The association between serum uric acid and diabetic complications in patients with type 2 diabetes mellitus by gender: a cross-sectional study. *PeerJ.* (2021) 9:e10691. doi: 10.7717/peerj.10691
26. Moher D, Liberati A, Tetzlaff J, Altman DG. Preferred reporting items for systematic reviews and meta-analyses: the PRISMA statement. *BMJ.* (2009) 339:b2535. doi: 10.1136/bmj.b2535
27. Stang A. Critical evaluation of the Newcastle-Ottawa scale for the assessment of the quality of nonrandomized studies in meta-analyses. *Eur J Epidemiol.* (2010) 25:603–5. doi: 10.1007/s10654-010-9491-z
28. Olukoga AO, Erasmus RT, Akinlade KS, Okesina AB, Alanamu AA, Abu EA. Plasma urate in diabetes: relationship to glycaemia, glucose disposal, microvascular complications and the variations following oral glucose. *Diabetes Res Clin Practice.* (1991) 14:99–105. doi: 10.1016/0168-8227(91)90115-T

29. Weitzman S, Maislos M, Bodner-Fishman B, Rosen S. Association of diabetic retinopathy, ischemic heart disease, and albuminuria with diabetic treatment in type 2 diabetic patients. A population-based study. *Acta Diabetol.* (1997) 34:275–9. doi: 10.1007/s005920050088
30. Huang EJ, Kuo WW, Chen YJ, Chen TH, Chang MH, Lu MC, et al. Homocysteine and other biochemical parameters in Type 2 diabetes mellitus with different diabetic duration or diabetic retinopathy. *Clin Chim Acta.* (2006) 366:293–8. doi: 10.1016/j.cca.2005.10.025
31. Cai XL, Wang F, Ji LN. Risk factors of diabetic retinopathy in type 2 diabetic patients. *Chin Med J.* (2006) 119:822–6. doi: 10.1097/00029330-200605020-00005
32. Navin S, Krishnamurthy N, Ashakiran S, Dayanand CD. The association of hypomagnesaemia, high normal uricaemia and dyslipidaemia in the patients with diabetic retinopathy [Article]. *J Clin Diagn Res.* (2013) 7:1852–4. doi: 10.7860/JCDR/2013/6106.3332
33. Longo-Mbenza B, Mvitu Muaka M, Masamba W, Muizila Kini L, Longo Phemba I, Kibokela Ndembe D, et al. Retinopathy in non diabetics, diabetic retinopathy and oxidative stress: a new phenotype in Central Africa? *Int J Ophthalmol.* (2014) 7:293–301. doi: 10.3980/j.issn.2222-3959.2014.02.18
34. Xia J, Wang Z, Zhang F. Association between related purine metabolites and diabetic retinopathy in type 2 diabetic patients. *Int J Endocrinol.* (2014) 2014:651050. doi: 10.1155/2014/651050
35. Chuengsamarn S, Rattanamongkolgul S, Jirawatnotai S. Association between serum uric acid level and microalbuminuria to chronic vascular complications in Thai patients with type 2 diabetes. *J Diabetes Compl.* (2014) 28:124–9. doi: 10.1016/j.jdiacomp.2013.12.002
36. Venkatachalam R, Krishnamoorthy RK, Kaliaperumal R, Anitha D, Anebaracy V, Buvana B, et al. Association of serum uric acid and lipid profile in type 2 diabetic patients with and without diabetic retinopathy [Article]. *Asian J Pharm Clin Res.* (2017) 10:112–4. doi: 10.22159/ajpcr.2017.v10i6.17029
37. Cui J, Ren JP, Chen DN, Xin Z, Yuan MX, Xu J, et al. Prevalence and associated factors of diabetic retinopathy in Beijing, China: a cross-sectional study. *BMJ Open.* (2017) 7:e015473. doi: 10.1136/bmjopen-2016-015473
38. Zhang D, Zhang W, Jin S, Wang W, Guo D, Wang L. Elevated serum total bilirubin concentrations are negatively associated with diabetic retinopathy among the chinese northeastern population. *Int J Endocrinol.* (2018) 2018:6539385. doi: 10.1155/2018/6539385
39. Pilemann-Lyberg S, Hansen TW, Persson F, Theilade S, Singh Ahluwalia T, Frystyk J, et al. Uric acid is not associated with diabetic nephropathy and other complications in type 1 diabetes. *Nephrol Dialysis Transpl.* (2019) 34:659–66. doi: 10.1093/ndt/gfy076
40. Chen D, Sun X, Zhao X, Liu Y. Associations of serum uric acid and urinary albumin with the severity of diabetic retinopathy in individuals with type 2 diabetes. *BMC Ophthalmol.* (2020) 20:467. doi: 10.1186/s12886-020-01713-5
41. Shawki HA, Elzehery R, Shahin M, Abo-Hashem EM, Youssef MM. Evaluation of some oxidative markers in diabetes and diabetic retinopathy. *Diabetol Int.* (2021) 12:108–17. doi: 10.1007/s13340-020-00450-w
42. Çakir I, Arifoglu HB, Günay NE, Pangal E, Sahin D, Sert GA, Duru N. Monocyte to high-density lipoprotein ratio: a novel inflammation marker related to diabetic retinopathy [Article]. *Erciyes Med J.* (2020) 42:190–4. doi: 10.14744/etd.2020.32549
43. Wakasugi S, Mita T, Katakami N, Okada Y, Yoshii H, Osonoi T, et al. Associations between continuous glucose monitoring-derived metrics and diabetic retinopathy and albuminuria in patients with type 2 diabetes. *BMJ Open Diabetes Res Care.* (2021) 9:e001923. doi: 10.1136/bmjdrc-2020-001923
44. Nakayama Y, Yamaguchi S, Shinzato Y, Okamoto S, Millman JF, Yamashiro K, et al. Retrospective exploratory analyses on gender differences in determinants for incidence and progression of diabetic retinopathy in Japanese patients with type 2 diabetes mellitus. *Endo J.* (2021) 68:655–69. doi: 10.1507/endocrj.EJ20-0630
45. Zhao X, Liu Y, Zhang W, Meng L, Lv B, Lv C, et al. Relationships between retinal vascular characteristics and renal function in patients with type 2 diabetes mellitus. *Transl Vision Sci Technol.* (2021) 10:20. doi: 10.1167/tvst.10.2.20
46. Chen B, Benedetti A. Quantifying heterogeneity in individual participant data meta-analysis with binary outcomes. *Syst Rev.* (2017) 6:243. doi: 10.1186/s13643-017-0630-4
47. Higgins JP, Thompson SG, Deeks JJ, Altman DG. Measuring inconsistency in meta-analyses. *BMJ.* (2003) 327:557–60. doi: 10.1136/bmj.327.7414.557
48. DerSimonian R, Laird N. Meta-analysis in clinical trials. *Control Clin Trials.* (1986) 7:177–88. doi: 10.1016/0197-2456(86)90046-2
49. Hayashino Y, Noguchi Y, Fukui T. Systematic evaluation and comparison of statistical tests for publication bias. *J Epidemiol.* (2005) 15:235–43. doi: 10.2188/jea.15.235
50. Begg CB, Mazumdar M. Operating characteristics of a rank correlation test for publication bias. *Biometrics.* (1994) 50:1088–101. doi: 10.2307/2533446
51. Lee JJ, Yang IH, Kuo HK, Chung MS, Chen YJ, Chen CH, et al. Serum uric acid concentration is associated with worsening in severity of diabetic retinopathy among type 2 diabetic patients in Taiwan–a 3-year prospective study. *Diabetes Res Clin Practice.* (2014) 106:366–72. doi: 10.1016/j.diabres.2014.07.027
52. Hou L, Shi Y, Wang S, Chen Q, Li Q, Zhao M, et al. Associations of serum uric acid level with diabetic retinopathy and albuminuria in patients with type 2 diabetes mellitus. *J Int Med Res.* (2020) 48:300060520963980. doi: 10.1177/0300060520963980
53. Xiong Q, Liu J, Xu Y. Effects of uric acid on diabetes mellitus and its chronic complications. *Int J Endocrinol.* (2019) 2019:9691345. doi: 10.1155/2019/9691345
54. Zhu DD, Wang YZ, Zou C, She XP, Zheng Z. The role of uric acid in the pathogenesis of diabetic retinopathy based on Notch pathway. *Biochem Biophys Res Commun.* (2018) 503:921–9. doi: 10.1016/j.bbrc.2018.06.097
55. Mazzali M, Hughes J, Kim YG, Jefferson JA, Kang DH, Gordon KL, et al. Elevated uric acid increases blood pressure in the rat by a novel crystal-independent mechanism. *Hypertension.* (2001) 38:1101–6. doi: 10.1161/hy1101.092839
56. Martinon F, Pétrilli V, Mayor A, Tardivel A, Tschopp J. Gout-associated uric acid crystals activate the NALP3 inflammasome. *Nature.* (2006) 440:237–41. doi: 10.1038/nature04516
57. Song J, Chen S, Liu X, Duan H, Kong J, Li Z. Relationship between C-reactive protein level and diabetic retinopathy: a systematic review and meta-analysis. *PLoS ONE.* (2015) 10:e0144406. doi: 10.1371/journal.pone.0144406
58. Yao Y, Li R, Du J, Li X, Zhao L, Long L, et al. Tumor necrosis factor-α and diabetic retinopathy: review and meta-analysis. *Clin Chim Acta.* (2018) 485:210–7. doi: 10.1016/j.cca.2018.06.028
59. Kinuthia UM, Wolf A, Langmann T. Microglia and inflammatory responses in diabetic retinopathy. *Front Immunol.* (2020) 11:564077. doi: 10.3389/fimmu.2020.564077
60. Mugisho OO, Rupenthal ID, Squirrell DM, Bould SJ, Danesh-Meyer HV, Zhang J, et al. Intravitreal pro-inflammatory cytokines in non-obese diabetic mice: modelling signs of diabetic retinopathy. *PLoS ONE.* (2018) 13:e0202156. doi: 10.1371/journal.pone.0202156
61. Thounaojam MC, Montemari A, Powell FL, Malla P, Gutsaeva DR, Bachettoni A, et al. Monosodium urate contributes to retinal inflammation and progression of diabetic retinopathy. *Diabetes.* (2019) 68:1014–25. doi: 10.2337/db18-0912
62. Carroll RM, Bracha P, Miller CG, Brucker AJ. Management of diabetic retinopathy in the anti-vascular endothelial growth factor era. *Retina.* (2021) 41:461–3. doi: 10.1097/IAE.0000000000003071
63. Li LX, Lu JX, Shuai HP, Xia HF, Zhang R, Wang JW, et al. Decreased urine uric acid excretion is associated with diabetic retinopathy but not with lower limb atherosclerosis in hospitalized patients with type 2 diabetes. *Atherosclerosis.* (2015) 242:13–8. doi: 10.1016/j.atherosclerosis.2015.06.051
64. Campbell L, Rössner S. Management of obesity in patients with type 2 diabetes. *Diabetic Med.* (2001) 18:345–54. doi: 10.1046/j.1464-5491.2001.00546.x
65. Stumvoll M, Goldstein BJ, van Haeften TW. Type 2 diabetes: principles of pathogenesis and therapy. *Lancet.* (2005) 365:1333–46. doi: 10.1016/S0140-6736(05)61032-X
66. Choukem SP, Mengue JA, Doualla MS, Donfack OT, Beyiha G, Luma HN. Hyperuricaemia in patients with type 2 diabetes in a tertiary healthcare centre in sub-Saharan Africa: prevalence and determinants. *Trop Doctor.* (2016) 46:216–21. doi: 10.1177/0049475515626030
67. Bjornstad P, Maahs DM, Rivard CJ, Pyle L, Rewers M, Johnson RJ, et al. Serum uric acid predicts vascular complications in adults with type 1 diabetes: the coronary artery calcification in type 1 diabetes study. *Acta Diabetol.* (2014) 51:783–91. doi: 10.1007/s00592-014-0611-1

68. Perna AF, Ingrosso D, De Santo NG. Homocysteine and oxidative stress. *Amino Acids.* (2003) 25:409–17. doi: 10.1007/s00726-003-0026-8
69. Shi Y, Wu Z, Wu J, Chen Z, Li P. Serum homocysteine level is positively correlated with serum uric acid level in U.S. Adolescents: a cross sectional study. *Front Nutr.* (2022) 9:818836. doi: 10.3389/fnut.2022.818836
70. Omae T, Nagaoka T, Tanano I, Yoshida A. Homocysteine inhibition of endothelium-dependent nitric oxide-mediated dilation of porcine retinal arterioles via enhanced superoxide production. *Invest Ophthalmol Visual Sci.* (2013) 54:2288–95. doi: 10.1167/iovs.12-11082

Conflict of Interest: The authors declare that the research was conducted in the absence of any commercial or financial relationships that could be construed as a potential conflict of interest.

Publisher's Note: All claims expressed in this article are solely those of the authors and do not necessarily represent those of their affiliated organizations, or those of the publisher, the editors and the reviewers. Any product that may be evaluated in this article, or claim that may be made by its manufacturer, is not guaranteed or endorsed by the publisher.

frontiers | Frontiers in Endocrinology

ORIGINAL RESEARCH
published: 01 June 2022
doi: 10.3389/fendo.2022.831909

Correlation Between Retinal Microstructure Detected by Optical Coherence Tomography and Best Corrected Visual Acuity in Diabetic Retinopathy Macular Edema

Siying Li[1], *Rui Hua*[2], *Zuoqian Jing*[2], *Lele Huang*[2] *and Lei Chen*[2]*

[1] Department of Ophthalmology, The First Affiliated Hospital of Jiamusi University, Jiamusi, China,
[2] Department of Ophthalmology, The First Affiliated Hospital of China Medical University, Shenyang, China

Objective: This study aimed to investigate the correlation between best corrected visual acuity (BCVA) and retinal microstructural parameters detected by optical coherence tomography (OCT) in diabetic retinopathy macular edema (DRME).

Methods: Thirty-nine patients (64 eyes) with DRME were enrolled in this study. These patients underwent OCT to measure the fracture distance of the external limiting membrane (ELM), junction between the inner and outer segments (IS/OS), central foveal thickness (CFT), and edema layer. The correlation between the above parameters and BCVA was discussed.

Results: CFT and the fracture distances of the ELM and IS/OS layers were negatively correlated with BCVA ($p<0.05$ for all). There was significant difference in Logarithm of the minimum angle of resolution (LogMAR) BCVA among patients with inner retinal edema, outer retinal edema, and mixed retinal edema ($F = 5.57$, $p = 0.01$). The LogMAR BCVA of inner retinal edema was the lowest ($p < 0.05$), and the LogMAR BCVA of outer retinal edema and mixed retinal edema were comparable ($p > 0.05$).

Conclusion: In eyes with DRME, thin CFT, intact ELM and IS/OS layers, and edema in inner retina is closely correlated with good BCVA.

Keywords: optical coherence tomography, photoreceptor layer, external limiting, central foveal thickness, diabetic retinopathy macular edema

OPEN ACCESS

Edited by:
Subrata Chakrabarti,
Western University, Canada

Reviewed by:
Prasanth Puthanveetil,
Midwestern University, United States
Eric Zirui Wang,
Western University, Canada

***Correspondence:**
Lei Chen
leichen_lc@163.com

Specialty section:
This article was submitted to Clinical Diabetes, a section of the journal Frontiers in Endocrinology

Received: *09 December 2021*
Accepted: *14 March 2022*
Published: *01 June 2022*

Citation:
Li S, Hua R, Jing Z, Huang L and Chen L (2022) Correlation Between Retinal Microstructure Detected by Optical Coherence Tomography and Best Corrected Visual Acuity in Diabetic Retinopathy Macular Edema. Front. Endocrinol. 13:831909. doi: 10.3389/fendo.2022.831909

1 INTRODUCTION

As a serious complication of diabetes, diabetic retinopathy macular edema (DRME) is a common eye disease that causes blindness and the main cause of vision loss in diabetic retinopathy (DR) (1). DR can destroy the blood-retina barrier, and the intravascular components such as proteins, lipids and inflammatory factors leak out the barrier, changing osmotic pressure and protein gradient (2). Metabolism of cell is thus affected, resulting in cellular edema or shrinking, ion disorder, membrane depolarization. These pathologic conditions lead to changes of microenvironment of the retina,

resulting in disruption of the retina especially the outer retina (3, 4). Clinical examination of DRME mainly depends on ophthalmoscopy, fundus fluorescein angiography, a slit lamp, and optical coherence tomography (OCT). Compared with other inspection methods, OCT can be used not only for tomography and interlayer positioning, but also for quantitative measurement; therefore, it is widely used in the clinical examination of retinal diseases such as branch retinal vein occlusion, chorioretinitis, and retinal detachment. This study was designed to inspect the retinal microstructure in DRME with OCT and analyze the correlation between retinal microstructure and best corrected visual acuity (BCVA) to demonstrate the pathological characteristics and provide a reference for treatment of DRME.

2 SUBJECTS AND METHODS

2.1 Subjects

Between September 2017 and March 2019, 39 patients (64 eyes) were diagnosed with DRME in our hospital and enrolled in this study. The average age of these patients was 58.6 ± 13.5 years. These patients included 19 males (48.72%) and 20 females (51.28%). Two patients had type I diabetes mellitus (5.13%), and 37 patients had type II diabetes mellitus (94.87%). The diseased eyes included 33 right eyes (51.56%) and 31 left eyes (48.44%). The course of disease was 11.4 ± 6.3 years. Inclusion criteria: (1) DRME was diagnosed according to the Early Treatment of Diabetic Retinopathy Study (ETDRS) evaluation criteria (5); and (2) in OCT images, the central foveal thickness (CFT) was ≥250 μm, and the junction between inner and outer segments (IS/OS) was involved. Exclusion criteria: (1) history of intraocular surgery; (2) refractive stromal opacity such as keratoleukoma and grade V sclerotic nuclei cataract; (3) macular edema associated with epimacular membrane, vitreoretinal proliferation, uveitis, and posterior vitreous detachment; (4) history of undergoing retinal laser photocoagulation, peribulbar vitreous cavity surgery, or injection of hormone drugs within 2 years.

2.2 Methods

2.2.1 Treatment

Two doctors with more than 3 years' experience in ophthalmic examination performed OCT and recorded the BCVA in 39 patients. The Heidelberg SPECTRALIS optical coherence tomoscanner (Spectarlis HRA + OCT; Heidelberg Engeneering, Heidelberg, Germany) with image resolution of more than 16 dB was used. The diseased macular area was scanned in four directions (0°, 45°, 90°, and 135°), with the fovea as the center and 1 mm as the radius. The distance of the accumulated fracture zone of the ELM layer and IS/OS layer was measured on the scanogram, and the mean was calculated. The CFT of each eye was measured and classified as follows: inner retinal edema, the inner five layers of the retina were affected; outer retinal edema, the outer five layers of the retina were affected; and mixed retinal edema, the inner and outer layers of the retina were affected. BCVA was obtained by optometry.

2.3 Statistical Analysis

The data analysis was conducted using SPSS 19.0. Measurement data, such as LogMAR BCVA and CFT, were evaluated using one-way analysis of variance (ANOVA). The correlation between data, such as the correlation between CFT and LogMAR BCVA, was evaluated using Pearson correlation. $P < 0.05$ was considered statistically significant.

3 RESULTS

3.1 Correlation Between CFT and BCVA

In 39 patients (64 eyes), LogMAR BCVA was 0.66 ± 0.37 and CFT was 430.48 ± 135.01 μm; therefore, CFT was positively correlated with LogMAR BCVA ($r = 0.58$, $p < 0.001$, **Figure 1**).

3.2 Correlation Between Fracture Distance of ELM Layer and BCVA

In 39 patients (64 eyes), the fracture distance of the ELM layer was 746.19 ± 631.01 μm, which was positively correlated with LogMAR BCVA ($r = 0.79$, $p < 0.001$, **Figure 2**).

3.3 Correlation Between Fracture Distance of IS/OS Layer and BCVA

In 39 patients (64 eyes), the fracture distance of the IS/OS layer was 997.00 ± 627.01 μm, which was positively correlated with LogMAR BCVA ($r = 0.85$, $p < 0.001$, **Figure 3**).

3.4 Correlation Between Edema Layer and BCVA

There was inner, outer, and mixed retinal edema in 18, 29, and 17 eyes, respectively, and the difference in LogMAR BCVA was

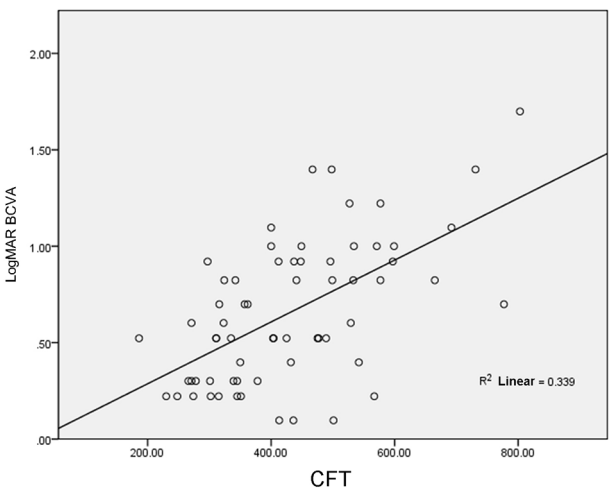

FIGURE 1 | Correlation between CFT and LogMAR BCVA.

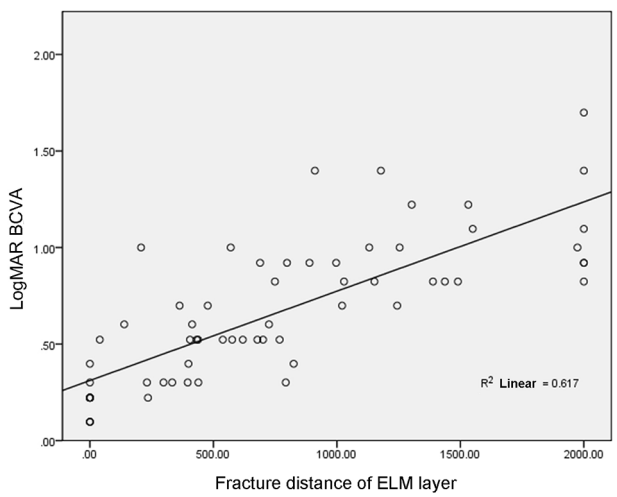

FIGURE 2 | Correlation between fracture distance of ELM layer and LogMAR BCVA.

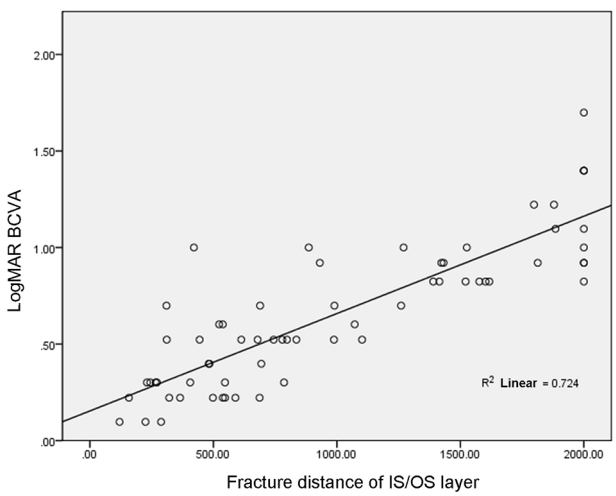

FIGURE 3 | Correlation between fracture distance of IS/OS layer and LogMAR BCVA.

statistically significant ([0.43 ± 0.24] vs. [0.72 ± 0.35] vs. [0.79 ± 0.43], F = 5.57, p = 0.01). The LogMAR BCVA of inner retinal edema was smaller than that of outer retinal edema ($p < 0.05$), the LogMAR BCVA of inner retinal edema was smaller than that of mixed retinal edema ($p < 0.05$), and there was no significant difference in LogMAR BCVA between outer retinal edema and mixed retinal edema ($p > 0.05$, **Figures 4–9**).

4 DISCUSSION

In related studies, in OCT examination, the correlation between CFT and LogMAR BCVA was different in DRME. For example, studies have revealed that there was a positive correlation between the two, and r values ranged from 0.39 to 0.79 (6–9). A study also revealed that CFT was negatively correlated with

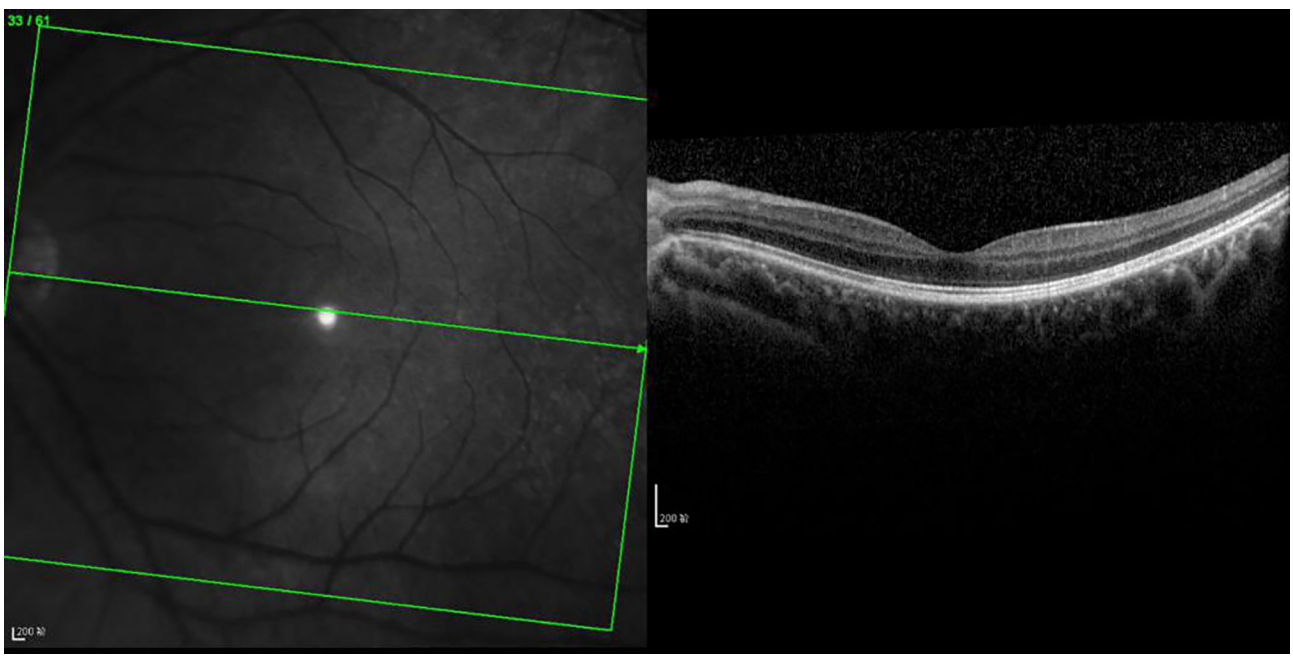

FIGURE 4 | OCT scanning of the ocular fundus in an individual without DRME. There is no edema in the macular area, the CFT value is 231 μm, and the ELM layer and IS/OS layer are continuous.

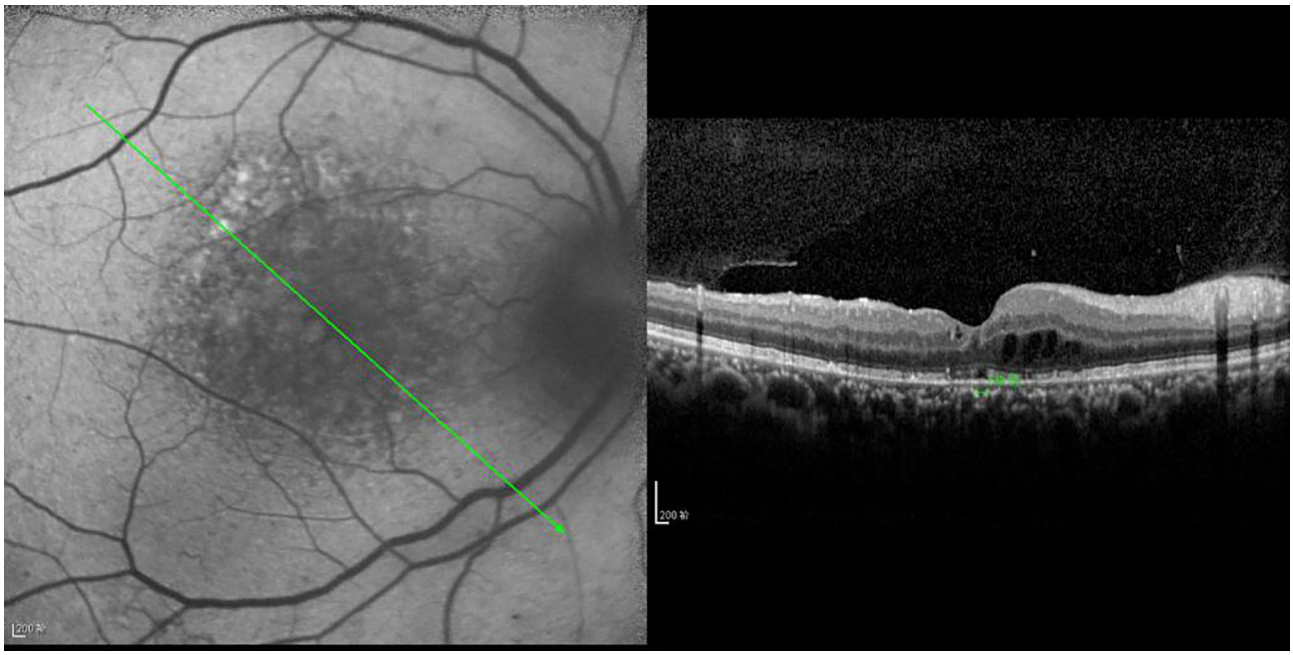

FIGURE 5 | OCT scanning of the ocular fundus in patients with DRME. The CFT value is 397 μm, the ELM layer is continuous, the fracture distance of the IS/OS layer is 139 μm, and there is outer retinal edema.

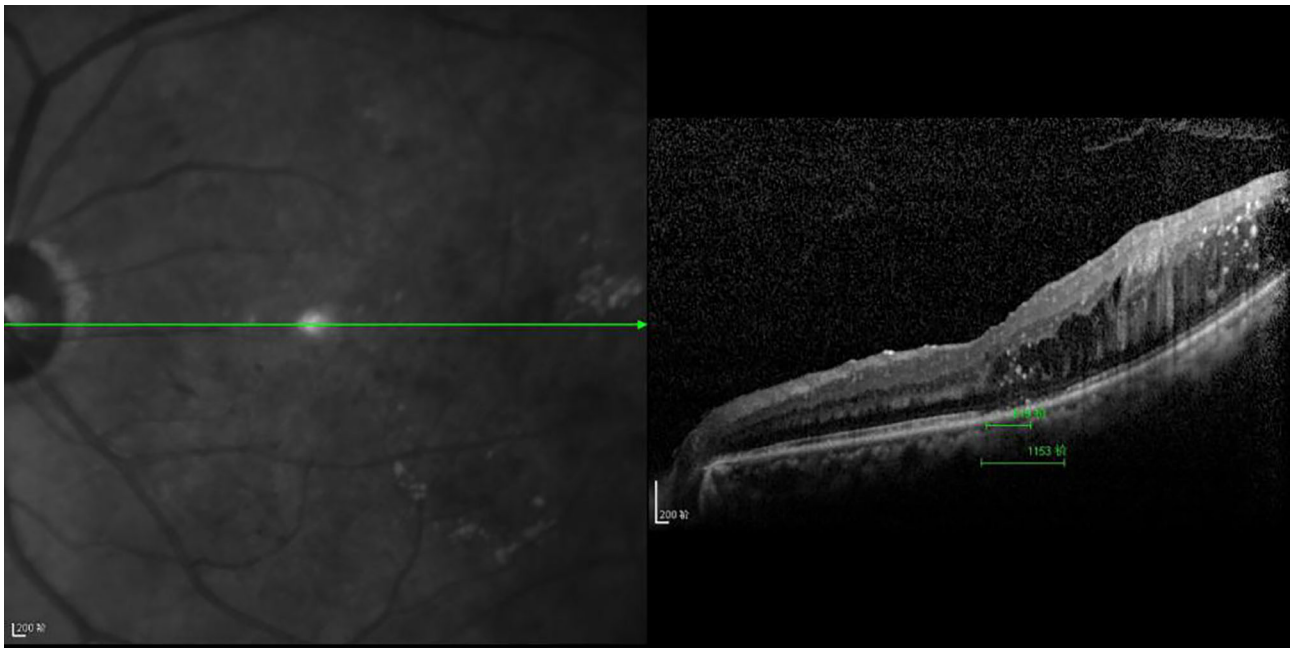

FIGURE 6 | The CFT value is 519 μm, the ELM layer is continuous, the fracture distance of the IS/OS layer is 1,153 μm, and there is outer retinal edema.

LogMAR BCVA in DRME (r = −0.23) (10). This study revealed that there was a negative correlation between CFT and BCVA, and the higher the CFT, the lower the BCVA is. CFT and LogMAR BCVA were used as baseline values and compared. It was found that BCVA increased with an increase in CFT in 17% of the eyes and decreased with a decrease in CFT in 16% of the eyes. However, this contradicts the overall results, and the reason may be that there were different degrees of ELM layer and/or IS/

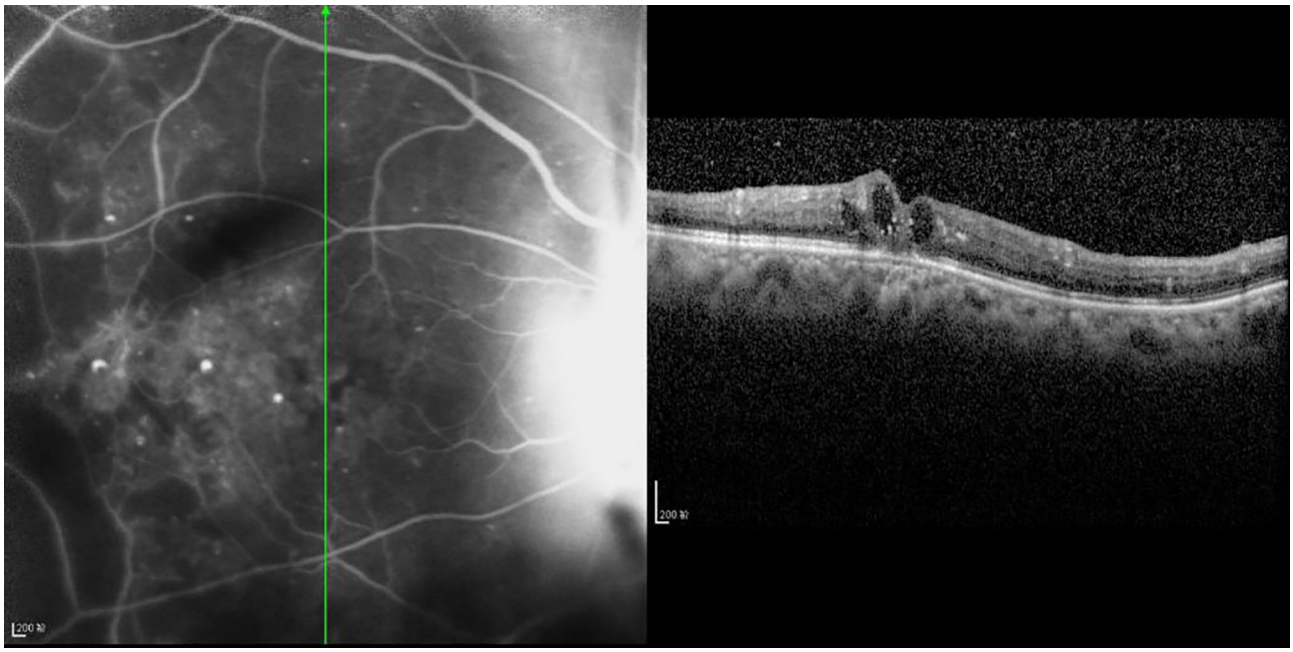

FIGURE 7 | The CFT value is 437 μm, the fracture distance of the ELM layer is 897 μm, the fracture distance of the IS/OS layer is 977 μm, and there is mixed retinal edema.

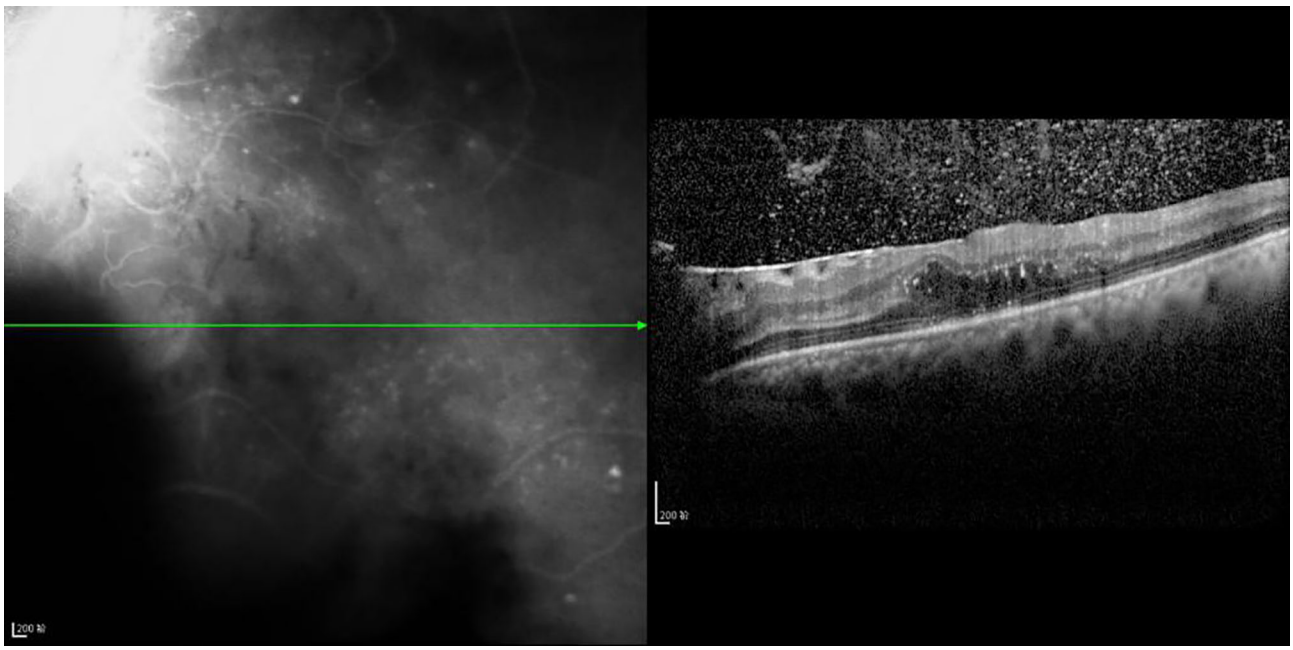

FIGURE 8 | The CFT value is 536 μm, the fracture distance of the ELM layer is 1,189 μm, the fracture distance of the IS/OS layer is >2,000 μm, and there is outer retinal edema.

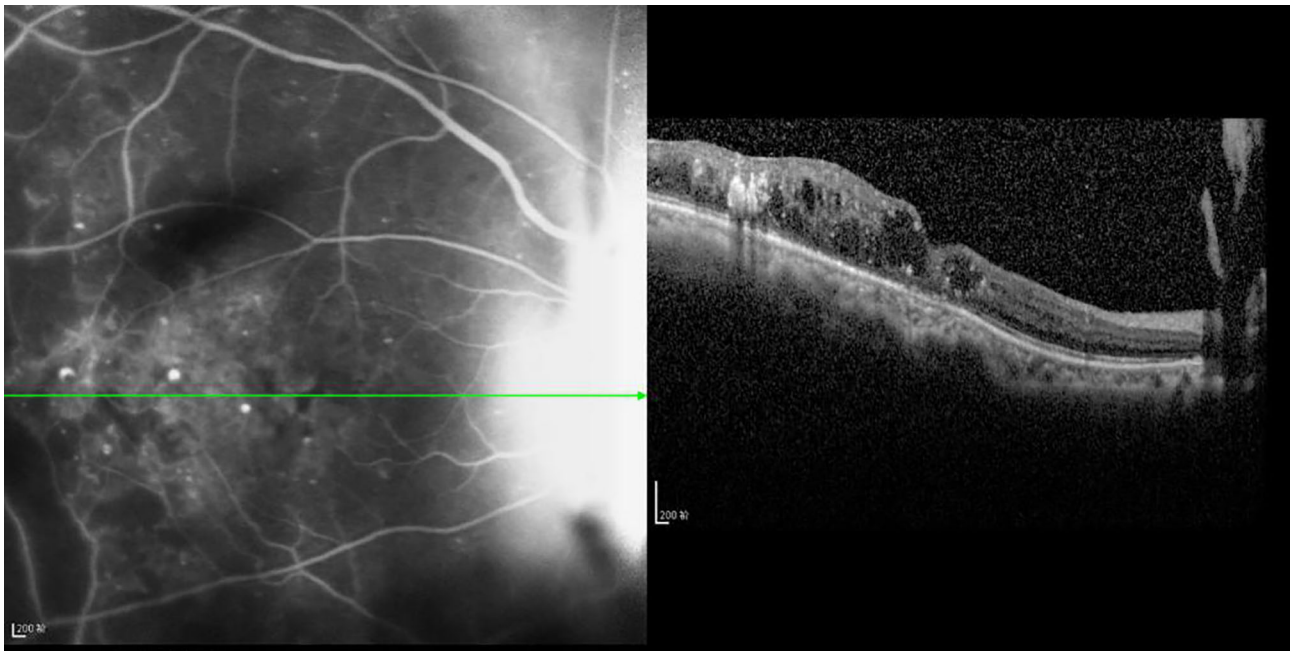

FIGURE 9 | The CFT value is 352 μm, the fracture distance of the ELM and IS/OS layers is >2,000 μm, and there is mixed retinal edema. R^2 Linear.

OS layer fracture in the eyes of the patients included in this study, which affected BCVA. Shen et al. (11) reached a similar conclusion, namely the severity of macular edema did not match BCVA; however, the integrity of photoreceptors plays a very important role in the limited vision in DRME.

In addition, this study revealed that the fracture distance of both the ELM layer and the IS/OS layer was statistically and negatively correlated with BCVA; this result is consistent with those reported in the related literature (12–14). However, most of the literature reflects the relationship between the integrity of the ELM layer and/or IS/OS layer with BCVA by classifying variables. For example, the continuity of the ELM layer and/or IS/OS layer was artificially divided into two groups (positive and negative) or three fractured groups, and then the difference in BCVA among different groups was compared. In this study, quantitative processing of the ELM layer and IS/OS layer was carried out to calculate the fracture distance in four directions, making the results of the ELM layer and IS/OS layer more reliable. The results of the present study revealed that the fracture distance of the ELM layer (746.19 μm) was shorter than that of the IS/OS layer (997.00 μm), which can provide a reference for the quantitative relationship between ELM layer fracture and the IS/OS layer. Regarding the correlation between the ELM layer and the IS/OS layer and visual acuity, Maheshwary et al. highlight that whether the IS/OS layer is damaged is a risk factor for BCVA (12). The present study supports the conclusion of the literature in that compared with the ELM layer, the IS/OS layer can affect visual acuity, namely compared with BCVA, the damage or fracture degree of the IS/OS layer has a stronger correlation with BCVA ($r = 0.851 > r = 0.786$).

The ELM of photoreceptor cells connecting Muller cells has a barrier function (15). Therefore, when Muller cells and glial cells become diseased, such as through degeneration or edema, the barrier function of the ELM layer is destroyed, causing large molecules, such as inflammatory cells in the blood, to be transferred to the outer retina through the damaged ELM layer, changing the protein concentration. Consequently, the osmotic pressure balance of the outer retina is damaged, the photoreceptor cells are destroyed, and the function of nerve signal transduction is reduced (14). The inner segment of the retinal photoreceptor is rich in mitochondria, and its damage and loss are considered to be a sign of decreased photoreceptor function, which is also associated with a decrease in BCVA (16). The ELM is a complex consisting of extended myoid photoreceptor cells and the foot plate of Muller cells, which is involved in the maturation and polarization of photoreceptor cells (17). A study highlights that the incompleteness of the IS/OS layer structure is closely related to the imperfection of the ELM layer (11), and ELM integrity recovery is earlier than IS/OS layer (18). Therefore, in patients with DRME, after treatment, the recovery of ELM is regarded as the key to BCVA recovery.

In OCT, when it scans the abnormal cells in the retinal pigment epithelial (RPE) layer, it indicates that macrophages in the RPE layer are activated or subjected to metaplasia or phagocytosis. The damaged RPE layer can indirectly reduce the activity or function of photoreceptor cells (19), which proves that the IS/OS layer is closely related to BCVA. A previous study revealed that compared with the other types, the damage to the integrity of ELM and IS/OS was mostly presented as cystic edema. Therefore, the visual acuity of patients with cystoid

macular edema is often weaker than that of healthy people of the same age, as cystic edema can affect glial components and destroy photoreceptor cells, which when severe, may cause blindness (14). According to the different pathological types of leakage, macular edema occurs in both the inner nuclear layer and the outer plexiform layer; therefore, the edema layer can be divided into three types: inner nuclear layer, outer plexiform layer, and mixed type. However, the three types of edema also have their own characteristics. For example, the BCVA of mixed and outer retinal edema is lower than that of inner layer edema. Previous studies have shown that blood components and wastes in the vesicles-like space may affect cell metabolism and cause changes in osmotic pressure, resulting in stretched axons and disfunction of bipolar cells with decreased photosensitivity and signal transduction (19). Similarly, photoreceptor cells are stressed and a similar cascade of changes occurs, leading to a decline in photographic function. In other studies, the vesicles with high density are mostly located in outer retinal edema since the component of the high density point is lipoprotein. Lipoproteins penetrate into the ELM layer, and the lipoproteins passing through the ELM layer can also destroy the IS/OS layer to directly induce photoreceptor degeneration (5). In DRME, there are inflammatory factors that lead to the destruction of the outer barrier, and then the edema of the outer retina is aggravated, and photoreceptor cells are damaged. In addition, the outer retinal edema is anatomically close to the IS/OS layer and ELM layer; therefore, edema can increase intracapsular pressure physically and further aggravate inner retinal edema. These factors reduce the BCVA visual acuity of outer retinal edema. Unlike outer and inner retinal edema, due to the presence of both inner and outer retinal edema, mixed retinal edema further enhances the edema effect and further reduces BCVA.

There are some limitations in this study, however; for example, the sample size was small, BCVA was not measured based on ETDRS, and it was difficult to exclude the influence of other factors on BCVA or retinal dysfunction. Therefore, it is still necessary to assess whether the retinal function is abnormal with the help of an electroretinogram. This study performed OCT scans of the macular area in four directions of 0, 45, 90, and 135 degrees in 64 eyes, and did not perform more refined scans, such as 8- or 16-equivalent scans. And the study area was only 1 mm as the radius and fovea as the center, and no larger area study was done. In addition, imaging with OCT scans in DME may have an impact on the imaging of the outer microstructure when there is hard exudate or hemorrhagic occlusion in the retina, leading to measurement errors.

In summary, according to OCT examination, the CFT is small, the ELM layer and IS/OS layer are relatively integral, and BCVA is closely correlated with inner retinal edema in DRME.

DATA AVAILABILITY STATEMENT

The original contributions presented in the study are included in the article/supplementary material. Further inquiries can be directed to the corresponding author.

ETHICS STATEMENT

The studies involving human participants were reviewed and approved by the ethics committee of The First Affiliated Hospital of China Medical University. The patients/participants provided their written informed consent to participate in this study.

AUTHOR CONTRIBUTIONS

SL and LC conceived the idea and conceptualized the study. RH collected the data. ZJ and LH analyzed the data. SL and LC drafted the manuscript. SL and LC reviewed the manuscript. All authors read and approved the final draft.

FUNDING

Project name: Basic Research Project of Heilongjiang Provincial Education Department. No. 2019-KYYWF1354.

REFERENCES

1. Bolinger MT, Antonetti DA. Moving Past Anti-VEGF: Novel Therapies for Treating Diabetic Retinopathy. *Int J Mol Sci* (2016) 17(9):1498. doi: 10.3390/ijms17091498
2. Das R, Spence G, Hogg RE, Stevenson M, Chakravarthy U. Disorganization of Inner Retina and Outer Retinal Morphology in Diabetic Macular Edema. *JAMA Ophthalmol* (2018) 136(2):202–8. doi: 10.1001/jamaophthalmol.2017.6256
3. Bizheva K, Pflug R, Hermann B, Povazay B, Sattman H, Qiu P, et al. Optophysiology: Depthresolved Probing of Retinal Physiology With Functional Ultrahighresolution Optical Coherence Tomography. *Proc Natl Acad Sci USA* (2006) 103(13):5066–71. doi: 10.1073/pnas.0506997103
4. Srinivasan VJ, Wojtkowski M, Fujimoto JG, Durker JS. *In Vivo* Measurement of Retinal Physiology With High-Speed Ultrahigh-Resolution Optical Coherence Tomography. *Opt Lett* (2006) 31(15):2308–10. doi: 10.1364/OL.31.002308
5. Relhan N, Flynn HWJr. The Early Treatment Diabetic Retinopathy Study Historical Review and Relevance to Today's Management of Diabetic Macular Edema. *Curr Opin Ophthalmol* (2017) 28(3):205–12. doi: 10.1097/ICU.0000000000000362
6. Campochiaro PA, Marcus DM, Awh CC, Regillo C, Adamis AP, Bantseev V, et al. The Port Delivery System With Ranibizumab for Neovascular Age-Related Macular Degeneration: Results From the Randomized Phase 2 Ladder Clinical Trial. *Ophthalmology* (2019) 126(8):1141–54. doi: 10.1016/j.ophtha.2019.03.036
7. Boyer DS, Nguyen QD, Brown DM, Basu K, Ehrlich JSRIDE and RISE Research Group. Outcomes With As-Needed Ranibizumab After Initial Monthly Therapy: Long-Term Outcomes of the Phase III RIDE and RISE Trials. *Ophthalmology* (2015) 122(12):2504–13.e1. doi: 10.1016/j.ophtha.2015.08.006
8. Catier A, Tadayoni R, Paques M, Erginay A, Haouchine B, Gaudric A, et al. Characterization of Macular Edema From Various Etiologies by Optical

Coherence Tomography. *Am J Ophthalmol* (2005) 140(2):200–6. doi: 10.1016/j.ajo.2005.02.053
9. Goebel W, Kretzchmar-Gross T. Retinal Thickness in Diabetic Retinopathy: A Study Using Optical Coherence Tomography (OCT). *Retina* (2002) 22 (6):759–67. doi: 10.1097/00006982-200212000-00012
10. Otani T, Yamaguchi Y, Kishi S. Correlation Between Visual Acuity and Foveal Microstructural Changes in Diabetic Macular Edema. *Retina* (2010) 30 (5):774–80. doi: 10.1097/IAE.0b013e3181c2e0d6
11. Shen Y, Liu K, Xu X. Correlation Between Visual Function and Photoreceptor Integrity in Diabetic Macular Edema: Spectral-Domain Optical Coherence Tomography. *Curr Eye Res* (2016) 41(3):391–9. doi: 10.3109/02713683.2015.1019003
12. Maheshwary AS, Oster SF, Yuson RM, Cheng L, Mojana F, Freeman WR. The Association Between Percent Disruption of the Photoreceptor Inner Segment-Outer Segment Junction and Visual Acuity in Diabetic Macular Edema. *Am J Ophthalmol* (2010) 150(1):63–67.e1. doi: 10.1016/j.ajo.2010.01.039
13. Murakami T, Nishijima K, Sakamoto A, Ota M, Horii T, Yoshimura N. Association of Pathomorphology, Photoreceptor Status, and Retinal Thickness With Visual Acuity in Diabetic Retinopathy. *Am J Ophthalmol* (2011) 151(2):310–7. doi: 10.1016/j.ajo.2010.08.022
14. Uji A, Murakami T, Nishijima K, Akagi T, Horii T, Arakawa N, et al. Association Between Hyperreflective Foci in the Outer Retina, Status of Photoreceptor Layer, and Visual Acuity in Diabetic Macular Edema. *Am J Ophthalmol* (2012) 153(4):710–7, 717.e1. doi: 10.1016/j.ajo.2011.08.041
15. Crim N, Velez-Montoya R, Morales-Canton V. Surgical Versus Medical Treatment for Diabetic Macular Edema: A Review. *Med Hypothesis Discovery Innov Ophthalmol* (2017) 6(4):136–42
16. Wilkerson JL, Stiles MA, Gurley JM, Grambergs RC, Gu X, Elliott MH, Proia RL, Mandal NA. Sphingosine Kinase-1 Is Essential for Maintaining External/Outer Limiting Membrane and Associated Adherens Junctions in the Aging Retina. *Mol Neurobiol* (2019) 56(10):7188–207. doi: 10.1007/s12035-019-1599-x
17. Cuenca N, Ortuño-Lizarán I, Pinilla I. Cellular Characterization of OCT and Outer Retinal Bands Using Specific Immunohistochemistry Markers and Clinical Implications. *Ophthalmology* (2018) 125(3):407–22. doi: 10.1016/j.ophtha.2017.09.016
18. Ooka E, Mitamura Y, Baba T, Kitahashi M, Oshitari T, Yamamoto S. Foveal Microstructure on Spectral-Domain Optical Coherence Tomographic Images and Visual Function After Macular Hole Surgery. *Am J Ophthalmol* (2011) 152(2):283–290.e1. doi: 10.1016/j.ajo.2011.02.001
19. Marmor MF. Mechanisms of Flfluid Accumulation in Retinal Edema. *Doc Ophthalmol* (1999) 97:239e249. doi: 10.1023/a:1002192829817

Conflict of Interest: The authors declare that the research was conducted in the absence of any commercial or financial relationships that could be construed as a potential conflict of interest.

frontiers | Frontiers in Endocrinology

ORIGINAL RESEARCH
published: 03 June 2022
doi: 10.3389/fendo.2022.869519

Secreted Protein Acidic and Rich in Cysteine Mediates the Development and Progression of Diabetic Retinopathy

Liying Luo[1†], Xi Sun[2], Min Tang[3,4], Jiahui Wu[3,4], Tianwei Qian[3,4], Shimei Chen[3,4], Zhiyuan Guan[5*†], Yanyun Jiang[1*†], Yang Fu[3,4*†] and Zhi Zheng[3,4*†]*

[1] Department of Ophthalmology, Tongren Hospital, Shanghai Jiao Tong University School of Medicine, Shanghai, China, [2] Department of Hematology, Shanghai General Hospital, Shanghai Jiao Tong University School of Medicine, Shanghai, China, [3] Department of Ophthalmology, Shanghai General Hospital, Shanghai Jiao Tong University School of Medicine, Shanghai, China, [4] Shanghai Key Laboratory of Ocular Fundus Diseases, Shanghai Engineering Center for Visual Science and Photomedicine, Shanghai, China, [5] Department of Orthopedics, The Shanghai Tenth People's Hospital of Tongji University, Shanghai, China

Backgrounds: Diabetic retinopathy (DR) is one of the most severe microvascular complications of diabetes mellitus (DM). Secreted protein acidic and rich in cysteine (SPARC) has been found to play an important role in many diseases, but its role and mechanism in DR remain unknown.

Methods: We studied the role of SPARC and integrin β1 in vascular pathophysiology and identified potential therapeutic translation. The SPARC levels were tested in human serum and vitreous by ELISA assay, and then the Gene Expression Omnibus (GEO) dataset was used to understand the key role of the target gene in DR. In human retinal capillary endothelial cells (HRCECs), we analyzed the mRNA and protein level by RT-PCR, immunohistochemistry, and Western blotting. The cell apoptosis, cell viability, and angiogenesis were analyzed by flow cytometry, CCK-8, and tube formation.

Results: In this study, we investigated the role of SPARC in the development and progression of human DR and high glucose-induced HRCEC cells and found that the SPARC-ITGB1 signaling pathway mimics early molecular and advanced neurovascular pathophysiology complications of DR. The result revealed that DR patients have a high-level SPARC expression in serum and vitreous. Knockdown of SPARC could decrease the expressions of inflammatory factors and VEGFR, inhibit cell apoptosis and angiogenesis, and increase cell viability by regulating integrin β1 in HRCECs.

Conclusion: SPARC promotes diabetic retinopathy *via* the regulation of integrin β1. The results of this study can provide a potential therapeutic application for the treatment of DR.

Keywords: SPARC, diabetic retinopathy, integrin β1, angiogenesis, HRCECs

OPEN ACCESS

Edited by:
Michele Lanza, University of Campania Luigi Vanvitelli, Italy

Reviewed by:
Norbert Nass, Städtische Klinikum Dessau, Germany
Yinan Jiang, University of Pittsburgh, United States

***Correspondence:**
Liying Luo, miss_lyluo@163.com
Zhi Zheng zzheng88@sjtu.edu.cn
Yang Fu fuyang_smile@126.com
Yanyun Jiang jyy3378@shtrhospital.com
Zhiyuan Guan gzy:2008@bjmu.edu.cn

†These authors have contributed equally to this work

Specialty section:
This article was submitted to Clinical Diabetes, a section of the journal Frontiers in Endocrinology

Received: *04 February 2022*
Accepted: *04 April 2022*
Published: *03 June 2022*

Citation:
Luo L, Sun X, Tang M, Wu J, Qian T, Chen S, Guan Z, Jiang Y, Fu Y and Zheng Z (2022) Secreted Protein Acidic and Rich in Cysteine Mediates the Development and Progression of Diabetic Retinopathy. Front. Endocrinol. 13:869519. doi: 10.3389/fendo.2022.869519

INTRODUCTION

Diabetic retinopathy (DR) is one of the most common microvascular complications of diabetes (types 1 and 2) and remains the leading cause of blindness and vision impairment worldwide (1). The global prevalence of DR is expected to remain high through 2034 in DR screening, treatment, and public healthcare strategies (2). In addition, DR is more common in women than men with type 2 diabetes, but men have more severe retinopathy, blurred vision, or blindness (3). The process consists of multiple events. In the early stages of diabetic retinopathy, hyperglycemia and altered metabolic pathways lead to oxidative stress and neurodegeneration (4). Ophthalmoscopy revealed a rupture of the blood–brain barrier, the release of various inflammatory cytokines and plasma proteins, and solid exudates (5). Therefore, when studying pathogenesis, more attention should be paid to molecular biology and molecular interventions targeting the disease. Understanding the changes and molecular biological signaling pathways of DR may represent valuable therapeutic targets for DR treatment.

Secreted protein acidic and rich in cysteine (SPARC, BM-40, osteonectin) is a stromal cellular protein (binding to the extracellular matrix) widely expressed in ocular tissue with multiple roles, including metabolic homeostasis, inflammation reduction, extracellular matrix remodeling, and collagen maturation (6). SPARC modulates tissue physiology by altering cell-ECM interactions, cell proliferation, and migration. Due to these properties, SPARC is involved in wound healing, angiogenesis, tumorigenesis, and inflammation (7). SPARC promotes these functions by affecting the activity of cytokines and growth factors such as vascular endothelial growth factor (VEGF), the most potent and widespread angiogenic mitogen in capillary endothelial cells (8). SPARC KO mice presented impaired glucose homeostasis and insulin section capacity and SPARC was confirmed as a key factor in the pathogenesis of diabetes (9). SPARC plays an important role in hyalocyte-to-myofibroblast transdifferentiation in proliferative diabetic retinopathy, and deletion of SPARC enhances retinal vaso-obliteration (10, 11). However, research has shown that the role of SPARC in the function of DR in humans and cellular is still lacking, and the exact mechanistic link between SPARC and disease development in DR has not been fully explored.

SPARC has been shown to modulate the mitogenic activity in normal endothelial cells in a dose-dependent manner (12) and play dual roles in tumor angiogenesis and tumor extravasation and mediate permeability that is related to endothelial barrier function (13). The expression of SPARC was significantly correlated with the expression of VEGF in colon tumors (14). SPARC regulates glioma growth by altering the tumor microenvironment and inhibiting tumor angiogenesis by suppression of VEGF expression and secretion (15). Furthermore, SPARC-secreted glycoprotein prevents deleterious cardiac inflammation by improving glycocalyx and endothelial barrier functions during viral myocarditis (16). However, the relationship between SPARC and angiogenesis and inflammation has not been investigated in DR.

Integrin β1 (ITGB1) belongs to the β-subfamily and forms dimers with multiple α-subunits. Previous studies found that inhibition of ITGB1 and focal adhesion kinase (FAK) inhibits the migration of bovine myeloid-derived suppressor cells (MDSCs) (17). In addition, ITGB1 signaling plays a significant role in pericyte apoptosis in DR (18). The high levels of glucose in diabetes increased VEGF expression in vascular endothelial cells through fibronectin and integrin β1 interaction (19). SPARC can affect the migration and differentiation of bovine muscle-derived satellite cells *via* the ITGB1-mediated cell signaling pathway (20). In the human lens epithelium-derived cell line SRA01/04, the expression of SPARC and ITGB1 exhibits as a molecular biology of lens cells (21).

This paper attempts to show the effect of SPARC expression in human samples and human cell lines. Our results suggest a unique mechanism for how SPARC-ITGB1 and hyperglycemia modulate VEGF signaling and inhibit neovascularization (NV) in DR. Thus, we aimed to provide direct and informative evidence of SPARC-ITGB1 expression and function involved in the development of DR.

MATERIALS AND METHODS

This study was approved by the ethics committee of Shanghai General Hospital and the institutional review board of the University (No. 2021-047). All patients were informed and signed an informed consent form. According to the CONSORT guidelines, these studies also comply with the Declaration of Helsinki.

Patients

We performed a prospective nonrandomized study at the Department of Ophthalmology, Shanghai General Hospital, Shanghai Jiao Tong University School of Medicine from January to December 2021. DR patients (12 patients) included in this study were diagnosed with diabetic retinopathy requiring surgery, with or without vitreous hemorrhage. Among the 7 control patients, five had macular epiretinal membranes and two had a macular hole, and they need surgery at the same time without hypertension and diabetes mellitus (DM).

At our clinic, patients who were clinically assessed as eligible were asked if they were interested in participating in the study. Before applying, they must decide on whether they would like to participate or not, and if so, they should provide written informed consent.

Inclusion and Exclusion Criteria

The minimum age of participants was 18 years old. Inclusion criteria included the diagnosis of diabetic retinopathy and either diabetes mellitus type 1 or type 2. The control group included patients diagnosed with macular epiretinal membranes or macular holes who needed pars plana vitrectomy.

Exclusion criteria included a history of subtotal or complete vitrectomy (3 port pars plana vitrectomy), treatment with an antiangiogenic agent, partial vitrectomy with drug administration, or laser coagulation within the 90 days before screening or treatment with a long-acting corticosteroid within the last 90 days

before screening. In addition, patients who had undergone a cataract operation or posterior capsule opacification treatment within the past 90 days or had any other eye disease or clinically significant glaucoma evident at the time of screening were excluded. Patients with uncontrolled intraocular pressure (≥30 mmHg) were excluded.

Additional exclusion criteria included patients with uncontrolled hypertension (>160/90 mmHg (systole/diastole), poorly controlled diabetes (HbA1c >10%), or those diagnosed with an autoimmune disease. Patients were excluded if pregnant or breastfeeding during the study, if they had participated in a clinical trial within 30 days before screening, and if they had any other condition, that at the discretion of the investigator, was deemed to be inconsistent with participation in the trial. Finally, patients who reported drug or alcohol abuse within the 180 days before screening were excluded.

Serum and Vitreous Sampling

A blood sample (5–10 ml blood) was taken before the surgery to determine the SPARC level. A minimally invasive 3-port partial pars plana vitrectomy was performed in all cases by one vitreoretinal surgeon in the operating room. The extracted vitreous sample was placed directly in the freezer at a temperature of −70°C. Once completed, the removal of the probe leaves a self-sealing wound, which reduces the risk of leakage from the eye and limits the penetration of pathogens from the outer ocular surface.

Analysis of Serum and Vitreous Samples

Serum and vitreous samples were sent for laboratory analysis following surgery. The laboratory received no information about whether each sample was part of the DR or control group. This was to allow for laboratory analysis to be conducted in a blinded fashion. The SPARC level was detected using an enzyme-linked immunosorbent assay (ELISA) (DY941-05, R&D, Minneapolis, USA).

HE Staining and Immunohistochemical Analysis

The sample of human proliferative membranes and epiretinal membranes were fixed in 2% PFA for 2 h and then frozen in isopentane (−55°C). Next, the eyes were embedded in paraffin and cut into 5-μm-thick sections, which were then mounted on glass slides. Paraffin-embedded sections were dewaxed with xylene, washed by gradient alcohol or distilled water, and stained with hematoxylin for 1–3 min. Sections were then differentiated by 1% hydrochloric alcohol, turned blue by PBS, stained by eosin, and dehydrated using gradient alcohol. After permeabilization with xylene, the tissues were photographed under microscopy (BX53, Olympus, Japan).

In addition, the tissues were processed for immunohistochemistry (IHC) analysis using an anti-SPARC antibody (ab225716, Abcam, Cambridge, the UK). Before the IHC procedure, sections were deparaffinized and rehydrated by immersing the slides in xylene and alcohol at descending concentrations. Colocalization of individual SPARC, TRIB3, and BRN3A, or GFAP and vimentin proteins in the retinal sections were detected using fluorescent confocal microscopy. Fluorescence intensity was measured using ImageJ software. Absorption control was performed using the recombinant human SPARC protein.

GEO Dataset and Data Processing

The RNA-sequencing data of DR patients and corresponding clinical information were obtained from the GEO dataset (GSE102485) on December 31, 2021. mRNA expression data of 11 DR patients and 3 healthy people were collected.

Difference Gene Expression and Functional Enrichment Analysis

The differential expression of mRNA in DR tissue and normal control samples was evaluated using the R software (Version 3.8; http://www.bioconductor.org/packages/release/bioc/html). The heatmap and volcano of these genes were plotted using the R software. Pearson correlation analyses were performed to identify gene-to-gene correlation. The p-value of 0.05 was considered the significant threshold in all tests.

GO and KEGG Analyses

Gene ontology (GO), including the biological process (BP), cellular component (CC), and molecular function (MF) categories, was conducted with the "ggplot2" package in the R software. Similarly, this package was also utilized to perform the Kyoto Encyclopedia of Genes and Genomes (KEGG) analysis.

The STRING website (https://string-db.org/) uses the protein–protein interaction network to study the interaction between protein names (SPARC) and organisms (*Homo sapiens*). The most important parameters are defined as follows: the minimum required interaction rating [low confidence (0,150)], the effectiveness of the network edge, the maximum number of interactions to be displayed (no more than 50 first shells), and the active interaction sources.

To further the function of SPARC, we used GeneMANIA tools (http://genemania.org/) to understand the coexpression, colocation, genetic interaction, pathway, physical interaction, and predicted and shared protein domains of SPARC.

Establishment of High Glucose-Induced Cell Model

Human retinal capillary endothelial cells (HRCECs; PriCells Biotechnological Co. Ltd., Wuhan, China) were cultured in DMEM (Gibco, Grand Island, NY, USA), 10% fetal bovine serum (FBS, Gibco), 100 IU/ml penicillin, and 100 μg/ml streptomycin (Gibco). All cells were incubated in a humidified atmosphere at 37°C under 5% CO_2 air. Subculturing was performed every 2 days, and cells were seeded into 96-well plates with the density of 4 × 105 cells/ml, cultured for 1 h, and detached with 0.25% trypsin. D-Glucose was added to the medium at a final concentration of 30 mmol/L to generate high-glucose (HG) conditions, while cells treated with DMEM (low glucose) with 5 mmol/L served as the low-glucose group. In addition, cells cultured in basal DMEM supplemented with 25 mmol/L glucose served as the normal medium conditions (control group).

siRNA and Plasmid Transfection in HRCECs

Overexpression plasmids for SPARC and ITGB1 as well as the silencing plasmids sh-NC, sh-SPARC, and sh-ITGB1 were synthesized by Shanghai GenePharma Biological Co. Ltd. (Shanghai, China). CDS sequences of SPARC and ITGB1 were obtained from NCBI, followed by polymerase chain reaction (PCR) amplification. Plasmids were established by cloning the corresponding sequences of SPARC to pcDNA3.1 (+) vector through restriction enzyme sites. Confluent cells were then transfected with 1 μg sh-SPARC plasmid according to the manufacturer's protocol in the Lipofectamine 2000 kit (Invitrogen, Carlsbad, CA, USA). Meanwhile, cells received treatment with vector + dimethyl sulfoxide (DMSO), sh-SPARC + DMSO, sh-ITGB1 + DMSO, and sh-SPARC + sh-ITGB1, followed by treatment with DMSO and 0.5 or 1.0 μM transmethylase inhibitor 5-Aza (Sigma) solution.

HRCECs were cultured at a density of 4 × 105 cells per 6-cm well, and they were 80%–90% confluent at the time of transfection. Two micrograms of each plasmid was transfected with 4 μl lipofectamine 2000 reagent (Invitrogen, Karlsruhe, Germany) according to the manufacturer's recommendations, and the empty vector was transfected into HRCECs as a control for comparison.

Cell Viability Assay

A Cell-Counting Kit-8 (CCK-8) assay was used to evaluate the cell viability. HRCECs were treated with sh-SPARC for 24 h. The cells were plated into 96-well plates for 48 h in the incubator. At the end of the incubation period, 10 μl CCK-8 solution was added to each well, and the plates were returned to the incubator for an additional 2 h at 37°C. Absorbance was measured at 450 nm using a microplate reader.

Tube Formation Assay

Tube formation assay was performed as we previously described (22). HRCECs were placed on the Matrigel and treated with sh-SPARC for 12 h. Tube formation was quantified by counting the number of connected cells in randomly selected fields and dividing by the total number of cells in the same field.

Western Blotting and RT-PCR Analyses

HRCECs were harvested, and total proteins were obtained using RIPA Lysis Buffer (Beyotime, Shanghai, China). The protein concentration was determined using the BCA Protein Quantitation kit (Beyotime, Shanghai, China). The proteins were then separated by SDS-PAGE and transferred to PVDF membranes. The membranes were blocked with 5% nonfat milk and 0.1% Tween-20 for 1 h at room temperature. Samples were then incubated with the primary antibodies overnight at 4°C, which were the primary antibodies against SPARC (66426-1-Ig, Proteintech), ITGB1 (ab199056 Abcam), vascular endothelial growth factor receptor (VEGFR) (ab134191, Abcam), integrin-linked kinase (ILK) (ab134179, Abcam), and fibronectin 1 (FN1) (ab52480, Abcam). After being washed three times with TBST buffer, the membranes were incubated with secondary antibodies (ab150077, Abcam) at 4°C for 3 h. Enhanced chemiluminescence (ECL) reaction reagents were used for visualization, and ImageJ software was employed to analyze the results. The protein bands were quantified and normalized to the expression of glyceraldehyde 3-phosphate dehydrogenase (GAPDH).

The total RNA was extracted using Trizol reagent (TaKaRa, Dalian, Liaoning, China), and the cDNA was synthesized with RNA Transcription Kit (TaKaRa). RT-qPCR was then performed using the SYBR Green RT-qPCR system. SPARC, ITGB1, VEGFR, ILK, and FN1 mRNA expression were tested in our study mRNA expression were tested in our study. The relative expressions of mRNAs were evaluated by the 2−ΔΔCq method, and the internal normalization control is GAPDH (**Supplementary Table S1**).

Flow Cytometry Apoptosis Detection Assay

HRCECs were seeded in 6-well plates, then collected by trypsinization, washed in 4°C PBS, and trypsinized into cell suspensions. Phosphatidyl-serine (PS) exposure due to the flipping of the plasma membrane, a concomitant feature during apoptosis, was evaluated by PE Annexin V Apoptosis Detection Kit (559763, BD Pharmingen) by flow cytometry analysis containing PE Annexin V and 7-AAD. The experiments were independently repeated three times.

Statistical Analysis

All results are expressed as the mean ± standard deviation (SD). Statistical differences were assessed by a 2-tailed Student's *t*-test or one-way ANOVA statistical analysis followed by Tukey's test. All results were repeated at least three times, and $p < 0.05$ was considered significant.

RESULTS

SPARC Is Highly Expressed in DR Patients' Serum, Vitreous, and Proliferative Membranes

Recent studies found that dysregulation of SPARC is associated with a variety of obesity-related diseases, including type 2 diabetes and its complications related to obesity, kidney and liver disease, cardiovascular disease, and cancer (23). Therefore, we investigated the SPARC expression in human serum and vitreous samples and histological results in proliferative membranes. The demographic data of the participants are shown in **Table 1**. HE staining showed that the epiretinal membrane is mainly composed of extracellular matrix (ECM) such as collagen fiber, and the nucleus is round and spindle shaped in the control group. DR group proliferation membrane is mainly manifested as vascular fiber membrane, which is characterized by more luminal structures surrounded by endothelioid cells (**Figure 1A**). To this end, we analyzed and quantitated SPARC level and immunoreactivity. Overall, the serum and vitreum SPARC levels in the DR group were highly increased significantly than in the control group (**Figures 1B, C**). Representative control and DR of a 67-year-old and 56-year-old

TABLE 1 | Demographic and clinical characteristics of patients.

Characteristics	Total	Control[a]	DR	*p*-value
Patients (No.)	19	7	12	–
Age (year)	57.8 ± 10.0	64.9 ± 6.5	52.8 ± 9.2	0.0940
Man/woman (%)	37 (7/19)	29 (2/7)	42 (5/12)	0.5681
Positive history of hypertension (%)	11 (2/19)	0 (0/7)	12 (2/17)	0.3432
Positive history of diabetes (%)	63 (12/19)	0 (0/7)	100 (12/12)	<0.0001*
SPARC (ng/ml)	17.12 ± 9.28	11.98 ± 4.31	22.22 ± 11.65	0.0405*

[a]*Diagnosed as macular hole or epiretinal membrane. DR, diabetic retinopathy; SPARC, secreted protein acidic and rich in cysteine. *Significant results.*

man are shown in **Figure 1D**. Strong evidence of DR immune responses in retinal endothelial cells, ganglia, and photoreceptor cells was observed in a 67-year-old nondiabetic man compared with the control (**Figure 1E**).

Differential Gene Expression and Pathway Signaling of SPARC

Further analysis showed the differential gene expression of DR patients in the GEO dataset. The heatmap and volcano map are shown in **Figures 2A, B**. SPARC and ITGB1 expressions are significant differences between DR patients and healthy patients. GO disease analysis also found that SPARC was correlated with electroretinogram abnormality, photophobia, rod-cone dystrophy, and disorder of the eye (**Supplementary Figure S1B**). GO target gene analysis investigated ZNF513, AUTS2, ZBTB44, and SUPT16H (**Supplementary Figure S1C**), and GO-regulated gene analysis also found that NRL, ETV7, PAX6, and CRX can regulate the expression of SPARC (**Supplementary Figure S1C**). GO enrichment and GO network found that SPARC plays an important role in retinal development in the camera-type eye (**Figure 2C**; **Supplementary Figure S1A**). The GeneMANIA network showed that SPARC significantly correlated with STAB1, FN1, VEGF, and ILK (**Figure 2C**). Protein–protein network also investigated the correlation of SPARC with ERBB4, ALB, COL1A1, and MMP2 (**Figures 2D, E**).

To verify these results, we test the mRNA of SPARC, ITGB1, ILK, and FN1 levels in DR and control tissues and found that the DR group has higher SPARC, ITGB1, ILK, and FN1 mRNA levels than the control group (**Figure 3A**). It is indicated that a high SPARC level is correlated with the development of DR, and the SPARC expression level also links to ITGB1 and ILK.

SPARC Is Highly Expressed in HG-Induced Cell Models

HG-induced retinal pigment epithelium can stimulate the development of DR. Therefore, we also analyzed the SPARC level in a different dose of HG-induced cell models. We found that the SPARC level can be increased significantly in HG medium (30 mmol/L) in than low glucose medium (5.5 mmol/L) after 7 days of incubation, and the effect of HG treatment on SPARC

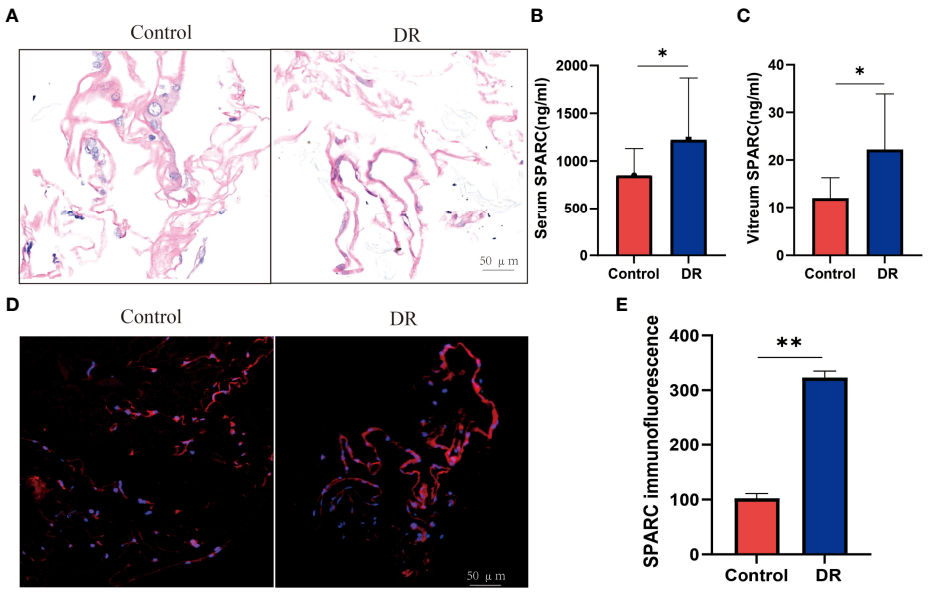

FIGURE 1 | The SPARC level is increased in diabetic retinopathy patient. **(A)** HE staining. **(B, C)** Serum and vitreum SPARC level. **(D, C)** Immunofluorescence staining of SPARC in control and diabetic retinopathy patient. **(E)** SPARC immunofluorescence between Control and DR group. *$p < 0.05$,**$p < 0.01$.

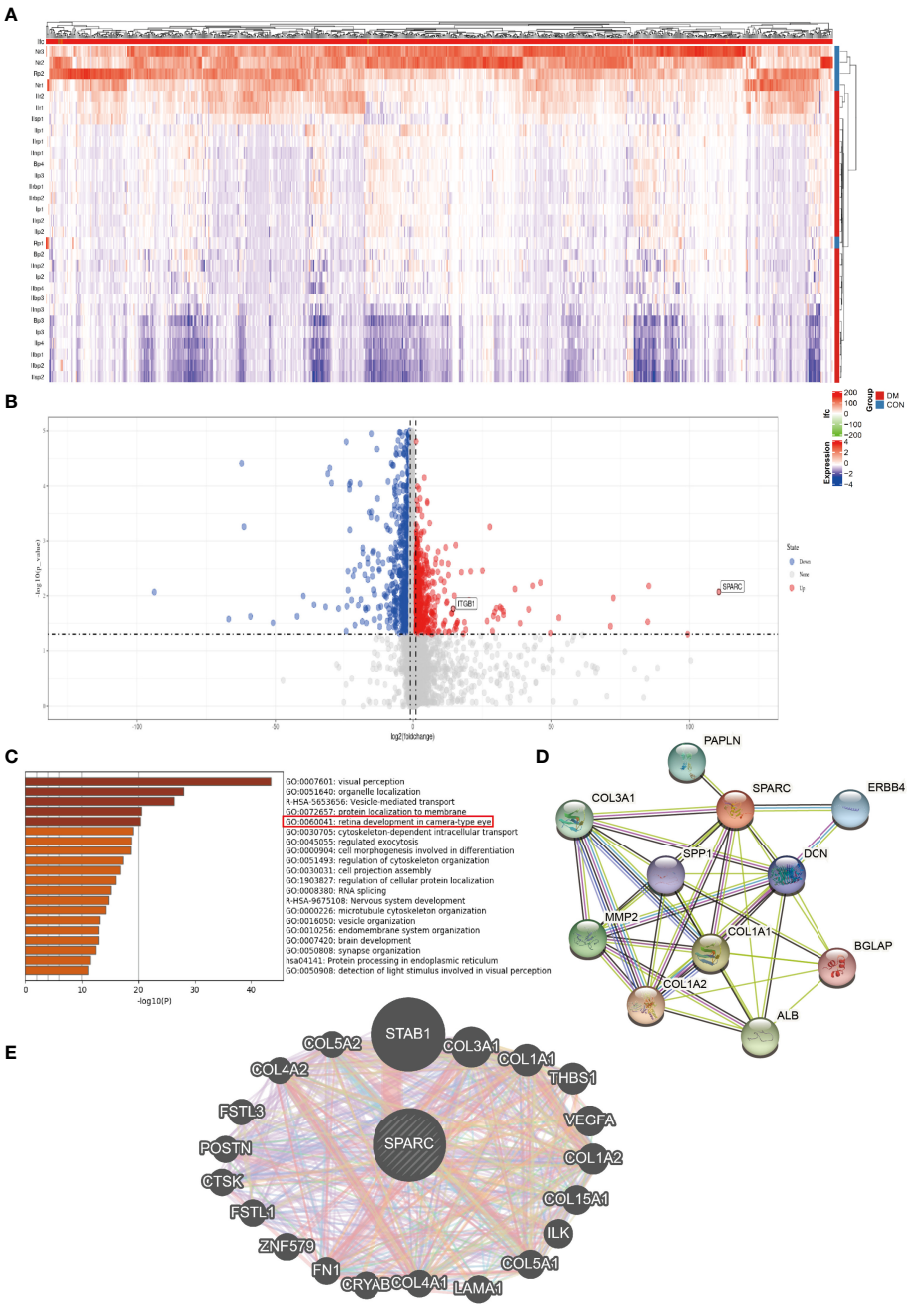

FIGURE 2 | The bioinformation analysis by GEO dataset. **(A)** Heatmap of DR patient. **(B)** Volcano map of DR patient. **(C)** GO pathway signaling. **(D)** Protein–protein network by the STRING analysis. **(E)** Target gene network by the GeneMANIA tool.

showed a dose-dependent manner. qPCR assay showed that the HG environment can also increase the SPARC, VEGFR, ITGB1, IL-6, TGF-β, and ILK mRNA levels than the low-glucose group (**Figure 3**). In this part, we further demonstrated that the expression of SPARC and related genes and proteins in the HRCEC cells were significantly increased under HG condition.

In addition, we also analyzed the protein level in the HG-induced HRCEC cell model. The HG environment increased the expression of ITGB1, ILK, FN1, and VEGFR compared with the low-glucose-induced HRCEC cells (**Figure 4A, B**).

Ablation of SPARC Suppresses ITGB1/ILK mRNA and Endothelial and Inflammation Cell Biomarkers

Subsequently, the study aimed to understand the role of SPARC and SPARC-related genes such as ITGB1 in the development

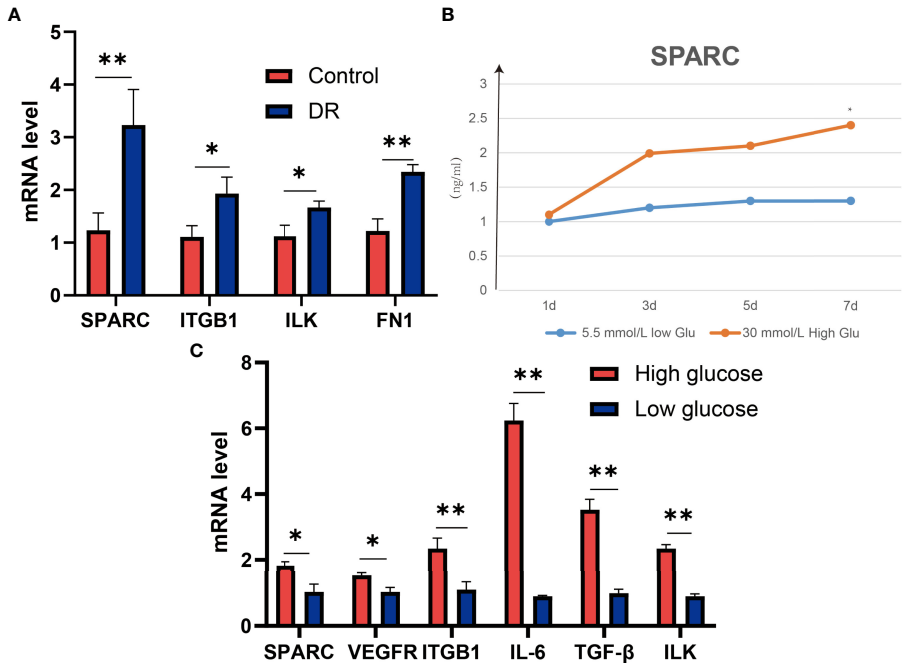

FIGURE 3 | SPARC regulates the expression of ITGB1, inflammation, and VEGF genes in high-glucose-induced HECEC cells. **(A)** The mRNA expression of SPARC, ITGB1, ILK, and FN1 in DR and control tissues. **(B)** SPARC level in different glucose-induced HECEC cells. **(C)** The mRNA expression in different glucose-induced HECEC cells. $^{*}p < 0.05$,$^{**}p < 0.01$.

of DR. We first transfected HRCECs with the sh-SPARC-interfered lentiviruses carrying red fluorescent protein. A representative figure of immunofluorescence has been shown in **Figure 5A**. The SPARC protein level has also been tested by Western blotting and was found to be significantly lower in the sh-SPARC group than in the control group, showing that the SPARC silence model is successful (**Figure 5**).

After the establishment of the cell silencing model, we detected the changes in SPARC-related gene expression. Firstly, the SPARC mRNA level was significantly decreased in the sh-SPARC group than in the sh-NC group, and then, the ITGB1, ILK, VEGFR, FN1, IL6, and TGF-β mRNA levels also markedly decreased in the sh-SPARC than in the sh-NC group.

Consisting with the mRNA expression of SPARC-related genes, SPARC knockdown could decrease the protein level of ITGB1, ILK, FN1, and VEGFR significantly than the control group (**Figure 4A, B**).

Overexpression and Ablation of ITGB1 in HG-Induced HRCEC Cells Suppress ITGB1/ILK mRNA and Endothelial and Inflammation Cell Biomarkers

ITGB1 overexpression and ablation demonstrate that the former can significantly increase the expression of VEGFR, FN1, IL6, and TGF-β in mRNA levels, whereas the latter could decrease the expression of VEGFR, FN1, IL6, and TGF-β in mRNA levels.

In addition, the ITGB1 overexpression or ablation could increase or significantly decrease the protein expression levels of ILK, FN1, and VEGFR. The sh-SPARC/ITGB1-OE group could also increase the ITGB1 protein level while the sh-SPARC/ITGB1-sh group decreased the ITGB1 protein level significantly. However, sh-SPARC/ITGB1-OE could only increase the protein level of FN1 and VEGFR compared with the sh-SPARC/ITGB1-sh group (**Figure 6**).

Ablation of SPARC and ITGB1 Inhibits the HG-Induced Apoptosis, Cell Viability, and Tube Formation of HRCECs

The cell apoptosis assay was conducted, and HG-induced HRCECs had a high apoptosis ratio when compared with the control group (**Figure 7A**). Firstly, HG-induced HRCECs can increase apoptosis levels in the control group more than normal glucose, and sh-SPACR can significantly decrease the apoptosis ratio in HG levels more than normal glucose (**Figure 7B**). In normal and HG (**Figure 7D**), the sh-ITGB1 group increased the apoptosis ratio significantly more than the sh-NC. In addition, sh-SPARC-ITGB1 also increased apoptosis significantly more than in the sh-SPARC-NC in HG (**Figure 7E**).

We analyze the cell viability by CCK-8 tests in **Figure 7A**. After 1 or 2 days postincubation (**Figures 8A, B**), sh-SPARC significantly decreased cell viability more than the sh-NC group (**Figures 8C–E**). Apoptosis analysis showed that sh-SPARC cells exhibit higher apoptosis levels than the sh-NC group in **Figure 7C**. Furthermore, ablation of ITGB1 decreased cell viability significantly more than the NC group, and overexpression of ITGB1 increased cell viability more than in the NC group (**Figures 9A–C**).

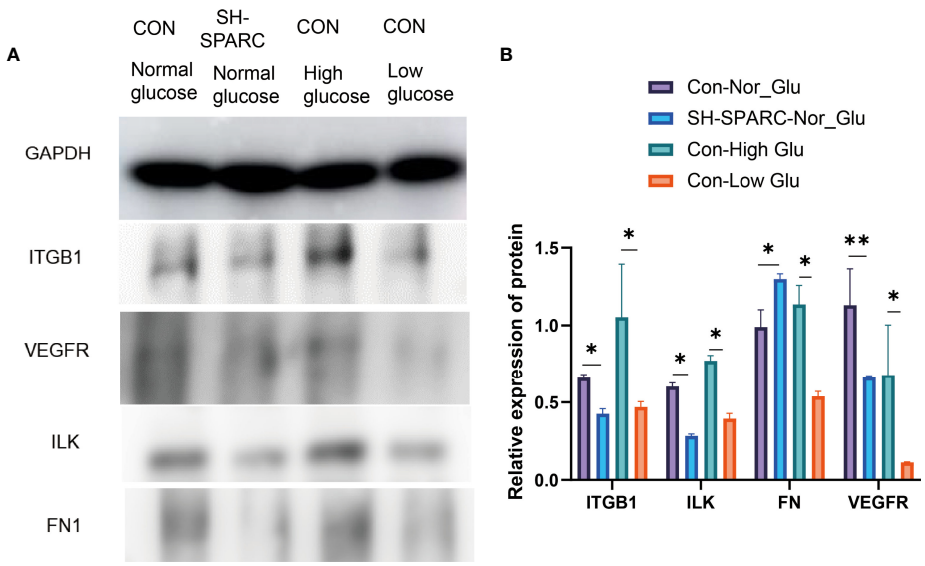

FIGURE 4 | The protein levels in HRCEC cells under high glucose and low glucose, sh-SPARC cells in normal condition, and control group. **(A)** Representative figure. **(B)** The expression of proteins such as ITGB1, ILK, FN1, and VEGFR in HECEC cells. *$p < 0.05$,**$p < 0.01$.

In **Figure 9A**, the tube formation test has been investigated among the NC, sh-SPARC, sh-ITGB1, and sh-SPARC-ITGB1 groups. The corresponding image was shown, and the results revealed that the sh-SPARC, sh-ITGB1, and sh-SPARC-ITGB1 groups could reduce tube formation rate and tube area covered than the NC group (**Figures 9B, C**).

DISCUSSION

DR is the most common complication of diabetes mellitus, and it is a leading cause of vision impairment and blindness (24). The present study firstly shows that high expression of SPARC has been detected in serum and vitreous samples of DR patients. The

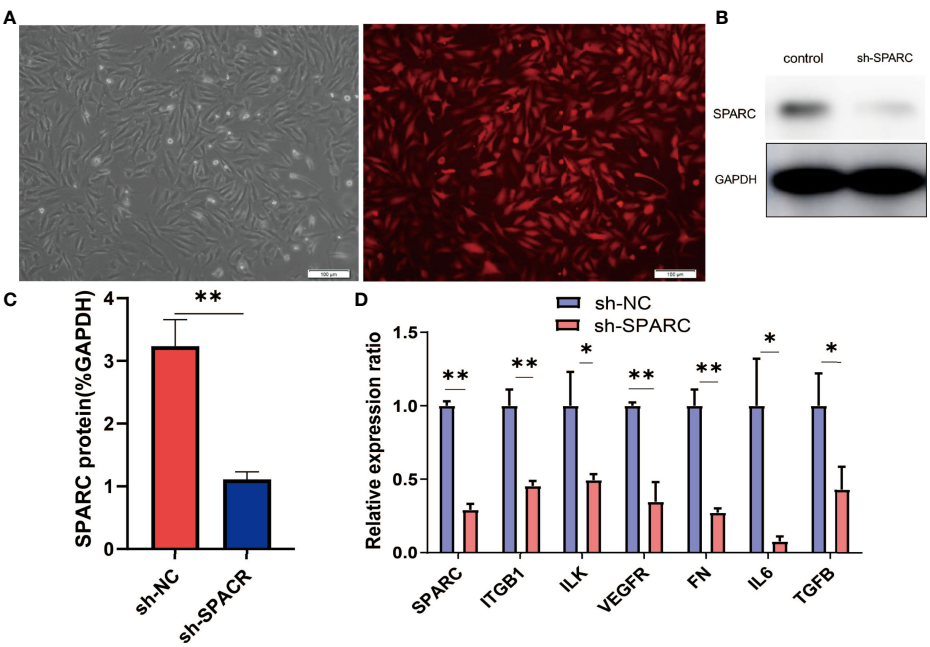

FIGURE 5 | The related gene expression in SPARC gene silencing experiments. **(A)** Representative fluorescence figure. **(B, C)** Protein level of SPARC in SPARC gene silencing experiments. **(D)** The mRNA level in SPARC gene silencing experiments. *:$p < 0.05$,**:$p < 0.01$.

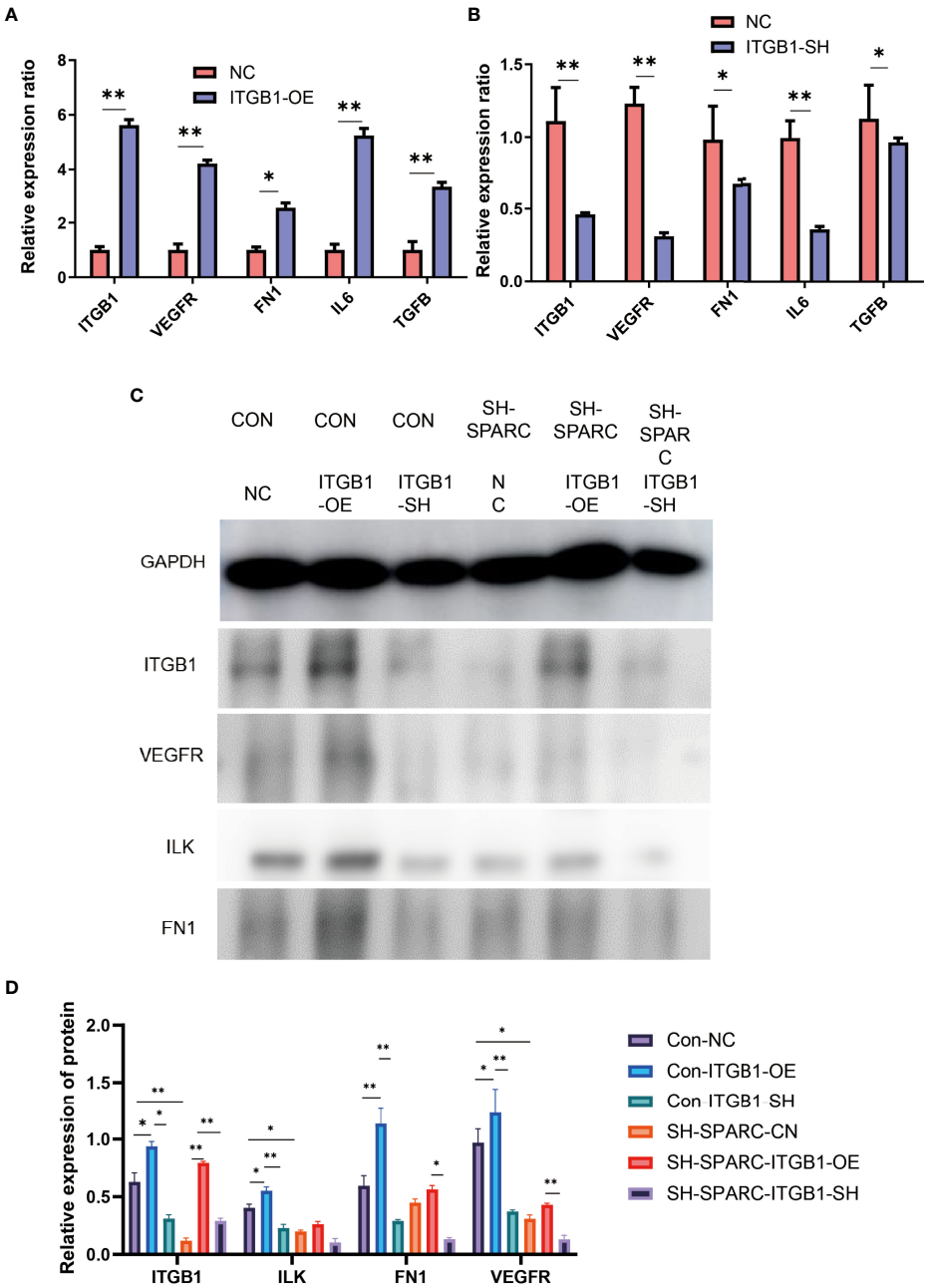

FIGURE 6 | The mRNA and protein levels in overexpression and ablation of ITGB1 experiments. **(A)** Overexpression of ITGB1 experiments. **(B)** Ablation of ITGB1 experiments. **(C, D)** Protein level in the overexpression and ablation of the ITGB1 experiments. *:$p < 0.05$,**:$p < 0.01$.

second part showed that HG-induced HRCEC cells could upregulate the SPARC/ITGB1 pathway signaling and inflammation biomarkers when combined with the GEO dataset. Finally, ablation of SPARC and ITGB1 can also regulate apoptosis, cell viability, and tube formation.

C-reactive protein, *N*-epsilon-carboxymethyl lysine (*N*-ϵ-CML), and pentosidine are just a few of the many circulating, vitreous, and genetic biomarkers that have been studied lately (25). VEGFR is a currently recognized biomarker of DR and plays a key role in the pathogenesis of DR by stimulating angiogenesis (26). However, not all patients respond to anti-VEGF therapy, and the treatment has side effects, such as short duration of action and the repetitive need for intraocular injection (27). Therefore, the identification of a new biomarker for DR is necessary to increase detection, risk stratification, and treatment for patients with DR.

SPARC plays a crucial role in the development of many diseases, including cancer and cardiovascular, osteoarticular, and metabolic diseases. Li et al. found that SPARC and FN1 are highly expressed

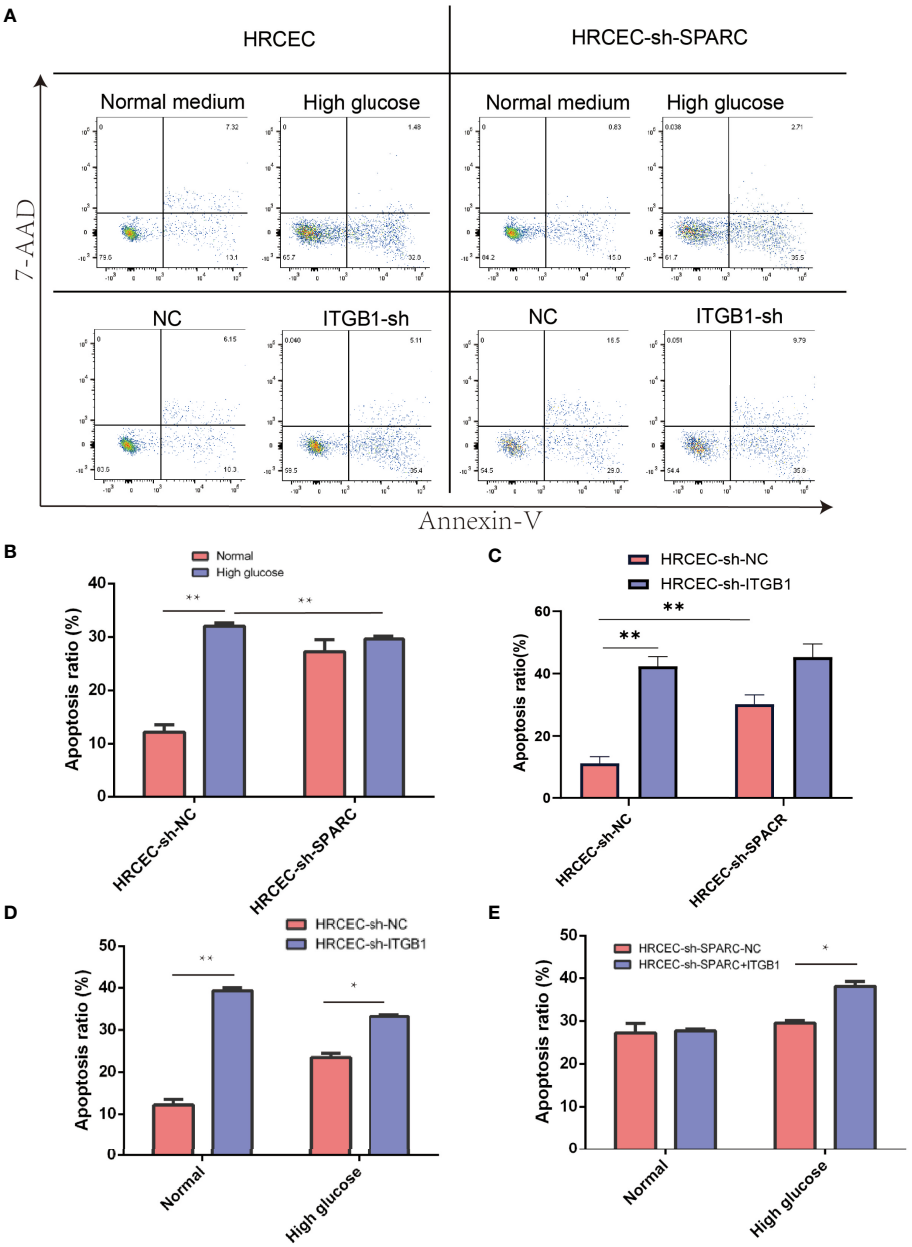

FIGURE 7 | Apoptosis level in ablation of SPARC and ITBG1 in different glucose-induced experiments. **(A)** Representative figure of flow cytometry. Annexin V/7-AAD assay was performed to determine the percentage of apoptotic cells. **(B–E)** Apoptosis ratio in ablation of SPARC and ITBG1 in different glucose-induced experiments. *:$p < 0.05$, **:$p < 0.01$.

and significantly related to the poor prognosis of gastric adenocarcinoma (28). Furthermore, SPARC is a key mediator of TGF-β-induced renal cancer and metastasis (29). In NAFLD-associated hepatocellular carcinoma, the inhibition of SPARC accelerates the development of cancer and cardiovascular disease (30). SPARC contributes to myocardial fibrosis in pressure overload (31). SPARC also plays a potential role in load-induced regulation of tendon homeostasis, vertebrate cartilage mineralization, and bone healing (32–34). SPARC is required to maintain glucose homeostasis and insulin secretion in mice with metabolic diseases such as obesity and type 2 diabetes (9). Previous studies found that SPARC plays an important role in hyalocyte-to-myofibroblast transdifferentiation in proliferative diabetic retinopathy (10). However, more in-depth studies on the role of SPARC in diabetic retinopathy are currently lacking.

In our studies, we found that ablation and overexpression of SPARC regulate the expression of ITGB1, inflammation, and VEGFR levels, which contribute to changes in apoptosis, cell viability, and tube formation. As mentioned in the literature review, SPARC influences skeletal muscle-derived satellite cell migration and

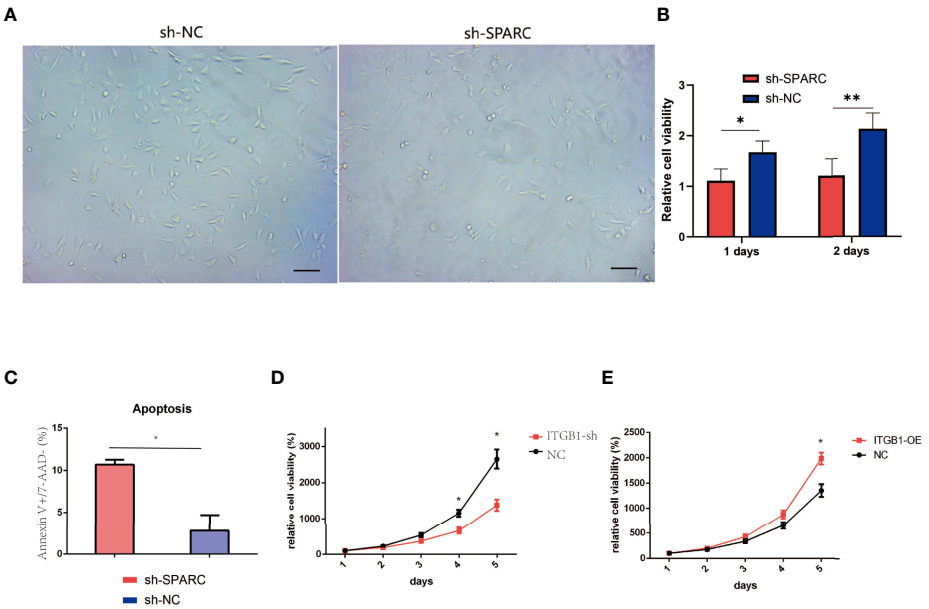

FIGURE 8 | Cell viability experiments test by CCK-8 analysis. **(A)** Representative figure of cell viability experiment. **(B)** The cell viability experiments in ablation of SPARC in 1 and 2 days. **(C)** Apoptosis of Annexin V+/7-AAD– experiment. **(D, E)** The cell viability experiments in 1, 2, 3, 4, 5 days with overexpression and ablation of ITGB1. *:$p < 0.05$, **:$p < 0.01$.

differentiation through the ITGB1-mediated signaling pathway (20). ITGB1 and SPARC exhibit lens epithelial cell-like characteristics in cataracts (21). These results corroborate the findings of a lot of our studies that SPARC may play an important role in regulating the ITGB1-mediated signaling pathway. SPARC also regulated the expression of VEGFR in DR. Previous studies have shown that SPARC regulates glioblastoma growth by altering the tumor microenvironment and inhibits tumor angiogenesis by inhibiting

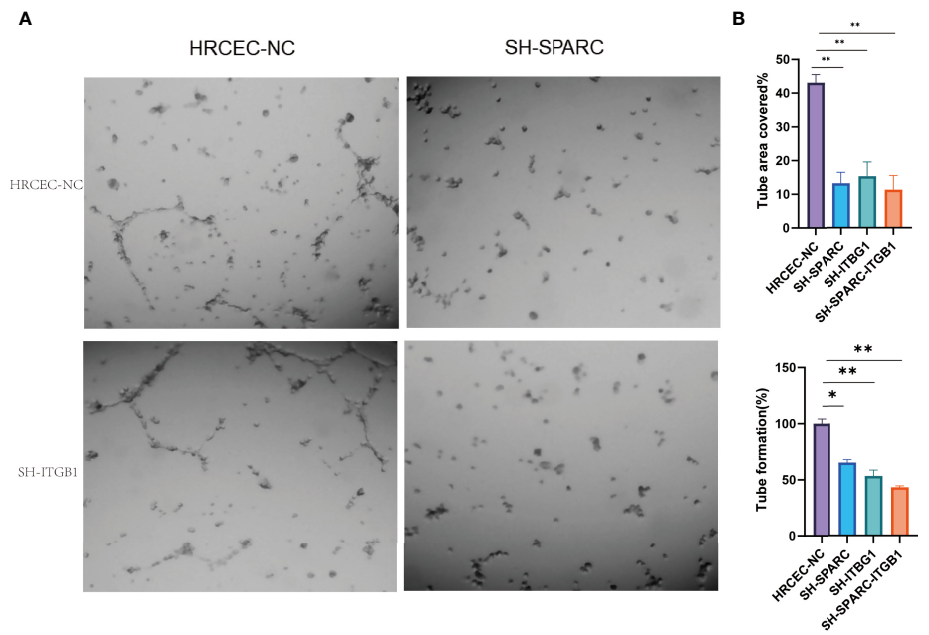

FIGURE 9 | The tube formation of ablation of SPARC and ITGB1 experiments. **(A)** Representative figure of tube formation. **(B)** Tube formation area covered. **(C)** Tube formation rate. *:$p < 0.05$,**:$p < 0.01$.

VEGF expression and secretion (15). Sachiko et al. investigated that SPARC activates fibroblasts only in the presence of fibronectin, which is abundantly secreted in endometrial cancer cells expressing SPARC, and SPARC-FN1-mediated fibroblast activation may be associated with increased cancer cell migration and invasiveness (35). In addition, fibronectin acts as a molecular switch that determines SPARC function in pancreatic cancer (36). SPARC also regulates the inflammation response *via* targeting TGF-β, which is also consistent with our results (37).

SPARC protein could also regulate cell apoptosis, cell viability, and tube formation. SPARC deficiency suppresses diabetes-stimulated increases in superoxide production and eliminates prominent features of hepatocyte damage, such as impaired cytoprotection, inflammation, apoptosis, and autophagy (38). SPARC increases NOX4 expression *via* a TGF-β1-dependent signaling pathway, leading to oxidative stress and proinflammatory matrix behavior and apoptosis in human brain smooth muscle cells (39). The downregulation of SPARC could decrease cell migration, invasion, and viability (40). SPARCs are targeted antiangiogenic proteins in dysfunctional endothelial colony-forming cells that have distinct proteomic profiles and phenotypic changes when compared with hyperangiogenic endothelial cells with impaired angiogenesis and dilation (41). SPARC promotes apoptosis of neurovascular cells, including astrocytes, and is implicated in the pathogenesis of neurovascular rupture-focused diseases (41). Furthermore, SPARC was confirmed to be extremely important in promoting vascular endothelial cell proliferation, motility, and capillary–like tube formation, as well as reducing apoptosis (42). Therefore, this finding broadly supports the findings of other studies in this field, which have linked SPARC with cell apoptosis, cell viability, and tube formation in DR.

In HG-induced retinal pigment epithelium in a dose-dependent manner, HG promoted reactive oxygen species (ROS) production and apoptosis and inhibited autophagy and proliferation, while low glucose induced ROS production and autophagy but had little effect on apoptosis and proliferation (43). Consistent with the literature, this research found that participants who reported using HG-induced retinal pigment epithelium played an important role in the development of DR. In addition, previous studies showed that HG-induced HRCEC inhibition of cell viability, migration, angiogenesis, and cell adhesion was reversed by inhibition of SPARC expression (44). In our studies, we found that HG-induced apoptosis can be reversed by ablation of SPARC.

We also use bioinformatic tools to analyze the key genes in DR as we previously described (45). These results revealed that SPARC is markedly associated with STAB1, VEGFR, ILK, and FN1. In-depth transcriptomic analysis of the human retina reveals molecular mechanisms such as SPARC underlying diabetic retinopathy (46). It is important to consider the possibility of bias in these responses from verified bioinformatic analysis.

CONCLUSION

Overall, our study indicates that SPARC mediates the expression of ITGB1, which plays an important role in regulating cell apoptosis, cell viability, and tube formation *in vitro* experiments. The results of this study will help in understanding the pathogenesis of DR, the development of effective drugs, and the development of a more comprehensive and effective strategy for the prevention and treatment of DR.

DATA AVAILABILITY STATEMENT

The datasets presented in this study can be found in online repositories. The names of the repository/repositories and accession number(s) can be found in the article/**Supplementary Material**.

ETHICS STATEMENT

The studies involving human participants were reviewed and approved by the ethics committee of Shanghai General Hospital. The patients/participants provided their written informed consent to participate in this study.

AUTHOR CONTRIBUTIONS

Conception and design: ZZ, YF, MT, and YYJ. Acquisition, analysis, and interpretation of the data: LYL, XS, JHW, SMC and TWQ. Drafting and writing: ZYG. Final approval of the article: LYL. All authors listed have made a substantial, direct, and intellectual contribution to the work and approved it for publication.

FUNDING

This project was qualified by the Reaserch Fund of Shanghai Tongren Hospital, Shanghai Jiaotong University School of Medicine (NO:TRYJ2021JC02).

ACKNOWLEDGMENTS

We would like to thank all participants and our hospital.

SUPPLEMENTARY MATERIAL

The Supplementary Material for this article can be found online at: https://www.frontiersin.org/articles/10.3389/fendo.2022.869519/full#supplementary-material

Supplementary Figure 1 | GO pathway signaling analysis in GEO dataset. **(A)** GO network analysis. **(B)** GO diseased analysis. **(C)** Target genes of GO anlayais. **(D)** The regulated genes analyzed by GO dataset.

REFERENCES

1. Ogurtsova K, da RochaFernandes JD, Huang Y, Linnenkamp U, Guariguata L, Cho NH, et al. IDF Diabetes Atlas: Global Estimates for the Prevalence of Diabetes for 2015 and 2040. *Diabetes Res Clin Pract* (2017) 128:40–50. doi: 10.1016/j.diabres.2017.03.024
2. Teo ZL, Tham YC, Yu M, Chee ML, Rim TH, Cheung N, et al. Global Prevalence of Diabetic Retinopathy and Projection of Burden Through 2045: Systematic Review and Meta-Analysis. *Ophthalmology* (2021) 128(11):1580–91. doi: 10.1016/j.ophtha.2021.04.027
3. Lin KY, Hsih WH, Lin YB, Wen CY, Chang TJ. Update in the Epidemiology, Risk Factors, Screening, and Treatment of Diabetic Retinopathy. *J Diabetes Investig* (2021) 12(8):1322–5. doi: 10.1111/jdi.13480
4. Wong TY, Cheung CM, Larsen M, Sharma S, Simó R. Diabetic Retinopathy. *Nat Rev Dis Primers* (2016) 2:16012. doi: 10.1038/nrdp.2016.12
5. Liu Y, Wu N. Progress of Nanotechnology in Diabetic Retinopathy Treatment. *Int J Nanomed* (2021) 16:1391–403. doi: 10.2147/IJN.S294807
6. Ghanemi A, Yoshioka M, St-Amand J. Secreted Protein Acidic and Rich in Cysteine as A Regeneration Factor: Beyond the Tissue Repair. *Life (Basel)* (2021) 11(1). doi: 10.3390/life11010038
7. Brekken RA, Sage EH. SPARC, a Matricellular Protein: At the Crossroads of Cell-Matrix Communication. *Matrix Biol* (2001) 19(8):816–27. doi: 10.1016/S0945-053X(00)00133-5
8. Kupprion C, Motamed K, Sage EH. SPARC (BM-40, Osteonectin) Inhibits the Mitogenic Effect of Vascular Endothelial Growth Factor on Microvascular Endothelial Cells. *J Biol Chem* (1998) 273(45):29635–40. doi: 10.1074/jbc.273.45.29635
9. Atorrasagasti C, Onorato A, Gimeno ML, Andreone L, Garcia M, Malvicini M, et al. SPARC is Required for the Maintenance of Glucose Homeostasis and Insulin Secretion In Mice. *Clin Sci (Lond)* (2019) 133(2):351–65. doi: 10.1042/CS20180714
10. Watanabe K, Okamoto F, Yokoo T, Iida KT, Suzuki H, Shimano H, et al. SPARC Is a Major Secretory Gene Expressed and Involved in the Development of Proliferative Diabetic Retinopathy. *J Atheroscler Thromb* (2009) 16(2):69–76. doi: 10.5551/jat.E711
11. Boneva SK, Wolf J, Hajdú RI, Prinz G, Salié H, Schlecht A, et al. In-Depth Molecular Characterization of Neovascular Membranes Suggests a Role for Hyalocyte-to-Myofibroblast Transdifferentiation in Proliferative Diabetic Retinopathy. *Front Immunol* (2021) 12:757607. doi: 10.3389/fimmu.2021.757607
12. Paley PJ, Goff BA, Gown AM, Greer BE, Sage EH. Alterations in SPARC and VEGF Immunoreactivity in Epithelial Ovarian Cancer. *Gynecol Oncol* (2000) 78(3 Pt 1):336–41. doi: 10.1006/gyno.2000.5894
13. Kato Y, Lewalle JM, Baba Y, Tsukuda M, Sakai N, Baba M, et al. Induction of SPARC by VEGF in Human Vascular Endothelial Cells. *Biochem Biophys Res Commun* (2001) 287(2):422–6. doi: 10.1006/bbrc.2001.5622
14. Liang JF, Wang HK, Xiao H, Li N, Cheng CX, Zhao YZ, et al. Relationship and Prognostic Significance of SPARC and VEGF Protein Expression in Colon Cancer. *J Exp Clin Cancer Res* (2010) 29(1):71. doi: 10.1186/1756-9966-29-71
15. Yunker CK, Golembieski W, Lemke N, Schultz CR, Cazacu S, Brodie C, et al. SPARC-Induced Increase in Glioma Matrix and Decrease in Vascularity Are Associated With Reduced VEGF Expression and Secretion. *Int J Cancer* (2008) 122(12):2735–43. doi: 10.1002/ijc.23450
16. Rienks M, Carai P, van Teeffelen J, Eskens B, Verhesen W, Hemmeryckx B, et al. SPARC Preserves Endothelial Glycocalyx Integrity, and Protects Against Adverse Cardiac Inflammation and Injury During Viral Myocarditis. *Matrix Biol* (2018) 74:21–34. doi: 10.1016/j.matbio.2018.04.015
17. Pang Y, Zhang Z, Wang Z, Wang Y, Yan Y, Li S, et al. Platelet Endothelial Aggregation Receptor-1 Regulates Bovine Muscle Satellite Cell Migration and Differentiation *via* Integrin Beta-1 and Focal Adhesion Kinase. *Cell Adh Migr* (2019) 13(1):192–202. doi: 10.1080/19336918.2019.1619434
18. Park SW, Yun JH, Kim JH, Kim KW, Cho CH, Kim JH. Angiopoietin 2 Induces Pericyte Apoptosis *via* α3β1 Integrin Signaling in Diabetic Retinopathy. *Diabetes* (2014) 63(9):3057–68. doi: 10.2337/db13-1942
19. Chen S, Chakrabarti R, Keats EC, Chen M, Chakrabarti S, Khan ZA. Regulation of Vascular Endothelial Growth Factor Expression by Extra Domain B Segment of Fibronectin in Endothelial Cells. *Invest Ophthalmol Vis Sci* (2012) 53(13):8333–43. doi: 10.1167/iovs.12-9766
20. Wang Y, Liu S, Yan Y, Li S, Tong H. SPARCL1 Influences Bovine Skeletal Muscle-Derived Satellite Cell Migration and Differentiation Through an ITGB1-Mediated Signaling Pathway. *Anim (Basel)* (2020) 10(8). doi: 10.3390/ani10081361
21. Weatherbee BAT, Barton JR, Siddam AD, Anand D, Lachke SA. Molecular Characterization of the Human Lens Epithelium-Derived Cell Line SRA01/04. *Exp Eye Res* (2019) 188:107787. doi: 10.1016/j.exer.2019.107787
22. Min JK, Cho YL, Choi JH, Kim Y, Kim JH, Yu YS, et al. Receptor Activator of Nuclear Factor (NF)-kappaB Ligand (RANKL) Increases Vascular Permeability: Impaired Permeability and Angiogenesis in eNOS-Deficient Mice. *Blood* (2007) 109(4):1495–502. doi: 10.1182/blood-2006-06-029298
23. Kos K, Wilding JP. SPARC: A Key Player in the Pathologies Associated With Obesity and Diabetes. *Nat Rev Endocrinol* (2010) 6(4):225–35. doi: 10.1038/nrendo.2010.18
24. Sabanayagam C, Banu R, Chee ML, Lee R, Wang YX, Tan G, et al. Incidence and Progression of Diabetic Retinopathy: A Systematic Review. *Lancet Diabetes Endocrinol* (2019) 7(2):140–9. doi: 10.1016/S2213-8587(18)30128-1
25. Kwan CC, Fawzi AA. Imaging and Biomarkers in Diabetic Macular Edema and Diabetic Retinopathy. *Curr Diabetes Rep* (2019) 19(10):95. doi: 10.1007/s11892-019-1226-2
26. Aiello LP, Avery RL, Arrigg PG, Keyt BA, Jampel HD, Shah ST, et al. Vascular Endothelial Growth Factor in Ocular Fluid of Patients With Diabetic Retinopathy and Other Retinal Disorders. *N Engl J Med* (1994) 331(22):1480–7. doi: 10.1056/NEJM199412013312203
27. Nicholson BP, Schachat AP. A Review of Clinical Trials of Anti-VEGF Agents for Diabetic Retinopathy. *Graefes Arch Clin Exp Ophthalmol* (2010) 248(7):915–30. doi: 10.1007/s00417-010-1315-z
28. Li L, Zhu Z, Zhao Y, Zhang Q, Wu X, Miao B, et al. FN1, SPARC, and SERPINE1 Are Highly Expressed and Significantly Related to a Poor Prognosis of Gastric Adenocarcinoma Revealed by Microarray and Bioinformatics. *Sci Rep* (2019) 9(1):7827. doi: 10.1038/s41598-019-43924-x
29. Bao JM, Dang Q, Lin CJ, Lo UG, Feldkoren B, Dang A, et al. SPARC Is a Key Mediator of TGF-β-Induced Renal Cancer Metastasis. *J Cell Physiol* (2021) 236(3):1926–38. doi: 10.1002/jcp.29975
30. Onorato AM, Fiore E, Bayo J, Casali C, Fernandez-Tomé M, Rodríguez M, et al. SPARC Inhibition Accelerates NAFLD-Associated Hepatocellular Carcinoma Development by Dysregulating Hepatic Lipid Metabolism. *Liver Int* (2021) 41(7):1677–93. doi: 10.1111/liv.14857
31. Riley HJ, Kelly RR, Van Laer AO, Neff LS, Dasgupta S, Baicu CF, et al. SPARC Production by Bone Marrow-Derived Cells Contributes to Myocardial Fibrosis in Pressure Overload. *Am J Physiol Heart Circ Physiol* (2021) 320(2):H604–h612. doi: 10.1152/ajpheart.00552.2020
32. Cassuto J, Folestad A, Göthlin J, Malchau H, Kärrholm J. The Key Role of Proinflammatory Cytokines, Matrix Proteins, RANKL/OPG and Wnt/β-Catenin in Bone Healing of Hip Arthroplasty Patients. *Bone* (2018) 107:66–77. doi: 10.1016/j.bone.2017.11.004
33. Romero A, Leurs N, Muñoz D, Debiais-Thibaud M, Marcellini S. Divergent Expression of SPARC, SPARC-L, and SCPP Genes During Jawed Vertebrate Cartilage Mineralization. *Front Genet* (2021) 12:788346. doi: 10.3389/fgene.2021.788346
34. Wang T, Wagner A, Gehwolf R, Yan W, Passini FS, Thien C, et al. Load-Induced Regulation of Tendon Homeostasis by SPARC, a Genetic Predisposition Factor for Tendon and Ligament Injuries. *Sci Transl Med* (2021) 13(582). doi: 10.1126/scitranslmed.abe5738
35. Yoshida S, Asanoma K, Yagi H, Onoyama I, Hori E, Matsumura Y, et al. Fibronectin Mediates Activation of Stromal Fibroblasts by SPARC in Endometrial Cancer Cells. *BMC Cancer* (2021) 21(1):156. doi: 10.1186/s12885-021-07875-9
36. Munasinghe A, Malik K, Mohamedi F, Moaraf S, Kocher H, Jones L, et al. Fibronectin Acts as a Molecular Switch to Determine SPARC Function in Pancreatic Cancer. *Cancer Lett* (2020) 477:88–96. doi: 10.1016/j.canlet.2020.02.031
37. Yuting Y, Lifeng F, Qiwei H. Secreted Modular Calcium-Binding Protein 2 Promotes High Fat Diet (HFD)-Induced Hepatic Steatosis Through Enhancing Lipid Deposition, Fibrosis and Inflammation *via* Targeting TGF-β1. *Biochem Biophys Res Commun* (2019) 509(1):48–55. doi: 10.1016/j.bbrc.2018.12.006
38. Aseer KR, Silvester AJ, Kumar A, Choi MS, Yun JW. SPARC Paucity Alleviates Superoxide-Mediated Oxidative Stress, Apoptosis, and Autophagy

in Diabetogenic Hepatocytes. *Free Radic Biol Med* (2017) 108:874–95. doi: 10.1016/j.freeradbiomed.2017.05.011
39. Tan X, Li T, Zhu S, Zhong W, Li F, Wang Y. Induction of SPARC on Oxidative Stress, Inflammatory Phenotype Transformation, and Apoptosis of Human Brain Smooth Muscle Cells *Via* TGF-β1-NOX4 Pathway. *J Mol Neurosci* (2020) 70(11):1728–41. doi: 10.1007/s12031-020-01566-z
40. Zhang F, Zhang Y, Da J, Jia Z, Wu H, Gu K. Downregulation of SPARC Expression Decreases Cell Migration and Invasion Involving Epithelial-Mesenchymal Transition Through the P-FAK/p-ERK Pathway in Esophageal Squamous Cell Carcinoma. *J Cancer* (2020) 11(2):414–20. doi: 10.7150/jca.31427
41. Tan CMJ, Lewandowski AJ, Williamson W, Huckstep OJ, Yu GZ, Fischer R, et al. Proteomic Signature of Dysfunctional Circulating Endothelial Colony-Forming Cells of Young Adults. *J Am Heart Assoc* (2021) 10(15):e021119. doi: 10.1161/JAHA.121.021119
42. Lyu Z, Jin H, Yan Z, Hu K, Jiang H, Peng H, et al. Effects of NRP1 on Angiogenesis and Vascular Maturity in Endothelial Cells Are Dependent on the Expression of SEMA4D. *Int J Mol Med* (2020) 46(4):1321–34. doi: 10.3892/ijmm.2020.4692
43. Zhang Y, Xi X, Mei Y, Zhao X, Zhou L, Ma M, et al. High-Glucose Induces Retinal Pigment Epithelium Mitochondrial Pathways of Apoptosis and Inhibits Mitophagy by Regulating ROS/PINK1/Parkin Signal Pathway. *BioMed Pharmacother* (2019) 111:1315–25. doi: 10.1016/j.biopha.2019.01.034
44. Fu Y, Tang M, Xiang X, Liu K, Xu X. Glucose Affects Cell Viability, Migration, Angiogenesis and Cellular Adhesion of Human Retinal Capillary Endothelial Cells *via* SPARC. *Exp Ther Med* (2019) 17(1):273–83. doi: 10.3892/etm.2018.6970
45. Guan X, Guan Z, Song C. Expression Profile Analysis Identifies Key Genes as Prognostic Markers for Metastasis of Osteosarcoma. *Cancer Cell Int* (2020) 20:104. doi: 10.1186/s12935-020-01179-x
46. Becker K, Klein H, Simon E, Viollet C, Haslinger C, Leparc G, et al. In-Depth Transcriptomic Analysis of Human Retina Reveals Molecular Mechanisms Underlying Diabetic Retinopathy. *Sci Rep* (2021) 11(1):10494. doi: 10.1038/s41598-021-88698-3

Conflict of Interest: The authors declare that the research was conducted in the absence of any commercial or financial relationships that could be construed as a potential conflict of interest.

Publisher's Note: All claims expressed in this article are solely those of the authors and do not necessarily represent those of their affiliated organizations, or those of the publisher, the editors and the reviewers. Any product that may be evaluated in this article, or claim that may be made by its manufacturer, is not guaranteed or endorsed by the publisher.

frontiers | Frontiers in Endocrinology

REVIEW
published: 06 June 2022
doi: 10.3389/fendo.2022.915031

Long Noncoding RNAs and Mitochondrial Homeostasis in the Development of Diabetic Retinopathy

Renu A. Kowluru *

Department of Ophthalmology, Visual and Anatomical Sciences, Wayne State University, Detroit, MI, United States

Retinopathy is one of the most devastating complications of diabetes, which a patient fears the most. Hyperglycemic environment results in many structural, functional, molecular and biochemical abnormalities in the retina, and overproduction of mitochondrial superoxide, induced by hyperglycemic milieu, is considered to play a central role in the development of diabetic retinopathy. Expression of many genes associated with maintaining mitochondrial homeostasis is also altered. Recent research has shown that several long noncoding RNAs, RNAs with more than 200 nucleotides but without any reading frames, are aberrantly expressed in diabetes, and altered expression of these long noncoding RNAs is now being implicated in the development of diabetes and its complications including retinopathy. This review focuses the role of long noncoding RNAs in the development of diabetic retinopathy, with a special emphasis on the maintenance of mitochondrial homeostasis.

Keywords: Diabetic retinopathy, long noncoding RNAs, mitochondria, epigenetics, diabetes

OPEN ACCESS

Edited by:
Michele Lanza,
University of Campania Luigi Vanvitelli, Italy

Reviewed by:
Subrata Chakrabarti,
Western University, Canada
Zhipeng You,
Affiliated Eye Hospital of Nanchang University, China
Manuela Bartoli,
Augusta University, United States

***Correspondence:**
Renu A. Kowluru
rkowluru@med.wayne.edu

Specialty section:
This article was submitted to Clinical Diabetes, a section of the journal Frontiers in Endocrinology

Received: *07 April 2022*
Accepted: *29 April 2022*
Published: *06 June 2022*

Citation:
Kowluru RA (2022) Long Noncoding RNAs and Mitochondrial Homeostasis in the Development of Diabetic Retinopathy. Front. Endocrinol. 13:915031. doi: 10.3389/fendo.2022.915031

INTRODUCTION

Incidence of diabetes is increasing at an alarming rate around the world; 151 million people had diabetes in 2000, this number is now 463 million adults, and is expected to pass 780 million by 2045 (1). Diabetes accounts for 6.7 million deaths in 2021-one death every 5 seconds, and this devastating disease does not know any social, economic or ethnic boundaries. Elevated blood glucose in the circulation, either due to impaired insulin production or resistance to properly use it, results in damaging small and large blood vessel in the body, resulting in many micro- and macro-vascular complications including nephropathy (kidney), neuropathy (nerve), retinopathy (retina, back of the eye) and cardiomyopathy (heart) (2). Over time, chronic high blood glucose affects almost every organ in the body, one in three adults with diabetes present chronic kidney disease, one in two peripheral nerve abnormalities and over 80% patients show some signs of retinopathy (3). Thus, diabetes is a whole-body chronic disease, and is commonly called as a 'disease of its complications'.

LONG NONCODING RNAs

Technological development in transcriptome-wide sequencing has now documented that although majority of the mammalian genome is actively transcribed into RNA, only 2-3% is further translated

into protein (4). Thus, most of the DNA does not code for the proteins, and this 'non-coding DNA' has a heterogeneous group of noncoding RNAs including transfer RNA, circular RNA, micro RNA (miRNA, less than 20 base pairs) and long noncoding RNA (LncRNAs, more than 200 base pairs) (**Figure 1**). The exact number of non-coding RNAs in the human genome is still not clear, but recent transcriptomic/bioinformatic studies have put their numbers in the tens of thousands (5). These noncoding RNAs, however, are not totally unfunctional, they can be alternatively spliced and/or processed into smaller products, and may have a hidden layer of internal signals (especially those derived from introns) that could control transcription, chromatin architecture etc. Noncoding RNAs are implicated in numerous cellular processes including cell cycle and metabolism (6–8). Thus far more than 2000 miRNAs and 30,000 LncRNAs have been discovered in humans, and these noncoding RNAs are responsible for regulating one third of the genes in the genome (9, 10). Although both miRNAs and LncRNAs RNAs are transcribed by RNAs polymerase II, miRNAs are better conserved than LncRNAs, and while miRNAs regulate mRNA at transcriptional and post-transcriptional levels, LncRNAs can remodel chromatin and genomic imprinting and regulate gene expression through sequence complementarity with RNAs or DNAs (11, 12). LncRNAs have four-fold higher tissue specificity compared to miRNAs (13, 14). LncRNAs are mRNA-like transcripts, but they do not possess any stable open reading frames, and compared to mRNAs, expression levels of LncRNAs are typically lower (14). Furthermore, while mRNAs have to be translated into proteins for carrying out specific cellular functions, LncRNAs are the functional unit and can function in different subcellular compartments based on local molecular interactions, and stronger tissue-specificity (15).

Based on their genomic location, LncRNAs are classified into various subclasses, 'intergenic LncRNAs' located between two protein coding-genes without intersecting with any protein-coding genes, 'intronic LncRNAs' transcribed from intronic region of a protein coding-gene and overlap with protein-coding genes, 'antisense LncRNAs' transcribed from complementary strand of either protein coding or non-protein coding genes, 'bidirectional LncRNA' initiating in a divergent fashion from a promoter of protein-coding gene, and 'enhancer LncRNA' synthesized at the enhancers (**Figure 2**). LncRNAs act as a guide *via* interacting with the modifying complexes or transcription factors, directing them to specific genes or loci, or they may function as a scaffold by binding its multiple effector partners at the same time with proteins. LncRNAs also act as 'decoy' by binding to the transcription factors or miRNAs, repressing gene expression, or as an 'enhancer' by changing chromatin architecture to recruit transcription factors and promote transcription (16). They bind to DNA or RNA in a sequence-specific manner, or can act as sponges for miRNAs or as scaffolds to provide stability, and facilitate transcription factor binding (7, 17, 18). Thus, LncRNAs are capable of interacting with RNA and DNA.

LncRNAs are mainly encoded by nuclear genome and are overall more numerous in the nucleus, a significant number is also present in the cytoplasm, where they are more stable than their nuclear counterparts (19–21). LncRNAs modulate chromatin interactions in the nucleus, and generally help in signal transduction and posttranscriptional control of gene expression in the cytoplasm (22). In addition to nuclear genome, ~15% of the human mitochondrial transcriptome is made of noncoding RNAs, including three LncRNAs- LncRNA *ND5*, LncRNA *ND6* and LncRNA *CytB*. Mitochondrial LncRNAs are located in the regions of the mtDNA complementary to the genes that encode

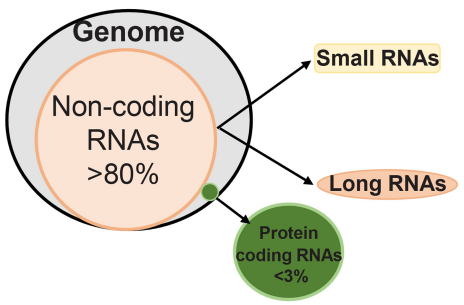

FIGURE 1 | Human genome has less than 3% RNAs that can code for proteins, and over 80% of RNAs are noncoding. Depending on the length of their transcripts, noncoding RNAs are classified as 'small' and 'long' noncoding RNAs. While small noncoding RNAs have less than 200 nucleotides, long noncoding RNAs have over 200 nucleotides.

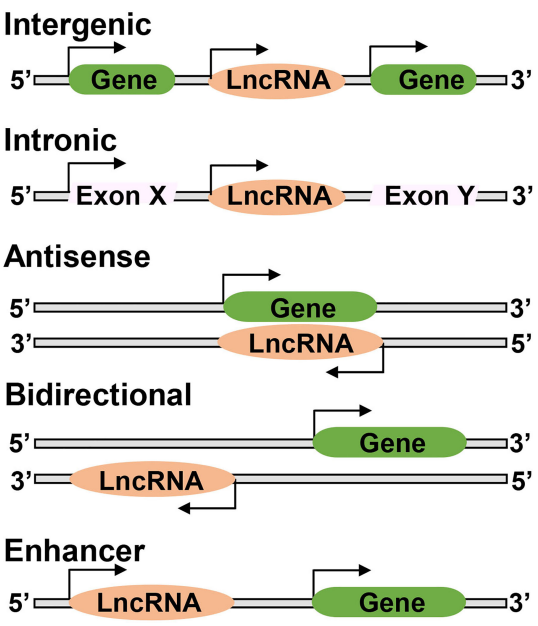

FIGURE 2 | Long noncoding RNAs may have different genomic locations; between two protein coding genes 'Intergenic', or located within an intron of a coding gene 'Intronic', or overlap with one or more introns and exons of a different transcript on the same or opposite strand, respectively 'Antisense', or be within 100 kb of a coding transcript of the opposite strand 'Bidirectional', or present in the enhancer regions close to the promoter 'Enhancer'.

for *ND5*, *ND6 of* complex I and *cytochrome* B of complex III respectively, and these mitochondrial genome encoded LncRNAs primarily form intermolecular duplexes with their respective complementary mRNAs (23, 24). However, these mitochondrial genome-encoded LncRNAs are not restricted to the mitochondria, instead, they can operate in the nucleus (24). Nuclear genome-encoded LncRNAs can also move from the nucleus to the mitochondria and the mitochondrial genome-encoded LncRNAs can be aberrantly transported to the nucleus, and this aberrant shuttling of crosstalk of LncRNAs is associated with abnormalities in energy metabolism (25). Accumulating research indicates that LncRNAs play important roles in diverse biological processes, and are identified as key regulators in pathological processes in a range of diseases including cancer, diabetes and Alzheimer (26–29), and their role in diabetic macro- and microvascular complications is an emerging area of research (30).

DIABETIC RETINOPATHY

High circulating glucose leads to increased risk of many eye problems, including increase in intraocular pressure and damage to the lens and the retina. Damage to the retinal microvasculature, commonly known as diabetic retinopathy, is the leading cause of acquired blindness in the working age adults in developing countries. In the initial stages of this progressing disease, patients may be asymptomatic, but their retinal microvasculature begins to become fragile, and as the duration of diabetes increases, retinopathy also progresses and the damaged retinal vasculature begins to leak. With time, lack of oxygen in the microvasculature leads to neovascularization, and ultimately, to vision loss (31, 32). Early diagnosis and treatment options of diabetic retinopathy, however, are limited, and it is critical to identify effective methods of its diagnosis and therapeutic targets to retard progression of this sight-threatening disease. In the first five years of diabetes, retinopathy is rare in type 1 diabetic patients, but after 20 years of diabetes, over 80% of patients develop retinopathy. In type 2 diabetic patients, 21% of patients present early signs of retinopathy at the time of their diagnosis of diabetes, and as with type 1 diabetic patients, most type 2 diabetic patients also develop some degree of retinopathy over time. In 2020, over 100 million diabetic adults had retinopathy, and among those, 28.5 million had vision-threatening retinopathy, and with increase in the incidence of diabetes, these numbers are expected to increase to over 160 million and 45 million, respectively in 2045 (33). Although pathological evidence is mainly seen in the retinal microvasculature, research has shown that nonvascular cells of the retina are also affected; they experience functional and structural alterations including retinal ganglion cell apoptosis, loss of contrast sensitivity and alterations in the electroretinogram (34, 35). Normal cell-cell interactions are also affected leading to the blood-retinal barrier breakdown and neuronal cell dysfunction (6, 36). In addition, Optical Coherence Tomography has also shown ganglion cell loss in the retina of diabetic patients with or without retinopathy, however, diabetic patients with moderate or severe retinopathy show more thinning of their ganglion cell-inner plexiform layers compared to patients without any retinopathy (37).

Impaired Mitochondrial Homeostasis

Diabetic retinopathy is a multifactorial disease with a complex etiology, and increase in oxidative stress-mitochondrial damage is considered to play a major role in the development of this blinding disease (2, 38–42). Retina is rich in polyunsaturated fatty acids and has a high oxygen uptake (43), making it a good target of increased oxidative stress in diabetes. In diabetes, increased cytosolic ROS, generated by activation of Ras-related C3 botulinum toxin substrate 1 (Rac1)-NADPH oxidase 2 (Nox2)-activation of gelatinase matrix metalloproteinases in diabetes damage mitochondria in retinal capillaries (44, 45). In addition, due to high circulating glucose, electron flux through the electron transport chain system is increased, and the complex III becomes dysfunctional, resulting in increased accumulation of ROS (40, 46). Mitochondrial structural and functional stability is impaired including increased production of superoxide radicals and damage to their membrane potential. Cytochrome C leaks out from the mitochondria in the cytosol, which accelerates capillary cell apoptosis, a phenomenon which is followed by the histopathology characteristic of retinopathy (38, 41, 47, 48). Mitochondria have their own DNA (mtDNA), which encodes genes for 13 proteins that are essential for the electron transport chain functioning; diabetes damages mtDNA and reduces the gene transcripts of mitochondrial genome-encoded *ND1* and *ND6* of complex I, and *cytochrome B* of complex III are reduced. In addition, mitochondrial dynamics is imbalanced, while fusion is decreased, fission is increased, and the removal of damaged mitochondria in impaired. Impairment in mitochondrial homeostasis in diabetes is further exacerbated by the suboptimal biogenesis of mtDNA (47, 49–52). Thus, instability in mitochondrial structure, function and genome plays a central role in the development of diabetic retinopathy.

Aldose reductase, an enzyme with a high 'Km' for glucose, using NADPH as a cofactor, converts glucose to sorbitol. This reduces availability of NADPH for glutathione biosynthesis, increasing oxidative stress. In diabetes, polyol pathway is activated in the retina and its capillary cells (53, 54). Diabetes increases non-enzymatic glycation of amino acids in proteins, lipids and nucleic acids, and this ultimately leads to advanced glycation end products (AGEs) (55); retinal capillaries have increased AGEs and their receptors (RAGEs), and AGEs-RAGEs are implicated in increased inflammation and capillary cell loss in diabetic retinopathy (56). Diacyl glycerol-protein kinase C cascade is also activated by high glucose, and protein kinase C activation in retinal vasculature is associated with increased vascular permeability, alterations in blood flow and stimulation of neovascularization seen in diabetic retinopathy (57). Furthermore, activation of protein kinase C, polyol pathway and increased AGEs accumulation can also increase oxidative stress, and can also be initiated by hyperglycemia-induced overproduction of mitochondrial superoxide, further strengthening the role of mitochondrial damage in diabetic

retinopathy (40, 58). In addition, many inflammatory markers including cytokines and leukostasis, are also elevated in diabetic retinopathy (59), and retinal glial cells, the cells that are between vasculature and neurons of the retina, also initiate the inflammatory cascade (60).

Hyperglycemia is the main instigator, but systemic factors, such as high blood pressure, cholesterol and smoking are also closely associated with the development and progression of diabetic retinopathy (61), and also in the exacerbated and accelerated mitochondrial damage (62). However, multifactorial nature and complex etiology of diabetic retinopathy makes it difficult to identify a link between any specific metabolic abnormality and the development of this progressive blinding disease.

Genetics and Diabetic Retinopathy

Genetic factors appear to play some role in diabetic retinopathy, but the exact role of genetic contribution in the development/progression of diabetic retinopathy has remained unclear. Significant association between the variations in the polyol pathway gene encoding aldo-keto reductase family 1-member B1, *AKR1B1*gene, has been documented by a meta-analysis (63). Type 2 diabetic patients in Pakistan with Pro12Ala polymorphism are at a reduced risk of developing diabetic retinopathy (64). Jackson Heart Study has shown an association between P-selectin and diabetic retinopathy (65). Another genome-wide association study (GWAS) has shown association with a zinc finger protein associated with transcriptional regulation, ZNF600. Polymorphisms at the regulatory regions of some of the genes including *VEGF* and endothelial nitric oxide synthase and paraoxonase1, have been considered as risk alleles for the susceptibility or progression of diabetic retinopathy (66). Genotyping of single nucleotide polymorphism has identified new loci on chromosome 6 associated with diabetic retinopathy, but none of the variants have shown any statistical significance (67). A recent GWAS meta-analyses of type 2 diabetic patients have shown enrichment of variants in the genes involved lipid catabolism and transport, oxidative stress and cell degeneration pathways and the risk of diabetic retinopathy (68). In addition, an association for the z-2 microsatellite and rs759853 on aldo-keto reductase family 1 member B, and some evidence for polymorphisms in *VEGF*, intercellular adhesion molecule 1 genes have also been documented by systemic meta-analyses, but a follow up of the analysis has not reported any loci after adjustment for multiple (69). A study of cohort from China with proliferative diabetic retinopathy has identified *INSR* gene as a possible susceptibility candidate for severe diabetic retinopathy, but this study is underpowered (70). Siblings of affected individuals has been shown to have three-fold higher risk of severe diabetic retinopathy, but diabetic patients with similar risk factors do not show the same range in the severity of retinopathy, when evaluated by Early Treatment Diabetic Retinopathy Study Grading System (71). Thus, despite recent technological advancement in the genetic field, multifactorial pathogenesis of this blinding disease has made it difficult to identify definite genetic associations. In addition, variations in the severity of hyperglycemia and other systemic factors such as hyperlipidemia and blood pressure in the diabetic population have further compounded the problem.

EPIGENETICS MODIFICATIONS

Gene function is expressed in the form of protein, and changes in the DNA sequence can alter how it is transcribed into RNA, which eventually is coded for a particular protein. The expression of a gene is also affected by external factors, such as environment and lifestyle, and these 'epigenetic' changes can turn a gene 'on' and 'off' without altering the DNA sequence. Although epigenetic processes are essential to many organism functions, their up- or down-regulation can have major adverse health and behavioral effects; they are now implicated in many diseases including cancer, cardiovascular diseases and diabetes and its complications. Some of the major epigenetic modifications include methylation of cytosine (DNA methylation), methylation and acetylation of histones and noncoding RNAs (72). Methylation of the 5′ position of the cytosine forms 5-methyl cytosine (5mC), and this process is facilitated by DNA methyl transferases (Dnmts) and condenses the chromatin, both genomic DNA and mitochondrial DNA undergo methylation. However, dioxygenases-ten-eleven translocation (Tets) can rapidly convert 5mC to hydroxymethylated to 5-hydroxymethyl cytosine (5hmC), resulting in transcriptional activation (73–75). Lysine in the histone proteins can be acetylated, relaxing the chromatin structure to allow transcription factors binding, and this is modulated by a balance between acetyl transferring and removing enzymes, histone acetyltransferases and histone deacetylases, respectively (76–78). Lysine or arginine residues in a histone can also be modified by the addition of one, two, or three methyl groups, and methylation status of histones is also maintained by opposing enzymes, addition of methyl group by histone methyltransferases and removal of methyl group by demethylases. Unlike histone acetylation, gene repression or activation is determined by the site of methylation and the number of methyl groups (79, 80). Moreover, epigenetics modifications have potential to modify the gene expression independently, or one modification can lead to the other, to ultimately regulate gene expression (75, 81). Noncoding RNAs may not be the main epigenetic components, but they can also regulate gene expression without altering the DNA sequence.

Epigenetics Modifications and Mitochondrial Damage

The role of epigenetic modifications in many chronic diseases, such as cancer and Alzheimer disease, is being investigated for several years, and their role in diabetes and its complications is now emerging (82–85). In diabetes, Dnmts and Tets are activated in the retina and its vasculature, and dynamic DNA methylation-hydroxymethylation at the promoters of *Rac1* and *matrix metalloproteinase 9* is associated with their activation and mitochondrial damage. Furthermore, DNA at the promoter of

polymerase gamma, a gene associated with mtDNA biogenesis, and at *MutLH1* (associated with mtDNA damage repair) is hypermethylated, further damaging the mitochondria. Mitochondrial DNA itself is also hypermethylated in diabetes, which impairs its transcription resulting in a compromised electron transport chain system (41, 86, 87). Thus, epigenetics plays a vital role in maintaining mitochondrial homeostasis in diabetic retinopathy.

LncRNAs are now considered as a new class of epigenetic regulators because they can regulate epigenetic modification by modulating histone or DNA modifications, and can also act as a scaffold that interacts with epigenetic enzymes or methylation and acetylation complexes. LncRNAs can regulate histone methylation and acetylation simultaneously, subsequently regulating the gene expression (88). Thus, LncRNAs can epigenetically modify the expression of a gene without altering its DNA sequence.

LONG NONCODING RNAs AND DIABETIC RETINOPATHY

Leading scientists in the field have reviewed how LncRNAs play a role in the development of diabetic retinopathy, focusing mainly on inflammation and angiogenesis, but the field is still in its infancy. Many laboratories are now focusing on identifying LncRNAs associated with various metabolic and functional abnormalities implicated in the development of diabetic retinopathy (89–94). LncRNA profiling performed in the retina of streptozotocin-induced diabetic mice has shown over 300 LncRNAs that are aberrantly expressed at two months of diabetes, with 214 showing downregulation and 89 upregulation (95), and profiling in the fibrovascular membranes of patients with diabetic retinopathy have identified 427 differentially expressed LncRNAs, 263 upregulated and 164 downregulated (96). Both of these profiling studies have identified differentially expressed LncRNAs that are enriched in inflammatory and angiogenic pathways including Metastasis-associated lung adenocarcinoma transcript 1 (MALAT1), Hypoxia-inducible factor 1 HIF-1 and tumor necrosis factor alpha.

In diabetic retinopathy, Lnc*MALAT1*, which is one of the most highly expressed and conserved LncRNAs, is upregulated in the *in vivo* and *in vitro* models, and also in the circulation of the patients with diabetic retinopathy (97). Aqueous humor and fibrovascular membranes of diabetic patients also have increased Lnc*MALAT1* (95). Inhibition of Lnc*MALAT1* protects retinal photoreceptors, and alleviate diabetic neurodegeneration (98). Although Lnc*MALAT1* is implicated in normal physiologic functions such as vascular growth (99), its elevation in diabetes is shown to act both as pro-inflammatory and apoptotic (100–102). *MALAT1* sequence has NF-*k*B transcription factor binding sites, and NF-*k*B is intimately associated with the induction of proinflammatory cytokines; in diabetic retinopathy, NF-*k*B is activated and many proinflammatory cytokines are upregulated (59, 103). Upregulation of cytokines is shown to play a major role in the development of diabetic retinopathy; in fact, diabetic retinopathy is also considered as a low grade chronic inflammatory disease. In experimental models of diabetic retinopathy, Lnc*MALAT1* expression is augmented by hypoxia contributing to the proliferative response in endothelial cells (104). In retinal endothelial cells Lnc*MALAT1* inhibition ameliorates cell migration-angiogenesis, neurodegeneration and monocyte chemotactic protein-1, and also prevents inactivation of the master transcription factor, nuclear factor erythroid 2-related factor, Nrf2 (91, 98, 105). Our recent studies have documented an antioxidant defense role of Lnc*MALAT1* in diabetic retinopathy; *via* affecting the interactions of nuclear factor erythroid 2-related factor 2 (Nrf2) and its intracellular inhibitor Kelch-like ECH-associated protein 1, Lnc*MALAT1* upregulation suppresses transcriptional activity of Nrf2, and this impairs the transcription of antioxidant defense genes, such as heme oxygenase 1 and superoxide dismutase (91). Inhibition of LncRNA *MALAT1* alleviates diabetes-induced neurodegeneration (98). LncRNA, antisense RNA to INK4 locus (Lnc*ANRIL*) with binding sites for NF-*k*B, is also upregulated in diabetes, and is implicated tube formation-proliferation in endothelial cells *via* regulation of VEGF expression (106). Another LncRNA Myocardial infarction associated transcript (Lnc*MIAT*), is also regulated by NF-*k*B; high glucose increases the NF-*k*B and *MIAT* binding, further regulating inflammatory cytokines and apoptosis (107). LncRNA maternally expressed gene 3 (Lnc*MEG3*), which increases endoplasmic reticulum stress and inhibits cell proliferation (108), is considered to negatively correlate with VEGF, and in patients with diabetic retinopathy, while the serum levels of VEGF are upregulated, Lnc*MEG3* are downregulated (109). Another LncRNA HOX antisense intergenic RNA (Lnc*HOTAIR*) is upregulated in the vitreous of diabetic retinopathy patients and in retinal endothelial cells by high glucose, and its inhibition is shown to prevent increase in retinal vascular permeability and VEGF in diabetic rodents (110). Thus, the role of LncRNAs in inflammation, oxidative stress and angiogenesis is now at the forefront of ongoing research.

LONG NONCODING RNAs AND MITOCHONDRIAL HOMEOSTASIS IN DIABETIC RETINOPATHY

Mitochondrial dysfunction plays a critical role in many diabetic complications, and as mentioned above, in diabetic retinopathy damaged mitochondria accelerate apoptosis of capillary cells, which precedes the development of histopathology (48, 111). Retinal mitochondrial homeostasis is impaired, they become swollen and their damaged membranes leak cytochrome C in the cytosol, superoxide levels are elevated, mitochondrial dynamics are disturbed, mtDNA is damaged and mitochondrial genome-encoded genes including *cytochrome B* is downregulated, and the complex III of the electron transport chain is inhibited (41, 47). LncRNAs, whether encoded by mitochondria or nuclear genome, are also implicated in mitochondrial homeostasis, nuclear genome encoded Lnc*MALAT1* is translocated in the mitochondria of hepatoma cells, where it is shown to regulate mitochondrial apoptosis and mitophagy (25), and Lnc*MEG3, via* mitochondrial pathway, is

shown to induce renal cell carcinoma apoptosis (112). Mice with *MALAT1* knocked out have lower levels of ROS and protein carbonylation in hepatocyte and islets (113). Furthermore, Lnc*MALAT1* is also shown to interact with multiple loci on the mtDNA in hepatoma cells (114). In addition, Lnc*HOTAIR* induces mitochondria-mediated apoptosis in head and neck squamous cell carcinoma *via* Bcl-2-BAX-Caspase-3 pathway (115), and cardiac apoptosis-related LncRNA (Lnc*CARL*) suppresses mitochondrial fission (116). In diabetic nephropathy, nuclear genome encoded LncRNA taurine-upregulated gene 1 is shown to modulate mitochondrial biogenesis by directly interacting with PGC1α (117), and depletion of Nuclear Enriched Abundant Transcript 1 (Lnc*NEAT1)* is shown to alter mitochondrial dynamics (118). This clearly shows that many nuclear genome-encoded LncRNAs have potential to regulate mitochondrial function.

Focusing on diabetic retinopathy, our recent work has suggested a role of nuclear genome encoded Lnc*MALAT1* and Lnc*NEAT1* in regulation of mitochondrial functions, we have demonstrated that high glucose increases their mitochondrial localization in retinal endothelial cells, and siRNA of Lnc*MALAT1* or Lnc*NEAT1* prevents increase in ROS and alterations in mitochondrial membrane potential. As mentioned earlier, diabetes damages retinal mtDNA and impairs the transcription of mitochondrial genome-encoded genes, important for the functioning of the electron transport chain, which results in a vicious cycle of free radicals (41, 42, 119). Lnc*MALAT1* is shown to interact with multiple loci on mtDNA in hepatoma cells (114), and regulation of Lnc*MALAT1* or Lnc*NEAT1* by their respective siRNAs in retinal endothelial cells, prevents glucose-induced mtDNA damage and decrease in its transcription (93). Although mtDNA does not contain histones, it has nucleoprotein complexes, the nucleoids, and these nucleoids provide a stable environment for replication and repair of mtDNA (120). In addition, nucleoids also help in controlling mitochondrial metabolism in response to cellular demands (121, 122). Regulation of Lnc*MALAT1* or Lnc*NEAT1* also protects glucose-induced decrease in mtDNA nucleoids in retinal endothelial cells, suggesting a close cross-talk between nuclear genome-encoded LncRNAs and mitochondrial stability *via* their role(s) in increasing the vulnerability of the histone-free mtDNA in hyperglycemic milieu (**Figure 3**).

As reported above, mtDNA itself also encodes three LncRNAs, two of them transcribed from its L strand, and one from the H strand, the regions of the mitochondrial genome that are complementary to the genes that encode *ND5*, *cytochrome B* and *ND6* mRNAs (23, 24). Lnc*ND5*, Lnc*ND6* and Lnc*CytB* are 58, 34 and 14% as abundant as their complementary coding *ND5*, *ND6*, and *cytochrome B* mRNAs, and these LncRNAs primarily form intermolecular duplexes with their respective complementary mRNAs, suggesting their functional role in either stabilizing or regulating their partner mRNAs (23, 24). Their role in metabolism/diseases, however, is still unclear. Our recent work (unpublished) has demonstrated decreased expression of Ln*CytB* in retinal endothelial cells in high glucose conditions, and shown its role in protecting mtDNA vulnerability to nuclease damage and *cytochrome B* expression; overexpression of Ln*CytB* ameliorates glucose-induced increase in mtDNA damage, decrease in mitochondrial genome-encoded nucleoids and decrease in *cytochrome B* expression. These studies have suggested that downregulation of Lnc*CytB* in the mitochondria in hyperglycemic milieu reduces the protective nucleoids, which makes mtDNA more susceptible to the damage. The damaged mtDNA compromises the electron transport chain and the vicious cycle of free radicals continues to self-propagate, thus implying an important role of this mitochondrial genome-encoded LncRNA in mitochondrial homeostasis in diabetic retinopathy. Although our initial results show significant decrease in Lnc*CytB*, we do not see any significant decrease in the other two mitochondrial genome-encoded LncRNAs-Lnc*ND5* or Lnc*ND6* in either *in vitro* or *in vivo* models of diabetic retinopathy. Despite significantly lower abundance of Lnc*CytB* is significantly lower compared to the other two mitochondrial genome-encoded LncRNAs, complex III is considered to play a major role in superoxide generation in diabetic retinopathy, and the activity of complex III, but not complex I, is downregulated (2, 38, 40)

As described above, nuclear genome-encoded LncRNAs can move inside the mitochondria and regulate mitochondrial homeostasis, and aberrant transport of mitochondrial genome-

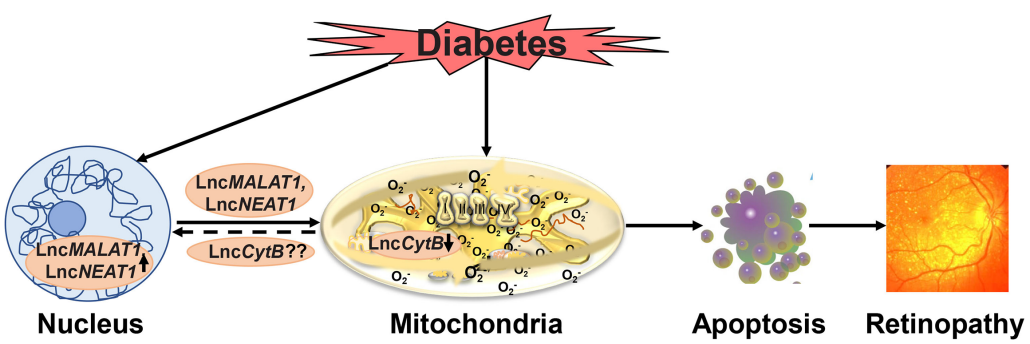

FIGURE 3 | Hyperglycemic environment damages mitochondria and also elevates levels of various nuclear genome encoded LncRNAs including Lnc*MALAT1* and Lnc*NEAT1*. These LncRNAs, in addition to affecting metabolic abnormalities associated with diabetic retinopathy including inflammation, also move inside the mitochondria, and damage mitochondrial structural, functional and genomic stability. Furthermore, possible decrease in the mitochondrial genome encoded Lnc*CytB* further damages the mitochondria, and the damaged mitochondria accelerates apoptosis, ultimately, resulting in the development of diabetic retinopathy.

encoded Lnc*CytB* in the nucleus of hepatoma HepG2 cells as compared with normal hepatic HL7702 cells suggests that the aberrant shuttling of LncRNAs in mitochondria-nucleus crosstalk could be important for abnormal energy metabolism in malignant cells (25). Weather mitochondrial genome-encoded LncRNAs also translocate outside the mitochondria in diabetic retinopathy needs investigation.

The focus of this review thus far has been on how LncRNAs can directly affect mitochondrial homeostasis in diabetic retinopathy, but many epigenetic modifications including histone modifications and methylation of DNA of many genes associated with mitochondrial metabolism and mitochondrial DNA itself, also affect mitochondrial stability (47, 87). Long noncoding RNAs are considered to play a significant role in regulating histone modifications and DNA methylation, for example, Lnc*HOTAIR* is shown to interact with the histone modifying polycomb repressive complex II and histone demethylase 1 (LSD1) (18). In diabetic retinopathy, LSD1 is activated, and its recruitment at the promoter of mitochondrial damaging matrix metalloproteinase-9 is increased. Silencing of LSD1 prevents hyperglycemia-induced damage to mitochondrial structure and function in retinal endothelial cells, suggesting an important role of this enzyme in mitochondrial homeostasis in diabetic retinopathy (123). Furthermore, in hyperglycemic milieu, *MALAT1* silencing directly reduces Enhancer of Zeste homolog 2 (Ezh2), an enzyme which catalyzes dimethylation/trimethylation of histone 3 lysine 27 (90), and Ezh2 activation in diabetes helps recruit DNA methylation enzymes at the promoter of *matrix metalloproteinase-9*, activating its transcription (124). Also, role of LncRNAs in regulating methylation of mtDNA or DNA at the promoters of other genes important genes associated with mitochondrial homeostasis needs further investigation. LncRNAs can also act as microRNA sponges, and in retinal pigment epithelium cells exposed to high glucose, upregulation of miR-34a is reversed by upregulation of MEG3 and Sirtuin 1 (125); overexpression of Sirtuin1 prevents mitochondrial damage and the development of retinopathy in diabetic mice (126). Lnc*MALAT1*, *via* targeting mi125b, inhibits glucose-induced angiogenesis in retinal endothelial cells (127). As the list of miRNAs implicated in the development of diabetic retinopathy grows, their interactions with LncRNAs in diabetic retinopathy is an open area that would need further attention.

LONG NONCODING RNAs AS BIOMARKERS AND THERAPEUTIC OPTIONS

Recent technical advances have allowed the LncRNA field to make great progress, the list of LncRNAs and their potential association with diseases is expanding rapidly, and their relatively stable nature in the body fluids, ease of obtaining body fluids and detecting them using commonly used molecular biology techniques makes them attractive biomarker candidates (128, 129). The results of a meta-analysis using data from over 1400 patients have shown that LncRNAs can serve as promising diagnostic biomarkers (130). For example, higher levels of LncRNA *LIPCAR* are associated with a higher risk of cardiovascular mortality (131), and LncRNA *NONHSAT112178* can be a possible predictive biomarkers for coronary artery disease (132), Lnc*HOTAIR* is highly expressed in saliva samples of oral squamous cells from carcinoma patients, making it a strong candidate for metastatic oral cancer diagnosis (133), and Lnc*MALAT1* is elevated in plasma and urine of prostate cancer patients (134). In diabetic retinopathy, Lnc*HOTAIR* and Lnc*MALAT1* have shown some discrimination between patients with nonproliferative and proliferative retinopathy (135) and plasma and aqueous humor levels of LncRNA small nucleolar RNA host gene 5 are negatively correlated with the development of diabetic macular edema (136). A recent study has shown a strong correlation between the differential expressions of nine LncRNAs including Lnc*ANRIL*, Lnc*HOTAIR* and Lnc*MIAT*, in the vitreous and serum samples of patients with or without diabetic retinopathy; these promising results suggest the possible use of serum LncRNAs as a potential biomarker of diabetic retinopathy, however, their validation in a larger cohort is needed (137). Thus, many LncRNA are now being implicated in regulating various pathways associated with the development of diabetic retinopathy, and future research and technical advancements may show us their role as biomarker or therapeutic target for its development, and/or its progression.

Like any new technology, LncRNA field also faces some challenges- the transcriptome studies suggest that ~80% of the genome is transcribed into RNA (138), but it is not clear how many of those LncRNAs are functional and what concentration of that LncRNA is required to achieve their biological effect. Also, LncRNAs can affect gene expression *via* many different mechanisms, it is difficult to predict how many different mechanisms one single LncRNA might use to control expression of a gene in a given disease. Fortunately, technical advances in genome editing and in surveying LncRNA molecular mechanisms have significantly advanced our ability to definitively characterize function of LncRNAs, making these molecules attractive targets for therapeutic intervention for diabetic retinopathy. LncRNAs in the mitochondria are also being investigated as potential blood-based biomarkers for cardiac remodeling in patients with hypertrophic cardiomyopathy (139), and with additional research in the field and technical advancements, their use in maintaining mitochondrial homeostasis in diabetic retinopathy is very optimistic, which will give diabetic patients hope of not losing their vision.

AUTHOR CONTRIBUTIONS

The author confirms being the sole contributor of this work and has approved it for publication.

FUNDING

This article based on the work supported in part by grants from the National Institutes of Health (EY014370, EY017313, and

EY022230) and from The Thomas Foundation to RK, and an unrestricted grant from Research to Prevent Blindness from the Department of Ophthalmology, Wayne State University.

ACKNOWLEDGMENTS

The author thanks her laboratory associates (past and present) for their contributions to the work cited in this review article.

REFERENCES

1. Sun H, Saeedi P, Karuranga S, Pinkepank M, Ogurtsova K, Duncan BB, et al. IDF Diabetes Atlas: Global, Regional and Country-Level Diabetes Prevalence Estimates for 2021 and Projections for 2045. *Diabetes Res Clin Pract* (2022) 183:109119. doi: 10.1016/j.diabres.2021.109119
2. Brownlee M. The Pathobiology of Diabetic Complications: A Unifying Mechanism. *Diabetes* (2005) 54:1615–25. doi: 10.2337/diabetes.54.6.1615
3. Deshpande AD, Harris-Hayes M, Schootman M. Epidemiology of Diabetes and Diabetes-Related Complications. *Phys Ther* (2008) 88:1254–64. doi: 10.2522/ptj.20080020
4. Bär C, Chatterjee S, Thum T. Long Noncoding RNAs in Cardiovascular Pathology, Diagnosis, and Therapy. *Circulation* (2016) 134:1484–99. doi: 10.1161/circulationaha.116.023686
5. Ma L, Cao J, Liu L, Du Q, Li Z, Zou D, et al. LncBook: A Curated Knowledgebase of Human Long Non-Coding RNAs. *Nucleic Acids Res* (2019) 47:D128–d134. doi: 10.1093/nar/gky960
6. Pescosolido N, Barbato A, Stefanucci A, Buomprisco G. Role of Electrophysiology in the Early Diagnosis and Follow-Up of Diabetic Retinopathy. *J Diabetes Res* (2015) 2015:319692. doi: 10.1155/2015/319692
7. Beermann J, Piccoli MT, Viereck J, Thum T. Non-Coding RNAs in Development and Disease: Background, Mechanisms, and Therapeutic Approaches. *Physiol Rev* (2016) 96:1297–325. doi: 10.1152/physrev.00041.2015
8. Chan JJ, Tay Y. Noncoding RNA:RNA Regulatory Networks in Cancer. *Int J Mol Sci* (2018) 19:1310. doi: 10.3390/ijms19051310
9. Hammond SM. An Overview of microRNAs. *Adv Drug Deliv Rev* (2015) 87:3–14. doi: 10.1016/j.addr.2015.05.001
10. Beck ZT, Xing Z, Tran EJ. LncRNAs: Bridging Environmental Sensing and Gene Expression. *RNA Biol* (2016) 13:1189–96. doi: 10.1080/15476286.2016.1240139
11. Fabian MR, Sonenberg N, Filipowicz W. Regulation of mRNA Translation and Stability by microRNAs. *Annu Rev Biochem* (2010) 79:351–79. doi: 10.1146/annurev-biochem-060308-103103
12. Rafiee A, Riazi-Rad F, Havaskary M, Nuri F. Long Noncoding RNAs: Regulation, Function and Cancer. *Biotechnol Genet Eng Rev* (2018) 34:153–80. doi: 10.1080/02648725.2018.1471566
13. Washietl S, Pedersen JS, Korbel JO, Stocsits C, Gruber AR, Hackermüller J, et al. Structured RNAs in the ENCODE Selected Regions of the Human Genome. *Genome Res* (2007) 17:852–64. doi: 10.1101/gr.5650707
14. Cabili MN, Trapnell C, Goff L, Koziol M, Tazon-Vega B, Regev A, et al. Integrative Annotation of Human Large Intergenic Noncoding RNAs Reveals Global Properties and Specific Subclasses. *Genes Dev* (2011) 25:1915–27. doi: 10.1101/gad.17446611
15. Cabili MN, Dunagin MC, McClanahan PD, Biaesch A, Padovan-Merhar O, Regev A, et al. Localization and Abundance Analysis of Human lncRNAs at Single-Cell and Single-Molecule Resolution. *Genome Biol* (2015) 16:20. doi: 10.1186/s13059-015-0586-4
16. Bhat SA, Ahmad SM, Mumtaz PT, Malik AA, Dar MA, Urwat U, et al. Long Non-Coding RNAs: Mechanism of Action and Functional Utility. *Noncoding RNA Res* (2016) 1:43–50. doi: 10.1016/j.ncrna.2016.11.002
17. Fang Y, Fullwood MJ. Roles, Functions, and Mechanisms of Long Non-Coding RNAs in Cancer. *Genomics Proteomics Bioinf* (2016) 14:42–54. doi: 10.1016/j.gpb.2015.09.006
18. Schmitz SU, Grote P, Herrmann BG. Mechanisms of Long Noncoding RNA Function in Development and Disease. *Cell Mol Life Sci* (2016) 73:2491–509. doi: 10.1007/s00018-016-2174-5
19. Dietrich A, Wallet C, Iqbal RK, Gualberto JM, Lotfi F. Organellar Non-Coding RNAs: Emerging Regulation Mechanisms. *Biochimie* (2015) 117:48–62. doi: 10.1016/j.biochi.2015.06.027
20. Gordon AD, Biswas S, Feng B, Chakrabarti S. MALAT1: A Regulator of Inflammatory Cytokines in Diabetic Complications. *Endocrinol Diabetes Metab* (2018) 1:e00010–0. doi: 10.1002/edm2.10
21. Han L, Yang L. Multidimensional Mechanistic Spectrum of Long Non-Coding RNAs in Heart Development and Disease. *Front Cardiovasc Med* (2021) 8:728746. doi: 10.3389/fcvm.2021.728746
22. Bridges MC, Daulagala AC, Kourtidis A. LNCcation: lncRNA Localization and Function. *J Cell Biol* (2021) 220:e202009045. doi: 10.1083/jcb.202009045
23. Mercer TR, Neph S, Dinger ME, Crawford J, Smith MA, Shearwood AM, et al. The Human Mitochondrial Transcriptome. *Cell* (2011) 146:645–58. doi: 10.1016/j.cell.2011.06.051
24. Dong Y, Yoshitomi T, Hu JF, Cui J. Long Noncoding RNAs Coordinate Functions Between Mitochondria and the Nucleus. *Epigenet Chromatin* (2017) 10:41. doi: 10.1186/s13072-017-0149-x
25. Zhao Y, Liu S, Zhou L, Li X, Meng Y, Li Y, et al. Aberrant Shuttling of Long Noncoding RNAs During the Mitochondria-Nuclear Crosstalk in Hepatocellular Carcinoma Cells. *Am J Cancer Res* (2019) 9:999–1008.
26. Faghihi MA, Modarresi F, Khalil AM, Wood DE, Sahagan BG, Morgan TE, et al. 3rd; Kenny, P.J.; Wahlestedt, C. Expression of a Noncoding RNA Is Elevated in Alzheimer's Disease and Drives Rapid Feed-Forward Regulation of Beta-Secretase. *Nat Med* (2008) 14:723–30. doi: 10.1038/nm1784
27. Sun M, Kraus WL. From Discovery to Function: The Expanding Roles of Long Noncoding RNAs in Physiology and Disease. *Endocr Rev* (2015) 36:25–64. doi: 10.1210/er.2014-1034
28. Singer RA, Sussel L. Islet Long Noncoding RNAs: A Playbook for Discovery and Characterization. *Diabetes* (2018) 67:1461–70. doi: 10.2337/dbi18-0001
29. Simion V, Haemmig S, Feinberg MW. LncRNAs in Vascular Biology and Disease. *Vascul Pharmacol* (2019) 114:145–56. doi: 10.1016/j.vph.2018.01.003
30. Tanwar VS, Reddy MA, Natarajan R. Emerging Role of Long Non-Coding RNAs in Diabetic Vascular Complications. *Front Endocrinol (Lausanne)* (2021) 12:665811. doi: 10.3389/fendo.2021.665811
31. Aiello LP, Gardner TW, King GL, Blankenship G, Cavallerano JD, Ferris FL, et al. Diabetic Retinopathy. *Diabetes Care* (1998) 21:143–56. doi: 10.2337/diacare.21.1.143
32. Cheung N, Mitchell P, Wong TY. Diabetic Retinopathy. *Lancet* (2010) 376:124–36. doi: 10.1016/S0140-6736(09)62124-3
33. Teo ZL, Tham YC, Yu M, Chee ML, Rim TH, Cheung N, et al. Global Prevalence of Diabetic Retinopathy and Projection of Burden through 2045: Systematic Review and Meta-analysis. *Ophthalmology* (2021) 128:1580–91. doi: 10.1016/j.ophtha.2021.04.027
34. Aung MH, Kim MK, Olson DE, Thule PM, Pardue MT. Early Visual Deficits in Streptozotocin-Induced Diabetic Long Evans Rats. *Invest Ophtahlmol Vis Sci* (2013) 54:1370–7. doi: 10.1167/iovs.12-10927
35. Barber AJ, Baccouche B. Neurodegeneration in Diabetic Retinopathy: Potential for Novel Therapies. *Vision Res* (2017) 139:82–92. doi: 10.1016/j.visres.2017.06.014
36. Antonetti DA, Silva PS, Stitt AW. Current Understanding of the Molecular and Cellular Pathology of Diabetic Retinopathy. *Nat Rev Endocrinol* (2021) 17:195–206. doi: 10.1038/s41574-020-00451-4
37. Ng DS, Chiang PP, Tan G, Cheung CG, Cheng CY, Cheung CY, et al. Retinal Ganglion Cell Neuronal Damage in Diabetes and Diabetic Retinopathy. *Clin Exp Ophthalmol* (2016) 44:243–50. doi: 10.1111/ceo.12724
38. Kanwar M, Chan PS, Kern TS, Kowluru RA. Oxidative Damage in the Retinal Mitochondria of Diabetic Mice: Possible Protection by Superoxide Dismutase. *Invest Ophtahlmol Vis Sci* (2007) 48:3805–11. doi: 10.1167/iovs.06-1280
39. Kowluru RA. Diabetic Retinopathy, Oxidative Stress and Antioxidants. *Curr Topics Nutraceutical Res* (2005) 3:209–18.
40. Giacco F, Brownlee M. Oxidative Stress and Diabetic Complications. *Circ Res* (2010) 107:1058–70. doi: 10.1161/CIRCRESAHA.110.223545

41. Kowluru RA. Mitochondrial Stability in Diabetic Retinopathy: Lessons Learned From Epigenetics. *Diabetes* (2019) 68:241–7. doi: 10.2337/dbi18-0016
42. Kowluru RA, Mishra M. Oxidative Stress, Mitochondrial Damage and Diabetic Retinopathy. *Biochim Biophys Acta* (2015) 1852:2474–83. doi: 10.1016/j.bbadis.2015.08.001
43. Anderson RE, Rapp LM, Wiegand RD. Lipid Peroxidation and Retinal Degeneration. *Curr Eye Res* (1984) 3:223–7. doi: 10.3109/02713688408997203
44. Kowluru RA, Mishra M. Regulation of Matrix Metalloproteinase in the Pathogenesis of Diabetic Retinopathy. *Prog Mol Biol Transl Sci* (2017) 148:67–85. doi: 10.1016/bs.pmbts.2017.02.004
45. Sahajpal N, Kowluru A, Kowluru RA. The Regulatory Role of Rac1, a Small Molecular Weight GTPase, in the Development of Diabetic Retinopathy. *J Clin Med* (2019) 8:965. doi: 10.3390/jcm8070965
46. Madsen-Bouterse SA, Mohammad G, Kanwar M, Kowluru RA. Role of Mitochondrial DNA Damage in the Development of Diabetic Retinopathy, and the Metabolic Memory Phenomenon Associated With Its Progression. *Antioxid Redox Signal* (2010) 13:797–805. doi: 10.1089/ars.2009.2932
47. Kowluru RA, Kowluru A, Mishra M, Kumar B. Oxidative Stress and Epigenetic Modifications in the Pathogenesis of Diabetic Retinopathy. *Prog Retin Eye Res* (2015) 48:40–61. doi: 10.1016/j.preteyeres.2015.05.001
48. Mizutani M, Kern TS, Lorenzi M. Accelerated Death of Retinal Microvascular Cells in Human and Experimental Diabetic Retinopathy. *J Clin Invest* (1996) 97:2883–90. doi: 10.1172/JCI118746
49. Tewari S, Santos JM, Kowluru RA. Damaged Mitochondrial DNA Replication System and the Development of Diabetic Retinopathy. *Antioxid Redox Signal* (2012) 17:492–504. doi: 10.1089/ars.2011.4333
50. Mohammad G, Radhakrishnan R, Kowluru RA. Epigenetic Modifications Compromise Mitochondrial DNA Quality Control in the Development of Diabetic Retinopathy. *Invest Ophthalmol Vis Sci* (2019) 60:3943–51. doi: 10.1167/iovs.19-27602
51. Duraisamy AJ, Mohammad G, Kowluru RA. Mitochondrial Fusion and Maintenance of Mitochondrial Homeostasis in Diabetic Retinopathy. *Biochim Biophys Acta Mol Basis Dis* (2019) 1865:1617–26. doi: 10.1016/j.bbadis.2019.03.013
52. Mohammad G, Kowluru RA. Mitochondrial Dynamics in the Metabolic Memory of Diabetic Retinopathy. *J Diabetes Res* (2022) 2022:3555889. doi: 10.1155/2022/3555889
53. Katakami N, Kaneto H, Takahara M, Matsuoka TA, Imamura K, Ishibashi F, et al. Aldose Reductase C-106T Gene Polymorphism Is Associated With Diabetic Retinopathy in Japanese Patients With Type 2 Diabetes. *Diabetes Res Clin Pract* (2011) 92:e57–60. doi: 10.1016/j.diabres.2011.02.017
54. Sorbinil Retinopathy Trial Research Group. A Randomized Trial of Sorbinil, an Aldose Reductase Inhibitor, in Diabetic Retinopathy. *Arch Ophthalmol* (1990) 108:1234–44. doi: 10.1001/archopht.1990.01070110050024
55. Ott C, Jacobs K, Haucke E, Navarrete Santos A, Grune T, Simm A. Role of Advanced Glycation End Products in Cellular Signaling. *Redox Biol* (2014) 2:411–29. doi: 10.1016/j.redox.2013.12.016
56. Stitt AW. AGEs and Diabetic Retinopathy. *Invest Ophtahlmol Vis Sci* (2010) 51:4867–74. doi: 10.1167/iovs.10-5881
57. Geraldes P, Hiraoka-Yamamoto J, Matsumoto M, Clermont A, Leitges M, Marette A, et al. Activation of PKC-Delta and SHP-1 by Hyperglycemia Causes Vascular Cell Apoptosis and Diabetic Retinopathy. *Nat Med* (2009) 15:1298–306. doi: 10.1038/nm.2052
58. Nishikawa T, Edelstein D, Brownlee M. THe Missing Link: A Single Unifying Mechanism for Diabetic Complications. *Kidney Int Supplement* (2000) 77:S26–30. doi: 10.1046/j.1523-1755.2000.07705.x
59. Kern TS. Contributions of Inflammatory Processes to the Development of the Early Stages of Diabetic Retinopathy. *Exp Diabetes Res* (2007) 2007:95103. doi: 10.1155/2007/95103
60. Rübsam A, Parikh S, Fort PE. Role of Inflammation in Diabetic Retinopathy. *Int J Mol Sci* (2018) 19:942. doi: 10.3390/ijms19040942
61. Frank RN. Diabetic Retinopathy and Systemic Factors. *Middle East Afr J Ophthalmol* (2015) 22:151–6. doi: 10.4103/0974-9233.154388
62. Kowluru RA. Diabetic Retinopathy and NADPH Oxidase-2: A Sweet Slippery Road. *Antioxid (Basel)* (2021) 10:783. doi: 10.3390/antiox10050783
63. Abhary S, Hewitt AW, Burdon KP, Craig JE. A Systematic Meta-Analysis of Genetic Association Studies for Diabetic Retinopathy. *Diabetes* (2009) 58:2137–47. doi: 10.2337/db09-0059
64. Tariq K, Malik SB, Ali SH, Maqsood SE, Azam A, Muslim I, et al. Association of Pro12Ala Polymorphism in Peroxisome Proliferator Activated Receptor Gamma With Proliferative Diabetic Retinopathy. *Mol Vision* (2013) 19:710–7.
65. Penman A, Hoadley S, Wilson JG, Taylor HA, Chen CJ, Sobrin L.. P-selectin Plasma Levels and Genetic Variant Associated With Diabetic Retinopathy in African Americans. *Am J Ophthalmol* (2015) 159:1152–1160.e1152. doi: 10.1016/j.ajo.2015.03.008
66. Cilensek I, Mankoc S, Globocnik Petrovic M, Petrovic D. The 4a/4a Genotype of the VNTR Polymorphism for Endothelial Nitric Oxide Synthase (eNOS) Gene Predicts Risk for Proliferative Diabetic Retinopathy in Slovenian Patients (Caucasians) With Type 2 Diabetes Mellitus. *Mol Biol Rep* (2012) 39:7061–7. doi: 10.1007/s11033-012-1537-8
67. Lin HJ, Huang YC, Lin JM, Wu JY, Chen LA, Tsai FJ. Association of Genes on Chromosome 6, GRIK2 , TMEM217 and TMEM63B (Linked to MRPL14) With Diabetic Retinopathy. *Ophthalmologica* (2013) 229:54–60. doi: 10.1159/000342616
68. Sobrin L, Susarla G, Stanwyck L, Rouhana JM, Li A, Pollack S, et al. Gene Set Enrichment Analsyes Identify Pathways Involved in Genetic Risk for Diabetic Retinopathy. *Am J Ophthalmol* (2022) 233:111–23. doi: 10.1016/j.ajo.2021.06.014
69. Dahlstrom E, Sandholm N. Progress in Defining the Genetic Basis of Diabetic Complications. *Curr Diabetes Rep* (2017) 17:80. doi: 10.1007/s11892-017-0906-z
70. Cheung CY, Hui EY, Lee CH, Kwok KH, Gangwani RA, Li KK, et al. Impact of Genetic Loci Identified in Genome-Wide Association Studies on Diabetic Retinopathy in Chinese Patients With Type 2 Diabetes. *Invest Ophtahlmol Vis Sci* (2016) 57:5518–24. doi: 10.1167/iovs.16-20094
71. Looker HC, Nelson RG, Chew E, Klein R, Klein BE, Knowler WC, et al. Genome-Wide Linkage Analyses to Identify Loci for Diabetic Retinopathy. *Diabetes* (2007) 56:1160–6. doi: 10.2337/db06-1299
72. Handy DE, Castro R, Loscalzo J. Epigenetic Modifications: Basic Mechanisms and Role in Cardiovascular Disease. *Circulation* (2011) 123:2145–56. doi: 10.1161/CIRCULATIONAHA.110.956839
73. Zhu JK. Active DNA Demethylation Mediated by DNA Glycosylases. *Annu Rev Genet* (2009) 43:143–66. doi: 10.1146/annurev-genet-102108-134205
74. Wu H, Zhang Y. Reversing DNA Methylation: Mechanisms, Genomics, and Biological Functions. *Cell* (2014) 156:45–68. doi: 10.1016/j.cell.2013.12.019
75. Du J, Johnson LM, Jacobsen SE, Patel DJ. DNA Methylation Pathways and Their Crosstalk With Histone Methylation. *Nat Rev Mol Cell Biol* (2015) 16:519–32. doi: 10.1038/nrm4043
76. Strahl BD, Allis CD. The Language of Covalent Histone Modifications. *Nature* (2000) 403:41–5. doi: 10.1038/47412
77. Vaissiere T, Sawan C, Herceg Z. Epigenetic Interplay Between Histone Modifications and DNA Methylation in Gene Silencing. *Mutat Res* (2008) 659:40–8. doi: 10.1016/j.mrrev.2008.02.004
78. Xu YM, Du JY, Lau AT. Posttranslational Modifications of Human Histone H3: An Update. *Proteomics* (2014) 14:2047–60. doi: 10.1002/pmic.201300435
79. Martin C, Zhang Y. The Diverse Functions of Histone Lysine Methylation. *Nat Rev Mol Cell Biol* (2005) 6:838–49. doi: 10.1038/nrm1761
80. Black JC, Van Rechem C, Whetstine JR. Histone Lysine Methylation Dynamics: Establishment, Regulation, and Biological Impact. *Mol Cell* (2012) 48:491–507. doi: 10.1016/j.molcel.2012.11.006
81. Molina-Serrano D, Schiza V, Kirmizis A. Cross-Talk Among Epigenetic Modifications: Lessons From Histone Arginine Methylation. *Biochem Soc Trans* (2013) 41:751–9. doi: 10.1042/bst20130003
82. Bird A. Perceptions of Epigenetics. *Nature* (2007) 447:396–8. doi: 10.1038/nature05913
83. Cooper ME, El-Osta A. Epigenetics: Mechanisms and Implications for Diabetic Complications. *Circ Res* (2010) 107:1403–13. doi: 10.1161/CIRCRESAHA.110.223552
84. Shanmugam MK, Sethi G. Role of Epigenetics in Inflammation-Associated Diseases. *Subcell Biochem* (2012) 61:627–57. doi: 10.1007/978-94-007-4525-4_27

85. Tammen SA, Friso S, Choi SW. Epigenetics: The Link Between Nature and Nurture. *Mol Aspects Med* (2013) 34:753–64. doi: 10.1016/j.mam.2012.07.018
86. Kowluru RA, Mohammad G. Epigenetic Modifications in Diabetes. *Metabolism* (2021) 126:154920. doi: 10.1016/j.metabol.2021.154920
87. Mishra M, Kowluru RA. Epigenetic Modification of Mitochondrial DNA in the Development of Diabetic Retinopathy. *Invest Ophthalmol Vis Sci* (2015) 56:5133–42. doi: 10.1167/iovs.15-16937
88. Zhang X, Wang W, Zhu W, Dong J, Cheng Y, Yin Z, et al. Mechanisms and Functions of Long Non-Coding RNAs at Multiple Regulatory Levels. *Int J Mol Sci* (2019) 20:5573. doi: 10.3390/ijms20225573
89. Raut SK, Khullar M. The Big Entity of New RNA World: Long Non-Coding RNAs in Microvascular Complications of Diabetes. *Front Endocrinol (Lausanne)* (2018) 9:300. doi: 10.3389/fendo.2018.00300
90. Biswas S, Sarabusky M, Chakrabarti S. Diabetic Retinopathy, lncRNAs, and Inflammation: A Dynamic, Interconnected Network. *J Clin Med* (2019) 8:1033. doi: 10.3390/jcm8071033
91. Radhakrishnan R, Kowluru RA. Long Noncoding RNA MALAT1 and Regulation of the Antioxidant Defense System in Diabetic Retinopathy. *Diabetes* (2021) 70:227–39. doi: 10.2337/db20-0375
92. Huang Q, Li J. Research Progress of lncRNAs in Diabetic Retinopathy. *Eur J Ophthalmol* (2021) 31:1606–17. doi: 10.1177/1120672120970401
93. Mohammad G, Kowluru RA. Nuclear Genome-Encoded Long Noncoding RNAs and Mitochondrial Damage in Diabetic Retinopathy. *Cells* (2021) 10:3271. doi: 10.3390/cells10123271
94. Lu X, Tan Q, Ma J, Zhang J, Yu P. Emerging Role of LncRNA Regulation for NLRP3 Inflammasome in Diabetes Complications. *Front Cell Dev Biol* (2021) 9:792401. doi: 10.3389/fcell.2021.792401
95. Yan B, Tao ZF, Li XM, Zhang H, Yao J, Jiang Q. Aberrant Expression of Long Noncoding RNAs in Early Diabetic Retinopathy. *Invest Ophthalmol Vis Sci* (2014) 55:941–51. doi: 10.1167/iovs.13-13221
96. Wang J, Gao X, Liu J, Wang J, Zhang Y, Zhang T, et al. Effect of Intravitreal Conbercept Treatment on the Expression of Long Noncoding RNAs and mRNAs in Proliferative Diabetic Retinopathy Patients. *Acta Ophthalmol* (2019) 97:e902–12. doi: 10.1111/aos.14083
97. Alfaifi M, Ali Beg MM, Alshahrani MY, Ahmad I, Alkhathami AG, Joshi PC, et al. Circulating Long Non-Coding RNAs NKILA, NEAT1, MALAT1, and MIAT Expression and Their Association in Type 2 Diabetes Mellitus. *BMJ Open Diabetes Res Care* (2021) 9:e001821. doi: 10.1136/bmjdrc-2020-001821
98. Zhang YL, Hu HY, You ZP, Li BY, Shi K. Targeting Long Non-Coding RNA MALAT1 Alleviates Retinal Neurodegeneration in Diabetic Mice. *Int J Ophthalmol* (2020) 13:213–9. doi: 10.18240/ijo.2020.02.03
99. Zhang X, Tang X, Liu K, Hamblin MH, Yin K-J. Long Noncoding RNA Malat1 Regulates Cerebrovascular Pathologies in Ischemic Stroke. *J Neurosci* (2017) 37:1797–806. doi: 10.1523/JNEUROSCI.3389-16.2017
100. Sathishkumar C, Prabu P, Mohan V, Balasubramanyam M. Linking a Role of lncRNAs (Long Non-Coding RNAs) With Insulin Resistance, Accelerated Senescence, and Inflammation in Patients With Type 2 Diabetes. *Hum Genomics* (2018) 12:41. doi: 10.1186/s40246-018-0173-3
101. Biswas S, Thomas AA, Chen S, Aref-Eshghi E, Feng B, Gonder J, et al. MALAT1: An Epigenetic Regulator of Inflammation in Diabetic Retinopathy. *Sci Rep* (2018) 8:6526. doi: 10.1038/s41598-018-24907-w
102. Abdulle LE, Hao JL, Pant OP, Liu XF, Zhou DD, Gao Y, et al. MALAT1 as a Diagnostic and Therapeutic Target in Diabetes-Related Complications: A Promising Long-Noncoding RNA. *Int J Med Sci* (2019) 16:548–55. doi: 10.7150/ijms.30097
103. Kowluru RA, Koppolu P, Chakrabarti S, Chen S. Diabetes-Induced Activation of Nuclear Transcriptional Factor in the Retina, and Its Inhibition by Antioxidants. *Free Radic Res* (2003) 37:1169–80. doi: 10.1080/10715760310001604189
104. Kolling M, Genschel C, Kaucsar T, Hubner A, Rong S, Schmitt R, et al. Hypoxia-Induced Long Non-Coding RNA Malat1 Is Dispensable for Renal Ischemia/reperfusion-Injury. *Sci Rep* (2018) 8:3438. doi: 10.1038/s41598-018-21720-3
105. Dong N, Xu B, Shi H. Long Noncoding RNA MALAT1 Acts as a Competing Endogenous RNA to Regulate Amadori-Glycated Albumin-Induced MCP-1 Expression in Retinal Microglia by a microRNA-124-Dependent Mechanism. *Inflammation Res* (2018) 67:913–25. doi: 10.1007/s00011-018-1184-1
106. Thomas AA, Feng B, Chakrabarti S. ANRIL: A Regulator of VEGF in Diabetic Retinopathy. *Invest Ophtahlmol Vis Sci* (2017) 58:470–80. doi: 10.1167/iovs.16-20569
107. Zhang J, Chen M, Chen J, Lin S, Cai D, Chen C, et al. Long Non-Coding RNA MIAT Acts as a Biomarker in Diabetic Retinopathy by Absorbing miR-29b and Regulating Cell Apoptosis. *Biosci Rep* (2017) 37:BSR20170036. doi: 10.1042/bsr20170036
108. Wang G, Ye Q, Ning S, Yang Z, Chen Y, Zhang L, et al. LncRNA MEG3 Promotes Endoplasmic Reticulum Stress and Suppresses Proliferation and Invasion of Colorectal Carcinoma Cells Through the MEG3/miR-103a-3p/PDHB ceRNA Pathway. *Neoplasma* (2021) 68:362–74. doi: 10.4149/neo_2020_200813N858
109. Zhang D, Qin H, Leng Y, Li X, Zhang L, Bai D, et al. LncRNA MEG3 Overexpression Inhibits the Development of Diabetic Retinopathy by Regulating TGF-β1 and VEGF. *Exp Ther Med* (2018) 16:2337–42. doi: 10.3892/etm.2018.6451
110. Biswas S, Feng B, Chen S, Liu J, Aref-Eshghi E, Gonder J, et al. The Long Non-Coding RNA HOTAIR Is a Critical Epigenetic Mediator of Angiogenesis in Diabetic Retinopathy. *Invest Ophtahlmol Vis Sci* (2021) 62:20. doi: 10.1167/iovs.62.3.20
111. Kowluru RA, Abbas SN. Diabetes-Induced Mitochondrial Dysfunction in the Retina. *Invest Ophtahlmol Vis Sci* (2003) 44:5327–34. doi: 10.1167/iovs.03-0353
112. Wang M, Huang T, Luo G, Huang C, Xiao X-Y, Wang L, et al. Long Non-Coding RNA MEG3 Induces Renal Cell Carcinoma Cells Apoptosis by Activating the Mitochondrial Pathway. *J Huazhong Univ Sci Technol [Med Sci]* (2015) 35:541–5. doi: 10.1007/s11596-015-1467-5
113. Gong W, Zhu G, Li J, Yang X. LncRNA MALAT1 Promotes the Apoptosis and Oxidative Stress of Human Lens Epithelial Cells *via* p38MAPK Pathway in Diabetic Cataract. *Diabetes Res Clin Pract* (2018) 144:314–21. doi: 10.1016/j.diabres.2018.06.020
114. Zhao Y, Zhou L, Li H, Sun T, Wen X, Li X, et al. Nuclear-Encoded lncRNA MALAT1 Epigenetically Controls Metabolic Reprogramming in HCC Cells Through the Mitophagy Pathway. *Mol Ther Nucleic Acids* (2021) 23:264–76. doi: 10.1016/j.omtn.2020.09.040
115. Kong L, Zhou X, Wu Y, Wang Y, Chen L, Li P, et al. Targeting HOTAIR Induces Mitochondria Related Apoptosis and Inhibits Tumor Growth in Head and Neck Squamous Cell Carcinoma *In Vitro* and *In Vivo*. *Curr Mol Med* (2015) 15:952–60. doi: 10.2174/1566524016666151123112716
116. Wang K, Long B, Zhou L-Y, Liu F, Zhou Q-Y, Liu C-Y, et al. CARL lncRNA Inhibits Anoxia-Induced Mitochondrial Fission and Apoptosis in Cardiomyocytes by Impairing miR-539-Dependent PHB2 Downregulation. *Nat Commun* (2014) 5:3596. doi: 10.1038/ncomms4596
117. Long J, Badal SS, Ye Z, Wang Y, Ayanga BA, Galvan DL, et al. Long Noncoding RNA Tug1 Regulates Mitochondrial Bioenergetics in Diabetic Nephropathy. *J Clin Invest* (2016) 126:4205–18. doi: 10.1172/jci87927
118. Wang Y, Hu SB, Wang MR, Yao RW, Wu D, Yang L, et al. Genome-Wide Screening of NEAT1 Regulators Reveals Cross-Regulation Between Paraspeckles and Mitochondria. *Nat Cell Biol* (2018) 20:1145–58. doi: 10.1038/s41556-018-0204-2
119. Kowluru RA, Mishra M. Therapeutic Targets for Altering Mitochondrial Dysfunction Associated With Diabetic Retinopathy. *Expert Opin Ther Targets* (2018) 22:233–45. doi: 10.1080/14728222.2018.1439921
120. Kolesnikov AA. The Mitochondrial Genome. The Nucleoid. *Biochem (Mosc)* (2016) 81:1057–65. doi: 10.1134/s0006297916100047
121. Sumitani M, Kasashima K, Ohta E, Kang D, Endo H. Association of a Novel Mitochondrial Protein M19 With Mitochondrial Nucleoids. *J Biochem* (2009) 146:725–32. doi: 10.1093/jb/mvp118
122. Kucej M, Kucejova B, Subramanian R, Chen XJ, Butow RA. Mitochondrial Nucleoids Undergo Remodeling in Response to Metabolic Cues. *J Cell Sci* (2008) 121:1861–8. doi: 10.1242/jcs.028605
123. Zhong Q, Kowluru RA. Regulation of Matrix Metalloproteinase-9 by Epigenetic Modifications and the Development of Diabetic Retinopathy. *Diabetes* (2013) 62:2559–68. doi: 10.2337/db12-1141
124. Duraisamy AJ, Mishra M, Kowluru RA. Crosstalk Between Histone and DNA Methylation in Regulation of Retinal Matrix Metalloproteinase-9 in

Diabetes. *Invest Ophtahlmol Vis Sci* (2017) 58:6440–8. doi: 10.1167/iovs.17-22706
125. Tong P, Peng QH, Gu LM, Xie WW, Li WJ. LncRNA-MEG3 Alleviates High Glucose Induced Inflammation and Apoptosis of Retina Epithelial Cells*via* regulating miR-34a/SIRT1 axis. *Exp Mol Pathol* (2019) 107:102–9. doi: 10.1016/j.yexmp.2018.12.003
126. Mishra M, Duraisamy AJ, Kowluru RA. Sirt1- a Guardian of the Development of Diabetic Retinopathy. *Diabetes* (2018) 67:745–54. doi: 10.2337/db17-0996
127. Liu P, Jia SB, Shi JM, Li WJ, Tang LS, Zhu XH, et al. LncRNA-MALAT1 Promotes Neovascularization in Diabetic Retinopathy Through Regulating miR-125b/VE-Cadherin Axis. *Biosci Rep* (2019) 39:BSR20170036. doi: 10.1042/bsr20181469
128. Boon RA, Jaé N, Holdt L, Dimmeler S. Long Noncoding RNAs: From Clinical Genetics to Therapeutic Targets? *J Am Coll Cardiol* (2016) 67:1214–26. doi: 10.1016/j.jacc.2015.12.051
129. Huang CK, Kafert-Kasting S, Thum T. Preclinical and Clinical Development of Noncoding RNA Therapeutics for Cardiovascular Disease. *Circ Res* (2020) 126:663–78. doi: 10.1161/circresaha.119.315856
130. Chen B, Zhang RN, Fan X, Wang J, Xu C, An B, et al. Clinical Diagnostic Value of Long Non-Coding RNAs in Colorectal Cancer: A Systematic Review and Meta-Analysis. *J Cancer* (2020) 11:5518–26. doi: 10.7150/jca.46358
131. Kumarswamy R, Bauters C, Volkmann I, Maury F, Fetisch J, Holzmann A, et al. Circulating Long Noncoding RNA, LIPCAR, Predicts Survival in Patients With Heart Failure. *Circ Res* (2014) 114:1569–75. doi: 10.1161/circresaha.114.303915
132. Cai Y, Yang Y, Chen X, He D, Zhang X, Wen X, et al. Circulating "LncPPARδ" From Monocytes as a Novel Biomarker for Coronary Artery Diseases. *Medicine* (2016) 95:e2360. doi: 10.1097/md.0000000000002360
133. Tang H, Wu Z, Zhang J, Su B. Salivary lncRNA as a Potential Marker for Oral Squamous Cell Carcinoma Diagnosis. *Mol Med Rep* (2013) 7:761–6. doi: 10.3892/mmr.2012.1254
134. Bolha L, Ravnik-Glavač M, Glavač D. Long Noncoding RNAs as Biomarkers in Cancer. *Dis Markers* (2017) 2017:7243968–7243968. doi: 10.1155/2017/7243968
135. Shaker OG, Abdelaleem OO, Mahmoud RH, Abdelghaffar NK, Ahmed TI, Said OM, et al. Diagnostic and Prognostic Role of Serum miR-20b, miR-17-3p, HOTAIR, and MALAT1 in Diabetic Retinopathy. *IUBMB Life* (2019) 71:310–20. doi: 10.1002/iub.1970
136. He J, Rui Z, Gao J, Chen Y, Li Y, Xu T, et al. Expression of Long Non-Coding RNA (lncRNA) SNHG5 in Patients with Refractory Diabetic Macular Edema and Its Regulatory Mechanism. *Med Sci Monit* (2022) 28:e932996. doi: 10.12659/msm.932996
137. Biswas S, Coyle A, Chen S, Gostimir M, Gonder J, Chakrabarti S. Expressions of Serum lncRNAs in Diabetic Retinopathy – A Potential Diagnostic Tool. *Front Endocrinol (Lausanne)* (2022) 13:851967. doi: 10.3389/fendo.2022.851967
138. Carninci P, Kasukawa T, Katayama S, Gough J, Frith MC, Maeda N, et al. The Transcriptional Landscape of the Mammalian Genome. *Science* (2005) 309:1559–63. doi: 10.1126/science.1112014
139. Kitow J, Derda AA, Beermann J, Kumarswarmy R, Pfanne A, Fendrich J, et al. Mitochondrial Long Noncoding RNAs as Blood Based Biomarkers for Cardiac Remodeling in Patients With Hypertrophic Cardiomyopathy. *Am J Physiol Heart Circulatory Physiol* (2016) 311:H707–712. doi: 10.1152/ajpheart.00194.2016

Conflict of Interest: The author declares that the research was conducted in the absence of any commercial or financial relationships that could be construed as a potential conflict of interest.

frontiers | Frontiers in Endocrinology

SYSTEMATIC REVIEW
published: 22 June 2022
doi: 10.3389/fendo.2022.922886

Meta-Analysis of Relationship of Sleep Quality and Duration With Risk of Diabetic Retinopathy

Zhenzhen Zheng[1†], Chaoyu Wang[2†], Chunhe Li[3†], Qinglan Wu[4†], Xiaojuan Chen[5†], Huimin Chen[1], Huizhao Liao[6], Jinru Zhu[1], Junyan Lin[6], Xudong Ou[6], Zhihong Zou[6], Jinhua Liang[1] and Riken Chen[6*]*

[1] Department of Respiratory and Critical Care Medicine, The Second Affiliated Hospital of Guangdong Medical University, Zhanjiang, China, [2] Department of Respiratory and Critical Care Medicine, Taishan Hospital of Traditional Chinese Medicine, Jiangmen, China, [3] Department of Critical Care Medicine, The First Affiliated Hospital of Guangzhou University of Chinese Medicine, Guangzhou, China, [4] Department of Respiratory and Critical Care Medicine, Central People's Hospital of Zhanjiang, Zhanjiang, China, [5] Medical College, Jiaying Uiversity, Meizhou, China, [6] Guangzhou Medical University, State Key Laboratory of Respiratory Disease, National Clinical Research Center for Respiratory Disease, Guangzhou Institute of Respiratory Health, The First Affiliated Hospital of Guangzhou Medical University, Guangzhou, China

OPEN ACCESS

Edited by:
Khalid Siddiqui,
King Saud University, Saudi Arabia

Reviewed by:
Xuefei Zhang,
Southern Medical University, China
Nanhong Li,
Southern Medical University, China

***Correspondence:**
Jinhua Liang
81446069@qq.com
Riken Chen
chenriken@126.com

[†]These authors have contributed equally to this work

Specialty section:
This article was submitted to Clinical Diabetes, a section of the journal Frontiers in Endocrinology

Received: 18 April 2022
Accepted: 18 May 2022
Published: 22 June 2022

Citation:
Zheng Z, Wang C, Li C, Wu Q, Chen X, Chen H, Liao H, Zhu J, Lin J, Ou X, Zou Z, Liang J and Chen R (2022) Meta-Analysis of Relationship of Sleep Quality and Duration With Risk of Diabetic Retinopathy. Front. Endocrinol. 13:922886. doi: 10.3389/fendo.2022.922886

Objective: A meta-analysis is used to explore the relationship of sleep quality and duration with the risk of diabetic retinopathy (DR).

Method: Cochrane Library, PubMed, Embase, and other databases are searched from their establishment to April 2022. Literature on the relationship of sleep quality and duration with DR risk published in various databases is collected, and two researchers independently screen the literature, extract data, and evaluate the quality of the included articles. The meta-analysis is performed with Review Manage 5.4.1 software.

Results: A total of 7 articles are selected, including 4,626 subjects. The results show a strong correlation between sleep quality and DR risk. When comparing the sleep quality scores of "DR" (experimental group) and "NO DR" (control group), the Pittsburgh sleep quality index(PSQI) score of the DR group is significantly higher than that of the NO DR group (MD = 2.85; 95% confidence interval [CI] 1.92, 3.78, P<0.001), while the ESS score of the DR group is also significantly higher than that of the NO DR group (MD = 1.17; 95% confidence interval [CI] 0.14 to 2.30, P=0.04), so the sleep quality score of the DR group is higher than that of the NO DR group in both the PSQI and ESS scores, which confirms that low sleep quality is a risk factor for DR. Long sleep duration is also associated with the risk of developing DR; the number of adverse events (DR prevalence) is higher for "long sleep duration" than "normal sleep duration" [OR = 1.83, 95%CI 1.36–2.47, P < 0.001], suggesting that long sleep duration can cause increased DR risk. Short sleep duration is also associated with the occurrence of DR [OR = 1.49, 95%CI 1.15–1.94), P = 0.003] and can increase DR risk.

Conclusion: Sleep quality and duration (including long and short sleep duration) are significantly associated with DR. To reduce DR risk, sleep intervention should be actively carried out, lifestyle changes should be made, and attention should be paid to the role of DR management.

Keywords: Pittsburgh sleep quality index, Epworth sleepiness scale, meta-analysis, diabetic retinopathy, sleep duration, sleep quality

Diabetes mellitus is one of the most common and frequently-occurring diseases in the world, and its rapidly rising prevalence has become a global public health problem. According to the International Diabetes Federation (1), there will be 700 million diabetes patients worldwide by 2045. Diabetic retinopathy (DR) is a serious complication of diabetes which may be caused by preventable insomnia in working-age people (2). Every year in the United States alone, 12,000 to 24,000 patients are blinded by DR (3), placing a heavy burden on individuals and society. Its incidence is related to the course of diabetes, age of onset, genetic factors, and control, and the longer the course of the disease, the higher the incidence. Most patients develop DR 10 to 15 years after the diagnosis of diabetes (4). Early intervention can effectively prevent the occurrence and development of DR, among which lifestyle intervention is the most cost-effective measure (5). Sleep disturbances have been found to be associated with abnormal glucose metabolism and an increased risk of diabetes (6). Sleep disturbances may be due to decreased sleep duration and/or decreased sleep quality (7). At present, the amount of clinical literature on the relationship of sleep quality and duration with DR is increasing year by year. However, there is a lack of randomized controlled trials with large multicenter samples, and few such evidence-based medical articles have been published in the world. Herein, a meta-analysis of observational studies on the relationship of sleep quality and duration with DR risk is carried out in order to provide medical evidence for the prevention and intervention of DR.

MATERIALS AND METHODS

Retrieval Strategy

Cochrane Library, PubMed, Embase, and other databases were searched by computer from their establishment to April 2022. English search terms included "sleep quality", "sleep wake disorders", "sleep score", "Pittsburgh sleep quality index", "PSQI", "Epworth Sleepiness Scale", "ESS", "sleep time", "sleep duration", "sleep amount", and "diabetic retinopathy".

Literature Inclusion and Exclusion Criteria

Inclusion criteria: ① The subjects of the study were diabetic patients. ② The study was a cohort study, case-control study, or cross-sectional study. ③ The exposure factors were sleep quality score and sleep duration, wherein sleep quality score included the Pittsburgh sleep quality index(PSQI) and Epworth Sleepiness Scale (ESS) scores, and sleep duration included long sleep duration and short sleep duration. ④ The outcome indicators included mean difference (MD), odds ratio (OR), and 95% confidence interval (CI) after multivariate adjustment. ⑤ Based on different reports on the same research population, the studies with the largest sample sizes were included.

Exclusion criteria: ① Languages other than English. ② Studies for which the effect sizes could not be extracted or calculated. ③ Studies for which the original author did not respond or could not provide meta-analysis data.

Literature Screening, Quality Assessment, and Data Extraction

Two researchers independently searched, selected, and screened the literature, then checked each other's work and provided articles with differences to a third researcher for analysis to decide whether they should be included. The evaluation was performed using the "Risk of Bias Assessment" tool recommended by the Cochrane Collaboration, which is divided into three levels: low risk, unclear, and high risk. The contents are: whether it is randomly assigned; whether to carry out allocation concealment; whether to use blinding; whether the outcome data is complete; whether the research results are selectively reported; and whether there is any other risk of bias. The extracted data included the first author, study area, publication time, study type, sample size, age, PSQI, ESS, sleep duration assessment method, sleep duration grouping, outcome measures, and adjustment for confounders.

Data Extraction and Definitions

The sleep quality scores of the research subjects were obtained by the PSQI and ESS questionnaires, and sleep duration was obtained by survey visits or questionnaires. DR was diagnosed by ophthalmologists through the analysis of fundus photos or conducting indirect ophthalmoscopy. In the included studies, DR included mild, moderate, severe, and any DR. The PSQI and ESS scoring standards of the sleep quality score were fixed and consistent, while the grouping and definition of sleep duration were not completely consistent. Long sleep duration was defined as > 8–9h, normal sleep duration as 6–8h, and short sleep duration as < 5–6h, all at night and within a 24h period.

Statistical Methods

Statistical analysis was performed using Review Manage 5.4.1 software. MD and OR values were used for effect evaluation, and 95%CI was calculated. The heterogeneity of the studies was analyzed using the I^2 statistic test and Q test. When $I^2 < 50\%$ and $P > 0.1$, this indicated that there was no significant heterogeneity among the studies; when $I^2 > 50\%$ and $P < 0.1$,

this indicated that there was statistical heterogeneity among the studies. If there was still heterogeneity, a random effect model was used, and if there was no obvious heterogeneity, a fixed effect model was used. Sensitivity analysis was used to judge the stability and reliability of the combined results. $P < 0.05$ indicated that the difference was statistically significant.

RESULTS

Literature Screening Results

A total of 513 articles were retrieved. A total of 437 papers were obtained after deduplication, and a total of 266 papers were excluded by reading the titles and abstracts. After reading the full texts, 7 papers were finally included (**Figure 1**), with a total of 4,626 research subjects. The study populations were from Korea, Singapore, India, Malaysia, Thailand, and Denmark. The basic characteristics of the articles included in the study are shown in **Table 1**.

Publication Bias and Sensitivity Analysis

By drawing funnel plots (**Figure 2**), the distribution of each study is shown to be basically symmetrical without any serious publication bias. The included studies showed a low risk of bias overall (**Figures 3**, **4**). Specifically: (1) two articles used the classification of subjects; (2) two articles did not have a clear degree of the non-concealment of subjects; (3) none of the articles mentioned blinding; (4) none of the articles mentioned the outcome indicators of selective reporting, and it was unclear whether there was any selective reporting of research results; (5) all articles and research data were complete.

The results of the sensitivity analysis showed that for DR risk in diabetic patients, all included studies had $I^2 < 50\%$ and $P > 0.1$, meaning they were all homogeneous, so a fixed effect model was used. Among the three studies (PSQI score study, long sleep duration study and short sleep duration study), any articles that had no significant effect on the combined effect size of the remaining literature were removed to confirm the stability of the results; for the ESS score study, only two articles were included, and the sensitivity analysis was not carried out for two studies, so the results of the ESS score analysis were unstable.

Statistical Analysis Results

Relationship Between Sleep Quality and DR Risk

A total of three (7, 12, 13) articles reported that the PSQI score for sleep quality revealed its relationship with DR risk. There was

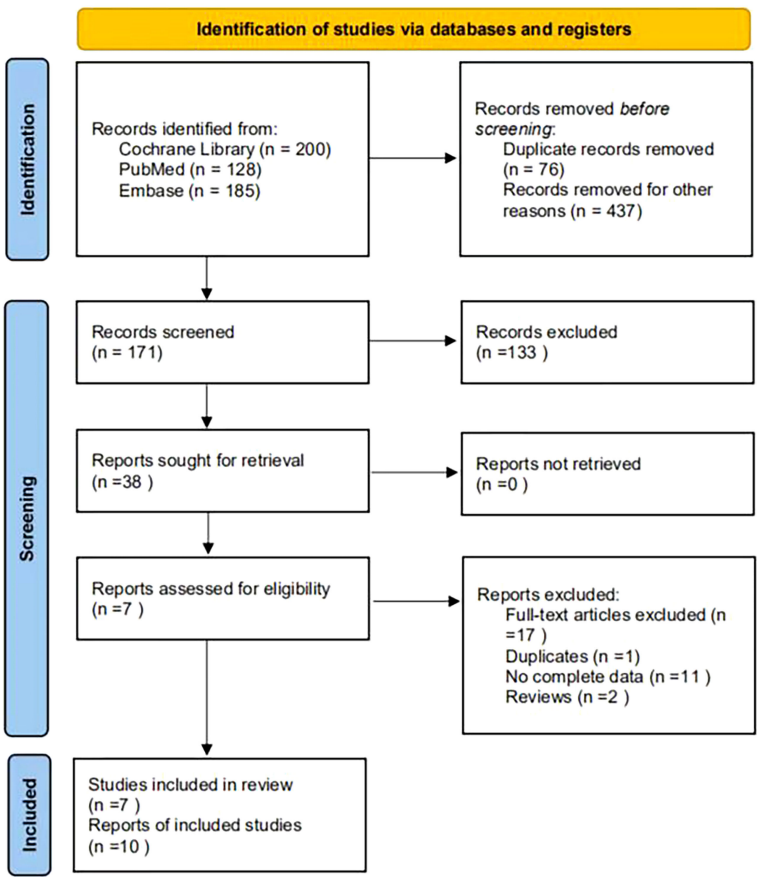

FIGURE 1 | Flow diagram of literature screening.

TABLE 1 | Characteristics of the included studies.

Study	Country	Sample Size	Mean age/year	Exposure assessment	Sleep duration/h	Global score (ESQI)	Global score (ESS)	Outcome	NOS score
Jee (8) 2017	Korean	1670	60.3	self-report	short(≦5) Long(≧9)	Not mentioned	Not mentioned	Any DR	7
Chew (9) 2020	Singapore	92	57.6+-8.3	self-report	short(<5)	Not mentioned	NO DR:4.8±2.5 DR:5.7±3.6	Moderate DR	7
Raman (10) 2012	India	1414	M:56.9±10.5 F:56.4±-8.9	self-report	short(<5) Long(>9)	Not mentioned	Not mentioned	Any DR	6
Tan (11) 2018	Malay India	1231	64.4±9.0	self-report	short(<6) Long(≧8)	Not mentioned	Not mentioned	Moderate DR	9
Dutta (7) 2020	India	140	NO DR:55.59 ±6.83 DR:57.51±5.82	self-report	Not mentioned	NO DR:4.30±3.26 DR:7.44±3.99	Not mentioned	Any DR	7
Sirisreet (12) 2020	Thailand	25	NO DR:51.1±11.5 DR:51.5±8.5	self-report	Not mentioned	NO DR:4.1±3.1 DR:7.4±3.5	Not mentioned	Any DR	7
Ba-Ali (13) 2018	Denmark	54	NO DR:63.1±8.3 DR:61.6±9.1	self-report	Not mentioned	NO DR:5.3±3.9 DR:7.2±4.5	NO DR:5.6±3.1 DR:7.2±3.6	Any DR	8

no homogeneity among the studies (P = 0.50, I^2 = 0%), so the fixed effect model was used. The results of the meta-analysis showed that the PSQI score of the diabetic population in the DR group (experimental group) was significantly higher than that in the NO DR group (control group), and the difference was statistically significant (MD = 2.85, 95%CI [1.92, 3.78], Z = 6.02, P < 0.00001), suggesting that the PSQI score is associated with DR risk and is a risk factor for DR. (**Figure 5**). Another two (9, 13) articles reported that the ESS score for sleep quality revealed its relationship with DR risk. There was no homogeneity among the studies (P = 0.55, I^2 = 0%), so the fixed effect model was also used. The results of the meta-analysis showed that the ESS score of the diabetic population in the DR group (experimental group) was significantly higher than that in the NO DR group (control group), and the difference was statistically significant (MD = 1.17, 95%CI [0.04, 2.30], Z = 2.04, P = 0.04), suggesting that the ESS score is associated with DR risk and is also a risk factor for DR (**Figure 6**). Therefore, in both the PSQI and ESS scores, the sleep quality score in the DR group was higher than that in the NO DR group, confirming that sleep quality is related to DR risk and is a risk factor for DR.

Relationship Between Sleep Duration and DR Risk

Long Sleep Duration and DR Risk

Long sleep duration and DR prevalence were included in 3 studies (8, 10, 11), and six studies provided the OR values and 95%CI of DR in diabetic patients in the long sleep duration group and control group. There was no heterogeneity among the

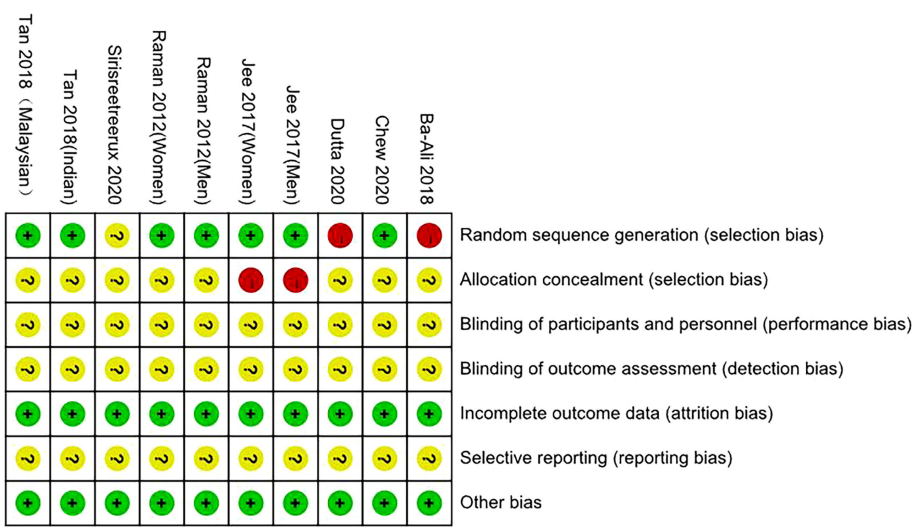

FIGURE 2 | Overview of bias risk assessment of included literature.

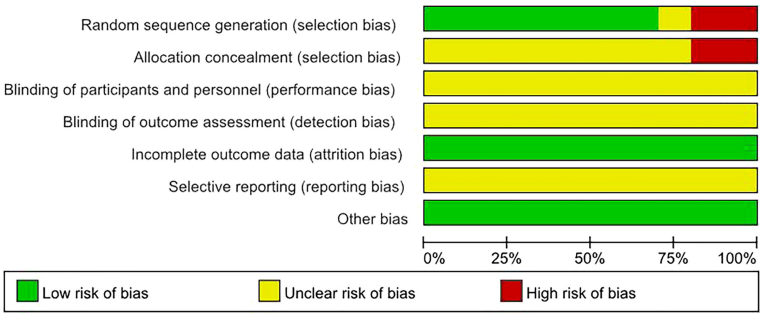

FIGURE 3 | Bias risk assessment chart of included literature.

studies (P = 0.93, I^2 = 0%), so the fixed effect model was used. The meta-analysis results showed that the fixed effect model was (OR = 1.83, 95%CI 1.36–2.47, P < 0.0001), suggesting that compared with patients with normal sleep duration, the prevalence of DR in diabetic patients with long sleep duration was significantly higher (**Figure 7**). This confirms that long sleep duration is related to DR risk and is a risk factor for DR.

Short sleep duration and DR risk

Short sleep duration and DR prevalence were included in 3 studies (8, 10, 11), and 6 studies provided the OR values and 95% CI of the incidence of DR in diabetic patients in the short sleep duration experimental group and normal sleep duration control group. There was no heterogeneity among the studies (P = 0.60, I^2 = 0%), so the fixed effect model was used. The meta-analysis results showed that the fixed effect model was (OR = 1.49, 95%CI (1.15, 1.94), P = 0.003), suggesting that compared with patients with normal sleep duration, the prevalence of DR in diabetic patients with short sleep duration was significantly higher (**Figure 8**). This confirms that short sleep duration is related to DR risk and is a risk factor for DR.

DISCUSSION

Given the rising prevalence of diabetes and the high burden of DR worldwide, the prevention and treatment of DR is an increasing public health challenge (14). Therefore, in addition to classic risk factors such as poor glycemic control, hypertension, and longer disease duration, it is important to identify other modifiable risk factors from clinical and public health perspectives (15). The increasing prevalence of poor sleep health, which shows a long-term trend as modern society changes, is an underestimated determinant of health outcomes. A recent accumulation of evidence from experimental and epidemiological studies has shown that sleep duration and quality are significantly associated with diabetes, insulin resistance, and poor glycemic control (16–19). Our findings suggest that both sleep quality and duration may have an impact on the presence of DR.

"Sleep disturbances" refers to abnormal sleep quality, such as difficulty falling asleep, early awakening, and disturbances of the normal rhythm of sleeping and waking. Continuous

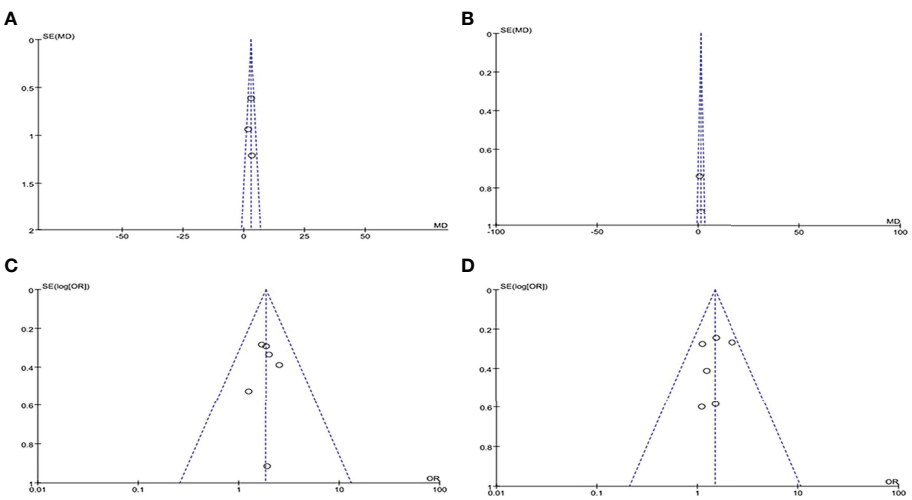

FIGURE 4 | Funnel plots of included literature: **(A)** PSQI score funnel plot; **(B)** ESS score funnel plot; **(C)** Long sleep duration DR funnel plot; **(D)** Short sleep duration DR funnel plot.

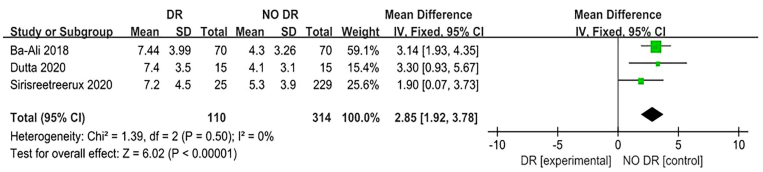

FIGURE 5 | Forest plot of PSQI score and DR risk relationship meta-analysis.

hyperglycemia and blood sugar fluctuations in diabetes can cause damage to the cerebral blood vessels, nerves, cells, etc., and disrupt the nerves that regulate sleep-wake rhythms, and the series of diabetes symptoms or complications also result in sleep problems. Evidence suggests that sleep deprivation itself contributes to the pathogenesis of DR and the development of proliferative DR. Another consideration is that sleep disturbances have been shown to negatively impact immune function and inflammation (20, 21), the latter of which is implicated in the pathogenesis of DR (22) and is a target for drug therapy in DR (23, 24). At present, there are many ways to evaluate sleep quality, including objective monitoring methods such as polysomnography and various subjective questionnaires such as PSQI (25), ESS (26), insomnia severity index (ISI) (27), Leeds sleep evaluation questionnaire (LSEQ) (28), etc. In this study, sleep quality was assessed by PSQI and ESS scores. The higher the score, the worse the sleep quality. PSQI was proposed by Buysse et al. (25) in 1989. The reliability test of PSQI showed that the scale has good internal consistency (Cronbach's alpha = 0.83) and test-retest reliability (r = 0.85). PSQI was developed on the basis of the analysis and evaluation of various scales related to assessing sleep quality. By organically combining the quality and quantity of sleep, it can not only evaluate the sleep behavior and habits of the general population, but also be used for the comprehensive evaluation of sleep quality in clinical patients (29). ESS item scores have been shown to be reliable, associated with sleepiness in everyday life, and effective in the assessment of sleep disturbances (30).

Through the analysis of the literature, it was found that more articles used the PSQI and ESS scores because they have good reliability and validity. Therefore, this study finally selected the PSQI and ESS scores as the outcome indicators. The PSQI and ESS scores of the DR experimental group were higher than those of the NO DR control group, meaning that sleep quality is significantly associated with DR and is a risk factor for DR. People with diabetes and poor sleep quality have a greater DR risk. Therefore, for DR patients with sleep disorders, in addition to specific problems that require symptomatic treatment, health education should be carried out at the same time, and clinical psychological and treatment intervention should be actively carried out to improve the sleep quality of patients, thereby improving their blood sugar control levels. Reducing the occurrence of diabetic complications and improving the quality of life of diabetic patients is of great significance.

A number of recent studies have found a relationship between sleep duration and diabetes risk (17) and its associated complications (10). The results of this study show that abnormal sleep duration, including long sleep duration and short sleep duration, is related to the occurrence of DR. Regarding the possible mechanism of the association between long sleep duration and DR: first, long sleep duration may be an indirect response of poor sleep quality, causing patients to require prolonged sleep; for example, obstructive sleep apnea is a known cause of increased sleep demand, and the resulting intermittent hypoxia may play an important role in the development of diabetes, and has been identified as a risk factor for insulin resistance and diabetes (16). Second, as with short sleep duration, long sleep duration also increases inflammatory biomarkers (31), and pro-inflammatory cytokines have sleep-inducing effects, so prolonged sleep may also be induced by diabetes itself and/or the resulting inflammatory states (32). Third, in a dark environment, the oxygen consumption of the outer retina increases, which leads to a sharp decrease in the retinal oxygen tension curve, aggravates retinal hypoxia, and stimulates the overproduction of vascular endothelial growth factor, which in turn promotes the occurrence of DR (33, 34). Fourth, long sleep duration is often clustered with other known risk factors for DR such as depression, low socioeconomic status, history of other medical diseases, and less physical activity (35, 36).

Short sleep duration may also affect the progression of DR through various mechanisms. First, short sleep duration is associated with poor glycemic control (37). Buxton et al. showed that sleep deprivation leads to decreased insulin

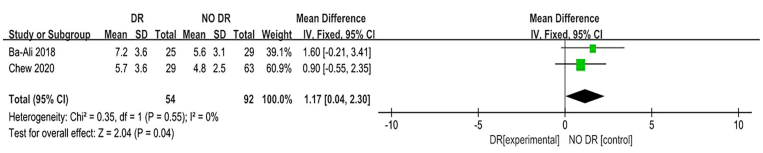

FIGURE 6 | Forest plot of ESS score and DR risk relationship meta-analysis.

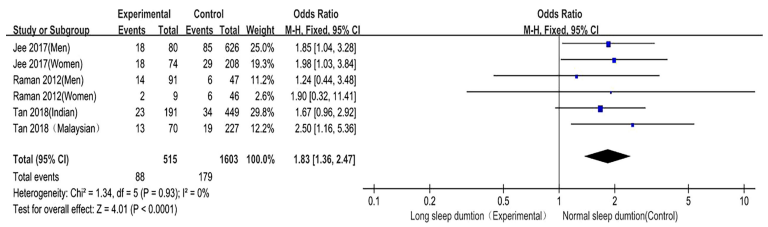

FIGURE 7 | Forest plot of long sleep duration and DR risk relationship.

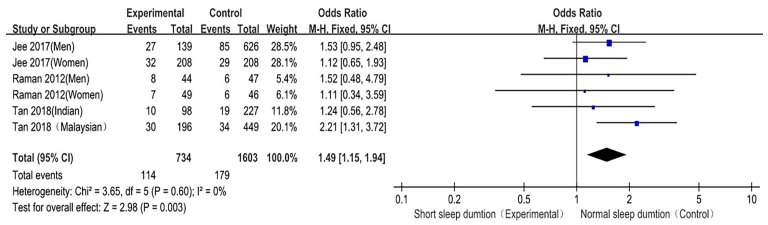

FIGURE 8 | Forest plot of short sleep duration and DR risk relationship meta-analysis.

sensitivity (18) and affects insulin secretion through the neuroendocrine system (38). Second, short sleep duration may be associated with inflammation (21). Third, short sleep duration may lead to vascular endothelial dysfunction by affecting nitric oxide, serum endothelin, etc. (39, 40). Fourth, sleep disruption affects melatonin levels (41), accelerating the progression of DR. At the same time, similar to long sleep duration, short sleep duration is often clustered with other DR-related risk factors such as low socioeconomic status and low education level (36).

It should be noted that DR itself also affects sleep duration and quality (42). Especially in elderly patients, the presence of diabetic complications is associated with depression and sleep duration (43). As there were insufficient studies on the association between DR and sleep stage, the relationship between the two could not be further investigated. Therefore, the causal relationship between the two remains to be determined through further research.

This study has several limitations: first, the sleep quality score was obtained in the form of a questionnaire, moreover, the results of the ESS score studies are not stable, the number of included studies is small, more studies are needed to further stabilize the study results; and sleep duration was mainly reported by patients, which is highly subjective. Moreover, the definitions of long and short sleep duration were not completely consistent among studies. Second, the methods of diagnosing and grading DR in each study were slightly different, and the study populations were from different ethnicities, which may have led to greater heterogeneity in the results. Third, the sample size was relatively small, and there was a lack of large-scale, multi-center, randomized controlled trials. Fourth, the quality of some included articles was not very high, so there may be selection bias. Therefore, the conclusions of this study should be interpreted with caution.

In conclusion, Our results suggest that both sleep quality and duration are related to the occurrence of DR. Among them, sleep quality and duration are both risk factors for DR, while the relationship between short sleep duration and DR needs to be further determined, and its causal relationship and biological mechanism also require further research for confirmation. Sleep quality and duration, as individual-level modifiable risk factors, should be of great concern to clinicians and patients.

DATA AVAILABILITY STATEMENT

The original contributions presented in the study are included in the article/supplementary material. Further inquiries can be directed to the corresponding author.

AUTHOR CONTRIBUTIONS

ZZZ, CW, CL, QW and XC are the guarantor of the manuscript and take responsibility for the content of this manuscript. JHL, ZZZ, RC and CW contributed to the design of the study. HC, JZ, JYL and XO were involved in the data analysis. ZHZ, XO and RC contributed to the acquisition of primary data. ZZZ, CW and RC wrote the initial draft of the manuscript. ZZZ, RC and JHL contributed significantly to the revision of the manuscript. All authors read and approved the final manuscript.

FUNDING

This study was funded by the Natural Science Foundation of Guangdong Province (2019A1515010981).

ACKNOWLEDGEMENTS

We would also like to thank Professor Nanshan Zhong from State Key Laboratory of Respiratory Disease for the constructive advice he gave.

REFERENCES

1. Arden GB, Sivaprasad S. The Pathogenesis of Early Retinal Changes of Diabetic Retinopathy. *Doc Ophthalmol* (2012) 124(1):15–26. doi: 10.1007/s10633-011-9305-y
2. Cheung N, Mitchell P, Wong TY. Diabetic Retinopathy. *LANCET* (2010) 376:124–36. doi: 10.1016/S0140-6736(09)62124-3
3. Pulido JE, Pulido JS, Erie JC, Arroyo J, Bertram K, Lu MJ, et al. A Role for Excitatory Amino Acids in Diabetic Eye Disease. *Exp Diabetes Res* (2007) 2007:36150. doi: 10.1155/2007/36150
4. Jampol LM, Glassman AR, Sun J. Evaluation and Care of Patients With Diabetic Retinopathy. *N Engl J Med* (2020) 382:1629–37. doi: 10.1056/NEJMra1909637
5. American Diabetes Association. 11. Microvascular Complications and Foot Care: Standards of Medical Care in Diabetes-2021. *Diabetes Care* (2021) 44: S151–67. doi: 10.2337/dc21-S011
6. Shamshirgaran SM, Ataei J, Malek A, Iranparvar-Alamdari M, Aminisani N. Quality of Sleep and its Determinants Among People With Type 2 Diabetes Mellitus In Northwest of Iran. *World J Diabetes* (2017) 8:358–64. doi: 10.4239/wjd.v8.i7.358
7. Dutta S, Ghosh S, Ghosh S. Association of Sleep Disturbance With Diabetic Retinopathy. *Eur J Ophthalmol* (2022) 32:468–74. doi: 10.1177/1120672120974296
8. Jee D, Keum N, Kang S, Arroyo JG. Sleep and Diabetic Retinopathy. *Acta Ophthalmol* (2017) 95:41–7. doi: 10.1111/aos.13169
9. Chew M, Tan N, Lamoureux E, Cheng CY, Wong TY, Sabanayagam C. The Associations of Objectively Measured Sleep Duration and Sleep Disturbances With Diabetic Retinopathy. *Diabetes Res Clin Pract* (2020) 159:107967. doi: 10.1016/j.diabres.2019.107967
10. Raman R, Gupta A, Venkatesh K, Kulothungan V, Sharma T. Abnormal Sleep Patterns in Subjects With Type II Diabetes Mellitus and its Effect on Diabetic Microangiopathies: Sankara Nethralaya Diabetic Retinopathy Epidemiology and Molecular Genetic Study (SN-DREAMS, Report 20). *Acta Diabetol* (2012) 49:255–61. doi: 10.1007/s00592-010-0240-2
11. Tan N, Chew M, Tham YC, Nguyen QD, Yasuda M, Cheng CY, et al. Associations Between Sleep Duration, Sleep Quality and Diabetic Retinopathy. *PloS One* (2018) 13:e196399. doi: 10.1371/journal.pone.0196399
12. Sirisreetreerux S, Sujirakul T, Nimitphong H, Pinyopodjanard S, Saetung S, Chailurkit LO, et al. Sleep Variability, 6-Sulfatoxymelatonin, and Diabetic Retinopathy. *SLEEP BREATH* (2021) 25:1069–74. doi: 10.1007/s11325-020-02165-3
13. Ba-Ali S, Brondsted AE, Andersen HU, Sander B, Jennum PJ, Lund-Andersen H. Assessment of Diurnal Melatonin, Cortisol, Activity, and Sleep-Wake Cycle in Patients With and Without Diabetic Retinopathy. *SLEEP Med* (2019) 54:35–42. doi: 10.1016/j.sleep.2018.10.018
14. Guariguata L, Whiting DR, Hambleton I, Beagley J, Linnenkamp U, Shaw JE. Global Estimates of Diabetes Prevalence for 2013 and Projections for 2035. *Diabetes Res Clin Pract* (2014) 103:137–49. doi: 10.1016/j.diabres.2013.11.002
15. Yau JW, Rogers SL, Kawasaki R, Lamoureux EL, Kowalski JW, Bek T, et al. Global Prevalence and Major Risk Factors of Diabetic Retinopathy. *Diabetes Care* (2012) 35:556–64. doi: 10.2337/dc11-1909
16. Wang X, Bi Y, Zhang Q, Pan F. Obstructive Sleep Apnoea and the Risk of Type 2 Diabetes: A Meta-Analysis of Prospective Cohort Studies. *RESPIROLOGY* (2013) 18:140–6. doi: 10.1111/j.1440-1843.2012.02267.x
17. Shan Z, Ma H, Xie M, Yan P, Guo Y, Bao W, et al. Sleep Duration and Risk of Type 2 Diabetes: A Meta-Analysis of Prospective Studies. *Diabetes Care* (2015) 38:529–37. doi: 10.2337/dc14-2073
18. Buxton OM, Pavlova M, Reid EW, Wang W, Simonson DC, Adler GK. Sleep Restriction for 1 Week Reduces Insulin Sensitivity in Healthy Men. *DIABETES* (2010) 59:2126–33. doi: 10.2337/db09-0699
19. Lee S, Ng KY, Chin WK. The Impact of Sleep Amount and Sleep Quality on Glycemic Control in Type 2 Diabetes: A Systematic Review and Meta-Analysis. *SLEEP Med Rev* (2017) 31:91–101. doi: 10.1016/j.smrv.2016.02.001
20. Besedovsky L, Lange T, Born J. Sleep and Immune Function. *Pflugers Arch* (2012) 463:121–37. doi: 10.1007/s00424-011-1044-0
21. Mullington JM, Simpson NS, Meier-Ewert HK, Haack M. Sleep Loss and Inflammation. *Best Pract Res Clin Endocrinol Metab* (2010) 24:775–84. doi: 10.1016/j.beem.2010.08.014
22. Joussen AM, Poulaki V, Le ML, Koizumi K, Esser C, Janicki H, et al. A Central Role for Inflammation in the Pathogenesis of Diabetic Retinopathy. *FASEB J* (2004) 18:1450–2. doi: 10.1096/fj.03-1476fje
23. Platania C, Leggio GM, Drago F, Salomone S, Bucolo C. Computational Systems Biology Approach to Identify Novel Pharmacological Targets for Diabetic Retinopathy. *Biochem Pharmacol* (2018) 158:13–26. doi: 10.1016/j.bcp.2018.09.016
24. Platania C, Giurdanella G, Di Paola L, Leggio GM, Drago F, Salomone S, et al. P2X7 Receptor Antagonism: Implications in Diabetic Retinopathy. *Biochem Pharmacol* (2017) 138:130–9. doi: 10.1016/j.bcp.2017.05.001
25. Buysse DJ, Reynolds CR, Monk TH, Berman SR, Kupfer DJ. The Pittsburgh Sleep Quality Index: A New Instrument for Psychiatric Practice and Research. *Psychiatry Res* (1989) 28:193–213. doi: 10.1016/0165-1781(89)90047-4
26. Johns MW. A New Method for Measuring Daytime Sleepiness: The Epworth Sleepiness Scale. *SLEEP* (1991) 14:540–5. doi: 10.1093/sleep/14.6.540
27. Albougami A, Manzar MD. Insomnia Severity Index: A Psychometric Investigation Among Saudi Nurses. *SLEEP BREATH* (2019) 23:987–96. doi: 10.1007/s11325-019-01812-8
28. Skrobik Y, Duprey MS, Hill NS, Devlin JW. Low-Dose Nocturnal Dexmedetomidine Prevents ICU Delirium. A Randomized, Placebo-Controlled Trial. *Am J Respir Crit Care Med* (2018) 197:1147–56. doi: 10.1164/rccm.201710-1995OC
29. Backhaus J, Junghanns K, Broocks A, Riemann D, Hohagen F. Test-Retest Reliability and Validity of the Pittsburgh Sleep Quality Index in Primary Insomnia. *J PSYCHOSOM Res* (2002) 53:737–40. doi: 10.1016/S0022-3999(02)00330-6
30. Johns MW. Sleepiness in Different Situations Measured by the Epworth Sleepiness Scale. *SLEEP* (1994) 17:703–10. doi: 10.1093/sleep/17.8.703
31. Williams CJ, Hu FB, Patel SR, Mantzoros CS. Sleep Duration and Snoring in Relation to Biomarkers of Cardiovascular Disease Risk Among Women With Type 2 Diabetes. *Diabetes Care* (2007) 30:1233–40. doi: 10.2337/dc06-2107
32. Zizi F, Jean-Louis G, Brown CD, Ogedegbe G, Boutin-Foster C, McFarlane SI. Sleep Duration and the Risk of Diabetes Mellitus: Epidemiologic Evidence and Pathophysiologic Insights. *Curr Diabetes Rep* (2010) 10:43–7. doi: 10.1007/s11892-009-0082-x
33. Linsenmeier RA. Effects of Light and Darkness on Oxygen Distribution and Consumption in the Cat Retina. *J Gen Physiol* (1986) 88:521–42. doi: 10.1085/jgp.88.4.521
34. Ramsey DJ, Arden GB. Hypoxia and Dark Adaptation in Diabetic Retinopathy: Interactions, Consequences, and Therapy. *Curr Diabetes Rep* (2015) 15:118. doi: 10.1007/s11892-015-0686-2
35. Patel SR, Malhotra A, Gottlieb DJ, White DP, Hu FB. Correlates of Long Sleep Duration. *SLEEP* (2006) 29:881–9. doi: 10.1093/sleep/29.7.881
36. Krueger PM, Friedman EM. Sleep Duration in the United States: A Cross-Sectional Population-Based Study. *Am J Epidemiol* (2009) 169:1052–63. doi: 10.1093/aje/kwp023
37. Whitaker KM, Lutsey PL, Ogilvie RP, Pankow JS, Bertoni A, Michos ED, et al. Associations Between Polysomnography and Actigraphy-Based Sleep Indices and Glycemic Control Among Those With and Without Type 2 Diabetes: The Multi-Ethnic Study of Atherosclerosis. *SLEEP* (2018) 41(11):zsy172. doi: 10.1093/sleep/zsy172

38. Buxton OM, Cain SW, O'Connor SP, Porter JH, Duffy JF, Wang W, et al. Adverse Metabolic Consequences in Humans of Prolonged Sleep Restriction Combined With Circadian Disruption. *Sci Transl Med* (2012) 4:129r–43r. doi: 10.1126/scitranslmed.3003200
39. Bain AR, Weil BR, Diehl KJ, Greiner JJ, Stauffer BL, DeSouza CA. Insufficient Sleep is Associated With Impaired Nitric Oxide-Mediated Endothelium-Dependent Vasodilation. *ATHEROSCLEROSIS* (2017) 265:41–6. doi: 10.1016/j.atherosclerosis.2017.08.001
40. Stockelman KA, Bain AR, Dow CA, Diehl KJ, Greiner JJ, Stauffer BL, et al. Regular Aerobic Exercise Counteracts Endothelial Vasomotor Dysfunction Associated With Insufficient Sleep. *Am J Physiol Heart Circ Physiol* (2021) 320:H1080–8. doi: 10.1152/ajpheart.00615.2020
41. Hikichi T, Tateda N, Miura T. Alteration of Melatonin Secretion in Patients With Type 2 Diabetes and Proliferative Diabetic Retinopathy. *Clin Ophthalmol* (2011) 5:655–60. doi: 10.2147/OPTH.S19559
42. Ida S, Kaneko R, Imataka K, Fujiwara R, Murata K. Are Diabetes-Related Factors Associated With the Social Roles of Elderly Patients With Diabetes? *J Diabetes Complications* (2021) 35:107759. doi: 10.1016/j.jdiacomp.2020.107759
43. Ozturk ZA, Yesil Y, Kuyumcu ME, Savas E, Uygun O, Sayiner ZA, et al. Association of Depression and Sleep Quality With Complications of Type 2 Diabetes in Geriatric Patients. *Aging Clin Exp Res* (2015) 27:533–8. doi: 10.1007/s40520-014-0293-0

Conflict of Interest: The authors declare that the research was conducted in the absence of any commercial or financial relationships that could be construed as a potential conflict of interest.

Publisher's Note: All claims expressed in this article are solely those of the authors and do not necessarily represent those of their affiliated organizations, or those of the publisher, the editors and the reviewers. Any product that may be evaluated in this article, or claim that may be made by its manufacturer, is not guaranteed or endorsed by the publisher.

frontiers | Frontiers in Endocrinology

ORIGINAL RESEARCH
published: 29 June 2022
doi: 10.3389/fendo.2022.883845

The Association of Homocysteine and Diabetic Retinopathy in Homocysteine Cycle in Chinese Patients With Type 2 Diabetes

Wei-Ming Luo[1†], Zhi-Peng Zhang[2†], Wei Zhang[1], Jing-Yang Su[1], Xiao-Qian Gao[1], Xu Liu[1], Wan-Ying Wang[1], Chang-Tao Jiang[3] and Zhong-Ze Fang[1,4]*

[1] Department of Toxicology and Sanitary Chemistry, School of Public Health, Tianjin Medical University, Tianjin, China, [2] Department of Surgery, Peking University Third Hospital, Beijing, China, [3] Key Laboratory of Molecular Cardiovascular Science, Department of Physiology and Pathophysiology, School of Basic Medical Sciences, Ministry of Education, Peking University, Beijing, China, [4] Tianjin Key Laboratory of Environment, Nutrition and Public Health, Tianjin, China

OPEN ACCESS

Edited by:
Khalid Siddiqui,
King Saud University, Saudi Arabia

Reviewed by:
Pranay Goel,
Indian Institute of Science Education and Research, India
Dario Rahelic,
Merkur University Hospital, Croatia

***Correspondence:**
Zhong-Ze Fang
fangzhongze@tmu.edu.cn

[†]These authors have contributed equally to this work

Specialty section:
This article was submitted to Clinical Diabetes, a section of the journal Frontiers in Endocrinology

Received: *25 February 2022*
Accepted: *25 May 2022*
Published: *29 June 2022*

Citation:
Luo W-M, Zhang Z-P, Zhang W, Su J-Y, Gao X-Q, Liu X, Wang W-Y, Jiang C-T and Fang Z-Z (2022) The Association of Homocysteine and Diabetic Retinopathy in Homocysteine Cycle in Chinese Patients With Type 2 Diabetes. Front. Endocrinol. 13:883845. doi: 10.3389/fendo.2022.883845

Objective: This study aimed to explore the relationship between homocysteine (Hcy) and diabetic retinopathy (DR) and the impacts of the Hcy pathway on this relationship against this background.

Methods: This study retrieved 1979 patients with type 2 diabetes (T2D) from the First Affiliated Hospital of Liaoning Medical University in Jinzhou, Liaoning Province, China. Multiple logistic regression was used to analyze the effects of Hcy cycle on the relationship between Hcy and DR. Spearman's rank correlation analysis was used to analyze the correlation between risk factors related to DR progression and Hcy. Finally, the results of logistic regression were supplemented by mediation analysis.

Results: We found there was a negative correlation between low concentration of Hcy and DR (OR : 0.83, 95%CI: 0.69-1). After stratifying all patients by cysteine (Cys) or Methionine (Met), this relationship remained significant only in low concentration of Cys (OR: 0.75, 95%CI: 0.61-0.94). Through the RCS curve, we found that the effect of Hcy on DR presents a U-shaped curve relationship. Mediating effect in Met and Hcy cycles was also significant [Total effect c (OR: 0.968, 95%CI: 0.938-0.998), Direct effect path c' (OR: 0.969, 95%CI: 0.940-0.999), Path a (OR: 1.047, 95%CI: 1.004-1.091), Path b (OR: 0.964, 95%CI: 0.932-0.998)].

Conclusions: The relationship between Hcy and DR presents a U-shaped curve and the homocysteine cycle pathway has an impact on it. And too low concentration of Hcy indicates a lack of other substances, such as vitamins. It is suggested that the progression of DR is the result of a combination of many risk factors. Further prospective studies are needed to determine the role of Hcy in the pathogenesis of DR.

Keywords: homocysteine, diabetic retinopathy, homocysteine cycle pathway, metabolism, type 2 diabetes

INTRODUCTION

Diabetes is a metabolic disorders illness caused by the absolute or relative lack of insulin secretion, and type 2 diabetes (T2D) is more common in patients. At present, the incidence of diabetes has risen sharply around the world and has become a global public health event. According to 10th Edition of International Diabetes Federation (IDF) in 2021 there were 537 million people aged 20-79 with diabetes worldwide. This number is expected to grow to 643 million by 2030, and it will rise to 783 million by 2045 (1). As a populous country with 110 million people living with diabetes, China has the largest number of diabetic patients in the world, posing a huge challenge to healthcare system in China (2). Diabetic retinopathy (DR), as a major microvascular complication, is one of the most dangerous complications of diabetes. The prevalence of DR among diabetic patients worldwide was 34.6%, and it can reach 40.3% in developed countries (3). There are 2.6 million people had been suffered from visual impairment due to DR until 2015 (4), and this number has been growing over time. In China, 40% of diabetic patients suffer from DR (5), and 1/10 of DR will develop into vision-threatening DR (6). So, DR is considered to be an important factor leading to visual impairment and even blindness in working-age diabetic patients.

Many studies have found that the development of DR is not solely due to hyperglycemia, many patients with well-controlled glycemia also developed DR (7–9). And there is no obvious symptoms in the early stage of DR (10), so most of the current effective treatments are aimed at the late stage of DR, which often accompanied by serious adverse reactions (11). Therefore, it is particularly important to discover early biomarkers of DR' development and carry out intervention in time.

Homocysteine (Hcy) is a sulfur-containing amino acid formed from methionine (Met) metabolism. In the Hcy cycle, a part of Hcy generates Cys through the trans-sulfurization pathway, and the other part is remethylated to regenerate Met. Hyperhomocysteinemia (HHcy) has been widely recognized as a risk factor for cardiovascular disease. Although the specific mechanism is unclear, studies have shown that Hcy causes cardiovascular disease by damaging the vascular endothelium (12, 13). As a microvascular disease, DR is also affected by Hcy to a certain extent. The Hcy cycle can regulate the balance of Met and Cys, linking the folate cycle to promote methylation (14), and the interaction between the various substances in the cycle can also affect the effect of Hcy on DR. In recent years, more and more researches about the effect of Hcy on DR have been carried out. At present, some published literatures have provided evidence for the effect of various risk factors on DR (15, 16), but the specific effect mechanism has been still not clear so far. Therefore, it is very important to understand the risk factors of DR, which provides the evidence for reducing the risk of DR in T2D and develops monitoring and intervention in high-risk groups and early-stage patients to reduce the risk of blindness in diabetic patients.

In this study, we aimed to explore the relationship between Hcy and DR and the impacts of Met and Cys involved in the Hcy cycle pathway on this relationship.

MATERIALS AND METHODS

Study Method and Population

The First Affiliated Hospital of Liaoning Medical University (FAHLMU) is a tertiary general hospital located in Jinzhou, Liaoning Province, China. Inclusion criteria for this study were: 1) Patients diagnosed as T2D or treated with antihyperglycemic therapy; 2) Complete Hcy cycle and DR prevalence information. Exclusion criteria were: 1) T2D patients under 18 years old; 2) Subjects lacked the research indicators, height, weight, and blood pressure. Finally, a total of 1797 subjects were included in the present study, including 232 DR patients. The specific screening steps are shown in **Figure 1**. The diagnosis and classification of T2D in the present study were based on the standard published by World Health Organization (WHO) or treated with antihyperglycemic therapy (17). DR diagnostic criteria based on eye exam results for T2D (18).

The Ethics Committee for Clinical Research of FAHLMU approved the ethics of the study, and informed consent was waivered due to the retrospective nature of the study, which is consistent with the Declaration of Helsinki.

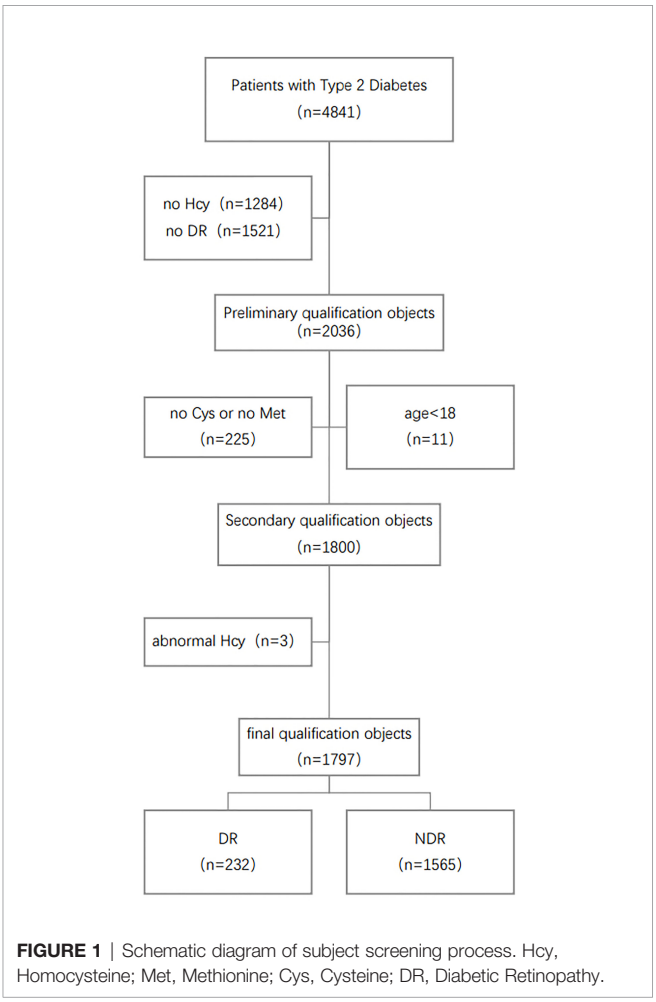

FIGURE 1 | Schematic diagram of subject screening process. Hcy, Homocysteine; Met, Methionine; Cys, Cysteine; DR, Diabetic Retinopathy.

Data Collection and Clinical Definitions

The data retrieved from the electronic medical records included demographic and anthropometric information, as well as current clinical factors and diabetic complications. Demographic included gender, age. Anthropometric measurements included height, weight, systolic blood pressure (SBP) and diastolic blood pressure (DBP). Clinical parameters included glycosylated hemoglobin (HbA1c), triglycerides (TG), total cholesterol (TC), high density lipoprotein cholesterol (HDL-C), low density lipoprotein cholesterol (LDL-C), urinary creatinine (UA), Serum creatinine (SCR), homocysteine (Hcy) concentration, methionine (Met) concentration and cysteine (Cys) concentration.

In the hospital, the measurements of anthropometric indicators were measured by using standardized procedures. Participants were allowed to wear light clothes and no shoes. Height and weight were measured to the nearest 0.5 cm and 0.1 kg, respectively. Blood pressure in adults was measured after a cuff on the right arm with a standard mercury sphygmomanometer and after a 10-minute rest in a seated position at an appropriate size. Age was obtained from the date of birth to the date of hospitalization or medical examination, and was calculated in years. The body mass index (BMI) was calculated as the ratio of body weight (kg) to squared height (m) and classified according to the overweight and obesity criteria recommended by the National Health Commission of China (19). DR was assessed by bilateral retinal photographs and defined as present if the following lesions were found: microaneurysm, retinal hemorrhage, soft exudate, hard exudate, or vitreous hemorrhage.

Based on the RCS curve, we defined the population with Cys concentration higher than 1.45 μmol/L as high Cys population, and the population with less than 1.45 μmol/L concentration as low Cys population (**Figure S1**); The population with higher than 16.9 μmol/L Met concentration was defined as the high Met population, and the population lower than 16.9 μmol/L was defined as the low Met population (**Figure S2**).

Laboratory Assay

Dried blood spots were used in the metabolomic assay, which were prepared from capillary whole blood through an 8-h fasting. We measured the metabolites by direct infusion mass spectrometry technology equipped with the AB Sciex 4000 QTrap system (AB Sciex, Framingham, MA, USA). High-purity water (7732–18–5) and acetonitrile (75-05-8) were purchased from Thermo Fisher (Waltham, MA, USA), and were utilized as diluting agent and mobile phase. 1-Butanol(71-36-3) and acetyl chloride(75-36-5) were obtained from Sigma-Aldrich (St Louis, MO, USA). Isotope-labeled internal standard samples of amino acids (NSK-A) were purchased from Cambridge Isotope Labo-ratories (Tewksbury, MA, USA), while standard samples of the Hcy(14857-77-3), Cys(52-90-4) and Met(63-68-3) were purchased from Chrom Systems (Grafelfing, Germany). In brief, 8.5 mL of venous blood was drawn from each participant at 08:00 to 09.30 h in the morning after an 8-h fasting. Laboratory tests were carried out at a specialized diagnostic laboratory. The level of lipid profiles was analyzed with an automatic biochemistry analyzer (Hitachi 7150, Tokyo, Japan). We also assayed the level of HDL-C and LDL-C by the selective solubilization.

Statistical Analysis

Continuous data were expressed as mean ± standard deviation (SD), non-normal distributed data were expressed as median (interquartile range), and categorical variables were expressed as numbers (percentages). In the four large groups divided by Cys and Met concentrations, it was tested whether there were differences between the patients in the DR group and the NDR group. The p-values of the repeated groups were FDR corrected. Continuous and normal distributed variables were tested with t-test or ANOVA, non-normal variables were analyzed by nonparametric test, and categorical variables were analyzed by chi-square test.

Binary logistic regression models were used to obtain odds ratios (OR) and the 95% confidence intervals (95%CI). Traditional risk factors for DR in T2D patients were adjusted through a structural adjustment program. Through the analysis, we obtained the unadjusted OR value and the adjusted OR value after adding traditional risk factors, including age, gender, body mass index, systolic blood pressure, diastolic blood pressure, low-density lipoprotein cholesterol, High-density lipoprotein cholesterol, triglyceride, total cholesterol, glycosylated hemoglobin, uric acid, serum creatinine.

Restrictive cubic spline (RCS) is a curve that can provide a more intuitive relationship. According to the change of the RCS curve, we select suitable nodes in the RCS. We used it to obtain cut-off values for metabolites associated with DR risk, and selected a cut-off point by visually inspecting the curves of DR probability. Then we repeated the logistic regression analysis in the Cys and Met populations to obtain the corresponding OR values to check whether the concentrations of Met or Cys would affect the relationship between Hcy and DR. Spearman correlation analysis confirmed the correlation between various factors in the Hcy cycle, Hcy and traditional related variables, and then through the mediation effect analysis, we analysis whether there is a mediating effect between Hcy cycle pathway and DR. We excluded patients with DR for >2 years to examine the effect of Hcy on the risk of DR. All analyses were performed using R version 4.1.0 and SAS 9.4.

RESULT

Description of Study Subjects

Table 1 summarizes the selected characteristics of the DR group and the control group in the total population and the population grouped by Cys and Met. The study included a total of 1797 participants with a mean age of 57.27 years (SD: 14.17) and a mean BMI of 26.14 kg/m^2 (SD: 4.66). 48.1% of subjects were male. 232 DR patients were included in the study, of which 119 (51.3%) were male. The power of all four groups was greater than 0.95.

TABLE 1 | Clinical and biochemical characteristics of participants according to the occurrence of diabetic retinopathy.

Variables	Total subjects	Low Cys		P	High Cys		P	Low Met		P	High Met		P
		Non-DR Mean/ number (SD or %)	DR Mean/ number (SD or %)		Non-DR Mean/ number (SD or %)	DR Mean/ number (SD or %)		Non-DR Mean/ number (SD or %)	DR Mean/ number (SD or %)		Non-DR Mean/ number (SD or %)	DR Mean/ number (SD or %)	
Age (years)	57.27 ± 14.17	56.66 ± 14.72	58.64 ± 11.05	0.158	57.67 ± 14.42	56.99 ± 11.28	0.632	57.11 ± 14.62	58.43 ± 10.66	0.341	57.24 ± 14.53	57.21 ± 11.71	0.981
Male sex	864 (48.1%)	361 (47.4%)	62 (51.7%)	0.445	384 (47.8%)	57 (50.9%)	0.603	348 (48.4%)	60 (49.6%)	0.886	397 (46.9%)	59 (53.2%)	0.257
Weight (kg)	71.73 ± 14.03	72.15 ± 14.49	70.58 ± 12.81	0.263	71.36 ± 14.52	69.53 ± 12.95	0.205	72.49 ± 14.63	70.69 ± 13.29	0.206	70.84 ± 13.65	69.36 ± 13.21	0.279
Height (cm)	165.00 (160.00, 172.00)	165.00 (160.00, 172.00)	164.00 (160.00, 171.00)	0.490	167.00 (160.00, 172.00)	165.00 (160.00, 170.00)	0.080	165.00 (160.00, 171.50)	163.00 (160.00, 172.00)	0.302	165.00 (160.00, 171.00)	164.00 (160.00, 171.00)	0.646
BMI (kg/m²)	26.14 ± 4.66	26.34 ± 5.18	25.72 ± 3.88	0.215	25.64 ± 4.63	25.33 ± 4.26	0.498	26.52 ± 5.25	26.01 ± 4.75	0.320	25.71 ± 4.31	25.18 ± 3.85	0.219
BMI<18.5	57 (3.2%)	20 (2.6%)	1 (0.9%)		37 (4.6%)	5 (4.5%)		26 (3.6%)	2 (1.7%)		33 (3.9%)	3 (2.7%)	
BMI≥18.5and<24.0	534 (29.7%)	235 (30.9%)	42 (35.0%)		251 (31.2%)	37 (33.0%)		209 (29.1%)	39 (32.2%)		254 (30.0%)	44 (39.6%)	
BMI≥24and<28.0	655 (36.4%)	275 (36.1%)	46 (38.3%)		308 (38.3%)	45 (40.2%)		243 (33.8%)	50 (41.3%)		334 (39.5%)	38 (34.2%)	
BMI≥28.0	551 ((30.7%)	231 (30.4%)	31 (25.8%)		208 (25.9%)	25 (22.3%)		241 (33.5%)	30 (24.8%)		225 (26.6%)	26 (23.5%)	
SBP (mmHg)	140.96 ± 23.92	140.55 ± 24.02	145.85 ± 25.09	0.026	140.14 ± 23.30	144.20 ± 24.58	0.087	139.04 ± 23.93	143.99 ± 24.37	0.036	141.42 ± 23.38	145.95 ± 25.21	0.058
DBP (mmHg)	83.24 ± 13.69	83.35 ± 13.18	83.91 ± 14.70	0.669	82.88 ± 13.89	84.25 ± 14.11	0.328	82.87 ± 14.29	83.78 ± 14.39	0.519	83.27 ± 12.93	84.17 ± 14.47	0.497
HbA1c (%)	9.62 ± 2.42	9.81 ± 2.47	9.31 ± 2.33	0.041	9.32 ± 2.36	9.84 ± 2.56	0.032	9.62 ± 2.37	9.74 ± 2.60	0.613	9.44 ± 2.36	9.37 ± 2.38	0.750
Triglyceride (mmol/L)	1.66 (1.12, 2.52)	1.69 (1.11, 2.54)	1.80 (1.21, 2.75)	0.267	1.67 (1.13, 2.55)	1.64 (1.17, 2.82)	0.441	1.71 (1.13, 2.59)	1.58 (1.11, 2.38)	0.376	1.62 (1.07, 2.43)	1.91 (1.33, 3.00)	0.005
TC (mmol/L)	4.76 (4.01, 5.54)	4.69 (4.01, 5.40)	4.80 (4.16, 5.74)	0.206	4.73 (3.95, 5.52)	5.11 (4.38, 5.98)	0.001	4.80 (3.98, 5.49)	4.96 (4.18, 5.74)	0.097	4.69 (3.93, 5.42)	4.88 (4.16, 5.65)	0.071
HDL-C (mmol/L)	1.11 ± 0.35	1.07 ± 0.32	1.12 ± 0.37	0.097	1.14 ± 0.38	1.15 ± 0.42	0.732	1.09 ± 0.34	1.16 ± 0.41	0.038	1.11 ± 0.36	1.11 ± 0.30	0.946
Male (HDL-C<1.0 mmol/L)	330 (18.4%)	161 (21.2%)	27 (22.5%)		131 (16.3%)	20 (17.9%)		138 (19.2%)	17 (14.1%)		147 (17.4%)	20 (18.0%)	
Female (HDL-C<1.3 mmol/L)	726 (40.4%)	330 (43.4%)	43 (35.8%)		313 (38.9%)	43 (38.4%)		296 (41.2%)	48 (39.7%)		347 (41.0%)	44 (39.6%)	
LDL-C (mmol/L)	2.83 (2.25, 3.46)	2.80 (2.28, 3.45)	2.80 (2.26, 3.50)	0.948	2.82 (2.24, 3.42)	3.13 (2.57, 3.51)	0.004	2.91 (2.32, 3.45)	2.81 (2.32, 3.40)	0.665	2.73 (2.22, 3.42)	2.89 (2.29, 3.46)	0.259
Hcy (μmol/L)	8.18 (7.47, 8.84)	7.98 (6.63, 8.55)	7.67 (6.46, 8.30)	0.007	8.41 (7.87, 9.19)	8.58 (7.88, 9.10)	0.507	8.16 (7.41, 8.71)	7.93 (7.05, 8.63)	0.109	8.24 (7.60, 8.97)	8.22 (6.95, 9.03)	0.656
<7.7μmol/L	536 (29.8%)	300 (39.4%)	62 (51.7%)		152 (18.9%)	22 (19.6%)		225 (31.3%)	46 (38.0%)		227 (26.8%)	38 (34.2%)	
≥7.7μmol/L	1261 (70.2%)	461 (60.6%)	58 (48.3%)		652 (81.1%)	90 (80.4%)		494 (68.7%)	75 (62.0%)		619 (73.2%)	73 (65.8%)	
UA	278.00 (181.00, 364.00)	284.20 (214.96, 371.00)	305.00 (238.25, 375.02)	0.149	265.70 (7.00, 358.00)	284.05 (175.03, 358.50)	0.460	282.00 (165.50, 369.50)	289.00 (196.00, 371.00)	0.779	273.55 (171.25, 360.00)	291.96 (228.50, 353.50)	0.178
SCR	59.00 (47.90, 75.51)	58.80 (47.52, 74.45)	56.12 (47.48, 75.26)	0.902	59.85 (47.03, 77.00)	59.52 (50.97, 74.22)	0.813	58.00 (46.05, 75.40)	56.74 (47.61, 74.89)	0.803	60.60 (49.16, 75.96)	57.00 (48.89, 72.43)	0.326

BMI, body mass index; SBP, systolic blood pressure; DBP, diastolic blood pressure; HbA1c, glycated hemoglobin; TG, triglyceride; HDL-C, high-density lipoprotein cholesterol; LDL-C, low-density lipoprotein cholesterol; Hcy, Homocysteine; UA, uric acid; SCR, serum creatinine.

Data are mean ± standard deviation, median (IQR), or n (%).

P values were derived from the t-test for normally distributed variables, Mann-Whitney U test for skewed distributions, Chi-square test (or fisher test if appropriate) for categorical variables. P < 0.05 was defined as statistically significant.

According to the Cys concentration, the population was divided into two groups. In the low Cys population, Only the differences of SBP, HbA1c and Hcy between two groups were statistically significant. DR patients had higher SBP, HbA1c concentration and lower Hcy concentration. In the high Cys population, the differences of HbA1c, TC and LDL-C between two groups among other indicators were statistically significant. The concentration of HbA1c, TC and HDL-C in the DR group were all higher.

We divided the general population into two groups according to the Met concentration of subjects in the same way. In the low Met population, the differences of SBP and HDL-C between two groups were statistically significant. The SBP and HDL-C concentrations in the DR group were higher. In the high Met population, except for TG, there was no significant difference in other indicators between the two groups, and the TG concentration was higher in the DR group.

The Association Between Homocysteine and Diabetic Retinopathy

The slope of the RCS curves of Hcy and DR have a process from large to small, and 7.7μmol/L is the junction point of the slope change. Among all subjects, 536 (29.8%) had plasma Hcy levels below 7.7 μmol/L (**Figure 2**).

For numerical Hcy, Hcy was inversely associated with DR risk in univariate regression, but the difference in this relationship was not significant (OR: 0.85, 95%CI: 0.71-1.03). After adjusting for traditional risk factors associated with DR, the negative correlation became significant and enhanced. After a step-by-step adjustment of the Model 1, we found that it was the adjustment of SBP that made the relationship between Hcy and DR significant. For the categorical Hcy (as reference), the relationship between Hcy and DR was significant in both univariate and multivariate regression (**Table 2**).

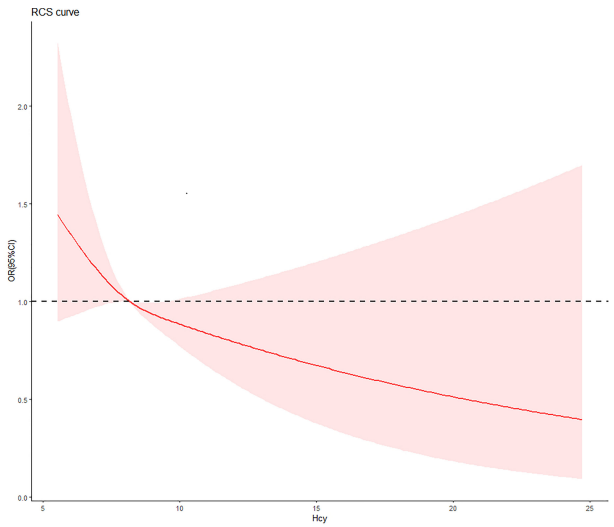

FIGURE 2 | The relationship between Hcy concentration and DR risk in T2D patients. The red curve was derived from multivariate analysis that adjusted for age, gender, body mass index, systolic blood pressure, diastolic blood pressure, low-density lipoprotein cholesterol, high-density lipoprotein cholesterol, triglyceride, glycosylated hemoglobin, urinary creatinine and serum creatine.

TABLE 2 | Odds ratio of Homocysteine (Hcy) for the risk of diabetic retinopathy.

	OR(95%CI)	P
Univariable model		
Hcy, per μmol/L	0.85 (0.71,1.03)	0.064
<7.7μmol/L	reference	
≥7.7μmol/L	0.72 (0.54-0.96)	0.025
Multivariable model1		
Hcy, per μmol/L	0.84 (0.7,1)	0.027
<7.7μmol/L	reference	
≥7.7μmol/L	0.73 (0.55,0.98)	0.04
Multivariable model2		
Hcy, per μmol/L	0.83 (0.69,1)	0.024
<7.7μmol/L	reference	
≥7.7μmol/L	0.72 (0.53-0.96)	0.029
Multivariable model3		
Hcy, per μmol/L	0.83 (0.69,1)	0.025
<7.7μmol/L	reference	
≥7.7μmol/L	0.73 (0.54-0.98)	0.04

In different models, the categorical Hcy divided into two groups by 7.7μmol/L was used as a reference, and then observed changes of numerical and categorical Hcy respectively.
Multivariable Model 1 was adjusted for age, gender, body mass index., systolic blood pressure, diastolic blood pressure.
Multivariable Model 2 was adjusted for variables in Model 1 and concentrations of low-density lipoprotein cholesterol, high-density lipoprotein cholesterol, triglyceride, total cholesterol, glycosylated hemoglobin.
Multivariable Model 3 was adjusted for variables in Model 2 and concentrations of uric acid, serum creatinine.

The Influence of Methionine and Cysteine Levels on the Association Between Homocysteine and Diabetic Retinopathy

In the population grouped by Cys concentration, the relationship between Hcy and DR was only significant in the low Cys population. Both univariate regression (OR: 0.77, 95%CI: 0.63-0.93) and multivariate regression (OR: 0.75, 95%CI: 0.61-0.94) showed a negative relationship between numerical Hcy and DR. For the binary Hcy, this negative relationship was still significant. This negative association enhanced after adjusting for traditional risk factors (univariate regression (OR: 0.61, 95%CI: 0.41-0.9), multivariate regression (OR: 0.6, 95%CI: 0.4-0.9). In the high Cys population, the relationship between Hcy and DR was no longer significant in both univariate and multivariate regression.

In addition, after grouping the total population by Met level, the relationship between Hcy and DR became no longer significant. The mediating effect of Hcy and Met cycle on DR was significant. It was suggested that the grouping of Met concealed the heterogeneity of Hcy levels in the same pathway (**Table 3**).

Correlation Between Homocysteine Cycle and Relevant Factors

We analyzed the correlation between three main factors involved in Hcy cycle pathway and other factors associated with the progression of DR, and only retained the factors that were significantly associated with Hcy (**Figure 3**). At first, the positive correlations between Hcy, Met and Cys were all significant, and the correlation between Hcy and Cys was the

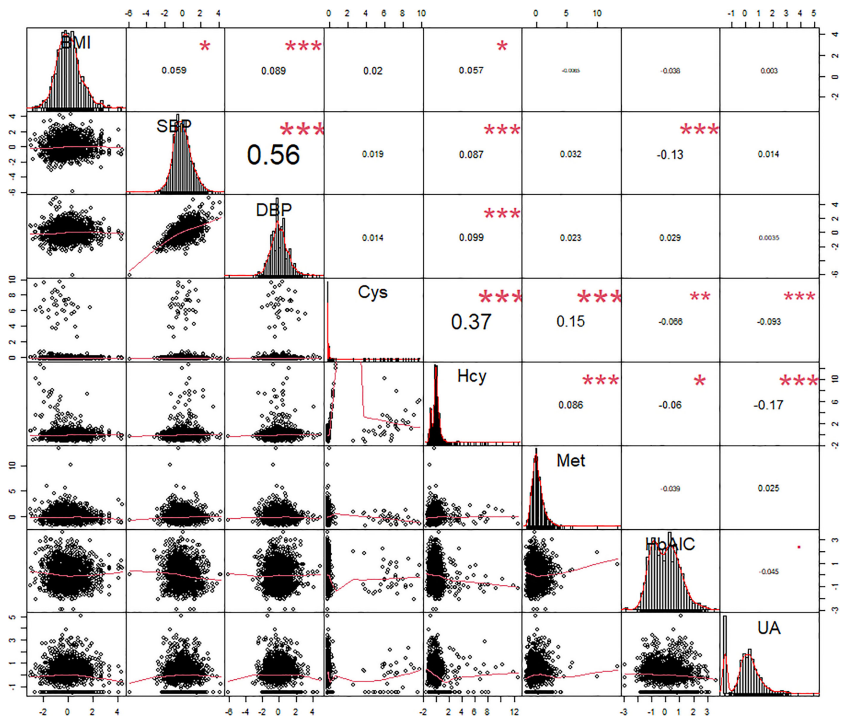

FIGURE 3 | Spearman correlation coefficients and probability density plots between plasma Hcy and risk factors of DR (n=1797). BMI, body mass index. SBP, systolic blood pressure. DBP, diastolic blood pressure; HbAlc, glycated hemoglobin; Hcy, Homocysteine; Met, Methionine; Cys, Cysteine; UA, uric acid. *p-value <0.05, **p-value <0.01, ***p-value <0.001.

largest, r=0.37. In addition, there were significant correlations between Hcy and BMI, SBP, DBP, HbA1c, and UA, among which HbA1c and UA were negatively correlated. In addition to the Hcy-related indicators, the factor with the strongest correlation with Hcy was UA, r=-0.17. The small correlation coefficient may be affected by other unadjusted factors, but the

TABLE 3 | Odds ratio of Homocysteine (Hcy) for the risk of diabetic retinopathy in different group by Met and Cys.

	Low Cys		High Cys		Low Met		High Met	
	OR (95%CI)	P	OR (95%CI)	P	OR (95%CI)	P	OR (95%CI)	P
Univariable model								
Hcy, per μmol/L	0.77 (0.63,0.93)	0.016	0.94 (0.75,1.17)	0.545	0.88 (0.69,1.13)	0.271	0.84 (0.64,1.11)	0.166
<7.7μmol/L	reference		reference		reference		reference	
≥7.7μmol/L	0.61 (0.41,0.9)	0.024	0.95 (0.58,1.57)	0.853	0.74 (0.5,1.11)	0.148	0.7 (0.46,1.07)	0.108
Multivariable model1								
Hcy, per μmol/L	0.76 (0.62,0.93)	0.016	0.91 (0.72,1.14)	0.374	0.87 (0.68,1.11)	0.208	0.83 (0.63,1.1)	0.152
<7.7μmol/L	reference		reference		reference		reference	
≥7.7μmol/L	0.6 (0.4,0.89)	0.022	0.96(0.58,1.58)	0.873	0.74 (0.5,1.12)	0.158	0.71 (0.46,1.08)	0.117
Multivariable model2								
Hcy, per μmol/L	0.76 (0.61,0.93)	0.016	0.93 (0.74,1.16)	0.498	0.87 (0.68,1.12)	0.239	0.84 (0.64,1.1)	0.162
<7.7μmol/L	reference		reference		reference		reference	
≥7.7μmol/L	0.59 (0.4,0.89)	0.022	1.01 (0.61,1.68)	0.938	0.73 (0.48,1.1)	0.138	0.71 (0.46,1.09)	0.12
Multivariable model3								
Hcy, per μmol/L	0.75 (0.61,0.94)	0.022	0.93 (0.74,1.16)	0.502	0.86 (0.66,1.12)	0.216	0.86 (0.66,1.13)	0.225
<7.7μmol/L	reference		reference		reference		reference	
≥7.7μmol/L	0.6 (0.4,0.9)	0.030	1.01 (0.61,1.69)	0.940	0.72 (0.47,1.1)	0.131	0.74 (0.48,1.14)	0.175

In different models, the categorical Hcy divided into two groups by 7.7μmol/L was used as reference, and then observed changes of numerical and categorical Hcy respectively.
Multivariable Model 1 was adjusted for age, gender, body mass index., systolic blood pressure, diastolic blood pressure.
Multivariable Model 2 was adjusted for variables in Model 1 and concentrations of low-density lipoprotein cholesterol, high-density lipoprotein cholesterol, triglyceride, total cholesterol, glycosylated hemoglobin.
Multivariable Model 3 was adjusted for variables in Model 2 and concentrations of uric acid, serum creatinine.
The p-values of the repeated groups were FDR corrected.

TABLE 4 | Mediation analysis of the relationship between Met and DR by Hcy.

	Met		
	Parameter estimate	**OR (95%CI)**	**P**
Total effect c	-0.0327	0.968 (0.938,0.998)	0.03826
Direct effect path c'	-0.0311	0.969 (0.940,0.999)	0.04882
Path a	0.0456	1.047 (1.004,1.091)	0.032820
Path b	-0.0367	0.964 (0.932,0.998)	0.03564

Adjusted for age, gender, body mass index., systolic blood pressure, diastolic blood pressure, low-density lipoprotein cholesterol, high-density lipoprotein cholesterol, triglyceride, total cholesterol, glycosylated hemoglobin, uric acid, serum creatinine.
Path c' indicated the path from Met to DR (Outcome) when controlled for Hcy (Mediator).
Path a indicated the path from Met to Hcy (Mediator).
Path b indicated the path from Hcy (Mediator) to DR (Outcome).

significance of its correlation indicates the significance of our inclusion of adjustment.

Mediating Effect of Homocysteine Cycle Pathway

We used the causal steps approach (20) to analyze the mediating effect of the Hcy cycle pathway. **Tables 4**, **5** showed the results of the mediation analysis. In Model 1 (Hcy as mediator), the total effect of Met concentration on DR was significant (OR: 0.968, 95%CI: 0.938-0.998). The interaction between Met and Hcy was significant (OR: 1.047, 95%CI: 1.004-1.091). The effect of Hcy on DR was significant (OR: 0.964, 95%CI: 0.932-0.998). Meanwhile, the direct effect of Met on DR remained significant (OR: 0.969, 95%CI: 0.940-0.999) after adjusting for the Hcy (**Figure 4**). It shows that the mediation effect is significant in Model 1, and it is incomplete mediation.

In model 2 (Cys as mediator), the total effect of Hcy on DR was significant (OR: 0.964, 95%CI: 0.932-0.998). The interaction between Hcy and Cys was significant (OR: 1.290, 95%CI: 1.227-1.355). However, the effect of Cys on DR was not significant (OR: 0.986, 95%CI: 0.956-0.1.017). After adjusting for Cys, the direct effect of Hcy on DR was still not significant (OR: 0.966, 95%CI: 0.932-1.000) (**Figure 5**). It shows that there is no mediation effect in the pathway of model 2.

DISCUSSION

We divided the study population according to the slope change point of the RCS curve, and we obtained that the Hcy and DR are negatively correlated. In the study, it can be seen from the changing direction of the RCS curve that in people with low concentrations of Hcy, even if it is not reached the level of traditional high Hcy, there can still have an impact on the development of DR. And after the changing point of slope (7.7 μmol/L), the effect of Hcy on the risk of DR tends to be gentle, and it can be seen that the intervention before this point is more effective in reducing the risk of DR.

At present, many scholars have carried out relevant researches about the prediction of disease risk by Hcy level in the body. Hcy is considered to be related to a variety of diseases, especially the relationship with cardiovascular disease has been confirmed many times. In recent years, many scholars have begun to explore the effect of Hcy on diabetes and its complications, but the results of the relationship between Hcy and diabetes and its complications are controversial. Mainstream results suggest that Hcy is a risk factor for DR. A cross-sectional study in Hoorn identified Hcy as a risk factor for DR (21), and then they did a prospective cohort study which found that Hcy affects DR possibly by reducing transmethylation *in vivo* (22). However, there are also some findings that are considered to be consistent with our results. A study found that Hcy above its threshold will increase the risk of DR (OR=1.66), while Hcy below the threshold become a protective factor for the DR (OR=0.83) (23). Although the result at low concentrations of Hcy was not statistically significant, this result was consistent with us in direction. We believe that the small sample sizes of the study (n=140) and the lack of adjustment for HDL-C, LDL-C, and UA may account for the no statistically significant results. Another study found that the median Hcy concentration in

TABLE 5 | Mediation analysis of the relationship between Hcy and DR by Cys.

	Cys		
	Parameter estimate (95%CI)	**OR (95%CI)**	**P**
Total effect	-0.0367	0.964 (0.932,0.998)	0.03564
Direct effect path c'	-0.0349	0.966 (0.932,1.000)	0.05175
Path a	0.2543	1.290 (1.227,1.355)	< 0. 01
Path b	-0.0143	0.986 (0.956,1.017)	0.36798

Adjusted for age, gender, body mass index., systolic blood pressure, diastolic blood pressure, low-density lipoprotein cholesterol, high-density lipoprotein cholesterol, triglyceride, total cholesterol, glycosylated hemoglobin, uric acid, serum creatinine.
Path c' indicated the path from Hcy to DR (Outcome) when controlled for Cys (Mediator).
Path a indicated the path from Hcy to Cys (Mediator).
Path b indicated the path from Cys (Mediator) to DR (Outcome).

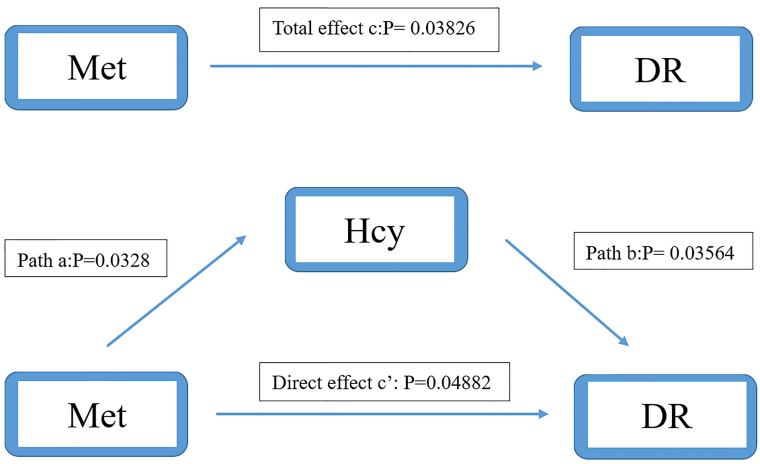

FIGURE 4 | Mediation analysis of the relationship between Met and DR by Hcy. The mediation analysis adjusted for age, gender, body max index, systolic blood pressure, diastolic blood pressure, low-density lipoprotein cholesterol, high-density lipoprotein cholesterol, triglyceride, glycosylated hemoglobin, urinary creatinine and serum creatinine.

healthy people was 7.8 μmol/L, and the Hcy concentration in diabetic patients increased to 10.2 μmol/L. And the Hcy concentration continued to increase in patients with DR (24). Although this article does not conduct in-depth research on the effect of lower concentrations of Hcy on the risk of DR, it is basically consistent with the range of DR risk reduction in our study. It can be seen that the effect of Hcy on the DR presents a U-shaped curve. We believe that the possible reasons for the discrepancy in the study results are as follows: 1. different definitions of the normal range of Hcy in different studies (25). 2. The lower Hcy level in T2D patients than in healthy subjects in this study is a partial reflection of the U-shaped curve for the effect of Hcy on DR.

Hcy is an important intermediate product in the metabolism of Met to Cys. *In vivo*, a part of Hcy will regenerate Met in two ways: 1) Remethylation under the action of Met synthase and VB_{12} to generate Met and Tetrahydrogen folic acid (THFA). 2) is catalyzed by Betaine-homocysteine S-methyltransferase to generate Met and dimethylglycine. Another part forms cystathionine under the action of cystathionine β-synthase (CBS) and VB_6 through the trans-sulfation pathway, and cystathionine forms Cys and α-ketobutyric acid under the action of γ-cystathionine lyase (26, 27). This is the main metabolic process of Hcy in the body. And the changes of Met and Cys *in vivo* also have influence on Hcy.

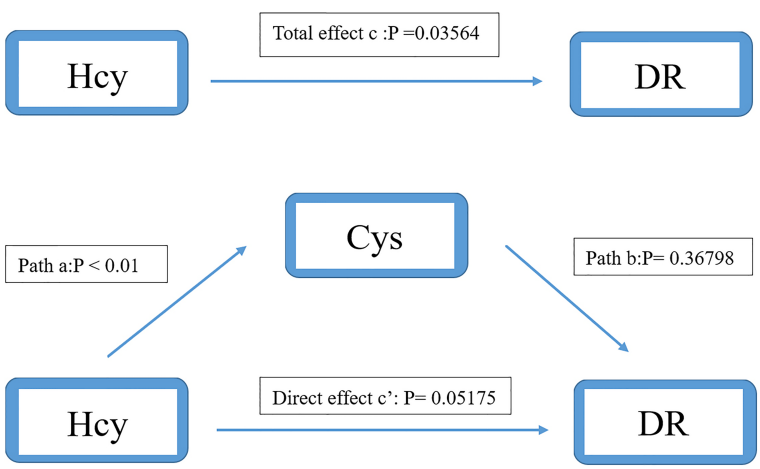

FIGURE 5 | Mediation analysis of the relationship between Hcy and DR by Cys. The mediation analysis adjusted for age, gender, body max index, systolic blood pressure, diastolic blood pressure, low-density lipoprotein cholesterol, high-density lipoprotein cholesterol, triglyceride, glycosylated hemoglobin, urinary creatinine and serum creatinine.

In the population grouped by Cys, low concentrations of Cys showed a significant additive interaction on the protective effect of Hcy on DR. It can be seen that low concentrations of Cys enhance the protective effect of Hcy [total population (OR: 0.83, 95%CI: 0.69-1), low Cys population (OR: 0.75, 95% CI: 0.61-0.94)]. Cys is a sulfur-containing amino acid that supports the occurrence of various reactions in the body, such as the transformation and synthesis of proteins and glutathione (GSH) (28). GSH is a tripeptide containing γ-amide bond and sulfhydryl, which has antioxidant and detoxification effects and maintains normal immune function of the body. Cys is indispensable in the synthesis of GSH. Insufficient Cys can lead to decreased GSH levels in the body, which in turn reduces the body's antioxidant capacity, leading to decreased immunity and aging of the body (29). It can be seen that the protective effect is stronger in the population with low Cys concentration, which means that the Hcy level is relatively higher in the normal range of our study. We believe that this additive effect on Hcy protection is temporary. Some studies have found that when the concentration of Hcy reaches about 10 μmol/L, the effect on the microvascular disease of the body becomes a negative effect (24). The conclusions obtained from our study are not in conflict with the existing results. In addition, the blood pressure of the case group was higher than that of the control group, and the difference between the systolic blood pressure was statistically significant. The result is consistent with previous studies showing that elevated blood pressure is a risk factor for diabetes and its complications (30, 31). Blood pressure control can reduce the risk of the disease.

In addition, the population grouped by Met concealed the heterogeneity of Hcy levels on the same pathway, making the relationship between Hcy and DR no longer significant. We think it is due to the mediating effect between Met, Hcy and DR pathway. We found a positive correlation between Met and Hcy concentration, indicating that the reduction of Met will synchronously lead to the decrease of Hcy concentration in individuals, and affect the difference of the real Hcy level in the actual population.

There are some published papers that are inconsistent with our results. We speculate that the heterogeneity of the population may had an impact on the differences in results. In addition, our study only reflects the relative changes of DR risk and does not represent the actual protection threshold. And due to the different definitions of population divisions, too low concentrations of Hcy may lead to changes in other metabolites in the body, resulting in inconsistent conclusions. In some published papers, most scholars use the definition of high Hcy (>15 μmol/L) to divide the population (32, 33) to study the effect of high Hcy on the human body. Few scholars have studied the relationship between the population with relatively low Hcy concentration and the pathogenesis of DR. And our research is based on this.

The accumulation of Hcy in the body may be caused by two reasons: excessive production or abnormal metabolism of Hcy. Disorders of Met metabolizing enzymes and Hcy metabolizing enzymes (CBS, MS, MTHFR) can lead to disorders of Hcy metabolism, resulting in elevated Hcy concentrations. Similarly, vitamins B_2, B_6, B_{12} and folic acid are important coenzymes in the process of Hcy metabolism, and deficiency of these vitamins can lead to abnormal Hcy metabolism, resulting in Hcy accumulation and causing HHcy (27). Studies have found that DR patients generally have lower concentrations of folic acid and VB_{12} (23), and folic acid is the main nutritional factor affecting Hcy concentration (34). Vitamin D deficiency is common in people with diabetes, and its deficiency increases the risk of microvascular disease (35). The retina is rich in polyunsaturated fatty acids and is very sensitive to oxidative stress. As an antioxidant, vitamin C can play a protective role in DR progression (36). In addition, studies have found that although the relationship between vitamin A and DR has shown inconsistent results in various countries, it has been demonstrated that V_A can significantly affect the development of DR (37). So, we believe that the protective phenomenon of Hcy in our study prompted other factors such as vitamin deficiency, drug use or disease state caused by abnormal Hcy metabolism. The use of metformin can reduce glycemia while leading to the deficiency of folic acid and VB_{12}. Meanwhile, the metformin may affect Hcy metabolism, which in turn affects the progression of DR (10). Therefore, it can be seen from our research results that the progression of DR is not only the effect of one certain factor, but also the result of the joint action of many factors.

In addition, studies have found that when the population was binarized by Hcy concentration, the difference in the prevalence of DR between two groups was not statistically significant (25). This phenomenon is related to our study, which indirectly confirms that the risk of DR in the population with low Hcy concentration is not lower than that in the high Hcy population. It is suggested that we should consider the adverse effects of low Hcy on the levels of other substances related to the pathogenesis of DR in the human body.

Our research has important implications for clinical practice. At present, the clinical significance of high Hcy is mostly considered in clinical practice while little attention is paid to the joint effect of other factors reflected by Hcy. The study pointed out that the lower the level of Hcy in the body is not the better, and we should pay attention to the changes of other indicators reflected behind the low Hcy.

Our research also has shortcomings. First, due to the nature of the cross-sectional study, we could not prove the existence of a causal relationship, which requires more prospective cohort studies to confirm. Considering that there is still a lack of population studies on the Hcy pathway and the risk of DR, our study which as a cross-sectional study with a larger sample size, can provide certain etiological clues. DR caused by change in Hcy concentration or the change of Hcy concentration caused by DR *in vivo* have been a controversial topic in academic circles. Secondly, because of a lack of vitamin concentration and drug use, it is impossible to verify the effect of vitamins on this cycle, and the effect of drugs on the relationship between Hcy and DR cannot be determined either. Furthermore, our cases did not distinguish the types of DR. The difference in Hcy concentrations

between patients with non-proliferating diabetic retinopathy (NPDR) and proliferative diabetic retinopathy (PDR) has been shown to be significant in some studies (24), and more detailed and in-depth studies are needed on the concentration of Hcy in patients with different types of DR.

In conclusion, we found an inverse relationship between low concentrations of Hcy and the risk of DR in T2D patients, suggesting that the influence curve of Hcy on DR may be U-shaped. This relationship was mainly influenced by the interaction of Cys *in vivo* and by changes in Met concentration. It may be a reflection of the lack of indicators such as vitamins in the body. Further experimental studies are needed to determine the role of Hcy in the pathogenesis of DR.

DATA AVAILABILITY STATEMENT

The raw data supporting the conclusions of this article will be made available by the authors, without undue reservation.

ETHICS STATEMENT

Ethical review and approval was not required for the study on human participants in accordance with the local legislation and institutional requirements. The patients/participants provided their written informed consent to participate in this study. Written informed consent was obtained from the individual(s) for the publication of any potentially identifiable images or data included in this article.

AUTHOR CONTRIBUTIONS

W-ML is mainly responsible for writing the article, Z-ZF provides data support, and all the members are responsible for data analysis and collection. All authors contributed to the article and approved the submitted version.

FUNDING

This work was supported by the national key research and development program of China (2021YFA1301200, 2021YFA1301202), Special Fund of State Key Joint Laboratory of Environment Simulation and Pollution Control. The funders had no role in study design, data collection and analysis, decision to publish, or preparation of the manuscript.

ACKNOWLEDGMENTS

The authors thank all doctors, nurses and research staff at the Liaoning Medical University in Jinzhou, for their participation in this study.

SUPPLEMENTARY MATERIAL

The Supplementary Material for this article can be found online at: https://www.frontiersin.org/articles/10.3389/fendo.2022.883845/full#supplementary-material

REFERENCES

1. International Diabetes Federation. (2021) *E. coli.* Available at: https://www.diabetesatlas.org [Accessed May 22, 2022].
2. Ma. Epidemiology of Diabetes and Diabetic Complications in China. *Diabetologia* (2018) 61:1249–60. doi: 10.1007/s00125-018-4557-7
3. Hou, Cai, Jia, Shi. Risk Factors and Prevalence of Diabetic Retinopathy: A Protocol for Meta-Analysis. *Med (Baltimore)* (2020) 99:e22695. doi: 10.1097/MD.0000000000022695
4. Flaxman, Bourne, Resnikoff, Ackland, Braithwaite, Cicinelli, et al. Taylor and Vision Loss Expert Group of the Global Burden of Disease. Global Causes of Blindness and Distance Vision Impairment 1990-2020: A Systematic Review and Meta-Analysis. *Lancet Glob Health* (2017) 5:e1221–34. doi: 10.1016/S2214-109X(17)30393-5
5. Yin, Zhang, Ren, Su, Sun. Prevalence and Risk Factors of Diabetic Retinopathy in Diabetic Patients: A Community Based Cross-Sectional Study. *Med (Baltimore)* (2020) 99:e19236. doi: 10.1097/MD.0000000000019236
6. Chen, Gardner. A Critical Review: Psychophysical Assessments of Diabetic Retinopathy. *Surv Ophthalmol* (2021) 66:213–30. doi: 10.1016/j.survophthal.2020.08.003
7. Satyanarayana, Balakrishna, Pitla, Reddy, Mudili, Lopamudra, et al. Status of B-Vitamins and Homocysteine in Diabetic Retinopathy: Association With Vitamin-B12 Deficiency and Hyperhomocysteinemia. *PloS One* (2011) 6: e26747. doi: 10.1371/journal.pone.0026747
8. Wang, Du, Wang, Zhang. Therapeutic Investigation of Quercetin Nanomedicine in a Zebrafish Model of Diabetic Retinopathy. *BioMed Pharmacother* (2020) 130:110573. doi: 10.1016/j.biopha.2020.110573
9. Simo-Servat, Hernandez, Simo. Diabetic Retinopathy in the Context of Patients With Diabetes. *Ophthalmic Res* (2019) 62:211–7. doi: 10.1159/000499541
10. Malaguarnera, Gagliano, Salomone, Giordano, Bucolo, Pappalardo, et al. Folate Status in Type 2 Diabetic Patients With and Without Retinopathy. *Clin Ophthalmol* (2015) 9:1437–42. doi: 10.2147/OPTH.S77538
11. Simo-Servat, Simo, Hernandez. Circulating Biomarkers of Diabetic Retinopathy: An Overview Based on Physiopathology. *J Diabetes Res* (2016) 2016:5263798. doi: 10.1155/2016/5263798
12. Keller, Klawitter, Hildreth, Christians, Putnam, Kohrt, et al. Elevated Plasma Homocysteine and Cysteine are Associated With Endothelial Dysfunction Across Menopausal Stages in Healthy Women. *J Appl Physiol 1985* (2019) 126:1533–40. doi: 10.1152/japplphysiol.00819.2018
13. He, Zeng, Li, Feng, Liu, Liu, et al. Homocysteine Impairs Coronary Artery Endothelial Function by Inhibiting Tetrahydrobiopterin in Patients With Hyperhomocysteinemia. *Am J Physiol Endocrinol Metab* (2010) 299:E1061–5. doi: 10.1152/ajpendo.00367.2010
14. Reed, Nijhout, Sparks, Ulrich. A Mathematical Model of the Methionine Cycle. *J Theor Biol* (2004) 226:33–43. doi: 10.1016/j.jtbi.2003.08.001
15. Xu, Wu, Liu, Liu, Wang, Yu. Relationship Between Homocysteine Level and Diabetic Retinopathy: A Systematic Review and Meta-Analysis. *Diagn Pathol* (2014) 9:167. doi: 10.1186/s13000-014-0167-y
16. Tawfik, Mohamed, Elsherbiny, DeAngelis, Bartoli, Al-Shabrawey. Homocysteine: A Potential Biomarker for Diabetic Retinopathy. *J Clin Med* (2019) 8:121. doi: 10.3390/jcm8010121
17. Alberti, Zimmet. Definition, Diagnosis and Classification of Diabetes Mellitus and its Complications. Part 1: Diagnosis and Classification of Diabetes Mellitus Provisional Report of a WHO Consultation. *Diabetes Med* (1998)

15:539–53. doi: 10.1002/(SICI)1096-9136(199807)15:7<539::AID-DIA668>3.0.CO;2-S
18. Faselis, Katsimardou, Imprialos, Deligkaris, Kallistratos, Dimitriadis. Microvascular Complications of Type 2 Diabetes Mellitus. *Curr Vasc Pharmacol* (2020) 18:117–24. doi: 10.2174/1570161117666190502103733
19. Chen, LuDepartment of Disease Control Ministry of Health. The Guidelines for Prevention and Control of Overweight and Obesity in Chinese Adults. *BioMed Environ Sci* (2004) 17:1–36.
20. MacKinnon, Fairchild, Fritz. Mediation Analysis. *Annu Rev Psychol* (2007) 58:593–614. doi: 10.1146/annurev.psych.58.110405.085542
21. Hoogeveen, Kostense, Eysink, Polak, Beks, Jakobs, et al. Hyperhomocysteinemia is Associated With the Presence of Retinopathy in Type 2 Diabetes Mellitus: The Hoorn Study. *Arch Intern Med* (2000) 160:2984–90. doi: 10.1001/archinte.160.19.2984
22. Van Hecke, Dekker, Nijpels, Teerlink, Jakobs, Stolk, et al. Homocysteine, S-Adenosylmethionine and S-Adenosylhomocysteine are Associated With Retinal Microvascular Abnormalities: The Hoorn Study. *Clin Sci (Lond)* (2008) 114:479–87. doi: 10.1042/CS20070275
23. Fotiou, Raptis, Apergis, Dimitriadis, Vergados, Theodossiadis. Vitamin Status as a Determinant of Serum Homocysteine Concentration in Type 2 Diabetic Retinopathy. *J Diabetes Res* (2014) 2014:807209. doi: 10.1155/2014/807209
24. Malaguarnera, Gagliano, Giordano, Salomone, Vacante, Bucolo, et al. Homocysteine Serum Levels in Diabetic Patients With non Proliferative, Proliferative and Without Retinopathy. *BioMed Res Int* (2014) 2014:191497. doi: 10.1155/2014/191497
25. Gupta, John, Rebekah, John. Role of Hyperhomocysteinemia in Proliferative Diabetic Retinopathy: A Case-Control Study. *Indian J Ophthalmol* (2018) 66:1435–40. doi: 10.4103/ijo.IJO_350_18
26. Kumar, Palfrey, Pathak, Kadowitz, Gettys, Murthy. The Metabolism and Significance of Homocysteine in Nutrition and Health. *Nutr Metab (Lond)* (2017) 14:78. doi: 10.1186/s12986-017-0233-z
27. Kim, Kim, Roh, Kwon. Causes of Hyperhomocysteinemia and its Pathological Significance. *Arch Pharm Res* (2018) 41:372–83. doi: 10.1007/s12272-018-1016-4
28. Stipanuk, Dominy, Lee, Coloso. Mammalian Cysteine Metabolism: New Insights Into Regulation of Cysteine Metabolism. *J Nutr* (2006) 136:1652S–9S. doi: 10.1093/jn/136.6.1652S
29. Forman, Zhang, Rinna. Glutathione: Overview of its Protective Roles, Measurement, and Biosynthesis. *Mol Aspects Med* (2009) 30:1–12. doi: 10.1016/j.mam.2008.08.006
30. Tight Blood Pressure Control and Risk of Macrovascular and Microvascular Complications in Type 2 Diabetes: UKPDS 38. UK Prospective Diabetes Study Group. *BMJ* (1998) 317:703–13.
31. Wang, Cui, Xu, Xu. Association Between Plasma Homocysteine and Progression of Early Nephropathy in Type 2 Diabetic Patients. *Int J Clin* (2015) 8:11174–80.
32. Tawfik, Samra, Elsherbiny, Al-Shabrawey. Implication of Hyperhomocysteinemia in Blood Retinal Barrier (BRB) Dysfunction. *Biomolecules* (2020) 10:1119. doi: 10.3390/biom10081119
33. Abdella, Mojiminiyi, Akanji, Moussa. Associations of Plasma Homocysteine Concentration in Subjects With Type 2 Diabetes Mellitus. *Acta Diabetol* (2002), 183–90. doi: 10.1007/s005920200033
34. Abuawad, Bozack, Saxena, Gamble. Nutrition, One-Carbon Metabolism and Arsenic Methylation. *Toxicology* (2021), 152803. doi: 10.1016/j.tox.2021.152803
35. Tecilazich, Formenti, Giustina. Role of Vitamin D in Diabetic Retinopathy: Pathophysiological and Clinical Aspects. *Rev Endocr Metab Disord* (2021), 715–27. doi: 10.1007/s11154-020-09575-4
36. Lopes de Jesus, Atallah, Valente, Moca Trevisani. Vitamin C and Superoxide Dismutase (SOD) for Diabetic Retinopathy. *Cochrane Database Syst Rev* (2008), CD006695. doi: 10.1002/14651858.CD006695.pub2
37. Zhang, Wang, Hu, Chen. Vitamin A and Diabetes. *J Med Food* (2021) 24(8), 775–85. doi: 10.1089/jmf.2020.0147

Conflict of Interest: The authors declare that the research was conducted in the absence of any commercial or financial relationships that could be construed as a potential conflict of interest.

Publisher's Note: All claims expressed in this article are solely those of the authors and do not necessarily represent those of their affiliated organizations, or those of the publisher, the editors and the reviewers. Any product that may be evaluated in this article, or claim that may be made by its manufacturer, is not guaranteed or endorsed by the publisher.

frontiers | Frontiers in Endocrinology

ORIGINAL RESEARCH
published: 12 July 2022
doi: 10.3389/fendo.2022.913370

Altered Expressions of Transfer RNA-Derived Small RNAs and microRNAs in the Vitreous Humor of Proliferative Diabetic Retinopathy

Yan Yang[1,2], *Wenyun Yue*[1,2], *Nan Wang*[1,2], *Zicong Wang*[1,2], *Bingyan Li*[1,2], *Jun Zeng*[1,2], *Shigeo Yoshida*[3], *Chun Ding*[1,2*] and *Yedi Zhou*[1,2*]

[1] Department of Ophthalmology, The Second Xiangya Hospital of Central South University, Changsha, China, [2] Hunan Clinical Research Center of Ophthalmic Disease, Changsha, China, [3] Department of Ophthalmology, Kurume University School of Medicine, Kurume, Japan

Purpose: We sought to reveal the expression profiles of transfer RNA-derived small RNAs (tsRNAs) and microRNAs (miRNAs) in the vitreous humor of patients with proliferative diabetic retinopathy (PDR).

Methods: Vitreous humor samples were obtained from PDR patients and a control group for this study. Sequencing of small RNAs was conducted to assess the expression profiles of tsRNAs and miRNAs in both groups, which was followed by validation using reverse transcription-quantitative real-time polymerase chain reaction (RT-qPCR). Bioinformatics analyses were conducted to predict the target genes and their potential biological functions and signaling pathways.

Results: A total of 37 tsRNAs and 70 miRNAs with significant differences were screened out from the vitreous humor samples of PDR patients compared to controls. Following validation by RT-qPCR, the target genes of the validated tsRNAs and miRNAs were predicted, and Gene Ontology analysis indicated that the target genes of the tsRNAs were most enriched in the cellular macromolecule metabolic process, cytoplasm, and ion-binding, while those of the miRNAs were most abundant in the regulation of major metabolic process, cytoplasm, and protein-binding. In addition, Kyoto Encyclopedia of Genes and Genomes pathway analysis showed that the target genes of said tsRNAs and miRNAs were most enriched in the adenosine monophosphate-activated protein kinase signaling pathway and Th17 cell differentiation, respectively.

Conclusions: The present study identified altered tsRNAs and miRNAs in vitreous humor samples of PDR patients, which may play important roles in the pathogenesis of PDR and could be considered potential therapeutic targets in the treatment of PDR.

Keywords: transfer RNA-derived small RNA, microRNA, proliferative diabetic retinopathy, retinal neovascularization, vitreous humor

OPEN ACCESS

Edited by:
Khalid Siddiqui,
King Saud University, Saudi Arabia

Reviewed by:
Enzhong Jin,
Peking University People's Hospital, China
Weihua Yang,
Nanjing Medical University, China
Han Zhang,
The First Affiliated Hospital of China Medical University, China
Zhipeng You,
Affiliated Eye Hospital of Nanchang University, China

***Correspondence:**
Yedi Zhou
zhouyedi@csu.edu.cn
Chun Ding
chunding@csu.edu.cn

Specialty section:
This article was submitted to Clinical Diabetes, a section of the journal Frontiers in Endocrinology

Received: *05 April 2022*
Accepted: *23 May 2022*
Published: *12 July 2022*

Citation:
Yang Y, Yue W, Wang N, Wang Z, Li B, Zeng J, Yoshida S, Ding C and Zhou Y (2022) Altered Expressions of Transfer RNA-Derived Small RNAs and microRNAs in the Vitreous Humor of Proliferative Diabetic Retinopathy. Front. Endocrinol. 13:913370. doi: 10.3389/fendo.2022.913370

INTRODUCTION

Diabetic retinopathy (DR) is a common complication of diabetes mellitus (DM), which has become a major cause of global blindness. With the aging of the population and the growing number of diabetic patients, DR has become a serious public health problem worldwide (1). As a more severe stage of DR, proliferative DR (PDR) is defined by retinal neovascularization, which may lead to serious loss of vision. Anti–vascular endothelial growth factor (VEGF) drugs have been widely applied clinically to inhibit pathological retinal neovascularization in PDR patients (2). However, these anti-VEGF drugs necessitate long-term repeated intravitreal injections, which greatly increases the medical economic burden. In addition, anti-VEGF drugs have a poor response in a considerable number of patients, as they are not capable of inhibiting all pathological neovascular tufts and may cause serious local and systemic complications in some cases (3). Ishikawa et al. identified gene-expression profile changes in the fibrovascular membranes of PDR patients and indicated that extracellular matrix–related molecules were involved in the development of said fibrovascular membranes (4). However, until now, the pathogenesis of PDR has remained unclear, and there is an urgent need to further explore the molecular mechanisms of retinal neovascularization in PDR and identify novel therapeutic targets with good safety and effectiveness so as to provide new methods for the diagnosis and treatment of PDR.

Recently, non-coding RNAs (ncRNAs) have emerged as research hotspots in medical and molecular biological studies. Although ncRNAs do not have the capability to translate genes to proteins, their regulatory roles in various physiological and pathological processes cannot be ignored (5). Small ncRNAs are important ncRNAs measuring < 200 nucleotides in length that include many types of RNAs, such as microRNAs (miRNAs), transfer RNA–derived small RNAs (tsRNAs), small nuclear RNAs, small nucleolar RNAs, and Piwi-interacting RNAs (6).

It has been reported that numerous miRNAs are involved in the development of DR (7). For instance, miR-15b attenuates angiogenesis by targeting VEGF (8), while miR-18a-5p inhibits retinal neovascularization *via* the downregulation of *FGF1* and *HIF1A* (9). On the other hand, another study indicated that miR-409-5p enhances retinal angiogenesis in DR (10).

Unlike miRNAs, tsRNAs are a novel type of small ncRNA that have been much less frequently explored. tsRNAs are derived from transfer RNAs and play regulatory roles in many biological processes and diseases (11, 12). According to the varying cleavage positions of precursor or mature tRNA transcripts, tsRNAs can be classified into 2 main subtypes, which are tRNA-derived fragments and tRNA-derived stress-induced RNAs (11). It has been revealed that tsRNAs contribute to different mechanisms in cancer, neurological disorders, and viral infections and can also serve as biomarkers for disease diagnosis and prognosis (13). We previously identified alterations in tsRNA expression profiles in mouse models of laser-induced choroidal neovascularization (14) and oxygen-induced retinopathy (OIR) (15). Although the OIR mouse model is widely used in the investigation of hypoxia-induced retinal neovascular diseases (16), the process of OIR modeling is very different from the clinical situation of PDR pathogenesis. Zhang et al. compared expression profiles of circular RNAs (circRNAs) in vitreous humor samples of patients with PDR and non-DM patients (17). Therefore, it is meaningful to reveal the expression profiles and possible functions of tsRNAs in clinical samples (such as vitreous humor samples) collected from patients with PDR.

In this study, we collected vitreous humor samples from PDR patients and controls, who were idiopathic macular hole (IMH) patients without DM. To identify the altered tsRNAs and miRNAs in samples from PDR patients, small RNA sequencing was conducted followed by validation with reverse transcription-quantitative real-time polymerase chain reaction (RT-qPCR). In addition, bioinformatics analyses were performed to predict the target genes and their potential biological functions and signaling pathways.

MATERIALS AND METHODS

Collection of Clinical Samples

Vitreous humor samples were collected from PDR patients and non-DM patients with IMH during plana vitrectomy surgeries. We diagnosed PDR by recognizing retinal neovascular tufts, vitreous hemorrhage, and fibrovascular membranes. Samples were collected from patients with severe vision loss because of PDR-induced vitreous hemorrhage, aged 50-70 years old, and patients were excluded when they had (1) PDR combined with neovascular glaucoma and rhegmatogenous retinal detachment; (2) a history of other vitreoretinal diseases, such as retinal vascular occlusion and age-related macular degeneration; (3) a history of intraocular surgery, laser treatment, or intravitreal injection medicine (including anti-VEGF and dexamethasone); (4) a history of systemic disease, including infectious, inflammatory, autoimmune, or immunosuppressive diseases and uncontrolled hypertension; (5) a history of myocardial infarction or cerebrovascular accidents, and coagulation abnormality or current use of an anticoagulative medication. The exact conditions and surgical indications of the included PDR patients were listed in **Supplementary Table 1**. Non-DM patients with IMH were considered to be the control group. A total of 1 mL of vitreous humor was collected from each individual, then stored in a refrigerator at -80°C after a quick freeze in liquid nitrogen.

This study adhered to the tenets of the Declaration of Helsinki, and the protocol of this study was approved by the ethics committee of the Second Xiangya Hospital of Central South University (number: 2021LY037). Informed consent was obtained from all participants before their recruitment into the study.

RNA Isolation From the Vitreous Humor

RNA was isolated from vitreous humor samples using a Trizol RNA extraction kit (Invitrogen, Carlsbad, CA, USA). The integrity and quantity of each RNA sample were assessed by agarose gel electrophoresis and NanoDrop ND-1000 spectrophotometry (Thermo Fisher Scientific, Waltham, MA, USA).

Library Preparation, Small RNA Sequencing, and Data Analysis

The protocols of library preparation, small RNA sequencing, and data analysis were adopted as previously described (14). In brief, first, total RNA was sequentially ligated to 3' and 5' small RNA adapters for each sample. Second, complementary DNA (cDNA) synthesis and amplification were conducted using Illumina's proprietary RT primers and amplification primers. Third, PCR-amplified fragments (~134–160 bp) were extracted from the polyacrylamide gel electrophoresis gel and purified. Finally, the completed libraries were quantified by the Agilent 2100 bioanalyzer (Agilent Technologies, Santa Clara, CA, USA). The libraries were denatured and diluted to a loading volume of 1.3 mL and loading concentration of 1.8 pM. Diluted libraries were loaded onto a reagent cartridge and forwarded for a sequencing run on the Illumina NextSeq 500 system using the NextSeq 500/550 V2 kit (Illumina, San Diego, CA, USA). Raw sequencing data, which were generated from the Illumina NextSeq 500 and passed the Illumina chastity filter, were used for the following analysis, and we also calculated the expression profiles of tsRNAs and miRNAs. The raw data of the small RNA sequencing were deposited in Gene Expression Omnibus database (Accession No. GSE199852).

Validation by RT-qPCR

The small RNA sequencing results were validated by RT-qPCR. To assess the expression of tsRNAs, RNA pre-treatment was performed by using the rtStar™ tRF and tiRNA pre-treatment kit (Arraystar, Rockville, MD, USA); then, the samples were transcribed into cDNA utilizing rtStar™ First-Strand cDNA Synthesis Kit (3' and 5' adaptor) (Arraystar). RT-qPCR was performed using 2 × PCR Master Mix (Arraystar) on the QuantStudio™ 5 real-time PCR system (Applied Biosystems, Foster City, CA, USA).

To evaluate miRNA expression levels, RNA was transcribed into cDNA using M-MuLV reverse transcriptase (Enzymatics, Beverly, MA, USA) as directed by the manufacturer with the Gene Amp PCR system 9700 (Applied Biosystems). RT-qPCR was performed using the ViiA 7 real-time PCR system (Applied Biosystems) with 2 × PCR Master Mix (Arraystar).

The reaction conditions of the 2 experiments were as follows: incubation at 95°C for 10 min, incubation at 95°C for 10 s, and incubation at 60°C for 60 s, with 40 cycles. Expression levels were calculated with a 2−ΔΔCt method (18) and normalized with U6. Primer sequences are shown in **Tables 1**, **2**.

Target Gene Prediction, Gene Ontology (GO), and Kyoto Encyclopedia of Genes and Genomes (KEGG) Pathway Analyses

The target prediction databases of miRanda and TargetScan were used to predict the target genes of validated miRNAs, and the common algorithms were used to predict the target genes of validated tsRNAs. The GO (http://www.geneontology.org/) and KEGG (http://www.genome.jp/kegg/) databases were used to predict the potential biological functions and involved pathways of the target genes.

Statistical Analyses

Data from small RNA sequencing were evaluated using counts per million reads mapped (CPM). The CPM values of the PDR group and the control group were calculated using a negative binomial generalized linear model, and p values were evaluated using a negative binomial distribution. A fold change ≥ 1.5 and $p < 0.05$ were used to screen for altered tsRNAs and miRNAs. RT-qPCR results were expressed as mean ± standard error of the mean values, and Student's t-test was used to evaluate the statistical difference. In all cases, $p < 0.05$ was considered to be statistically different.

RESULTS

Clinical Characteristics of the Enrolled Subjects

Eight patents were included in this study, including 4 PDR patients and 4 non-DM patients with IMH as controls, respectively. The demographic features of the recruited patients are shown in **Table 3**. There was no significant difference in age, gender, body mass index, or intraocular pressure between the groups. However, the fasting blood glucose level in the PDR

TABLE 1 | The sequences of primers used for RT-qPCR validation of tsRNAs.

tsRNA	Primer sequence	Tm (°C)	Product length (bp)
U6	F:5'GCTTCGGCAGCACATATACTAAAAT3' R:5'CGCTTCACGAATTTGCGTGTCAT3'	60	89
tRF-57:75-Pro-AGG-1-M7	F:5'AGTCCGACGATCAATCCCG3' R:5'CTCTTCCGATCTTGGGGGC3'	60	43
tRF-1:24-Val-AAC-1-M7	F:5'CGATCGTTTCCGTAGTGTAGTG3' R:5'GTGTGCTCTTCCGATCTTGATA3'	60	46
tRF-+1:T16-Thr-TGT-2	F:5'CGACGATCCCTGTTGGCTTA3' R:5'GACGTGTGCTCTTCCGATCTAA3'	60	44
tRF-56:72-chrM.Val-TAC	F:5'AGTTCTACAGTCCGACGATCCTT3' R:5'TTCCGATCTTGGTCAGAGCG3'	60	46
tRF-57:76-Tyr-GTA-1-M2	F:5'CTACAGTCCGACGATCGAATCC3' R:5'GCTCTTCCGATCTTGGTCCTT3'	60	49
tRF-55:76-Arg-ACG-1-M2	F:5'GATCTCGACTCCTGGCTGGC3' R:5'TGTGCTCTTCCGATCTTGGC3'	60	42

TABLE 2 | The sequences of primers used for RT-qPCR validation of miRNAs.

miRNA	Primer sequence	Tm (°C)	Product length (bp)
U6	F:5'GCTTCGGCAGCACATATACTAAAAT3' R:5'CGCTTCACGAATTTGCGTGTCAT3'	60	89
hsa-miR-889-3p	GSP:5'GGGGGTTAATATCGGACAAC3' R:5'GTGCGTGTCGTGGAGTCG3'	60	64
hsa-miR-939-5p	GSP:5'GTGGGGAGCTGAGGCTCT3' R:5'GTGCGTGTCGTGGAGTCG3'	60	63
hsa-miR-1469	GSP:5'AATCTCGGCGCGGGG3' R:5'GTGCGTGTCGTGGAGTCG3'	60	63
hsa-miR-4755-3p	GSP:5'GCAGCCAGGCTCTGAAGG3' R:5'GTGCGTGTCGTGGAGTCG3'	60	62
hsa-miR-411-5p	GSP:5'GGACAGCAGACCGCACAG3' R:5'GTGCGTGTCGTGGAGTCG3'	60	62
hsa-miR-369-3p	GSP:5'GGGGAATAATACATGGTTG R:5'CAGTGCGTGTCGTGGA3'	60	65
hsa-miR-181d-5p	GSP:5'GGGGCATTCATTGTTGTCG3' R:5'GTGCGTGTCGTGGAGTCG3'	60	63
hsa-miR-125a-5p	GSP:5'GCTCCCTGAGACCCTTTA3' R:5'CAGTGCGTGTCGTGGAGT3'	60	66

group was significantly higher than that of the control group. All patients in the PDR group had type 2 diabetes with an average disease duration of 12.50 ± 3.70 years, and the glycated hemoglobin value of the PDR group was 8.20% ± 1.75%.

Catalog of tsRNA Expressions in Vitreous Humor Samples

A principal component analysis plot was used to overview the small RNA sequencing data and revealed an obvious distinction between the groups (**Figure 1A**). The Venn diagram in **Figure 1B** demonstrates that, in total, 450 kinds of tsRNAs were detected in this study, of which 67 tsRNAs are known from the tRFdb database. As shown in **Figure 1C**, 169 tsRNAs were commonly expressed in both PDR and control samples, 123 tsRNAs were only expressed in PDR samples, and 76 were only expressed in control samples (CPM ≥ 20).

The pie chart shows the distribution of each expressed tsRNA subtype (**Figures 1D, E**). A total of 38 tRF-1, 7 tRF-2, 52 tRF-3a, 38 tRF-3b, 50 tRF-5a, 23 tRF-5b, 66 tRF-5c, 1 tiRNA-3, and 17 tiRNA-5 RNA(s) were identified in the PDR group (**Figure 1D**). On the other hand, 27 tRF-1, 7 tRF-2, 48 tRF-3a, 34 tRF-3b, 39 tRF-5a, 19 tRF-5b, 57 tRF-5c, and 14 tiRNA-5 RNAs were identified in the control group, while no tiRNA-3 RNA was recognized (**Figure 1E**). The numbers of subtype tsRNAs against tRNA isodecoders of the PDR group and control group are also shown (**Figures 1F, G**).

Altered Expression Profiles of tsRNAs and miRNAs in Vitreous Humor Samples of PDR Patients

To reveal the expression alterations of tsRNAs and miRNAs in the vitreous humor samples from PDR patients, a threshold of a fold change ≥ 1.5 and $p < 0.05$ were applied to identify the significantly different expressions.

The variation in tsRNA expression levels between the PDR and control groups is shown as a scatterplot (**Figure 2A**) and a volcano plot (**Figure 2C**). The results indicated that 20 tsRNAs were up-regulated and 17 were down-regulated in the PDR group compared to the control group (**Figure 2E**). The top 10 up- and down-regulated tsRNAs are listed in **Table 4**. In particular, tRF-1:22-chrM.Ser-GCT and tRF-+1:T24-Leu-AAG-1 were the most significantly up- and down-regulated tsRNAs in the PDR group, respectively.

In addition, the variation in miRNA expression levels between the PDR and control groups is shown as a scatterplot (**Figure 2B**) and a volcano plot (**Figure 2D**). As shown in the heatmap, 34 and 36 miRNAs were significantly increased and decreased in the PDR samples, respectively (**Figure 2F**). The top 10 up- and down-regulated miRNAs are listed in **Table 5**. According to the fold changes, hsa-miR-6734-5p and hsa-miR-1297 were the most significantly up- and down-regulated miRNAs in the PDR group, respectively.

TABLE 3 | Clinical characteristics of included subjects of the study.

Characteristics	PDR Group (n=4)	Control Group (n=4)	P-value
Age (y)	58.00 ± 4.83	59.75 ± 6.85	0.691
Gender (male/female)	2/2	2/2	–
Diabetic duration (y)	12.50 ± 3.70	n.a.	–
BMI (kg/m^2)	21.77 ± 4.48	23.03 ± 4.25	0.698
Fasting blood glucose (mmol/L)	8.02 ± 1.45	4.94 ± 0.23	0.006**
HbA1c%	8.20 ± 1.75	n.a.	–
IOP (mmHg)	17.00 ± 1.41	17.00 ± 1.41	1.000

*BMI, Body Mass Index; HbA1c, glycated hemoglobin; IOP, Intraocular Pressure. **p < 0.01, na; no applicable.*

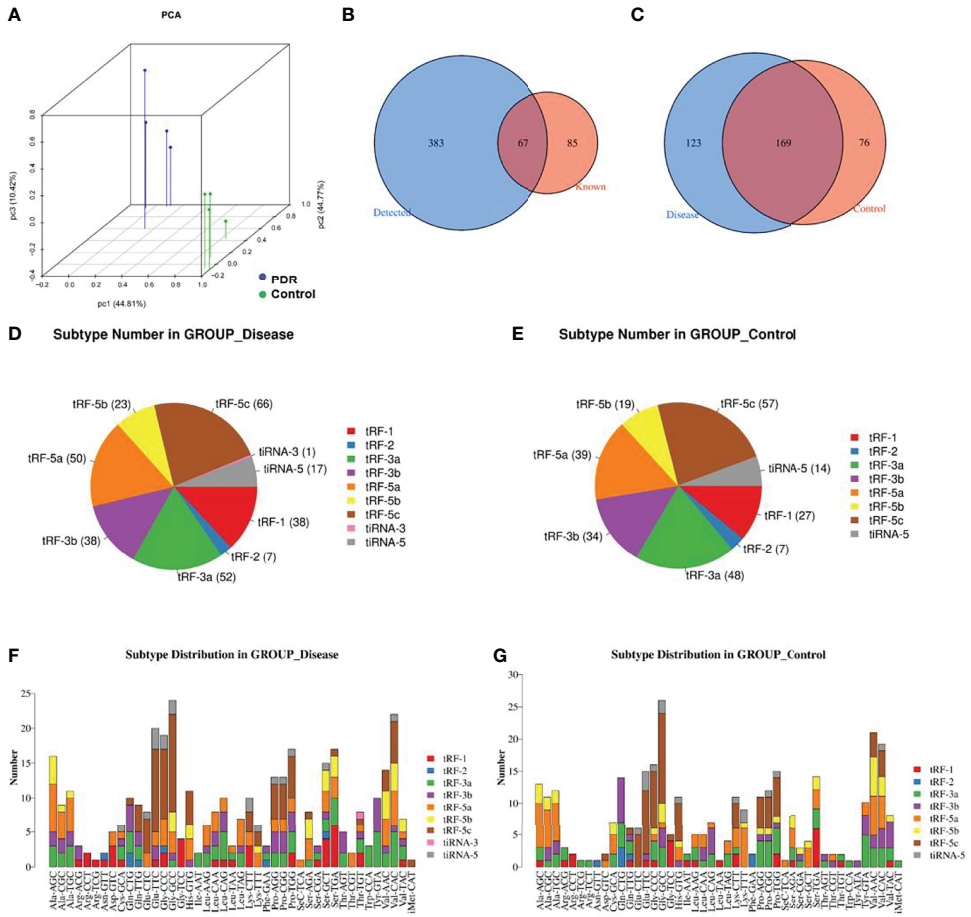

FIGURE 1 | Catalog of tsRNA expressions in vitreous humor samples. **(A)** Primary component analysis was performed by principal component analysis, which was conducted using tsRNAs. **(B)** The Venn diagram shows the number of detected tsRNAs and the known tsRNAs. **(C)** The Venn diagram shows the number of commonly expressed and specifically expressed tsRNAs in the PDR (disease) and control groups. **(D, E)** Pie charts display the numbers of different tsRNA subtypes in the PDR **(D)** and control **(E)** groups. **(F, G)** Different subtype distributions of tsRNAs in the PDR **(F)** and control **(G)** groups.

Validation of the Altered tsRNAs and miRNAs by RT-qPCR

To validate the reliability of the small RNA sequencing, RT-qPCR was performed to assess the expressions of selected tsRNAs and miRNAs. As shown in **Figure 3A**, tRF-57:75-Pro-AGG-1-M7, tRF-1:24-Val-AAC-1-M7, tRF-+1:T16-Thr-TGT-2, tRF-57:76-Tyr-GTA-1-M2, and tRF-55:76-Arg-ACG-1-M2 were significantly increased in the PDR samples compared to the control samples, while tRF-56:72-chrM.Val-TAC was significantly decreased. In addition, the expression levels of hsa-miR-889-3p, hsa-miR-939-5p, hsa-miR-4755-3p, hsa-miR-411-5p, hsa-miR-369-3p, hsa-miR-181d-5p, and hsa-miR-125a-5p were significantly enhanced, while that of hsa-miR-1469 was dramatically attenuated in the PDR samples (**Figure 3B**). The results of RT-qPCR indicated that the trend of these changes were similar to the results of the small RNA sequencing.

Target Gene Prediction

To illustrate the prediction of ncRNA-messenger RNA (mRNA) interaction, target gene networks of the validated tsRNAs and miRNAs were constructed according to the databases (miRanda and TargetScan). In total, there were 2,950 target genes associated with the 6 validated tsRNAs by 3,195 edges (**Supplementary Figure 1**), while 700 target genes were associated with 7 of the 8 altered miRNAs by 721 edges (**Supplementary Figure 2**).

GO and KEGG Analyses of the Target Genes

To further identify the potential biological functions and involved signaling pathways of the predicted target genes mentioned above, GO and KEGG analyses were performed. The GO analysis

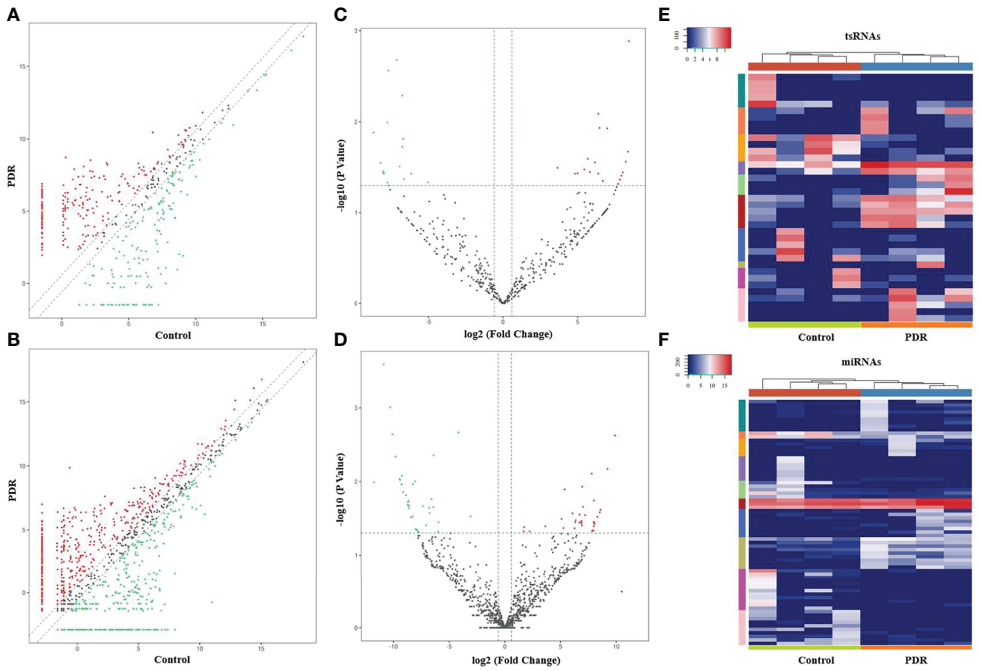

FIGURE 2 | Altered expression profiles of tsRNAs and miRNAs in vitreous humor samples from PDR patients compared to controls. **(A, B)** The scatterplots of altered tsRNAs **(A)** and miRNAs **(B)**. The red and green dots represent the up- and down-regulated tsRNAs/miRNAs, respectively (fold change ≥ 1.5). **(C, D)** The volcano plots of significantly altered tsRNAs **(C)** and miRNAs **(D)**. The red and green dots represent the significantly up- and down-regulated tsRNAs/miRNAs, respectively (fold change ≥ 1.5, $p < 0.05$). **(E, F)** A heatmap and hierarchical clustering analysis of significantly altered tsRNAs **(E)** and miRNAs **(F)** in vitreous humor samples of the PDR and control groups.

indicated that the target genes of these 6 tsRNAs were most enriched in the cellular macromolecule metabolic process, cytoplasm, and ion-binding (**Figure 4A**), while the target genes of the 7 miRNAs were most enriched in the regulation of primary metabolic process, cytoplasm, and protein-binding (**Figure 5A**).

On the other hand, the KEGG pathway analysis demonstrated that the target genes of those tsRNAs were most enriched in the adenosine monophosphate–activated protein kinase (AMPK) signaling pathway (**Figure 4B**), while those of tsRNAs were most enriched in Th17 cell differentiation (**Figure 5B**).

TABLE 4 | Top 10 up- and down-regulated tsRNAs in vitreous humor samples of PDR patients.

tsRNA	Type	Length	Regulation	log2FC	P-value
tRF-1:22-chrM.Ser-GCT	tRF-5b	22	up	8.443880	0.001304
tRF-+1:T25-Leu-CAG-1-6	tRF-1	25	up	8.389052	0.021170
tRF-1:31-Ser-AGA-1-M6	tRF-5c	31	up	8.227896	0.027329
tRF-61:77-Ile-AAT-2-M3	tRF-3a	17	up	8.032453	0.035820
tRF-1:14-chrM.Ala-TGC	tRF-5a	14	up	7.939212	0.038880
tRF-56:77-Thr-AGT-3	tRF-3b	22	up	7.838917	0.042854
tiRNA-1:20-chrM.Ser-GCT	tiRNA-5	20	up	7.829087	0.043066
tRF-1:16-Leu-TAA-1	tRF-5a	16	up	7.715198	0.047983
tRF-57:76-Tyr-GTA-1-M2	tRF-3b	20	up	6.988874	0.011771
tRF-68:86-Leu-CAG-1	tRF-3b	19	up	6.693507	0.044548
tRF-+1:T24-Leu-AAG-1	tRF-1	24	down	-8.688740	0.013120
tRF-1:14-Tyr-GTA-1-M7	tRF-5a	14	down	-8.215016	0.028057
tRF-56:75-Thr-CGT-2-M2	tRF-3b	20	down	-8.058716	0.034978
tRF-56:75-Gln-CTG-2	tRF-3b	20	down	-8.035050	0.035697
tRF-55:75-Gln-TTG-1-M2	tRF-3b	21	down	-7.998365	0.036983
tRF-1:32-Gly-TCC-3	tRF-5c	32	down	-7.757781	0.010194
tRF-66:86-Leu-CAG-1	tRF-3b	21	down	-7.756151	0.046285
tRF-58:76-Tyr-ATA-1	tRF-3b	19	down	-7.679754	0.049904
tRF-56:72-chrM.Val-TAC	tRF-3a	17	down	-7.679407	0.002737
tRF-1:28-Glu-TTC-2	tRF-5c	28	down	-7.138055	0.002093

TABLE 5 | Top 10 up- and down-regulated miRNAs in vitreous humor samples of PDR patients.

miRNA	Length	Regulation	log2FC	P-value
hsa-miR-6734-5p	23	up	9.899317	0.002366
hsa-miR-4755-3p	22	up	9.221942	0.006720
hsa-miR-518f-5p	22	up	8.592911	0.024083
hsa-miR-137-3p	23	up	8.523897	0.026054
hsa-miR-369-5p	22	up	8.305219	0.029994
hsa-miR-6877-5p	22	up	8.050634	0.037353
hsa-miR-1287-5p	22	up	8.022825	0.036348
hsa-miR-6794-5p	20	up	8.010205	0.017993
hsa-miR-642b-3p	22	up	7.999533	0.035298
hsa-miR-1297	17	up	7.998397	0.040450
hsa-miR-4316	17	down	-11.741562	0.010238
hsa-miR-1183	27	down	-10.871765	0.000252
hsa-miR-11401	20	down	-10.267196	0.000981
hsa-miR-7156-5p	23	down	-10.073930	0.002273
hsa-miR-520g-5p	23	down	-9.785546	0.004598
hsa-miR-5693	22	down	-9.448693	0.009282
hsa-miR-501-5p	22	down	-9.374017	0.009450
hsa-miR-99a-3p	22	down	-9.260094	0.010906
hsa-miR-1323	22	down	-9.232822	0.008348
hsa-miR-2278	22	down	-9.115166	0.013852

DISCUSSION

Evidence has accumulated that ncRNAs, including miRNAs, long ncRNAs (lncRNAs), and circRNAs, have an essential role in the occurrence and development of DR (19). Several miRNAs, such as hsa-miR-3184-3p, hsa-miR-24-3p, and hsa-miR-197-3p, are overexpressed in the vitreous humor of PDR patients, and intravitreal injection of anti-VEGF drugs inhibits the increase of these miRNAs (20). Despite the direct regulatory actions of target genes on mRNA expression levels, miRNAs also serve as targets of the competitive endogenous RNA (ceRNA) network, which is constructed using lncRNAs or circRNAs (21). For example, knockdown of the lncRNA TUG1 inhibited the migration and tube-formation capabilities of retinal microvascular endothelial cells under high glucose-stimulation by targeting miR-145; in other words, lncRNA TUG1 serves as a ceRNA by sponging miR-145 (22).

Compared to miRNAs, tsRNAs are novel and remain more unknown. It has been reported that the tsRNA tRF-Gly-GCC is involved in the pathogenesis of atherosclerosis *via* functional regulation in human umbilical vein endothelial cells and vascular smooth muscle cells (23). Until now, few studies have investigated the role of tsRNAs in ocular disorders.

In this study, the expression profiles of tsRNAs and miRNAs were assessed in vitreous humor samples of PDR and control patients by small RNA sequencing, followed by RT-qPCR. In addition, bioinformatics analysis revealed the predicted biological functions and involved pathways of the target genes.

As GO analysis indicated (**Figures 4A**, **5A**), metabolic processes were involved in the target genes of both tsRNAs and miRNAs. Our previous study reported different levels of metabolites (especially amino acids and their derivatives) in retinal tissues of an OIR mouse model, and the impact on the metabolite changes may be a long-term one (24). It has been demonstrated that the metabolic profiles of plasma and vitreous humor are significantly altered in PDR patients (25–27). Thus, it is interesting to further study the correlations of altered tsRNAs/miRNAs and the changes in metabolites in PDR.

AMP-activated protein kinase (AMPK) pathway activation is a well-known mechanism which plays dual roles in angiogenesis (28).

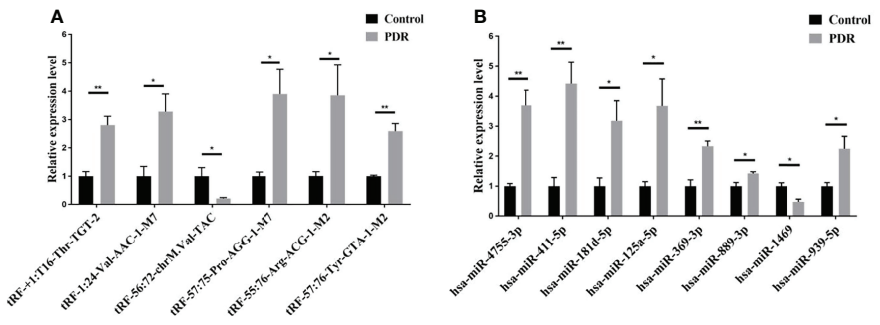

FIGURE 3 | RT-qPCR validation of the significantly altered tsRNAs and miRNAs. **(A)** Relative expression levels of the tsRNAs by RT-qPCR. **(B)** Relative expression levels of the miRNAs by RT-qPCR. *, $p < 0.05$; **, $p < 0.01$.

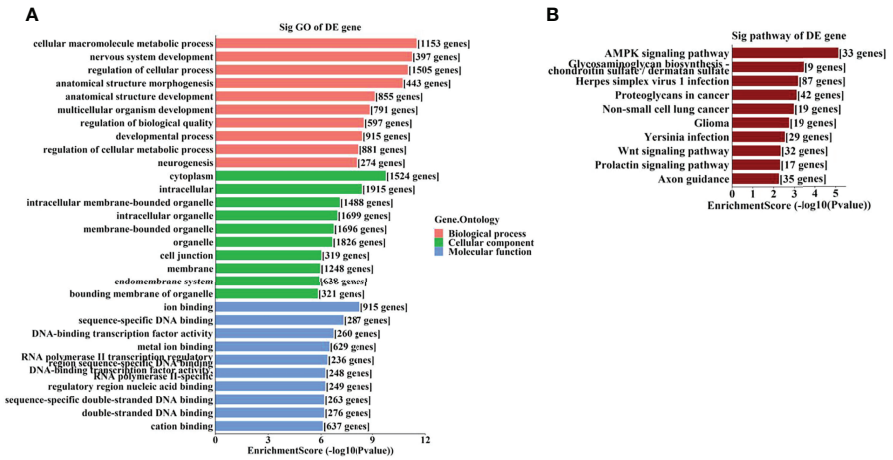

FIGURE 4 | The GO and KEGG analyses by target genes of tsRNAs. The GO analysis **(A)** and KEGG pathway analysis **(B)** of targets based on 6 validated tsRNAs.

AMPK pathway also regulates metabolism and protects cells from pathogenic alterations in DR (29). It has been reported that the AMPK signaling pathway is involved in the etiopathogenesis of many ocular diseases, including DR (30). Song et al. demonstrated that stimulation of AMPK signaling pathway attenuate diabetes-induced photoreceptor degeneration through regulation of autophagy and mitochondrial function (31). AMPK phosphorylation is required in the regulation of HMGB1 induced by Epac1 in the diabetic retinal vasculature (32). In this study, we identified the AMPK signaling pathway as a leading enriched pathway associated with the altered tsRNAs (**Figure 4B**), which also suggested that these tsRNAs might have regulatory functions in the pathogenesis of DR.

It has been revealed that the Th17 immune response as well as the related cytokines (such as IL-17 and IL-23) play important regulatory roles in retinal neovascular diseases (33, 34). Th17 immune response may also be involved in promoting functional and morphological changes in retinas of spontaneously developing diabetes (35). Th17 cell differentiation is a leading enriched pathway of the target genes of the altered miRNAs in this study, it is also interesting to explore the potential roles of these miRNAs associated with Th17 immune response.

This is an innovational study to report the expression profiles of tsRNAs from human clinical samples of PDR, which indicated a huge alteration of tsRNAs in the vitreous humor of PDR patients. Moreover, this study also predicted the target genes of the significantly changed tsRNAs, as well as the potential biological functions and involved pathways, which shed light on future investigations into the roles and mechanisms of those specific tsRNAs in PDR pathogenesis.

Limitations exist in this study. First, IMH patients were included as the control group, and their vitreous humor might be different from the normal population. Second, it is necessary

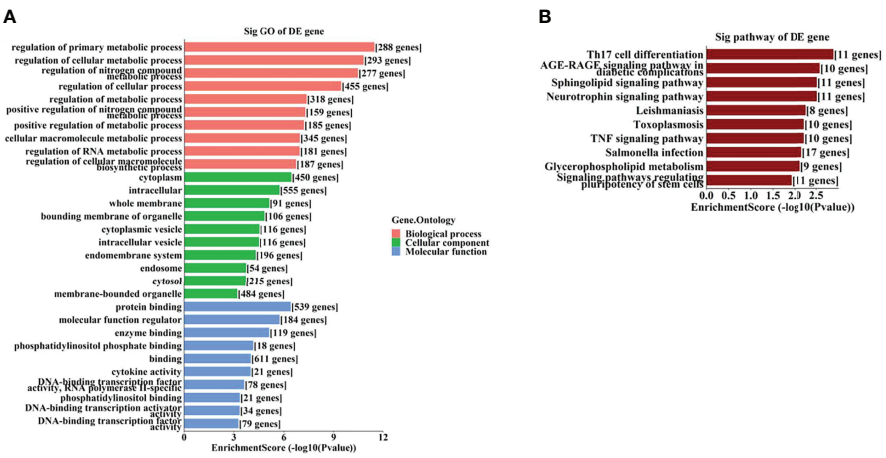

FIGURE 5 | The GO and KEGG analyses by target genes of miRNAs. The GO analysis **(A)** and KEGG pathway analysis **(B)** of targets based on 7 validated tsRNAs.

to increase the number of included subjects to validate the altered tsRNAs and miRNAs. Third, functional experiments are necessary to further explore the roles and mechanisms of the altered tsRNAs and miRNAs in PDR pathogenesis.

In conclusion, the present study indicated the altered expression profiles of tsRNAs and miRNAs, and the significantly altered tsRNAs and miRNAs, as well as the predicted signaling pathways, might be involved in the development and pathogenesis of PDR. Therefore, these tsRNAs/miRNAs have a potential for clinical application and could become novel therapeutic targets in the treatment of PDR.

DATA AVAILABILITY STATEMENT

The datasets presented in this study can be found in online repositories. The names of the repository/repositories and accession number(s) can be found below: GEO, GSE199852.

ETHICS STATEMENT

The studies involving human participants were reviewed and approved by the ethics committee of the Second Xiangya Hospital of Central South University. The patients/participants provided their written informed consent to participate in this study. Written informed consent was obtained from the individual(s) for the publication of any potentially identifiable images or data included in this article.

AUTHOR CONTRIBUTIONS

YZ and CD conceived and designed the study. YY, YZ, CD, and BL analyzed the data and wrote the manuscript. YY, WY, NW, ZW, and JZ obtained the samples and clinical records. JZ and SY reviewed and revised the manuscript. All authors contributed to the article and approved the final version of the manuscript.

FUNDING

This work was supported by National Natural Science Foundation of China (No. 81800855), Natural Science Foundation of Hunan Province (No. 2021JJ40885), Scientific Research Project of Hunan Provincial Health Commission (No. 202207022574), Development Project of Hunan Development and Reform Commission (No. 2021-212), and New Technology Incubation Funds in Ophthalmology.

SUPPLEMENTARY MATERIAL

The Supplementary Material for this article can be found online at: https://www.frontiersin.org/articles/10.3389/fendo.2022.913370/full#supplementary-material

Supplementary Figure 1 | The network of validated tsRNAs and the target genes. The pink diamond nodes represent tsRNAs, the green circular nodes represent target genes (mRNAs), and the T-shaped edges represent targets.

Supplementary Figure 2 | The network of validated miRNAs and the target genes. The pink diamond nodes represent miRNAs, the green circular nodes represent target genes (mRNAs), the gray lines represent targets without experimental validation by miRTarBase7.0, and the blue lines represent targets with experimental validation by miRTarBase7.0.

REFERENCES

1. Sabanayagam C, Banu R, Chee M L, Lee R, Wang Y X, Tan G, et al. Incidence and Progression of Diabetic Retinopathy: A Systematic Review. *Lancet Diabetes Endocrinol* (2019) 7(2):140–9. doi: 10.1016/S2213-8587(18)30128-1
2. Osaadon P, Fagan X J, Lifshitz T, Levy J. A Review of Anti-VEGF Agents for Proliferative Diabetic Retinopathy. *Eye (Lond)* (2014) 28(5):510–20. doi: 10.1038/eye.2014.13
3. Salam A, Mathew R, Sivaprasad S. Treatment of Proliferative Diabetic Retinopathy With Anti-VEGF Agents. *Acta Ophthalmol* (2011) 89(5):405–11. doi: 10.1111/j.1755-3768.2010.02079.x
4. Ishikawa K, Yoshida S, Kobayashi Y, Zhou Y, Nakama T, Nakao S, et al. Microarray Analysis of Gene Expression in Fibrovascular Membranes Excised From Patients With Proliferative Diabetic Retinopathy. *Invest Ophthalmol Vis Sci* (2015) 56(2):932–46. doi: 10.1167/iovs.14-15589
5. Patil VS, Zhou R, Rana TM. Gene Regulation by non-Coding RNAs. *Crit Rev Biochem Mol Biol* (2014) 49(1):16–32. doi: 10.3109/10409238.2013.844092
6. Watson CN, Belli A, Di Pietro V. Small Non-Coding RNAs: New Class of Biomarkers and Potential Therapeutic Targets in Neurodegenerative Disease. *Front Genet* (2019) 10:364. doi: 10.3389/fgene.2019.00364
7. Satari M, Aghadavod E, Mirhosseini N, Asemi Z. The Effects of microRNAs in Activating Neovascularization Pathways in Diabetic Retinopathy. *J Cell Biochem* (2019) 120(6):9514–21. doi: 10.1002/jcb.28227
8. Yang Y, et al. MicroRNA-15b Targets VEGF and Inhibits Angiogenesis in Proliferative Diabetic Retinopathy. *J Clin Endocrinol Metab* (2020) 105 (11):3404–15. doi: 10.1210/clinem/dgaa538
9. Guan J T, Li X X, Peng D W, Zhang W M, Qu J, Lu F, et al. MicroRNA-18a-5p Administration Suppresses Retinal Neovascularization by Targeting FGF1 and HIF1A. *Front Pharmacol* (2020) 11:276. doi: 10.3389/fphar.2020.00276
10. Wang Y, Lin W, Ju J. MicroRNA-409-5p Promotes Retinal Neovascularization in Diabetic Retinopathy. *Cell Cycle* (2020) 19(11):1314–25. doi: 10.1080/15384101.2020.1749484
11. Li S, Xu Z, Sheng J. tRNA-Derived Small RNA: A Novel Regulatory Small Non-Coding RNA. *Genes (Basel)* (2018) 9(5):246. doi: 10.3390/genes9050246
12. Shen Y, Yu X, Zhu L, Li T, Yan Z, Guo J. Transfer RNA-Derived Fragments and tRNA Halves: Biogenesis, Biological Functions and Their Roles in Diseases. *J Mol Med (Berl)* (2018) 96(11):1167–76. doi: 10.1007/s00109-018-1693-y
13. Jia Y, Tan W, Zhou Y. Transfer RNA-Derived Small RNAs: Potential Applications as Novel Biomarkers for Disease Diagnosis and Prognosis. *Ann Transl Med* (2020) 8(17):1092. doi: 10.21037/atm-20-2797
14. Zhang L, Liu S, Wang J H, Zou J, Zeng H, Zhao H, et al. Differential Expressions of microRNAs and Transfer RNA-Derived Small RNAs: Potential Targets of Choroidal Neovascularization. *Curr Eye Res* (2019) 44(11):1226–35. doi: 10.1080/02713683.2019.1625407
15. Peng Y, Zou J, Wang J H, Zeng H, Tan W, Yoshida S, et al. Small RNA Sequencing Reveals Transfer RNA-Derived Small RNA Expression Profiles in Retinal Neovascularization. *Int J Med Sci* (2020) 17(12):1713–22. doi: 10.7150/ijms.46209
16. Connor KM, Krah NM, Dennison RJ, Aderman CM, Chen J, Guerin KI, et al. Quantification of Oxygen-Induced Retinopathy in the Mouse: A Model of Vessel Loss, Vessel Regrowth and Pathological Angiogenesis. *Nat Protoc* (2009) 4(11):1565–73. doi: 10.1038/nprot.2009.187

17. He M, Wang W, Yu H, Wang D, Cao D, Zeng Y, et al. Comparison of Expression Profiling of Circular RNAs in Vitreous Humour Between Diabetic Retinopathy and non-Diabetes Mellitus Patients. *Acta Diabetol* (2020) 57 (4):479–89. doi: 10.1007/s00592-019-01448-w
18. Livak KJ, Schmittgen TD. Analysis of Relative Gene Expression Data Using Real-Time Quantitative PCR and the 2(T)(-Delta Delta C) Method. *Methods* (2001) 25(4):402–8. doi: 10.1006/meth.2001.1262
19. Chang X, Zhu G, Cai Z, Wang Y, Lian R, Tang X, et al. miRNA, lncRNA and circRNA: Targeted Molecules Full of Therapeutic Prospects in the Development of Diabetic Retinopathy. *Front Endocrinol (Lausanne)* (2021) 12:771552. doi: 10.3389/fendo.2021.771552
20. Guo J, Zhou P, Liu Z, Dai F, Pan M, An G, et al. The Aflibercept-Induced MicroRNA Profile in the Vitreous of Proliferative Diabetic Retinopathy Patients Detected by Next-Generation Sequencing. *Front Pharmacol* (2021) 12:781276. doi: 10.3389/fphar.2021.781276
21. Virciglio C, Abel Y, Rederstorff M. Regulatory Non-Coding RNAs: An Overview. *Methods Mol Biol* (2021) 2300:3–9. doi: 10.1007/978-1-0716-1386-3_1
22. Shi Q, Tang J, Wang M, Xu L, Shi L. Knockdown of Long Non-Coding RNA TUG1 Suppresses Migration and Tube Formation in High Glucose-Stimulated Human Retinal Microvascular Endothelial Cells by Sponging miRNA-145. *Mol Biotechnol* (2022) 64(2):171–7. doi: 10.1007/s12033-021-00398-5
23. He X, Yang Y, Wang Q, Wang J, Li S, Li C, et al. Expression Profiles and Potential Roles of Transfer RNA-Derived Small RNAs in Atherosclerosis. *J Cell Mol Med* (2021) 25(14):7052–65. doi: 10.1111/jcmm.16719
24. Zhou Y, Tan W, Zou J, Cao J, Huang Q, Jiang B, et al. Metabolomics Analyses of Mouse Retinas in Oxygen-Induced Retinopathy. *Invest Ophthalmol Vis Sci* (2021) 62(10):9. doi: 10.1167/iovs.62.10.9
25. Wang H, Li S, Wang C, Wang Y, Fang J, Liu K. Plasma and Vitreous Metabolomics Profiling of Proliferative Diabetic Retinopathy. *Invest Ophthalmol Vis Sci* (2022) 63(2):17. doi: 10.1167/iovs.63.2.17
26. Sun Y, Zou H, Li X, Xu S, Liu C. Plasma Metabolomics Reveals Metabolic Profiling For Diabetic Retinopathy and Disease Progression. *Front Endocrinol (Lausanne)* (2021) 12:757088. doi: 10.3389/fendo.2021.757088
27. Tomita Y, Cagnone G, Fu Z, Cakir B, Kotoda Y, Asakage M, et al. Vitreous Metabolomics Profiling of Proliferative Diabetic Retinopathy. *Diabetologia* (2021) 64(1):70–82. doi: 10.1007/s00125-020-05309-y
28. Li Y, Sun R, Zou J, Ying Y, Luo Z. Dual Roles of the AMP-Activated Protein Kinase Pathway in Angiogenesis. *Cells* (2019) 8(7):752. doi: 10.3390/cells8070752
29. Hsu SK, Cheng KC, Mgbeahuruike MO, Lin YH, Wu CY, Wang HD, et al. New Insight Into the Effects of Metformin on Diabetic Retinopathy, Aging and Cancer: Nonapoptotic Cell Death, Immunosuppression, and Effects Beyond the AMPK Pathway. *Int J Mol Sci* (2021) 22(17):9453. doi: 10.3390/ijms22179453
30. Shukal DK, Malaviya PB, Sharma T. Role of the AMPK Signalling Pathway in the Aetiopathogenesis of Ocular Diseases. *Hum Exp Toxicol* (2022) 41:9603271211063165. doi: 10.1177/09603271211063165
31. Song S, Bao S, Zhang C, Zhang J, Lv J, Li X, et al. Stimulation of AMPK Prevents Diabetes-Induced Photoreceptor Cell Degeneration. *Oxid Med Cell Longev* (2021) 2021:5587340. doi: 10.1155/2021/5587340
32. Jiang Y, Steinle JJ. Epac1 Requires AMPK Phosphorylation to Regulate HMGB1 in the Retinal Vasculature. *Invest Ophthalmol Vis Sci* (2020) 61 (11):33. doi: 10.1167/iovs.61.11.33
33. Li Y, Zhou Y. Interleukin-17: The Role for Pathological Angiogenesis in Ocular Neovascular Diseases. *Tohoku J Exp Med* (2019) 247(2):87–98. doi: 10.1620/tjem.247.87
34. Sui A, Chen X, Yao Y, Yao Y, Shen X, Zhu Y, et al. The IL-23/IL-17 Axis Promotes the Formation of Retinal Neovascularization by Activating the NLRP3 Inflammasome in Macrophages in an Experimental Retinopathy Mouse Model. *Immunology* (2021) 164(4):803–16. doi: 10.1111/imm.13402
35. Taguchi M, Someya H, Inada M, Nishio Y, Takayama K, Harimoto K, et al. Retinal Changes in Mice Spontaneously Developing Diabetes by Th17-Cell Deviation. *Exp Eye Res* (2020) 198:108155. doi: 10.1016/j.exer.2020.108155

Conflict of Interest: The authors declare that the research was conducted in the absence of any commercial or financial relationships that could be construed as a potential conflict of interest.

Publisher's Note: All claims expressed in this article are solely those of the authors and do not necessarily represent those of their affiliated organizations, or those of the publisher, the editors and the reviewers. Any product that may be evaluated in this article, or claim that may be made by its manufacturer, is not guaranteed or endorsed by the publisher.

frontiers | Frontiers in Public Health

ORIGINAL RESEARCH
published: 18 July 2022
doi: 10.3389/fpubh.2022.922289

The Association Between Diabetic Retinopathy and the Prevalence of Age-Related Macular Degeneration—The Kailuan Eye Study

*Zhang Yongpeng[1], Wang Yaxing[2], Zhou Jinqiong[1], Wang Qian[1], Yan Yanni[1], Yang Xuan[1], Yang Jingyan[1], Zhou Wenjia[1], Wang Ping[1], Shen Chang[1], Yang Ming[1], Luan Yanan[1], Wang Jinyuan[1], Wu Shouling[3], Chen Shuohua[4], Wang Haiwei[5], Fang Lijian[6], Wan Qianqian[7], Zhu Jingyuan[1], Nie Zihan[1], Chen Yuning[1], Xie Ying[8], Jost B. Jonas[9] and Wei Wenbin[1]**

[1] Beijing Key Laboratory of Intraocular Tumor Diagnosis and Treatment, Beijing Ophthalmology and Visual Sciences Key Lab, Medical Artificial Intelligence Research and Verification Key Laboratory of the Ministry of Industry and Information Technology, Beijing Tongren Eye Center, Beijing Tongren Hospital, Capital Medical University, Beijing, China, [2] Beijing Key Laboratory of Ophthalmology and Visual Sciences, Beijing Tongren Eye Center, Beijing Institute of Ophthalmology, Beijing Tongren Hospital, Capital Medical University, Beijing, China, [3] Cardiology Department, Kailuan General Hospital, Tangshan, China, [4] Health Care Center, Kailuan Group, Tangshan, China, [5] Department of Ophthalmology, Fuxing Hospital, Capital Medical University, Beijing, China, [6] Department of Ophthalmology, Beijing Liangxiang Hospital, Capital Medical University, Beijing, China, [7] Department of Ophthalmology, The Second Hospital of Anhui Medical University, Hefei, China, [8] Department of Ophthalmology, Shanxi Provincial People's Hospital, Taiyuan, China, [9] Department of Ophthalmology, Medical Faculty Mannheim of the Ruprecht-Karls-University of Heidelberg, Heidelberg, Germany

This study aimed to investigate the prevalence of age-related macular degeneration (AMD) in patients with diabetes mellitus (DM) and diabetic retinopathy (DR) and analyze whether DR is a risk factor for AMD. This population-based epidemiological study included 14,440 people from the Kailuan Eye Study in 2016, of whom 1,618 were patients with type 2 DM aged over 50 years, and 409 had DM with DR. We analyzed whether there were differences in the prevalence of AMD between DM with DR and DM without DR, and conducted a hierarchical statistical analysis according to different stages of DR. Using variable regression analysis, we explored whether DR constituted a risk factor for AMD. In the DM population, the prevalence of wet AMD in patients with DM with and without DR was 0. 3 and 0.2%, respectively, with no significant difference ($P = 0.607$). Meanwhile, the prevalence of dry AMD in patients with DM with and without DR was 20.8 and 16.0%, respectively, with a significant difference. In the subgroup analysis of dry AMD, the prevalence of early, middle, and late dry AMD in DM with DR was 14.4, 5.9, and 0.5%, respectively. In DM without DR, the prevalence of early, middle, and late dry AMD was 10.5, 4.8, and 0.7%, respectively ($P = 0.031$). In the subgroup analysis of DR staging, statistical analysis could not be performed because of the limited number of patients with PDR. In the variable regression analysis of risk factors for dry AMD, after

OPEN ACCESS

Edited by:
Khalid Siddiqui,
King Saud University, Saudi Arabia

Reviewed by:
Hu Bojie,
Tianjin Medical University Eye Hospital, China
Qisheng You,
Wayne State University, United States

***Correspondence:**
Wei Wenbin
weiwenbintr@163.com

Specialty section:
This article was submitted to Clinical Diabetes, a section of the journal Frontiers in Public Health

Received: *17 April 2022*
Accepted: *10 June 2022*
Published: *18 July 2022*

Citation:
Yongpeng Z, Yaxing W, Jinqiong Z, Qian W, Yanni Y, Xuan Y, Jingyan Y, Wenjia Z, Ping W, Chang S, Ming Y, Yanan L, Jinyuan W, Shouling W, Shuohua C, Haiwei W, Lijian F, Qianqian W, Jingyuan Z, Zihan N, Yuning C, Ying X, Jonas JB and Wenbin W (2022) The Association Between Diabetic Retinopathy and the Prevalence of Age-Related Macular Degeneration—The Kailuan Eye Study. Front. Public Health 10:922289. doi: 10.3389/fpubh.2022.922289

adjusting for age, sex, body mass index, hypertension, and dyslipidemia, DR constituted the risk factor for dry AMD. In conclusion, DM did not constitute a risk factor for AMD, and the prevalence of wet AMD and dry AMD in patients with DM and DR was higher than that in patients with DM without DR (among which dry AMD was statistically significant). Multivariate regression analysis confirmed that DR is an independent risk factor for dry AMD. Reasonable control of DM and slowing down the occurrence and development of DR may effectively reduce the prevalence of AMD in patients with DM.

Keywords: diabetes mellitus, diabetic retinopathy, age-related macular degeneration, prevalence, epidemiology

INTRODUCTION

Diabetes mellitus (DM), a metabolic disorder, can affect multiple systems of the body. The eye is an important organ that can be affected by DM, and almost every ocular structure may be involved. Diabetic retinopathy (DR), which seriously affects visual function, is associated with the progression of DR and DM. The prevalence of DR increases with the duration of DM. After 10–15 years from the diagnosis of DM, patients develop DR (1). The prevalence of DM has increased in both developing and developed countries (1).

In China, the prevalence of DM increased from <1% in 1980 to 11.6% in 2013, with 114 million people affected (2). As a major complication of DM, DR is the leading cause of blindness in the working-age population. The duration of DM and glycemic control levels have a major effect on the development of DM complications. The prevalence of DR increases with the aging of the Chinese population. In the adult DM population in northern China, the prevalence of DR is as high as 37.1–43.1%, that is, more than one-third of patients with DM have DR, of which the prevalence of DR threatening vision is 5–6.3%. As an irreversible blinding eye disease, DR is a heavy burden on society and families (3–6).

However, more attention should be paid to age-related macular degeneration (AMD). AMD can be dry (non-exudative) or wet (exudative). The late stages of AMD include geographic atrophy (GA) and wet AMD. Globally, AMD is the leading cause of blindness in people over 50 years of age. Moreover, 8.7% of the worldwide population has AMD, and the projected number of people with the disease is approximately 196 million in 2020 and 288 million in 2040 (7, 8). Epidemiological studies on the prevalence of AMD in northern China show that the prevalence of early AMD is 1.4%-3.0%, and that of late AMD is 0.1–0.2% (9–11). The treatment of advanced AMD is difficult and expensive, placing a heavy economic burden on families and society.

As the country with the largest population in the world, China has begun to enter an aging society. Visual quality is an important aspect of improving the sense of acquisition of quality of life in the elderly. DR and AMD, two important blinding eye diseases, seriously affect the quality of life of patients, and their prevention and treatment are urgently needed. Patients with DM will eventually reach the age group of more than 50 years. What are the results when the two diseases are superimposed? The conclusions drawn from different studies were controversial. Some studies have shown that DM and DR can increase the prevalence of AMD (12–21), whereas some have shown that DM and DR are not related to the onset of AMD (22–27) and that DM or DR might be protective factors against AMD (28–32). The research methods adopted, such as epidemiological research, medical insurance data, case-control, sampling population, age setting, disease classification, and staging standards, the number of cases, and race, may have affected the differences in research conclusions.

This population-based epidemiological study in northern China aimed to explore the relationship between the prevalence of AMD in DR and non-DR populations and provide a scientific basis for the comprehensive prevention and control of the two ocular diseases with a high blindness rate.

MATERIALS AND METHODS

The Kailuan Eye Study was introduced previously (33–36). This retrospective cross-sectional study included 14,440 people who had undergone ophthalmologic and general examinations from the longitudinal Kailuan Study in 2016.

The body mass index (BMI) was calculated for all study participants. BP was assessed with the participants sitting for at least 5 min. Blood samples were collected under fasting conditions to determine the blood glucose, high-density lipoprotein cholesterol (HDL-C), low-density lipoprotein cholesterol (LDL-C), triglyceride (TC), and total cholesterol (TG) concentrations.

Ophthalmological examinations included measurement of visual acuity, intraocular pressure, and slit-lamp-assisted biomicroscopy of the eye. Using a non-mydriatic fundus camera (CR6-45 NM; Canon, Inc, Osta, Tokyo, Japan), we obtained two 45° fundus photographs centered on the optic nerve head and macula. If the pupil diameter did not allow fundus photography with sufficient photographic quality, the pupil was dilated medically by applying eye drops containing 0.5% tropicamide and 0.5% phenylephrine hydrochloride. Using fundus photographs, DR was assessed in a masked manner without knowledge of other ocular or systemic parameters of the study participants. Both eyes were evaluated.

The diagnosis of DM was based on any of the following three criteria: measurement of the fasting blood glucose concentration of 7.0 mM, a self-reported history of DM, or a history of medication with hypoglycemic agents.

The diagnostic criteria for hypertension were blood pressure of ≥140/90 mmHg, positive history of hypertension, or the use of antihypertensive drugs.

The clinical classification of hyperlipidemia included hypercholesterolemia (TC≥6.2 mmol/L), hyperglycemia (TG≥2.3 mmol/L), mixed hyperlipidemia (TC ≥6.2 mmol /L and TG≥2.3 mmol/L), and low HDL-C levels (<1.0 mmol/L).

The diagnostic criteria for BMI were based on the guidelines for prevention and control of overweight and obesity in Chinese adults as follows: underweight (BMI, <18.5 kg/m^2), normal (BMI, 18.5–23.9 kg/m^2), overweight (BMI, 24.0–27.9 kg/m^2), obese (BMI, ≥28 kg/m^2).

The diagnostic criteria for AMD were based on the Beckman Macular Research Classification System. The lesions were assessed within two optic disc diameters of the fovea of either eye. AMD was classified as follows: no apparent aging changes (no drusen and no AMD pigmentary abnormalities), normal aging changes (small drusen of ≤ 63γm and no AMD pigmentary abnormalities), early AMD (medium drusen of > 63 γm, ≤125 γm, and no AMD pigmentary abnormalities), intermediate AMD (large drusen of >125 γm or any AMD pigmentary abnormalities), and late AMD (neovascular AMD or any geographic atrophy).

DR grading was performed according to the Early Treatment of Diabetic Retinopathy Study (ETDRS) criteria. DR severity was graded as mild non-proliferative DR (20 ETDRS levels of <43 with at least one microaneurysm), moderate non-proliferative DR (43 ETDRS levels of <53), severe non-proliferative DR (53 ETDRS levels of <61), and proliferative DR (ETDRS level of 61). An experienced and trained ophthalmologist assessed the photographs. In cases of doubt, photographs were reassessed by a panel that included several ophthalmologists.

Statistical analysis was performed using the R software. The results were expressed as mean and standard deviation or as mean and 95% CI. Logistic regression models were used to estimate the odds ratios (ORs) and their 95% CIs for each risk factor for DR. Statistical significance was set at $P < 0.05$.

Ethics Statement

This study adhered to the tenets of the Declaration of Helsinki. The Medical Ethics Committee of Beijing Tongren Hospital approved the study protocol, and informed consent was obtained from all patients after an explanation of the nature and possible consequences of the study.

RESULTS

A total of 14,440 participants were enrolled in the Kailuan Eye Study, of whom 9,627 were older than 50 years old. Fifteen were excluded for having type 1 DM and 717 for an unclear diagnosis of AMD. Finally, 8,895 were included in the analysis group. Among them, the number of patients with type 2 DM was 1,618, 409 of whom had DM combined with DR, and 1,191 had DM without DR, excluding 18 people diagnosed with unclear DR. The prevalence of DM aged 50 years was 16.83%. The prevalence of DR was 25.28% in the population with DM aged > 50 years (**Figure 1**).

Notably, among the 7,277 non-DM participants, 13 were excluded from image unrecognition, and 259 people were found to have DR image characteristics, including microaneurysm, retinal hemorrhage, hard exudation, cotton–wool, and retinal neovascularization, in the non-DM group, with a prevalence of 3.56%. There are two possibilities; one is that in epidemiological field screening, although the random blood glucose level is normal, there may be abnormal glucose tolerance or low insulin function; and another reason is that the current diagnostic criteria for DM are not suitable for this group of people; that is, the blood glucose level for the normal population is already high.

The Prevalence of AMD in Diabetic and Non-DM Participants

The prevalence of wet and dry AMD was 0.5% and 16.4%, respectively, in the non-DM population (7,277 people). In the patients with type 2 DM (1,618 people), the prevalence of wet AMD and dry AMD was 0.3 and 17%, respectively. There was no significant difference in the prevalence of wet and dry AMD between the diabetic and non-diabetic participants.

In a staging study of dry AMD, the prevalence of dry AMD in the early, middle, and late stages without DM was 11.7, 4.4, and 0.3%, respectively. The prevalence of dry AMD in the early, moderate, and late stages of DM was 11.4, 5, and 0.6%, respectively, with no significant differences (**Table 1**).

The Prevalence of AMD in DM With DR and DM Without DR

In the population with DM without DR (1191 people), the prevalence of wet AMD and dry AMD was 0.3 and 16.0%, respectively. In the population of patients with DM and DR (409 people), the prevalence of wet and dry AMD was 0.5 and 20.8%, respectively. The Fisher's exact probability method showed that there was no significant difference in the prevalence of wet AMD between the DR and non-DR groups ($P = 0.607$ and $\alpha = 0.05$), whereas there was a significant difference in the prevalence of dry AMD between the DR and non-DR groups when $\alpha = 0.05$ ($\chi^2 = 4.655$ and $P = 0.031$). The prevalence of dry AMD was higher in the DR group than in the non-DR group.

In a staging study of dry AMD in the non-DM population, the prevalence of early, middle, and late dry AMD was 10.5, 4.8, and 0.7%, respectively, in the DM population, the prevalence of early, middle, and late dry AMD was 14.4, 5.9, and 0.5%, respectively, with significant differences (**Table 2**).

The Prevalence of AMD in Different DR Stages of DM

In different stages of DM, because wet AMD did not combine with moderate NPDR ($n = 66$) and severe NPDR ($n = 2$), it was impossible to calculate the difference in the prevalence of dry and wet AMD (**Table 3**).

The Prevalence of AMD in Different "DR" Stages of Non-DM

In non-DM participants, some patients with "DR" were also staged according to DR. Because moderate NPDR ($n = 44$),

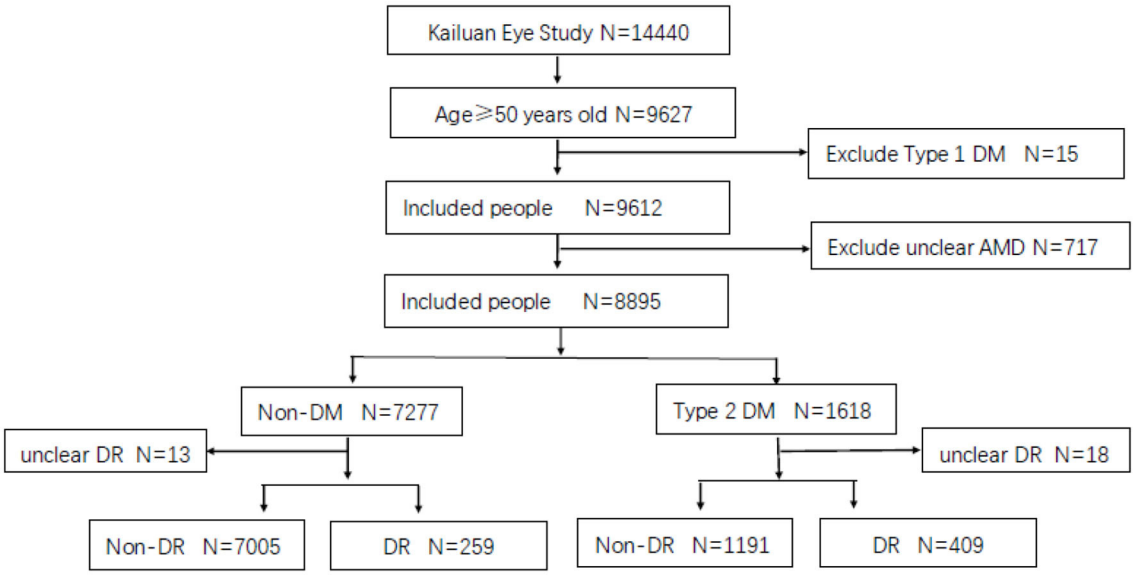

FIGURE 1 | Flow chart of included and excluded population.

TABLE 1 | The prevalence of AMD in diabetic and non-diabetic people.

	Wet AMD (%)*	Dry AMD (%)**	Dry AMD (n = 1,469)		
			Early dry AMD (%)	Middle dry AMD (%)	Late dry AMD (%)
Non-DM n = 7,277	33 (0.5)	1,194 (16.4)	850 (11.7)	321 (4.4)	23 (0.3)
DM n = 1,618	5 (0.3)	275 (17.0)	184 (11.4)	81 (5.0)	10 (0.6)
Total n = 8,895	38	1,469	1,034	402	33

*$\chi^2 = 0.354$, $P = 0.551$. When test level $\alpha = 0.05$, there is no difference of the prevalence of wet AMD between diabetic and non-diabetic people.
**$\chi^2 = 0.291$, $P = 0.590$. When test level $\alpha = 0.05$, there is no difference of the prevalence of dry AMD between diabetic and non-diabetic people.
AMD, age-related macular degeneration.

TABLE 2 | The prevalence of AMD in DM with DR and DM without DR.

	Wet AMD (%)*	Dry AMD (%)**	Dry AMD (n = 275)		
			Early dry AMD (%)	Middle dry AMD (%)	Late dry AMD (%)
Non-DR N = 1,191	3 (0.3)	190 (16.0)	125 (10.5)	57 (4.8)	8 (0.7)
DR n = 409	2 (0.5)	85 (20.8)	59 (14.4)	24 (5.9)	2 (0.5)
Total n = 1,600	5	275	184	81	10

*Fisher $P = 0.607$, when test level $\alpha = 0.05$, the prevalence of wet AMD in DR and non-DR is not statistical significance.
**$\chi^2 = 4.655$, $P = 0.031$, when test level $\alpha = 0.05$, the prevalence of dry AMD in DR is higher than that of non-DR with statistical significance.
AMD, age-related macular degeneration; DR, diabetic retinopathy; DM, diabetes mellitus.

severe NPDR (n = 1), and PDR (n = 1) were not combined with wet AMD, it is impossible to count the difference in the prevalence of dry and wet AMD in the different "DR" stages of non-DM (**Table 4**).

Multivariate Analysis of Influencing Factors of Dry AMD

In the analysis of risk factors for dry AMD, the following three models were established: Model 1, corrected age; Model 2, corrected for age, sex, and BMI (< 8.5, 18.5–23.9, 24–27.9, ≥ 28); and Model 3, adjusted for age, sex, BMI, hypertension (yes or no), and dyslipidemia (yes or no).

The results showed that DR is a risk factor for dry AMD, and male sex and age were risk factors for dry AMD. Meanwhile, BMI, hypertension, and hyperlipidemia were not identified as risk factors for dry AMD (**Table 5**).

DISCUSSION

The global crude prevalence of avoidable vision impairment and blindness in adults aged ≥ 50 years did not change between 2010 and 2019 (37). The leading global cause of blindness in those aged 50 years and older in 2020 was cataracts, followed by glaucoma, under-corrected refractive error, AMD, and DR (37). Although DR was the fifth leading cause of blindness in 2020, it was the only cause of blindness that showed a global increase in age-standardized prevalence between 1990 and 2020. Furthermore, more than 600 million people are projected to

TABLE 3 | The prevalence of AMD in different stages of DR with DM.

	Wet AMD (%)	Dry AMD (%)	Dry AMD (n=85)		
			Early dry AMD (%)	Middle dry AMD (%)	Late dry AMD (%)
Mild NPDR $n = 341$	2 (0.6)	77 (22.6)	54 (15.8)	22 (6.5)	1 (0.3)
Moderate NPDR $n = 66$	0 (0.0)	8 (12.1)	5 (7.6)	2 (3.0)	1 (1.5)
PDR $n = 2$	0 (0.0)	0 (0.0)	0 (0.0)	0 (0.0)	0 (0.0)
Total $n = 409$	2	85	59	24	2

AMD, age-related macular degeneration; DR, diabetic retinopathy, DM, diabetes mellitus.

TABLE 4 | The prevalence of AMD in different stages of "DR" with non-DM.

	Wet AMD (%)	Dry AMD (%)	Dry AMD ($n = 57$)		
			Early dry AMD (%)	Middle dry AMD (%)	Late dry AMD (%)
Mild NPDR $n = 216$	1 (0.5)	48 (22.2)	30 (13.9)	16 (7.4)	2 (0.9)
Moderate NPDR $n = 41$	0 (0.0)	9 (22.0)	5 (12.2)	4 (9.8)	0 (0.0)
Severe NPDR $n = 1$	0 (0.0)	0 (0.0)	0 (0.0)	0 (0.0)	0 (0.0)
PDR $n = 1$	0 (0.0)	0 (0.0)	0 (0.0)	0 (0.0)	0 (0.0)
Total $n = 259$	1	57	35	20	2

AMD, age-related macular degeneration; DR, diabetic retinopathy; DM, diabetes mellitus.

live with diabetes by 2040 (38). Because people with DM live increasingly longer with improvements in medical conditions, the number of people with DR and vision impairment is expected to increase rapidly, especially in China. DR management requires a disproportionate amount of social and economic resources. The prevalence of blindness due to AMD has declined by almost 30% from 1990 to 2020. This decrease is probably associated with the widespread clinical introduction of anti-VEGF therapy for wet AMD. However, most patients with AMD have untreatable dry AMD that can progress to GA (37). DR and AMD remain the most important ocular public health problems in China and worldwide.

International Diabetes Federation (IDF) estimated the global population with DM to be 463 million in 2019 and projected it to be 700 million by 2045 (2). As the most common and specific complication of DM, DR is one of the leading causes of preventable blindness in the adult working population (39). A declining trend in DR prevalence has been suggested, particularly in developed countries (40–42). This is the result of systemic control in patients with DM. It has been estimated that 51% of all the patients with blindness due to DR come from the Asia-Pacific region. The prevalence of DR among patients with DM ranges from 10% in India to 43% in Indonesia within the Asia-Pacific (43, 44). The highest number of people with DM is in China (116 million), which reflects the rapid economic growth and urbanization in China with significant lifestyle and dietary changes (39). In China, a large-scale population-based study conducted on 46,239 adults reported a 14-fold increase in DM prevalence over 30 years (0.67% in 1980 vs. 9.7% in 2008) (45).

Globally, AMD is the leading cause of blindness among people over 50 years old (7, 8). Epidemiological studies on the prevalence of AMD in northern China show that the prevalence of early AMD is 1.4–3.0%, and that of late AMD is 0.1–0.2% (9–11). The prevalence of early AMD in the Chinese sample was similar to that in white individuals in the Blue Mountains Eye Study (BMES) and other studies (10).

Today's working-age group will become tomorrow's elderly group. What is the relationship between DM, DR, and AMD in the Chinese population? Some research has been conducted on this topic, but the conclusion is contradictory.

The research methods on the relationship between DM or DR and AMD include longitudinal studies (prospective cohort study and retrospective cohort study), cross-sectional studies (cross-sectional population-based study and observational analysis of randomized clinical trial), case-control studies (retrospective descriptive observational case-control and case-control studies), and systematic reviews and meta-analyses. The study design that we used was cross-sectional population-based epidemiology. Every method has its advantages but also has limitations. In this study, AMD included early, middle, and late stages, and late-stage AMD included GA and wet AMD. DR includes NPDR and PDR, whereas NPDR includes mild, moderate, and severe NPDR. It is difficult to correlate each stage of DR to each stage and type of AMD individually, which requires epidemiological research with a large sample size and long-term longitudinal follow-up.

The relationship between DR and AMD remains inconsistent because of different research methods and sample sizes; that is, some studies have shown that DM and DR can increase the prevalence of AMD (12–21), some have shown that DM and DR are not related to AMD (22–27), and some have shown that DM or DR might protect against AMD (28–32).

Early studies did not find a relationship between DM and AMD (12–21). Later, the Beaver Dam Eye Study (BDES) (17) and BMES (15) found that DM and AMD were correlated, but their conclusions were contradictory. The BDES showed that DM was not associated with early AMD or GA. However, the prevalence of exudative AMD among people with DM was higher (9.4%) than that of those without DM (4.7%) who were older than 75 years. The BMES showed that DM was only associated with GA but not with wet AMD or early AMD. In 2013, Medicare data from 6,621 patients over the age of 69 years with newly diagnosed DM (1995–2005) in the United States showed that NPDR significantly increased the risk of dry AMD and wet AMD, whereas PDR can only increase the risk of wet AMD. The risk of dry AMD and wet AMD did not increase in patients with

TABLE 5 | The risk factor for dry AMD ($n = 8,857$).

	Model 1 OR (95% CI)[a]	Model 2 OR (95% CI)[b]	Model 3 OR (95% CI)[c]
Ref=non-DR			
DR	1.35 (1.05, 1.72)	1.38 (1.07, 1.78)	1.38 (1.07, 1.78)
Ref=female			
Male	1.33 (1.17, 1.52)	1.32 (1.13, 1.55)	1.33 (1.13, 1.56)
Ref=lower than 60 years old			
60–69 years old	1.62 (1.43, 1.84)	1.62 (1.40, 1.89)	1.62 (1.39, 1.89)
≥70 years	2.11 (1.79, 2.50)	2.36 (1.90, 2.92)	2.35 (1.89, 2.92)
Ref=normal weight (BMI: 18.5–23.9)			
Low weight (BMI: <18.5)	-	0.57 (0.26, 1.10)	0.57 (0.26, 1.10)
Overweight (BMI: 24.0–27.9)	-	0.95 (0.82, 1.11)	0.95 (0.81, 1.10)
Obesity (BMI:≥28.0)	-	1.12 (0.92, 1.37)	1.10 (0.90, 1.35)
Ref=non hypertension			
Hypertension	-	-	1.01 (0.88, 1.17)
Ref=non hyperlipidemia			
Hyperlipdemia	-	-	1.11 (0.95, 1.31)

[a]*Model 1: corrected age (50–59, 60–69, ≥70) and gender (male, female).*
[b]*Model 2: corrected age, gender, and BMI (<18.5, 18.5–23.9, 24–27.9, ≥28).*
[c]*Model 3: corrected age, gender, BMI, hypertension (yes or no), hyperlipidemia (yes or no).*
AMD, age-related macular degeneration; DR, diabetic retinopathy; DM, diabetes mellitus.

DM, but not without DR. There was no difference in the risk of wet AMD between PDR and NPDR (12). A retrospective study of the longitudinal health insurance database of Taiwan (1997–2012) showed that patients with DM had a 1.4-fold increase in dry and wet AMD compared to matched patients without DM, although the difference was not significant. In contrast, patients with DM and DR had a 4 and 3.9-fold increased incidence of dry and wet AMD, respectively. The HR for the development of dry AMD and wet AMD was 3.89 and 3.42 for patients with DM and DR and those without DR, respectively ($P < 0.001$) (14). This is consistent with the conclusion of our study that DM may not be a risk factor for increasing the prevalence of AMD, but DR does.

However, studies have shown that the incidence rate of AMD in the DM population is lower than that in the general population (28–31). Recent research has shown that the prevalence of neovascular AMD of the eyes in people with DR is low (0.04%). Moreover, the prevalence of choroidal neovascularization (CNV) in eyes with DR is low, with a lower prevalence of AMD. Diabetic choroidopathy plays a significant role in CNV formation in eyes with DR (32).

The findings of our study showed that DM had no effect on the prevalence of AMD, but DR could promote the development of dry AMD. The prevalence of wet AMD and dry AMD was 0.5 and 16.4%, respectively, in the non-DM population and 0.3 and 17%, respectively, in the DM population. There was no significant difference in the prevalence of wet and dry AMD between the diabetic and non-diabetic individuals.

The prevalence of wet AMD and dry AMD was 0.3% and 16.0%, respectively, in the population with DM without DR and 0.5 and 20.8%, respectively, in the population with DM and DR. There was no significant difference in the prevalence of wet AMD between the DR and non-DR groups. The prevalence of dry AMD was significantly higher in the DR group than in the non-DR group.

In the Kailuan Eye Study, we also found another finding of "DR" in the non-DM population. Among the 7,277 non-DM subjects, 259 people were found to have "DR" image characteristics, including microaneurysm, retinal hemorrhage, hard exudation, cotton-wool, and retinal neovascularization in no-DM, and the prevalence was 3.56%. There have been reports of retinopathy in persons without DM in the Handan Eye Study (46). The prevalence of retinopathy among participants without DM was 13.6%, and the age and sex-standardized prevalence of retinopathy in the Chinese adult population (aged 30 years) without DM was estimated to be 12.1%. Its association with fasting plasma glucose and BP suggests that early microvascular damage occurs at "high normal" levels of blood.

Why can DR accelerate the onset of AMD? DR may share common pathogenic pathways with AMD. The biological interplay between DR and AMD is complicated and not fully understood (13). First, DM may lead to the accumulation of highly stable advanced glycation end products (AGEs) in multiple tissues, including the retinal pigment epithelium (RPE) cell layers and photoreceptors, which are implicated in the pathogenesis of AMD (47–50). Second, hyperglycemia and dyslipidemia in patients with disturbed homeostasis of the retina by inducing inflammatory responses, which might play a role in AMD (51–53). Third, VEGF plays an important role in both DR and AMD, and both benefit from anti-VEGF treatment (13, 14). Fourth, swept-source optical coherence tomography demonstrated a significant reduction in central macular thickness in PDR compared to controls (54). Understanding diabetic choroidopathy may improve our knowledge of the mechanisms underlying DR and AMD. Finally, structural retinal changes

occur with aging. Retinal thickness decreases with age, especially in the inner nuclear layer. The macular blood flow was reduced by an average of 20%. Microglia are less motile and respond more slowly to injury. RPE decreases melanin production and increases lipofuscin accumulation. Müller cells are more susceptible to oxidative stress (55). These anatomical changes may contribute to the pathogenesis of DR combined with AMD in the elderly population.

DR is a major complication of DM. Globally, DR is the leading cause of preventable blindness in adults aged 20–74 years. Because it is avoidable blindness, slowing down the occurrence of DR after the occurrence of DM should be the key point. In most patients, retinopathy develops 10–15 years after the diagnosis of DM (1). The most common modifiable risk factors for DR in the Asia–Pacific region are hyperglycemia, BP, dyslipidemia, and obesity (43). Data from the UK Prospective Diabetes Study (UPDS) and the Diabetes Control and Complications Trial (DCCT) showed that controlling blood glucose (glycated hemoglobin A1c, HbA1c<7%) and BP levels slowed the onset and progression of DR (56–59). In China, a 5-year community-based prospective study on patients with type 2 DM showed DR regression in 24% of patients, which occurred mostly in patients with lower glucose levels (60). In Hong Kong, the regression rate was 13.2% and was also associated with lower HbA1c levels and the absence of albuminuria (61). These data suggest that the onset and progression of DR may be slowed down by reasonably controlling DM to reduce the prevalence of AMD in patients with DM.

The limitation of this study is its cross-sectional design rather than a longitudinal study. Therefore, the prevalence can only be discussed, and its incidence cannot be analyzed. Although our study was a population-based epidemiological study, the sample size was limited. Some diseases require hierarchical research, and some studies cannot be conducted owing to the limited number of cases. For example, in the study of DM combined with different DR stages, there were only two cases of PDR, and neither was combined with dry nor wet AMD; therefore, the study of PDR combined with dry and wet AMD cannot be counted. The stages of AMD include early, middle, and late stages, such as GA and wet AMD. The stages of DR included NPDR and PDR, and NPDR included mild, moderate, and severe NPDR. It is very difficult to correlate each stage of DR to each stage and type of AMD individually; therefore, epidemiological research or meta-analysis with a larger sample size is needed.

In conclusion, to our knowledge, this is the first epidemiological population-based study to discuss the relationship between DR and AMD in the northern mainland China. This study confirmed that the prevalence of dry AMD in DM complicated with DR was increased, and DR was a risk factor for dry AMD.

For patients with DM, how to screen for DR early and how to reduce or delay the occurrence of DR to effectively reduce the prevalence of AMD is an important topic. Future research aims to use new screening techniques combined with the in-depth learning artificial intelligence technique, to screen for early DR (62–65). The precise changes in choroidal thickness and structure of DR and AMD may provide evidence for the common pathogenesis of DR and AMD, although it is complex and unclear and needs to be discovered. An animal model of diabetic choroidopathy and the construction of animal models for DR combined with CNV are needed in the future (66). Whether PRP and anti-VEGF therapy can delay AMD occurrence in patients with DR should be investigated. Larger and longitudinal population-based epidemiological studies are needed to determine the exact relationship between the different stages of DR and AMD.

DATA AVAILABILITY STATEMENT

The datasets presented in this study can be found in online repositories. The names of the repository/repositories and accession number(s) can be found in the article/supplementary material.

ETHICS STATEMENT

The studies involving human participants were reviewed and approved by Beijing Tongren Hospital. The patients/participants provided their written informed consent to participate in this study.

AUTHOR CONTRIBUTIONS

ZY, ZJinq, and WW contributed to the interpretation of data and drafting of the report. WW contributed to the study design and review. All authors contributed to the article and approved the submitted version.

ACKNOWLEDGMENTS

The authors thank Xiuhua Guo and Haiping Zhang for statistical assistance.

REFERENCES

1. Jampol LM, Glassman AR, Sun J. Evaluation and care of patients with diabetic retinopathy. *N Engl J Med.* (2020) 382:1629–37. doi: 10.1056/NEJMra1909637
2. Saeedi P, Petersohn I, Salpea P, Malanda B, Karuranga S, Unwin N, et al. Global and regional diabetes prevalence estimates for 2019 and projections for 2030 and 2045: Results from the International Diabetes Federation Diabetes Atlas, 9th edition. *Diabetes Res Clin Pract.* (2019) 157:107843. doi: 10.1016/j.diabres.2019.107843
3. Xie XW, Xu L, Jonas JB, Wang YX. Prevalence of diabetic retinopathy among subjects with known diabetes in China: the Beijing Eye Study. *Eur J Ophthalmol.* (2009) 19:91–9. doi: 10.1177/112067210901900114
4. Wang FH, Liang YB, Zhang F, Wang JJ, Wei WB, Tao QS, et al. Prevalence of diabetic retinopathy in rural China: the Handan Eye Study. *Ophthalmology.* (2009)116:461–7. doi: 10.1016/j.ophtha.2008.10.003
5. Cao K, Wang B, Friedman DS, Hao J, Zhang Y, Hu A, et al. Handan Eye Study Group. Diabetic retinopathy, visual impairment, and the risk of six-year

death: a cohort study of a rural population in China. *Ophthalmic Res*. (2021) 64:983–90. doi: 10.1159/000512667
6. Wang FH, Liang YB, Peng XY, Wang JJ, Zhang F, Wei WB, et al. Handan Eye Study Group. Risk factors for diabetic retinopathy in a rural Chinese population with type 2 diabetes: the Handan Eye Study. *Acta Ophthalmol*. (2011) 89:e336–343. doi: 10.1111/j.1755-3768.2010.02062.x
7. Wong WL, Su X, Li X. Global prevalence of age-related macular degeneration and disease burden projection for 2020 and 2040: a systematic review and meta-analysis. *Lancet Glob Health*. (2014) 2:e106–116. doi: 10.1016/S2214-109X(13)70145-1
8. Jonas JB. Global prevalence of age-related macular degeneration. *Lancet Glob Health*. (2014) 2:e65–66. doi: 10.1016/S2214-109X(13)70163-3
9. You QS, Xu L, Yang H, Li YB, Wang S, Wang JD, et al. Five-year incidence of age-related macular degeneration: the Beijing Eye Study. *Ophthalmology*. (2012) 119:2519–25. doi: 10.1016/j.ophtha.2012.06.043
10. Liang YB, Gao LQ, Peng Y, Shen R, Duan XR, Friedman DS, et al. Prevalence of age-related macular degeneration in a rural Chinese population: the Handan Eye Study. *Ophthalmology*. (2011) 118:1395–401. doi: 10.1016/j.ophtha.2010.12.030
11. Xu L, Wang S, Li Y, Jonas JB. Retinal vascular abnormalities and prevalence of age-related macular degeneration in adult Chinese: the Beijing Eye Study. *Am J Ophthalmol*. (2006) 142:688–9. doi: 10.1016/j.ajo.2006.05.028
12. Cousins SW, Lee PP, Sloan FA. Ten-year incidence of age-related macular degeneration according to diabetic retinopathy classification among medicare beneficiaries. *Retina*. (2013) 33:911–9. doi: 10.1097/IAE.0b013e3182831248
13. Chen X, Rong SS, Xu Q, Tang FY, Liu Y, Gu H, et al. Diabetes mellitus and risk of age-related macular degeneration: a systematic review and meta-analysis. *PLoS ONE*. (2014) 19:e108196. doi: 10.1371/journal.pone.0108196
14. He MS, Chang FL, Lin HZ, Wu JL, Hsieh TC, Lee YC. The association between diabetes and age-related macular degeneration among the elderly in Taiwan. *Diabetes Care*. (2018) 41:2202–11. doi: 10.2337/dc18-0707
15. Mitchell P, Wang JJ. Diabetes, fasting blood glucose and age-related maculopathy: the Blue Mountains Eye Study. *Aust N Z J Ophthalmol*. (1999) 27:197–9. doi: 10.1046/j.1440-1606.1999.00211.x
16. Clemons TE, Milton RC, Klein R, Seddon JM, Ferris FL 3rd. Age-Related Eye Disease Study Research Group Risk factors for the incidence of advanced age-related macular degeneration in the Age-Related Eye Disease Study (AREDS): AREDS report no 19. *Ophthalmology*. (2005) 112:533–9. doi: 10.1016/j.ophtha.2004.10.047
17. Klein R, Klein BE, Moss SE. Diabetes, hyperglycemia, and age-related maculopathy. The Beaver Dam Eye Study. *Ophthalmology*. (1992) 99:1527–34. doi: 10.1016/S0161-6420(92)31770-1
18. Leske MC, Wu SY, Hennis A, Nemesure B, Yang L, Hyman L, et al. Barbados Eye Studies Group Nine-year incidence of age-related macular degeneration in the Barbados Eye Studies. *Ophthalmology*. (2006) 113:29–35. doi: 10.1016/j.ophtha.2005.08.012
19. Topouzis F, Anastasopoulos E, Augood C, Bentham GC, Chakravarthy U, de Jong PT, et al. Association of diabetes with age-related macular degeneration in the EUREYE study. *Br J Ophthalmol*. (2009) 93:1037–41. doi: 10.1136/bjo.2008.146316
20. Choi JK, Lym YL, Moon JW, Shin HJ, Cho B. Diabetes mellitus and early age-related macular degeneration. *Arch Ophthalmol*. (2011) 129:196–9. doi: 10.1001/archophthalmol.2010.355
21. Klein R, Deng Y, Klein BE, Hyman L, Seddon J, Frank RN, et al. Cardiovascular disease, its risk factors and treatment,and age-related macular degeneration: Women's Health Initiative Sight Exam ancillary study. *Am J Ophthalmol*. (2007) 143:473–83. doi: 10.1016/j.ajo.2006.11.058
22. Maltzman BA, Mulvihill MN, Greenbaum A. Senile macular degeneration and risk factors: a case-control study. *Ann Ophthalmol*. (1979) 11:1197–201.
23. Hyman LG, Lilienfeld AM, Ferris FL 3rd, Fine SL. Senile macular degeneration: a case-control study. *Am J Epidemiol*. (1983) 118:213–27. doi: 10.1093/oxfordjournals.aje.a113629
24. Blumenkranz MS, Russell SR, Robey MG, Kott-Blumenkranz R, Penneys N. Risk factors in age-related maculopathy complicated by choroidal neovascularization. *Ophthalmology*. (1986) 93:552–8. doi: 10.1016/S0161-6420(86)33702-3
25. Voutilainen-Kaunisto RM, Teräsvirta ME, Uusitupa MI, Niskanen LK. Age-related macular degeneration in newly diagnosed type 2 diabetic patients and control subjects: a 10-year follow-up on evolution, risk factors, and prognostic significance. *Diabetes Care*. (2000) 23:1672–8. doi: 10.2337/diacare.23.11.1672
26. Kahn HA, Leibowitz HM, Ganley JP, Kini MM, Colton T, Nickerson RS, et al. The Framingham Eye Study II Association of ophthalmic pathology with single variables previously measured in the Framingham Heart Study. *Am J Epidemiol*. (1977) 106:33–41. doi: 10.1093/oxfordjournals.aje.a112429
27. Cackett P, Yeo I, Cheung CM, Vithana EN, Wong D, Tay WT, et al. Relationship of smoking and cardiovascular risk factors with polypoidal choroidal vasculopathy and age-related macular degeneration in Chinese persons. *Ophthalmology*. (2011) 118:846–52. doi: 10.1016/j.ophtha.2010.09.026
28. Borrone R, Saravia M, Bar D. Age related maculopathy and diabetes. *Eur J Ophthalmol*. (2008) 18:949–54. doi: 10.1177/112067210801800615
29. Proctor B, Ambati J. Age-related macular degeneration and diabetic retinopathy: is diabetic retinopathy protective against ARMD? *ARVO*. (2007) 48:2149.
30. Zylbermann R, Landau D, Rozenman Y, Abrahami S, Pollack A. Exudative age related macular degeneration in patients with diabetic retinopathy and its relation to retinal laser photocoagulation. *Eye*. (1997) 11(Pt 3):872–5. doi: 10.1038/eye.1997.224
31. Chakravarthy U, Wong TY, Fletcher A, Piault E, Evans C, Zlateva G, et al. Clinical risk factors for age-related macular degeneration: a systematic review and meta-analysis. *BMC Ophthalmol*. (2010) 10:31. doi: 10.1186/1471-2415-10-31
32. Singh SR, Parameswarappa DC, Govindahari V, Lupidi M, Chhablani J. Clinical and angiographic characterization of choroidal neovascularization in diabetic retinopathy. *Eur J Ophthalmol*. (2021) 31:584–91. doi: 10.1177/1120672120902027
33. Wang Q, Wang YX, Wu SL, Chen SH, Yan YN, Yang MC, et al. Ocular axial length and diabetic retinopathy: the Kailuan Eye Study. *Invest Ophthalmol Vis Sci*. (2019) 60:3689–95. doi: 10.1167/iovs.19-27531
34. Wang Q, Liu L, Jonas JB, Gao B, Wu SL, Chen SH, et al. Albuminuria and retinal vessel density in diabetes without diabetic retinopathy: the Kailuan Eye Study. *Acta Ophthalmol*. (2021) 99:669–78. doi: 10.1111/aos.14670
35. Yang MC, Zhu XB, Wang YX, Wu SL, Wang Q, Yan YN, et al. Influencing factors for peripheral and posterior lesions in mild non-proliferative diabetic retinopathy-the Kailuan Eye Study. *Int J Ophthalmol*. (2020) 13:1467–6. doi: 10.18240/ijo.2020.09.20
36. Zhou W, Yang J, Wang Q, Wang Y, Yan Y, Wu S, et al. Systemic Stressors and retinal microvascular alterations in people without diabetes: the Kailuan Eye Study. *Invest Ophthalmol Vis Sci*. (2021) 62:20. doi: 10.1167/iovs.62.2.20
37. GBD 2019 Blindness and Vision Impairment Collaborators; Vision Loss Expert Group of the Global Burden of Disease Study. Causes of blindness and vision impairment in 2020 and trends over 30 years, and prevalence of avoidable blindness in relation to VISION 2020: the Right to Sight: an analysis for the Global Burden of Disease Study. *Lancet Glob Health*. (2021) 9:144–60.
38. Ogurtsova K, da Rocha Fernandes JD, Huang Y, Linnenkamp U, Guariguata L, Cho NH, et al. IDF Diabetes Atlas: global estimates for the prevalence of diabetes for 2015 and 2040. *Diabetes Res Clin Pract*. (2017) 128: 40–50. doi: 10.1016/j.diabres.2017.03.024
39. Teo ZL, Tham YC, Yu M, Chee ML, Rim TH, Cheung N, et al. Global Prevalence of Diabetic Retinopathy and Projection of Burden through 2045: Systematic Review and Meta-analysis. *Ophthalmology*. (2021) 128:1580–91. doi: 10.1016/j.ophtha.2021.04.027
40. Claessen H, Kvitkina T, Narres M, Trautner C, Zöllner I, Bertram B, et al. Markedly decreasing incidence of blindness in people with and without diabetes in southern Germany. *Diabetes Care*. (2018) 41:478–84. doi: 10.2337/dc17-2031
41. Zhang X, Saaddine JB, Chou CF, Cotch MF, Cheng YJ, Geiss LS, et al. Prevalence of diabetic retinopathy in the United States, 2005-2008. *JAMA*. (2010) 304:649–56. doi: 10.1001/jama.2010.1111
42. Cheung N, Wong TY. Changing trends of blindness: the initial harvest from translational public health and clinical research in ophthalmology. *Am J Ophthalmol*. (2012) 153:193–5. doi: 10.1016/j.ajo.2011.11.022
43. Chua J, Lim CXY, Wong TY, Sabanayagam C. Diabetic retinopathy in the Asia-Pacific. *Asia Pac J Ophthalmol (Phila)*. (2018) 7:3–16. doi: 10.22608/APO.2017511

44. Rizwan A, Sufyan A, Asghar A, Khan H, Ahmad B, Rabbani MH. Awareness of diabetic retinopathy among diabetic patients. *J Pak Med Assoc.* (2021) 71:651–5. doi: 10.47391/JPMA.897
45. Yang SH, Dou KF, Song WJ. Prevalence of diabetes among men and women in China. *N Engl J Med*. (2010) 362:2425–6. doi: 10.1056/NEJMoa0908292
46. Peng XY, Wang FH, Liang YB, Wang JJ, Sun LP, Peng Y, et al. Retinopathy in persons without diabetes: the Handan Eye Study. *Ophthalmology*. (2010) 117:531–7. doi: 10.1016/j.ophtha.2009.07.045
47. Stitt AW. AGEs and diabetic retinopathy. *Invest Ophthalmol Vis Sci.* (2010) 51:4867–74. doi: 10.1167/iovs.10-5881
48. Hammes HP, Hoerauf H, Alt A, Schleicher E, Clausen JT, Bretzel RG, et al. N(epsilon) (carboxymethyl)lysin and the AGE receptor RAGE colocalize in age-related macular degeneration. *Invest Ophthalmol Vis Sci.* (1999) 40:1855–9.
49. Soulis T, Thallas V, Youssef S, Gilbert RE, McWilliam BG, Murray-McIntosh RP, et al. Advanced glycation end products and their receptors co-localise in rat organs susceptible to diabetic microvascular injury. *Diabetologia*. (1997) 40:619–28. doi: 10.1007/s001250050725
50. Howes KA, Liu Y, Dunaief JL, Milam A, Frederick JM, Marks A, et al. Receptor for advanced glycation end products and age-related macular degeneration. *Invest Ophthalmol Vis Sci*. (2004) 45:3713–20. doi: 10.1167/iovs.04-0404
51. Zhang W, Liu H, Al-Shabrawey M, Caldwell RW, Caldwell RB. Inflammation and diabetic retinal microvascular complications. *J Cardiovasc Dis Res*. (2011) 2: 96–103. doi: 10.4103/0975-3583.83035
52. Totan Y, Yagci R, Bardak Y, Ozyurt H, Kendir F, Yilmaz G, et al. Oxidative macromolecular damage in age-related macular degeneration. *Curr Eye Res*. (2009) 34:1089–93. doi: 10.3109/02713680903353772
53. Venza I, Visalli M, Cucinotta M, Teti D, Venza M. Association between oxidative stress and macromolecular damage in elderly patients with age-related macular degeneration. *Aging Clin Exp Res*. (2012) 24:21–7. doi: 10.3275/7659
54. Laíns I, Talcott KE, Santos AR, Marques JH, Gil P, Gil J, et al. Choroidal thickness in diabetic retinopathy assessed with swept-source optical coherence tomography. *Retina*. (2018) 38:173–82. doi: 10.1097/IAE.0000000000001516
55. Leley SP, Ciulla TA, Bhatwadekar AD. Diabetic retinopathy in the aging population: a perspective of pathogenesis and treatment. *Clin Interv Aging*. (2021) 16:1367–78. doi: 10.2147/CIA.S297494
56. Mohamed Q, Gillies MC, Wong TY. Management of diabetic retinopathy: a systematic review. *JAMA*. (2007) 298:902–16. doi: 10.1001/jama.298.8.902
57. Diabetes Control and Complications Trial Research Group, Nathan DM, Genuth S, Lachin J, et al. The effect of intensive treatment of diabetes on the development and progression of long-term complications in insulin-dependent diabetes mellitus. *N Engl J Med*. (1993) 329:977–86. doi: 10.1056/NEJM199309303291401
58. Matthews DR, Stratton IM, Aldington SJ, Holman RR, Kohner EM. Risks of progression of retinopathy and vision loss related to tight blood pressure control in type 2 diabetes mellitus: UKPDS 69. *Arch Ophthalmol*. (2004) 122:1631–40. doi: 10.1001/archopht.122.11.1631
59. Estacio RO, Jeffers BW, Gifford N, Schrier RW. Effect of blood pressure control on diabetic microvascular complications in patients with hypertension and type 2 diabetes. *Diabetes Care*. (2000) 23(Suppl 2): B54–B64.
60. Jin P, Peng J, Zou H, Wang W, Fu J, Shen B, et al. The 5-year onset and regression of diabetic retinopathy in Chinese type 2 diabetes patients. *PLoS ONE*. (2014) 9:e113359. doi: 10.1371/journal.pone.0113359
61. Tam VH, Lam EP, Chu BC, Tse KK, Fung LM. Incidence and progression of diabetic retinopathy in Hong Kong Chinese with type 2 diabetes mellitus. *J Diabetes Complications*. (2009) 23:185–93. doi: 10.1016/j.jdiacomp.2008.03.001
62. Vujosevic S, Aldington SJ, Silva P, Hernández C, Scanlon P, Peto T, et al. Screening for diabetic retinopathy: new perspectives and challenges. *Lancet Diabetes Endocrinol*. (2020) 8:337–47. doi: 10.1016/S2213-8587(19)30411-5
63. Xie Y, Nguyen QD, Hamzah H, Lim G, Bellemo V, Gunasekeran DV, et al. Artificial intelligence for teleophthalmology-based diabetic retinopathy screening in a national programme: an economic analysis modelling study. *Lancet Digit Health*. (2020) 2:e240–9. doi: 10.1016/S2589-7500(20)30060-1
64. Bora A, Balasubramanian S, Babenko B, Virmani S, Venugopalan S, Mitani A, et al. Predicting the risk of developing diabetic retinopathy using deep learning. *Lancet Digit Health*. (2021)3:e10–e19. doi: 10.1016/S2589-7500(20)30250-8
65. Bandello F, Cicinelli MV. 19th EURETINA Congress Keynote Lecture: Diabetic Retinopathy Today. *Ophthalmologica*. (2020) 243:163–71. doi: 10.1159/000506312
66. Olivares AM, Althoff K, Chen GF, Wu S, Morrisson MA, DeAngelis MM, et al. Animal models of diabetic retinopathy. *Curr Diab Rep*. (2017) 17:93. doi: 10.1007/s11892-017-0913-0

Conflict of Interest: CS was employed by Kailuan Group.

The remaining authors declare that the research was conducted in the absence of any commercial or financial relationships that could be construed as a potential conflict of interest.

Publisher's Note: All claims expressed in this article are solely those of the authors and do not necessarily represent those of their affiliated organizations, or those of the publisher, the editors and the reviewers. Any product that may be evaluated in this article, or claim that may be made by its manufacturer, is not guaranteed or endorsed by the publisher.

frontiers | Frontiers in Endocrinology

TYPE Review
PUBLISHED 09 August 2022
DOI 10.3389/fendo.2022.935244

OPEN ACCESS

EDITED BY
Michele Lanza,
University of Campania Luigi Vanvitelli, Italy

REVIEWED BY
Bertrand Kaeffer,
Institut National de recherche pour l'agriculture, l'alimentation et l'environnement (INRAE), France
Eleni Anastasiadou,
Sapienza University of Rome, Italy

*CORRESPONDENCE
Shu Lin
shulin1956@126.com
Yu Hong
15985998008@163.com

SPECIALTY SECTION
This article was submitted to Clinical Diabetes, a section of the journal Frontiers in Endocrinology

RECEIVED 03 May 2022
ACCEPTED 11 July 2022
PUBLISHED 09 August 2022

CITATION
Niu S-r, Hu J-m, Lin S and Hong Y (2022) Research progress on exosomes/microRNAs in the treatment of diabetic retinopathy. *Front. Endocrinol.* 13:935244. doi: 10.3389/fendo.2022.935244

Research progress on exosomes/microRNAs in the treatment of diabetic retinopathy

Si-ru Niu[1], Jian-min Hu[1,2], Shu Lin[3,4]* and Yu Hong[1]*

[1]Department of Ophthalmology, The Second Affiliated Hospital of Fujian Medical University, Quanzhou, China, [2]The School of Medical Technology and Engineering, Fujian Medical University, Fuzhou, China, [3]Centre of Neurological and Metabolic Research, The Second Affiliated Hospital of Fujian Medical University, Quanzhou, China, [4]Group of Neuroendocrinology, Garvan Institute of Medical Research, Sydney, NSW, Australia

Diabetic retinopathy (DR) is the leakage and obstruction of retinal microvessels caused by chronic progressive diabetes that leads to a series of fundus lesions. If not treated or controlled, it will affect vision and even cause blindness. DR is caused by a variety of factors, and its pathogenesis is complex. Pericyte-related diseases are considered to be an important factor for DR in many pathogeneses, which can lead to DR development through direct or indirect mechanisms, but the specific mechanism remains unclear. Exosomes are small vesicles of 40–100 nm. Most cells can produce exosomes. They mediate intercellular communication by transporting microRNAs (miRNAs), proteins, mRNAs, DNA, or lipids to target cells. In humans, intermittent hypoxia has been reported to alter circulating excretory carriers, increase endothelial cell permeability, and promote dysfunction *in vivo*. Therefore, we believe that the changes in circulating exocrine secretion caused by hypoxia in DR may be involved in its progress. This article examines the possible roles of miRNAs, proteins, and DNA in DR occurrence and development and discusses their possible mechanisms and therapy. This may help to provide basic proof for the use of exocrine hormones to cure DR.

KEYWORDS

Diabetic retinopathy, pericyte, microRNA, exosomes, treatment

Abbreviations: DR, diabetic retinopathy; miRNA, microRNA; ECs, endothelial cells; MVBs, multivesicular bodies; miRNAs, microRNAs; NC RNA, noncoding RNA; MSCs, mesenchymal stem cells; HRMECs, human retinal microvascular endothelial cells; HG, high glucose; HUVECs, human umbilical vein endothelial cells; EndMT, endothelial mesenchymal transformation; VSMCs, vascular smooth muscle cells; HUVEC-Exo, human umbilical vein endothelial cell exosome; ROS, reactive oxygen species; AGE, advanced glycation end products; ALE, advanced lipid oxidation end products; RAGE, AGE receptor; CTGF, connective tissue growth factor; PRP-Exos, exosomes derived from platelet-rich plasma; CXCL10, CXCchemokineligand-10; BSCB, Blood spinal cord barrier; BMSC-EVs, Extracellular vesicles derived from bone marrow mesenchymal stem cells; TGF-β 2, transforming growth factor-β 2; VEGF, vascular endothelial growth factor; REC, retinal microvascular endothelial cells; DKD, development of diabetic nephropathy; IR, ischemia and reperfusion; MI, myocardial infarction; EPCs, endothelial progenitor cells.

1 Introduction

Microvascular complications are one of the most common complications of diabetes mellitus. Persistent high blood sugar levels can harm a range of organs, including the heart, kidneys, and retina. The most common complications of diabetes are microvascular complications, particularly diabetic nephropathy (DN) and retinopathy (1). Diabetic retinopathy (DR) is chronic retinopathy that causes leakage and blockage of retinal blood vessels, which can result in a range of fundus lesions, including microangiomas, hard exudates, cotton spots, neovascularization, vitreous hyperplasia, macular edema, and retinal detachment, among others. In recent years, with the advancement of medical technology, particularly the emergence of antiangiogenic drugs, there have been more options for DR treatment; however, it remains an important cause of impaired vision and even blindness.

The etiology of DR is associated with several morphological alterations, including pericyte loss, basement membrane thickening, increased vascular permeability, and microaneurysms. Pericytes and endothelial cells (ECs) are the most common retinal vascular cells. Communication between these two cell types is important for microvascular stabilization and remodeling. Pericyte loss is an early pathological feature of DR and frequently occurs in diabetic patients and animals (2). These two cell types share the same basement membrane on the vessel wall. There is communication between them due to the discontinuity of the basement membrane. ECs and pericytes communicate through the gap junctions between PEG sockets with other paracrine signaling factors, including growth factors, secreted cytokines, and extracellular secretions (2–5). Because pericytes are an abundant cell type in microvessels, their dysfunction can result in a variety of vascular-related diseases, including stroke and renal infarction, among others. Studies have shown that diseases associated with the diabetic retina are closely associated with pericytes. For example, pericytes create cPWWP2A (circ RNAs - PWWP2A), which is subsequently transferred to ECs *via* exosomes (5). CPWWP2A silencing can exacerbate diabetic retinal microvascular damage and dysfunction, such as pericyte loss, acellular capillary microaneurysm, vascular leakage, and inflammation (5).

Exosomes refer to small membrane vesicles containing complex RNAs and proteins. Under normal and pathological conditions, many cells secrete exosomes. They are primarily sourced in the multivesicles formed by the invagination of intracellular lysosomal granules, and the outer membranes of the multivesicles are released into the extracellular matrix following fusion with the cell membrane. Exosomes are considered to be membrane vesicles that are secreted exclusively and play a role in intercellular communication. Studies have shown that exosomes can maintain stable blood sugar levels in the body through multiple mechanisms and slow the development of diabetes and the associated microvessel formation, reducing the progression of this diabetic complication. However, the specific mechanism of exosome action remains unclear (1, 2). Many biological effects of exosomes are expressed by microRNA (miRNA), and miRNAs regulate different pathological alterations during DR, which include cell proliferation, apoptosis, inflammation responses, microcirculation impairments, oxidative stress, and cellular death by controlling the key molecules, particularly vascular endothelial growth factor (VEGF) (6). Therefore, miRNA antagonists or mimics as a novel class of drugs could be potentially helpful to control the occurrence and progression of pathological changes during DR.

This article examines the role and possible mechanisms of DR and the occurrence of exosomes and their possible use in its treatment. To reverse the chronic consequences of DR, we might use exosome substances to treat this disease, for example, miRNA-21 and miR-200a-3p.

2 Diabetic retinopathy and pericytes

DR is characterized by a severe deterioration of the retinal microvasculature, resulting in hypoperfusion, increased capillary permeability, abnormal proliferation of retinal blood vessels, and ultimately even blindness (7). DR can be classified into two types according to fundus changes: non-proliferative and proliferative phases (7, 8). The non-proliferative phase is confined to the retina; blood vessels undergo microaneurysms and bleeding and display vascular instability, macular edema, basement membrane thickening, and vascular degeneration (9). By comparison, the proliferative phase is characterized by neovascularization. New blood vessels are prone to rupture, which may eventually lead to retinal bleeding and detachment (8).

Although DR is primarily considered to be a disease caused by decreased EC function, there is significant evidence from animal studies that its pathogenesis begins with pericyte loss. Studies of diabetic complications in humans have shown that pericyte exfoliation in DR is associated with microvascular lesion development, including microaneurysms, acellular capillaries, vascular distortion, increased permeability, and capillary perfusion (4). The early pericyte loss is rapidly accompanied by EC loss and capillary network collapse, resulting in reduced retinal blood flow. It is proposed that the initial pericyte loss is driven by angpt-2 (10). The regeneration and plasticity of pericytes allow possible treatment of diseases associated with vascular malnutrition, including muscular dystrophy, ischemic stroke, and DR. To facilitate intercellular communication, the tight binding of pericytes and ECs occurs through direct contact, with ion exchange by gap junctions such as connexin43 (11) and the exchange of other paracrine molecules such as cathepsin D

(12) and sphingosine 1-phosphate (13). Pericytes may serve as targets to treat microvascular diseases such as diabetic pathological angiogenesis and complications (14).

3 Effects of exosomes on diabetic retinopathy

Exosomes are released into the extracellular space from many cell types. These exosomes are broadly distributed in the body fluids. In recent years, mRNA and miRNA have been identified *in vitro*, which can be absorbed by nearby or distant cells, and regulate the receptor cells, thus playing a role in the occurrence and development of related diseases.

3.1 Exosomes

3.1.1 Concept and classification of exosomes

Exosomes currently refers specifically to discoid vesicles with a diameter of 40–100 nm. They are common membrane-bound nanovesicles which transport proteins, lipids, DNA, mRNA, and miRNA among other biomolecules. They are initially formed by endocytosis. Above all, internalization of the cell membrane produces endosomes. Subsequently, many small vesicles are formed in the inner body through the invaginated part of the inner body membrane. Such endosomes are termed multivesicular bodies (MVBs). Finally, MVBs fuse with the cell membrane, releasing endosome vesicles outside the cell as exosomes. Exosomes are produced by cells *via* exocytosis and are taken up by target cells. They transport substances and messages between cells through the circulation of body fluids. Therefore, exosomes play a role in different physiological and pathological processes in the human body (15, 16). Many biological effects of exosomes are expressed through miRNAs. miRNAs are a class of endogenous short non-coding single-stranded RNA molecules of 19–23 nucleotides in length which are from genome regions that do not code for proteins (17). They can be found in human fluids in a stable state, according to increasing data. Extracellular miRNAs can be loaded into high-density lipoprotein or bound by argonaute-2 protein outside vesicles, in addition to being packed into exosomes or microvesicles. All three mechanisms protect miRNAs against degradation and ensure their long-term stability (16). miRNAs negatively regulate the expression levels of target genes and confer characteristic changes on them, playing a regulatory role in almost all cellular processes. When miRNAs are analyzed as exosome miRNAs rather than intracellular miRNAs, researchers discovered a new role in certain cases, being exported inside extracellular vesicles, with Toll-like receptor (TLR)–binding miRNA released by cells from injured or stressed tissues able to reach the endosomal compartment and propagate inflammatory signals in distant recipient cells (17). Exosomal miR-21 and miR-29a were initially revealed to have the ability to attach to TLRs and activate immune cells, in addition to their traditional action of targeting miRNA (18). The quantity and composition of secreted miRNAs vary between diseased and healthy individuals (16, 19–21). To date, hundreds of miRNAs have been found in eye tissue, which may become a new biomarker for the early diagnosis of non-invasive ocular diseases (22).

3.1.2 Regulation of exosomes secretion

Exosomes are primarily derived from multivesicles formed by the invagination of lysosomal granules in cells, and the outer membranes of multivesicular vesicles are released into the extracellular environment after fusion with the cell surface. Although many cells are able to secrete exosomes under normal or abnormal conditions, under pathological conditions, exosome secretions may increase or their content may change.

On the one hand, it has been found that the RAB family (a member of the RAS oncogene family) of small GTPase proteins controls different steps of vesicle transport in cells (23), such as vesicle budding, mobility of vesicles and organelle interaction through the cytoskeleton, and the junction of vesicles with target chambers to form membrane fusion (24). Since the first proteomic study, endosomal-related members of this family have been identified in exosomes (25). For example, RAB-11 has been implicated in the control of TfR and Hsc70 released from exosomes in K562 cells (26).

On the other hand, in some studies, cellular stress enhanced exosome release (27–29). For example, studies found that radiotherapy-induced cellular senescence is associated with a significant rise in the release of exosome-like microvesicles. In premature aging, this new secretory phenotype depends on p53 activation. Radiation therapy can induce increased DNA damage, such as p53-dependent vesicle increase (28). At present, the specific mechanism of increased secretion caused by cellular stress is unclear, but the increased secretion may act on adjacent cells, leading to pathological changes in these cells.

3.2 Regulation of endothelial function

The two main cellular components of retinal microvessels are pericytes and ECs. The formation, maturation, and stabilization of microvessels require the interaction of these two cell types. Endothelial dysfunction is among the risk variables for DR development. Studies have shown that pericytes activated by the hypoxia-inducible factor (HIF) pathway can secrete exosomes under hypoxia and can regulate EC migration, germination, and angiogenesis (30). In addition to those from pericytes, exosomes from neurons, glial cells, ECs, and the circulation can modulate EC integrity and intercellular cross-talk in the neurovascular unit under physiological and

pathological conditions (31–33). Gong et al. found that exosomes from mesenchymal stem cells (MSCs) were found to facilitate the transfer of miRNA from MSCs to human umbilical vein ECs (HUVECs) and promote angiogenesis. Their findings demonstrated that MSCs secrete exosomes containing proteins, cytokines, and chemicals that promote HUVEC-mediated tubular formation, increase the bud number of HUVEC spheroids, and attract ECs and promote their proliferation (34). Zhu et al. found that retinal astrocytes may release exosomes to transmit autophagy-inducing signals and regulate EC proliferation and migration; thus, they participate in the occurrence and development of retinal vascular-related diseases (35).

Endothelial-mesenchymal transition (EndMT) has been found to contribute to pathological fibrosis in proliferative DR (PDR). Gu et al. discovered that miR-202-5p secreted by retinal pigment epithelial cells (ARPE) can act as an important mediator of intercellular cross-talk and transfer miR-202-5p *via* the TGF/Smad pathway to inhibit EndMT (36). Cao et al. reported that MSC-derived exosomal SNHG7 can inhibit EndMT and tube formation by human retinal microvascular ECs (HRMECs) stimulated by high glucose (HG) by interacting with the miR-34a-5p/XBP1 signaling pathway, providing a viable treatment approach for DR therapy (37).

3.3 Smooth muscle cell proliferation and differentiation

Vascular smooth muscle cells (VSMCs) are a special cell type with abnormal plasticity in response to environmental stressors. Because abnormally increased VSMC proliferation is associated with a variety of vascular disorders, controlling its phenotype may have important implications for delaying DR development. In DR development caused by microvascular diseases caused by microcirculation disorders, hypoxia frequently occurs. Hypoxia promotes VSMC growth. New research suggests that miRNAs are key regulators of the VSMC hypoxia response. Previous studies have shown that miR-1260b is among the more upregulated hypoxia-related amines in VSMCs (38). GDF11-Smad–dependent signaling mediated by miR-1260b is an important signaling method for VSMC proliferation, and hypoxia controls this axis, which promotes aberrant VSMC proliferation (39). The new findings demonstrated that miR-1260b downregulation reduces VSMC proliferation. Consequently, hypoxia-induced increased miR-1260b expression may stimulate VSMC proliferation (39). Research has also shown that HG can induce VSMC calcification/aging, which in turn leads to diabetes-related vascular calcification/aging. Studies have shown that Notch3 is abundant in HG-stimulated HUVECs (HG-HUVEC-Exo). In addition, Notch3 expression in VSMCs was clearly increased in HG-stimulated HUVECs compared with the HG-stimulated HUVEC treatment group. When Notch3 inhibitors act *in vivo* to inhibit Notch3 expression, the capacity of HG-stimulated HUVECs to stimulate calcification/senescence of VSMCs is reduced (40).

Therefore, miR-1260b downregulation can inhibit VSMC proliferation and Notch3 expression, which may consequently delay VSMC calcification/aging and aid in the treatment of DR.

3.4 Macrophage activation

Inflammation is the central component of the pathogenesis of diabetes and metabolic syndrome, particularly in the development of complications. DR is considered a vascular and neurodegenerative disease that develops after periods of inadequate blood glucose control. Retinal microvascular disease is the early pathogenesis, which is caused by low-level, persistent leukocyte activation, resulting in recurrent capillary blockage and gradual retinal-depleting ischemia. At the molecular level, macrophage-restricted protein tyrosine phosphatase 1B (PTP1B) is a critical moderator of metabolic syndrome inflammation involving insulin resistance. PTP1B imbalance may underlie retinal microangiopathy (41). Hyperglycemia in patients with diabetes leads to an increased generation of reactive oxygen species (ROS) and the accumulation of advanced glycation or lipid oxidation end products (AGE and ALE, respectively), affecting the physiological functions of the retina (42). AGE and AGE receptor (RAGE) interaction induces a pro-inflammatory phenotype in microglia, resulting in an enhanced release of inflammatory cytokines (TNF-α and IL-6) (43, 44). Elevated TNF-α and IL-1β levels are consistent with increased intraretinal neovascularization in DR and increased microvascular degeneration in ischemic retinopathy (45, 46). Hyperglycemia could activate VEGF expression, and HIF-1 is translocated to the extracellular signal–regulated kinase (ERK)1/2–nuclear factor κB (NF-κB) signaling pathway in the nucleus and microglia (47, 48). VEGF overexpression contributes to retinal neovascularization, whereas translocation of HIF-1 increases the transcription of angiogenesis-related genes (49).

3.5 Platelet activation

Vascular fibrosis is the main pathological feature of the proliferative stage of DR. However, the molecular mechanism of its occurrence remains unclear. Connective tissue growth factor (CTGF), a main fibrotic factor, is highly expressed in DR and plays a key role in retinal endothelial membrane thickening (50). The study showed that exosomes of platelet plasma in diabetic rats (DM-PRP-Exos) considerably elevated Müller cell growth and metastasis compared with exosomes of platelet plasma from normal control rats (Nor-PRP-Exos). The above results suggest that platelet plasma secretion–induced fibrogenesis may be triggered by activating the phosphoinositide-3 kinase-serine/threonine kinase (PI3K/Akt) signaling pathway (51). Therefore,

under hyperglycemia, platelets are stimulated to produce PRP-Exos, which activate the PI3K/Akt signaling pathway (52).

Platelet plasma exosomes (PRP-Exos) mediate hyperglycemia-induced retinal endothelial damage *via* upregulating the TLR4 signaling pathway. They can transfer platelet cytokines, alter protein expression, and cause retinal endothelial dysfunction and early DR. A study found that the PRP-Exo levels in the circulation of diabetic rats were significantly increased. At the same time, it was further proved that HG effectively enhances the capacity of platelets to produce PRP-Exos *in vitro*. It was shown that PRP-Exos can promote TLR4 expression and that of its downstream proteins MyD88, p-NF-κB/P65, and NF-κB/P65 and activate the TLR4 pathway (53). Accumulating evidence suggests that TLR4 has a vital function in regulating retinal homeostasis and is engaged in DR progression (54). The new study found that CXCL10 may activate the TLR4 pathway *in vitro*. CXCL10 blockade can downregulate the TLR4 signaling pathway and diminish PRP-Exo–induced retinal inflammation. These results suggested that CXCL10 appears to be a key regulator of PRP-Exo–derived retinal endothelial damage in DR (53). Consequently, inhibiting the TLR4 signaling pathway provides a new therapeutic idea for reducing the early vascular DR complications induced by PRP-Exo.

3.6 In summary

As described above, circulating exosome action on various related cells leads to DR. Figure 1 shows the effect of exosomes on cells associated with DR.

4 Effects of exosomes on pericytes

Long-term hyperglycemia causes DR, a frequent microvascular condition. Intercommunication of pericytes and ECs is critical for maintaining vascular homeostasis and remodeling. Hypoxia was found to upregulate circEhmt1 production in pericytes, which can subsequently be transported to ECs by exosomes. In addition, circEhmt1 overexpression has a protective effect against HG-induced EC damage *in vitro*. Mechanistically, circEhmt1, which is strongly expressed in pericyte nuclei, upregulates NFIA (transcription factor) levels and inhibits NLRP3-mediated inflammatory bodies (55).

Diabetes-related stress enhanced cPWWP2A expression in pericytes but had no effect on ECs, according to the findings. Pericytes create cPWWP2A, which is delivered to ECs through exosomes. *In vitro* studies demonstrated that cPWWP2A directly regulates pericyte biology, whereas EC biology is directly regulated by cPWWP2A-carrying exosomes.

CPWWP2A acts as an endogenous miR-579 sponge, isolating and inhibiting the activity of miR-579. Diabetes-induced retinal vascular dysfunction was reduced *in vivo* when cPWWP2A overexpression or miR-579 suppression was used. Furthermore, suppressing cPWWP2A or overexpressing miR-579 can exacerbate microvascular dysfunction by inhibiting the cPWWP2A-mediated signaling pathway. This study suggests that intervention at the level of cPWWP2A or miR-579 expression could provide an opportunity for the treatment of diabetic microvascular complications (2).

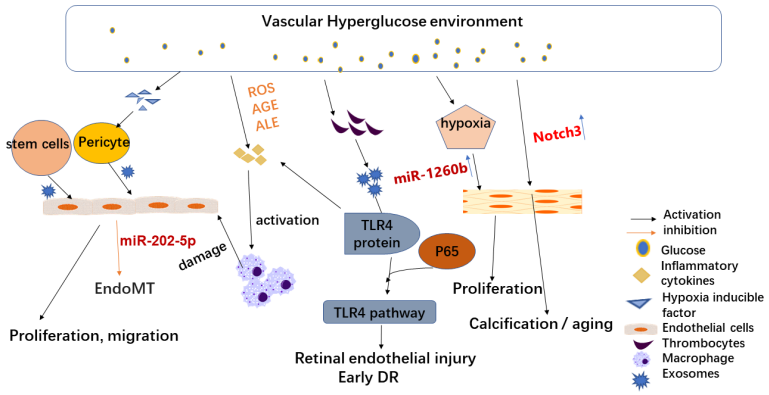

FIGURE 1
Effects of exosomes on diabetic retinopathy-related cells. High-glucose environment and hypoxia alter circulating exosomes and play a key role in DR development. Therefore, stem cell exosomes may be an effective treatment for DR. Hypoxia-induced increased secretion of hypoxia-inducible factors can lead to endothelial dysfunction (ED) and promote endothelial cell permeability *in vitro*. Hypoxia also leads to changes in circulating exosomes (such as miR-1260b), resulting in the proliferation of vascular smooth muscle cells. A high-glucose microenvironment also leads to a greater generation of reactive oxygen species (ROS) and the build-up of advanced glycation or lipid oxidation end products (AGE or ALE), which in turn leads to inflammatory increased cytokines (TNF-α, the secretion of IL-6) and thus to inflammation and exacerbates the harm of DR. PRP-Exos participate in early DR formation *via* mediating hyperglycemia-induced retinal endothelial damage by upregulating the TLR4 signaling pathway.

Exosomes reduce pericyte migration by downregulating NF-κB p65 signaling, thereby maintaining the function of the blood spinal cord barrier (BSCB). Studies have found that bone marrow MSC–derived extracellular vesicles prevent pericyte migration by inhibiting the activation of the NF-κB signaling pathway. This improves the integrity of the BSCB (56).

Pericyte activation is a key pathogenic characteristic of interstitial fibrosis (RIF). It was found that MSC-derived exosomes deliver the miR-34c-5p by inhibiting core focusing (CF) to reduce cellular activation and help exosomal miR-34c-5p enter pericytes through the RIFcd81–epidermal growth factor receptor (EGFR) ligand receptor complex. The findings of this study offer a potential therapy option for renal fibrosis (57).

5 Possible mechanisms of exosome-mediated diabetic retinopathy

Although studies have demonstrated exosome involvement in DR progression, including multiple cascades and interconnections, the specific processes remain unknown. The mechanisms associated with exosomes and DR are mainly hypoxia, inflammation, and stress intensification. As mentioned above, exosomes are extensively involved in DR development and progression. Next, we will attempt to explain the signaling pathways and molecular mechanisms by which exosomes, mainly through miRNAs, may be involved in DR development and progression.

5.1 TGF-β–mediated pathways

TGF-β and TGF-β–mediated signaling pathways play an exacerbating role in DR pathogenesis (58). Further research has revealed that they are essential regulators of cell growth and mid-differentiation. For example, as key inducers of tissue fibrosis, they can promote fibroblast proliferation, ultimately leading to tissue fibrosis (59, 60). Lou et al. reported that the miR-21 expression level in the retina of rats with DR was considerably higher than the normal rats, implying that abnormal retinal miR-21 expression may participate in DR pathogenesis. Moreover, the analysis results of this study showed that TGF-β signaling pathway inhibitors greatly reduced the effect of miR-21 in DR in rats and improved ocular hemodynamics in these animals. This suggests that miR-21 controls the TGF-β signaling pathway involved in the pathogenesis of DR. Therefore, TGF-β signaling pathway regulation by miR-21 affects hemodynamics in rats with PDR (61). Li et al. found that inhibiting the TGF-β2/Smad pathway increased miR-200a-3p, which prevented DR development. It was also found that miR-200a-3p was significantly downregulated in both ARPE-19 cells and retinal tissues of rats with DR after HG treatment, whereas TGF-β2 expression was upregulated. Subsequently, miR-200a-3p overexpression greatly accelerated cell proliferation, decreased apoptosis, and reduced the level of secreted inflammatory cytokines and VEGF in HG-injured ARPE-19 cells. MiR-200a-3p overexpression attenuated HG-induced damage in ARPE-19 cells, decreased the secretion of inflammatory cytokines, and downregulated VEGF expression through inactivation of the TGF-β2/Smad pathway. *In vivo*, miR-200a-3p upregulation improved retinal angiogenesis and inflammation in DR in rats, thus providing a novel target for DR therapy. However, it is unclear how miR-200a-3p expression was upregulated *in vivo* (62).

5.2 PI3K/Akt signaling pathway

The PI3K/Akt signaling pathway is a downstream signal of a variety of cell-surface receptors that regulate cell proliferation, survival, and death (63). Zhang et al. discovered that miR-183 was markedly upregulated in a rat model of DR with activation of the PI3K/Akt/VEGF signaling pathway. It was observed that miR-183 expression was upregulated and BTG1 expression was downregulated in retinal tissue in DR in rats. MiR-183 overexpression activated the PI3K/Akt/VEGF signaling pathway to inhibit BTG1 and promote EC proliferation but inhibit apoptosis. According to the findings, miR-183 inhibition could inhibit vascular EC proliferation and angiogenesis by downregulating BTG1 and inactivating the PI3K/Akt/VEGF signaling pathway (64).

It is known that, in PDR, miR-21 expression is increased and can promote retinal pigment epithelial cell proliferation and migration (65). Lu et al. found that miR-21 may be a target for DR therapy because it has the potential to block DR. Downregulation of miR-21 disrupts the survival of retinal vascular ECs (RVECs), inducing apoptosis of these cells, and attenuates angiogenesis by inhibiting the PI3K/Akt/VEGF signaling pathway and upregulating phosphatase and tensin homolog (PTEN). The results indicated that miR-21 overexpression may activate the PI3K/Akt/VEGF signaling pathway by inhibiting PTEN expression, thereby stimulating RVEC activity and angiogenesis in DR in rats, suggesting that miR-21 may be a target of DR treatment (66).

According to Wang et al., HG decreased the relative miR-199a-3p expression level in HRMECs and apre-19 cells but increased VEGF expression. Upregulation of miR-199a-3p not only significantly alleviated HG-induced cell proliferation and migration but also significantly inhibited the PI3K/Akt signaling pathway and HG-induced angiogenesis. MiR-199a-3p upregulation can control the PI3K/Akt pathway by suppressing VEGF and promoting HG-induced angiogenesis in HRMECs (67).

5.3 p38 MAPK signaling pathway

The MAPK signaling pathway is present in many cells, delivering extracellular stimuli that elicit biological responses. The P38 signal transduction pathway (MAPK pathway) regulates a wide range of biological functions (68). Li et al. found that miR-141-3p inhibited retinal angiogenesis in glaucoma mice by preventing activation of the docking protein 5 (DOK5)–mediated MAPK signaling pathway. The DOK5 gene was repressed by miR-141-3p, which activated the MAPK pathway. The findings revealed that miR-141-3p reduced the proliferation and angiogenesis of retinal vascular epithelial cells and promoted RGC apoptosis (69). Chen et al. found that MSC-derived exosomes prevented hypoxia-induced cell death by carrying miR-21 and inhibiting p38 MAPK signaling (70). MSC exosomes may aid patients with diabetes, according to their findings. Dai et al. reported that baicalin (BAI) inhibited the activation of the NF-κB and p38 MAPK pathways by upregulating miR-145 and had a protective effect on HG-induced injury of human retinal pigment epithelial cells (71).

5.4 NF-κB pathway

NF-κB functions primarily in biological processes, including the inflammatory response and immunity. It was demonstrated to be activated in the diabetic retina in numerous studies, its activation increasing capillary apoptosis (72), which is a precursor to the development of DR characteristics. The activity of the NF-κB signaling pathway has been reported to be enhanced in diabetic rat studies. In turn, NF-κB p65 expression upregulation increases ROS production, which leads to microaneurysms, retinal neovascularization, and vitreous hemorrhage in diabetic rats, and promotes DR progression (73, 74).

According to Li et al., the number of pericytes in retinal capillaries of miR-874 mimics-treated DR in rats rose, whereas EC proliferation was reduced. MiR-874 inhibitor exacerbates DR in diabetic rats after treatment. The results showed that miR-874 overexpression suppressed NF-κB signaling pathway expression and alleviated DR in diabetic rats (75). Li et al. demonstrated low miR-486-3p expression and high TLR4 and NF-κB expression in HG-treated Müller cells. TLR4 is the action site of miR-486-3p. In HG-treated Müller cells, miR-486-3p upregulation or TLR4 downregulation prevented oxidative damage, inflammation, and apoptosis while promoting proliferation. This study highlighted that the protective role of exosomal-induced miR-486-3p upregulation in DR mice is by TLR4/NF-κB axis inhibition (76).

Hui et al. found that miR-145 was downregulated in HG-treated retinal microvascular ECs (RECs), while miR-145 overexpression suppressed enhanced TLR4 expression and NF-κB p65 nuclear translocation in HG-treated RECs. More importantly, miR-145 overexpression reduced REC apoptosis, oxidative stress, and inflammatory cytokine release in HG environments. These findings revealed that miR-145 may exert antioxidant and anti-inflammatory effects in DR (54). Ye and Steinle reported decreased miR-146a expression in human RECs cultured with HG. Overexpression of miR-146a with a miR-146a mimic reduced TLR4/NF-κB and TNF expression in RECs induced by HG. Overexpression of miR-146a in RECs reduced MyD88-dependent and -independent signaling under HG conditions. The results showed that miR-146a suppressed TLR4/NF-κB and TNF-α, the potential site of action for reducing REC inflammation (77).

5.5 Summary

Exosomes have multiple mechanisms of action in DR, but the specific mechanisms remain unclear. However, exosomes might have a critical role in this process and its treatment. Figure 2 shows the possible signaling pathways and molecular mechanisms involving miRNA in DR formation and development. Table 1 shows exosome-derived proteins and RNA involved in DR.

6 Exosomes and diabetes-related cardiovascular and cerebrovascular events

The vascular complications of diabetes include macrovascular and microvascular complications. In recent years, many studies have proved that miRNA has a good therapeutic effect in the treatment not only of DR but also of other complications of diabetes. There is increasing evidence that exosomes change in the blood of patients with diabetes and are implicated in the progression of diabetes, including microvascular complications, inflammation, and changes in coagulation (78, 79). Next, we briefly introduce the role of miRNA in the treatment of other complications of diabetes. Figure 3 shows the exosomes related to cardiovascular and cerebrovascular risk events, such as DN, myocardial infarction (MI), and stroke.

6.1 Diabetic nephropathy

It was found that rapamycin (mTOR) is a core component of cell growth signaling, and, when its activity is enhanced, it can promote protein translation and autophagy. Autophagy protects against renal injury induced by hyperglycemia (80). Ebrahim et al. found that BMSC-derived exosomes enhanced autophagy *via* blocking the mTOR signaling pathway in a model of DR. In addition, they found that when using MSC-derived exosomes to treat mice with DN, the histological morphology of the kidneys was restored and fibrosis markers were reduced (81).

The development of DN is also associated with podocyte injury (82). VEGF produced by podocytes is not beneficial in

10.3389/fendo.2022.935244

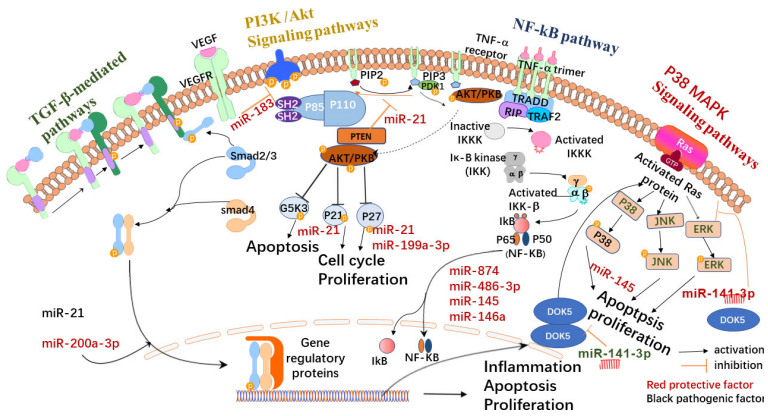

FIGURE 2
Possible exosome-mediated signaling pathways in DR. Exosomes are synthesized in various cells. Under physiological or pathological conditions, their carriers may change and participate in the formation of the collective pathological state. They may activate TGF-β, the signaling pathway that mediates the hemodynamics of individuals with PDR. By blocking TGF-β, the activation of the signaling pathway promotes cell proliferation and reduces apoptosis and the inflammatory response. Exosomes (such as miR-141-3p) may also inhibit retinal neovascularization by preventing the activation of the p38/MAPK signaling pathway. Exosomes can also be detected by the PI3K/Akt signaling pathway, which can induce vascular endothelial cell proliferation while preventing cell apoptosis, as well as cell proliferation and migration of the retinal pigment epithelium cell. The stimulation of the signaling system may also aid in the reduction of HG-induced cell proliferation, migration, and angiogenesis. In diabetic rats, the activity of the NF-κB signaling pathway rose dramatically, and inhibiting the NF-κB signaling pathway can reduce inflammation, apoptosis, and oxidative stress.

treating DN (83). MiR-16-5p could reduce VEGF expression. Hyperglycemia reduces podocyte miR-16-5p production and stimulates VEGF release. Following miR-16-5p overexpression in human embryonic stem cells, exosomes might deliver it to HG-treated podocytes, reducing the degree of podocyte apoptosis and expressing VEGF, thereby delaying the occurrence and development of DN (84).

6.2 Ischemic myocardial infarction

MI is a major cause of mortality in all cardiovascular diseases. Ischemia and reperfusion damage is an inevitable adverse reaction after MI. There is presently no effective treatment to reduce the damage to the heart from MI. Recent research has shown that miRNAs in the heart and circulation are markedly altered after MI

TABLE 1 List of exocrine derived proteins and RNA involved in diabetic retinopathy.

Classification	Component	Effect	Reference
Protein	SNHG7	EndMT ↓	(37)
	Notch3	Calcification/aging of VSMCs ↓	(40)
RNA	miR–202–5p	EndMT ↓	(36)
	miR–1260b	Abnormal VSMC proliferation ↑	(39)
	miR–21	Proliferation and migration of RPEC↑	(65)
	miR–200a–3p	Cell proliferation↑ Apoptosis↓, Inflammatory cytokines ↓ VEGF ↓	(62)
	miR–183	Endothelial cell proliferation ↑ Apoptosis↓	(64)
	miR–199a–3p	Neovascularization ↓	(67)
	miR–141–3p	Retinal neovascularization ↓	(69)
	miR–145	RECs Apoptosis↓ oxidative stress↓ Inflammatory cytokines↓	(54, 71)
	miR–874	Number of retinal capillary pericytes↑ Endothelial cell proliferation↓	(75)
	miR–486–3p	Oxidative stress↓ inflammation ↓ Apoptosis↓	(75)
	miR–146a	REC inflammation↓	(77)

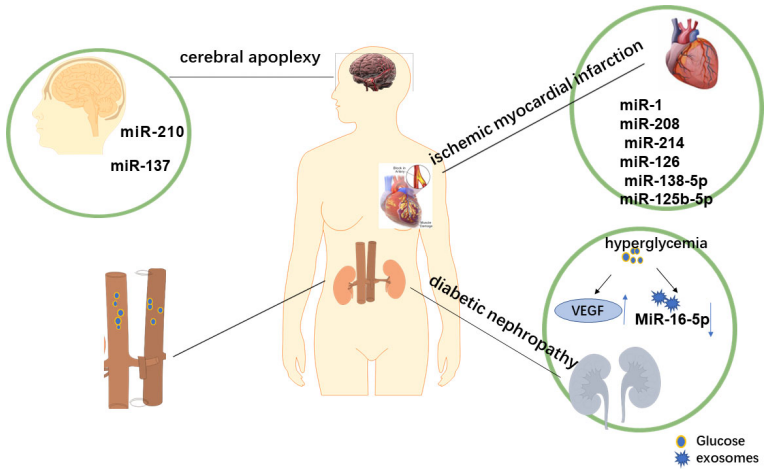

FIGURE 3
Exocrine-related complications of diabetes. During the development t of diabetes mellitus, changes in the microenvironment also lead to alterations in exocrine bodies, which are involved in cardiovascular and cerebrovascular risk events, such as diabetic nephropathy, myocardial infarction, and stroke. Ever-increasing evidence suggests that the level of exosomes in the blood of patients with diabetes is elevated and is involved in the pathophysiology of diabetes-related diseases. Therefore, we concluded that the overexpression and downregulation of specific miRNA might be a new method to treat diabetes and its related complications.

(85). For example, Cheng et al. found significantly increased miR-1 and miR-208 levels in the urine of patients with acute MI and in the circulating blood of rats after acute MI (86). Mao et al. found that KLF3-AS1 mediates Sirt1 expression by serving as a ceRNA to sponge miR-138-5p, thereby regulating cardiomyocyte pyroptosis and MI progression (87). Furthermore, miR-125b-5p inhibited p53 and BAK1 production, which reduced apoptosis. In addition, increased miR-125b-5p expression in macrophages alleviated hypoxia/reperfusion-induced cellular damage. Enhanced miR-125b-5p production in the myocardium significantly reduced the size of the MI (88, 89). The findings of Zhu et al. showed a unique method, whereby cell-free hypo-exo promotes ischemic heart repair *via* anti-apoptotic miR-125b-5p (89). The role of exosomes in MI is increasingly recognized, but the mechanisms involved and their role in improving cardiac function remain unclear (90).

6.3 Stroke

Reflex mechanisms are engaged to protect cerebral perfusion in early hemorrhagic strokes, such as intracerebral hemorrhage and subarachnoid hemorrhage, but the corresponding secondary injury and malfunction can lead to cerebral ischemia, hypoxia, and ultimately neuronal cell death (91). Recent evidence suggests that exosomes may perform various functions in brain repair and as biomarkers for stroke (92). In a previous research, exosome extraction from MSCs was reported to ameliorate specific brain tissue damage in an experimental animal model (93). Exosomes generated by endothelial progenitor cells (EPCs) have been shown to protect ECs from hypoxia/reoxidation injury, which is partially due to the role of miR-210 (94). According to Liu et al., miR-137 upregulation promoted EPC proliferation and angiogenesis in mice with ischemic stroke by the Notch pathway (95). Taken together, exosomes are implicated in the occurrence and progression of stroke through various mechanisms, providing new ideas for stroke treatment.

7 Conclusion and prospects

In recent years, exosomes have been studied as a new biological entity engaged in intercellular communication in a variety of physiological and pathological processes. Ongoing technological and experimental advances have the potential to uncover cellular and molecular mechanisms of intercellular communication, organ homeostasis, and disease, enhancing our ability to use these mechanisms as therapeutic and diagnostic tools. DR increases the risk for blindness in those with diabetes. Previous studies have found that exosomes may play a role in both the pathogenesis and treatment of DR. Earlier studies have found that circulatory miRNAs are differentially expressed in subjects with diabetes (96), suggesting that miRNAs could be used as new biomarkers for detecting or predicting the overall progression of the disease, as well as the progression of retinopathy from mild to sight-threatening (97–99). For example, miR-221, an antiangiogenic miRNA found in blood as a biomarker for DR in individuals with T2DM and PDR, was found to be implicated in the physiopathology of T2DM and macrovascular problems (100–102). RNA sequencing has established the potential biomarkers let-7a and miR-151 in serum for early-stage and late-stage DR in patients with T2DM. The

previous study has discovered that using multiple miRNAs and anti-miRNAs in a combinational therapy is a unique method that involves targeting numerous pathways with different drugs and may provide a synergistic angiostatic effect that can help to prevent DR pathologic angiogenesis problems. Overexpression of miR-216a, for example, protected against HRMEC damage in DR by inhibiting the NOS2/JAK/STAT axis in the DR rat retina (103). Simultaneously, miRNA-29b-3p increases HRMEC apoptosis in DR by inhibiting SIRT1 (104). Upregulation of miR-203a-3p, which targets VEGFA and HIF-1, may decrease retinal neovascularization in the oxygen-induced retinopathy rat model (105). In DR development, the involvement of exosomes and the role of pericytes have separately been widely studied. However, limited studies have investigated the role of pericyte-related exosomes in the occurrence and development of DR, particularly its biological mechanism. Consequently, future studies should focus on the effect of exocytosis on pericytes and thus its potential role in DR. The use of stem cell exosomes for the treatment of DR requires further basic and clinical research.

In conclusion, exosomes, particularly their miRNAs, are involved in the pathophysiological process of DR and establish multilevel connections. Exosomes have broad application prospects in the treatment and prognostic evaluation of DR.

Author contributions

S-rN is responsible for writing the manuscript. J-mH is responsible for data collection. YH and SL are mainly responsible for reviewing and revising the article. All authors contributed to the article and approved the submitted version.

Funding

This work was supported by the Science and Technology Bureau of Quanzhou (grant number 2020CT003 and 2021N036S).

Conflict of interest

The authors declare that the research was conducted in the absence of any commercial or financial relationships that could be construed as a potential conflict of interest.

Publisher's note

References

1. Cui X, Zhu L, Zhai R, Zhang B, Zhang F. Mesenchymal stem cell-derived exosomes: a promising vector in treatment for diabetes and its microvascular complications. *Am J Transl Med* (2021) 13(5):3942–53.

2. Liu C, Ge HM, Liu BH, Dong R, Shan K, Chen X, et al. Targeting pericyte-endothelial cell crosstalk by circular RNA-cPWWP2A inhibition aggravates diabetes-induced microvascular dysfunction. *Proc Natl Acad Sci U.S.A.* (2019) 116(15):7455–64. doi: 10.1073/pnas.1814874116

3. van Dijk CG, Nieuweboer FE, Pei JY, Xu YJ, Burgisser P, van Mulligen E, et al. The complex mural cell: pericyte function in health and disease. *Int J Cardiol* (2015) 190:75–89. doi: 10.1016/j.ijcard.2015.03.258

4. Arboleda-Velasquez JF, Valdez CN, Marko CK, D'Amore PA. From pathobiology to the targeting of pericytes for the treatment of diabetic retinopathy. *Curr Diabetes Rep* (2015) 15(2):573. doi: 10.1007/s11892-014-0573-2

5. Huang H. Pericyte-endothelial interactions in the retinal microvasculature. *Int J Mol Sci* (2020) 21(19):7413. doi: 10.3390/ijms21197413

6. Akbari Kordkheyli V, Amir Mishan M, Khonakdar Tarsi A, Mahrooz A, Rezaei Kanavi M, Hafezi-Moghadam A, et al. MicroRNAs may provide new strategies in the treatment and diagnosis of diabetic retinopathy: Importance of VEGF. *Iran J Basic Med Sci* (2021) 24(3):267–79. doi: 10.22038/ijbms.2021.52164.11807

7. Hammes HP, Feng Y, Pfister F, Brownlee M. Diabetic retinopathy: targeting vasoregression. *Diabetes* (2011) 60(1):9–16. doi: 10.2337/db10-0454

8. Winkler EA, Bell RD, Zlokovic BV. Central nervous system pericytes in health and disease. *Nat Neurosci* (2011) 14(11):1398–405. doi: 10.1038/nn.2946

9. Frank R. Diabetic retinopathy. *New Engl J Med* (2004) 350(1):48–58. doi: 10.1056/NEJMra021678

10. Hammes H, Lin J, Wagner P, Feng Y, Vom Hagen F, Krzizok T, et al. Angiopoietin-2 causes pericyte dropout in the normal retina: evidence for involvement in diabetic retinopathy. *J Clin Med* (2004) 53(4):1104–10. doi: 10.2337/diabetes.53.4.1104

11. Li AF, Sato T, Haimovici R, Okamoto T, Roy S. High glucose alters connexin 43 expression and gap junction intercellular communication activity in retinal pericytes. *Invest Ophthalmol Vis Sci* (2003) 44(12):5376–82. doi: 10.1167/iovs.03-0360

12. Monickaraj F, McGuire P, Das A. Cathepsin d plays a role in endothelial-pericyte interactions during alteration of the blood-retinal barrier in diabetic retinopathy. *FASEB J* (2018) 32(5):2539–48. doi: 10.1096/fj.201700781RR

13. McGuire PG, Rangasamy S, Maestas J, Das A. Pericyte-derived sphingosine 1-phosphate induces the expression of adhesion proteins and modulates the retinal endothelial cell barrier. *Arterioscler Thromb Vasc Biol* (2011) 31(12):e107–115. doi: 10.1161/ATVBAHA.111.235408

14. Caporali A, Martello A, Miscianinov V, Maselli D, Vono R, Spinetti G. Contribution of pericyte paracrine regulation of the endothelium to angiogenesis. *Pharmacol Ther* (2017) 171:56–64. doi: 10.1016/j.pharmthera.2016.10.001

15. He C, Zheng S, Luo Y, Wang B. Exosome theranostics: Biology and translational medicine. *Theranostics* (2018) 8(1):237–55. doi: 10.7150/thno.21945

16. Zhang J, Li S, Li L, Li M, Guo C, Yao J, et al. Exosome and exosomal microRNA: trafficking, sorting, and function. *Genomics Proteomics Bioinf* (2015) 13(1):17–24. doi: 10.1016/j.gpb.2015.02.001

17. Bosch S, Young NA, Mignot G, Bach JM. Epigenetic mechanisms in immune disease: The significance of toll-like receptor-binding extracellular vesicle-encapsulated microRNA. *Front Genet* (2020) 11:578335. doi: 10.3389/fgene.2020.578335

18. Fabbri M, Paone A, Calore F, Galli R, Gaudio E, Santhanam R, et al. MicroRNAs bind to toll-like receptors to induce prometastatic inflammatory response. *Proc Natl Acad Sci U.S.A.* (2012) 109(31):E2110–2116. doi: 10.1073/pnas.1209414109

19. Ambros V. The functions of animal microRNAs. *Nature* (2004) 431 (7006):350–5. doi: 10.1038/nature02871

20. Doench JG, Sharp PA. Specificity of microRNA target selection in translational repression. *Genes Dev* (2004) 18(5):504–11. doi: 10.1101/gad.1184404

21. Sevignani C, Calin GA, Siracusa LD, Croce CM. Mammalian microRNAs: a small world for fine-tuning gene expression. *Mamm Genome* (2006) 17(3):189–202. doi: 10.1007/s00335-005-0066-3

22. Guo R, Shen W, Su C, Jiang S, Wang J. Relationship between the pathogenesis of glaucoma and miRNA. *Ophthalmic Res* (2017) 57(3):194–9. doi: 10.1159/000450957

23. Kowal J, Tkach M, Thery C. Biogenesis and secretion of exosomes. *Curr Opin Cell Biol* (2014) 29:116–25. doi: 10.1016/j.ceb.2014.05.004

24. Stenmark H. Rab GTPases as coordinators of vesicle traffic. *Nat Rev Mol Cell Biol* (2009) 10(8):513–25. doi: 10.1038/nrm2728

25. Thery C, Boussac M, Veron P, Ricciardi-Castagnoli P, Raposo G, Garin J, et al. Proteomic analysis of dendritic cell-derived exosomes: a secreted subcellular compartment distinct from apoptotic vesicles. *J Immunol* (2001) 166(12):7309–18. doi: 10.4049/jimmunol.166.12.7309

26. Savina A, Fader CM, Damiani MT, Colombo MI. Rab11 promotes docking and fusion of multivesicular bodies in a calcium-dependent manner. *Traffic* (2005) 6(2):131–43. doi: 10.1111/j.1600-0854.2004.00257.x

27. Kanemoto S, Nitani R, Murakami T, Kaneko M, Asada R, Matsuhisa K, et al. Multivesicular body formation enhancement and exosome release during endoplasmic reticulum stress. *Biochem Biophys Res Commun* (2016) 480(2):166–72. doi: 10.1016/j.bbrc.2016.10.019

28. Lehmann BD, Paine MS, Brooks AM, McCubrey JA, Renegar RH, Wang R, et al. Senescence-associated exosome release from human prostate cancer cells. *Cancer Res* (2008) 68(19):7864–71. doi: 10.1158/0008-5472.CAN-07-6538

29. Beer L, Zimmermann M, Mitterbauer A, Ellinger A, Gruber F, Narzt MS, et al. Analysis of the secretome of apoptotic peripheral blood mononuclear cells: Impact of released proteins and exosomes for tissue regeneration. *Sci Rep* (2015) 5:16662. doi: 10.1038/srep16662

30. Mayo JN, Bearden SE. Driving the hypoxia-inducible pathway in human pericytes promotes vascular density in an exosome-dependent manner. *Microcirculation* (2015) 22(8):711–23. doi: 10.1111/micc.12227

31. Zagrean AM, Hermann DM, Opris I, Zagrean L, Popa-Wagner A. Multicellular crosstalk between exosomes and the neurovascular unit after cerebral ischemia. therapeutic implications. *Front Neurosci* (2018) 12:811. doi: 10.3389/fnins.2018.00811

32. Huang C, Fisher KP, Hammer SS, Navitskaya S, Blanchard GJ, Busik JV. Plasma exosomes contribute to microvascular damage in diabetic retinopathy by activating the classical complement pathway. *Diabetes* (2018) 67(8):1639–49. doi: 10.2337/db17-1587

33. Xu B, Zhang Y, Du XF, Li J, Zi HX, Bu JW, et al. Neurons secrete miR-132-containing exosomes to regulate brain vascular integrity. *Cell Res* (2017) 27(7):882–97. doi: 10.1038/cr.2017.62

34. Gong M, Yu B, Wang J, Wang Y, Liu M, Paul C, et al. Mesenchymal stem cells release exosomes that transfer miRNAs to endothelial cells and promote angiogenesis. *Oncotarget* (2017) 8(28):45200–12. doi: 10.18632/oncotarget.16778

35. Zhu L, Zang J, Liu B, Yu G, Hao L, Liu L, et al. Oxidative stress-induced RAC autophagy can improve the HUVEC functions by releasing exosomes. *J Cell Physiol* (2020) 235(10):7392–409. doi: 10.1002/jcp.29641

36. Gu S, Liu Y, Zou J, Wang W, Wei T, Wang X, et al. Retinal pigment epithelial cells secrete miR-202-5p-containing exosomes to protect against proliferative diabetic retinopathy. *Exp Eye Res* (2020) 201:108271. doi: 10.1016/j.exer.2020.108271

37. Cao X, Xue LD, Di Y, Li T, Tian YJ, Song Y. MSC-derived exosomal lncRNA SNHG7 suppresses endothelial-mesenchymal transition and tube formation in diabetic retinopathy *via* miR-34a-5p/XBP1 axis. *Life Sci* (2021) 272:119232. doi: 10.1016/j.lfs.2021.119232

38. Lee J, Heo J, Kang H. miR-92b-3p-TSC1 axis is critical for mTOR signaling-mediated vascular smooth muscle cell proliferation induced by hypoxia. *Cell Death Differ* (2019) 26(9):1782–95. doi: 10.1038/s41418-018-0243-z

39. Seong M, Kang H. Hypoxia-induced miR-1260b regulates vascular smooth muscle cell proliferation by targeting GDF11. *BMB Rep* (2020) 53(4):206–11. doi: 10.5483/BMBRep.2020.53.4.136

40. Lin X, Li S, Wang YJ, Wang Y, Zhong JY, He JY, et al. Exosomal Notch3 from high glucose-stimulated endothelial cells regulates vascular smooth muscle cells calcification/aging. *Life Sci* (2019) 232:116582. doi: 10.1016/j.lfs.2019.116582

41. Forrester JV, Kuffova L, Delibegovic M. The role of inflammation in diabetic retinopathy. *Front Immunol* (2020) 11:583687. doi: 10.3389/fimmu.2020.583687

42. Sharma Y, Saxena S, Mishra A, Saxena A, Natu SM. Advanced glycation end products and diabetic retinopathy. *J Ocul Biol Dis Infor* (2012) 5(3-4):63–9. doi: 10.1007/s12177-013-9104-7

43. Chen J, Sun Z, Jin M, Tu Y, Wang S, Yang X, et al. Inhibition of AGEs/RAGE/Rho/ROCK pathway suppresses non-specific neuroinflammation by regulating BV2 microglial M1/M2 polarization through the NF-kappaB pathway. *J Neuroimmunol* (2017) 305:108–14. doi: 10.1016/j.jneuroim.2017.02.010

44. Subedi L, Lee JH, Gaire BP, Kim SY. Sulforaphane inhibits MGO-AGE-Mediated neuroinflammation by suppressing NF-kappaB, MAPK, and AGE-RAGE signaling pathways in microglial cells. *Antioxidants (Basel)* (2020) 9 (9):792. doi: 10.3390/antiox9090792

45. Rivera JC, Sitaras N, Noueihed B, Hamel D, Madaan A, Zhou T, et al. Microglia and interleukin-1beta in ischemic retinopathy elicit microvascular degeneration through neuronal semaphorin-3A. *Arterioscler Thromb Vasc Biol* (2013) 33(8):1881–91. doi: 10.1161/ATVBAHA.113.301331

46. Yoshida S, Yoshida A, Ishibashi T. Induction of IL-8, MCP-1, and bFGF by TNF-alpha in retinal glial cells: implications for retinal neovascularization during post-ischemic inflammation. *Graefes Arch Clin Exp Ophthalmol* (2004) 242 (5):409–13. doi: 10.1007/s00417-004-0874-2

47. Zhang T, Ouyang H, Mei X, Lu B, Yu Z, Chen K, et al. Erianin alleviates diabetic retinopathy by reducing retinal inflammation initiated by microglial cells *via* inhibiting hyperglycemia-mediated ERK1/2-NF-kappaB signaling pathway. *FASEB J* (2019) 33(11):11776–90. doi: 10.1096/fj.201802614RRR

48. Yu Z, Zhang T, Gong C, Sheng Y, Lu B, Zhou L, et al. Erianin inhibits high glucose-induced retinal angiogenesis *via* blocking ERK1/2-regulated HIF-1alpha-VEGF/VEGFR2 signaling pathway. *Sci Rep* (2016) 6:34306. doi: 10.1038/srep34306

49. Hachana S, Pouliot M, Couture R, Vaucher E. Diabetes-induced inflammation and vascular alterations in the goto-kakizaki rat retina. *Curr Eye Res* (2020) 45(8):965–74. doi: 10.1080/02713683.2020.1712730

50. Kang GY, Bang JY, Choi AJ, Yoon J, Lee WC, Choi S, et al. Exosomal proteins in the aqueous humor as novel biomarkers in patients with neovascular age-related macular degeneration. *J Proteome Res* (2014) 13(2):581–95. doi: 10.1021/pr400751k

51. Jin X, Zhao W, Zhou P, Niu T. YAP knockdown inhibits proliferation and induces apoptosis of human prostate cancer DU145 cells. *Mol Med Rep* (2018) 17 (3):3783–8. doi: 10.3892/mmr.2017.8352

52. Zhang W, Jiang H, Kong Y. Exosomes derived from platelet-rich plasma activate YAP and promote the fibrogenic activity of Muller cells *via* the PI3K/Akt pathway. *Exp Eye Res* (2020) 193:107973. doi: 10.1016/j.exer.2020.107973

53. Zhang W, Dong X, Wang T, Kong Y. Exosomes derived from platelet-rich plasma mediate hyperglycemia-induced retinal endothelial injury *via* targeting the TLR4 signaling pathway. *Exp Eye Res* (2019) 189:107813. doi: 10.1016/j.exer.2019.107813

54. Hui Y, Yin Y. MicroRNA-145 attenuates high glucose-induced oxidative stress and inflammation in retinal endothelial cells through regulating TLR4/NF-kappaB signaling. *Life Sci* (2018) 207:212–8. doi: 10.1016/j.lfs.2018.06.005

55. Ye L, Guo H, Wang Y, Peng Y, Zhang Y, Li S, et al. Exosomal circEhmt1 released from hypoxia-pretreated pericytes regulates high glucose-induced microvascular dysfunction *via* the NFIA/NLRP3 pathway. *Oxid Med Cell Longev* (2021) 2021:8833098. doi: 10.1155/2021/8833098

56. Lu Y, Zhou Y, Zhang R, Wen L, Wu K, Li Y, et al. Bone mesenchymal stem cell-derived extracellular vesicles promote recovery following spinal cord injury via improvement of the integrity of the blood-spinal cord barrier. *Front Neurosci* (2019) 13:209. doi: 10.3389/fnins.2019.00209

57. Hu X, Shen N, Liu A, Wang W, Zhang L, Sui Z, et al. Bone marrow mesenchymal stem cell-derived exosomal miR-34c-5p ameliorates RIF by inhibiting the core fucosylation of multiple proteins. *Mol Ther* (2022) 30(2):763–81. doi: 10.1016/j.ymthe.2021.10.012

58. Kim DJ, Kang JM, Park SH, Kwon HK, Song SJ, Moon H, et al. Diabetes aggravates post-ischaemic renal fibrosis through persistent activation of TGF-beta1 and shh signalling. *Sci Rep* (2017) 7(1):16782. doi: 10.1038/s41598-017-16977-z

59. Kilari S, Yang B, Sharma A, McCall DL, Misra SJ. Increased transforming growth factor beta (TGF-β) and pSMAD3 signaling in a murine model for contrast induced kidney injury. *Sci Rep* (2018) 8(1):1–12. doi: 10.1038/s41598-018-24340-z

60. van der Velden JL, Wagner DE, Lahue KG, Abdalla ST, Lam YW, Weiss DJ, et al. TGF-beta1-induced deposition of provisional extracellular matrix by tracheal basal cells promotes epithelial-to-mesenchymal transition in a c-jun NH2-terminal kinase-1-dependent manner. *Am J Physiol Lung Cell Mol Physiol* (2018) 314(6): L984–97. doi: 10.1152/ajplung.00053.2017

61. Lou H, Wang S, Guo T, Yang Y. Role of miR-21 in rats with proliferative diabetic retinopathy *via* TGF-β signaling pathway. *Eur Rev Med Pharmacol Sci* (2019) 23(3 Suppl):9–16. doi: 10.26355/eurrev_201908_18621

62. Xue L, Xiong C, Li J, Ren Y, Zhang L, Jiao K, et al. miR-200-3p suppresses cell proliferation and reduces apoptosis in diabetic retinopathy via blocking the TGF-β2/Smad pathway. *Biosci Rep* (2020) 40(11):BSR20201545. doi: 10.1042/BSR20201545

63. Fruman DA, Chiu H, Hopkins BD, Bagrodia S, Cantley LC, Abraham RT. The PI3K pathway in human disease. *Cell* (2017) 170(4):605–35. doi: 10.1016/j.cell.2017.07.029

64. Zhang Z-Z, Qin X-H, Zhang J. Metabolism. MicroRNA-183 inhibition exerts suppressive effects on diabetic retinopathy by inactivating BTG1-mediated PI3K/Akt/VEGF signaling pathway. *Am J Physiol Endocrinol Metab* (2019) 316(6): E1050–60. doi: 10.1152/ajpendo.00444.2018

65. Usui-Ouchi A, Ouchi Y, Kiyokawa M, Sakuma T, Ito R, Ebihara N. Upregulation of mir-21 levels in the vitreous humor is associated with development of proliferative vitreoretinal disease. *PloS One* (2016) 11(6): e0158043. doi: 10.1371/journal.pone.0158043

66. Lu JM, Zhang ZZ, Ma X, Fang SF, Qin XH. Repression of microRNA-21 inhibits retinal vascular endothelial cell growth and angiogenesis *via* PTEN dependent-PI3K/Akt/VEGF signaling pathway in diabetic retinopathy. *Exp Eye Res* (2020) 190:107886. doi: 10.1016/j.exer.2019.107886

67. Wang L, Liu W, Huang XJE. MicroRNA-199a-3p inhibits angiogenesis by targeting the VEGF/PI3K/AKT signalling pathway in an *in vitro* model of diabetic retinopathy. *Pathol M* (2020) 116:104488. doi: 10.1016/j.yexmp.2020.104488

68. Qi R, Liu H, Wang Q, Wang J, Yang F, Long D, et al. Expressions and regulatory effects of P38/ERK/JNK mapks in the adipogenic trans-differentiation of C2C12 myoblasts. *Cell Physiol Biochem* (2017) 44(6):2467–75. doi: 10.1159/000486169

69. Zhang LQ, Cui H, Yu YB, Shi HQ, Zhou Y, Liu MJ. MicroRNA-141-3p inhibits retinal neovascularization and retinal ganglion cell apoptosis in glaucoma mice through the inactivation of docking protein 5-dependent mitogen-activated protein kinase signaling pathway. *J Cell Physiol* (2019) 234(6):8873–87. doi: 10.1002/jcp.27549

70. Chen J, Chen J, Cheng Y, Fu Y, Zhao H, Tang M, et al. Mesenchymal stem cell-derived exosomes protect beta cells against hypoxia-induced apoptosis *via* miR-21 by alleviating ER stress and inhibiting p38 MAPK phosphorylation. *Stem Cell Res Ther* (2020) 11(1):97. doi: 10.1186/s13287-020-01610-0

71. Dai C, Jiang S, Chu C, Xin M, Song X, Zhao B. Baicalin protects human retinal pigment epithelial cell lines against high glucose-induced cell injury by up-regulation of microRNA-145. *Exp Mol Pathol* (2019) 106:123–30. doi: 10.1016/j.yexmp.2019.01.002

72. Antzelevitch C. Genetic, molecular and cellular mechanisms underlying the J wave syndromes. *Circ J* (2012) 76(5):1054–65. doi: 10.1253/circj.CJ-12-0284

73. Chen F, Zhang H-Q, Zhu J, Liu K-Y, Cheng H, Li G-L, et al. Puerarin enhances superoxide dismutase activity and inhibits RAGE and VEGF expression in retinas of STZ–induced early diabetic rats. *Asian Pacific J Trop Med* (2012) 5 (11):891–6. doi: 10.1016/S1995-7645(12)60166-7

74. Yin Y, Chen F, Wang W, Wang H, Zhang X. Resolvin D1 inhibits inflammatory response in STZ-induced diabetic retinopathy rats: Possible involvement of NLRP3 inflammasome and NF-κB signaling pathway. *Mol Vis* (2017) 23:242.

75. Li R, Yuan H, Zhao T, Yan Y, Liu Z, Cai J, et al. miR-874 ameliorates retinopathy in diabetic rats by NF-kappaB signaling pathway. *Adv Clin Exp Med* (2021) 30(4):421–30. doi: 10.17219/acem/130602

76. Li W, Jin L, Cui Y, Nie A, Xie N, Liang G. Bone marrow mesenchymal stem cells-induced exosomal microRNA-486-3p protects against diabetic retinopathy through TLR4/NF-kappaB axis repression. *J Endocrinol Invest* (2021) 44(6):1193–207. doi: 10.1007/s40618-020-01405-3

77. Ye EA, Steinle JJ. miR-146a attenuates inflammatory pathways mediated by TLR4/NF-kappaB and TNFalpha to protect primary human retinal microvascular endothelial cells grown in high glucose. *Mediators Inflammation* (2016) 2016:3958453. doi: 10.1155/2016/3958453

78. Freeman D, Noren Hooten N, Eitan E, Green J, Mode N, Bodogai M, et al. Altered extracellular vesicle concentration, cargo, and function in diabetes. *Diabetes* (2018) 67(11):2377–88. doi: 10.2337/db17-1308

79. O'Neill S, Bohl M, Gregersen S, Hermansen K, O'Driscoll L. Blood-based biomarkers for metabolic syndrome. *Trends Endocrinol Metab* (2016) 27(6):363–74. doi: 10.1016/j.tem.2016.03.012

80. De Rechter S, Decuypere JP, Ivanova E, van den Heuvel LP, De Smedt H, Levtchenko E, et al. Autophagy in renal diseases. *Pediatr Nephrol* (2016) 31(5):737–52. doi: 10.1007/s00467-015-3134-2

81. Ebrahim N, Ahmed IA, Hussien NI, Dessouky AA, Farid AS, Elshazly AM, et al. Mesenchymal stem cell-derived exosomes ameliorated diabetic nephropathy by autophagy induction through the mTOR signaling pathway. *Cells* (2018) 7 (12):556. doi: 10.3390/cells7120226

82. Zhang X, Song Z, Guo Y, Zhou M. The novel role of TRPC6 in vitamin d ameliorating podocyte injury in STZ-induced diabetic rats. *Mol Cell Biochem* (2015) 399(1-2):155–65. doi: 10.1007/s11010-014-2242-9

83. Bus P, Scharpfenecker M, van der Wilk P, Wolterbeek R, Bruijn JA, Baelde HJ. The VEGF-a inhibitor sFLT-1 improves renal function by reducing endothelial activation and inflammation in a mouse model of type 1 diabetes. *Diabetologia* (2017) 60(9):1813–21. doi: 10.1007/s00125-017-4322-3

84. Duan YR, Chen BP, Chen F, Yang SX, Zhu CY, Ma YL, et al. Exosomal microRNA-16-5p from human urine-derived stem cells ameliorates diabetic nephropathy through protection of podocyte. *J Cell Mol Med* (2021) 25 (23):10798–813. doi: 10.1111/jcmm.14558

85. Sahoo S, Losordo DW. Exosomes and cardiac repair after myocardial infarction. *Circ Res* (2014) 114(2):333–44. doi: 10.1161/CIRCRESAHA.114.300639

86. Cheng Y, Wang X, Yang J, Duan X, Yao Y, Shi X, et al. A translational study of urine miRNAs in acute myocardial infarction. *J Mol Cell Cardiol* (2012) 53 (5):668–76. doi: 10.1016/j.yjmcc.2012.08.010

87. Mao Q, Liang XL, Zhang CL, Pang YH, Lu YX. LncRNA KLF3-AS1 in human mesenchymal stem cell-derived exosomes ameliorates pyroptosis of cardiomyocytes and myocardial infarction through miR-138-5p/Sirt1 axis. *Stem Cell Res Ther* (2019) 10(1):393. doi: 10.1186/s13287-019-1522-4

88. Wang X, Ha T, Zou J, Ren D, Liu L, Zhang X, et al. MicroRNA-125b protects against myocardial ischaemia/reperfusion injury *via* targeting p53-mediated apoptotic signalling and TRAF6. *Cardiovasc Res* (2014) 102(3):385–95. doi: 10.1093/cvr/cvu044

89. Zhu LP, Tian T, Wang JY, He JN, Chen T, Pan M, et al. Hypoxia-elicited mesenchymal stem cell-derived exosomes facilitates cardiac repair through miR-125b-mediated prevention of cell death in myocardial infarction. *Theranostics* (2018) 8(22):6163–77. doi: 10.7150/thno.28021

90. Davidson SM, Padro T, Bollini S, Vilahur G, Duncker DJ, Evans PC, et al. Progress in cardiac research: from rebooting cardiac regeneration to a complete cell atlas of the heart. *Cardiovasc Res* (2021) 117(10):2161–74. doi: 10.1093/cvr/cvab200

91. Xiao M, Li Q, Feng H, Zhang L, Chen Y. Neural vascular mechanism for the cerebral blood flow autoregulation after hemorrhagic stroke. *Neural Plast* (2017) 2017:5819514. doi: 10.1155/2017/5819514

92. Otero-Ortega L, Laso-Garcia F, Gomez-de Frutos M, Fuentes B, Diekhorst L, Diez-Tejedor E, et al. Role of exosomes as a treatment and potential biomarker for stroke. *Transl Stroke Res* (2019) 10(3):241–9. doi: 10.1007/s12975-018-0654-7

93. Otero-Ortega L, Gomez de Frutos MC, Laso-Garcia F, Rodriguez-Frutos B, Medina-Gutierrez E, Lopez JA, et al. Exosomes promote restoration after an experimental animal model of intracerebral hemorrhage. *J Cereb Blood Flow Metab* (2018) 38(5):767–79. doi: 10.1177/0271678X17708917

94. Ma X, Wang J, Li J, Ma C, Chen S, Lei W, et al. Loading MiR-210 in endothelial progenitor cells derived exosomes boosts their beneficial effects on Hypoxia/Reoxygeneation-injured human endothelial cells *via* protecting mitochondrial function. *Cell Physiol Biochem* (2018) 46(2):664–75. doi: 10.1159/000488635

95. Liu XL, Wang G, Song W, Yang WX, Hua J, Lyu L. microRNA-137 promotes endothelial progenitor cell proliferation and angiogenesis in cerebral ischemic stroke mice by targeting NR4A2 through the notch pathway. *J Cell Physiol* (2018) 233(7):5255–66. doi: 10.1002/jcp.26312

96. Zampetaki A, Kiechl S, Drozdov I, Willeit P, Mayr U, Prokopi M, et al. Plasma microRNA profiling reveals loss of endothelial miR-126 and other microRNAs in type 2 diabetes. *Circ Res* (2010) 107(6):810–7. doi: 10.1161/CIRCRESAHA.110.226357

97. Jimenez-Lucena R, Camargo A, Alcala-Diaz JF, Romero-Baldonado C, Luque RM, van Ommen B, et al. A plasma circulating miRNAs profile predicts type 2 diabetes mellitus and prediabetes: from the CORDIOPREV study. *Exp Mol Med* (2018) 50(12):1–12. doi: 10.1038/s12276-018-0194-y

98. Jimenez-Lucena R, Rangel-Zuniga OA, Alcala-Diaz JF, Lopez-Moreno J, Roncero-Ramos I, Molina-Abril H, et al. Circulating miRNAs as predictive biomarkers of type 2 diabetes mellitus development in coronary heart disease patients from the CORDIOPREV study. *Mol Ther Nucleic Acids* (2018) 12:146–57. doi: 10.1016/j.omtn.2018.05.002

99. Barutta F, Bellini S, Mastrocola R, Bruno G, Gruden G. MicroRNA and microvascular complications of diabetes. *Int J Endocrinol* (2018) 2018:6890501. doi: 10.1155/2018/6890501

100. Martinez B, Peplow PV. MicroRNAs as biomarkers of diabetic retinopathy and disease progression. *Neural Regener Res* (2019) 14(11):1858–69. doi: 10.4103/1673-5374.259602

101. Mammadzada P, Bayle J, Gudmundsson J, Kvanta A, Andre H. Identification of diagnostic and prognostic microRNAs for recurrent vitreous hemorrhage in patients with proliferative diabetic retinopathy. *J Clin Med* (2019) 8(12):2217. doi: 10.3390/jcm8122217

102. Chen S, Yuan M, Liu Y, Zhao X, Lian P, Chen Y, et al. Landscape of microRNA in the aqueous humour of proliferative diabetic retinopathy as assessed by next-generation sequencing. *Clin Exp Ophthalmol* (2019) 47(7):925–36. doi: 10.1111/ceo.13554

103. Liu Y, Xiao J, Zhao Y, Zhao C, Yang Q, Du X, et al. microRNA-216a protects against human retinal microvascular endothelial cell injury in diabetic retinopathy by suppressing the NOS2/JAK/STAT axis. *Exp Mol Pathol* (2020) 115:104445. doi: 10.1016/j.yexmp.2020.104445

104. Zeng Y, Cui Z, Liu J, Chen J, Tang S. MicroRNA-29b-3p promotes human retinal microvascular endothelial cell apoptosis *via* blocking SIRT1 in diabetic retinopathy. *Front Physiol* (2019) 10:1621. doi: 10.3389/fphys.2019.01621

105. Han N, Xu H, Yu N, Wu Y, Yu L. MiR-203a-3p inhibits retinal angiogenesis and alleviates proliferative diabetic retinopathy in oxygen-induced retinopathy (OIR) rat model *via* targeting VEGFA and HIF-1alpha. *Clin Exp Pharmacol Physiol* (2020) 47(1):85–94. doi: 10.1111/1440-1681.13163

Advantages of publishing in Frontiers

OPEN ACCESS
Articles are free to read for greatest visibility and readership

FAST PUBLICATION
Around 90 days from submission to decision

HIGH QUALITY PEER-REVIEW
Rigorous, collaborative, and constructive peer-review

TRANSPARENT PEER-REVIEW
Editors and reviewers acknowledged by name on published articles

Frontiers
Avenue du Tribunal-Fédéral 34
1005 Lausanne | Switzerland

Visit us: www.frontiersin.org
Contact us: frontiersin.org/about/contact`

REPRODUCIBILITY OF RESEARCH
Support open data and methods to enhance research reproducibility

DIGITAL PUBLISHING
Articles designed for optimal readership across devices

FOLLOW US
@frontiersin

IMPACT METRICS
Advanced article metrics track visibility across digital media

EXTENSIVE PROMOTION
Marketing and promotion of impactful research

LOOP RESEARCH NETWORK
Our network increases your article's readership